Author:
Kharnoob, H. H

Title:
Trace metals as pollutants

TRACE METALS AS POLLUTANTS

by

HUSSIAN HASSAN KHARNOOB, M.Sc.

Submitted in April 1986 for the degree of DOCTOR OF PHILOSOPHY in the Department of Chemistry at the University of Bristol.

MEMORANDUM

The research described in this dissertation was conducted in the Department of Inorganic Chemistry at the University of Bristol, under the supervision of Dr. G. Nickless, between April 1983 and September 1985. It was the independent work of the author and has not been described in any other dissertation except where otherwise stated.

HUSSAIN HASSAN KHARNOOB

ACKNOWLEDGEMENTS

The author wishes to accord his gratitude to the following :-

Dr. Nickless, for his patient supervision and encouragement during the research for and compilation of this thesis;

Dr. Martin, for his helpful classification of plant species, and permission to use GFAAS;

Dr. Bennett and Mr. Kemp of the Geology Department for their assistance with XRF analysis;

Mr. Scott and Dr. Hein for their help in computing and statistical analysis of results;

Colleagues of W503 for their useful discussion and advice;

Wessex Water Authority for permission to use Dcp and ICP/MS;

The Iraqi Government for financial support;

Lastly, Mrs. Cottrell who has so kindly typed this thesis.

To my parents

ABSTRACT

The dissertation consists of four Experimental chapters entitled :-

1) Metal Speciation Studies,

2) Thallium : Determination and Effects,

3) Aluminium, Silver and Lanthanum : Determination, Effects and Fractionation Studies;

4) Response Surface Methodology,

preceded by an Introduction of a general nature.

The Introduction is a survey emphasising the occurrence of heavy metals (and other metals used in this study) in the environment, their toxicity, chemical forms, as well as the uptake of metals by plants. In general, because of the low levels of toxic metals found within the environment, sensitive methods of analysis are necessary for their determination in a variety of matrices. The second chapter is concerned with a series of comments concerning the suitability of a number of instrumental methods for these tasks. The techniques used included FAAS, GFAAS, XRF, GLC, DPASV and emission plasma spectroscopy.

Membrane filters were used in sequence to separate the lead species into different groups. The sequential leaching schemes which differentiate the metal format present in sediments were employed to indicate the bio-availability of Ca, Mn, Fe, Cu, Zn and Pb.

Aluminium was chelated with trifluoroacetylacetonate and determined by GLC, while other trivalent metals such as chromium, iron and lanthanum were treated similarly; but their chromatography suffered from a number of practical difficulties. The technique was reliable for aluminium; however, although very sensitive was quite time consuming. Therefore aluminium in plant tissue was determined by GFAAS using pyrolytic graphite system.

The oxidation potential of silver is higher than that of mercury, hence silver was determined by RGCE. However, the level of silver in environmental samples was low and in most samples was not detected.

Three procedures for thallium determination in rock samples were used to evaluate the efficiency of each procedure. A study of interaction of humic acid with thallium ions was carried out. The results obtained indicated that thallium is not affected by the presence of humic acids.

Lanthanum, a most refractory element, was extremely difficult to determine by AAS and therefore Dcp and ICP/MS were used for the determination of lanthanum in plant tissues.

The toxicity of aluminium, silver, lanthanum and thallium to Lolium perenne seedlings was investigated by means of their critical levels. Fractionation of aluminium and lanthanum in plant tissues indicated that most lanthanum was associated with α-cellulose and aluminium with hemicellulose in the roots of Lolium perenne seedlings.

By use of a 5^2 factorial design the interaction between pH and time on the desorption of metals from a Restronguet Creek sediment was studied. The interactive effect of metals in plants was studied using three variable composite rotatable designs. The data were fitted to second-order polynomials and analysed by Minitab and SAS packages. Contour and 3-D plots were used to display the surfaces produced.

Very detailed discussions of the results so obtained are presented, some indicating only additive effects of toxic metals, while others suggest a more involved system of responses.

CONTENTS

LIST OF ABBREVIATIONS

AAS	Atomic Absorption Spectrometry
AES	Atomic Emission Spectrometry
ASV	Anodic Stripping Voltammetry
B.pt.	boiling point
conc.	concentrated
cys.	cysteine
DC	Direct Current
DC-ASV	Direct Current Anodic Stripping Voltammetry
DCP	Direct Current Polarography
Dcp	Direct current plasma
DDW	double distilled water
DPASV	Differential Pulse Anodic Stripping Voltammetry
DPP	Differential Pulse Polarography
DWOM	Dry weight of material
$E_{\frac{1}{2}}$	Half wave potential
EDTA Na_2	Ethylene diamine tetra acetic acid disodium
E_h	Redox potential
EPMA	Electron Probe Microanalysis
FAAS	Flame Atomic Absorption Spectrometry
GCE	Glassy Carbon Electrode
GFAAS	Graphite Furnace Atomic Absorption Spectrometry
GTA	Graphite Tube Atomiser
HMDE	Hanging Mercury Drop Electrode
HFA	Hexafluoroacetylacetone
ICP	Inductively Coupled Plasma
ICP/MS	Inductively Coupled Plasma/Mass Spectrometry
i_d	Diffusion Current

ILL	Instrumental Laboratories Limited
IR	Infrared
ISE	Ion Selective Electrode
MDE	Mercury Drop Electrode
MIBK	Methyl Isobutyl Ketone
M.pt.	Melting point
M.wt.	Molecular Weight
N.D.	Not Detected
NPP	Normal Pulse Polarography
PARC	Princeton Applied Research Corporation
pH	Activity of Hydrogen Ion ($-\log_{10} H^+$)
PP	Pulse Polarography
RGCE	Rotating Glassy Carbon Electrode
RSM	Response Surface Methodology
SCE	Standard Calomel Electrode
SRM	Standard Reference Material
TFA	Trifluoroacetylacetone
TFME	Thin Film Mercury Electrode
TPPS	Triphenyl phosphine sulphide
UV	Ultra violet
v/v	volume to volume (ratio)
vs.	versus
w/w	weight to weight (ratio)

UNITS

km	kilometre
cm^3	cubic centimetre
μg	microgram
$\mu g/cm^3$	microgram/cubic centimetre
L	litre
ms	millisecond
μA	microamp
mA	milliamp
$\mu g/L$	microgram/litre
mv	millivolt
mg	milligram
g	gram
r/min	revolutions per minute
%	percentage
^oC	degree Centigrade
^oK	degree Kelvin
t/yr	tons per year
mM/L	millimolar/litre
v	volt
h	hour
g/g	microgram/gram
MHz	megahertz
M	molar concentration
mv/s	millivolts/second
g/L	grams/litre
ng	nanogram
KW	kilowatt

INDEX TO TABLES

INDEX TO FIGURES

CHAPTER 1

GENERAL INTRODUCTION

CONTENTS

1.1 ENVIRONMENTAL POLLUTION BY HEAVY METALS

Heavy metals have been defined as those metals with specific gravity greater than 4 or 5. These metals are principally located from Atomic Numbers 22 to 34, 40 to 52 and 72 to 84 of the Periodic Table, as well as the lanthanide and actinide series (1-3). During the last twenty years there has been increasing interest in environmental contamination by heavy metals because some are essential for maintenance of normal growth and development, while others are toxic (4,5). Heavy metals have also received special attention because they are immutable, i.e. not biodegradable in the biogeochemical cycle (2), and so can enter the food chain via plant uptake or contamination of fresh waters (6). Recently, the association between heavy metal accumulation in man and the incidence of diseases has been recognised (7,8). It is important to realise that trace metal pollution of any medium represents subtly different forms of pollution to that generally considered in an environmental context. The situation does not represent the unique occurrence of a material within a component, but the level of increase relative to the natural occurrence of that material. The latter fraction is referred to as the 'normal' or 'back' background concentration. There are several different sources of metal pollution in the environment (5). The major natural sources originate from :

1) geological weathering of rocks and minerals;

2) animal and human excretion (which contains heavy metals)

Man's activities have increased the quantity and distribution of heavy metals into the environment. The major anthropogenic sources for

the environment are generally classified as:-

1) those involved with metal smelting and refining

2) emissions from coal/oil fired power generating plants

3) disposal of metal containing wastes

4) solid waste incineration

5) burning of leaded petrol

6) manufacture of cement

7) chemical processing operations.

The most important natural sources of entry of heavy metals in the atmosphere are from:-

1) sea water evaporating leaving salt particles

2) soil particles or continental dust; some of these may be volcanic in origin

3) organic particles evaporating from forest vegetation together with pollen and spores

4) soot particles and forest fires (9,10)

Table 1.1 gives an estimate of the natural emission of heavy metals to the atmosphere. Due to the increasing use of such metals in industrial processes, emissions of these metals has increased considerably in the last 60 years. Table 1.2 indicates the consumption and anthropogenic emissions of heavy metals to the atmosphere on a global scale.

Table 1.1 : Worldwide Emissions of Heavy Metals from Natural Sources (10)

Source	Global production ($\times 10^9$ kg yr^{-1})	Worldwide annual emission ($\times 10^6$ kg)				
		Cd	Cu	Ni	Pb	Zn
Windblow dust	500	0.1	12.00	20.00	16.00	25.00
Forest fires	36	0.012	0.3	0.6	0.5	2.1
Soil particles	10	0.52	3.6	3.8	6.4	7.0
Organic particles	75	0.2	25.00	1.6	1.6	9.4
Salt particles	1,000	0.001	0.08	0.04	0.02	0.01
Total		0.83	18.5	26.00	24.5	43.5

In river systems, heavy metals originate to a large extent from :

1. the abundance of metals in the rocks and soils of a river's catchment area and by their geochemical mobility. Thus, a catchment area containing mineralised rocks will usually have elevated metal levels in the sediment and water of rivers draining into it (11).
2. mining and smelting activity; because of river run-off over waste tips, and through mines, the heavy metals discharge to the waters. The pollution by such metals may continue long after the mine and smelting activities have ceased (11,12).
3. wastewater treatment plants (13). Table 1.3 shows the effect of a discharge from municipal wastewater treatment plants on dissolved heavy metal concentration in the River Derwent in the UK during 1979-1980. When metal concentrations are compared with admissible concentrations stated by the EEC directive intended for drinking water, it is apparent that the level of cadmium significantly exceeded the Directive value.

Table 1.2 : Worldwide Consumption and Anthropogenic Emissions of Heavy Metals (10)

Period	Global metal consumption (x 10^9 kg)					Global metal emission (10^6 kg)				
	Cd	Cu	Pb	Ni	Zn	Cd	Cu	Pb	Ni	Zn
pre-1850	-	45	55	-	50	63	319	2,420	12	2,844
1850-1900	-	13	25	0.2	15	19	92	1,100	12	841
1901-1910	-	7.5	10.7	0.14	7.0	89	53	471	8.2	392
1911-1920	0.001	11.3	11.2	0.35	8.8	11	80	493	21	493
1921-1930	0.007	13.5	14.2	0.36	11.1	14	96	1,120	21	622
1931-1940	0.026	16.3	14.6	0.83	13.3	17	116	1,639	49	746
1941-1950	0.048	23.8	14.9	1.37	17.1	22	169	1,672	80	959
1951-1960	0.084	32.4	24	2.38	27	34	230	2,694	140	1,514
1961-1970	0.14	61.4	33	4.37	42.3	54	435	3,704	257	2,372
1971-1980	0.15	82.5	38	7.07	58	74	585	4,265	415	3,252
Total (all time)	0.50	307	241	17	250	316	2,175	19,578	1,003	13,995

Table 1.3 : Heavy Metal Concentrations Recorded Above and Below a Sewage Effluent Discharge into the River Derwent (UK)

Metal	Concentration above effluent discharge (mg L^{-1})	Concentration below effluent discharge near point at abstraction (mg L^{-1})	EEC Directive on surface water quality 75/440/CEC MAC (mg L^{-1})
Cd	< 0.01[a] (< 0.01)[b]	0.02 (< 0.01)	0.0005
Cr	0.02 (< 0.01)	0.09 (0.01)	0.05
Cu	0.02 (< 0.01)	0.05 (0.02)	-
Pb	0.12 (< 0.02)	0.06 (0.02)	0.05
Mn	-	0.19 (0.09)	-
Ni	0.01 (< 0.01)	0.11 (0.01)	-
Zn	0.13 (0.06)	0.16 (0.08)	5.00

a = Maximum Recorded Concentration

b = Mean Recorded Concentration

EEC = European Economic Community

MAC = Maximum Admissible Concentration

Heavy metals in river water reach the sediment in three principal ways :-

i) in or on particles which settle on the bottom

ii) in or on particles which are transported along the bottom

iii) by the sorption of dissolved metal from the water in contact with the sediment (14).

It can be seen that heavy metals discharge to sediments either from metals present in river waters (as above) or directly from the activity of man (15). Some investigations have shown that the sediments are excellent hosts for trace metals (16,17). Greig et alia (18) reported

that 99% of the total amount of a metal in a marine environment was held by the sediments. The total concentration of heavy metal in sediments indicates the degree of contamination (17).

The soil is the primary supplier of trace metal to the soil-plant animal system and the soil-foodstuff-water human system (19,20). In these systems, the occurrence and concentration of heavy metals in any individual component depends largely on the source of the heavy metal. In this context, the sources of heavy metals to the ecosystems will be either via the soil or by deposition of aerial particulates (21), i.e. the two recognised routes of uptake are from :-

i) soil sources through the roots, and

ii) atmospheric sources through aerial portions of the plant (22).

1.2 TRACE METAL SPECIES IN THE ENVIRONMENT

Speciation of metal is the determination of the individual physico-chemical forms of that metal which together make up its total concentration in a sample (23). From a public health viewpoint it is important whether trace metals are :-

1. in solution or adsorbed on solids, where they are readily available.
2. in organic matter or on precipitated hydrous manganese and iron oxides. On such a surface chemical changes e.g. oxidation of organic matter or reduction of iron and manganese hydroxide are required before heavy metals are released, so that they are termed less available.
3. in the crystal structure of suspended material where they are almost unavailable in nature (24).

It is now well established that speciation measurements are necessary to ascertain the :-

i) availability of heavy metals to aquatic organisms, plants and microorganisms;

ii) interaction of trace metals in waters with sediments and suspended particulates. Most studies of river, estuarine and marine sediments have shown that many trace metals are concentrated in sedimentary material in natural aquatic systems (25). Figure 1.1 illustrates some of the major reaction pathways for metal removal from water with eventual deposition in the sediment. Removal of trace metals is known to be related to adsorption or other surface phenomena with hydrous metal oxide, clays and organic matter (25);

iii) toxicity; most studies of toxicity of heavy metals for fish have shown that the free (Hydrated) metal ion is the most

FIG.1.1 A MAJOR REACTION PATHWAYS OF TRACE METAL TRANSPORT AND DEPOSITION IN SEDIMENTS IN NATURAL AQUATIC SYSTEMS

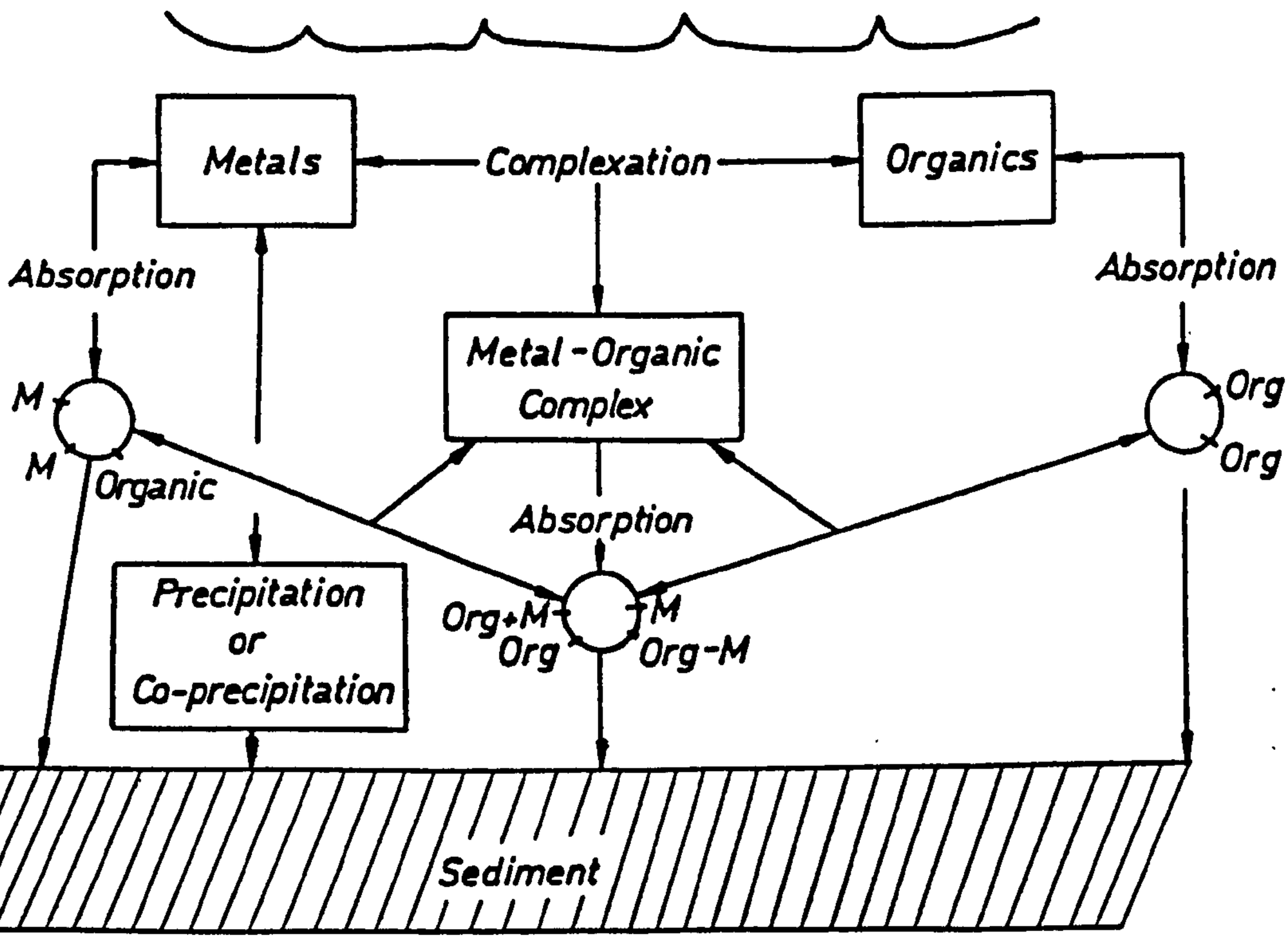

toxic form (23). Strong complexes and species associated with colloidal particles are usually assumed to be non-toxic (23).

Most heavy metals act through their soluble forms, thus water must be regarded as the most important medium for distribution of these metals (26). Dissolved metal ions in natural waters may be present as several species (27). For example :

1. simple aquated metal ions
2. metal ions complexed by inorganic anions, such as chloro, carbonato and hydroxo complexes, i.e. more or less labile complexes
3. metal ions complexed by organic ligands such as amino, fulvic acid, humic acid, nucleic acid, proteins plus chelating agents of anthropogenic origin (27).

There is evidence (23) that colloidal particles such as iron oxide and clay coated with humic acid strongly adsorb heavy metal ions and control their concentrations in natural waters. Although disssolved metal ions have been defined as metal species which pass through 0.45 μm filters; the majority of colloidal particles pass through this filter and are thus included in the dissolved fraction. "Filterable" metal ions may be a better term than "dissolved". Table 1.4 describes the possible physico-chemical forms of metals in natural waters. Selected aquatic biota have been known to accumulate metal concentrations, the routes of transportation of metals in water to biota have been suggested and include :-

i) particulate ingestion of aqueous suspended matter
ii) ingestion within food material
iii) complexation by chelating agents
iv) incorporation into the physiological system (28).

Table 1.4 : Possible Physico-Chemical Forms of Metals in Natural Waters

Physico-Chemical Forms	Example	Approximate diameter (nm)
Particulate	Retained by 0.45 μm filter	> 450
Simple hydrate metal ion	$[Cd(H_2O)_6]^{+2}$	0.8
Simple inorganic complex	$Pb(H_2O)_4Cl_2$	1
Simple organic complex	Cu-glycinate	1-2
Stable inorganic complex	PbS, $ZnCO_3$	1-2
Stable organic complex	Cu-fulvate	2-4
Adsorbed on inorganic colloids	Cu^{2+}-Fe_2O_3	10-500
Adsorbed on organic colloids	Cu^{2+}-humic acid	10-500
Adsorbed on mixed organic/ inorganic colloids	Cu^{2+}-humic acid/Fe_2O_3	10-500

Association of trace metals within the sediment can be classified into :-

1. lattice held (or residual) trace metals; trace metals can only be released into solutions by digestion with mineral acids, thus are not released into the environment under any conditions (17,29).

2. non-lattice held (or non-residual) trace metals; which are the most important since such metals can be released into the environment under certain conditions and taken up by biota (17). The non-residual trace metal burden in sediments indicate the level of metal originally in polluted water and the type of mechanisms which it has followed during its transportation from water to sediment. Within a sediment the non-residual trace metal can originate to a large extent from being :-

i) adsorbed on the surface of particles; most suspended particles in natural waters are negatively charged and cations are attracted to their surface. In addition the metals may be adsorbed at the ion exchange positions in the clay minerals and hydrous oxides of iron and manganese. Both types of adsorbed ions are readily leached when the surrounding solution becomes acidic (30).

ii) coprecipitated with iron and manganese in hydrous oxide coatings; during weathering iron is released to the solution as Fe(II), but due to the presence of dissolved oxygen Fe(II) is oxidised to Fe(III) and so precipitates as a hydrated oxide. The oxidation process of Fe^{2+} to Fe^{3+} takes a few hours at pH = 5, while at pH = 7, only a few minutes is required (31). Manganese in solution is commonly coprecipitated with iron. These oxides are excellent scavengers for trace metals either by coprecipitation or sorption but they are unstable under reducing conditions.

iii) complexed or adsorbed with organic matter; under oxidising conditions organic matter can be degraded, leading to release of the soluble trace metals (29-31).

In soil, the total concentration of heavy metals indicates the extent of contamination but not the significance (19), the proportion of such metals in various chemical forms can demonstrate how the metal is bound in soil as a basis for assessing potential availability (32). In soil solution heavy metal may be present as free ion and/or as soluble inorganic and organic complexes, while in the solid phase, they may occur in exchangeable forms being specifically adsorbed, bound to organic soil constituents, occluded in amorphous materials and associated with primary and secondary clay minerals (32).

Humic substances, the major organic constituent of soil and sediments, are widely distributed over the earth's surface. They arise from the chemical and biological degradation of plant and animal residues, and through the biological activity of microorganisms. The most important characteristic of humic substances (Figures 1.2 and 1.3) are their ability to form water-soluble and water-insoluble complexes with metal ions (33), thus the major fraction of metal ions in soil are complexed with these materials. The most important chelating groups in order of decreasing affinity for metal ions are (30) :-

O^-	>	NH_2	>	N=N	>	- N -	>	COO^-	>	- O -	>	C=O
phenoxy		amine		azo		ring-N		carboxylate		ether		carboxy

Inorganic cations such as a heavy metal can be coordinated to these functional groups in humic material to form stable linkages (34). The pH of the soil influences metal ion mobility, thus affecting the chelation with humic material (35). Although the mechanisms by which humic substances bind metal ions remains uncertain (36), the complexing properties have been attributed to the phenoxy and other functional groups (33). The fact that metal complexation by humic substances results in the release of protons indicates to some extent that the same ligands are involved in proton as well as metal binding (37). Copper in soil has high affinity to form complexes with fulvic and humic acids while the complex formation is pH dependent (Figure 1.4). It may be that most copper in soil is associated with the organic matter. Little is known about the forms in which heavy metals occur in plants. It is generally accepted that mineral elements are present as free ionic as well as organo-mineral complexes. The complexation of essential and non-essential heavy metals is connected with their ability to coordinate with plant constituents which are :-

FIG. 1.2 FULVIC ACID STRUCTURE

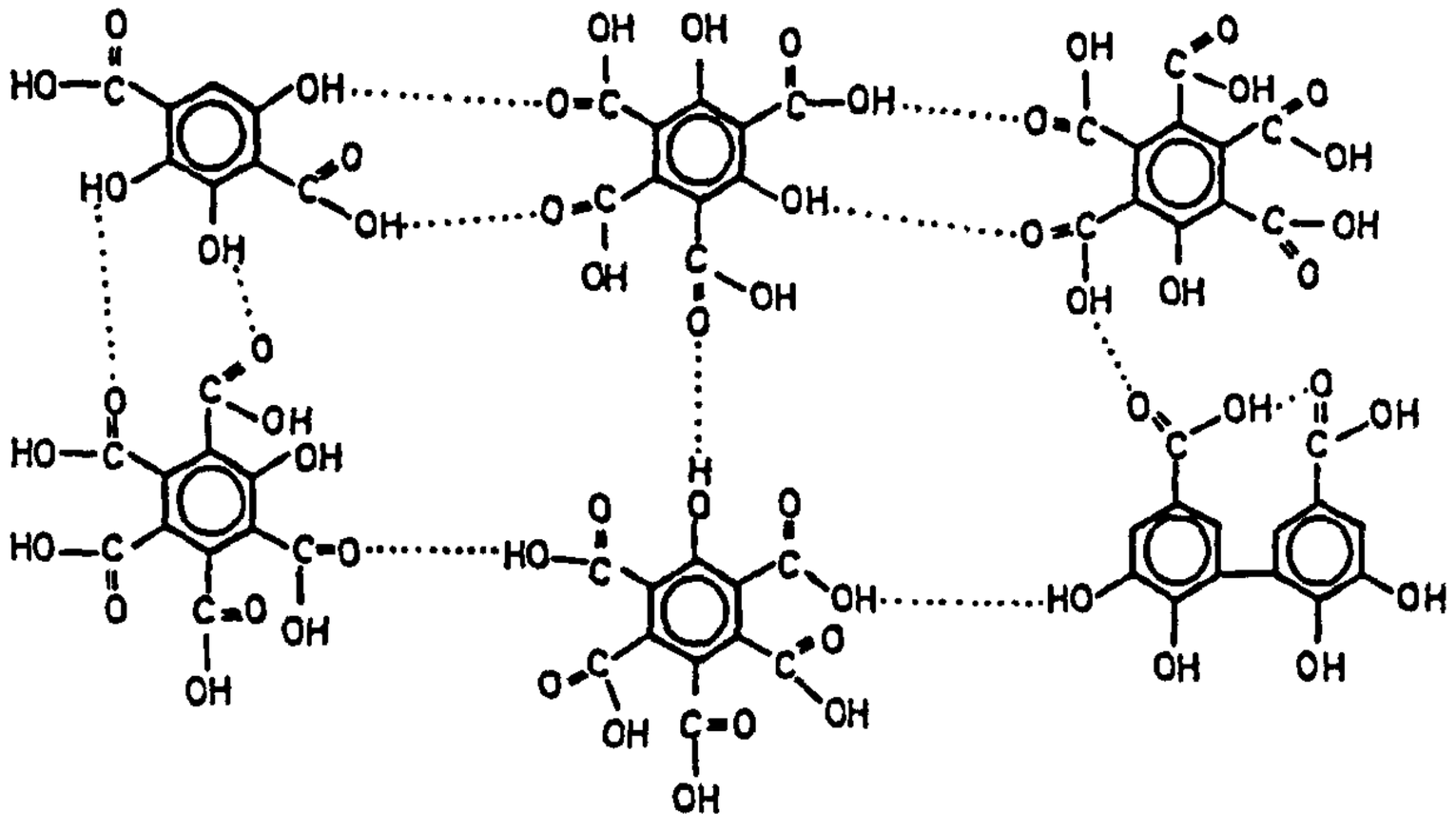

FIG. 1.3 POSSIBLE BONDING SITES IN HUMIC ACID

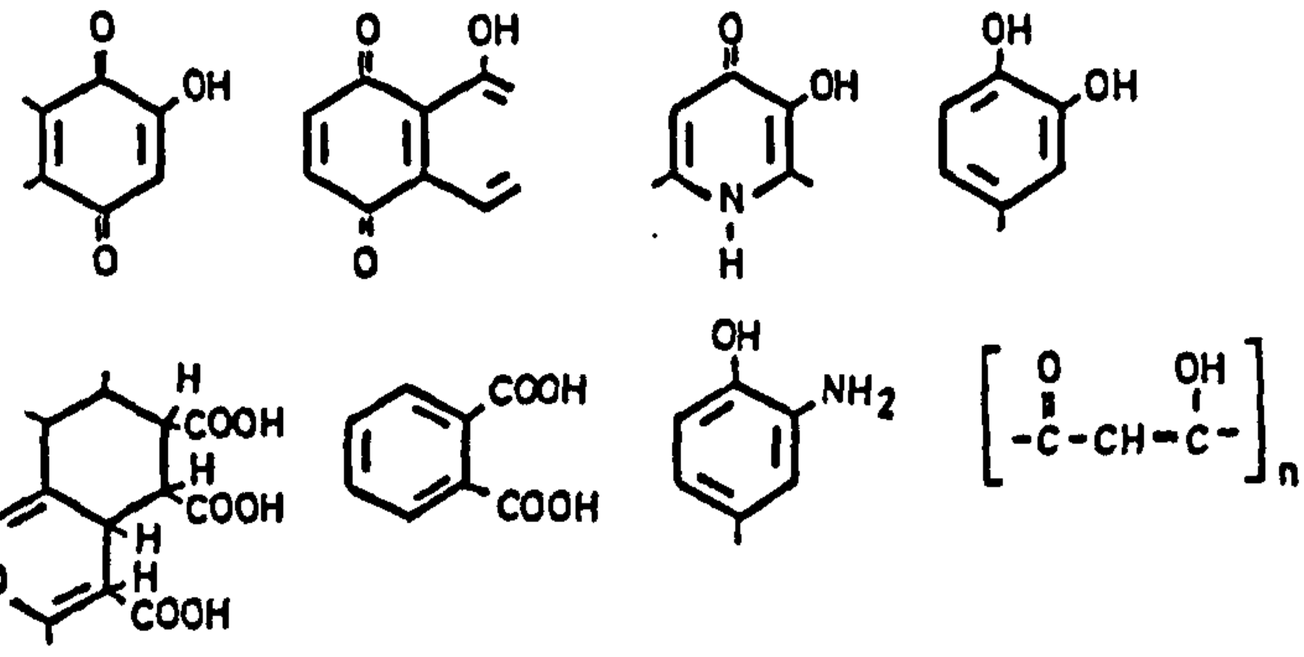

FIG. 1.4 COMPLEXATION OF COPPER WITH HUMIC MATERIAL (33)

a) humic acid

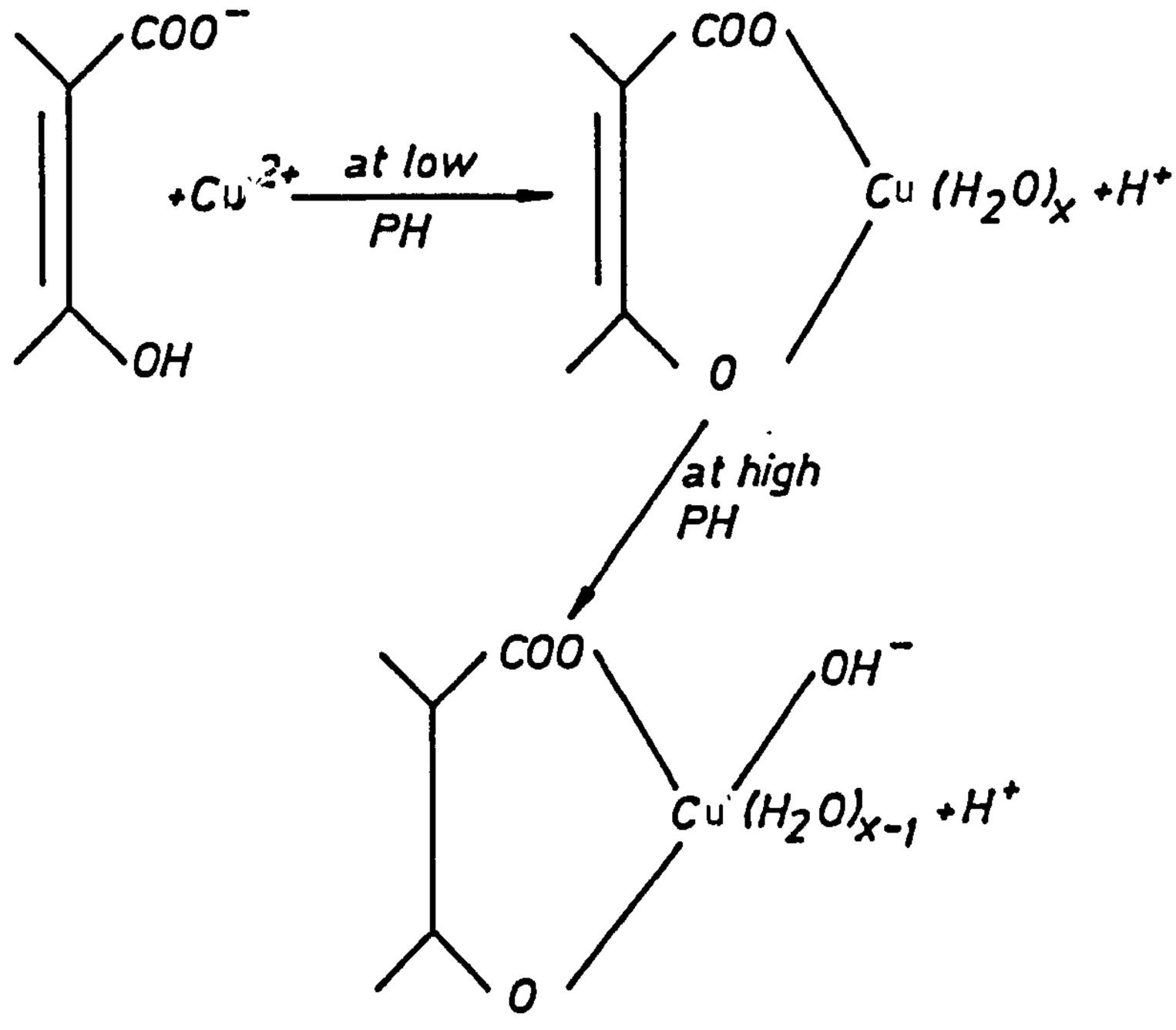

b) fulvic acid

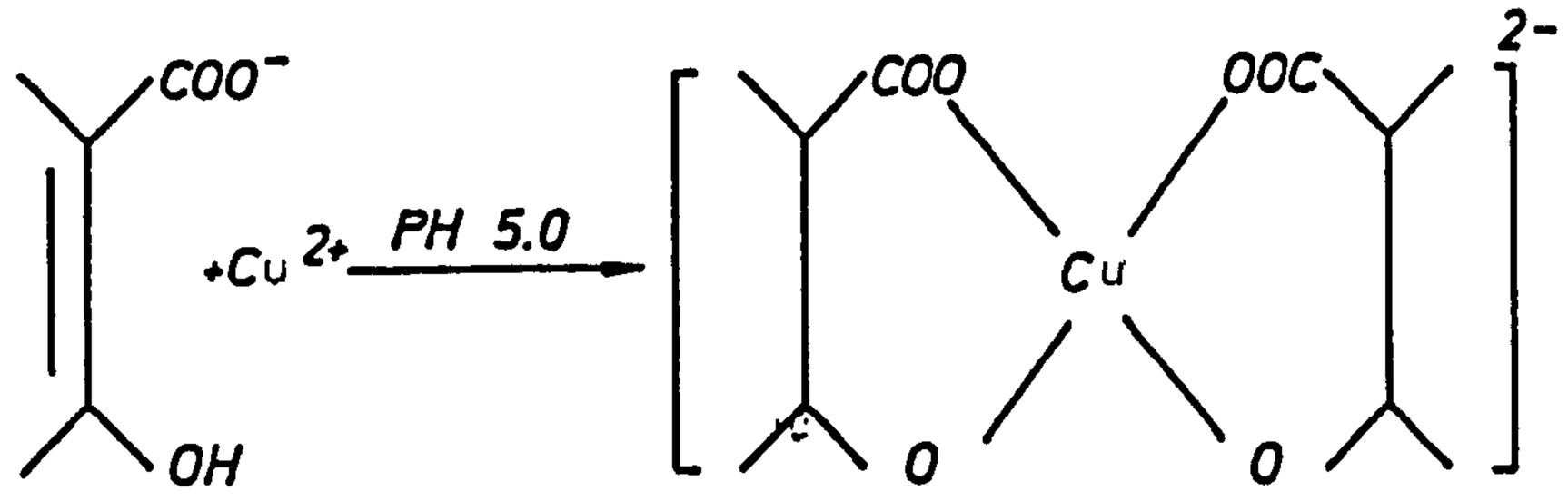

i) organic acids; it is thought that metal tolerance in plants can be based on the complexing of metal with organic compounds including organic acids, thus reducing the activity coefficient of free metal ions and hence their toxicity (38). In the nickel accumulator species Sebertia acuminata, it has been found that the nickel is chelated by two molecules of citrate (39). At least two tridentate citrato-nickel complexes can be imagined in cis or trans configurations (Figure 1.5). However, if organic acids play an important role in tolerance mechanisms, the tolerant plants must produce more of such organic acids. Even if this is so, it is not clear how tolerant plants are able to respond in this way whilst non tolerant ones are unable to do so.

ii) carboxyl groups in the cell wall; heavy metals especially copper have higher affinity to coordinate with carboxyl groups than other metals (40). Again this type of complexation is thought to play an important role in the biochemistry of metal tolerant plants. If this is so, then zinc tolerant plants should also be copper tolerant, but they are not. For example, clones of A. stolonifera were found to be zinc tolerant but not copper tolerant (40).

iii) thioneins; this type of protein is cysteine rich and has the ability to bind with metals such as Zn, Cu, Cd, Hg, Ag (38) and so form metallothioneins (Figure 1.6). Their metal binding capacity has led to the suggestion that such complexes could play a role in the mechanisms responsible for metal tolerance in higher plants (38).

In general, metals may be complexed with other organic compounds within plants. For example (41) :-

1) pigments

2) soluble protein

3) soluble pectate

4) low molecular weight material

FIG. 1.5 COORDINATION OF NICKEL BY CITRATE

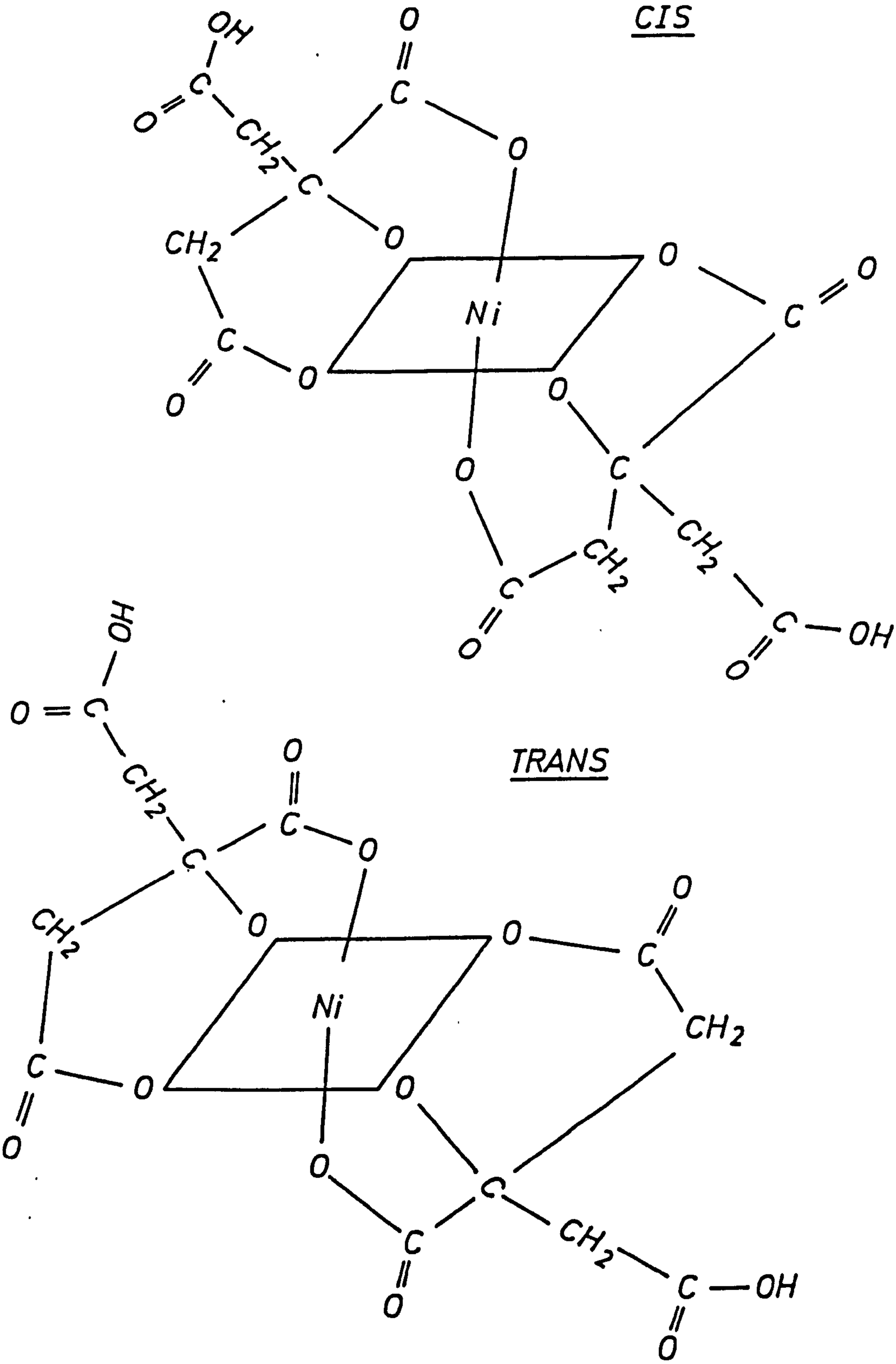

FIG. 1.6 METAL-THIOLATE CHROMOPHORES IN METALLOTHIONEINS

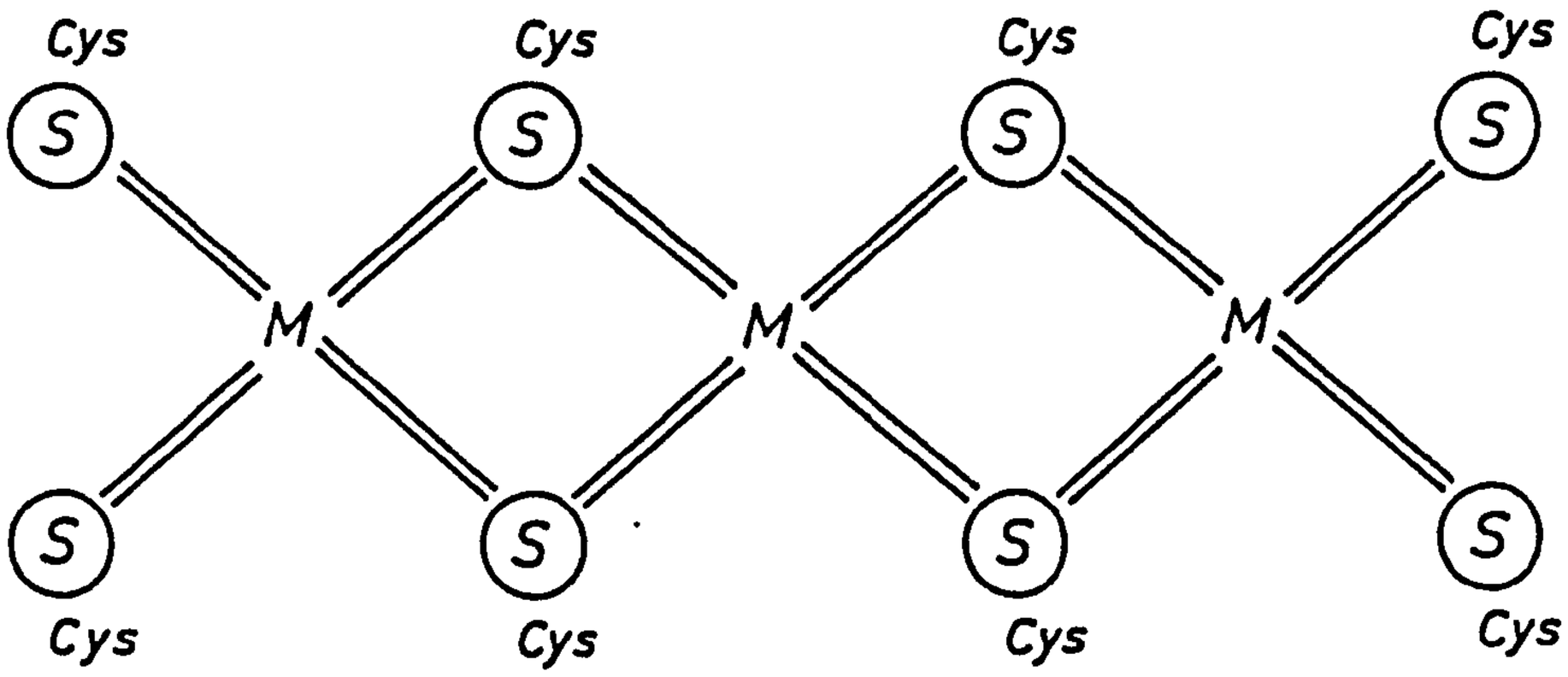

M = Zn or Cd - Thionein

5) polar low molecular weight material

6) proteins and amino acids

7) insoluble pectates

8) protopectates

9) α-cellulose

10) hemicellulose

11) polysaccharides

12) lignin

1.3 TOXICITY OF HEAVY METALS

The heavy metals in the environment can reach toxic levels in living organisms by accumulation. i.e. by building up over a period of time (42). Although traces of certain heavy metals are essential as key components of enzyme systems, other heavy metals, however, may compete for these sites and cause deformation in and inhibit enzyme systems (39). Enzymes have active groups such as amino, imino and sulphydryl types which have great affinity for the more electronegative metals. The greater electronegativity of the inhibitor metal, as well as the more stable metal chelate so formed, then the higher the toxicity (43). Table 1.5 shows that most toxic metals behave as soft acceptors. These metals form particularly stable bonds with soft donors. The various factors (5) which influence the toxicity of trace metals are listed in Table 1.6. It shows that the potential toxicity of metals is controlled to a large extent by their physico-chemical forms (23). Toxicity of heavy metals is not restricted to those metals thought to be non-essential ones. All elements, including essential ones, are toxic at high concentrations (5).

Table 1.5 : Classification of Acceptor and Donor Electrons
(R = alkyl or aryl)

Hard acceptor	Intermediate	Soft acceptor
H^+, Na^+, K^+, Be^{2+}, Mg^{2+}, Ca^{2+}, Mn^{2+}, Al^{3+}, Cr^{3+}, Co^{3+}, Fe^{3+}, As^{3+}	Fe^{2+}, Co^{2+}, Ni^{2+}, Cu^{2+}, Zn^{2+}, Pb^{2+}	Cu^+, Ag^+, Au^+, Ti^+, Hg^{2+}, CH_3Hg^+
Hard donor	**Intermediate**	**Soft donor**
H_2O, OH^-, F^-, Cl^-, PO_3^-, SO_4^{2-}, CO_3^{2-}, O^{2-}	Br^-, NO_2^-, SO_3^{2-}	SH^-, S^{2-}, RS^-, CN^-, SCN^-, CO, R_2SRSH

Table 1.6 : Factors Influencing the Toxicity of Heavy Metals in Solution

1. Form of metal in water
   - inorganic
     - soluble
       - Ion (free)
       - Complex ion
       - Chelate ion
       - Molecule
     - particulate
       - Colloidal
       - Precipitated
       - Adsorbed
   - organic

2. Presence of other metals or poisons
   - joint action
   - interaction

3. Factors influencing physiology of organism and possibly form of metal in water
   - Temperature
   - pH
   - Dissolved oxygen
   - Light
   - Salinity

4. Factors influencing uptake of metal ions by living cells
   - charge
   - ionic radius
   - coordination of metal to certain organic ligands
   - available concentration of metal ions in aqueous environment
   - binding and chemical reactivities of metal ion in solution

Figure 1.7a shows the biological response curve for essential heavy metal ions; below a certain concentration level of nutrient, there is retardation of the growth of an organism. As the concentration of nutrient increases, the beneficial effect of the nutrient reaches an optimum. Any further increase in the concentration causes an adverse effect and finally a lethal dose may be reached. The shape of the curve will vary with the organisms and heavy metal. Figure 1.7b shows the biological response for non-essential heavy metals; it indicates that the curve does not follow the first part of the curve for the essential metals, but depicts a tolerant range followed by the toxic and lethal regions.

In natural waters, the toxicity of metal ions and the rate of uptake by organisms is predominantly controlled by the concentration of the "free", hydrated ion, and not by the total concentration (23). The toxicity of particulate dissolved metal species is probably related to its ability to react with biological membranes. The alkyl compounds of mercury and lead are especially dangerous because they are lipid-soluble, and material such as the lead halide aerosols emitted by automobiles can enter the lungs and be absorbed directly into the blood stream (23).

In soil-plant systems, the toxicity of metal ions and the rate of uptake by plants depends upon their solubility in soil solution (44). For example, aluminium in acid soil is toxic due to formation of free aluminium ion, soluble $AlSO_4^+$ and $AlOH^+$, which are easily taken up by plants (45). Some plants can grow in soils that contain levels of toxic ions lethal to other species. At present, four main mechanisms of plant resistance to toxic metals are suggested, as follows (46) :

1. phenological escape; where the stress is seasonal the plants may adjust their life-cycle so as to grow in the most favourable season.

FIG. 1.7 DEFICIENCY AND TOXICITY OF ESSENTIAL AND NON-ESSENTIAL HEAVY METALS

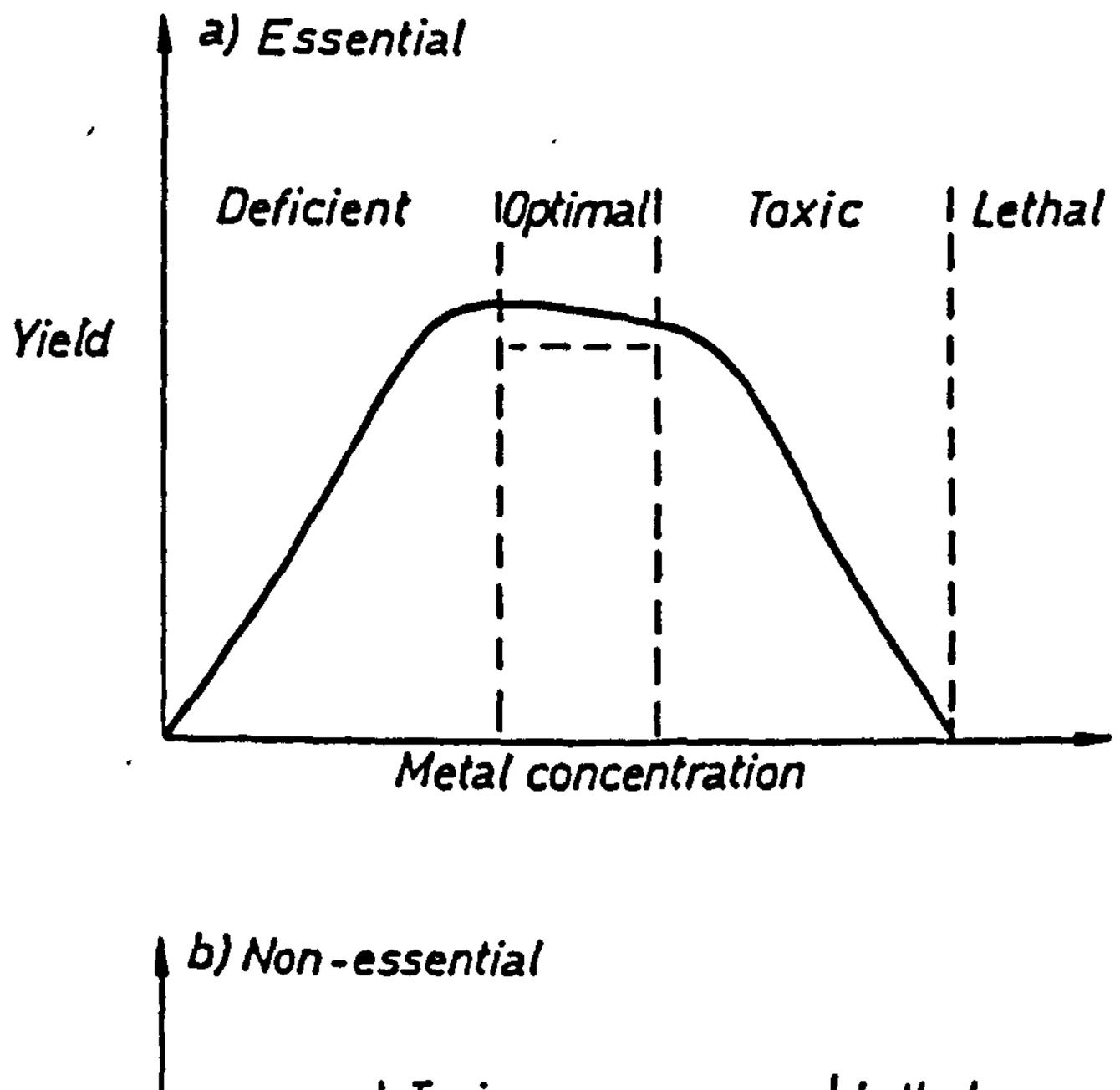

2. exclusion; the plant may be able to recognise the toxic ion and prevent its uptake, and so not experience the toxicity.
3. amelioration; the plant may absorb the ion but act upon it in such a way as to minimise its effect. Variously this may involve chelation, dilution, localisation, or even excretion.
4. tolerance - the plant may have evolved a metabolic system which can function at potentially toxic concentrations, possibly by means of distinct enzyme molecules.

An understanding of the biochemical basis for resistance to metal ion toxicity has been started, but it is complicated by different resistance mechanisms. For example, some mechanisms for microbial resistance to heavy metals are (43) :-

i) development of energy driven efflux pumps that keep the toxic element level low in the interior of the cell
ii) oxidation or reduction and intracellular conversion of a more toxic form of an element to a less toxic form
iii) biosynthesis of intracellular polymers that serve as a trap for removal of metal ions from solution
iv) the binding of metal ions to cell surfaces
v) precipitation of insoluble metal complex at cell surface
vi) biomethylation and transport through cell membranes by diffusion controlled processes.

1.4 UPTAKE OF HEAVY METALS BY PLANTS

To date, the mechanism of uptake of elements by plants is not known, however it has been proposed that :-

1. plant roots excrete hydronium ion H_3O^+ at their surface so that exchange with cation can occur. Similarly it would be expected that roots would excrete hydroxyl or bicarbonate ions to exchange with anions (47).
2. metal ions move to the root surface by diffusion so that adsorption of ions on the root surface occurs whether it is dead or alive (48).

However, when the metal ion is taken up by the roots, it can either remain at the roots or is translocated to the shoots. For example, lead remains in the roots whereas potassium ions are translocated in major part to the shoots (49). The movement of metal ions from soil to shoots via roots in plants may occur in the way suggested by Fried et alia (50) as follows :-

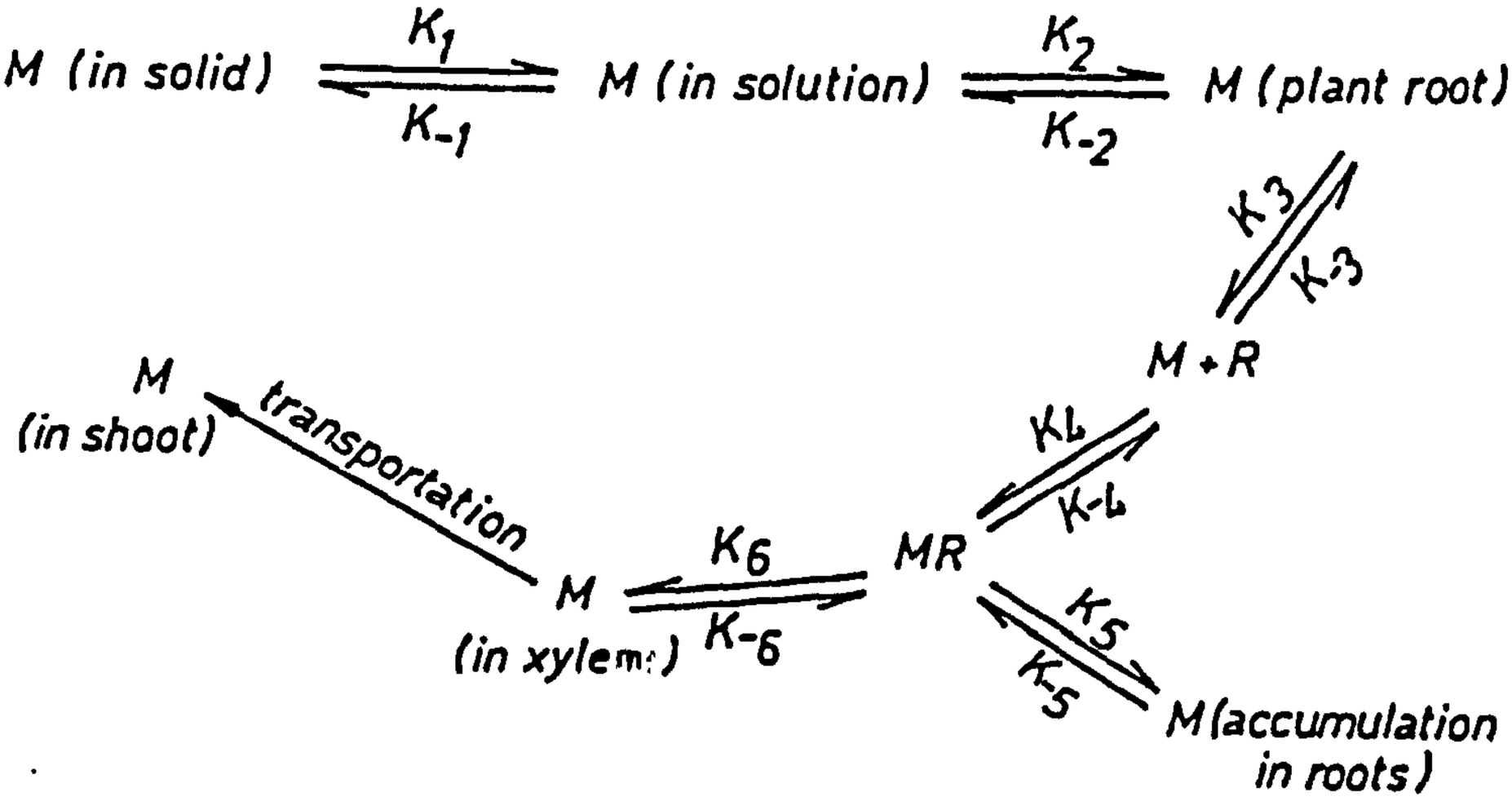

Where M = nutrient

R = carrier

MR = carrier nutrient complex

The availability of heavy metals to plants in soil depends on a number of factors (51,52). The major factor is the solubility and the activity of the uncomplexed ion. In order for root uptake to occur, a soluble species must exist adjacent to the root membrane for some finite period (44). The rate of release and form of this soluble species will have a strong influence on the rate and the extent of uptake. The plant uptake of chemical species from soil solution is dependent on a number of plant/soil interactions. These include :-

i) physical processes such as root intrusion (44)

ii) soil factors, including : forms of the metal, solubility type of soil, pH, Eh, inorganic material, organic matter, cation exchange capacity of the soil, availability of other heavy metals and soil temperature (4,21,51,52)

iii) water and ion fluxes and their relationship to the kinetics of metal solubilisation in soils (48)

iv) biological parameters, including kinetics of membrane transport and the ability of plants to adapt metabolically to changing metabolic stresses in the environment (53).

Three types of plant/soil relationships have been proposed, where plants are described as (53) :-

i) excluders or plants which restrict transport

ii) index plants which reflect soil concentrations

iii) accumulators - these plants can be defined as concentrating metals within their above ground plant parts from low or high soil levels.

Heavy metal tolerance in plants is a well documented but a poorly understood phenomenon (54). Over the past several years, studies on heavy metal tolerance have become more broadly based, which has resulted

in the accumulation of information along a wider front, rather than a marked advancement in any one particular area (40). To date, the suggested mechanisms of tolerance to heavy metals are shown in Table 1.7. It shows two mechanisms, firstly an external mechanism of tolerance represents those circumstances which prevent entry of metal ions, secondly an internal mechanism indicates that a toxic level of the metal ion is taken up by the plant and the response by the plant to that toxic level (3,55). The tolerance of plants to toxic metals is frequently measured by comparing the rates of root growth in culture solution with and without the addition of the metal (55,56).

Heavy metal uptake and distribution in tolerant and non-tolerant populations of plants depends on the species and the metal. For example, Coughtrey *et alia* (57) have found that the root:shoot ratio::concentration of cadmium in tolerant *Holcus lanatus* is significantly higher than in the non-tolerant form. It appears that the localisation of cadmium within the roots forms the basis of cadmium tolerance in the tolerant population of *H. lanatus*, thus preventing the toxic effect. Brookes *et alia* (58) found that zinc accumulated in the tolerant roots of *Anthoxanthum odoratum* to a higher extent than in the non-tolerant roots of *Deschampsia caespitosa*. The zinc content of the shoots of both clones were similar and contained less zinc than the roots. It is clear from these two studies (57,58) that heavy metals accumulate in the roots of tolerant species, this may involve the internal mechanisms and decrease the toxicity of heavy metals to plants.

Table 1.7 : Possible Mechanisms of Metal Tolerance

(i) External	(ii) Internal
(A) Form of metal ion is not soluble in water and/or if dissolved is then rapidly diluted by surrounding water	(A) Removal of metal ions from metabolism by deposition in vacuole
(B) Actual amount of freely diffusable metal ions is small compared to total amount	(B) Removal of metal ions from metabolism by conversion into an innocuous form
(C) Lack of permeability to heavy metals under specific conditions	(C) Greater requirement of enzyme systems for metal ions
(D) Metal ion antagonism	(D) Alternative metabolic pathway by-passing inhibited site
	(E) Decrease permeability of cell or subcellular units to metal ions

1.5 METALS USED IN THE PRESENT WORK

The metals include Al, Ag, La, Tl, Pb; silver and thallium are monovalent, lead is a divalent, aluminium and lanthanum are trivalent metals respectively, and were used to provide a comparative assessment of uptake of these metals by plants in relation to their valency.

It is best to discuss individually the occurrence and the toxicity of each of the above elements, in the order of their Atomic Numbers.

a) Aluminium

The commonest metallic element in the earth's crust (8.8 mass %) occurs widely in nature in silicates such as the hydroxo oxide (bauxite) and as cryolite (Na_3AlF_6). It is a hard, strong, white metal. Aluminium salts are used to remove natural organic substances from water (59), as coagulants in water treatment to remove turbidity and colour (60) and in the manufacture of anti-rust coatings.

Until recently there was very little interest in the environmental chemistry of aluminium, the metal generally being considered relatively non-toxic under all normal conditions (23). This situation has changed since clinical toxicologists documented that consumption of Al compounds has caused neurological degeneration (61). The common symptoms for Al toxicity are skin lesions, nervous afflictions, gastro-intestinal disturbance, growth retardation, perihepatic granulomas and fibrous peritonitis (61). Furthermore, aluminium is responsible for phosphorylation reactions in the tissue (61). From these symptoms of Al toxicity, one of the major questions to be asked is, how do biota live on earth surrounded with so much aluminium silicate? The very low solubility of aluminium has led to the consideration that aluminium is immobile during weathering processes. All studies (62) indicate that aluminium exists

at very low concentrations in sea waters and fresh waters.

The aluminium(III) species in aqueous environments is pH dependent. Table 1.8 gives the possible aluminium (III) species present in solution at different pHs. Atmospheric inputs of sulphuric acid and nitric acid to soils can increase soil aluminium leaching. This aluminium may be transported to waterways and lead to aquatic biota mortality (63).

Table 1.8 : Possible Al(III) Species Present in Solution

Species	pH	Reference
$Al(OH)_4^-$, $Al(OH)_4(H_2O)_2^-$, AlO_2^-, $H_2AlO_3^-$	> 7	64,65
$[Al(H_2O)_6]^{3+}$, $[Al_6(OH)_{12}]^{6+}$	< 4	64,65
$AlOH^{2+}$, $Al(OH)_2^+$, $Al(OH)_3^o$, $Al_n(OH)_m^{(3n-m)+}$	4-7	65

It would be expected that aluminium concentrations in solution decrease as the pH increases, and vice versa, due to precipitation as aluminium hydroxide. However, aluminium is always present in acidic soils. The resulting drop in pH of the soil may arise from exchange desorption of H_3O^+ ion or from the hydrolysis of desorbed Al^{3+} ions. The first stage can be represented by (66) :-

$$[Al(H_2O)_6]^{3+} + H_2O \longrightarrow [Al(H_2O)_5OH]^{2+} + H_3O^+ \qquad [1.1]$$

Soil acidity has been known (67) as a factor influencing plant growth. The effect may be due to one of the following components of the acidity complex :-

i) low pH

ii) deficiency of phosphorus, calcium and molybdenum

iii) greatly increased release of aluminium and manganese to the point of toxicity.

Most studies on Al toxicity are often reported for plants grown in acid soils. In fact, the reduced yield of crops on acid soils is often due to availability of Al rather than H^+ concentration. For example, Pavan et alia (68) has investigated the effect of available Al on the growth and mineral nutrients of Coffee (Coffea arabica L.) seedlings grown in different acid soils. It was shown that aluminium reduces the growth of roots and the uptake of mineral nutrition. Although the physiological function of Al in plants is not clear at the present time, Lee et alia (45) has suggested the possible physiological mechanisms of Al toxicity is due to inhibition of uptake of the following essential cations :-

1. divalent cations which were inhibited in the order Ca > Mg > Mn > Fe > Zn and Ca > Zn > Mn > Mg > Fe respectively in shoots and roots of Trifolium repens L.
2. monovalent cations such as potassium.

The Al in plants also strongly affected nodulation in the plant by delaying nodule appearance and reducing the number and the dry weight of nodules. For example, Asher et alia (69) have found that the effects of Al on nodules of Stylosanthes hamata cf. Verano and Stylosanthes hamata cf. Fitzroy occurred before any significant effect of Al on top growth and root elongation. The effects of aluminium on plants depend upon the pH of the solution. It has been found by Wood et alia (70-72) that the same concentration of aluminium at pH 4.3 and pH 4.7 inhibited root elongation and root hair formation in Trifolium repens L., while pH 5.5 inhibited rhizobium multiplication in the rhizosphere and reduced nodule formation, but root elongation and root hair formation were unaffected. It is possible that aluminium may be precipitated on the root as $Al(OH)_3$ by hydrolysis of the ions $Al(OH)^{2+}$ and $Al(OH)_2^+$ by free carboxyl groups. Amorphous aluminium hydroxide surfaces are positively

charged below pH 6.5. Such surfaces are known to adsorb and precipitate phosphates from solution, resulting in the formation of $Al(OH)_2H_2PO_4$ (73). It may be this complex that reduces nodule formation. The interaction of Al and P may play an important role in the mechanisms of Al toxicity. It has been reported that there is a P deficiency with excess of Al in plants (74). Conversely, it is expected that phosphate is an effective agent for detoxifying excess of Al by complexation with it and precipitation as phosphate complexes, so removing the offending aluminium.

At the present time, the mechanism of Al tolerance in plants seems to be unclear. However, it may be that the mechanisms of Al tolerance in plants are related to genetic controls. Therefore, there is most probably a selection mechanism by plants involving genetic adaptation to face the problem of Al stress in acid soils.

b) Silver

The electronic configuration of silver is a single 5s electron outside and a completed 4d shell. The monovalent silver ion, Ag^+, is the most stable cation. The element is chemically less reactive than copper, except towards sulphide and hydrogen sulphide, which rapidly blacken silver surfaces (75). The principal silver minerals are argentite, Ag_2S, pyroustite, Ag_3AsS_3, and pyrargrite, Ag_3SbS_3. It is present with galena, PbS, pyrites, FeS_2, sphalerite, ZnS and chalcopyrite, Cu_2FeS_2 (76).

Silver is emitted to the environment and exists in different forms. The major anthropogenic sources of traces of silver in the environment are from :

1. mining and smelting operations (77)
2. combustion of fossil fuels (78,79)

3. photographic uses (80).

Silver forms many insoluble compounds which reduces the element's importance as an environmental contamination (81). However, silver is distributed within the sediment as reducible, oxidisable and resistant forms (82). In natural waters, the element is associated with suspended particles. Some silver may be redissolved from suspended particles when the ammonia content of the water is sufficiently high (from agricultural runoff), but become insoluble again when the ammonia is ultimately oxidised to nitrate (83). Silver in municipal treatment effluents is probably present as thiosulphate complexes, colloidal silver chloride and sulphide, or as soluble organic complexes (83). In plants, the forms of silver in tissue are most probably protein complexes with bonding via sulphur and/or nitrogen of the amino acids (83). The silver ion is one of the most toxic of heavy metals and is particularly toxic to humans (84), plants (83), marine animals (85) and blue-green algae (83). Every type of silver compound in common usage has caused argyria to humans. The argyria is a discolouration on the face, hands and fingernails. Silver may be deposited in the body as metallic silver or as silver oxide, while only trace amounts are excreted in the faeces and especially the urine (84). In plants, the silver ion stimulates the root growth of watercress, onion and Holcus lanatus (86).

In marine animals such as hard clams, Mercenaria mercenaria, the effects of silver nitrate and silver acetate was studied by Calabres et alia (85). Gill-tissue respiration was depressed by both salts, with no significant difference in their effects. However, liver transaminase activity was higher when the acetate salt was used rather than the nitrate. The activity in the liver was significantly depressed with the nitrate group, but not with the acetate group.

The blue-green algae Phormidium mundatum is commonly found in

swimming pools. Silver nitrate (0.14 $\mu g/cm^3$) or silver sulphate (0.08 $\mu g/L$) can reduce the growth of this algae (83).

To date, there is little published work available for the uptake of silver from soil by plants. It was mentioned in Section 1.4 that the uptake of metals depends on their solubility, so that silver present in an insoluble form will have a decreased availability to plants. However, silver is taken up by plants and accumulates in specific species to higher levels than in soil. Table 1.9 gives the typical level of silver in soils and plants. The marine and freshwater plants concentrate silver by a factor of 200. The silver concentrations of marine and freshwater plants, respectively, are approximately 0.06 and 0.026 $\mu g/g$ (86). From the above it is clear that silver is accumulated by plants and other organisms and can reach the toxic level. The toxicity of silver ion may be due to the formation of an unionised complex with the inorganic groups of the enzyme system such as phosphate, carboxyl, and especially the sulfhydryl groups present. Binding of silver ions to -SH groups is the most important mechanism by which silver ions inhibits enzyme activity. Silver and mercury are generally considered among the most specific reagents for these groups and are especially effective in very low concentrations (81).

Table 1.9 : Silver Contents of Some Plants and Soils (87)

Order	Plant Species	Ag ($\mu g/g$) Dry weight	Ag ($\mu g/g$) in Soils
Psilotales	Psilotum triquetrum	0.31	0.04
Bryidae	Hyperium cypressiforme	0.03	0.09
Lycopodiales	Lycopodium circinatum	1.0	0.03
Cycadales	Encephalartos lehmanii	0.15	0.09
Coniferales	Juniperus communis	1.5	0.09
Gnetates	Ephedra gerardiana	8	0.08

c) Lanthanum

The element belongs to rare earth elements and has an electronic configuration $4f^{o}\ 5d^{1}\ 6s^{2}$. Lanthanum occurs mainly as the +3 cation, and is thus expected to behave the same as aluminium in the environment, but it seems not to do so. The presence of lanthanum in soils, rocks and sediments has been shown to range from 0.01 to 0.08 per cent lanthanium oxide in American soils (88). The mobility of lanthanum is low in neutural and alkaline soils, where it is precipitated as the carbonate and hydroxide while in acidic soils, lanthanum is strongly absorbed onto clay present in the soil (89). Lanthanum salts are more soluble than other elements of the lanthanide series (90). Table 110 gives the concentration of lanthanide elements in the central Atlantic Ocean and indicates a higher concentration of lanthanum than other lanthanides; which may be a direct reflection of the higher solubility of lanthanum than other elements in the series.

Yliruokanen (89) has investigated that hickory trees (Carya sp., Juglandaceae family) contained no less than 0.2 per cent lanthanum oxide in their dry leaves, which indicates that lanthanum is present in the plants as one of their components, thus it may be an essential element. Lanthanum is taken up by plants; Cowgill et alia (91) have reported that lanthanum was not detected in a water sample taken from Linsley Pond, but a high concentration of lanthanum was found in the immersed roots of plants grown in the pond, so suggesting that the roots of plants extract the lanthanum from the water. Cowgill et alia (91) have also reported that lanthanum is taken up from soils by plants and varying quantities of lanthanum are present in different parts of the plant.

Neither the uptake of lanthanum nor its physiological properties have received much attention. It is probable that lanthanum is slightly

toxic on the one hand, or on the other trace concentrations of lanthanum may play a part in normal metabolism. However, there is little published information on the element's inhibitory effects on plants, but it may be that lanthanum inhibits the action of the divalent essential cations such as calcium.

Table 1.10: Concentration of Lanthanide Elements in the Central Atlantic Ocean between 16°N (Depth below 1000 m)

Rare Earth Elements	Concentration (μg/litre)
La	0.0034
Nd	0.0028
Gd	0.00070
Ho	0.00022
Yb	0.00082
Ce	0.0012
Sm	0.00045
Tb	0.00014
Er	0.00087
Lu	0.00015
Pr	0.00063
Eu	0.00013
Dy	0.000091
Tm	0.00017
Y	0.0133

d) Thallium

The electronic configuration of thallium is $4f^{14}\ 5d^{10}\ 6s^2\ 6p^1$. It belongs to group IIIb. Thallium exists in two forms, monovalent and trivalent states. Because of chemical affinity, size and valency, thallium (I) associates with silicate minerals rich in the alkali metals such as potassium, rubidium and cesium (92,93), i.e. Tl^+ (ionic radius 1.49 A) fits readily into K^+ (1.33) sites in minerals (92). Thallium ores, crobkesite, $(Cu, Tl, Ag)_2Se$, hutchinsonite $(Pb, Tl)_2(Cu, Ag)As_5S_{10}$, lorandite, $TlAsS_2$, and urbaite, $Hg_3Tl_4As_8Sb_2S_{20}$, are extremely rare (92,94). Thallium is generally present in sphalerite, pyrite and other sulphide minerals (95).

Because of the toxicity of thallium, its uses are limited. However, the metal or salts have been used in :-

i) electrical and electronic applications

ii) catalysis in organic synthesis

iii) rodenticides and insecticides (92)

iv) thallium halides are added in glass to increase the refractive index (95).

Figure 1.8 shows the US consumption of thallium between 1920 and 1980. The temporary increase in consumption during the Second World War was due to the greater need for the protection of stored and transported foodstuffs during the war years. Due to its high toxicity, use of the metal for such purposes was prohibited in the USA from 1972 onwards (96).

Thallium pollution is much less widespread than that of other heavy metals. The contamination of the environment with thallium results chiefly from mines, coal combustion, steel and manganese production or emissions from cement plants (96). The thallium compounds assumed to be contained in emitted dust particulates such as Tl(I) chloride,

bromide, sulphate and oxide are stable under normal atmospheric conditions, with the exception of Tl(II) oxide which may react with moist air to form Tl(I) hydroxide. Therefore, chemical reactions are not very likely to occur in the atmosphere (92).

Thallium is probably transported in solution as Tl^{+}. In strong oxidising conditions, Tl^{+} will be removed from solution as Tl^{3+} by precipitation with manganese and/or iron salts (92). Thallium (III) forms compounds with nearly all ligands that are more stable than those of monovalent forms (96). The redox reaction between Tl(I) and Tl(III) in natural waters is :-

$$Tl(OH)_2Cl + 2H^{+} + 2e \rightleftharpoons TlCl + 2H_2O \qquad [1.2]$$

Batley et alia (97) have suggested that thallium is present in natural waters as Tl^{3+} and the chloride ions control solution transport by forming chloride complexes, which are either stable with respect to reduction to Tl(I) or precipitated. Table 1.11 gives the concentrations of thallium found in natural waters.

Thallium also occurs in sediments. Table 1.12 shows the concentration of thallium in different types of sediments and indicates low concentrations of thallium in calcareous sediments but high concentrations of thallium in sediment containing abundant ferro-manganese nodules (98). Thallium in soil occurs in chemical forms that do not wash out rapidly from soil. For example, after injection of thallium at a rate of 2.5 mg/kg into the soil in easily soluble forms, only 40% were determined to be still in this form (96); so indicating that thallium in soil is not readily available to be taken up by plants. However, Zyka et alia (99) have found extremely high Tl contents in ashes derived from plants (Table 1.13) from the Alsar deposits.

Table 1.11 : Concentration of Thallium in Natural Waters

Source		[Tl] ng/litre	Ref.
Pacific Ocean	Gunnamatta Bay	15.3,12.9	97
	North Cronulla Beach	12.2,12.0	
	Wattamolla Beach	13.0,12.8	
	Wattamolla Beach	11.5,10.3,12.5	
	Wattamolla Beach	15.5,13.8,15.1,12.0	
	Pacific Ocean, 10 mile station	13.4	
	Woronora Weir	5.1,2.8,3.3	
	North Atlantic depth 2 m	9.4	98
	North Atlantic depth 500 m	16.6	
	North Atlantic depth 1000 m	10.0	
	North Atlantic depth 2000 m	10.2	
	North Atlantic depth 2500 m	10.9	
Canadian Rivers	South Tomogonops (April)	20.0	101
	South Tomogonops (May)	5.8	
	South Little (July)	88.3	
	South Little (September)	51.0	
	South Little (November)	9.0	
	Little	42.4	

Table 1.12 : Concentration of Thallium in Marine Sediments in the North Atlantic (98)

Type of sediment	Station	Latitude	Longitude	Depth (m)	Tl (μg/g)
Globigerina ooze	Discovery 154	07°06'N	22°21'W	3,900	0.17
Globigerina ooze	Discovery 2896	001°06'N	85°36'E	4,464	0.35
Calcareous	Discovery 6045	35°50'N	19°22'W	3,532	0.08
Siliceous - manganiferous	Downwind DWHD81	22°07'S	115°14'W	3,200	4.9*
Siliceous - calcareous	Eltanin 11-3 E196A	56°54'S	115°14'W	5,000	0.47
Glauconitic mud	Eltanin -	16°51'N	25°08'W	720	0.09
Red clay	Cusp 15p	37°15'N	143°07'W	5,220	1.8
Brown volcanic clay	Mid-Pacific 20-2	19°46'N	154°58'W	5,408	0.12
Chocolate volcanic clay	Capricorn H24	16°44'S	161°22'W	4,685	2.2
Volcanic muddy sand	Mid-Pacific 18A-1	19°46'N	154°58'W	359	0.31

* Sample from sediment surface; 5.7 ppm at a depth 5 cm below sediment surface.

Table 1.13 : Thallium Contents of Plants (99)

Plants	Tl content in ashes (mg/kg)
Lavatera sp. Malvaceae (leaves)	128
Lavatera sp. Malvaceae (flowers)	45
Dianthus sp. Caryophyllaceae (flowers)	5,200
Galium sp. Rubiaceae (flowers)	17,000
Centaurea sp. Compositae (fruit)	75
Centaurea sp. Compositae (leaves)	105
Eryngium sp. Umbelliferae (leaves)	03
Eryngium sp. Umbelliferae (flowers)	01
Campanula sp. Campanulaceae (flowers, leaves)	59,990
Echinops sp. Compositae (leaves)	15

Thallium and its compounds are highly toxic to biota. Thallium is absorbed through the skin and mucous membrane. It is widely distributed through the body and accumulates in the central nervous system. The effects of thallium on rats are behaviour disorders, hair loss and histological alteration of the liver, kidneys and stomach membrane (96).

Thallium is also toxic to plants and inhibits chlorophyll formation and seed germination. Thallium uptake via roots shows discolouration in the leaf which results from degradation of chlorophyll, beginning at the base of the leaf vein, progressing along the vein, reaching the tip and spreading over the whole leaf blade until it is totally covered by intercostal chloroses (95).

Thallium is toxic to aquatic animals such as clams (Mya arenaria)

and mussels (Mytilus edulis) (100), juvenile Atlantic salmon (Salmo salar) (101) and embryos and larvae of fathead minnows (Pimephales promelas) (102). However, thallium may be accumulated in these animals, thus entering the body of humans via ingestion of such animals. Zitko et alia (100) reported that the degree of thallium accumulation is low in clams and mussels, which indicates that only small amounts of thallium will enter the body of humans via ingestion of these foodstuffs.

In general, the effects of thallium on living organisms originate from :-

i) oxidation of Tl(I) to Tl(III) which inhibits the ATpase of amine-storing granules, thus causing alteration in the catecholamine metabolism (95);

ii) thallium (I) is able to substitute monovalent cations, particularly potassium, in enzyme reactions. Thallium is isomorphic with potassium, but has approximately 10 times higher affinity than potassium for the enzymes. The increased affinity may cause toxic effects (92);

iii) reduction of mitosis (96);

iv) effects on transport mechanisms (92).

FIG. 1.8 U.S. CONSUMPTION OF THALLIUM BETWEEN 1920 AND 1980 (96)

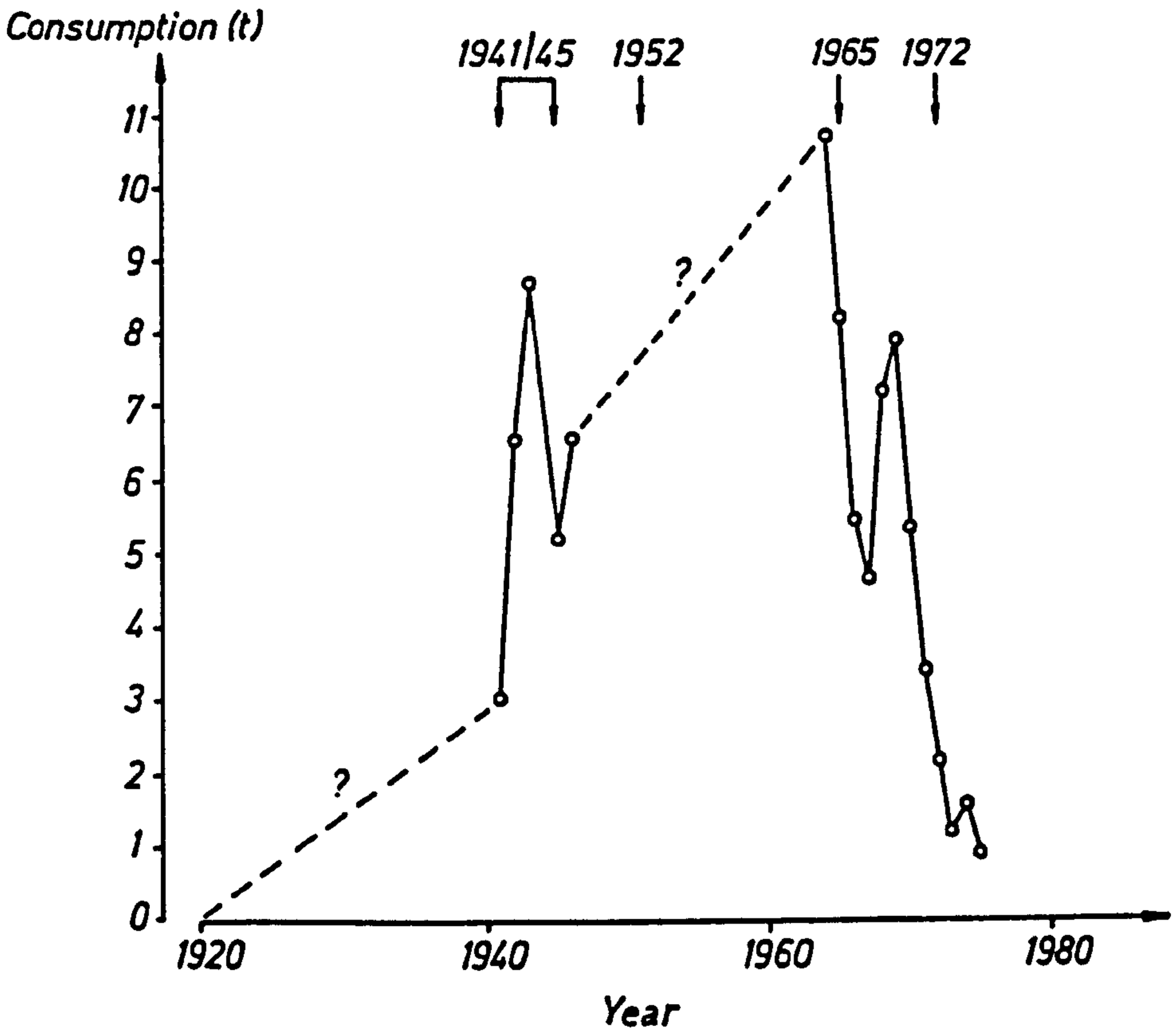

e) Lead

The electronic configuration of lead is $4f^{14}\ 5d^{10}\ 6s^2\ 6p^2$. The primary form of lead in the natural state is galena, PbS, but it is also found as plattnerite, PbO_2, cerussite, $PbCO_3$, and anglesite, $PbSO_4$ (14).

The major anthropogenic sources of lead emission into the environment originate from :-

i) smelting and refining processes

ii) combustion of coal and oil

iii) industrial effluent discharge

iv) combustion of petrol containing alkyl lead compounds

v) direct use of elemental lead and lead compounds e.g. fungicides, insecticides, and anti-fouling paints (103).

The combustion of leaded petrol is probably the major source of lead emissions. Ward et alia (104) reported higher concentrations of lead on leaves of unwashed grass species than on the washed ones (Table 1.14) along the major motorways in New Zealand. Although lead occurs naturally in soil, enhanced levels of lead were found and correlated with heavily utilised highways in New Zealand. The concentration of lead in soil decreased with the depth (Figure 1.9). The lead contents of soil and grass species tend to increase with traffic volume and decrease with distance from the highway (105). The source of this lead is aerial deposition from the motor vehicles, derived from the tetraethyl lead that is added to petrol and used as an "anti-knocking" agent. Other lead compounds are added to lubrication oils, grease and light mineral oil and used as an anti-oxidant. Figure 1.10 gives the structure of these compounds (106). Some tetraethyl lead and lead halides are emitted to the atmosphere when the petrol is combusted by vehicles and eventually returns to the earth as particulate

fall-out or washed out with the rain. When the lead returns over soil it may be immobilised by soil microorganisms, precipitation, sorption or ion exchange interaction with soils, or fixation by organic matter. It may also be taken up by plants, thereby entering the food chain (107).

Table 1.14 : Mean Concentration (μg/g Dry Weight) of Lead in Unwashed Pasture Species at Greenlane Interchange of Auckland Motorway, New Zealand (104)

Species	Lead (μg/g)
Poa annua L.	
Root	460
Leaves	546
Holcus lanatus L.	
Root	408
Leaves	553
Flatweeds	
Roots	225
Leaves	1044
Bellis perennis L.	
Roots	165
Leaves	313
Paspalum dilatatum L.	
Roots	213
Leaves	305

FIG. 1.9 LEAD CONCENTRATION OF SOIL AS A FUNCTION OF DEPTH AT VARIOUS DISTANCES FROM HIGHWAY (105)

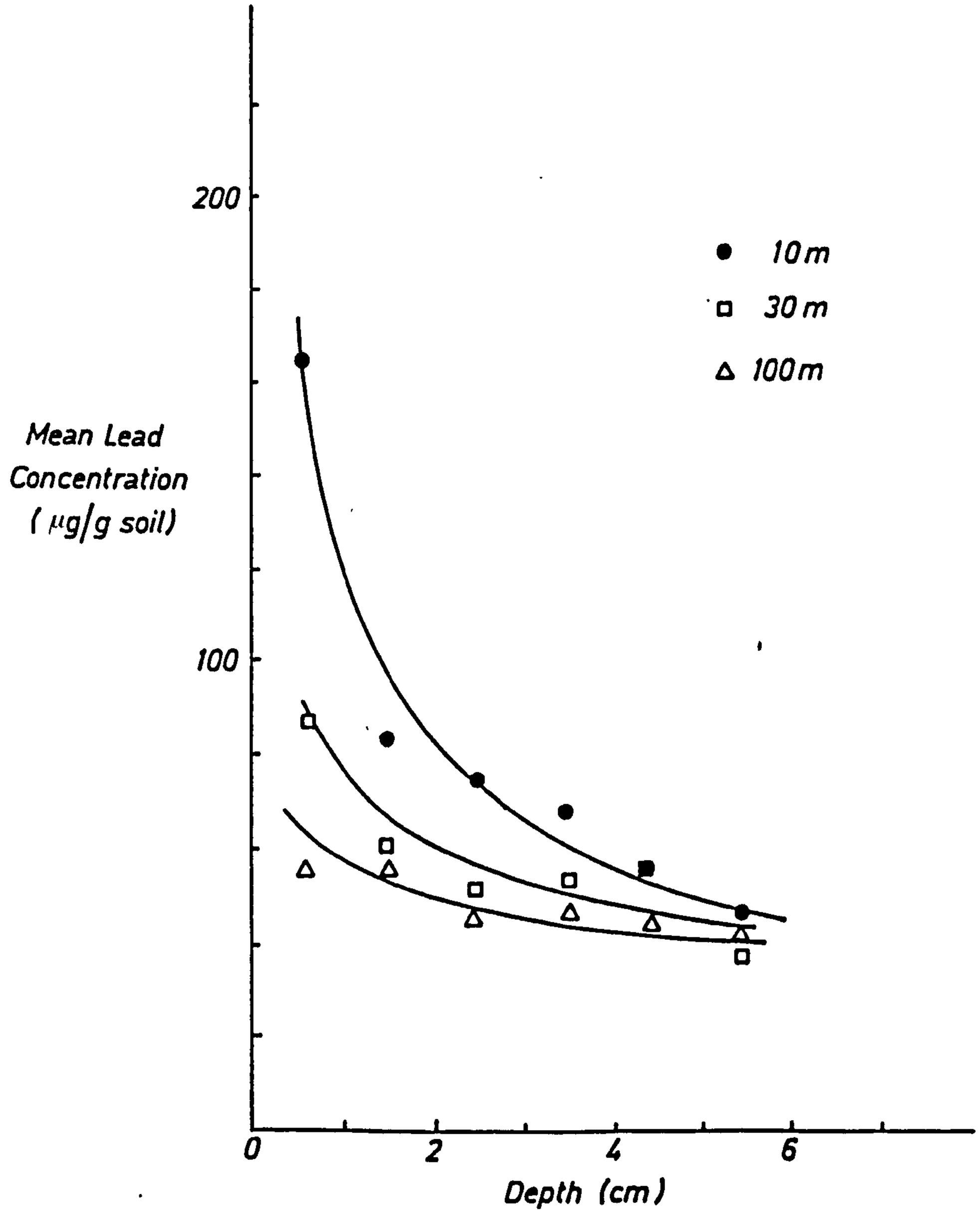

FIG. 1.10 STRUCTURE OF VARIOUS LEAD COMPOUNDS USED AS PETROLEUM ADDITIVES (106)

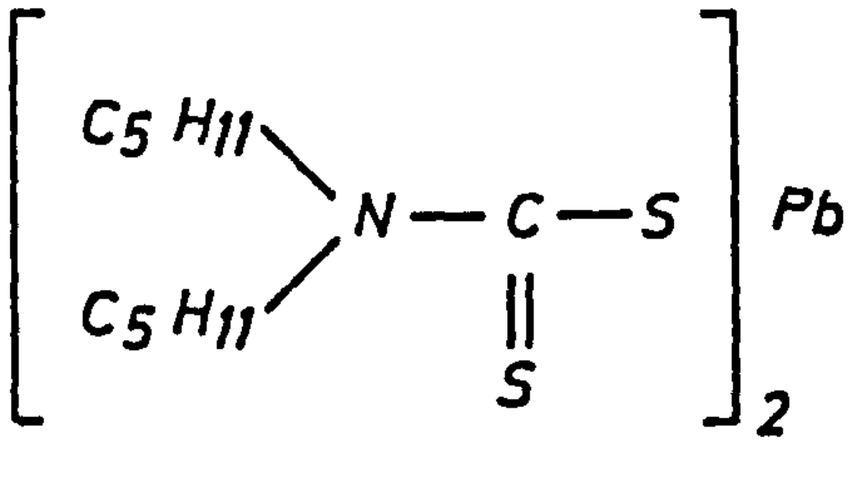

LEAD DIAMYLDITHIOCARBOMATE

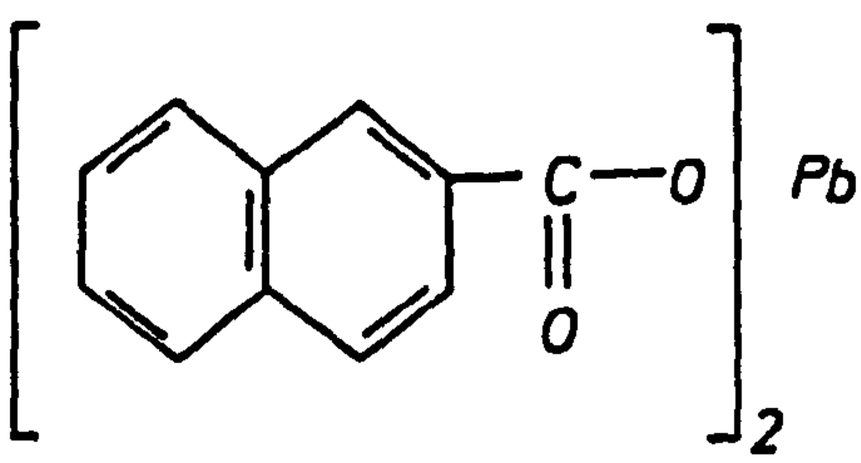

LEAD NAPHTHENATE

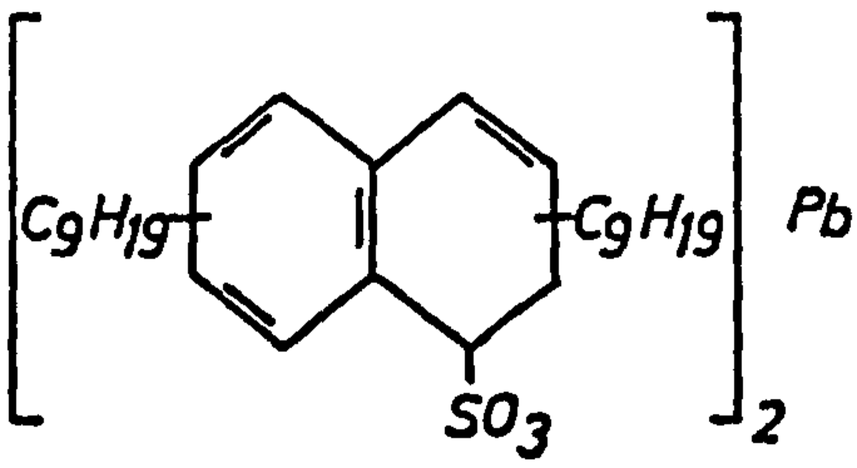

LEAD DINONYLNAPHTHALENE

Harrison et alia (108) have reported that six lead species were found in street dusts and these include $PbSO_4$, Pb^{o}, $PbSO_4.(NH_4)_2SO_4$, Pb_3O_4, $PbO.PbSO_4$ and $2PbCO_3.Pb(OH)_2$. Again this study indicates that the lead is deposited from the atmosphere as a result of combustion of petrol by vehicles.

The major anthropogenic source of lead in river systems is industrial effluents, especially those arising from lead mines. However, the chemical form of lead in natural waters below pH 7 may be Pb^{2+}, $PbCO_4$, $Pb(CO)_3^{2-}$, $PbOH^{+}$ and $Pb(OH)_2$ (28). The main species of lead in seawater are thought to be $PbOH^{+}$ and $PbCl^{+}$. Chloride, hydroxide and dissolved carbon dioxide play an important role in the control of soluble forms of lead in the interstitial water (28). Figure 1.11 gives the possible lead species in water classified according to their size association (109). Lead species may exist in different chemical forms in drinking water. The most important are the soluble forms which are harmful to humans. Lead carbonate $2PbCO_3.Pb(OH)_2$ is the most stable insoluble lead compound formed in the conditions apertaining to most potable waters in Britain (110). However, lead present in drinking water in Britain comes mainly from lead water pipes, soldered joints and atmospheric fall-out (111).

Lead, in soil or in solution culture, is taken up by plants and is accumulated in roots rather than in other parts of the plants (22). The addition of EDTA to soils increases the uptake of lead by plants (103), so indicating that the uptake depends on the chemical form of the lead. The environmental consequences of lead in the environment has been the subject of major reviews (22,103). Lead generally has effects on plants such as inhibition of growth (112), reduction of photosynthesis, mitosis, water absorption and can contribute to copper deficiency (103).

FIG. 1.11 THE RANGE OF FORMS OF LEAD IN WATER CLASSIFIED ACCORDING TO SIZE ASSOCIATION (109)

Size/nm ← 1 — 10 — 100 — 1000

	Soluble			Colloidal		Particulate	
Metal species	Free metal ions	Inorganic ion pairs organic chelates	Organic complexes	Metal species bound to high molecular weight organic material	Metal species absorbed on colloids	Metals incorporated with organic particles and remains of living organisms	Mineral solids metals absorbed on solids: precipitates co-precipitates
Example	Pb^{2+}	$PbHCO_3^+$ Pb EDTA	Pb-fulvic acid	Pb-humic acid	Pb-Fe(OH)$_3$ Pb-MnO_2	Pb-organic solids	Pb-clay $PbCO_{3(s)}$

The chemical form of lead in plants may be complexed with organic compounds, however the lead compounds have been identified in Soybean and Pintobean as orthophosphate and pyrophosphate respectively (22).

The toxicology of lead is very complex. Inorganic lead, Pb^{2+}, is a general metabolic poison and is cumulative in humans. Lead inhibits enzyme systems necessary for the formation of haemoglobin through its strong interaction with -SH groups (111). Lead (II) can replace Ca^{2+} in bones, so tending to accumulate over long periods. Lead alkyls such as tetraethyl-lead are even more poisonous than Pb^{2+}, the effects are probably due to the R_3Pb^+ species which is readily absorbed from the respiratory tract, gastrointestinal tract and skin, whereas the insoluble but stable lead sulphate, sulphide and chromate are poorly absorbed from the gastrointestinal tract (14).

1.6 OBJECTIVES

The objectives of the present work were :-

i) to determine the reproducibility of the determination of Al, Ag, La, Tl and Pb by ASV, XRF, AAS, plasma emission and gas chromatographic techniques;

ii) to determine the most suitable methods for the determination of these metals in natural samples;

iii) to investigate the effects of these metals on Lolium pérenne by measuring critical and lethal levels;

iv) to investigate the speciation of lead in water by means of sequential filtration and estimation by DPASV and GFAAS;

v) to investigate the association of Pb, Cu, Zn, Mn, Fe, Ca in sediments using the Tessier scheme;

vi) to investigate the best supporting electrolyte for the determination of Tl by DPASV and to determine the detection limit;

vii) to investigate the differences in the sensitivity between HMDE and TFME for the determination;

viii) to investigate the availability of Ag, Tl and Pb in soils for plants;

ix) to investigate the best supporting electrolyte for the determination of Ag by DC-ASV;

x) to investigate the association of La and Al uptake by plants using the Farago scheme;

xi) to investigate the interactions (if any) between metal uptake by plants using response surface methodology;

xii) to study the effect of pH and time on heavy metals released from sediment using response surface methodology.

1.7 REFERENCES

1. Murphy, C.B. and Speigel, S.J., J. Water Pollut. Control Fed., 54, 849 (1982).
2. Waldichuk, M., Some Biological Concerns in Heavy Metals Pollution, in "Pollution and Physiology of Marine Organisms", Academic Press, Inc., New York, p. 8 (1974).
3. Antonovics, J., Bradshaw, A.D.and Turner, R.G., Adv. Ecol. Res., 7, 1 (1971).
4. Martin, M.H., Ducan, E.M. and Coughtrey, P.J., Environ. Pollut. (B), 3, 147 (1982).
5. Wittman, G.T.W., Toxic Metals, Chap. B, in "Metal Pollution in the Aquatic Environment", Forstner, U. and Wittman, G.T.W. (Eds.), Springer-Verlag, London, p. 12-30 (1979).
6. Goulden, P.D., "Environmental Pollution Analysis", Heyden & Son, Ltd., p. xi (1978).
7. Warren, H.V., J. Biosoc. Sci., 6, 223 (1974).
8. Williams, D.R., Chem. Rev., 72, 203 (1974).
9. Bowen, H.J.M., Environmental Chemistry of the Elements, Academic Press, London, p. 9 (1979).
10. Nriague, J.O., Nature, 279 409 (1979).
11. Vivian, C.M.G. and Massie, K.S., Environ. Pollut., 14, 47 (1977).
12. Ireland, M.P., Environ. Pollut., 4, 27 (1973).
13. Kirk, P.W.W. and Lester, J.N., Sci. Total Environ., 40, 1 (1984).
14. Randall, L., "Fractionation of Heavy Metals in Natural Samples", Ph:D.Thesis, University of Bristol, p. 32 (1984).
15. Hershelman, G.P., Schafer, H.A., Jan, T.K. and Young, D.R.,. Marine Pollut. Bull., 12, 231 (1981).
16. Taylor, D., Estuar. Coast. Mar. Sci., 2, 417 (1974).

17. Chester, R., Kudoja, W.M., Thomas, A. and Towner, J., Environ. Pollut. (B), 10, 213 (1985).

18. Grieg, R.A., Reid, R.N. and Wenzloff, D.R., Marine Pollut. Bull., 8, 183 (1977).

19. Water Research Council, Technical Report TR 140. Crops as Indicators of the Significance of Contamination of the Soil by Heavy Metals.

20. Thornton, I., Geochemical Aspect of Distribution and Forms of Heavy Metals in Soils, Chap. 1, p. 1, in "Effect of Heavy Metal Pollution on Plants", Lepp, N.W. (Eds.), Vol. 2, Applied Science Publishers, London (1981).

21. Martin, M.H. and Coughtrey, P.J., Impact of Metals on Ecosystem Function and Productivity, Chap. 4, p. 119, in "Effect of Heavy Metals on Plants", Lepp, N.W. (Ed.), Applied Science Publishers, London (1981).

22. Zimdahl, R.L. and Koeppe, D.E., Uptake by Plants, in "Lead in the Environment", Boggess, W.R. and Wixson, B.G. (Eds.), Castle House Publication Ltd., p. 99 (1979).

23. Florence, T.M., Talanta, 29, 345 (1982).

24. Gibbs, R.J., Science, 180, 71 (1973).

25. Davis, J.A. and Leckie, J.O., Environ. Sci. Technol., 12, 1309 (1978).

26. Gennaro, M.C., Balocchi, C., Campi, E., Mentasti, E. and Aruga, R., Anal. Chim. Acta, 151, 339 (1983).

27. Guy, R.D. and Chakrabarti, C.L., Analytical Techniques for Speciation of Trace Metals, in "International Conference on Heavy Metals in the Environment", Symposium Recording, Vol. 1, p. 276, Toronto, (1975).

28. Jorado, C.P., "Chemical Availability of Heavy Metals in Aquatic Environments", Ph.D. Thesis, University of Bristol, p. 28 (1983).

29. Harrison, R.M., Laxen, D.P.H. and Wilson, S.J., Environ. Sci. Technol., 15, 1378 (1981).

30. Thorne, L., "Metal Speciation in Severn Estuary Sediments", Ph.D. Thesis, University of Bristol, p. 47 (1978).

31. Forstner, U., Metal Transfer between Solid and Aqueous Phases, Chap. E, in "Metal Pollution in the Aquatic Environment", Springer-Verlag, Berlin, p. 215 (1979).

32. Kiekens, L. and Cottenie, A., Characterization of Chemical and Biological Activity of Heavy Metals in the Soil, in "International Conference on Heavy Metals in the Environment", Heidelberg, Sept. (1983), CEP, Consultants (Edinburgh).

33. Schnitzer, M., Humic Substances: Chemistry and Reaction, Chap. 1, p. 1, in "Soil Organic Matter", Schnitzer, M. and Kahn, S.U. (Eds.), Elsevier Scientific Publishing Company, Amsterdam (1978).

34. Yen, T.F. and Tang, I.S., Chemical Aspects of Marine Sediments, in "Chemistry of Marine Sediments", Ann Arbor Science, p. 1 (1977).

35. Saar, R.A. and Weber, J.H., Environ. Sci. Technol., 14, 877 (1980).

36. Tovar-Grau, J., Graham, C.L. and Hayes, M.H.B., J., Anal. Proc., (London), 20, 125 (1983).

37. Perdue, E.M. and Lytle, C.R., Environ. Sci. Technol., 17, 654 (1983).

38. Thurman, D.A. and Collins, J.C., Metal Tolerance Mechanisms in Higher Plants - A Review, in "International Conference on Heavy Metals in the Environment", Heidelberg, Sept. (1983), CEP, Consultants (Edinburgh).

39. Hewitt, E.J., A Perspective of Mineral Nutrition : Essential and Functional Metals in Plants, Chap. 14, p. 277, in "Metals and Micronutrients : Uptake and Utilization by Plants", Robb, R.A.

and Pierpoint, W.S. (Eds.), Academic Press, London (1983).

40. Thurman, D.A., Mechanism of Metal Tolerance in Higher Plants, Chap. 8, p. 239, in "Effect of Heavy Metal Pollution on Plants", Vol. 2, Lepp, N.W. (Ed.), Applied Science Publishers, London (1981).

41. Farago, M.E., Mullen, W.A., Cole, M.M. and Smith, R.F., Environ. Pollut., 21, 225 (1980).

42. Burton, K.W. and John, E., Water, Air and Soil Pollut., 7, 45 (1977).

43. Wood, J.M. and Wang, H.K., Environ. Sci. Technol., 17, 582A (1983).

44. Cataldo, D.A. and Wildung, Environ. Health Persp., 27, 149 (1978).

45. Lee, J. and Pritchard, M.W., Plant and Soil, 82, 101 (1984).

46. Fitter, A.H. and Hay, R.K.M., "Environmental Physiology of Plants", Academic Press, London, p. 200 (1981).

47. Morgan, E., "The Influence of Heavy Metals upon Tree Growth in South Wales Forests", PhD Thesis, Polytechnic of Wales, p. 160 (1983).

48. Barber, S.A. and Claassen, N., A Mathematical Model to Simulate Metal Uptake by Plant Growing in Soil, p. 358, in "Biological Implication of Metals in the Environment", Drucker, H. and Wildung, R.E. (Eds.), published by Technical Center, USA (1977).

49. Barker, D.A., Uptake of Cations and Their Transport within the Plant, Chap. 1, in "Metals and Micronutrients : Uptake and Utilization by Plants", Robb, D.A. and Pierpoint, W.S.,(Eds.), Academic Press, London, p. 4 (1983).

50. Fried, M. and Broeshart, H., The Soil-Plant Systems in Relation to Inorganic Nutrition, published by Academic Press, p. 109 (1967).

51. Burton, K.W., Morgan, E. and Roig, A., Plant and Soil., 78, 271 (1984).

52. Esser, J. and Bassam, N. El., Environ. Pollut., 26, 15 (1981).

53. Peterson, P.J., Adaptation of Toxic Metals, Chap. 4, in "Metals

and Micronutrients, Uptake and Utilization by Plants", Robb, D.A. and Pierpoint, W.S. (Eds.), Academic Press, London, p. 51 (1983).

54. Brown, H. and Martin, M.H., New Phytol., 89, 621 (1981).

55. Woolhouse, H.W., Chem. Br., 16, 72 (1980).

56. Wilkins, D.A., New Phytol., 80, 623 (1978).

57. Coughtrey, P.J. and Martin, M.H., OIKOS, 30, 555 (1978).

58. Brookes, A., Collins, J.C. and Thurman, D.A., J. Plant Nutr., 3, 695 (1981).

59. Diamadopoulos, E. and Woods, D.R., Water Res., 18, 1455 (1984).

60. Snodgrass, W.J., Clark, M.M. and O'Mella, C.R., Water Res., 18, 479 (1984).

61. Caster, W.O. and Wang, M., Sci. Total Environ., 17, 31 (1981).

62. Hydes, D.J. and Liss, P.S., Estuar. Coast. Mar. Sci., 5, 755 (1977).

63. Cronan, C.S. and Schofield, C.L., Science, 204, 305 (1979).

64. Smith, R.W., Adv. Chem. Ser., 106, 250 (1971).

65. Campbell, P.G.C., Bisson, M., Bougie, R., Tessier, A. and Villeneuve, J.P., Anal. Chem., 55, 2252 (1983).

66. Bache, B.W., J. Soil Sci., 25, 320 (1974).

67. De Manzi, J.M. and Cartwright, P.M., Plant and Soil, 80, 423 (1984).

68. Pavan, M.A., Bingham, F.T. and Pratt, P.F., Soil Sci. Soc. Am. J., 46, 1201 (1982).

69. Asher, C.J., Edwards, D.G. and Carvalho, M.M. De, Plant and Soil, 64, 141 (1982).

70. Wood, M., Cooper, J.E. and Holding, A.J., Soil Biol. Biochem., 15, 123 (1983).

71. Wood, M., Cooper, J.E. and Holding, A.J., Plant and Soil, 78, 367 (1984).

72. Wood, M., Cooper, J.E. and Holding, A.J., Plant and Soil, 78, 381 (1984).

73. Clarkson, D.T., Plant and Soil, 27, 347 (1967).

74. Keyser, H.H. and Munns, D.N., Soil Sci. Soc. Am. J., 43, 519 (1979).

75. Cotton, F.A. and Wilkinson, G., Advanced Inorganic Chemistry, John Wiley & Sons Inc., (1980).

76. Krauskopf, K.B., Introduction to Geochemistry, McGraw-Hill Book Company, London (1967).

77. Maxfield, D., Rodriguez, J.M., Buettner, M., Davis, J., Forbes, L., Kovacs, R., Russel, W., Schultz, L., Smith, R., Stanfon, J. and Wal, C.M., Environ. Pollut., 7, 1 (1974).

78. Klein, D.H. and Russell, P., Environ. Sci. Technol., 7, 357 (1973).

79. Bertine, K.K., Goldberg, E.D., Science, 173, 233 (1971).

80. Encyclopedia of Chemical Technology, Third Edition, John Wiley & Sons, New York, Vol. 17, 611 (1982).

81. Cooper, C.F. and Jolly, W.C., Water Resources Res., 6, 88 (1970).

82. Bruland, K.W., Bertine, K., Koide, M. and Goldberg, E.D., Environ. Sci. Technol., 8, 425 (1974).

83. Smith, I.C. and Carson, B.L., Trace Metals in the Environment, Vol. 2, Sliver, Ann Arbor Science, Michigan, p. 324 (1977).

84. Buckley, W.R., Arch. Dermatol., 88, 531 (1963).

85. Calabrese, A., Thurberg, F.P. and Gould, E., Marine Fish. Rev., 39, 5 (1977).

86. Benkhayal, A.A., "Silver as Pollutant", M.Sc. Thesis, University of Bristol, p. 49 (1983).

87. Horovitz, C.T., Schock, H.H. and Horovitz-Kisimova, L.A., Plant and Soil, 40, 397 (1974).

88. Hutchinson, G.E., Quart, Rev. Biol., 18, 255 (1943).

89. Yliruokanen, I., A Chemical Study on the Occurrence of Rare Earths in Plants, Ph.D. Thesis , University of Helsinki, p. 20 (1975).

90. Høgdahl, O.T., Melsom, S. and Bowen, V.T., Neutron Activation Analysis of Lanthanide Elements in Sea Water, in "Trace Inorganics in Water", Baker, R.A. (Ed.), Chap. 19, published by American Chemical Society, Washington, p. 308 (1968).

91. Cowgill, U.M., Geochim. et Cosmochim. Acta, 37, 2329 (1973).

92. Smith, I.C. and Carson, B.L., Trace Metals in the Environment, Vol. 1, Thallium, Ann Arbor Science, Michigan, p. 185 (1977).

93. Robinson, K., U.S. Geol. Survey Prof. Paper 820.

94. Lee, A.G., The Chemistry of Thallium, Elsevier Publishing Company, London (1971).

95. Zitko, V., Chemistry, Applications, Toxicity and Pollution Potential of Thallium, Technical Report No. 518, p. 21 (1975).

96. Schoer, J., Thallium, in "The Handbook of Environmental Chemistry", Hutzinger, O. (Ed.), Vol. 3, Part C, Springer-Verlag, New York, p. 147 (1984).

97. Batley, G.E. and Florence, T.M., J. Electroanal. Chem., 61, 205 (1975).

98. Matthews, A.D. and Riley, J.P., Chem. Geol., 6, 149 (1970).

99. Zyka, V., Sbor. Geol. Ved. Technol., 10, 91 (1975).

100. Zitko, V. and Carson, W.V., Bull. Environ. Contam. Toxicol., 14, 530 (1975).

101. Zitko, V., Carson, W.V., Carson, W.G., Bull. Environ. Contam. Toxicol., 13, 23 (1975).

102. Leblanc, G.A. and Dean, J.W., Bull. Environ. Contam. Toxicol., 32, 565 (1984).

103. Martinson, D.M., "The Determination of Lead in the Environment", Ph.D.Thesis, University of Bristol, p. 30 (1979).

104. Ward, N.I., Brooks, R.R., Roberts, E. and Boswell, C.R., Environ. Sci. Technol., 11, 917 (1977).

105. Ward, N.I., Reeves, R.D. and Brooks, R.R., Environ. Pollut., 9, 243 (1975).

106. Supp, G.R., Gibbs, I. and Juszli, M., At. Absorp. News., 12, 66 (1973).

107. Zimdahi, R.L. and Skogerboe, R.K., Environ. Sci. Technol., 11, 1202 (1977).

108. Biggins, P.D.E. and Harrison, R.M., Environ. Sci. Technol., 14, 336 (1980).

109. Harrison, R.M. and Laxen, D.P.H., Chem. Br., 16, 316 (1980).

110. Harrison, R.M. and Laxen, D.P.H., Nature, 286, 791 (1980).

111. Smith, D.B., Chem. Br., 7, 54 (1971).

112. Wilkins, D.A., Nature, 180, 37 (1957).

CHAPTER 2

DETERMINATION OF TRACE METALS

CONTENTS

2.1 INTRODUCTION

Prior to the quantitative determination of trace metals in natural samples, preparation of samples is needed. These preparations may be performed by conversion of the sample constituents into forms more amenable to detection and measurement, using pre-concentration via solution techniques or matrix modification procedures to homogenise the solid sample (1,2). The choice of the most suitable method for trace metal determination is governed by the availability, sensitivity and selectivity of analytical method. Many different analytical methods are available for trace metal determination and are often based on different principles.

Colorimetric methods depend upon reaction of specific reagents or ligands with a metal ion at a certain pH to form a coloured metal-complex, thus the metal ion can then be determined by visible spectrophotometry at certain wavelengths. For example, Sn, Zn, Tl can react with Pyrocatechol Violet (3), Alizarin (4) and Brilliant green (5) respectively to form such complexes of quantitative analytical significance.

In neutron activation analysis, the sample is bombarded with neutrons, some of which are captured by the atomic nuclei of the same element to produce radioactive isotopes. These activated nuclei may then emit radiation which can be exploited to determine specific elements. The method is sensitive but expensive (6-8).

These two methods of trace metal determinations are not used in the present work due to lack of sensitivity in the former case and unavailability in the second.

2.2 METHODS OF TRACE METAL DETERMINATION IN THE PRESENT WORK

2.2.1 Atomic Absorption Spectrometry (AAS)

AAS is the determination of absorption of radiation by free atoms. The population of free atoms exists at various electronic energy levels (9). The distribution of atoms in such energy levels is given by the Boltzman distribution as follows:-

$$\frac{N_2 E}{\tau} = \frac{N_1 E g_1}{g_2} e^{-E/kt} \quad \ldots\ldots \quad [2.1]$$

where: N_1 = number of atoms in ground state

N_2 = number of atoms in excited state

E = energy difference between the ground and excited states

g_1, g_2 = statistical weight of atoms in ground and excited states

τ = life time in excited state

K = Boltzmann distribution constant

T = absolute temperature of system

The atom is called in the ground state when all the valence electrons are in orbitals with low energy levels (E_o), but the valence electrons move to higher energy levels (E_1), i.e. the atom is called in an excited state. The difference in energy between the ground and excited states is called the energy of excitation. Normally atoms will remain in the ground state unless they absorb energy and are converted to the excited state (9-11). In atomic absorption analysis, the sample is converted to atomic vapour by an atomiser system (normally by flame or electrothermal energy) and irradiated at a specific wavelength by light from a source which is usually a hollow cathode lamp (HCL) of the specific metal being determined. Absorption of radiation from the HCL is measured according to the Beer-Lambert Law

$$A = abc \qquad \ldots\ldots \quad [2.2]$$

where: A = absorbance

a = absorptivity constant

b = cell path length

c = sample concentration

The sample cell in atomic absorption analysis is the atomiser length and percentage absorption is converted to absorbance which is a logarithmic function (9) equal to :-

$$A = \log \frac{I_o}{I} \qquad \ldots\ldots \quad [2.3]$$

where: I_o = the radiation from HCL without sample in the sample cell

I = the radiation from HCL with sample in the sample cell

$I_o - I$ = amount of radiation absorbed by the sample

The attractions of the AAS technique to analytical chemists are sensitivity, reproducibility, low cost and nearly 70 metallic elements of the Periodic Table may be determined by this technique. The metals may be determined by AAS by measuring the absorbance of a number of standard solutions containing known concentrations of the analyte, then drawing a calibration graph by plotting absorbance against concentration. The linear regression relationship between the absorbance and known concentration is used to find the concentration of the analyte in the unknown; within the range of standard solutions.

The major disadvantages of AAS are its single channel operation and the interferences mainly caused by molecular absorption. If the appropriate energy source is employed, the molecular absorption is corrected for by the use of background correction (9). Deuterium or

hydrogen lamps have been used very successfully as background correction in AAS, but it is limited to correction in the range 0-1 A in the wavelength range 200-400 nm (12,13). Figure 2.1 gives the spectrum of a deuterium lamp, which indicates the low intensity at or above 350 nm. For resonance lines at visible wavelengths either a tungsten-halogen lamp or Zeeman background correction system affects the absorption response only at the exact analyte wavelength. The Zeeman effect refers to the phenomenon of the splitting of atomic spectral lines when subjected to a strong magnetic field. The Zeeman effect is applied to the absorber to discriminate pure atomic absorption from background effects due to molecular absorption (13). The atomic absorption Zeeman spectrophotometer is depicted schematically in Figure 2.2 (14), which indicates that the atomiser is situated between poles of an electromagnet.

It is best to discuss the AAS atomiser systems, namely flame and furnace, individually.

a) Flame Atomic Absorption Spectrometry (FAAS)

Since the introduction of atomic absorption spectrometry in 1955, the main developments have been in the design and performance of atomisation systems. When a flame is used in AAS, the technique is said to be FAAS. Figure 2.3 depicts a typical flame atomic absorption spectrophotometer. Flames are produced by combustion of a mixture of two gases (fuel and oxidant). The temperature of the flame depends upon the mixture of gases used.

The total concentration of metals in samples can be extracted by mineral acids. Most mineral acids, such as hydrochloric, nitric, sulphuric acid, perchloric and hydrofluoric acids individually or as mixtures have been widely used in atomic absorption spectrometry determinations (15). Hydrochloric acid dissolves adsorbed and

FIG. 2.1 SPECTRUM OF DEUTERIUM LAMP

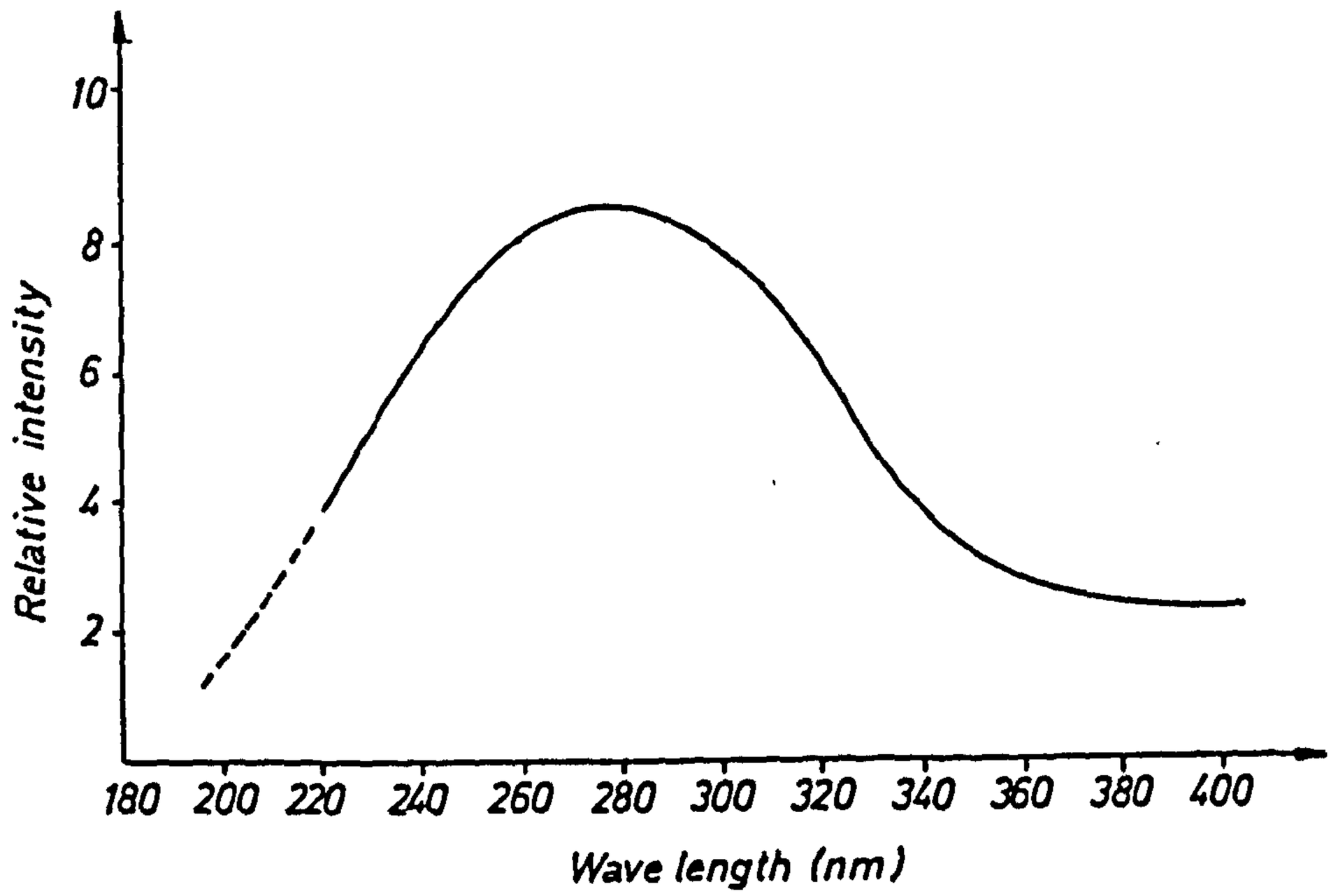

FIG. 2.2 ATOMIC ABSORPTION ZEEMAN SPECTROPHOTOMETER WITH TUNGSTEN ATOMISER

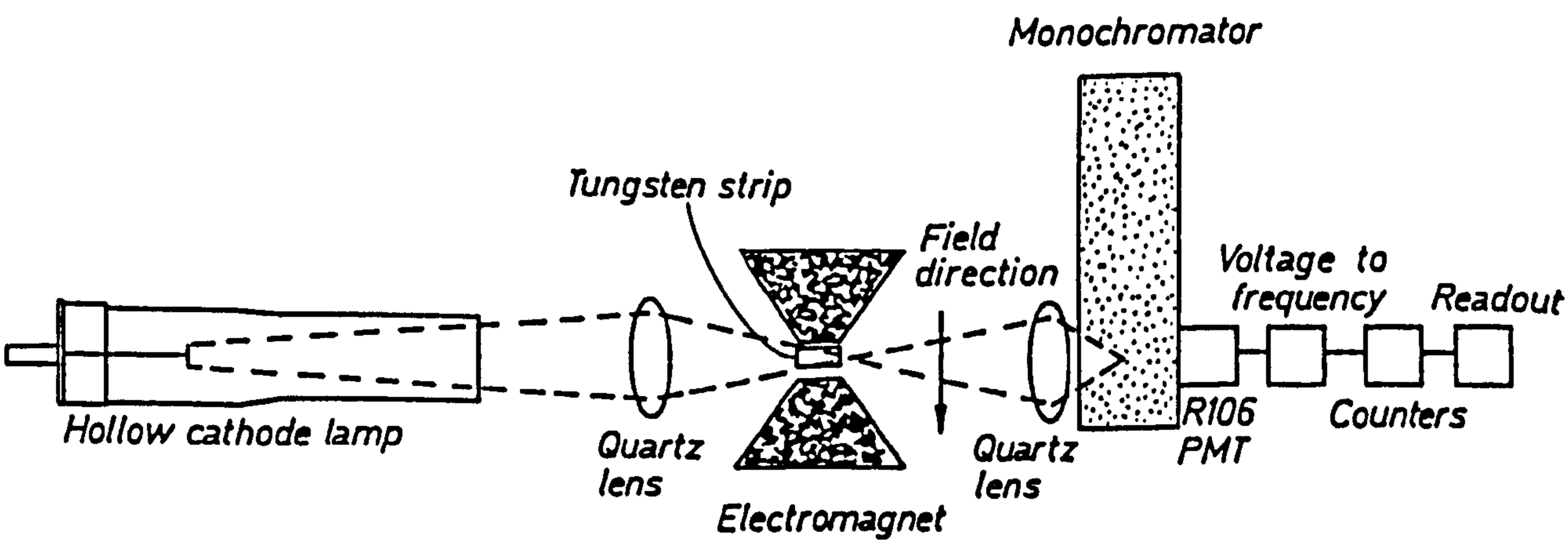

FIG. 2.3 SCHEMATIC OF A SIMPLE FLAME ATOMIC ABSORPTION SPECTROMETER

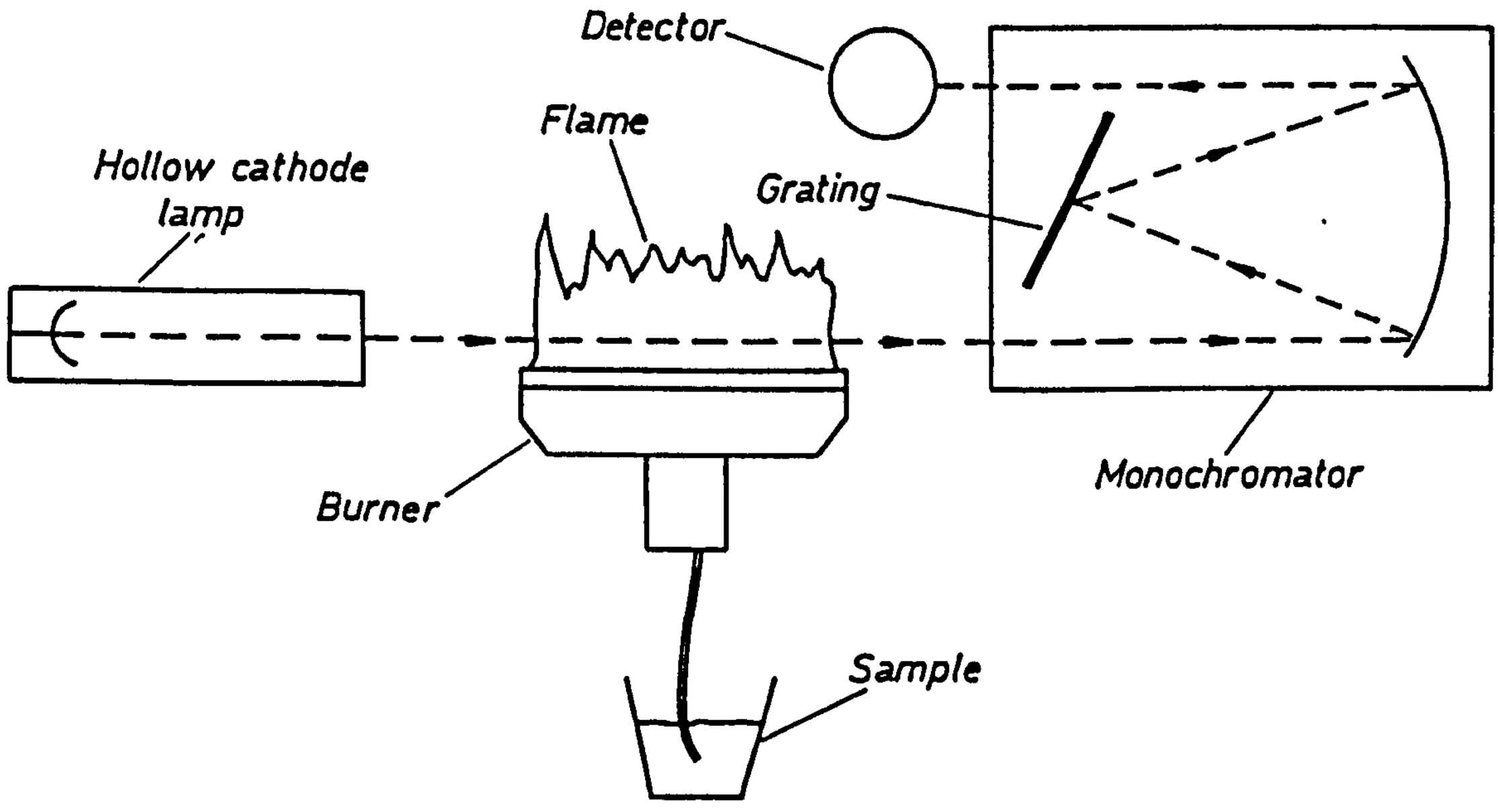

precipitated metals, but it has little effect on metals obonded to silicates. Nitric acid has been recommended for the extraction of trace metals, mainly due to the fact that most nitrates are soluble and the acid is a good medium for atomic absorption spectrophotometry causing few interferences (16). Sulphuric acid forms several insoluble sulphates, while the sulphate ions tend to interfere with the FAAS determination of metals, by forming a salt which is difficult to dissociate and atomise in the flame (17). Perchloric acid is a very good oxidising agent and forms soluble perchlorates, but the acid may cause explosions when it is used to digest samples which contain high levels of organic materials (18). Hydrofluoric acid dissolves metal silicates and releases metals by volatilisation of the major elements of the matrix :-

$$SiO_2 + 4HF \longrightarrow SiF_4 + 2H_2O \qquad \ldots\ldots \qquad [2.4]$$

The chloride, fluoride and iodide ions in major amounts tend to interfere in FAAS determination of metals, by forming molecules, with alkali and alkaline earth elements, which can give rise to background effects when vaporised in the flame, either by particulates scattering light or by molecular absorption within the bandpass of the monochromator (19).

In FAAS interference due to the sample matrix can be reduced by using one or more of the following techniques:

i) standard addition methods

ii) matching the matrix of standards with that of the sample

iii) solvent extraction to remove the metal to be determined from the interfering matrix. The principle of this method is that the metal, after being complexed with a chelating agent, is extracted into an organic solvent. Thus the extraction of

a metal-diethyl dithocarbamate complex into methyl isobutyl ketone (MIBK) is widely used for separation of metal ions from the matrix. The effective solvents for use in AAS are of medium molecular weight, such as volatile oxygen-containing aliphatics, with low viscosity and surface tension. Frequently used solvents are MIBK and ethyl propionate.

. The chlorinated solvents are not suitable for use due to the formation of toxic gases such as phosgene in the flame (20).

iv) ion exchange. Anion and cation exchange resins have limited usage for analytical separation of trace metal from the matrix, because of their lack of selectivity (20). However, Chelex-100 has been used to remove ionic metal forms from natural water matrices through chelation as follows (21):-

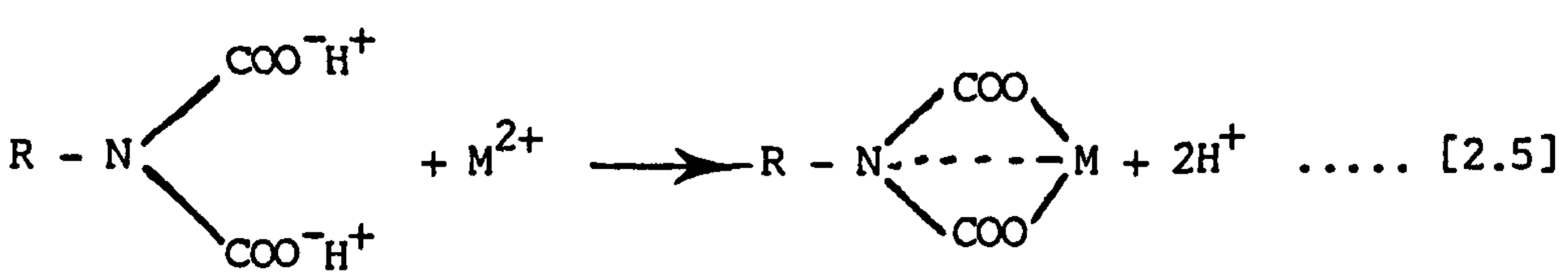

..... [2.5]

Where R = styrene-divinyl benzene copolymer matrix.

Ion-exchange and solvent extraction methods have been used for pre-concentration of trace metals (in addition to removal of metal ions from the matrix), thus the sensitivity of the analytical technique used for the examination of samples can be increased.

v) metals, where appropriate, are separated from the matrices by conversion to volatile hydrides (22,23) or co-precipitation (20).

A major disadvantage of FAAS is that the sample vapour always contains molecular species in addition to analyte atoms. These species

may interfere with the metal to be measured (24). Interference effects in FAAS may be divided into six main headings (20). Table 2.1 lists the type of interference effect, the interference problem caused and the amelioration of the problem in FAAS.

Many reviews have been published on FAAS and its uses in the trace determination of metals in natural samples (25,26). There are many applications of FAAS in agriculture, pollution, food, petroleum and other areas (27).

Table 2.1 : Selected Approach for Avoiding Interference Effects in FAAS

Type of Interference Effects	Interference Problem	Solution
1. Spectral	Two metals, one effect on other due to close proximity of resonance wavelengths	Choose an alternative absorption line
2. Emission	Emission and absorption at the same wavelength	Increase the source current, close down the slit
3. Chemical	Anything which prevents formation of ground state atom in flame	i) Chelate the metal ion with EDTA and leave the anion unassociated ii) Add releasing agent such as $La(NO_3)_3$ iii) Use high temperature flames such as $(N_2O + C_2H_2)$
4. Matrix	Samples and standard are different matrices	i) Remove the metal ion to be determined from matrix by solvent extraction ii) Use standard addition
5. Non-specific	Due to presence of dried particles in the flame which both scatter and absorb the incident radiation from the source	i) Use deuterium background correction ii) Use solvent extraction to remove metal ion

Table 2.1 continued

Type of Interference	Interference Problem	Solution
6. Ionisation	The problem arises from the energetic nature of the flame which gives both ground state atom and ionic state	Add ionised salt such as KCl (or more easily ionised salt) to produce free electron to react with ionised state and convert to free atom

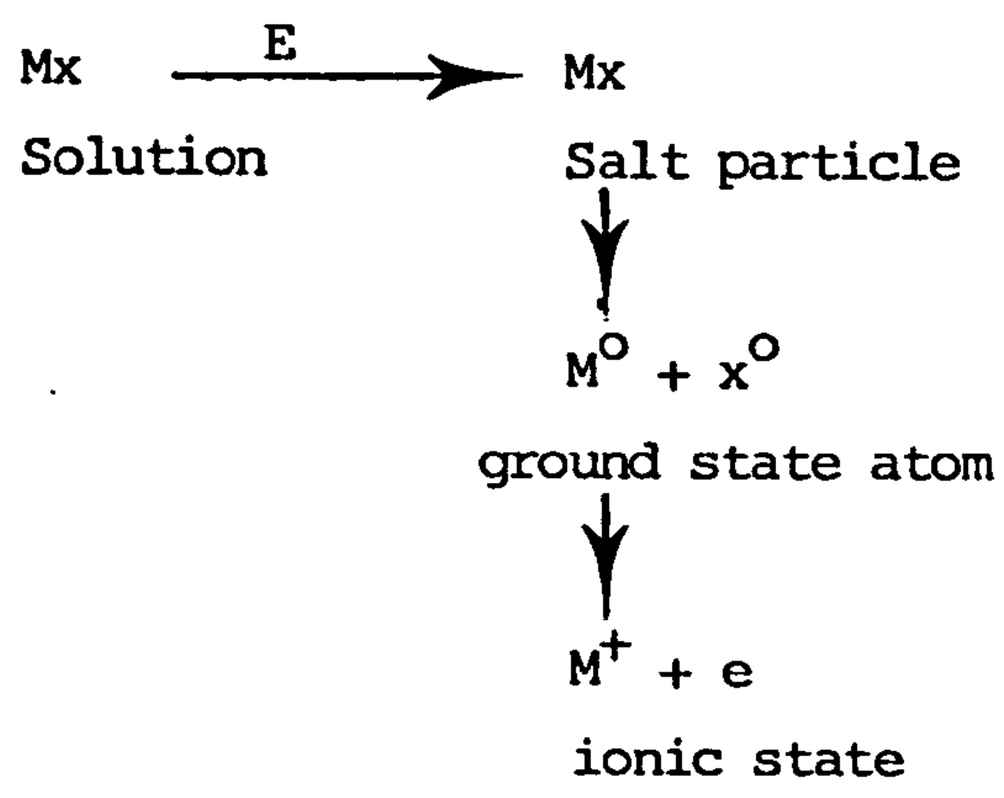

b) Atom Trap Flame Atomic Absorption Spectrometry

The technique involves collection of free atoms in the flame on a water-cooled silica tube or tubes. Upon aspiration of sample solution, analyte atoms are condensed on the tube for the time required to build up a measurable concentration to give an atomic absorption signal. They are released by shutting off the water and allowing the silica tube to be heated in the flame (28). This technique is shown diagrammatically in Figure 2.4. It has been used in different flames (29) and applied to determine extractable metal in soils (30). The mechanisms of collection and release of elements in this technique were examined by Khalighie et alia (31). Aluminium has a significant effect on the collection of atoms on silica tubes. This enhancement in the signal for copper has been observed when aluminium was added to the copper solution and then aspirated in the flame (32). The enhancement may be due to the formation of aluminium oxide which coated the tube and increased the active surface area for atom trapping.

Although the technique is more sensitive than FAAS (28), it needs more attention to adjust the silica tube or tubes in the beam of light from the source. The major problem with this technique is the scattering of light by the silica tube. This scattering interferes with the atomic absorption signal.

c) Flameless Atomic Absorption Spectrometry

The principle of this technique is quite simple, an electrically heated tubular furnace, shown diagrammatically in Figure 2.5, is placed in the beam of an HCL. The tube is protected from atmospheric oxidation by a stream of inert gas (33). The graphite tube atomisers (GTA) are the most widely used for production of atom vapours in commercially available flameless spectrometers. For atomisation the parameters of

FIG. 2.4 ATOM TRAP AND COOLING SYSTEM

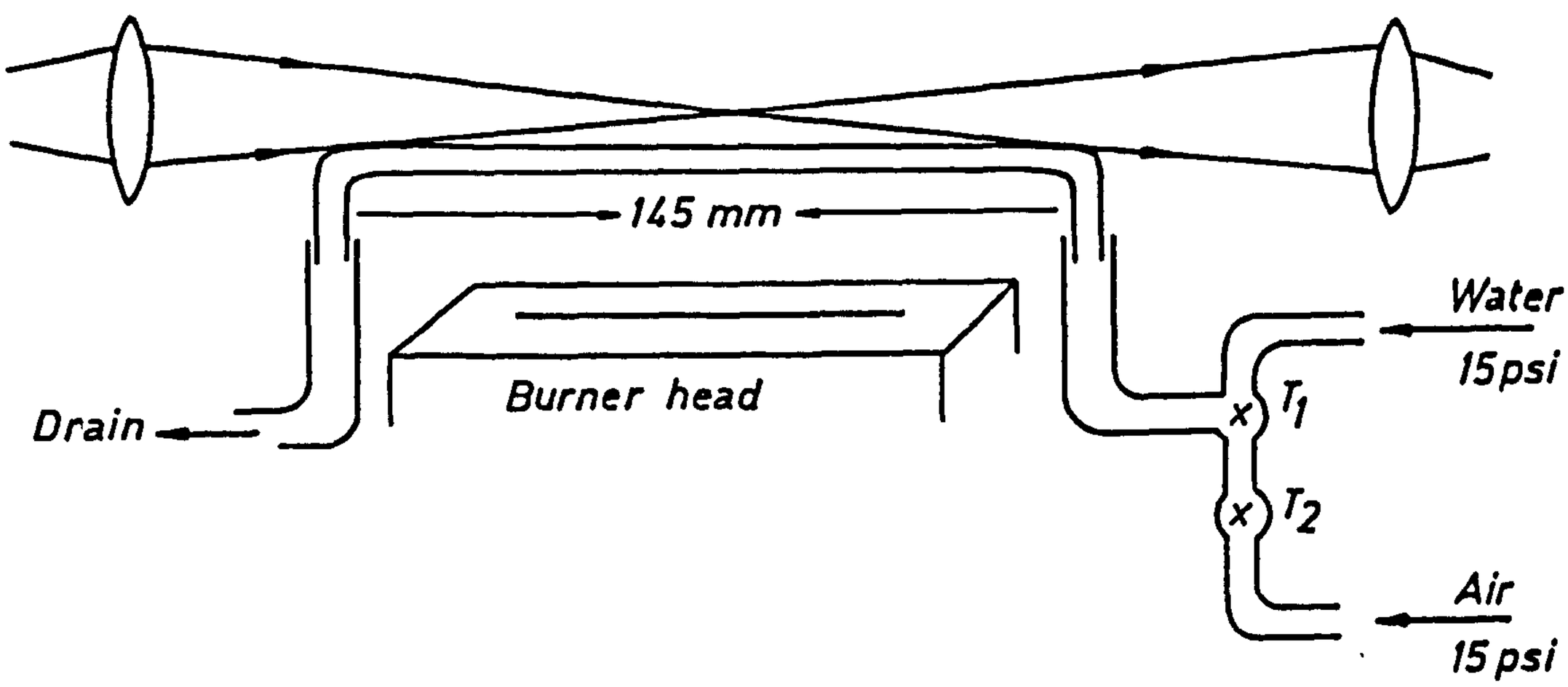

FIG. 2.5 GRAPHITE FURNACE ATOMIC ABSORPTION SPECTROMETER

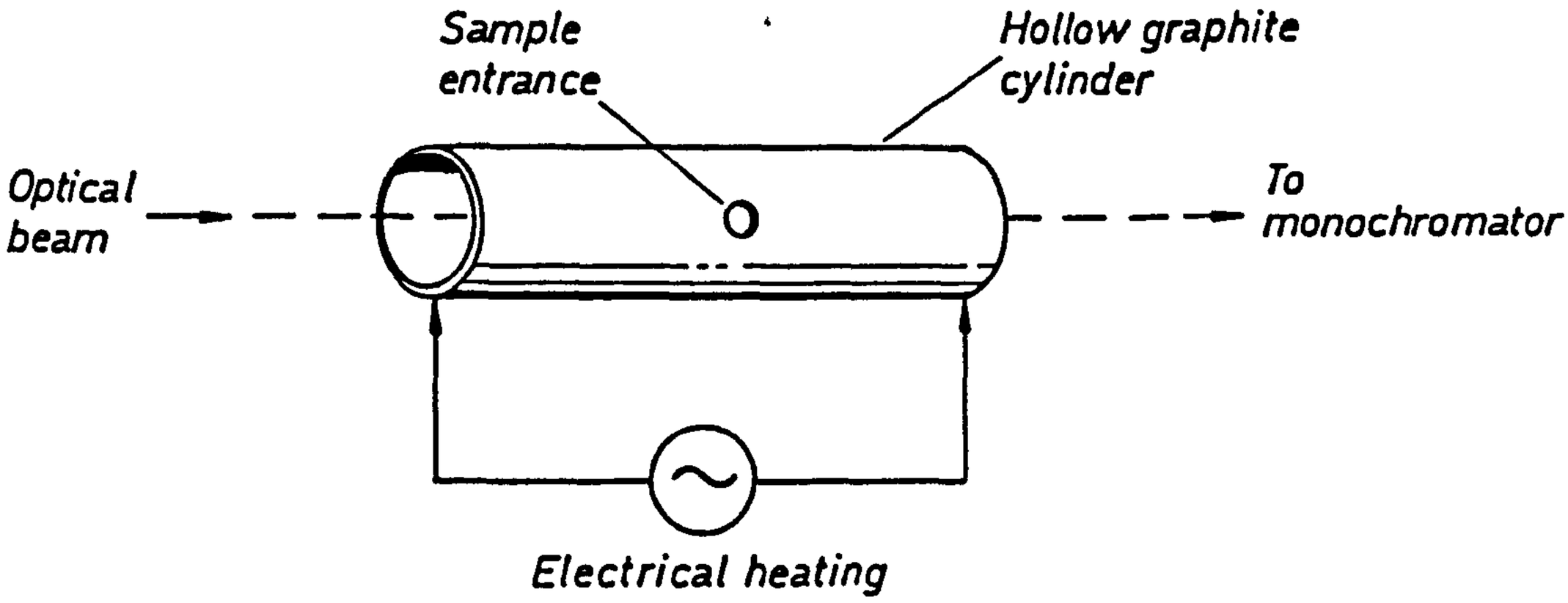

heating programmes and the type and flow rate of inert gas need to be determined for the maximum AA signal in flameless atomisation (33). The resultant signal is a sharp narrow peak for volatile metals, while the peak height is the most widely accepted method for evaluating flameless signals.

Very recently a technique has been described for coating graphite tubes with pyrolytic material which increases the sensitivity of the technique (34). The coated materials have low permeability to gases, high thermal conductivity, high resistance, high sublimation point and small coefficient of thermal expansion (35).

The mechanisms of atom formation in graphite furnace atomic absorption spectrometry (GFAAS) are either reduction of metal oxide by carbon with subsequent sublimation of the metal or vaporisation of the oxide and thermal decomposition of oxide in the gas phase (12,36,37) as follows :-

$$MO_{(g)} + C \xrightarrow{\text{Reduction}} M_{(g)} + CO_{(g)} \quad \ldots\ldots\ldots \quad [2.7]$$

$$MO_{(s)} \xrightarrow{\text{Dissociation}} MO_{(g)} \longrightarrow M_{(g)} \quad \ldots\ldots\ldots \quad [2.8]$$

The disadvantage of the graphite tube system is that hot gases pass quite easily through the wall so that losses of atomic vapour can occur. To avoid this problem, the graphite tube is impregnated with carbide forming elements such as Si, Ti, V and U. By firing at high temperatures, the metal forms the respective metal carbide layer which prevents the permeation of atomic vapour (33) through the wall of the tube.

Many workers (33,38,39) have tried to improve the production of free atoms in graphite tubes either by inserting metal foil liners inside the tube or using tubes made of high melting point metals such as Ta, W, Mo, Pt.

Although background effects are a major source of error in GFAAS, there are other interference effects which can cause problems. They are physical, chemical and spectral. Table 2.2 illustrates the mechanism by which they are produced (12,33,40,41). The technique of "Matrix modification" has been successfully employed in many cases to overcome the chemical interference effects (12). In this technique, a reagent is added to the sample (in the graphite tube) which enables a more effective ashing procedure to be used. The addition is designed to either decrease the volatility of a normally volatile element or to increase the volatility of a matrix (41). For example, ammonium phosphate is used as matrix modifier in the determination of silver in samples (42). The phosphate ion holds the silver ion and prevents the loss of silver during the ashing period. The well proven example of removal of a relatively involatile matrix is that of removing sodium chloride from sea water and other chloride-containing matrices. This can be successfully done to a large degree by addition of 50% ammonium nitrate solution which converts the chloride to nitrate (12). The nitrate compounds have lower boiling points than chloride compounds and thus they are removed at the ashing stage (41). The mechanism of this method is shown below :-

$$NaCl + NH_4NO_3 \longrightarrow NaNO_3 + NH_4Cl \quad \ldots\ldots [2.6]$$

Boiling point	1413°C	210°C decomposes	380°C decomposes	335°C sublimes

A platform made of pyrolytic graphite within furnace tube has been studied in recent years to overcome the vapour-phase interferences (43). The platform works in the following way. As the furnace wall rises in temperature, the actual temperature of the platform is lower than the walls. When the sample finally vaporises, the atmosphere within the

furnace has reached a more isothermal and hotter temperature than the platform. During the vaporisation of the sample, the temperature in the platform furnace tube is in the following order (41) :-

tube wall > atmosphere > platform

Such an order indicates that sample vapour does not meet any cool phase, thus condensation will not occur with this technique and is the great advantage of the platform furnace tube system. The graphite tubes with platform, probe or microboat systems have been studied by several groups of workers (44-47). From these studies, it is clear that there is a difference in peak height absorbance recorded for the metal in the three systems. The differences may be due partly to the differences in the thickness of the platform, probe and microboat, which results in different vaporising rates, and partly to the difference in their effective areas (which are heated) and hence the shape factor. The major disadvantages of the graphite tubes with platform, probe or microboat systems, is that they cannot be used with severely refractory elements like Mo, Pt or Ti due to the atomisation temperature of these elements being too close to the maximum temperature of the furnace.

Flameless atomic absorption spectrophotometry has tended to replace FAAS due to the high sensitivity and low sample size. Table 2.3 offers a comparison between flame and graphite furnaces as atomisers (48).

Table 2.2 : Selected Approach for Avoiding Interference Effects in GFAAS

Type of Interference Effect	Interference Problem	Solution
1. Physical It may result from different behaviour of sample in the atomiser during the dry stage of sample due to the surface tension, viscosity, volatility or volume of sample	Different response will be obtained from same injected volume of the same concentration of metal, i.e. results are irreproducible with low precision and accuracy	i) Match physical properties of sample to that of the standard ii) Use an automatic sampling to inject the mixed varying volumes of standard or sample with the blank to give the same total volume of solution. This procedure eliminates variation in the amount of spreading between samples of different volume. iii) Dilute viscous samples with a suitable solvent to reduce the irreproducibility in the result.
2. Spectral	i) Large concentrations of matrix vaporised during the atomisation stage and can cause scattering of the incident light beam ii) Molecular species which vaporise during the atomisation stage can cause molecular absorption by their band structure	i) Use a long ashing period to eliminate matrix vaporisation during the atomisation stage ii) Use background-correction technique to eliminate molecular absorption

Table 2.2 continued

Type of Interference Effects	Interference Problem	Solution
3. Chemical		
It may result either from a matrix component which can chemically combine with the metal, altering the ground state atom population within the absorption or from reactions taking place in the graphite tubes prior to, and during, the atomisation stage of a furnace cycle. This type of interference effects originate from:-	Changes in the sensitivity of the method and high error in the accuracy of measurement	
i) pyrolysis loss	Metal may be present in the sample in volatile form at pyrolysis temperature employed	Add matrix modifier reagent to decrease the volatility of normally volatile compound
ii) condensation	When the atomised metal leaves the hot surface of an atomiser, it is transported into a much cooler region where condensation of atomic species can occur	Use platform technique
iii) carbide formation	Formation of stable carbide which prevents formation of the atom population	Use pyrolytically coated tubes
iv) nitride formation	When nitrogen is used as an inert gas, some metal may form stable nitrides and so reduce the analytical sensitivity	Use argon as inert gas
v) memory effect	Incomplete atomisation of a metal causes an enhancement in subsequent analytical determinations	Use higher atomisation temperatures or long atomisation time

Table 2.3 : Comparison between FAAS and GFAAS

FAAS	GFAAS
1. Continuous atomisation	1. Discrete, transient atomisation
2. Requires 5 cm^3 sample	2. Requires 10-20 μl
3. A small proportion of sample is measured (2-10%)	3. Total mass response
4. Low solid compatibility, slurries may be atomised	4. Compatible with solid samples
5. Sample heated by gas from from flame	5. Sample heated by graphite tube wall and gas
6. Temperature of flame is different according to gas and mixture	6. Temperature is programmed from ambient to 3000 ^{o}C at variable heating rates and steps
7. Background interference low	7. Background interference high

2.2.2 Atomic Emission Spectrometry (AES)

Atomic emission involves the measurement of the radiation emitted when an excited atom loses energy and returns to the ground state (6,9). Generally samples are excited in arcs and sparks. occasionally in flames, but increasingly plasmas are being used (27).

In the last decade analytical chemists have chosen plasmas as energy sources for trace metal determinations due to the greatly increased detection limits. Table 2.4 gives the detection limits for different plasma sources compared with FAAS and GFAAS. Furthermore, plasmas have been chosen due to :-

i) low interference effects

ii) simultaneous multi-element determination

iii) suitability for a large number of samples

iv) small volumes of sample are needed

v) the high temperature of plasma results in wide applicability

Table 2.4 : Comparison of Detection Limits ($\mu g/L$) of Flame, Flameless and Plasma for Metals

Metal	[a]FAAS (73)	[a]FAAS (49)	[a]FAES (59)	GFAAS (73)	GFAAS (49)	ICP (73)	DCP (68)	MIP (52)
Al	25	20	8	0.01	0.01	10	1	50
Ag	1.2	2	5	0.001	0.001	3	2	1
Pb	9	20	0.1	0.007	0.007	25	5	1
Cu	1.8	2	0.01	0.005	0.005	1	1	1
Zn	1.2	0.6	50	0.001	0.001	2	1	1
Cd	1	1	0.8	0.0002	0.0002	1.5	5	0.6
Fe	5	5	0.03	0.01	0.01	2	2	10
Ca	2	1	0.0001	0.01	1	0.2	0.1	1
Mn	0.3	3	0.0005	0.0002	0.0005	0.1	0.1	1
La	2000	1	1	0.5	1	2	1	1
Tl	30	1	0.2	0.01	1	27	1	1

a = nitrous oxide - acetylene flame

FAES = flame atomic emission

for the determinations of elements in the Periodic Table (49). The plasma is a gas in which a significant proportion of the population of atoms or molecules are in an ionised state (50). There are three sources of plasma generation, namely :

(1) inductively-coupled plasma (51)

(2) direct-current plasma (51)

(3) microwave plasma (52).

The ICP is the favoured form of plasma because of its stability and the higher operating temperature (27). The microwave plasma is produced by the interaction of a microwave frequency (usually 2450 MHz) electrical field with gases such as Ar, N_2 or He (52). Two general types of microwave frequency have been used to produce microwave plasmas (52). In one, the microwave energy is generated from a magnetron and conducted through a coaxial wave-guide to the top of a coaxial (conductive) electrode which is used to form plasma at the electrode. This type of source is used to generate a plasma called the coupled microwave plasma (CMP) system. Another system which is electrodeless is known as microwave induced plasma (MIP) system, shown diagrammatically in Figure 2.6 (53). In the latter system, the microwave energy is coupled to the gas stream contained in a quartz tube (non-conductive) within an external cavity (53). The high sensitivity and selectivity of the combination of GLC-MIP has led to its use for the determination of organometallic compounds in the environment (52,53).

FIG. 2.6 MIP SOURCE FOR ELEMENTAL EMISSION SPECTROSCOPY

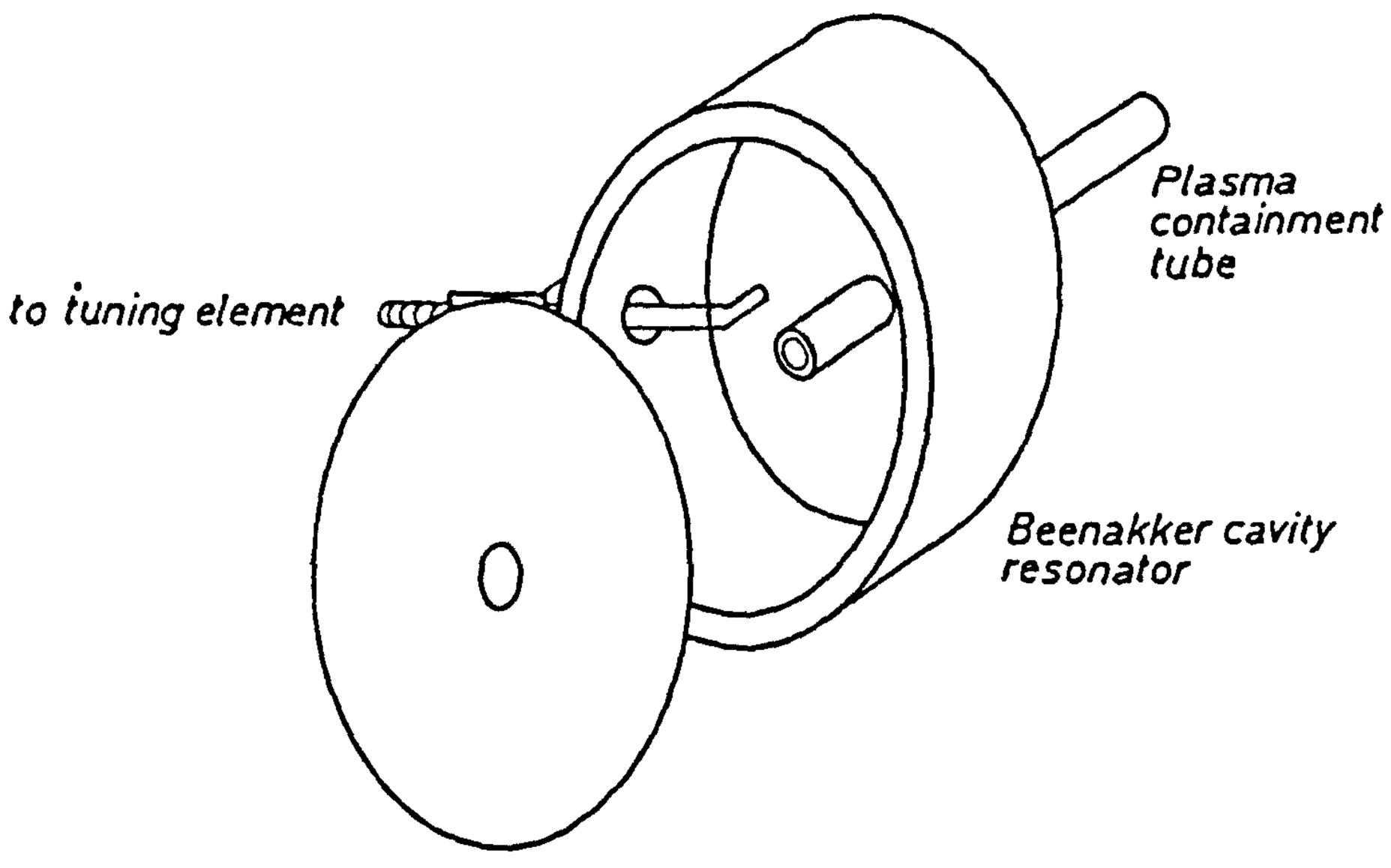

a) Inductively Coupled Plasma (ICP)

An ICP torch is shown diagrammatically in Figure 2.7, it consists of three concentric quartz tubes and an induction coil. The argon is supplied to the quartz tubes in three capacities as the coolant, auxiliary and nebuliser flow (54). The induction coil is connected to a high frequency generator operating typically in the 40 to 50 MHz range to generate output levels between 2-5 KW (54). Argon gas is introduced to the tube so that it swirls around before reaching the induction coil. At this point the gas experiences the oscillating magnetic fields generated at the coil whose line of force is axially oriented inside the quartz tube and follows elliptical close path outside the coil (55). The ionisation of argon has to be initiated electrically from an external source e.g. the Tesla coil. The ionisation process produces a few ions to "seed" the process. The ions formed are then accelerated in alternative directions with each change in the magnetic field (52). The accelerated electrons and ions meet resistance to their flow, heating and additional ionisation occurs. This step leads to formation of the plasma. The temperature of an ICP is in the range 7000-10000^{o}K. It can be maintained indirectly via inductive heating of the gas by means of the electromagnetic field established using the power generated at radio frequencies (54). The actual shape of the plasma produced depends upon the argon flow rates which are in the range 10-13 L min^{-1}, 0-1 L min^{-1} and 0.5-1 L min^{-1} for the coolant, auxiliary and nebuliser respectively (56). At higher coolant flows around 15 L min^{-1} the plasma becomes more elongated and may tend back towards the torch and cause severe damage. The auxiliary flow has the effect of pushing the discharge away from the nebuliser tip to prevent heat damage occurring. At low frequencies, less than 10 MHz, the plasma appears as a "teardrop" with the hottest region at

FIG. 2.7 ICP SOURCE FOR ELEMENTAL EMISSION SPECTROSCOPY

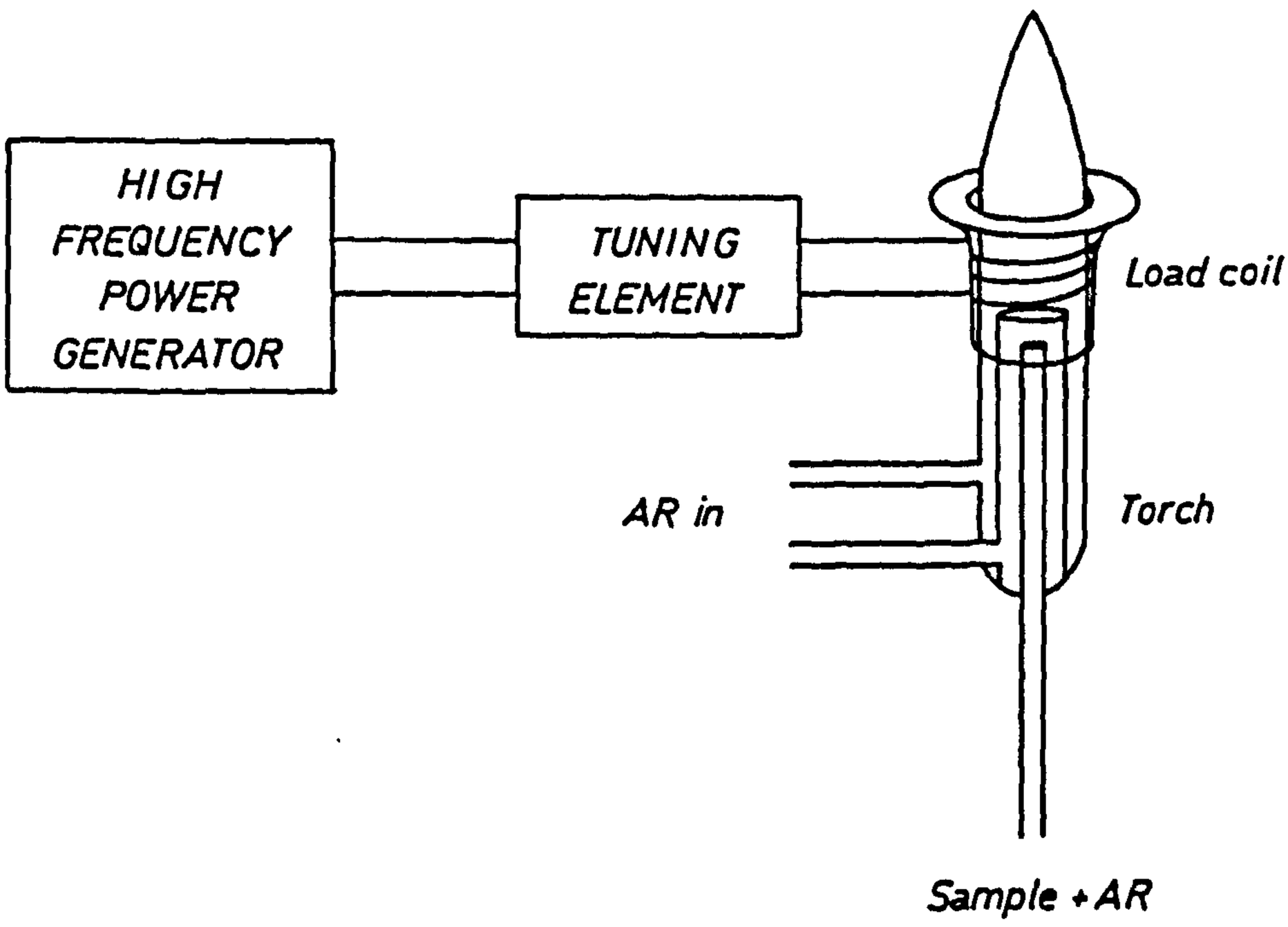

the centre of the plasma. However, at higher frequency, around 30 MHz, the plasma appears as a "doughnut" shape also containing the highest temperature while a slightly cooler region is held at the centre (55).

ICP has mainly been used as a source of excitation for simultaneous multi-element determination with atomic emission spectrometry (57-59). Figure 2.8 illustrates ICP as excitation source for atomic emission spectrometry (49). In addition to those uses mentioned above, ICP has been employed with :-

i) atomic fluorescence spectrometry (60)

ii) chromatographic technique as an element-selective detector (53,61).

Although the mass spectrometer using principally spark sources has been used for the determination of elemental composition for solids and sediments, the procedure is tedious and requires careful calculation (62). The mass spectrometer has also been used for trace metal determination when connected to other analytical techniques (63). When connected with ICP, the technique of inductively coupled plasma mass spectrometer (ICP/MS) is produced. The principles of this technique are extraction of ions from an ICP into the mass spectrometer (64), i.e. the sample is rapidly dissociated and ionised in the plasma. The resulting ions are then admitted through a very narrow aperture into the vacuum system of a quadrupole mass spectrometer, where the mass spectrum of the ions is obtained (65). Although ICP/MS is a combination of two existing analytical systems which is designed to utilise the advantage of both, it has many problems. The major problem is the formation of a cool boundary layer of molecular ions, such as oxides between the plasma and the orifice to mass spectrometer which removes the opportunity of ion formation, so decreasing the sensitivity (66,67).

FIG. 2.8 INDUCTIVELY COUPLED PLASMA EMISSION SPECTROMETER

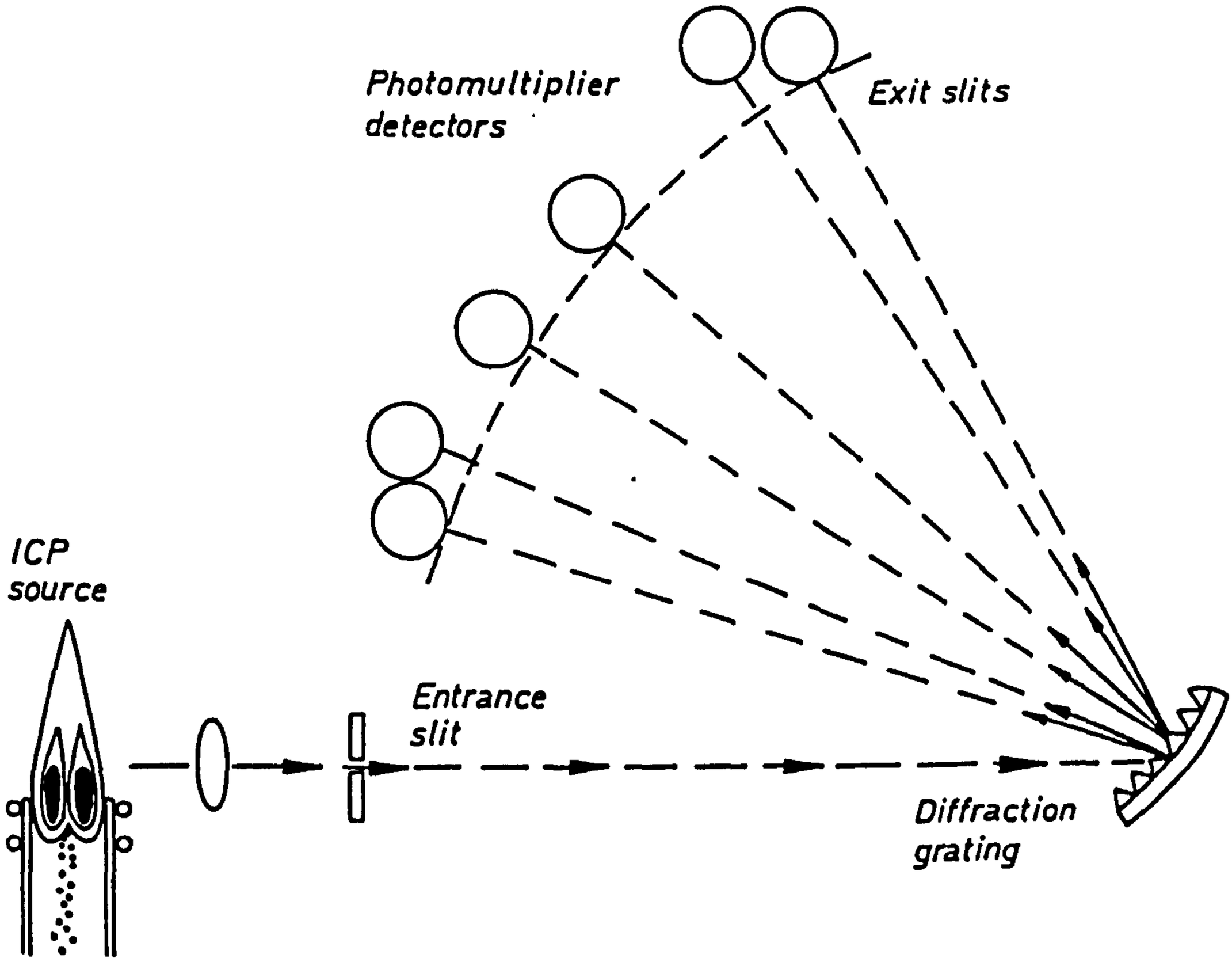

b) Direct Current Plasma (Dcp)

The Dcp has been operated in several forms as an excitation source; the major Dcp source used at present is illustrated in Figure 2.9. It consists of two graphite carbon anodes and a tungsten cathode in an inverted Y-configuration (68).

Greenfield et alia (51) connected a thoriated tungsten rod to tungsten to act as a stabiliser electrode. In Dcp, a flow of argon gas is required for each electrode and the nebuliser. The energy necessary to generate the plasma is produced by a high current electric arc burning at 500 amp and at a potential of 40 volts DC current between the electrodes. In these conditions the arc temperature is about 6000^{o}K and results from collision between electrons accelerated in the electromagnetic field of the discharge and atoms or molecules of argon in the discharge (69). The plasma is maintained directly by an electrical discharge through the argon gas (53).

Dcp has been used in elemental analysis in the emission mode (70,71) and as a coupled system with mass spectrometry (72).

2.2.3 X-Ray Spectrometry

In this technique, the sample is bombarded with a beam of photons from an X-ray source. When the beam of X-rays interact with the sample, the X-ray beam is attenuated and a decrease in the intensity of the incident beam of X-ray can occur (74). However, provided that the X-ray photons have sufficient energy, on interaction they eject an electron from an inner but appropriate atomic level of element to a higher and more excited state (74,75). X-ray fluorescence (XRF) involves the measurement of the intensity of an emitted X-ray from the sample due to the movement of an electron into the vacancy (76,77). When the sample contains several elements the X-ray fluorescence spectrum

FIG. 2.9 Dcp SOURCE FOR ELEMENTAL EMISSION SPECTROSCOPY

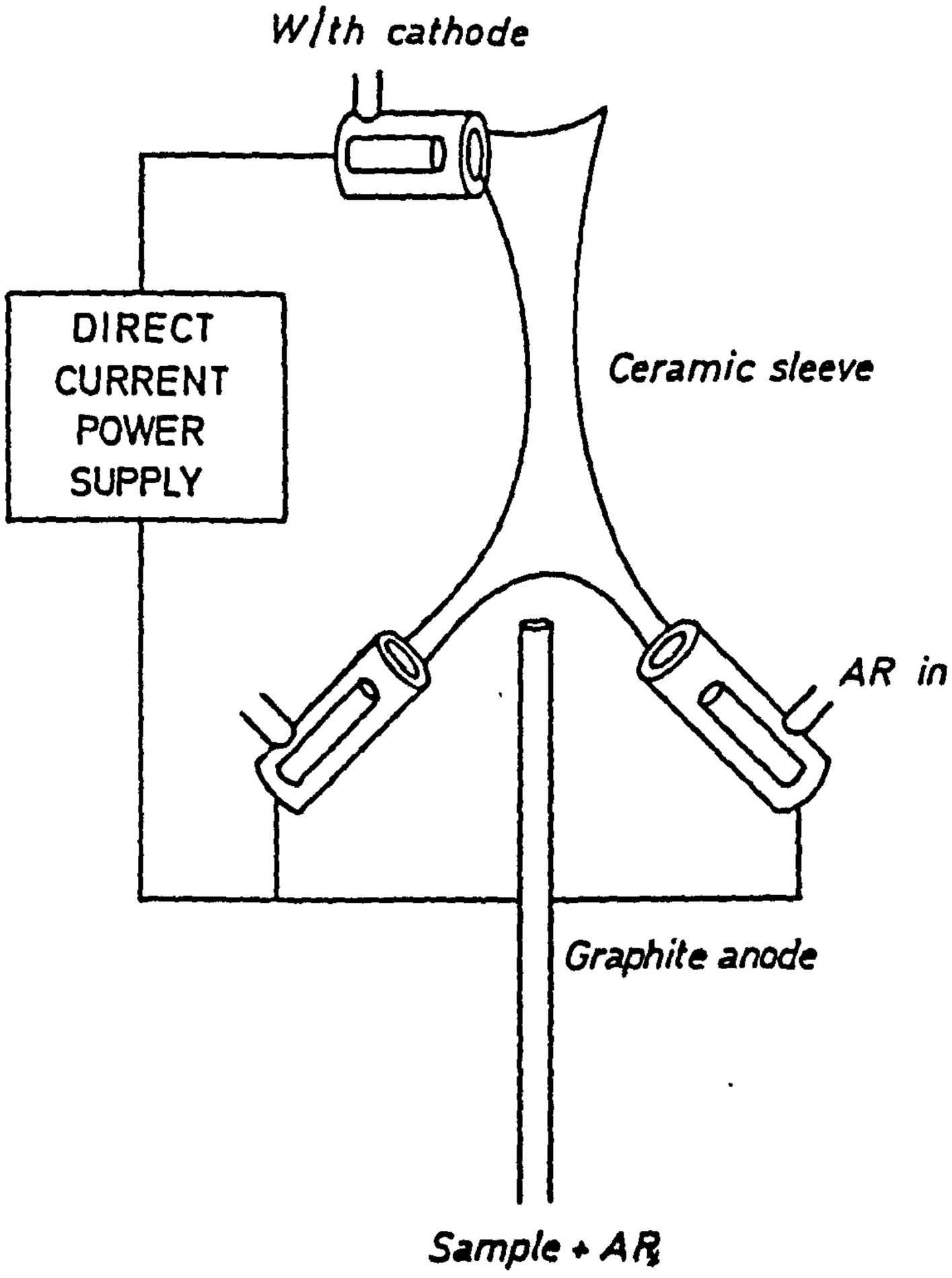

exhibits several peaks. The frequency of the peak is characteristic of the elements present while the intensities indicate the concentration. The intensity is affected by various factors such as the target material, target angle, sample matrix, tube focus and tube window (78). Figure 2.10 illustrates diagrammatically XRF spectrometer. XRF is a very suitable technique for both major and trace element determination of a wide range of geological materials (79,80) requiring only relatively simple sample preparation, although calibration is lengthy and tedious. The preparation of what are essentially solid samples requires care and much attention to detail. The electron-probe microanalysis (EPMA) consists essentially a focussed beam of electrons to produce the X-ray fluorescence spectra of the element in the sample but in an area as small as one micron in diameter on the sample surface. Thus the purpose of the technique is to measure local variations in composition rather than the average composition of the whole sample (76,81). EPMA is not a sensitive technique for determination of trace metals, however, when coupled with electron microscopy it has been used to study the release of Zn, Ca, Ba, Cu Pb from Fe-Mn oxide phases on treatment with hydroxylamine hydrochloride (82).

The major advantage of X-ray spectrometry is that it may be used for multichannel quantitative and qualitative determination of metals and is a non-destructive technique. Additionally, the costs of X-ray spectrometry are high in terms of instrumentation cost while the sensitivity and detection limits are not as good as in atomic spectroscopy.

FIG. 2.10 GEOMETRY OF A PLANE-CRYSTAL X-RAY FLUORESCENCE SPECTROMETER

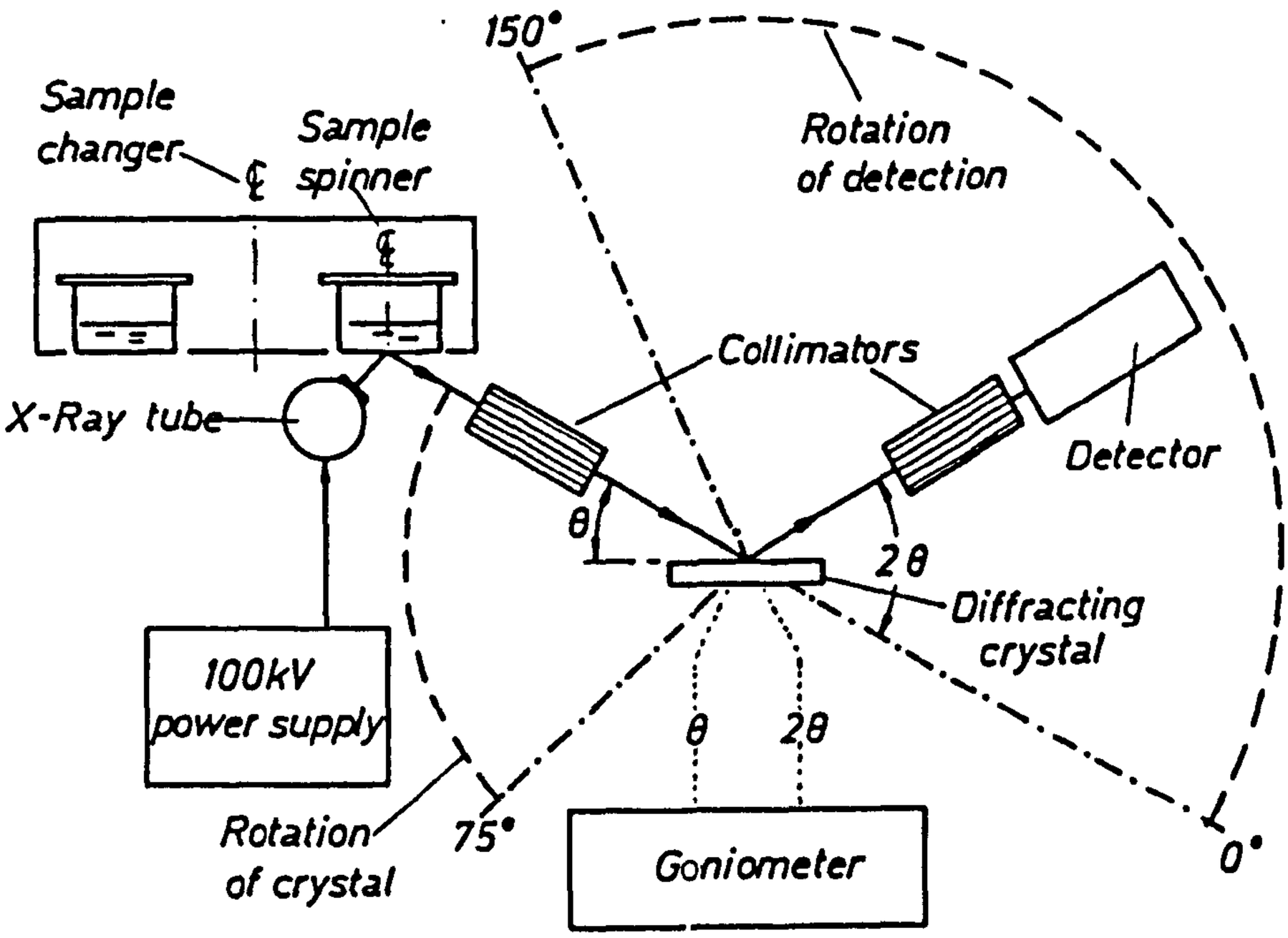

2.2.4 Electroanalytical Techniques

These techniques depend upon the exploitation of the current-voltage relationships to determine the concentration of electroactive species in solution. Advances in modern electronics which allow the measurement of current and voltage at low levels have led to significant advances in the sensitivity of these techniques. Determination of most components in solution that can be electrochemically oxidised or reduced are now possible. Most metal ions are reduced at some form of mercury cathode to form an amalgam with the mercury.

a) Polarography

The principles of polarography were established around 1925 by Heyrovsky and formed the basis for the instrumental method (83). In polarographic methods, under the influence of a potential applied to usually the dropping mercury electrode, ions in the sample solution will tend to be reduced at the surface of the electrode, which results in an increase in the current. The potential at which the current reaches half the limiting diffusion value defines so-called "half-wave potential" which is quite characteristic of the nature of ionic species undergoing reaction at the surface of the mercury drop electrode (83, 84). The current-potential relationship is described by the Nernst equation (84) as follows :

$$E = E^{O} + \frac{RT}{nF} \ln \left(\frac{i_d - i}{i}\right) \left(\frac{D_R}{D_O}\right)^{\frac{1}{2}} \quad \ldots\ldots\ldots \quad [2.7]$$

Where : i = current at potential E

i_d = limiting diffusion current

E^{O} = standard redox potential for the system

D_R and D_O = diffusion coefficients of reduced and oxidised forms of the electroactive species respectively

$\frac{RT}{F}$ = thermodynamic factor equal to 0.0592

n = number of electrons involved in the electrode reaction

The diffusion current at the mercury drop electrode (MDE) is affected by both the parameters of the DME and the properties of electroactive species in solution as shown in the Ilkovic equation (85).

$$i_d = 7.06 \times 10^3 \, n \, m^{\frac{2}{3}} \, t^{1/6} \, D^{\frac{1}{2}} \, C \qquad \ldots\ldots \qquad [2.8]$$

where : i_d = diffusion current (μA)

D = diffusion coefficient of reducible ion in solution (cm^2/s)

C = concentration of the reactant (mM/L)

m = mass of mercury flowing (mg/s)

t = drop time (s).

From the Ilkovic equation, clearly the diffusion current is directly proportional to the concentration and hence provides quantitative information about the reducible cations.

The migration current which is due to movement of charge and particles in electric field set up between MDE and reference electrode can be removed by addition of a large excess of an indifferent (inert) supporting electrolyte (84). The charging (or capacitance) current is caused by the changing potential on the mercury drop and is independent of concentration. This type of current represents noise in the current-voltage curve (86).

Polarography is always performed at the MDE, and when the input voltage used as DC voltage the technique was called direct current polarography (DCP). The DCP current represents a response which is a direct reflection of current variation during the lifetime of each mercury drop (87). DCP involves measurement of the diffusion current when an applied potential is changed by typically 100 mV min^{-1} in a

linear but negative direction from -0.1 to -1.80 volts w.r to Ag/AgCl. Due to the double layer formation at the MDE-solution interface by electrostatic attraction of cation and anion respectively, a significant background current is observed in the current-applied potential and the phenomenon effectively limits the sensitivity of DCP (84) which has a detection limit of around 10^{-5} M.

In normal pulse polarography (NPP), the MDE is held at initial potential until there are only about 60 millisecond (ms) left in the lifetime of an individual drop. The potential is then stepped to a new value and held there for the remainder of drop life. During the last 17 ms of the pulse the current is measured and plotted versus the applied potential (88). Since the charging current is allowed to decay before the measurement of Faradic current, the sensitivity is greater than DCP (83,84,87,88).

In differential pulse polarography (DPP), pulses of equal amplitude are superimposed on the linearly increasing ramp applied in DCP. The current is sampled twice during each drop lifetime; once just before and once at the end of the pulse period. The difference between these two current values is amplified and fed to recorder producing peak output (83). The sensitivity of differential pulse lies between that of DCP and NPP but is often preferred because DPP discriminates more effectively against charging current (87) (see Table 2.5).

Table 2.5 : Typical Sensitivity and Detection Limits for DCP, NPP and DPP

Technique	Sensitivity μA/mM	Detection Limit (M)
DCP	5	10^{-5}
NPP	30	10^{-6}
DPP	20	10^{-7}

b) Anodic Stripping Voltammetry (ASV)

The use of ASV has increased rapidly during the last few years due to its ability to simultaneously determine several metals at concentrations in the range $\mu g/L$ or less with relatively inexpensive instrumentation (89). In the ASV technique. the initial deposition potential is more negative than half wave of the most negative metal to be determined. All ASV measurements involve two discrete steps. The analyte, usually a metal, is reduced (electrodeposited) on the working electrode and then oxidised (stripped) back into the electrolyte solution (90) :

$$M^{n+} + ne^- \xrightarrow{Red} M(Hg) \quad \ldots\ldots \quad [2.9]$$

$$M(Hg) \xrightarrow{oxid} M^{n+} + ne^- \quad \ldots\ldots \quad [2.10]$$

In the reduction step, the metal is pre-concentrated from solution into an electrode of small volume (usually mercury) by formation of an amalgam. The oxidation step consists of the application of an anodic voltage scan to the electrode and the current-potential curve is recorded (89-93).

Oxygen is capable of dissolving in aqueous solution to the extent of forming millimolar solution at room temperature. Problems arise from both the voltammetric behaviour of oxygen and from the associated chemical reactions which take place, oxygen is reduced either to (94):

$$O_2 + 2H^+ + 2e^- \longrightarrow H_2O_2 \quad \ldots\ldots \quad [2.11]$$

acid media

$$O_2 + 2H_2O + 2e^- \longrightarrow H_2O_2 + 2OH^- \quad \ldots\ldots \quad [2.12]$$

neutral or alkaline media

$$E_{\frac{1}{2}} = -0.05 \text{ V vs SCE}$$

or

$$O_2 + 4H^+ + 4e^- \longrightarrow 2H_2O \quad \text{acid media} \qquad \ldots\ldots \qquad [2.13]$$

$$O_2 + 2H_2O + 4e^- \longrightarrow 4OH^- \quad \text{neutral or alkaline media} \qquad \ldots\ldots \qquad [2.14]$$

$E_{\frac{1}{2}}$ = -0.5 to -1.3 V vs SCE

Oxygen must, therefore, be removed by purging the analyte solution with pre-purified nitrogen, using an oxygen scrubbing system. Figure 2.11 illustrates a typical oxygen scrubbing system. The system contains vanadous chloride solution which is prepared from ammonium metavanadate and concentrated hydrochlorid acid. Amalgamated zinc is added to the solution to reduce the vanadium to the vanadous (+2) state. The nitrogen gas brings the solution into contact with the amalgamated zinc and causes the reduction to take place (94).

The electrodes used with differential pulse anodic stripping voltammetry (DPASV) are both the hanging mercury drop (HMDE) and various forms of thin film mercury electrodes (TFME). The static mercury drop electrode (SMDE), recently developed by EG & G Princeton Applied Research, utilises a method of drop formation in which the mercury drop is dispensed rapidly and then allowed to hang stationary at the capillary tip. The SMDE is shown diagrammatically in Figure 2.12, the electrode can be used in an MDE Mode for all forms of polarography but as an HMDE for DPASV (95). HMDE is the best working electrode for routine DPASV because of its extremely reproducible surface area. The DPASV using an HMDE is performed on one drop, that drop is then dislodged and a new drop is dispensed for the next experiment (90). The use of mercury is nearly an ideal choice for the operation of the working electrode for several reasons (86,95) :

FIG. 2.11 OXYGEN SCRUBBING SYSTEM

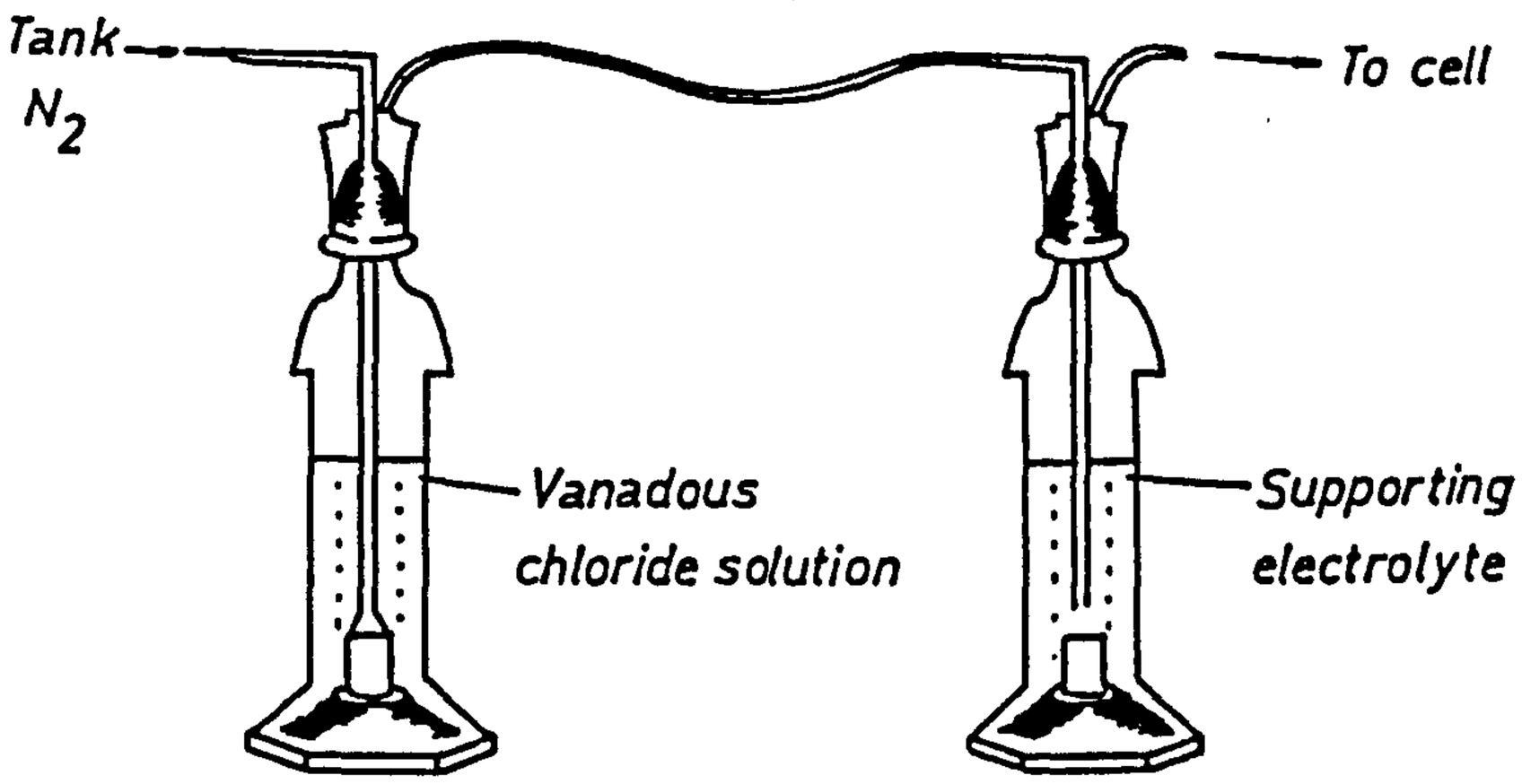

FIG. 2.12 EG & G PARC MODEL 303 STATIC MERCURY DROP ELECTRODE

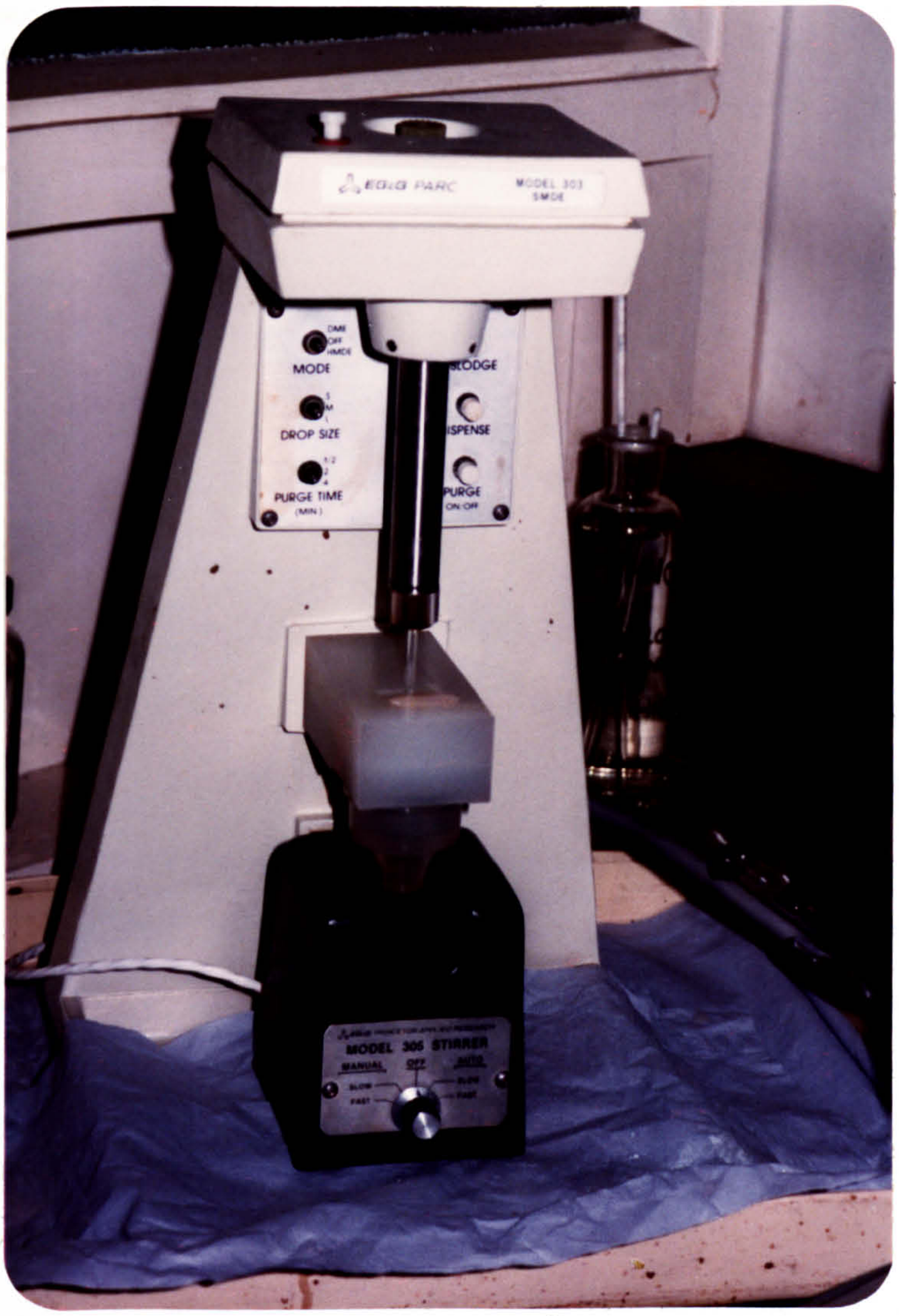

i) mercury has a large liquid range (-38.9 to 356.9°C at normal pressures) and therefore electrodes of various shapes may be easily prepared;

ii) the surface area of such electrode is highly uniform and reproducible (if the mercury is clean);

iii) the high hydrogen overvoltage of mercury allows the analyst to reach more negative potentials than any other metal before the reduction of hydrogen ion commences;

iv) mercury behaves as an inert electrode in most aqueous solutions.

The most important application of DPASV using an HMDE lies in the determination of trace metals in natural water samples (96-98), sea water (99,100), plankton (101), estuarine water (102,103) and bovine liver (104). The technique has provided the greatest amounts of information available concerning the speciation of heavy metals in sea water (105).

The disadvantages of the HMDE originate from :

1) mercury is a toxic material and the oxidation of mercury occurs at +0.4 V, preventing the determination of materials that are oxidised at more positive potentials (95).

2) interferences caused by intermetallic compound formation and overlapping stripping peaks have occurred (91). Table 2.6 lists some common interferences encountered DPASV measurements using HMDE in natural samples and the methods to avoid them (91).

In order to avoid some problems encountered with the HMDE, the TFME has been used with DPASV. The TFME are prepared by depositing a film of mercury onto solid electrodes such as gold, silver, platinum and carbon in different various forms. The noble metal solid electrodes exhibit a tendency to form intermetallic compounds, so various forms of carbon are often now used (90). These principal forms are glassy carbon,

wax-impregnated graphite (106), carbon paste (107) and the pyrolytic graphite electrodes (108). A TFME can be prepared on glassy carbon electrodes by one of the following methods :

i) placing a glassy carbon tip in a well-stirred solution of 1×10^{-5} M Hg^{2+} (as $Hg(NO_3)_2$) made slightly acidic with nitric acid and plating at -0.4 V ws SCE for 5 minutes (90);

ii) adding 1×10^{-5} M Hg^{2+} directly to the sample solution and allowing the deposition of mercury and the analyte to occur simultaneously (90).

Once the TFME is generated it must be protected from oxygen to prevent oxidation of the film. The use of the TFME should be limited to analyte concentrations less than 10^{-7} M due to the thinness (1-100 μm) and hence capacity of the deposited mercury layer (109). TFME using a rotating glassy carbon electrode is affected by the pH of supporting electrode (110,111), any organic compounds present (112), intermetallic formation (113) and surface active substance (114,115), so changing the current-potential curve.

Although deposited TFME on solid substrates avoids some limitations of the HMDE, it also suffers from disadvantages. Table 2.7 shows a comparison between HMDE and TFME using the DPASV mode (109,116). The major problems with the TFME which is deposited on rotating glassy carbon (RGC) electrodes are changes in the surface of solid substrate and the deposited film. These changes result in the irreproducible and often multiple or split stripping peaks (117,118). A Metrohm 628 rotating glassy carbon electrode is shown in Figure 2.13.

Table 2.6 : Selected Approaches for Avoiding Interference Effects in DPASV using HMDE

Measured Metal	Interference Problem	Solution
Tl in the presence of Pb and Cd	Overlapping peak	Add EDTA to mask Cd and Pb
Cu in the presence of Fe	Combined DPASV peaks	Subtract the iron peak measured at zero deposition time from the combined peak
Pb and Cd in sewage effluents	Irreproducible results due to sorption of organic matter on the electrode	Use ozone oxidation or UV irradiation to destroy organic matter
Zn in the presence of Cu	Cu-Zn intermetallic compound (poor precision and sensitivity)	Add Ga ions to combine with Cu
Cu in sea water	Reduced sensitivity due to the formation of $CuCl_2^-$ at the electrode	Acidify the sample to prevent the formation
Zn in the presence of Ni	Ni-Zn intermetallic compound (poor precision and sensitivity)	Use citrate to complex with Ni

FIG. 2.13 METROHM 628 ROTATING GLASSY CARBON ELECTRODE ASSEMBLY

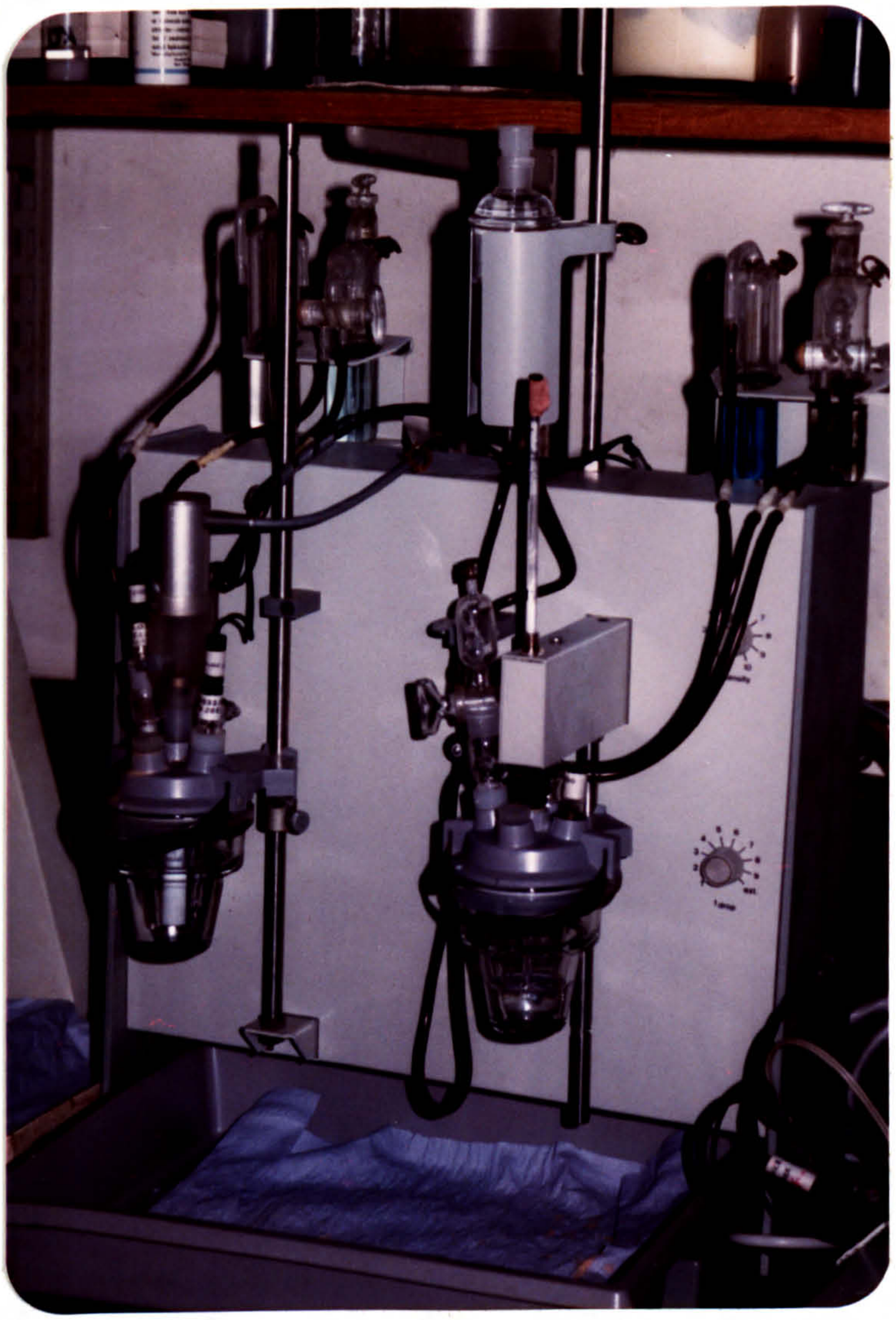

Table 2.7 : A Comparison between HMDE and TFME (on RGCE) using DPASV Mode

HMDE	TFME
(1) A low surface area to volume ratio	(1) A higher surface area to volume ratio
(2) Less sensitive	(2) More sensitive
(3) Interferences are less as a result of the greater volume of hanging drop which leads to lower intermetallic compound formation	(3) Interferences are more as a result of precipitation of metals with the mercury film on RGC
(4) Results are generally more reproducible at high concentrations	(4) Results are more reproducible at very low concentrations
(5) Voltammetric cell can be deoxygenated relatively fast	(5) Voltammetric cell can be deoxygenated relatively slowly
(6) Contamination of hanging drop occurs, but it can be removed by dislodging the drop. The capillary is then washed with diluted HNO_3	(6) No contamination problems
(7) Pure 100% mercury used as hanging drop and that is toxic and causes health hazard from its vapour	(7) Dilute mercury 1 x 10^{-5} M and use as thin film precursor
(8) It is not used with positive potentials due to oxidation of mercury at +0.4 V	(8) TFME is also not used but RGCE can be used
(9) Less time for analysis	(9) More time is required for analysis due to preparation of film and polishing the rotating glassy carbon surface
(10) Tl and Cd are better separated	(10) Tl and Cd are not separated
(11) Tl and Pb are not separated	(11) Tl and Pb are separated
(12) Stirring of the solution by magnetic bar	(12) Rotation of the electrode provides more reproducible stirring of solution than magnetic stirring bar system

2.2.5 Gas Chromatography of Metal Chelates

The application of gas chromatography to metal determination requires that the metal compounds which are usually ionic be converted to volatile compounds which can then be subjected to gas chromatographic separation and measurement (119). The formation of volatile compounds (metal chelates) is an important aspect of the analytical technique, it is necessary that the metal chelates be formed quantitatively, rapidly and also be easy to extract into organic solvents in order to facilitate introduction in gas chromatography.

The metal chelates of fluorinated β-diketones are suitable for determination in gas chromatography using the electron capture detector. Fluorinated β-diketones, unfluorinated β-diketones, β-thioketones and β-aminoketones can all form metallocycles with metal ions. The formation of metallocpmplexes is dependent upon the coordination number of the metal (120). The oxygen donor atom in such β-diketones reacts by complexation with 6-coordinate metallic elements to form cis and trans isomers of the corresponding metal chelates (120). The enolisation and subsequent ionisation of β-diketone is shown in Figure 2.14 (120). The enolate anion can form a 6-membered metallocycle with metals whose coordination number is twice their oxidation state. The enolate of many metals has six π-electrons available for delocalisation in a metallocyclic structure forming a theoretical analogy to the resonance stabilised six π-electron carbocycle benzene (120,121). Figure 2.15 gives the chemical structure of a metal hexafluoroacetylacetonate. The fluorinated β-diketones have low boiling points, i.e. they are volatile. The volatility of these ligands is a function of the degree of fluorination rather than that of the molecular weight. Table 2.8 lists the properties of some β-diketone compounds (122). A reduction in Van der Waals forces and a decrease in the intermolecular hydrogen

FIG. 2.14 MECHANISM OF ENOLISATION AND SUBSEQUENT IONISATION OF β-DIKETONES

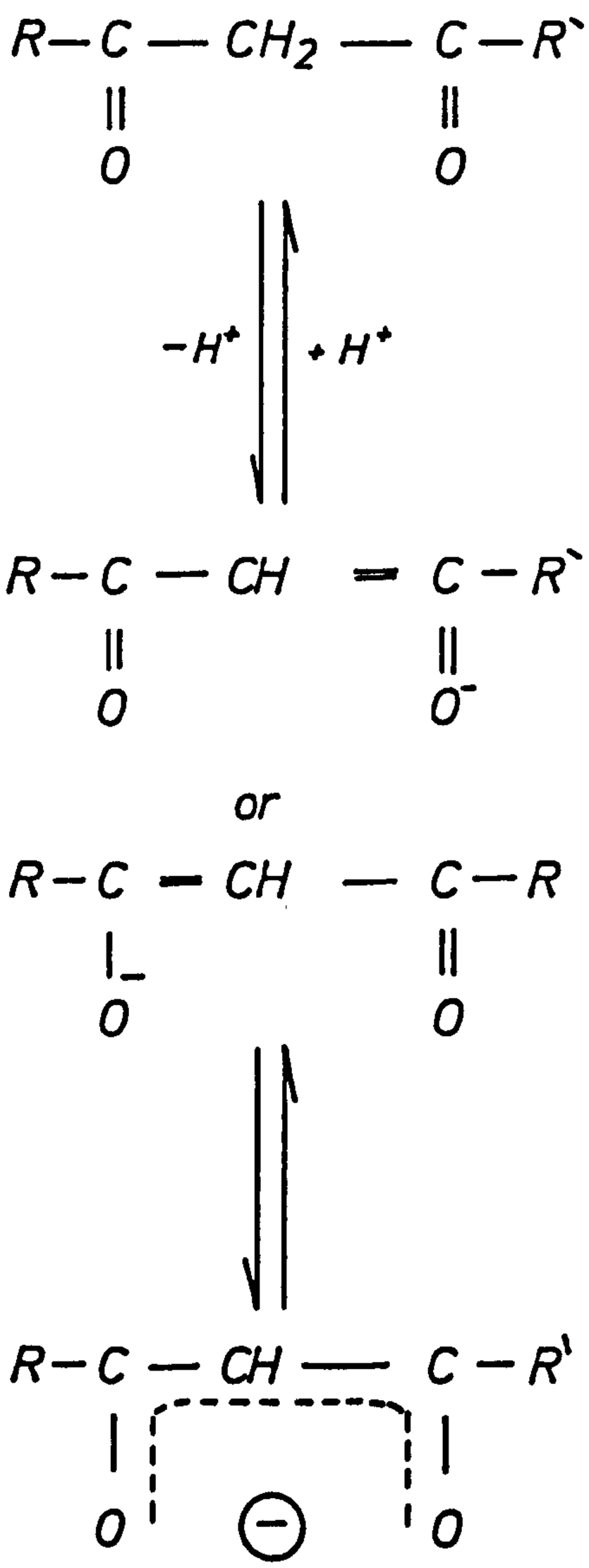

FIG. 2.15 CHEMICAL STRUCTURE OF METAL HEXAFLUOROACETYLACETONATE

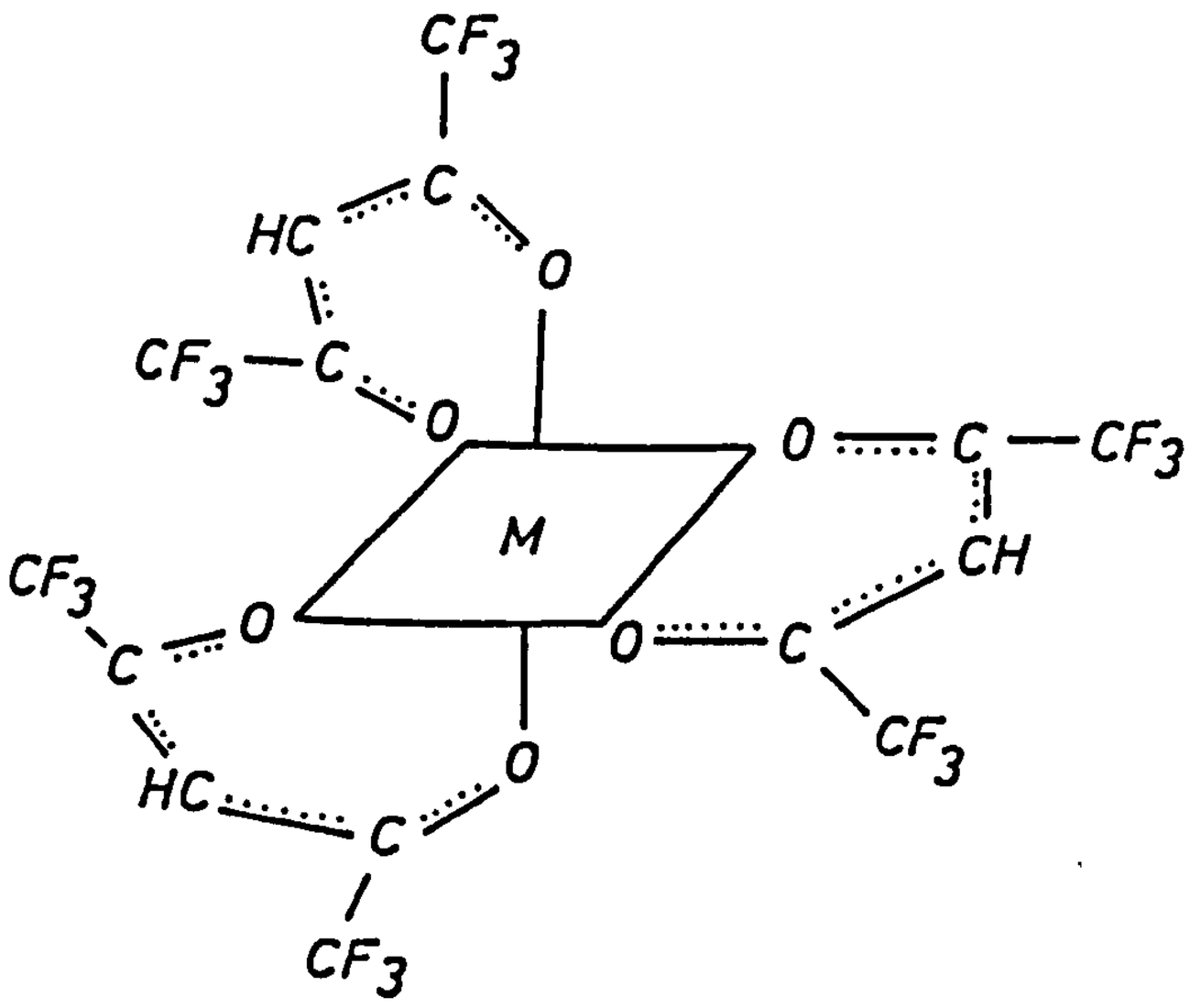

bonding have been offered as possible reasons for the increased volatility of fluorine containing chelates (122).

Table 2.8 : Properties of Some β-diketone Compounds

Ligand	Structural Formula	B. point ^{o}C	M. wt
Acetylacetone (AA)	$H_3C - \underset{\underset{O}{\|}}{C} - CH_2 - \underset{\underset{O}{\|}}{C} - CH_3$	137	100
1,1,1-trifluoro-acetylacetone (TFA)	$F_3C - \underset{\underset{O}{\|}}{C} - CH_2 - \underset{\underset{O}{\|}}{C} - CH_3$	104	154
1,1,1,5,5,5-Hexa-fluoroacetylacetone (HFA)	$F_3C - \underset{\underset{O}{\|}}{C} - CH_2 - \underset{\underset{O}{\|}}{C} - CF_3$	66	208

The determination of metal chelates by gas chromatography is dependent upon the choice of support, stationary phase and type of detector (120,121). The stability and polarity of the various metal β-diketones affects the choice of stationary phase to be made. The support must be as inert as possible. Most columns for metal determination are glass because they are very inert, cheap and can be used at higher operating temperatures than stainless steel because of the catalytic activity of the latter (121). TFA and HFA have been the most widely studied ligands in gas chromatography of metal chelates. Table 2.9 lists some of the reactions of TFA and HFA with different metals. Gas chromatography of TFA in conjunction with an electron capture detector (which is sensitive for halogenated compounds) lends itself particularly well to the determination of metals at ultra-trace

levels. Table 2.10 compares the detection limits obtained in the determination of aluminium, beryllium, chromium and rhodium by gas-liquid chromatography combined with solvent extraction and other methods of analysis (123).

Table 2.9 : Gas Chromatography of Metal Trifluoroacetylacetone and Hexafluoroacetylacetone Complexes

Metal	Ligand	Reference
Rare earths	TFA	144,148,136
La, Nd, Sm, Cu	HFA	136
Y, Nd, Lu	HFA	122
Th	TFA	136,150
Th, U	HFA	139
Rare earths	HFA	141,148
Be, Al, Sc, V, Cr, Ni, Co	TFA	147
Mn	TFA	146
Co, Fe, In, Zn	TFA	125
Al, Cr	TFA	134
Al	TFA	133
Al, Cr, Fe	TFA	132
Al, Fe	TFA	130
Al, Cu, Fe	TFA	129,131

Table 2.10 : Comparison of Detection Limits of Some Methods for Ultra-trace Analysis

Metal	Gas Chromatography (g)	Atomic Absorption (g)	Neutron Activation (g)
Be	4×10^{-13}	1×10^{-8}	-
Cr	2×10^{-12}	2×10^{-9}	1×10^{-6}
Rh	2×10^{-12}	2×10^{-8}	5×10^{-11}
Al	7×10^{-11}	1×10^{-6}	1×10^{-9}

It is clear that all the fluorinated complexes are good electron-capturing species and should afford detection limits in the nanogram range (120,124,125). The ECD response is simply the ratio of decrease in standing current to remaining current, i.e., if I_b is designated as standing current and I_e as the current observed during the passage of a capturing compound, then (126,127) :

$$\frac{I_b - I_e}{I_e} = K.\ A \qquad \ldots\ldots \qquad [2.15]$$

where : K = electron attachment coefficient

A = sample concentration

The trivalent metals such as Al, Ga, In, Cr, Fe form complexes with TFA and HFA. These metal chelates can be determined and separated by gas chromatography (128-132). The formation of $Al(TFA)_3$ is pH dependent, thus the pH of solution should be adjusted between 5-6 to prevent precipitation of aluminium. Aluminium has been determined as $Al(TFA)_3$ by gas chromatography in freshwaters (133) and in uranium (134). Ferric ion also has been determined as $Fe(TFA)_3$ in sea water (135).

The lanthanide elements form chelate compounds with fluorinated β-diketone ligands (136-138). These metal chelates occur in the hydrated form which is difficult to extract in organic solvents as well as not being volatile. To increase the percentage of extraction in organic solvents and volatility, organophosphorus compounds (139) or organosulphur compounds have been used as a mixed ligand phase (140). Tri-n-butylphosphate (TBP) and di-n-butylsulphoxide (DBSO) have been widely used in mixed ligand systems for the extraction of lanthanide chelates (141-143).

The major problem in the gas chromatography of metal chelates is the dissociation of metal chelates on the column while on passage to the detector. To avoid this problem, the carrier gas is often saturated before the injection with the ligand in question (144-148).

In general, the problem of decomposition and adsorption of the volatile chelates has not been solved and still remains a major obstacle to the extensive use of GLC for the determination of metals, particularly at the trace level, so resulting in trailing peaks (to the rear), which seems to be irreproducible in magnitude as well as varying with the concentration of metal ion.

The technique is eminently suitable for the purpose, provided that the correct ligands to render stability and volatility to the complexed metal ions are available. Instead of the β-diketones, the family of coordinating ligands based on the dithiocarbamate grouping has been extensively investigated (149). The grouping offers the possibility of chelation with many sulphur-seeking metals e.g. Cd, Pb, Ni, etc.; which if coupled with a specific electron-capturing ligand promises simultaneous determination of several metals at extremely high sensitivity using capillary gas chromatography on Flexisil columns.

The use of the recently synthesised reagent trifluoroethyl-dithio-carbamate ligand offers much hope in this direction; regretfully, however, the ligand is not available commercially, is prepared in only low yield (c. 20%) and therefore presents considerable difficulties for its exploitation (149).

2.3 References

1. Mitchell, J.W., J. Radioanal. Chem., 69, 47 (1982).
2. Berman, E., Toxic Metals and their Analysis, Heyden & Son Ltd. (1980).
3. Corbin, H.B., Anal. Chem., 45, 534 (1973).
4. Xing, W. and Ingman, F., Talanta, 29, 707 (1982).
5. Schoer, J., Thallium, in "The Handbook of Environmental Chemistry", Vol. 3, Part C, Hutzinger, O., (Ed.), Springer-Verlag, New York (1984).
6. Minear, R.A. and Murray, B.B., Method of Trace Metal Analysis in Aquatic Systems, in "Trace Metal and Metal-Organic Interaction in Natural Waters", Singer, P.C. (Ed.), Ann Arbor Science, Michigan, Chap. 1 (1973).
7. Skoog, D.A. and West, D.M., Principles of Instrumental Analysis, Saunder College/Holt, Rinehart & Winston (1980).
8. Mitchell, J.W., Am. Lab., November, p. 16 (1981).
9. Robinson, J.W., Basic Principles, in "Techniques and Instrumentation in Analytical Chemistry", Vol. 5, Atomic Absorption Spectrometry, Chap. 1, Cantle, J.E. (Ed.), Elsevier Scientific Publishing Company, New York (1982).

PAGE
MISSING
IN
ORIGINAL

10. Bioteux, H., "Basic Concepts of Spectroscopy", Principles of Atomic Absorption", in "Atomic Absorption Spectrometry", Pinta, M. (Ed), Adam Hilger, London (1975).

11. Price, W.J., Spectrochemical Analysis by Atomic Absorption, Heyden & Son Ltd., London (1979).

12. Brodie, K., "Furnace Atomization" in "Analytical Method for Graphite Tube Atomizers", Rothery, E. (Ed.), Varian Techtron Pty. Ltd., Mulgrave Victoria, Australia, Chap. 1 (1982).

13. Technical Description of the Zeeman Modulated Atomic Absorption Spectrophotometer, Scintrex Company, Canada.

14. Zinger, M., Inter. Lab., May, 81 (1985).

15. Carrondo, M.J.T., Reboredo, F., Ganho, R.M.B. and Oliveira, J.F.S.; Talanta, 31, 561 (1984).

16. Jordao, C.P., "Chemical Availability of Heavy Metals in Aquatic Environments", PhD Thesis, University of Bristol (1983).

17. Randall, L., "Fractionation of Heavy Metals in Natural Samples", PhD Thesis, University of Bristol (1984).

18. Forstner, U., Metal Pollution Assessment from Sediment Analysis, in "Metal Pollution in the Aquatic Environment", Forstner, U. and Wittman, G.T.W. (Eds.), Springer-Verlag, New York, p. 118 (1979).

19. Dymott, T.C., Atomic Absorption with Electrothermal Atomisation, Pye Unicam Ltd.,(1985).

20. Cantle, J.E., Practical Techniques, in "Techniques and Instrumentation in Analytical Chemistry", Vol. 5, Atomic Absorption Spectrometry, Chap. 3, Cantle, J.E. (Ed.), Elsevier Scientific Publishing Company, New York (1982).

21. Riley, J.P. and Taylor, D., Anal. Chim. Acta, 40, 479 (1968).

22. Hahn, M.H., Wolnik, K.A. and Fricke, F.L., Anal. Chem., 54, 1048 (1982).

23. Thompson, K.C. and Thomerson, D.R., Analyst, 99, 595 (1974).

24. Barbooti, M.M. and Jasim, F., J. Iraqi Chem. Soc., 8, 1 (1983).

25. Horlick, G., Anal. Chem., 54, 277R (1982).

26. Horlick, G., Anal. Chem., 56, 278R (1984).

27. Cresser, M.S. and Sharp, B.L. (Eds.), Annual Reports on Analytical Atomic Spectroscopy, Vol. II, Published by the Royal Society of Chemistry (1981).

28. Lau, C., Held, A. and Stephens, R., Can. J. Spectro., 21, 100 (1976).

29. Khalighie, J., Ure, A.M. and West, T.S., Anal. Chim. Acta, 131, 27 (1981).

30. Lau, C.M., Ure, A.M. and West, T.S., Anal. Chim. Acta, 146, 171 (1983).

31. Khalighie, J., Ure, A.M. and West, T.S., Anal. Chim. Acta, 117, 257 (1980).

32. Khalighie, J., Ure, A.M. and West, T.S., Anal. Chim. Acta, 107, 191 (1979).

33. Barbooti, M.M.,and Jasim, F., J. Iraqi Chem. Soc., 8, 19 (1983).

34. Littlejohn, D., Duncan, I., Marshall, J. and Ottaway, J.M., Anal. Chim. Acta, 157, 291 (1984).

35. Dymott, T.C., Wassall, M.P. and Whiteside, P.J., Totally Pyrolytic Cuvettes (TPC) for Electrothermal Atomic Absorption Spectrometry, Pye Unicam Ltd. (1984).

36. Chung, C.H., Anal. Chem., 56, 2714 (1984).

37. Wahab, S.H, and Chakrabartic, C.L., 6th Arab Chemical Conference, Baghdad, p. 19 (1980).

38. Gupta, J.G.S., Talanta, 31, 1053 (1984).

39. Gupta, J.G.S., Talanta, 32, 1 (1985).

40. Fuller, C.W., Analytical Science Monograph No. 4, Electrothermal Atomisation for Atomic Absorption Spectrometry, published by the Chemical Society, London, p. 61 (1977).

41. Doidge, P., Development of Analytical Programs, in "Analytical Method for Graphite Tube Atomizers", Rothery, E.,(Ed.), Varian Techtron Pty. Ltd., Mulgrave, Victoria, Australia, Chap. 2 (1982).

42. Bloom, N., At. Spectro., 4, 204 (1983).

43. Sotera, J.J., Cristiano, L.C., Conley, M.K. and Kahn, H.L., Anal. Chem., 55, 204 (1983).

44. Fuavao, V.A. and Sneddon, J., At. Spectro., 4, 179 (1983).

45. Slavin, W., Carnrick, G.R., Manning, D.C. and Pruszkowska, E., At. Spectro., 4, 69 (1983).

46. Vollkopf, U., Grobenski, Z. and Welz, B., At. Spectro., 4, 165 (1983).

47. Chakrabarti, C.L., Wu, S., Karwowska, R., Chang, S.B. and Bertels, P.C., At. Spectro., 5, 69 (1985).

48. Routh, M.W., Doidge, P.S.,,Chidzey, J. and Frary, B., Int. Lab., May, 101 (1982).

49. Khan, H.L., AAS or ICP? Each Technique has Its Own Advantages, Instrumentation Laboratory Inc.,Wilmington, Aid I75 (1982).

50. Fassel, V.A., Science, 202, 183 (1978).

51. Greenfield, S., Jones, I.L. and Berry, C.T., Analyst, 713 (1964).

52. Skogerboe, R.K. and Coleman, G.N., Anal. Chem., 48, 611A (1976).

53. Carnahan, J.W., Mulligan, K.J. and Caruso, J.A., Anal. Chem. Acta, 130, 227 (1981).

54. Greenfield, S., McGeachin, H.M. and Smith, P.B., Talanta, 23, 1 (1976).

55. Watson, K.P., A Comparison of Detection Parameters, M.Sc. Thesis, University of Bristol (1985).

56. Boulos, M.I., Pure & Appl. Chem., 57, 1321 (1985).

57. Nygaard, D.D., Chase, D.S. and Leight, D.A., Analysis of Waste-water by ICP Spectrometry, Instrumentation Laboratory, Wilmington, Aid 177 (1984).

58. Fabec, J.L. and Ruschak, M.L., Anal. Chem., 55, 2241 (1983).

59. Fassel, V.A. and Kniseley, R.N., Anal. Chem., 46, 1110A (1974).

60. Demers, D.R., Busch, D.A. and Allemand, C.D., Int. Lab., May, 40 (1982).

61. Yoshida, K. and Haraguchi, H., Anal. Chem., 56, 5280 (1984).

62. Johnson, J.V. and Yost, R.A., Anal. Chem., 57, 758A (1985).

63. Schulten, H.R. and Monkhouse, P.B., Int. Lab., July/August, 70 (1983).

64. Houk, R.S., Fassel, V.A., Flesch, G.D., Svec, H.J., Gray, A.L. and Taylor, C.E., Anal. Chem., 52, 2283 (1980).

65. Focus:- VG Instruments Debuts ICP/MS, Anal. Chem., 56, 801A (1984).

66. Date, A.R. and Gray, A.L., Analyst, 106, 1255 (1981).

67. Date, A.R. and Gray, A.L., Analyst, 108, 159 (1983).

68. Reednick, J., Am. Lab., 11, 53 (1979).

69. Mavrodineann, R. and Boiteux, H., Flame Spectroscopy, John Wiley & Sons Inc., p. 53 (1965).

70. Cantillo, A.Y., Sinex, S.A. and Helz, G.R., Anal. Chem., 56, 33 (1984).

71. Debolt, D.C., J. Assoc. Off. Anal. Chem., 63, 802 (1980).

72. Gray, A.L., Analyst, 100, 289 (1975).

73. Guide to Analytical Values for IL Spectrometers, Instrumentation Laboratory, AID 91.

74. Deduke, D., Could, R.W.,and Jenkins, R., Quantitative X-Ray Spectrometry, Marcel Dekker Inc., New York, p. 19 (1981).

75. Jenkins, R. and De Vries, J.L., Practical X-Ray Spectrometry, Macmillan Press Ltd., p. 11 (1970).

76. Bertin, E.P., Introduction to X-Ray Spectrometric Analysis, Plenum Press, New York, p. 49,(1978).

77. Hercules, D.M., Anal. Chem., 42, 21A (1970).

78. Gurvich, Y.M., Int. Lab., January/February, 24 (1985).

79. Coetzee, P.P. and Zyle de Villiers, W.V., S.Afr. J. Chem., 38, 37 (1985).

80. Sweileh, J.A., Determination of Some Trace Elements in Phosphate Rock, MSc Thesis, University of Bristol,(1979).

81. Birks, L.S., X-Ray Spectrochemical Analysis, John Wiley & Sons, New York, p. 111 (1969).

82. Tipping, E., Hetherington, N.B., Hilton, J., Emma, B., Thompson, D.W. and Taylor, J.H., Anal. Chem., 57, 1944 (1985).

83. Ray, T.H., Modern Polarography and Its Applications, Lab. Equip., April (1984).

84. Smyth, W.F., Goold, L., Dadgor, D., Jan, M.R. and Smyth, R.M., Int. Lab., September, 40 (1983).

85. Vassos, B.H. and Ewing, G.W., Electroanalytical Chemistry, John Wiley & Sons, New York, p. 40 (1983).

86. Peterson, W.M., EG & G PARC Application Note T-2 (1982).

87. Borman, S.A., Anal. Chem., 54, 698A (1982).

88. EG & G Princeton Applied Research, Application Note P-2 (1978).

89. Copeland, T.R. and Skogerboe, R.K., Anal. Chem., 46, 1258A (1974).

90. Peterson, W.M. and Wong, R.V., Am. Lab., November, 116 (1981).

91. Wang, J., Environ. Sci. Technol., 16, 104A (1982).

92. Vassos, B.H. and Ewing, G.W., Electroanalytical Chemistry, John Wiley & Sons, New York, p. 176 (1983).

93. Vydra, E., Stulik, K. and Julakova, E., Electrochemical Stripping Analysis, Ellis Horwood Limited, Chichester, p. 18 (1976).

94. Model 315 Automated Electroanalysis Controller Operation and Service Manual, P.A.R. Corp., (1974).

95. Claus, Z., Mercury Electrode, in "Laboratory Techniques in Electroanalytical Chemistry", Kissinger, P.T. and Heinemann, W.R. (Eds.), Marcel Dekker Inc., New York, p. 267 (1984).

96. Princeton Applied Research, Application Note An-107. (1978).

97. Zirino, A. and Healy, M.L., Environ. Sci. Technol., 6, 245 (1972).

98. Nurnberg, H.W., Sci. Total Environ., 37, 9 (1984).

99. Whitnack, G.C. and Sasselli, R., Anal. Chim. Acta, 47, 267 (1969).

100. Nurnberg, H.W. and Raspor, B., Environ. Technol. Lett., 2, 457 (1981).

101. Gillan, G., Talänta, 29, 651 (1982).

102. Nelson, A. and Mantoura, R.F.C., Electroanal. Chem.,164, 237 (1984).

103. Nelson, A. and Mantoura, R.F.C., Electroanal. Chem., 164, 253 (1984).

104. Adeloju, S.B., Bond, A.M. and Hughes, H.C., Anal. Chim. Acta, 148, 59 (1983).

105. Hasle, J.R. and Abdullah, M.I., Mar. Chem., 10, 487 (1981).

106. Crosmun, S.T., Dean, J.A. and Stokely, J.R., Anal. Chim. Acta, 75, 421 (1975).

107. Zara, A.J. and Bulhoes, L.O., Anal. Letters, 15, 775 (1982).

108. Gustavsson, I. and Lundstrom, K., Talanta, 30, 959 (1983).

109. Lee, A.F., The Application of Anodic Stripping Voltammetry to the Determination of Trace Element in Standard Reference Materials, Ph.D. Thesis, Rand Afrikaans University (1981).

110. Gunasingham, J. and Fleet, B., Analyst, 108, 316 (1983).

111. Stewart, E.E. and Smart, R.B., Anal. Chem., 56, 1131 (1984).

112. Smart, R.B. and Stewart, E.E., Environ. Sci. Technol., 19, 137, (1985).

113. Wang, J., Farias, P.A.M., Luo, D., Anal. Chem., 56, 2379 (1984).

114. Sagberg, P. and Lund, W., Talanta, 29, 457 (1982).

115. Wang, J. and Luo, D., Talanta, 31, 703 (1984).

116. Batley, G.E. and Florence, T.M., Electroanal. Chem.,55, 23 (1974).

117. Brainina, K.Z., Talanta, 18, 513 (1971).

118. Dryhurst, C.D. and McAllister, D.L., Carbon Electrode, in

"Laboratory Techniques in Electroanalytical Chemistry", Kissinger, P.T. and Heinemann, W.R. (Eds.), Marcel Dekker Inc., New York, p. 289 (1984).

119. Moshier, R.W. and Sievers, R.F., Gas Chromatography of Metal Chelates, Pergamon Press, Oxford, p. 1 (1965).

120. Uden, P.C. and Henderson, D.E., Analyst, 102, 889 (1977).

121. Mushak, P., The Gas-Liquid Chromatography of Metal Ions via Chelation and Non-Chelation Techniques, in "Handbook of Derivatives for Chromatography", Blau, K. and King, G.S. (Eds.), Heyden, London, Chap. 12, p. 433 (1978).

122. Butts, W.C., Gas Chromatography of Some Metal Chelates of Benzoytrifluoroacetone and Thenoyltrifluoroacetone of the Complexes of the Rare Earths with the Mixed Ligands Hexafluoro-acetylacetone and Tri-n-butylphosphate, Ph.D. Thesis, Iowa State University (1968).

123. Guiochon, G. and Pommier, C., Gas Chromatography of Inorganics and Organometallics, Ann Arbor Science Publishers Inc., p. 207, (1974).

124. Lovelock, J.E. and Watson, A.J., J. Chromatogr., 155, 23 (1978).

125. Lovelock, J.E., J. Chromatogr., 99, 3 (1974).

126. Fenimore, D.C. and Davis, C.M., J. Chromatogr. Sci., 8, 519 (1970).

127. Perry, J.A., Chromatographic Science Series, Vol. 14, Introduction to Analysis Gas Chromatography, Marcel Dekker Inc., New York, p. 164 (1981).

128. Morie, G.P. and Sweet, T.R., Anal. Chem., 37, 1552 (1965).

129. Moshier, R.W. and Schwarberg, J.E., Talanta, 13, 445 (1966).

130. Morie, G.P. and Sweet, T.R., Anal. Chim. Acta, 34, 314 (1966).

131. Scribner, W.G., Treat, W.J. and Weis, J.D., Anal. Chem., 37, 1136 (1965).

132. Belcher, R., Jenkins, C.R., Stephen, W.I. and Uden, P.C., Talanta, 17, 455 (1970).

133. Lee, M.L. and Burrell, D.C., Anal. Chim. Acta, 66, 245 (1973).

134. Genty, C., Colette, H., Malherbe, P. and Schott, R., Anal. Chem., 43, 235 (1971).

135. Lee, M.L.,and Burrell, D.C., Anal. Chim. Acta, 62, 153 (1972).

136. Staniforth, R.A., Chelate Compounds of the Rare Earth Methods, Ph.D. Thesis,School of the Ohio State University (1943).

137. Berg, E.W. and Acosta, J.J.C., Anal. Chim. Acta, 40, 101 (1968).

138. Stites, J.G., McCarthy, C.N. and Quill, L.L., J. Am. Chem. Soc., 71, 3142 (1948).

139. Mitchell, J.W. and Banks, C.V., Anal. Chim. Acta, 57, 415 (1971).

140. Burget, C.A. and Fritz, J.S., Anal. Chem., 44, 1738 (1972).

141. Butts, W.C. and Banks, C.V., Anal. Chem., 42, 133 (1970).

142. Sieck, R.F. and Banks, C.V., Anal. Chem., 44, 2307.

143. Burgett, C.A. and Fritz, J.S., Talanta, 20, 363 (1973).

144. Fujinaga, T., Kuwamoto, T. and Kimoto, T., Talanta, 23, 753 (1976).

145. Fujinaga, T., Kuwamoto, T. and Murai, S., Talanta, 18, 429 (1971).

146. Fujinaga, T., Kuwamoto, T., Sugiura, K. and Matsubara, N., Anal. Chim. Acta, 136, 175 (1982).

147. Matsubara, N. and Kuwamoto, T., Anal. Chim. Acta, 161, 101 (1984).

148. Fujinaga, T., Kuwamoto, T., Sugiura, K. and Ichiki, S., Talanta, 28, 295 (1981).

149. Neeb, R., Pure & Appl. Chem., 54, 847 (1982).

150. Fujinaga, T., Kuwamoto, T. and Murai, S., Anal. Chim. Acta, 71, 141 (1974).

CHAPTER 3

METAL SPECIATION STUDIES

CONTENTS

3.1 INTRODUCTION

The total concentration of heavy metals in natural waters is often below 1 μg/L, and sometimes below 0.1 μg/L. Chemical analysis at these concentration levels is difficult. There are severe problems with contamination from a multitude of sources and serious losses of metal can occur by adsorption on the walls of sample bottles or analysis vessels (1).

To study the speciation of trace metal in natural waters requires an analytical technique which not only can detect trace metals at their natural concentration levels but also can differentiate the various chemical species of a given trace metal (2). A great many techniques have been used to study trace metal speciation. These include (3) :

i) ion-selective electrodes
ii) dialysis
iii) ion-exchange resins
iv) ultrafiltration
v) U.V. irradiation
vi) anodic stripping voltammetry

Batley *et alia* (4) have suggested a speciation scheme which employs a combination of the latter four techniques. The speciation scheme suggested by Batley *et alia* (4) is shown in Figure 3.1 for metals in natural waters. The species are classified into seven groups according to their behaviour rather than chemical differences between metal species.

Ion-selective electrode potentiometry (ISE) is widely used in speciation measurements because of its ability to measure selectivity in the activity of the free metal ion in the presence of a large number of metal complexes. Unfortunately, ISE often does not have sufficient

FIG. 3.1 ANALYTICAL SCHEME FOR SPECIATION OF TRACE METALS IN NATURAL WATERS

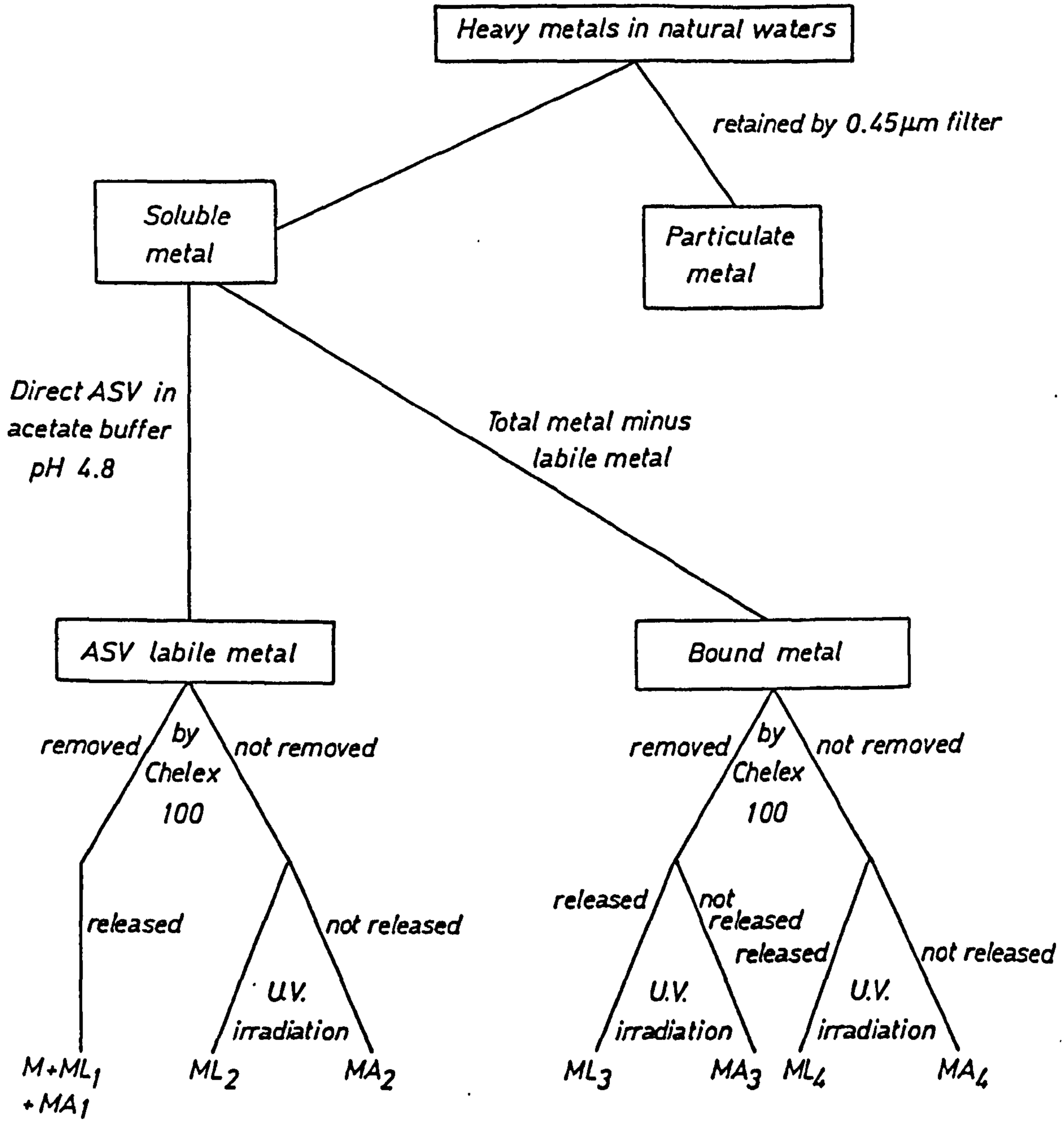

Figure 3.1 continued

Class 1

M + ML1 + MA1: Free metal ions + ASV-labile organic complexes dissociated by Chelex-100 + ASV-labile inorganic complexes dissociated by Chelex-100.

Class 2

ML2: ASV-labile organic complexes plus labile metal adsorbed on organic colloids - not dissociated by Chelex-100.

MA2: ASV-labile inorganic complexes plus labile metal adsorbed on inorganic colloids - not dissociated by Chelex-100.

Class 3

ML3: Non-labile organic complexes dissociable by Chelex-100.

MA3: Non-labile inorganic complexes dissociable by Chelex-100.

Class 4

ML4: Non-labile organic complexes plus non-labile metal adsorbed on organic species - not dissociable by Chelex-100.

MA4: Non-labile inorganic complexes plus non-labile metal adsorbed on inorganic species - not dissociable by Chelex-100.

sensitivity for the analysis of natural waters (2,3).

Dialysis membranes which have pore diameters 1-5 nm can be used to separate colloidal and molecular species. The technique suffers from metal contamination, metal adsorption and dissociation of metal complexes at the membrane surface (1).

Many speciation studies (5,6) have employed Chelex-100 to determine what is called Chelex-labile metal. The resin has a pore diameter of about 2 mm, colloidal particles are therefore excluded from the resin matrix, providing a simple and contamination-free method for separating ionic and colloidally-associated metals. The resin labile metal can be calculated as the difference between the total and effluent metal concentrations.

Filtration has become a universally applied first step in the preparation of water samples for trace metal determination. The filtration is usually performed with 0.45 μm membrane filters, the resultant fractions usually being termed particulate and dissolved (7).

Although U.V. irradiation and ozone have also been used for speciation studies, the technique is not suitable for quantitative work (6,8). U.V. irradiation destroys organic matter which then allows iron oxide to coagulate and precipitate from metal solutions. When ozone is used to destroy organic matter, metals may be precipitated as oxides and so be removed from the soluble phase (6).

Anodic stripping voltammetry is one of the very few analytical techniques that is sufficiently sensitive for direct determination of heavy metals in natural waters but also has an intrinsic capability for speciation work (1). A complex is designated as an ASV labile metal complex when dissociation of metal complex into free metal ions plus the representative ligand occurs rapidly at the electrode surface in the electroreduction process (Equation 3.1). When the dissociation of

the complex occurs slowly, this type of complex is termed as a non-labile metal complex (Equation 3.2). The difference between the total and labile metal has been called bound metal (i.e. metal present as a strong complex). Bound metal may be considered as bound metal in an inert complex and other inert forms such as colloidal particles (9).

$$M(LL) \longrightarrow M^{n+} + LL \quad \ldots\ldots \quad [3.1]$$

$$M(NL) \longrightarrow M^{n+} + NL \quad \ldots\ldots \quad [3.2]$$

where (LL) and (NL) are labile and non-labile ligands respectively

ASV-labile metal determinations at natural pH measures that metal present as the free ion, as simple complexes and possibly the weak organic complexes. Acidification should release that metal tied up in strong organic, organic and inorganic colloids and that portion adsorbed on particulate matter (10).

Recently, speciation has been studied by applying computer modelling, the concentration of each species of given metal can be calculated on the basis of thermodynamics, provided that the following parameters are known (11) :

i) the total concentrations of all the elements in the solution used for study;

ii) the equilibrium constants of all the reactions occurring between the various species.

Models for the chemical speciation of inorganic lead in sea water, the stability constants and free ligand concentration have been studied by Turner et alia (12). However, computer modelling is a powerful technique, and will make an important contribution towards an understanding of speciation in waters once the necessary thermodynamic data are available. The main obstacle to the successful use of computer modelling

of trace metal speciation in waters is the lack, even dearth, of reliable thermodynamic data (1).

Many workers have determined the trace metal distribution associated with the suspension material in street dusts, roadside soil (13), sludge ash (14) and sediment (15) by sequential extraction procedures. Some of these procedures have classified the associated metal into five fractions. For example, Tessier et alia (16) designed a procedure to differentiate between the various forms of residual and non-residual metal. The procedure involves the sequential chemical extraction for the partition of particulate trace metal into five fractions. The Tessier et alia (16) scheme is shown in Figure 3.2. Gupta et alia (17) selected a specific procedure to study the partition of trace metals in sediment (see Figure 3.3). Gupta et alia (17) claimed that the selective extraction procedures can be used successfully in determining different geochemical fractions for most trace metals. Chester et alia (18) have also determined the total non-residual trace metal in sediments by extraction with 0.5 N HCl, while the distribution of trace metals within the sediment was also divided into five fractions shown in Figure 3.4. This particular scheme is similar to other schemes (mentioned previously), but the organic fraction is divided into two forms; humic materials associated with trace metal (which is extracted with $Na_4P_2O_7$) and the trace metal associated mainly with residual organics and sulphides which is extracted by 30% (v/v) H_2O_2 (pH 2), followed by 1 M CH_3COONH_4. Engler et alia (19) have also reported a specific scheme for the extraction of trace metals associated with each geochemical phase within the sediment (see Figure 3.5). The Tessier et alia (16) scheme seems to be simple, rapid and gives reliable information about the speciation of trace metals in sediment and soils, therefore it was used in later work in this dissertation.

Figure 3.2 : Tessier et alia (16) Scheme for Speciation of Particulate Trace Metals in Sediments

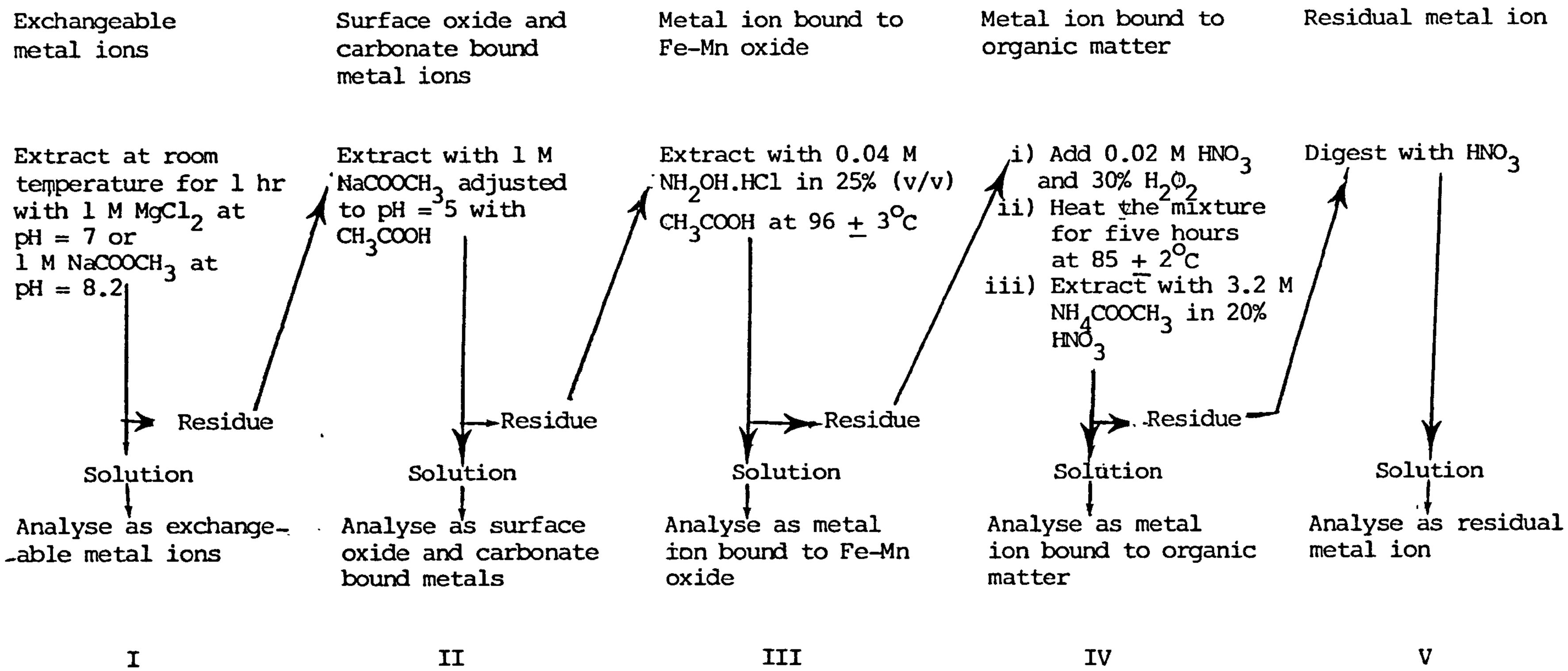

Figure 3.3 : Gupta et alia (17) Scheme for Speciation of Trace Metals in Sediments

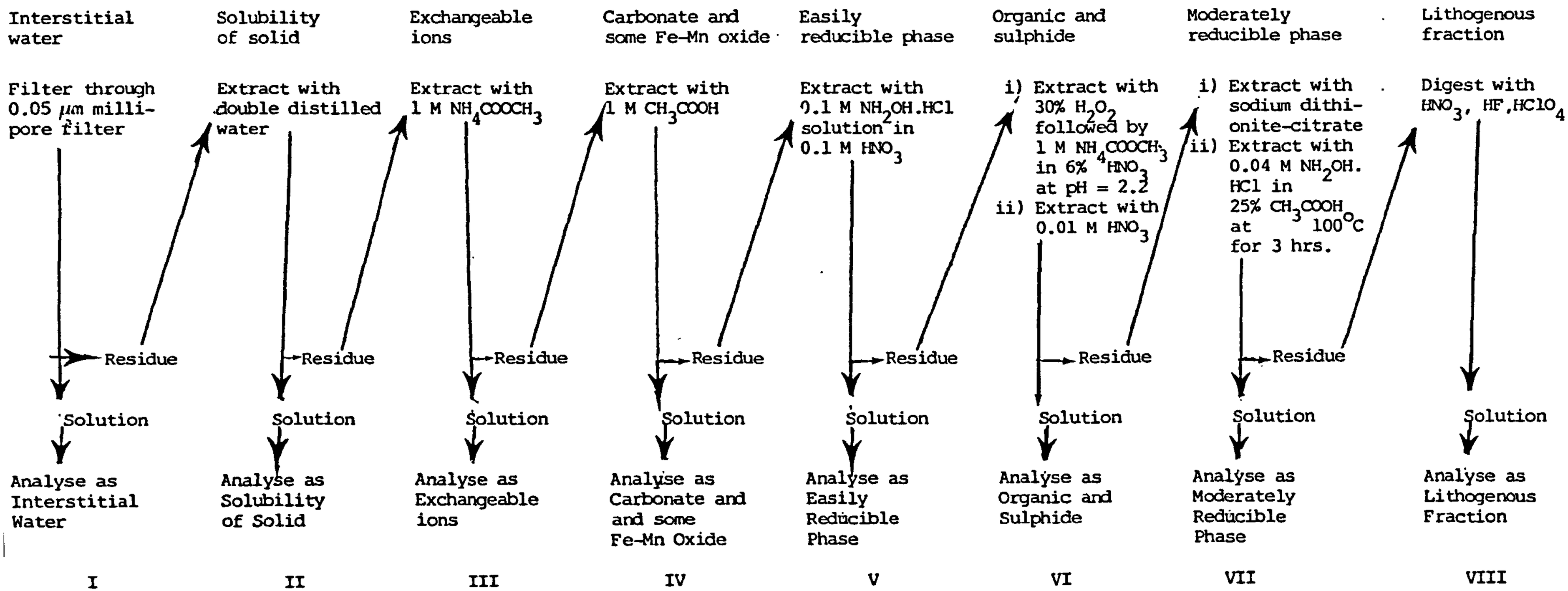

Figure 3.4 : Chester *et alia* (18) Scheme for Speciation of Non-Residual Trace Metal in Sediments

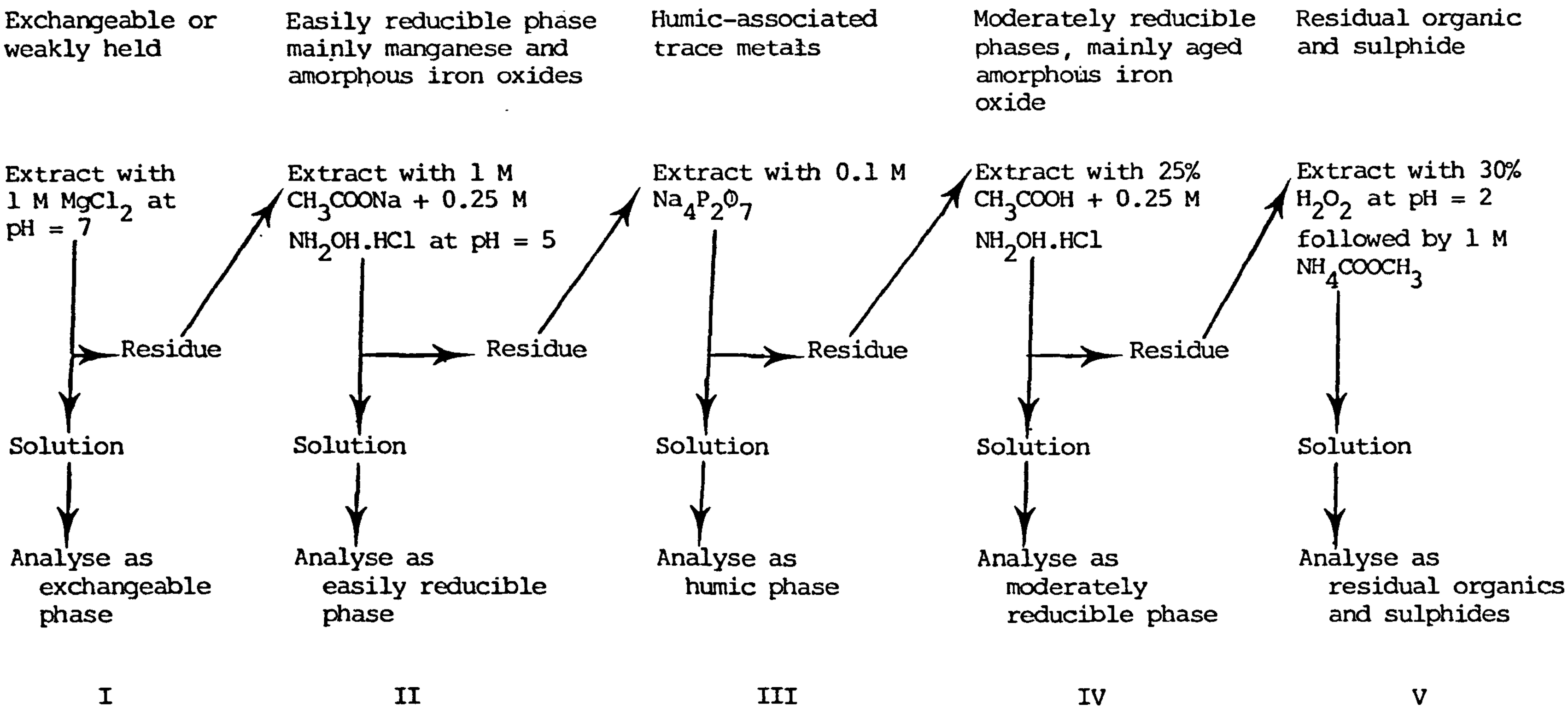

Figure 3.5 : Engler et alia (19) for Speciation of Trace Metals in Sediment

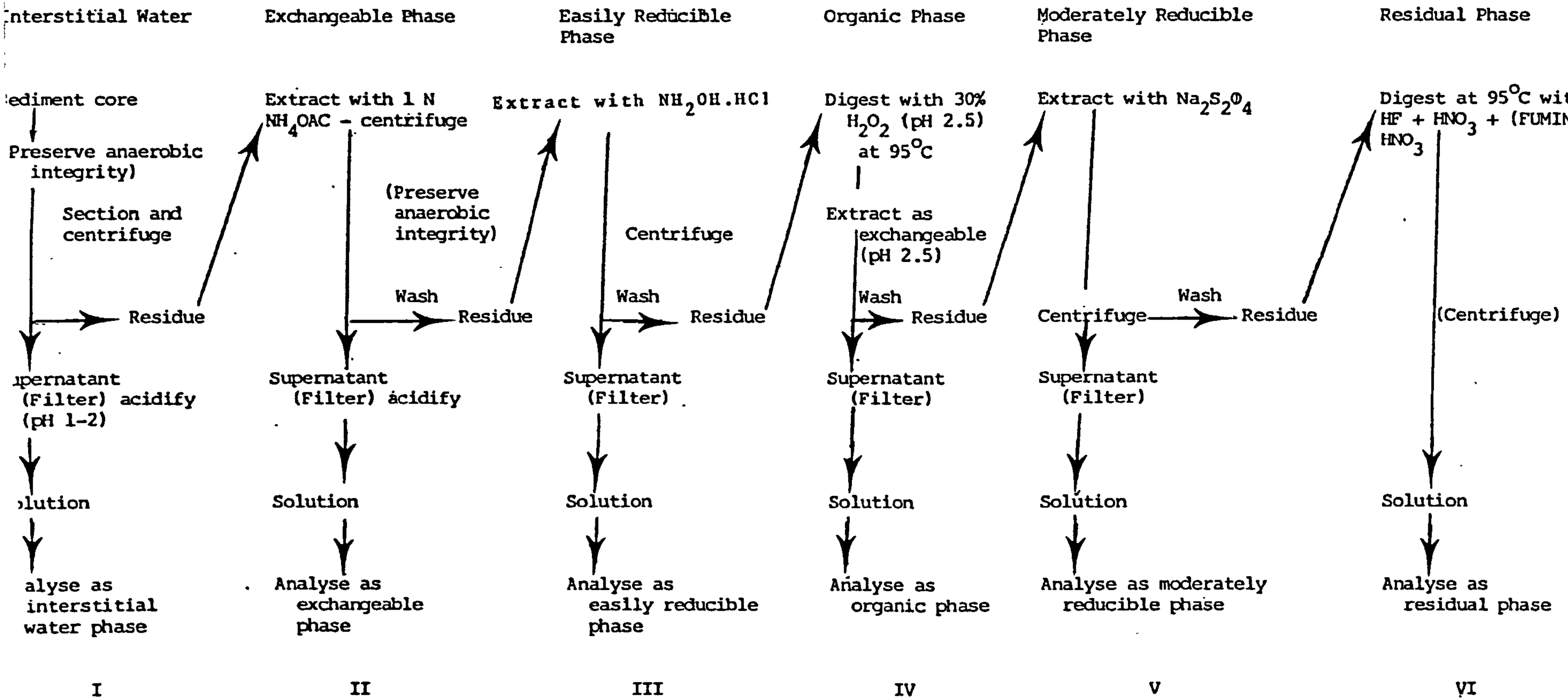

3.2 EXPERIMENTAL AND RESULTS

a) Site Description and Sample Collection

Samples of waters, sediments, soils and vegetation were collected from Mendip streams at Waldegrave Pool and Fair Lady Well at the end of June, 1983 (see Figure 3.6). A sample from Restronguet Creek No. 3 was collected from OS 204 (794389) on 12/2/85. On the same day, samples at Adit Bridge No. 8, OS 200 (839564) and Adit No. 8, OS 200 (839569) were collected from the Penhallow Moor area near to Newquay, a scene of earlier mining activity. The Luckett soil sample, OS 201 (387736) and Caradon stream sediments,(OS 201 (264700) had been collected two years previously. The location of these sample sites is shown in Figures 3.7 to 3.9. Samples of waters, sediments and soils were collected from Iraq at the end of December 1983 (see Figure 3.10).

The water samples were collected in polyethene bottles, previously rinsed with nitric acid and again with DDW. The polyethene bottles (2.5 L) were rinsed three times with the stream water and then filled. After return to the laboratory, the water samples were immediately analysed for metal content whenever possible or stored at the natural pH at $4^{o}C$ in a refrigerator.

The sediment, soil and vegetation samples were collected in plastic bags. The Iraqi samples (water, sediment and soils) were collected the day prior to flying to Bristol.

FIG. 3.6 LOCATION OF SAMPLE SITES NEAR PRIDDY, MENDIP HILL

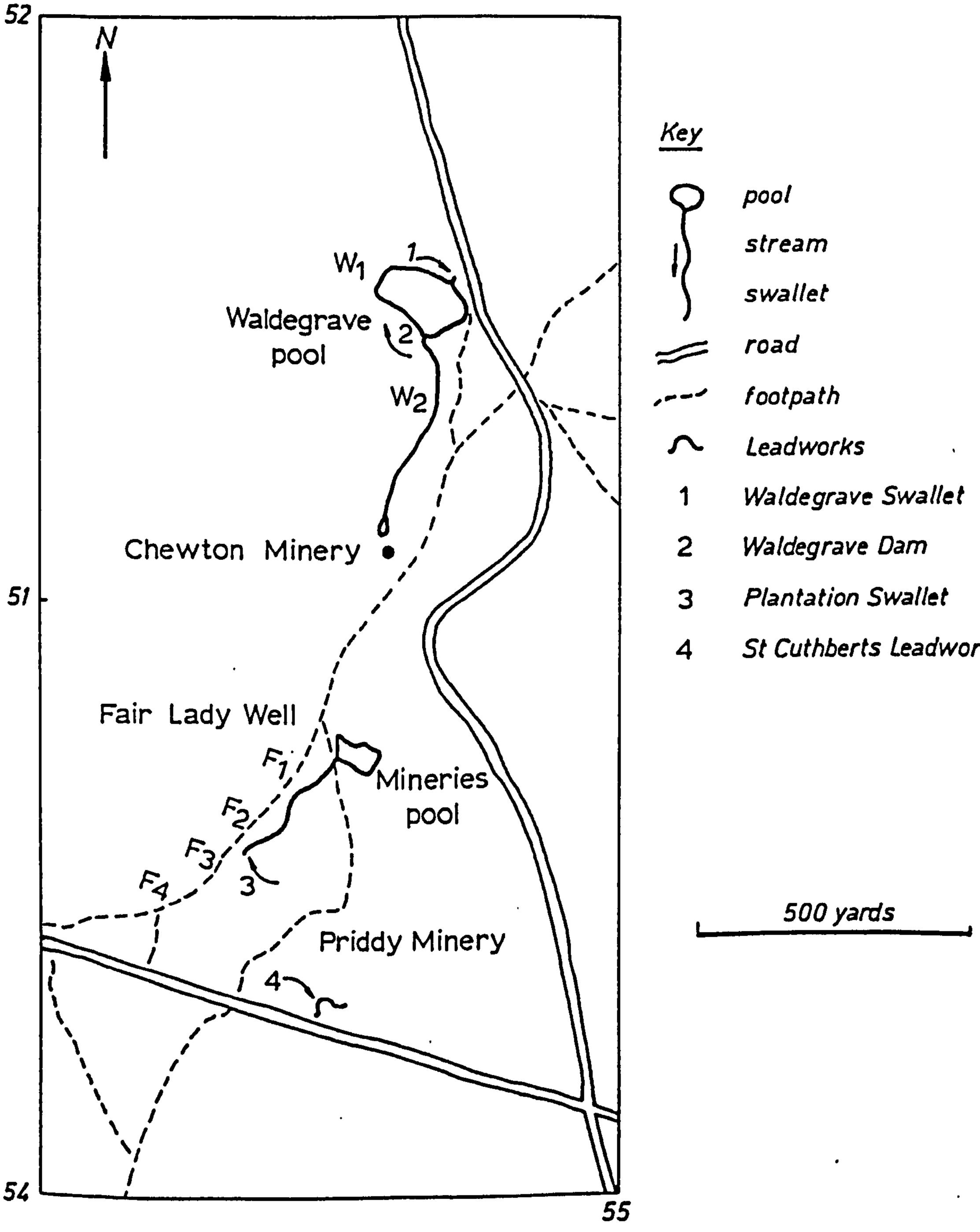

FIG. 3.7 LOCATION OF SAMPLE SITE ON PENHALLOW MOOR

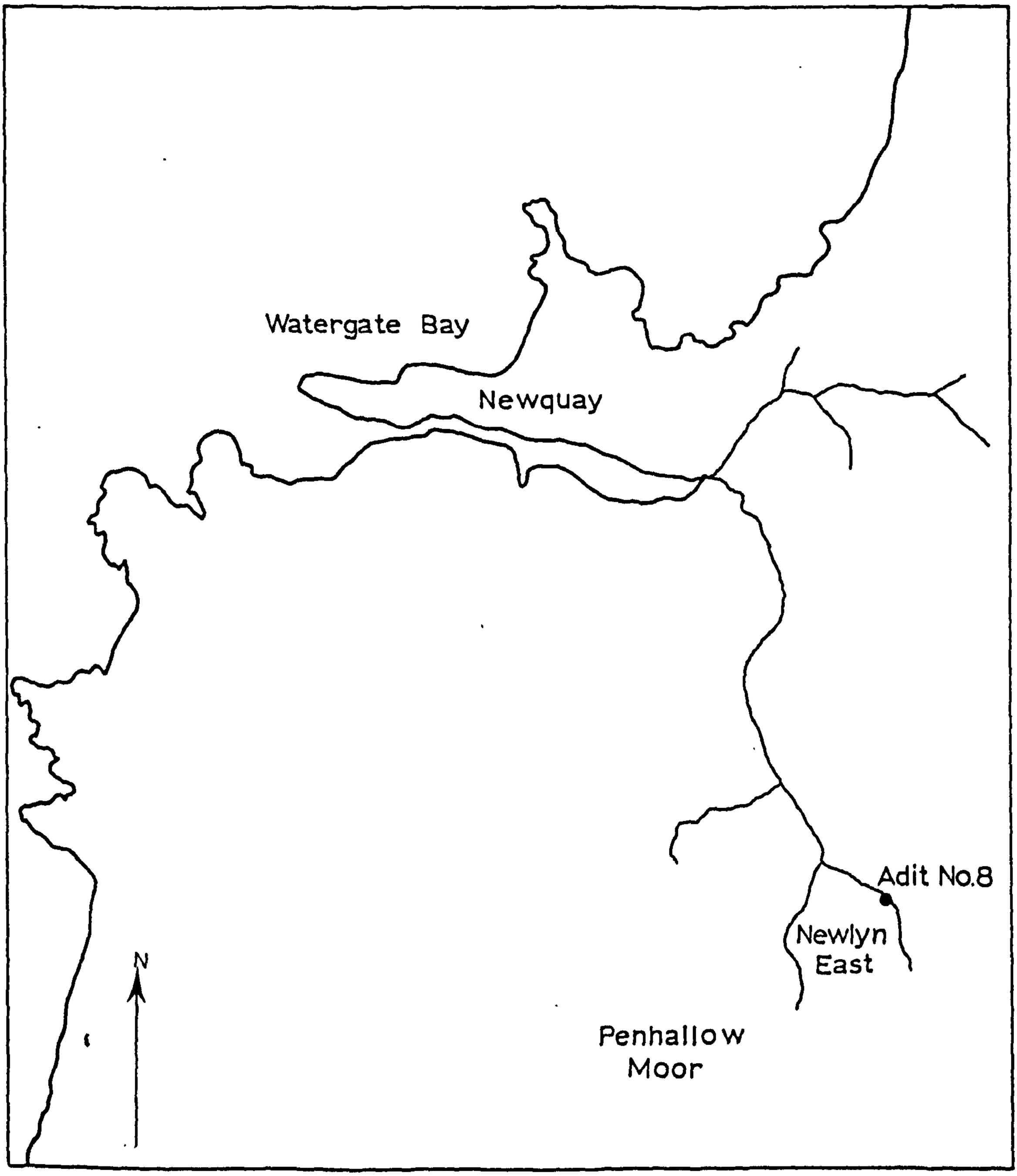

SCALE 1:500 0 0

FIG. 3.8 LOCATION OF SAMPLE SITES ON RESTRONGUET CREEK

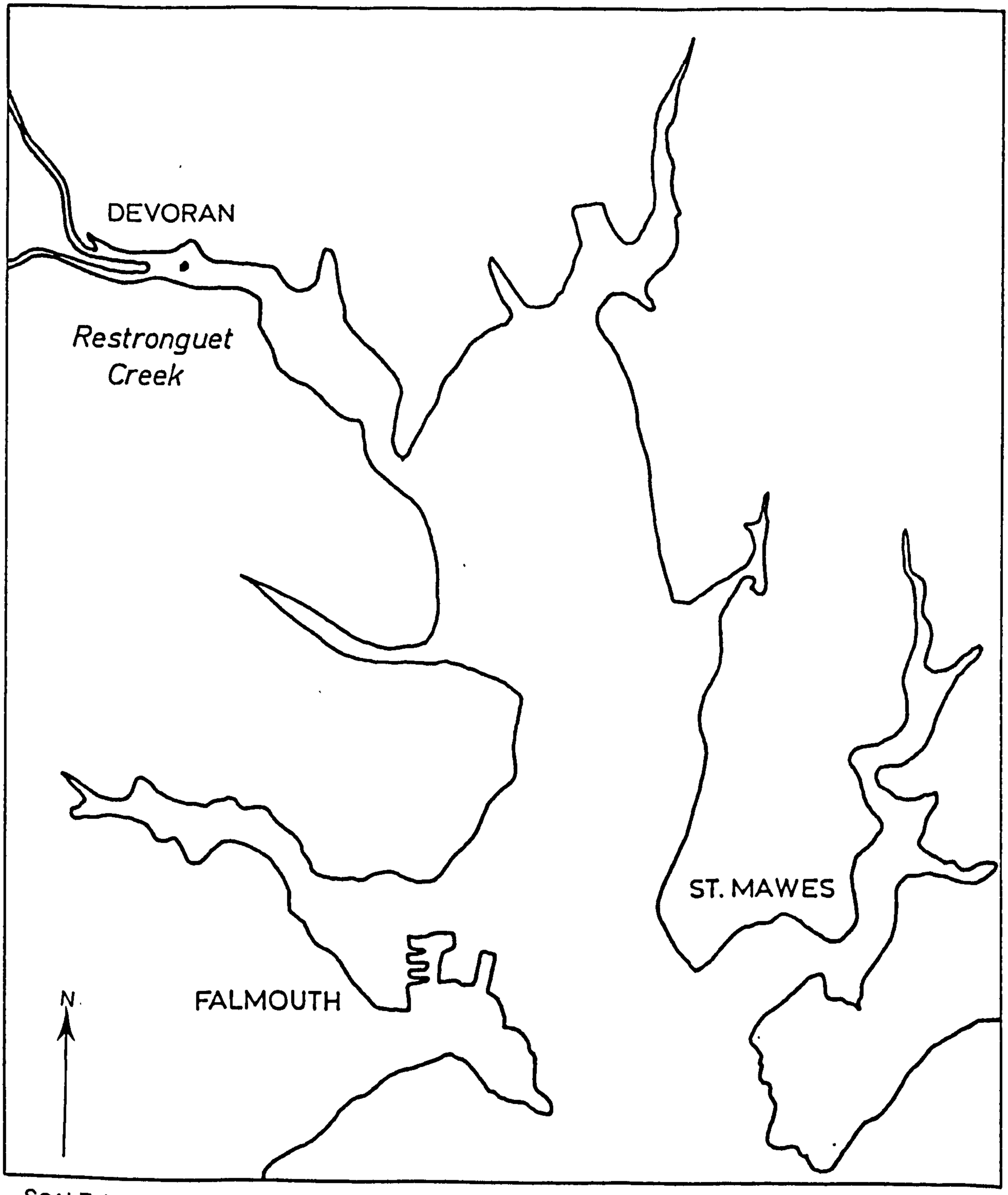

FIG. 3.9 LOCATION OF SAMPLE SITES
(a) Near Caradon Hill
(b) Near Luckett

(a)

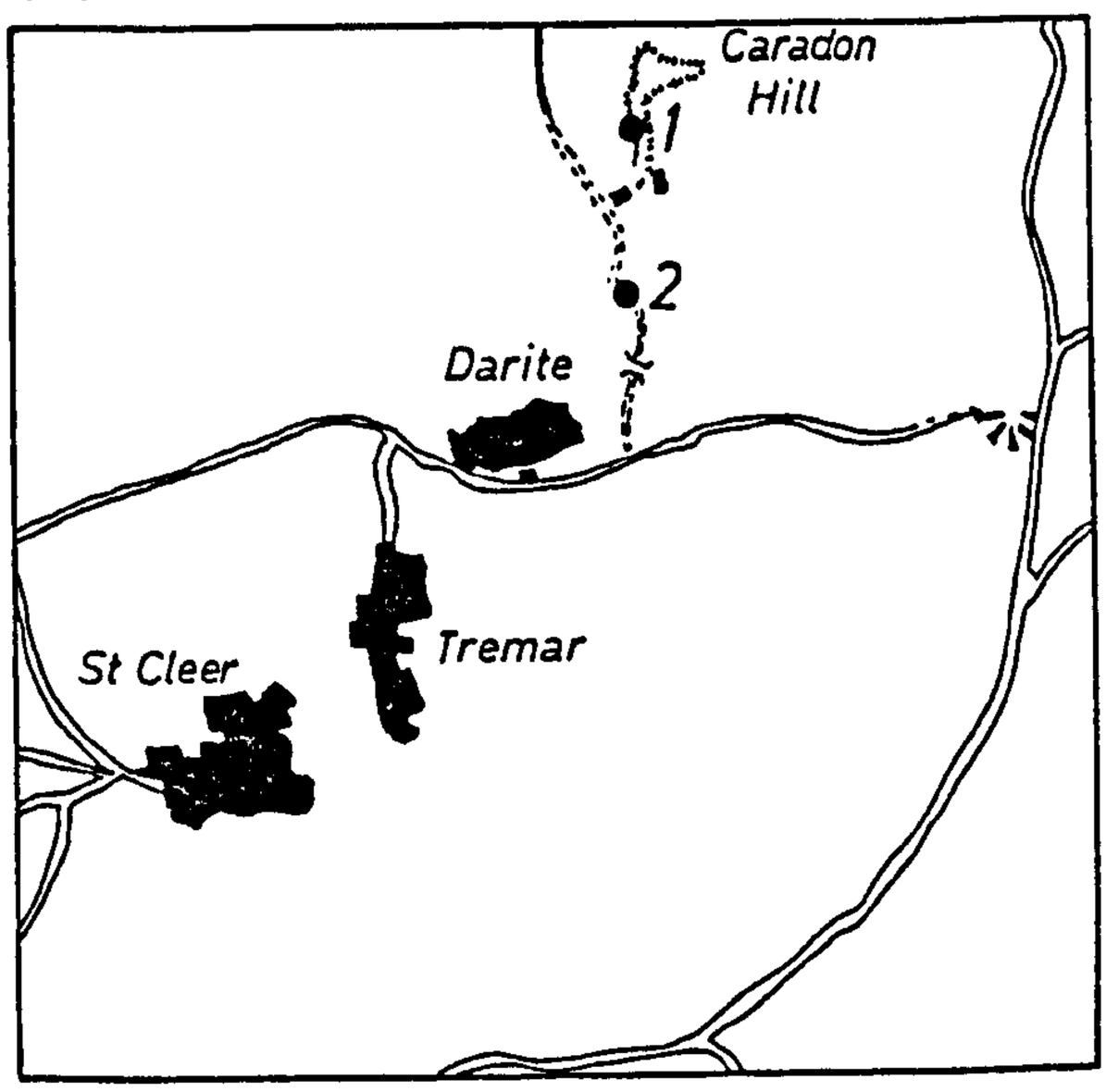

(b)

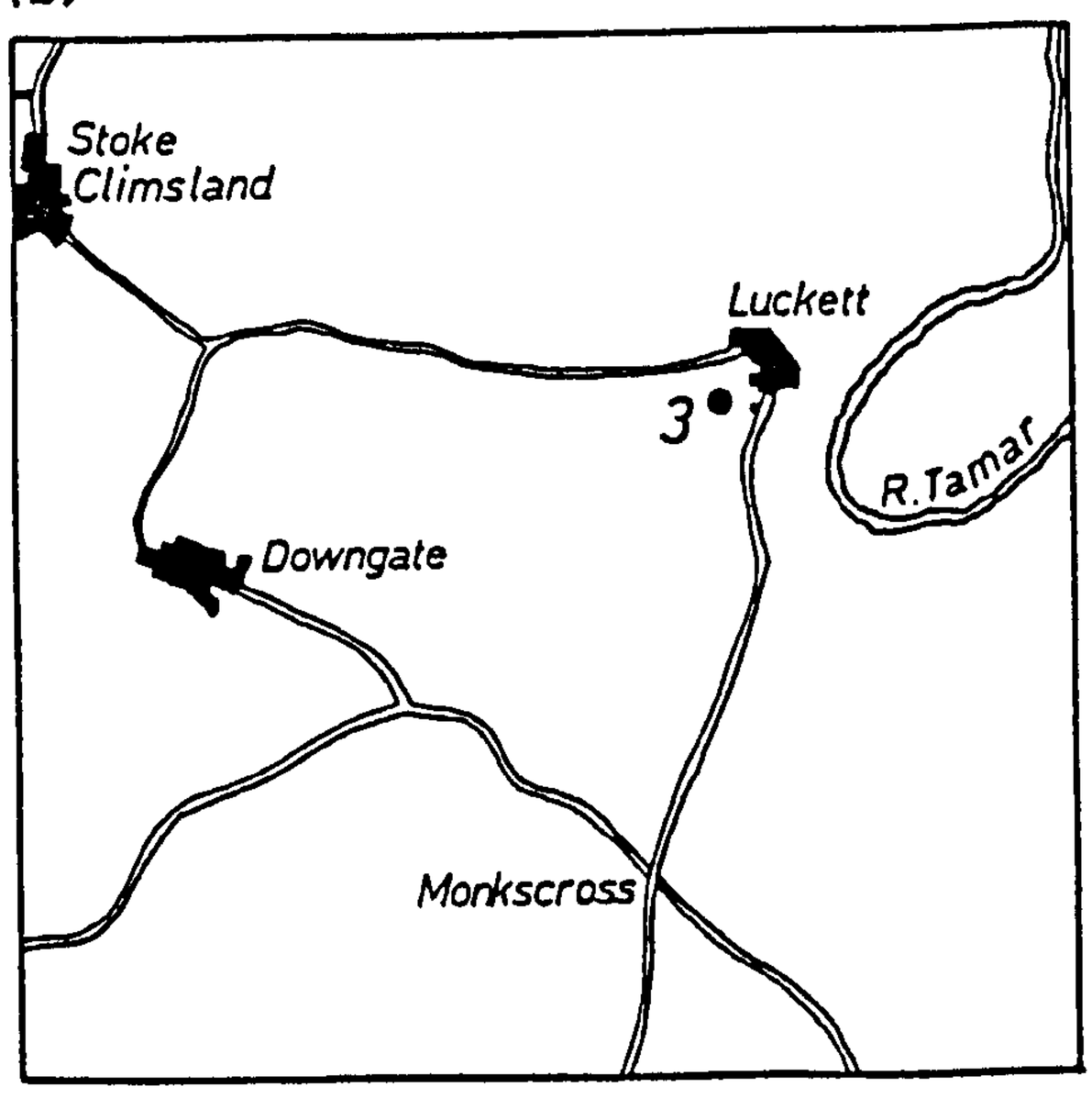

Key

1 = Caradon Native Sediment
2 = Caradon Secondary Rock
3 = Orain Luckett Sediment

FIG. 3.10 LOCATION OF SAMPLE SITE IN IRAQ

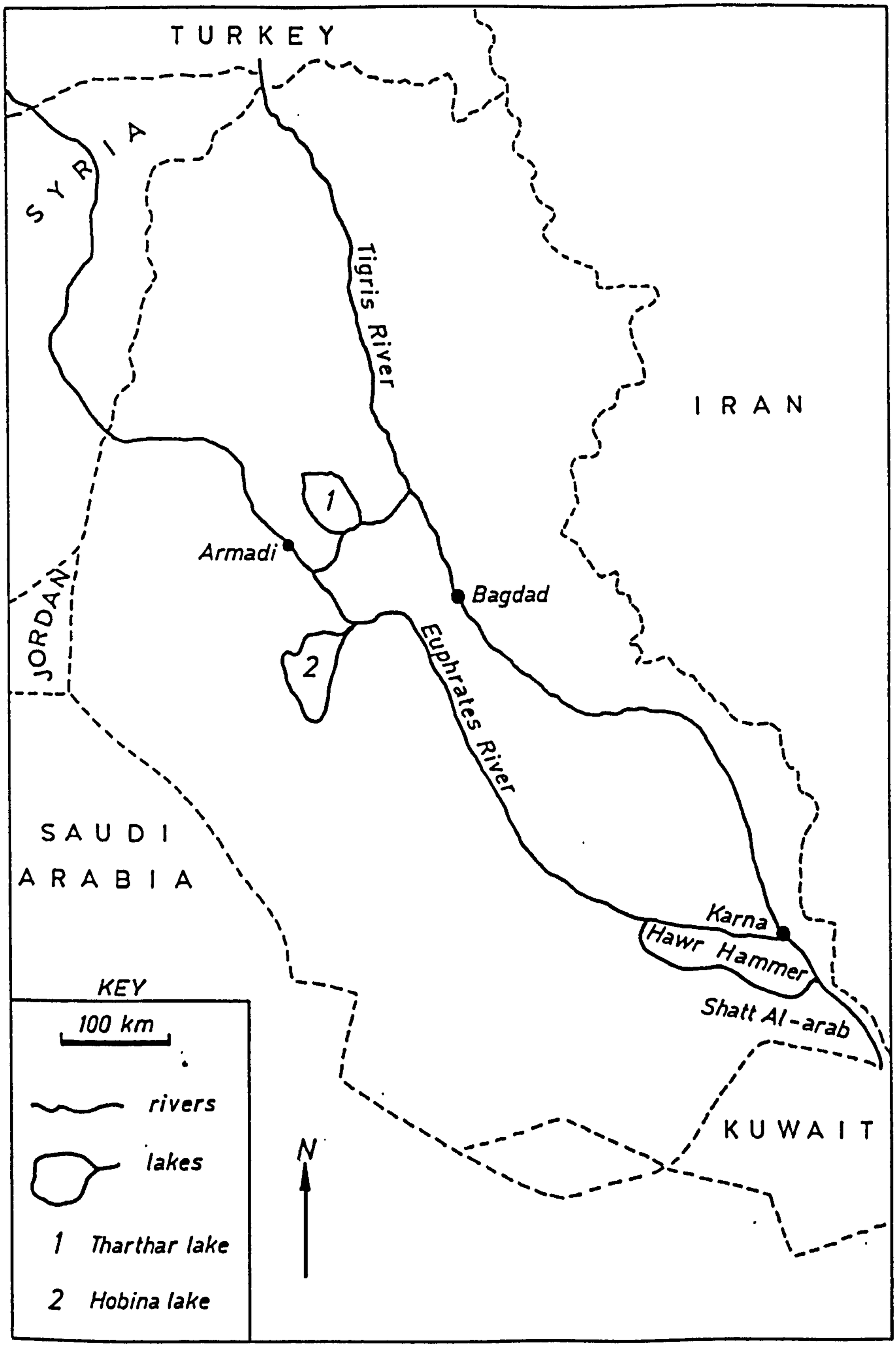

b) Experimental Preparation

i) Reagents

The following Analar reagents were employed in the water analysis procedures: nitric acid, sodium acetate, glacial acetic acid and lead nitrate. Double distilled water (DDW) was used for dilution and other purposes. AnalaR reagents were also used for the sediment, soil and plant analyses. These included: nitric acid, acetic acid, lead nitrate, copper nitrate, zinc nitrate, manganese nitrate, nickel nitrate, ammonium acetate, magnesium chloride, hydroxylamine-hydrochloride, hydrogen peroxide and hydrofluoric acid.

ii) Glassware

Glassware was washed with "Teepol" detergent, rinsed with tap-water and distilled water and placed in 40% v/v nitric acid for at least 48 hours. The glassware was rinsed with DDW and oven dried.

iii) Preparation of Solutions

A stock solution (1000 $\mu g/cm^3$) of some metals (Cu, Zn, Pb, Cd) was prepared by dissolving the appropriate weight of the metal nitrate in 5 cm^3 of 20% v/v HNO_3 and diluting to 500 cm^3 with 20% v/v HNO_3. The stock metal solutions were maintained for an extended period. Commercially prepared stock solutions of Ca, Mg, Mn, Fe and Ni were used and further dilutions were made when needed to prepare the appropriate working standard solutions.

The background electrolyte was a pH 5.0 acetate solution prepared by mixing 30 cm^3 of 0.2 M acetic acid and 70 cm^3 of 0.2 M sodium acetate. The chelating resin used to purify the acetate buffer solution (removal of heavy metals) was Chelex-100 (Bio-Rad Laboratories, Richmond, California), with a size range of 50-100 mesh, supplied in the hydrogen

form. Portions of resin were slurry packed to a height of 11 cm in a glass column and were converted to the ammonium form using a 1 M ammonium acetate solution. The resin was washed with sufficient DDW prior to use. The background electrolyte was passed through the resin at a rate of 2 cm^3/minute. Figure 3.11 illustrates the voltammogram of the background electrolyte before and after passage through the resin.

c) Sample Treatment, Analysis and Results

i) Waters

Six samples were collected along the length of the Mendip streams, two samples were collected at Waldegrave Pool (W_1 and W_2) and four samples at the Fair Lady Well (F_1, F_2, F_3, F_4). Two aliquots of unfiltered samples from the sites of Waldegrave Pool and Fair Lady Well were used to study the total and labile lead in Mendip streams. The first sample (25 cm^3) was acidified to pH 2.3 with 2 M HNO_3 and examined at pH 5 by DPASV for labile lead. The resultant voltammogram from the Waldegrave Pool (W_1) is shown in Figure 3.12. A second sample (25 cm^3) was acidified to pH 0.7 with 2 M HNO_3 and heated for 10 minutes under an IR lamp; the sample was examined by GFAAS for total lead. The results are listed in Table 3.1.

An attempt to fractionate the lead species by size fraction was carried out on each sample from each site in the Mendip streams, by using membrane filters of 0.45 μm and 0.1 μm pore size respectively. Analysis was carried out by GFAAS. The results are given in Table 3.2.

FIG. 3.11 VOLTAMMOGRAM OF ACETATE BUFFER

A = Before passage through the resin

B = After passage through the resin

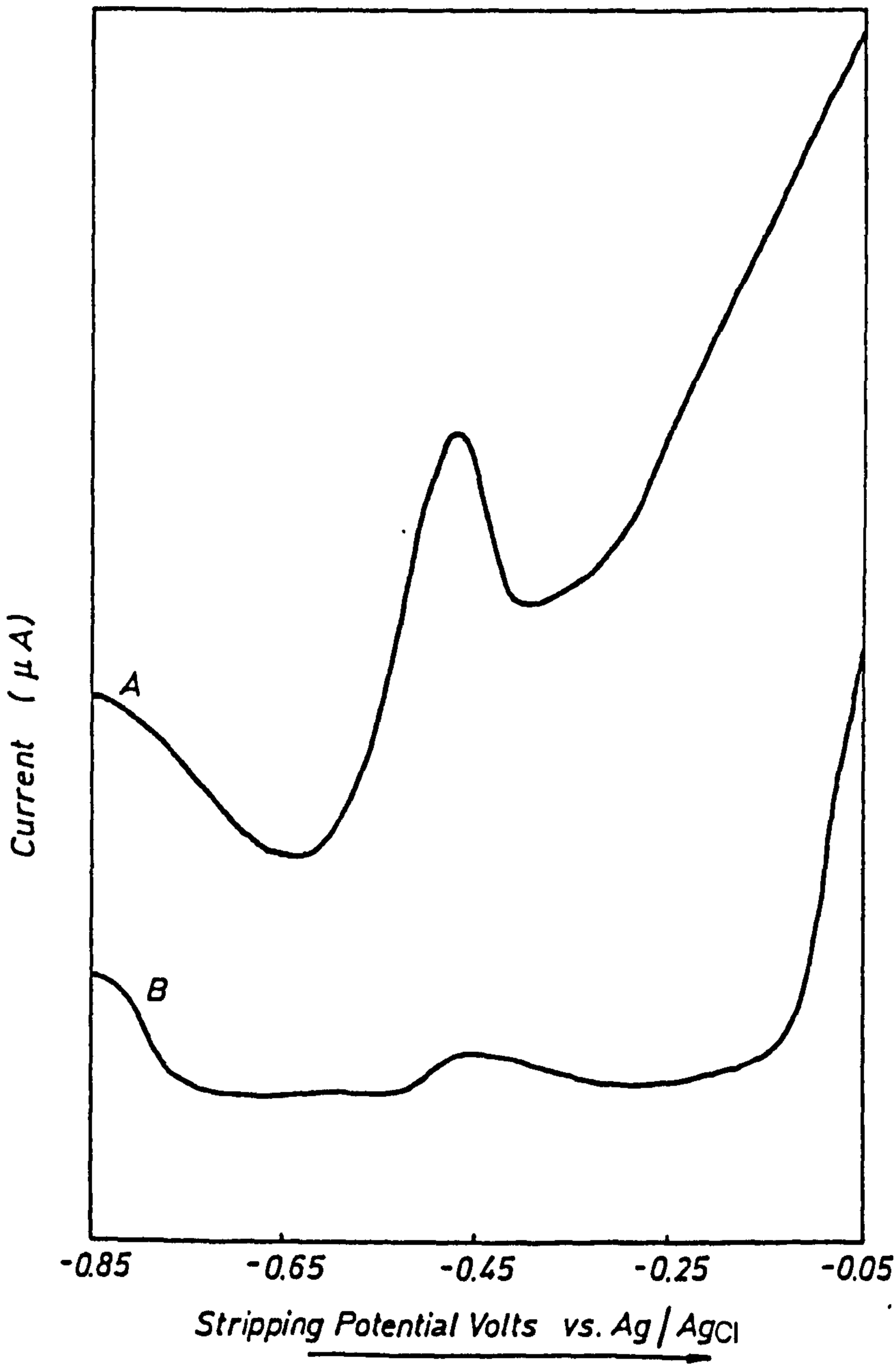

FIG. 3.12 VOLTAMMOGRAM OF WALDEGRAVE POOL (W_1)

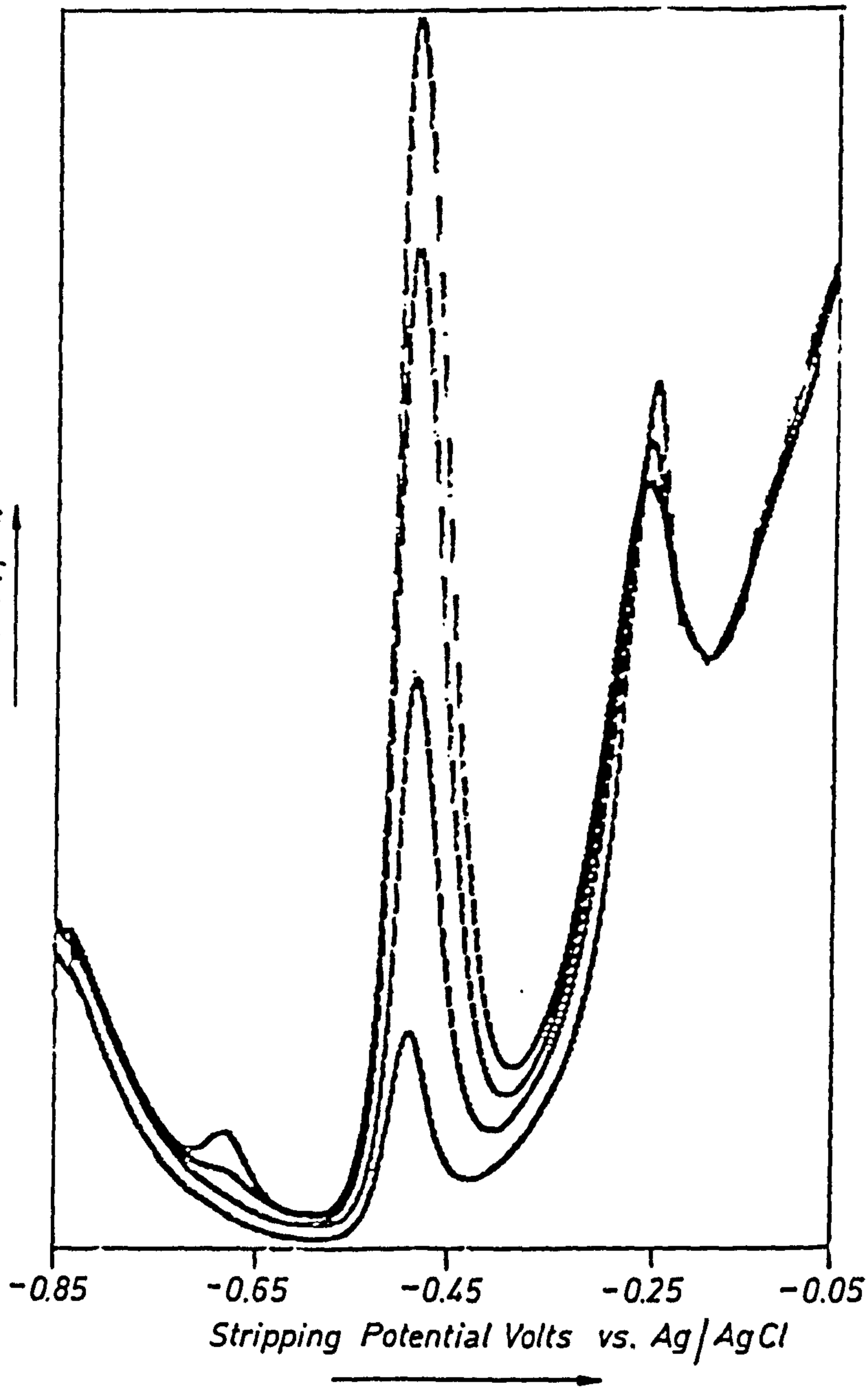

Table 3.1 : Lead Concentration in Mendip Streams (μg/L), Analysis by GFAAS for Total Lead and DPASV for Labile Lead

Sample Site		Total	Labile	Bound
i) Waldegrave Pool				
	W_1	160	24.77	135.23
	W_2	65.87	N.D.	65.87
ii) Fair Lady Well				
Top	F_1	140.77	112.79	27.98
	F_2	182.41	69.83	112.58
	F_3	85.40	60.96	24.44
Bottom	F_4	81.0	N.D.	81.00

Table 3.2 : Lead Concentration in Mendip Streams (μg/L), Filtered at Different Size Fraction, Analysis by GFAAS

Sample Site		Size Fraction	Concentration
i) Waldegrave Pool			
	W_1	0.45	101.43
		0.1	64.65
	W_2	0.45	145.12
		0.1	153.98
ii) Fair Lady Well			
	F_1	0.45	N.D.
		0.1	25.23
	F_2	0.45	180.26
		0.1	195.70
	F_3	0.45	3.89
		0.1	48.23
	F_4	0.45	15.05
		0.1	N.D.

Five samples were collected from Iraqi waters, two samples from the Tigris River (south Baghdad (TS) and north Baghdad (TN)) and three samples were also collected from the following sites:

1) Tharthar Lake (TH)

2) Euphrates River (EU) near Aramadi

3) Hobina Lake (HO).

Each sample (125 cm^3) was digested with 1 cm^3 of concentrated HNO_3 and heated for 10 minutes under an IR lamp. The sample, after cooling, was passed through the 11 x 0.5 cm of glass column which contained Chelex-100 in calcium form. Lead was eluted with 15 cm^3 of 10% (v/v) HNO_3. The effluent volume was diluted to 25 cm^3 with DDW and the determination was carried out by GFAAS. The results are given in Table 3.3.

Table 3.3 : Lead Concentration (μg/L) in Iraqi Water Samples

Sample Site	Total Lead
TS	2.04
TN	N.D.
TH	1.60
EU	0.230
HO	1.52

The figures are the mean of two determinations.

ii) Sediments and Soils

The collected sediments and soils from the Mendip Hills, Iraq, and other sites were oven dried at 105°C for 24 hrs; the samples were finely ground by means of a Tema mill. The determinations were performed on the 105 mesh portion of the sample, 0.5 g of Mendip Hill samples or 2 g of Iraqi samples were digested in 10 cm^3 of hot concentrated Analar nitric acid under IR lamps and reduced in volume to 2 cm^3; 10 cm^3 of DDW was added. The samples were filtered through a Whatman 541 filter paper to remove insoluble silica material and the volume was diluted to 25 cm^3 with DDW. The analysis was carried out by FAAS for lead. The results obtained are presented in Tables 3.4 and 3.5.

Table 3.4 : Concentration of Lead in Soils and Slag Samples Collected from the Mendip Hills. Analysis by FAAS

Sample Site	Lead Concentration ($\mu g/g$)
Mineries Pool Exit	13,563
St. Cuthbert's Leadwork (Slag No. 1)	38,923
St. Cuthbert's Leadwork (Slag No. 2)	3,000
Fair Lady Well Dam	41,325
Waldegrave Swallet	38,688
Waldegrave Pool	21,938
Waldegrave Dam	43,437
Plantation Swallet	55,375

The figures are the means of five determinations

Table 3.5 : Concentration of Lead (μg/g) in Soils and Sediment Samples Collected from Iraq. Analysis by FAAS

Sample Site	Lead Concentration
Baghdad Soil (Al-Rashied Road)	51
Tigris Sediment (Republic Bridge)	27
Euphrates Sediment (Al-Ramida)	40

The figures are the mean of two determinations

Vegetation samples were also collected from the Mendip Hills, the samples were carefully separated from the soil, washed with DDW, dried between two filter papers and finally dried at 105°C for 24 hrs; the dry weights were recorded. The samples were digested in concentrated nitric acid and the analysis was carried out as for the sediment and soil samples. The results obtained are presented in Table 3.6.

Table 3.6 : Concentration of Lead (μg/g) in Vegetation Samples Collected from the Mendip Hills. Analysis by FAAS

Vegetation Samples	Lead Concentration
Juncus effusus	1,175
Elodea canadensis	6,650
Ranunculus peltatus	375
Pseudoscleropodium purum	50
Cladonia rangiformis	75

The figures are the mean of two determinations

The Tessier et alia (16) extraction scheme was performed on the following samples:

1) Caradon native sediment

2) Caradon secondary rock

3) Drain Luckett sediment

4) Restronguet Creek No. 3 sediment

5) Adit Bridge No. 8 sediment

6) Adit No. 8 sediment.

The first three samples were examined for copper, while the others were examined for Ca, Mn, Fe, Ni, Cu, Zn, Cd and Pb. The analysis was carried out on duplicate subsamples of the same material and blanks were run to control any contamination. The scheme most often used is outlined in Figure 3.13. The sequential extraction procedure was applied to 0.5 g of each sample contained in 50 cm^3 polypropylene centrifuge tubes. The extracts were examined by FAAS for the trace metals. The results obtained are given in Tables 3.7 - 3.12.

gure 3.13 : Sequential Extraction Procedure for the Speciation of Metals in Sediments

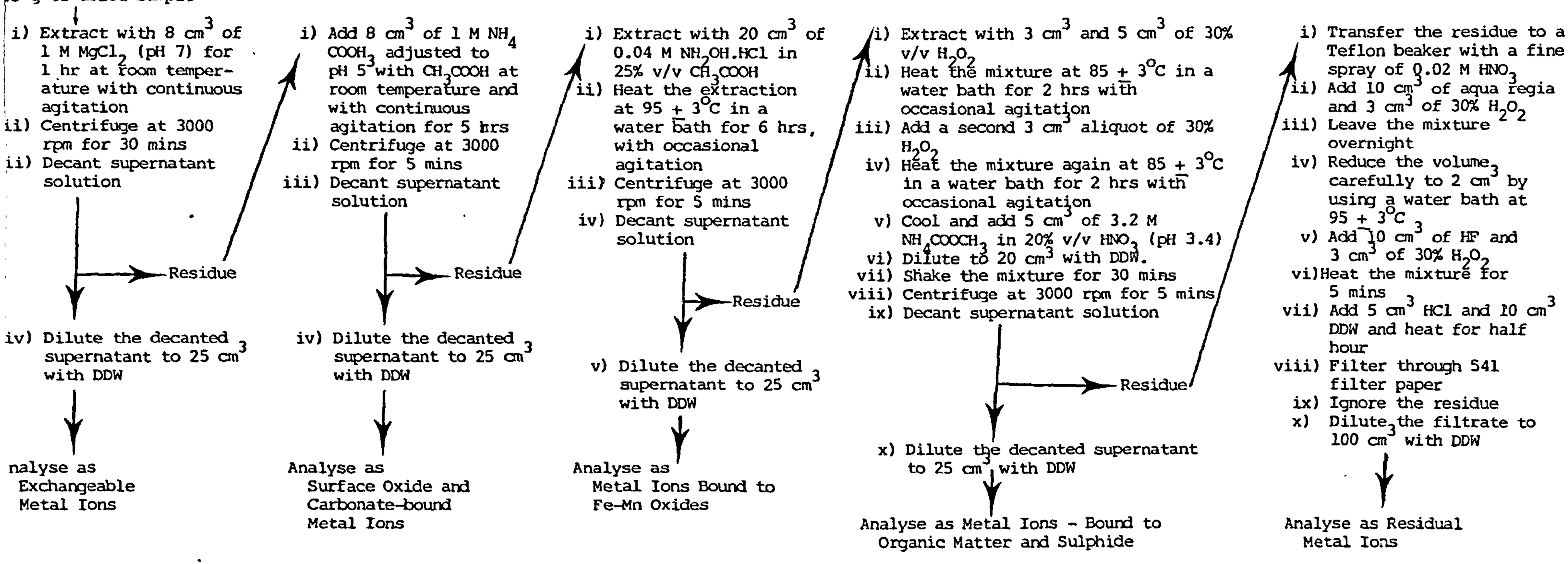

Table 3.7 : Sequential Extraction of Copper from Caradon Native Sediment (Analysis by FAAS)

Fraction	Cu (μg/g)	Percentage Association
Exchangeable	53	0.564
Carbonate	103	1.096
Fe-Mn oxides	N.D.	
Organic	138	1.469
Residual	9,100,[a] 17,420[b]	96.870
Total	9,394	
HNO_3 acid digest	35,772	

Table 3.8 : Sequential Extraction of Copper from Caradon Secondary Rock (Analysis by FAAS)

Fraction	Cu (μg/g)	Percentage Association
Exchangeable	325	0.788
Carbonate	1,250	3.033
Fe-Mn oxides	N.D.	
Organic	10,625,[a] 15,500[b]	25.788
Residual	29,000,[a] 53,100[b]	70.388
Total	41,200	
HNO_3 acid digest	46,200	

a = sequential extraction

b = direct extraction

N.D. = Cu < 25 μg/g

Table 3.9 : Sequential Extraction of Copper from Drain Luckett Sediment (Analysis by FAAS)

Fraction	Cu (μg/g)	Percentage Association
Exchangeable	425	1.626
Carbonate	2,063	7.894
Fe-Mn oxides	21,250	81.321
Organic	1,988	7.607
Residual	405	1.549
Total	26,131	
HNO_3 acid digest	51,230	

Table 3.10 : Sequential Extraction of Ca, Mn, Fe, Ni, Cu, Zn, Cd, Pb (μg/g) from Restronguet Creek No. 3 Sediment (Analysis by FAAS)

Fraction	Ca	Mn	Fe	Ni	Cu	Zn	Cd	Pb
Exchangeable	1,359	7	N.D.	N.D.	N.D.	218	51	6
Carbonate	76	N.D.	N.D.	N.D.	50	128	N.D.	40
Fe-Mn oxides	1,340	50	13,360	N.D.	215	770	N.D.	231
Organic	1,247	16	11,250	N.D.	650	1,185	N.D.	12
Residual	370	63	29,282	N.D.	975	5,400	N.D.	198
Total	4,392	136	53,890	N.D.	1,890	7,701	51	487
HNO_3 acid digest	5,371	310	55,850	N.D.	3,270	29,315	58	501

N.D. = Ni < 50 μg/g, Mn < 5 μg/g, Cd < 5 μg/g, Cu < 25 μg/g, Fe < 25 μg/g

Table 3.11 : Sequential Extraction of Ca, Mn, Fe, Ni, Cu, Zn, Cd and Pb (μg/g) from Adit No. 8 Sediment (Analysis by FAAS)

Fraction	Ca	Mn	Fe	Ni	Cu	Zn	Cd	Pb
Exchangeable	1,205	100	N.D.	N.D.	N.D.	23	N.D.	N.D.
Carbonate	1,433	140	73	N.D.	N.D.	41	N,D.	N.D.
Fe-Mn oxides	202	130	4,000	N.D.	N.D.	86	N.D.	126
Organic	1,153	61	3,500	N.D.	100	78	N.D.	114
Residual	286	26	17,800	N.D.	75	85	N.D.	N.D.
Total	4,279	457	25,373	N.D.	175	313	N.D.	240
HNO_3 acid digest	4,861	763	32,850	N.D.	90	303	N.D.	368

N.D. = Fe < 25 μg/g, Pb < 10 μg/g, Ni = 50 μg/g, Cd < 5 μg/g

Table 3.12 : Sequential Extraction of Ca, Mn, Fe, Ni, Cu, Zn, Cd and Pb (μg/g) from Adit Bridge No. 8 Sediment (Analysis by FAAS)

Fraction	Ca	Mn	Fe	Ni	Cu	Zn	Cd	Pb
Exchangeable	854	263	57	N.D.	35	84	N.D.	401
Carbonate	1,265	3.0	89	N.D.	953	291	N.D.	252
Fe-Mn oxides	380	394	14,860	N.D.	132	1,900	N.D.	1,175
Organic	1,467	1.0	487	N.D.	1,406	62	N.D.	N.D.
Residual	40	43	11,083	N.D.	156	14	N.D.	N.D.
Total	7,426	704	26,576	N.D.	2,682	2,351	N.D.	1,828
HNO_3 acid digest	7,616	967	29,144	N.D.	84	2,405	N.D.	2,405

N.D. = Ni < 50 μg/g, Cd < 5 μg/g, Fe < 25 μg/g

Electron microscopy was used to check the efficiency of the chemical extractants used in the Tessier scheme. Five treated samples of Restronguet Creek No. 3 sediment using the Tessier scheme and untreated sample were examined. The results were recorded in the form of photographs (Figures 3.14 - 3.17) and X-ray spectra (Figures 3.18 - 3.21).

The sediment samples were also prepared for microanalytical determination of C, H, N by grinding and mixing. The technique only requires a small sample weight (1-3 mg), and therefore the sample must be as homogeneous as possible to produce a representative sample. The sample was placed into a platinum boat and placed in the combustion tube. The sample was flooded with oxygen and heated to 1000^{o}C. The gaseous combustion products were flushed by a stream of helium through the reduction tube. The gases, N_2, CO_2, H_2O were measure by passage through a sensitive thermal conductivity cell. The sample was allowedtto cool and then reweighed. The method was used for total carbon determination. The inorganic carbon was measured by addition of dilute acid such as phosphoric acid and measuring inorganic carbon as CO_2. The results obtained are presented in Table 3.13

Table 3.13 : Fraction of Carbon in Sediments

Sample	% C[a]	% C[b]	% C[c]	% H	% N
Adit Bridge No. 8	0.72	0.32	0.40	0.33	0.10
Restronguet Creek No. 3	0.94	0.56	0.38	0.51	0.14
Adit No. 8	5.49	0.56	4.93	0.91	0.39
Luckett Drain	0.56	0.30	0.26	0.46	0.07
Caradon secondary rock	0.69	0.22	0.47	0.21	0.04
Mineries Pool exit	3.34	2.05	1.29	0.30	0.13

a = Total Carbon; b = Inorganic Carbon; c = Organic Carbon (Total - Inorganic)

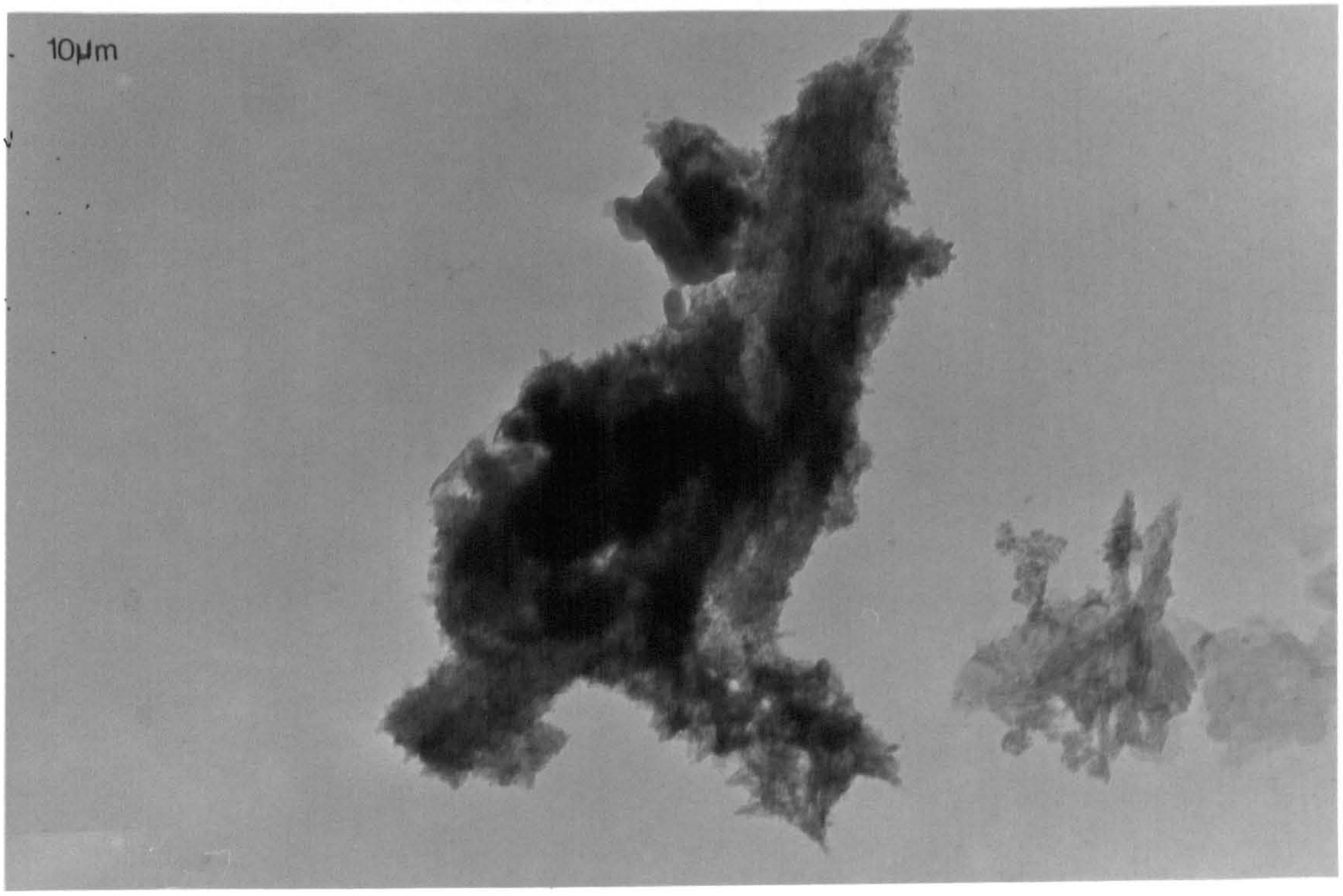

FIG. 3.14 ELECTRON MICROGRAPH OF RESTRONGUET CREEK No. 3 SEDIMENT (GEL-LIKE MATERIAL)

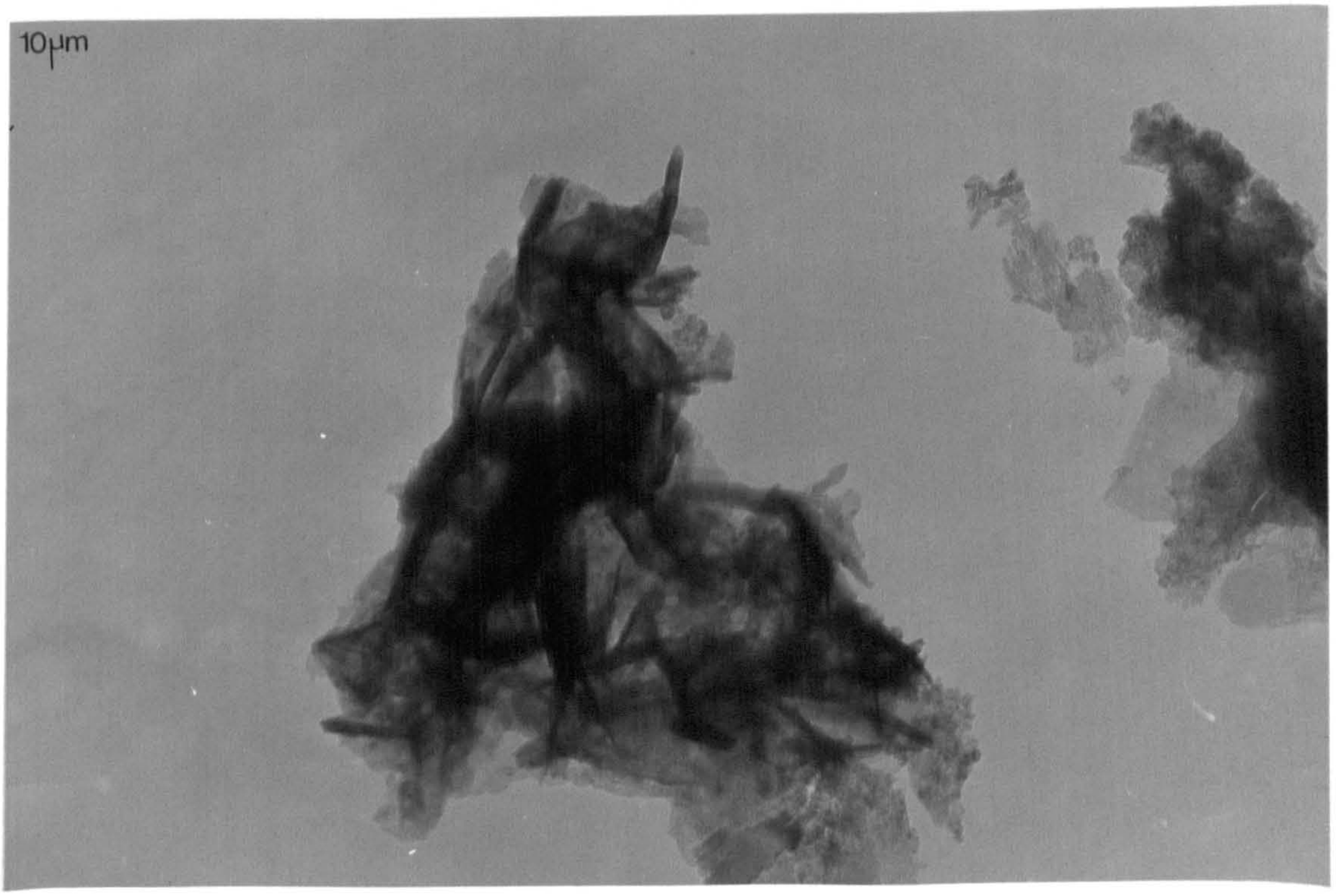

FIG. 3.15 ELECTRON MICROGRAPH OF RESTRONGUET CREEK No. 3 SEDIMENT (SHEET-LIKE CRYSTAL)

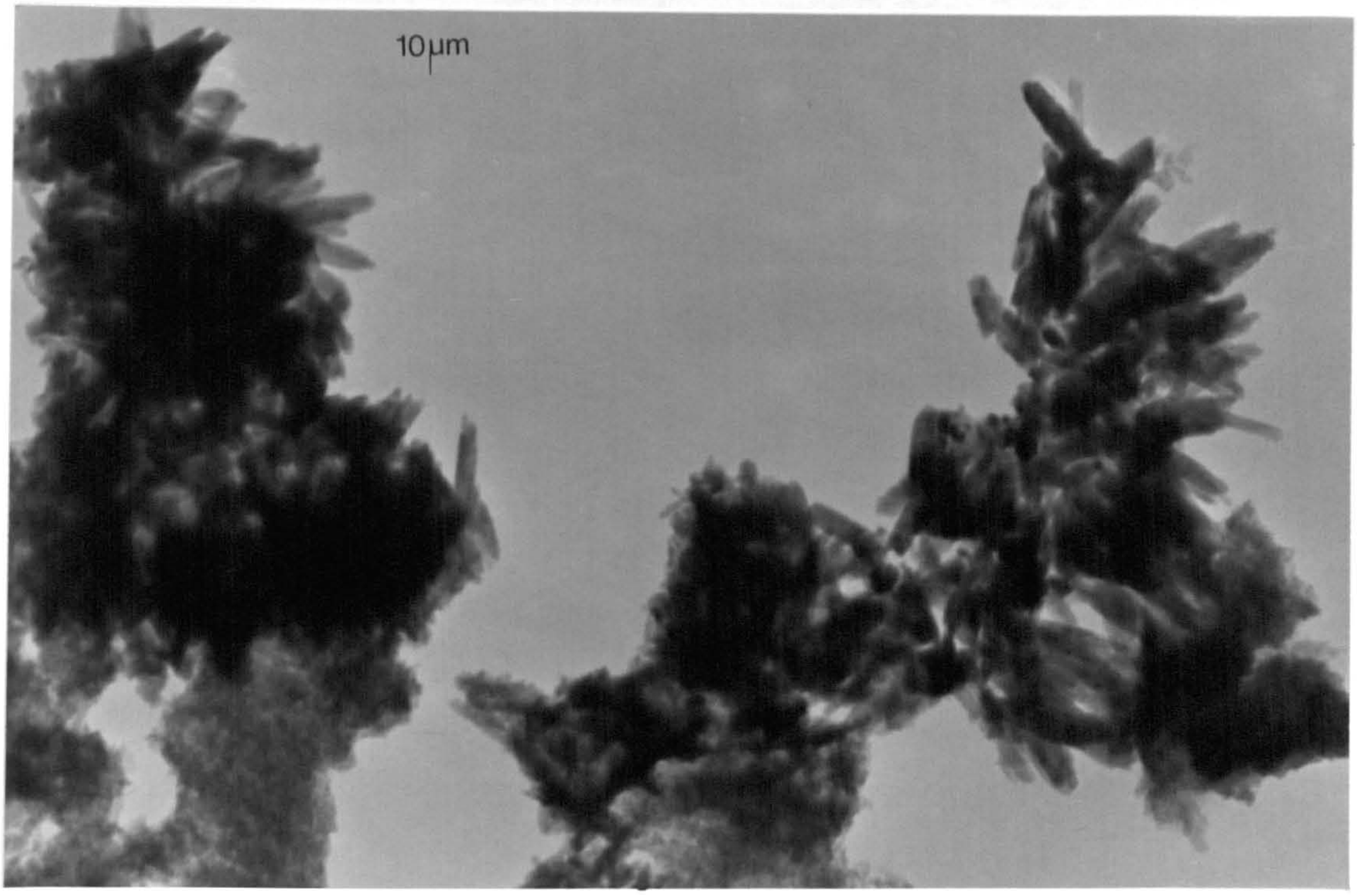

FIG. 3.16 ELECTRON MICROGRAPH OF RESTRONGUET CREEK No. 3 SEDIMENT (ACICULAR CRYSTAL)

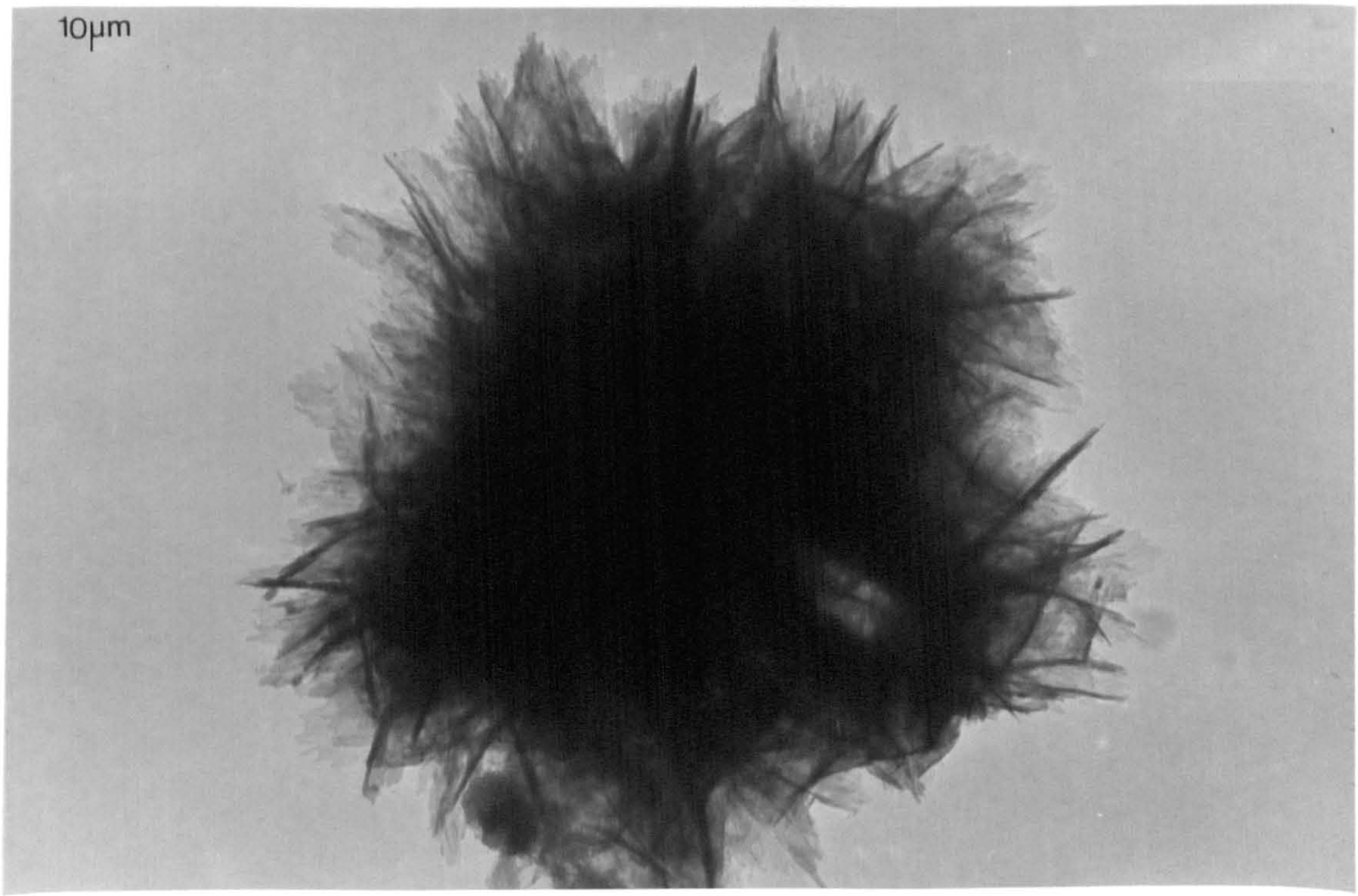

FIG. 3.17 ELECTRON MICROGRAPH OF RESTRONGUET CREEK No. 3 SEDIMENT (HAIRY SPHERE)

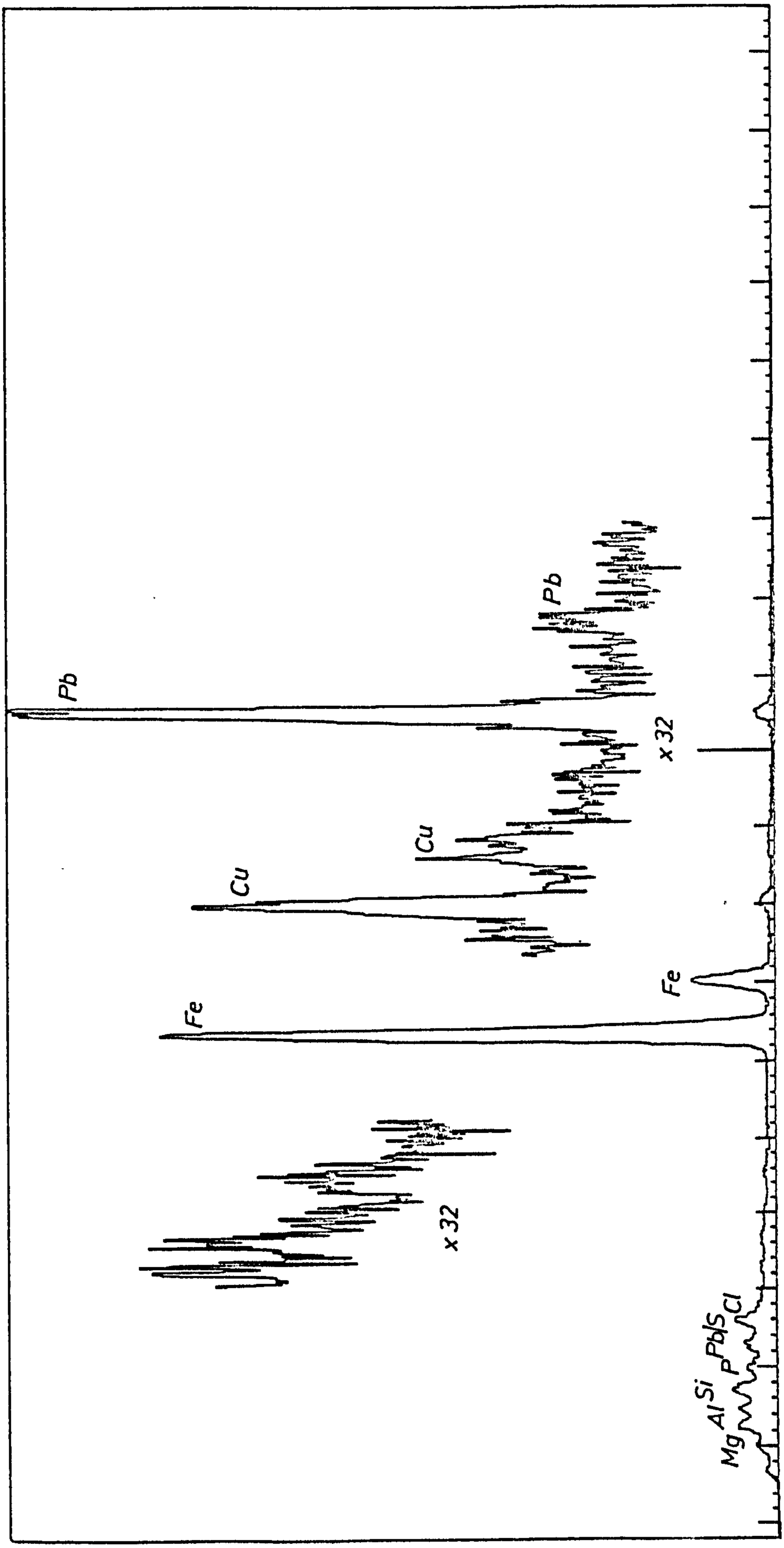

FIG. 3.18 ELECTRON MICROGRAPH SPECTRUM OF UNTREATED RESTRONGUET CREEK No. 3 SEDIMENT

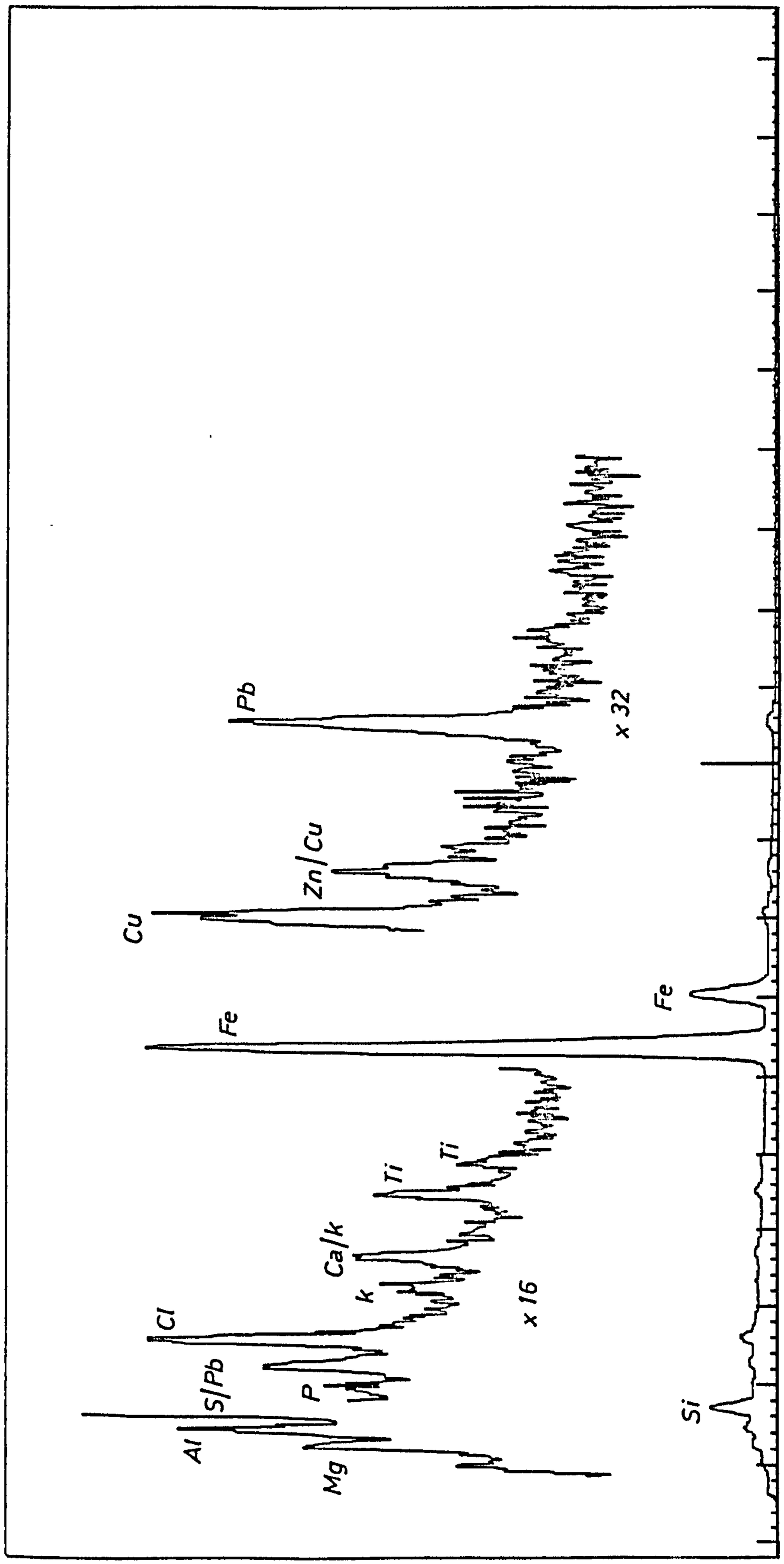

FIG. 3.19 ELECTRON MICROGRAPH SPECTRUM OF RESTRONGUET CREEK No.3 SEDIMENT TREATED WITH IM $MgCl_2$ (pH 7)

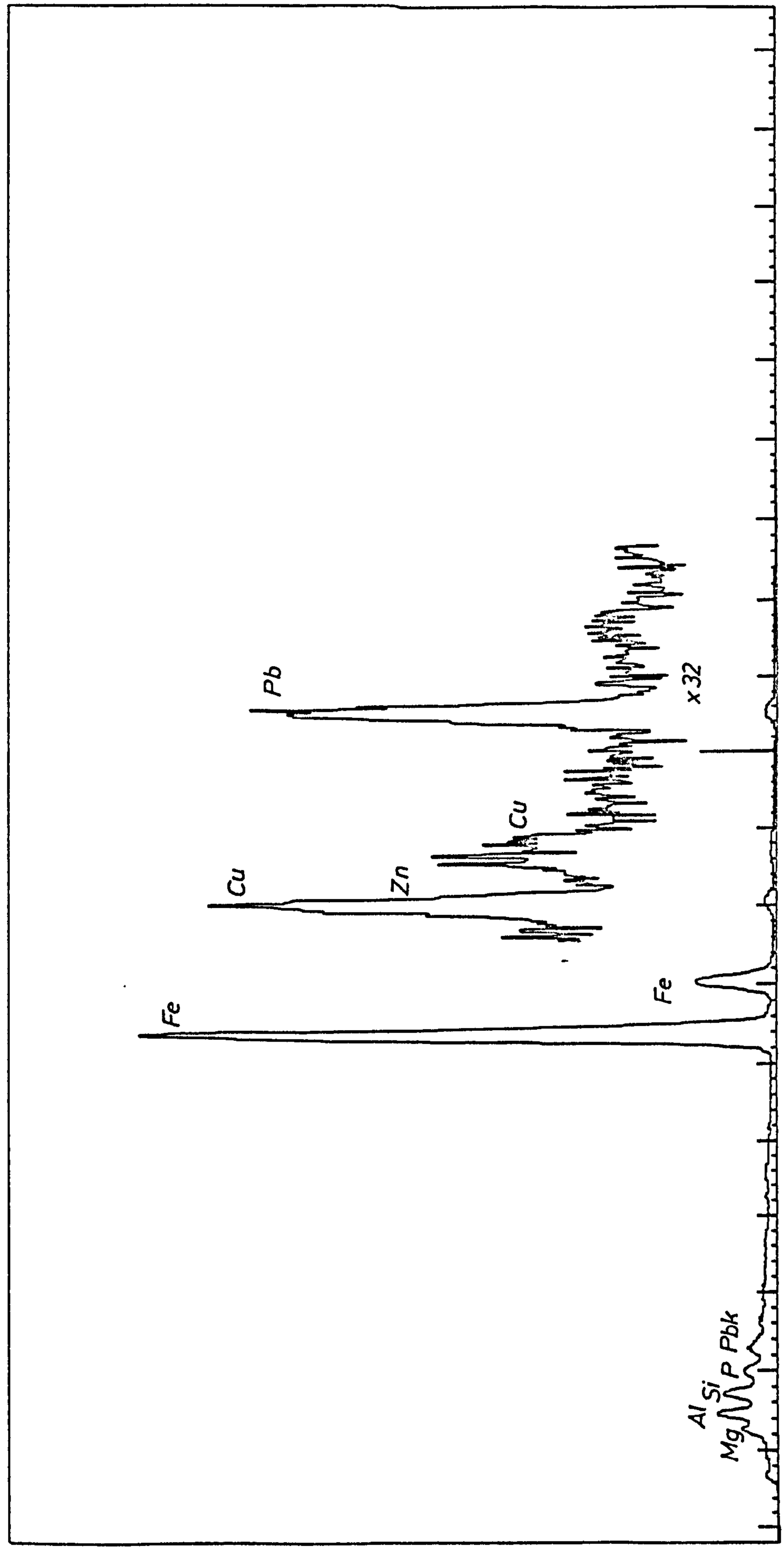

FIG. 3.20 ELECTRON MICROGRAPH SPECTRUM OF RESTRONGUET CREEK. No. 3 SEDIMENT TREATED WITH $1M\ NH_4\ COOCH_3$ (pH5)

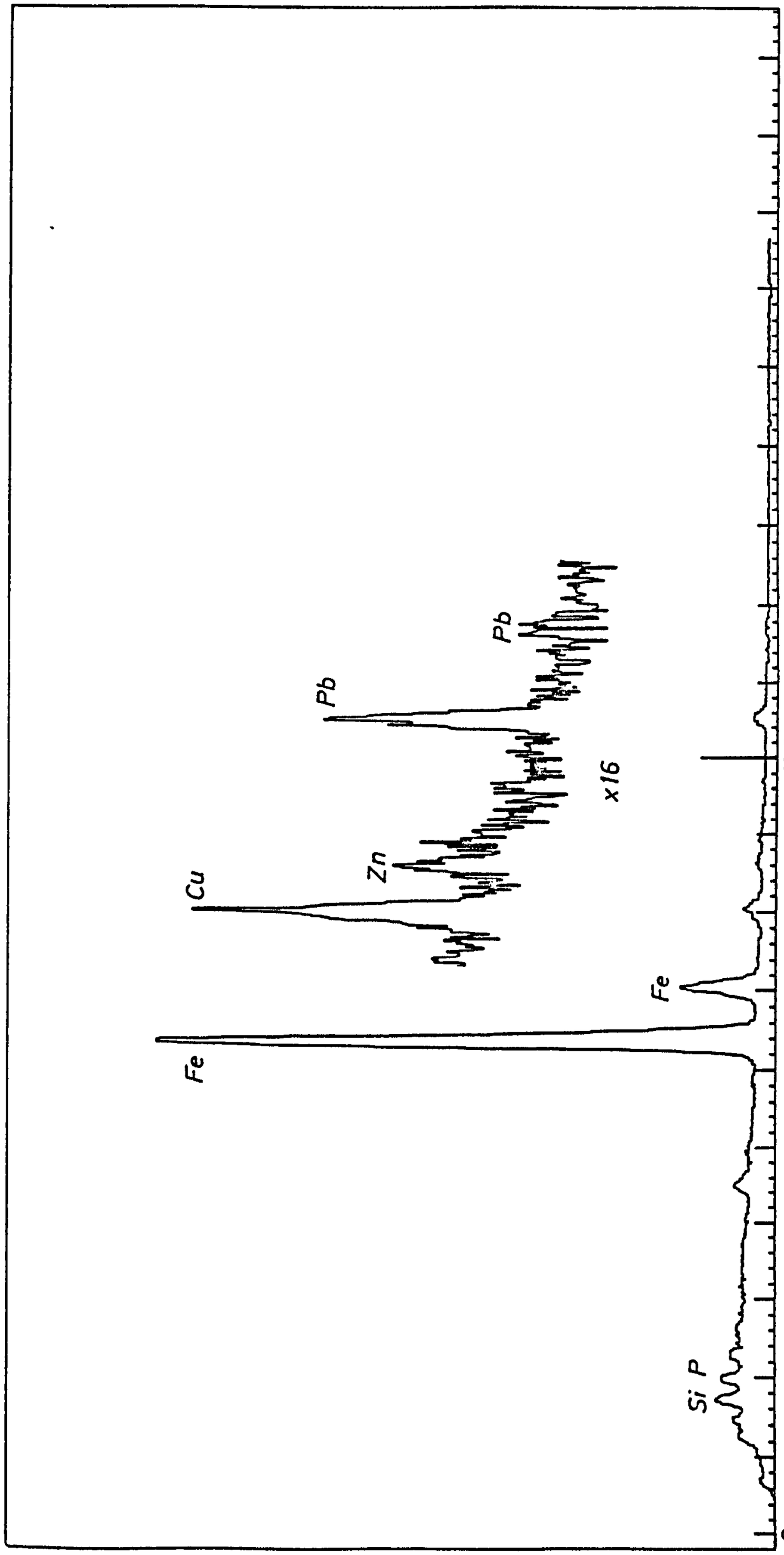

FIG. 3.21 ELECTRON MICROGRAPH SPECTRUM OF RESTRONGUET CREEK No. 3 SEDIMENT TREATED WITH 30% (v/v) H_2O_2

d) Apparatus and Instrumental Parameters

. The determination of total lead in water samples was carried out by GFAAS using a Pye Unicam system SP-9, which comprised the following instrumentation :-

1. SP-9 atomic absorption spectrophotometer, equipped with graphite cuvette
2. SP-9 Computer
3. SP-9 Video furnace programmer
4. SP-9 Autoanalyser

The instrumental conditions for determination are given in Table 3.14.

Table 3.14 : Instrumental Conditions for Analysis by GFAAS

(a) Spectrometer Parameters

	wavelength, nm	lamp current	band pass, nm
Lead	217.0	5	0.5

(b) Electrothermal Heating Process

	phase	process	temperature ^{o}C	time(s)	ramp ($^{o}C/s$)
Lead	1	Drying	125	20	0
	2	Ashing	500	40	0
	3	Atomisation	1600	3	0
	4	Cleaning	2500	3	0

A PAR 174A polarographic analyser with Model 315A automated electroanalysis controller was used for DPASV, the voltammograms were recorded on a Hewlett-Packard 7040A X-Y recorder. DPASV was used for the

determination of labile lead in water, the instrumental parameters selected for voltammetric measurement are given in Table 3.15.

Table 3.15 : Instrumental Conditions for Analysis by DPASV

Electrolyte	:	5 cm^3 of acetate buffer (pH 5)
Initial Potential	:	-0.85 V / Ag/AgCl
Final Potential	:	-0.05 V / Ag/AgCl
Condition Potential	:	+0.00 V
Purge time	:	5 minutes
Deposition time	:	120 sec
Equilibration time	:	30 sec
Working electrode	:	HMDE
Current range	:	5 uA
Potential range	:	3.0 V
Modulation amplitude	:	25 mv
Scan rate	:	5 mv/sec
Pulse Repetition period	:	0.5 sec
Auxiliary electrode	:	platinum wire
Reference electrode	:	Ag/AgCl saturated with 3 M KNO_3
Low pass filter	:	off
Scan direction	:	" + "
Display direction	:	" - "
Mode	:	Differential pulse

An Instrumental Laboratory Ltd. atomic absorption spectrometer model 151 (IL 151) with background correction was used for the determination of lead in sediments, soils and vegetation samples collected from the Mendip Hills. The IL 151 was also used for the determination of lead in the Iraqi soils and sediments, as were the variety of elements in the Restronguet Creek No. 3, Adit No. 8 and Adit Bridge No. 8 samples. The instrumental conditions used were as in Table 3.16.

Table 3.16 : Atomic Absorption Operating Conditions and Statistical Information Obtained using LSQ Analyses

Metal	Wavelength (nm)	Flame	Correlation Coefficient	Equation of Regression Line y = mx + c
Ca	422.7	Air - Acetylene	0.9890	y = 0.051x + 0.008
Mn	279.5		0.9940	y = 0.433x + 0.048
Fe	248.3		0.9970	y = 0.125x + 0.1081
Ni	232.0		0.9874	y = 0.0920x + 0.3617
Cu	324.7		0.9969	y = 0.430x - 0.1690
Zn	213.9		0.9837	y = 0.7684x + 0.1994
Pb	217.0		0.9995	y = 0.1409x + 0.0334
Cd	228.8		0.9991	y = 0.924x + 1.1840

An unsuccessful attempt was made to determine Cu and Cd by fitting a silica tube (Figure 2.4) on a Varian AA5 spectrophotometer. The failure may have been due to the smooth surface silica tube having insufficient surface area to trap a large enough number of atoms to produce an atomic absorption signal.

The AAS determination of trace metals involved the use of standard solutions for a direct comparison measurement with the unknown sample. The standards were prepared by dilution of the 1000 $\mu g/cm^3$ to give a range of standards suitable for the calibration plots. Figures 3.22 and 3.23 show the calibration graphs for cadmium and lead. Since the working curve can change from day to day due to small variations in lamp and flame conditions, the instruments had to be recalibrated for each batch of samples. The analyte concentration in sediment, soil and vegetation samples were determined by the equation :-

$$y = \frac{xVI}{W} \qquad \ldots\ldots \quad [3.3]$$

where y = concentration in ug/g of metal in sample

x = concentration in ug/cm^3 of metal determined from the calibration graph

V = final volume (cm^3) of analyte solution

I = dilution factor (if any)

W = weight of sample (g)

The DPASV analyses were performed on 5 cm^3 aliquots of the water samples diluted with 5 cm^3 of acetate buffer, in a polarographic cell. Sample calculation for the DPASV results are shown in Table 3.17.

FIG. 3.22 AAS CALIBRATION GRAPH FOR CADMIUM

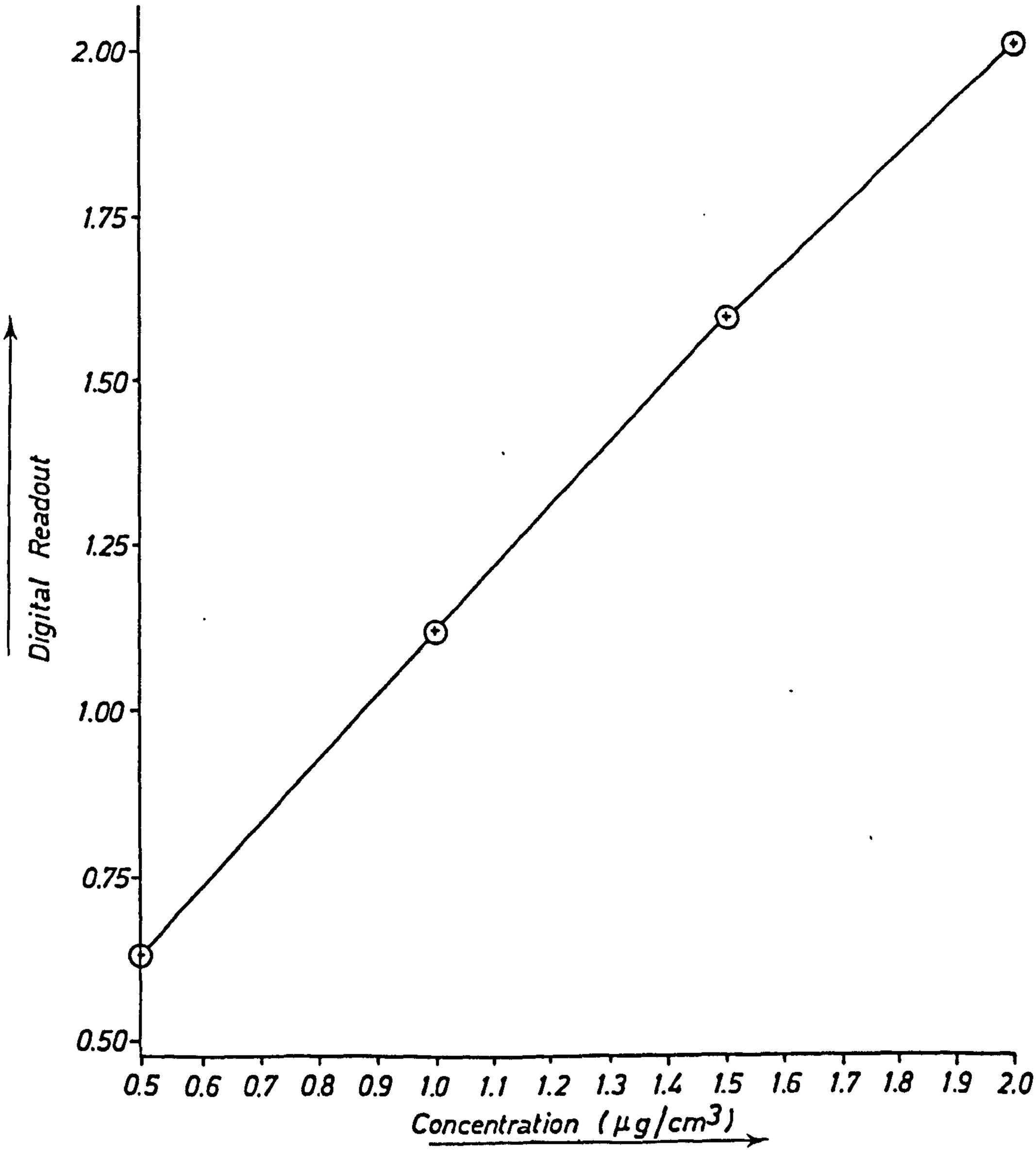

FIG. 3.23 AAS CALIBRATION GRAPH FOR LEAD

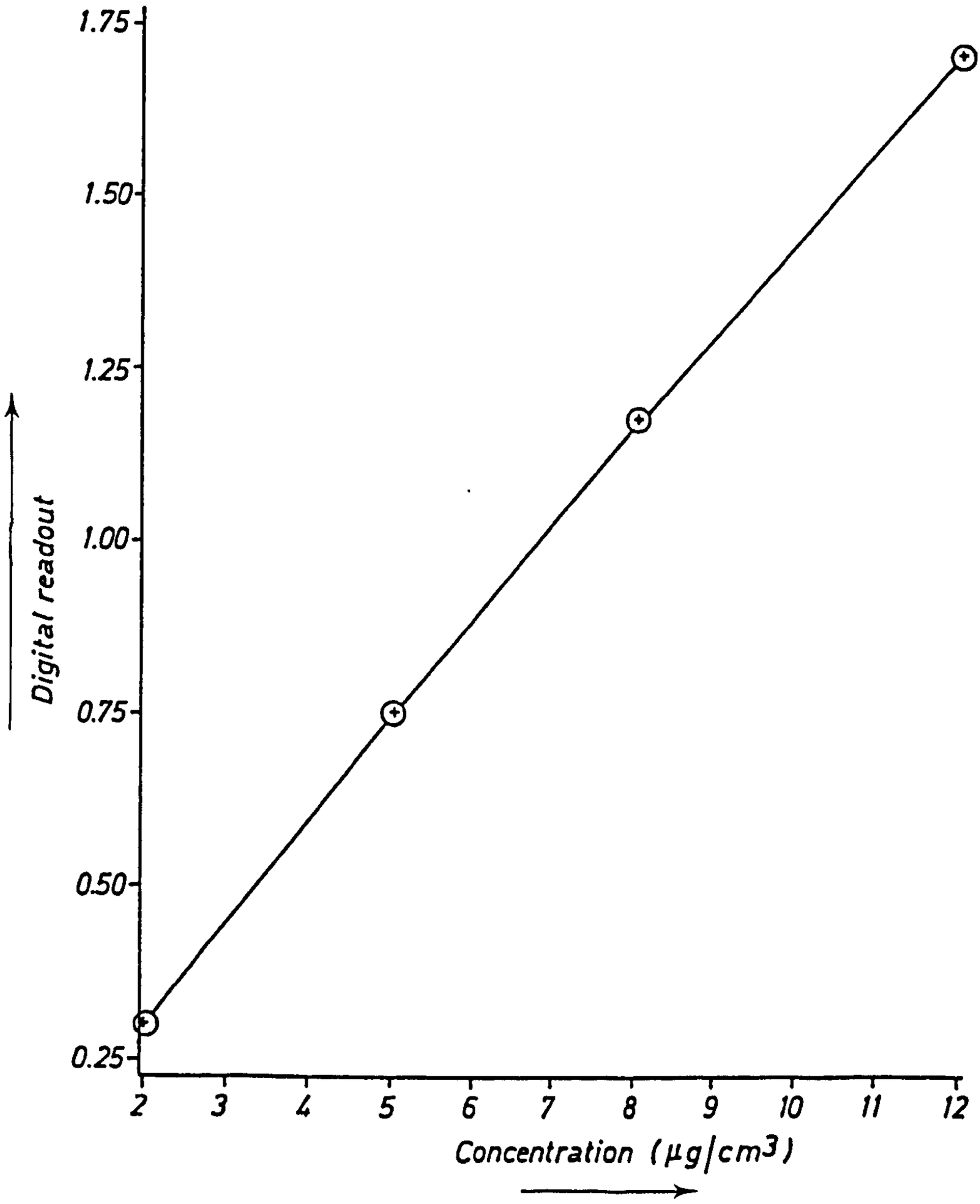

Table 3.17 : Sample calculation for DPASV Results. For example, Concentration of Lead in Waldegrave Pool (W_1)

Peak Height on voltammogram, cm

Addition of 10 $\mu g/cm^3$ of lead solution

Vol, μl	Lead, μg	Peak height
0	0	2.6
20	200	6.5
40	400	11.8
60	600	14.8

For regression line,* $y = mx + c$

m, ng cm^{-1}	0.0210
c, cm	2.6083
correlation coefficient	0.9949
Lead content (-x) of original sample + buffer, ng (for y = 0)	123.878
Lead content (-x) of 5 cm^3 buffer, ng	< 0
Lead concentration of original sample, ng/cm^3	24.77

* The regression line was calculated from the true lead contents of the addition, calculated from the actual concentration. The line was obtained by the least squares method using a "PET" computer.

3.3 DISCUSSION

a) Water Analysis

Table 3.1 indicates the GFAAS and DPASV determination of lead. GFAAS determination gives total lead while DPASV indicates that lead is present as an electroactive species. Florence et alia (20) determined the total and labile lead in sea water by DPASV after concentration on Chelex-100. The determination of total lead needs an acid digested sample, thus analysis by DPASV is not suitable due to the hydrogen peak swamping the position of the lead potential. For this reason GFAAS analysis was chosen. However, GFAAS determination of total lead caused considerable problems; two determinations of the sample had high standard deviations. The problems were possibly caused by background interference due to the radiation from the heated cuvette. DPASV with pH 5.0 has been employed for the determination of labile metal by many workers (21-23); pH 5.0 is the optimum for the formation of many electroactive species. At higher pH values an electroinactive carbonate species will be formed (23), so DPASV with pH 5.0 was used in the present work for determination of labile lead. Table 3.1 shows that lead determined by DPASV was lower than the lead level obtained by GFAAS. Thus the release of lead by GFAAS indicated that bound lead was present; the lead was probably present as colloidal or other non-electroactive species. The levels of total and labile lead are represented as histograms in Figure 3.24. Lead levels in the water of the Mendip streams were found to be much lower than in the sediments (Table 3.4), which may be due to the alkaline pH of Mendip water, the lead being precipitated from the water. In view of the limestone nature of the Mendip streams, lead being trapped, probably as the carbonate, is most likely.

In water samples, the general rule is that the metal level decreases

FIG. 3.24 DISTRIBUTION OF LEAD SPECIES IN MENDIP STREAMS

T = Total lead

L = Labile lead

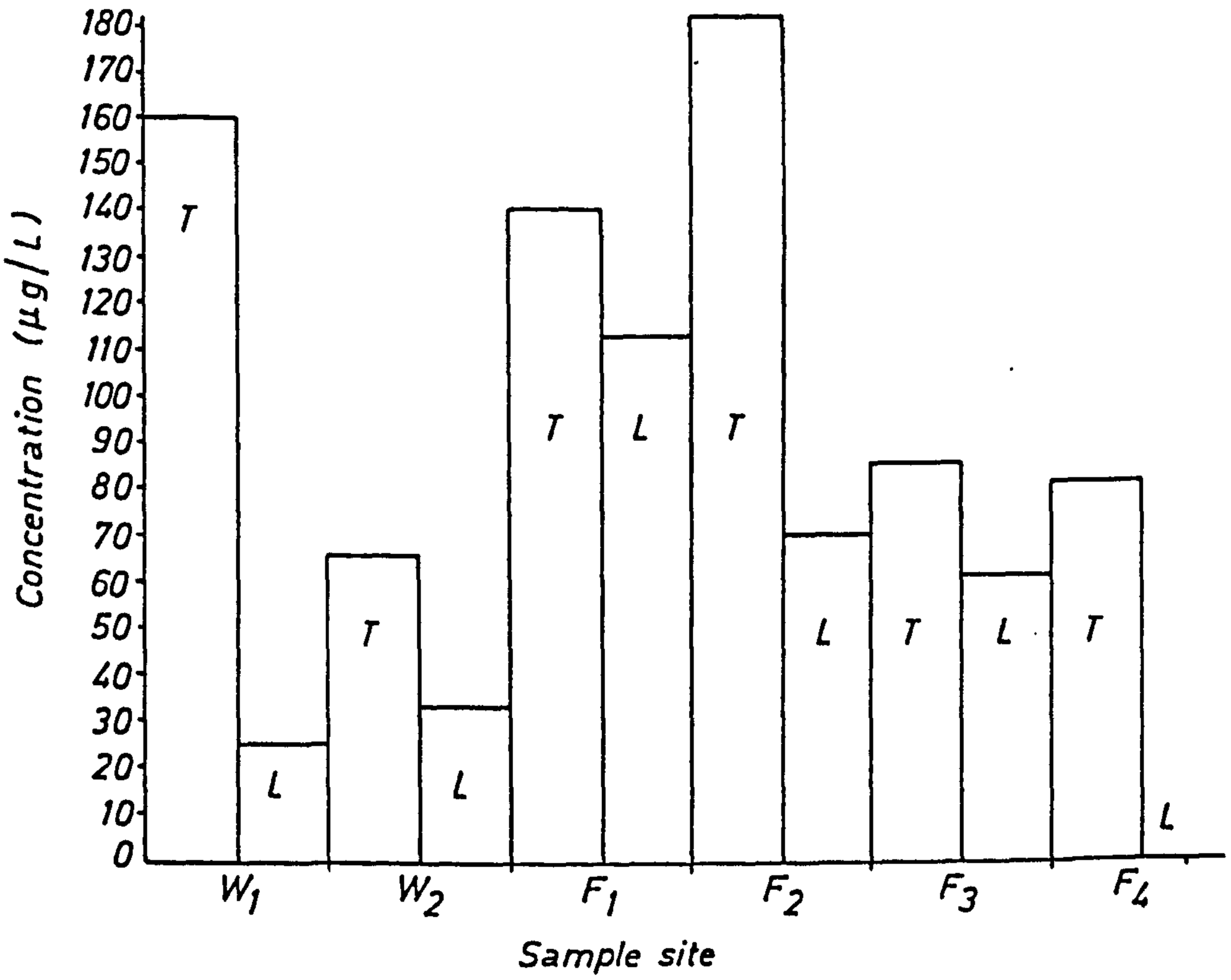

with decrease of filtered size fraction; this is due to removal of particulate metal fractions from the solution. The results in Table 3.2 deviate from this rule except W_1 and F_4 samples. The deviation from the rule may be due to sample contamination with Pb or organic material leached from the filter. Table 3.2 indicates high sample contamination with Pb, in particular samples W_2 and F_2 when the results are compared with total concentration of lead in Table 3.1. When the results in Table 3.2 are compared with the results of other workers (Table 3.18), significant differences may be observed. The difference may be due to different geographical locations and methods of analysis used. Figure 3.25 depicts histogrammatically the results in Table 3.2.

Table 3.3 gives the lead concentration in Iraqi water; a high concentration was found at sample site TS, which may arise from a localised discharge of effluent from Baghdad city. The results in Table 3.3 are 10 times higher than the lead levels found by Abaychi et alia (24) at Shatt Al-Arab river which originates from the confluence of two major rivers of Iraq (Tigris and Euphrates) at Qurna, but the level of lead in the Iraqi water was so low as to prevent the possibility of speciation studies. Comparison between the results obtained by this work and Abaychi et alia (24) indicates that the lead concentration decreased as the two rivers join together due to a dilution effect. Because of the low concentration of lead in Iraqi water, concentration was needed. Since the chelation is pH dependent, many workers (25-27) have used Chelex-100 in forms other than the hydrogen format to concentrate trace metal in natural water, thus Chelex-100 in calcium form was used in the present work.

Figure 3.26 shows histogrammatically the results in Table 3.3.

FIG. 2.25 DISTRIBUTION OF LEAD IN MENDIP STREAM FILTERED AT DIFFERENT FRACTION SIZES

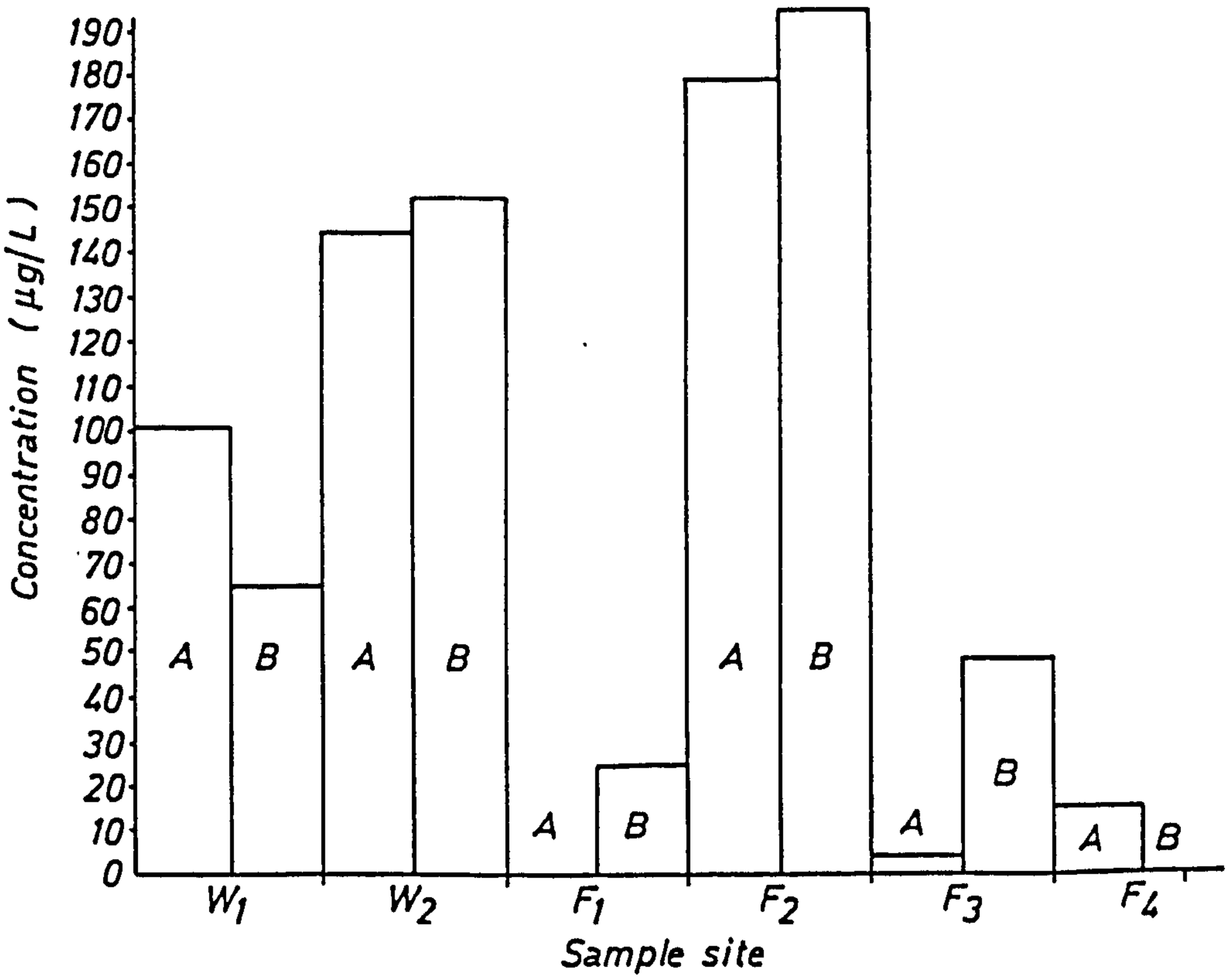

A = 0.45 µm
B = 0.1 µm

FIG. 3.26 DISTRIBUTION OF TOTAL LEAD IN IRAQI WATER SAMPLES

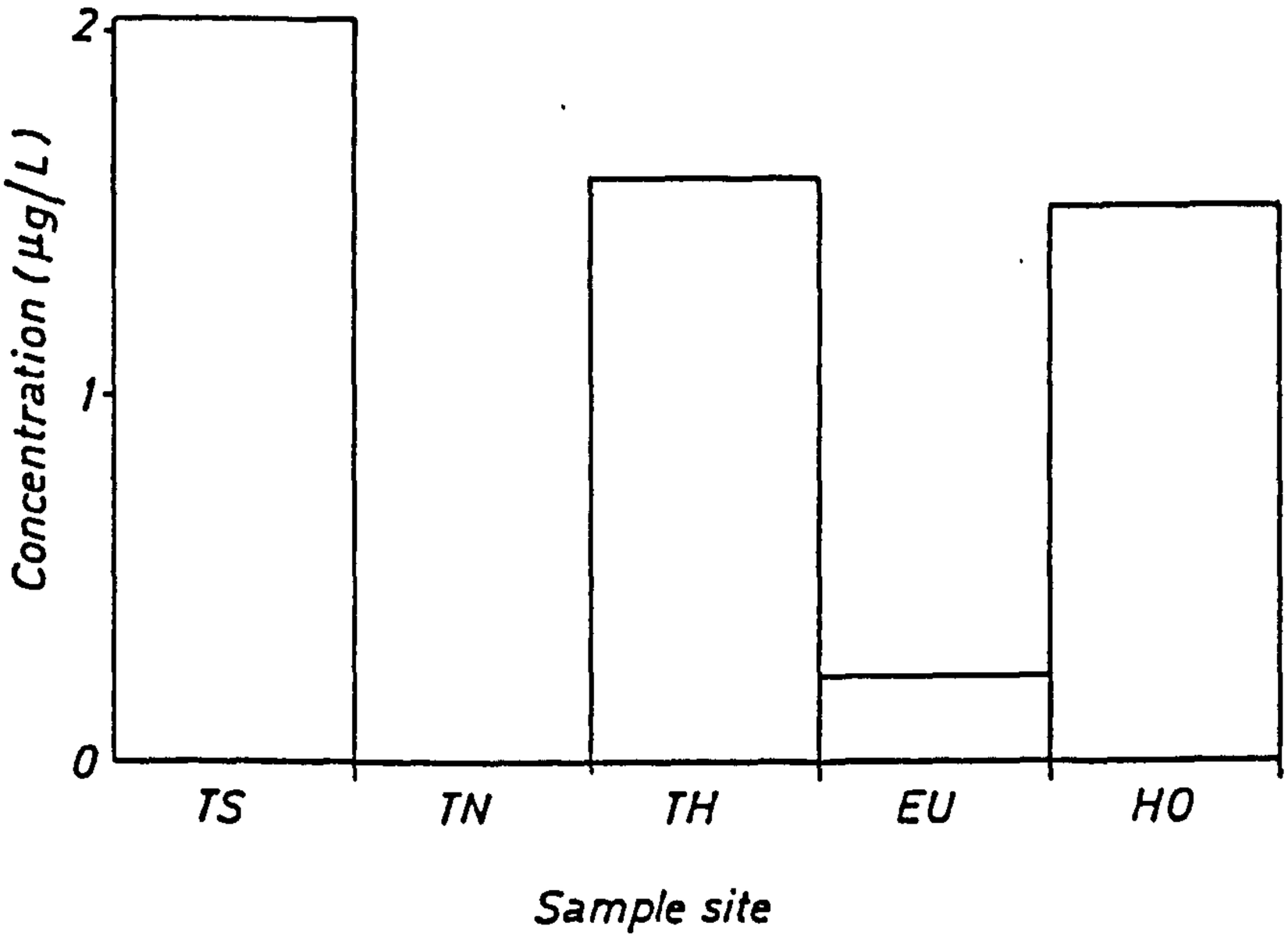

Table 3.18 : Comparison of Results with Salter (23) and Jordao (28)

Sample Site	Size Fraction (μm)	Concentration of Lead (μg/L)	Reference
Waldegrave Pool	0.45	24	(23)
	0.45	165	(28)
	0.45	101.43	This work
	0.1	1	(23)
	0.1	N.D.	(28)
	0.1	64.65	This work

b) Sediments and Soils Analysis

i) Acid Extractable Metal Content of Samples

The results in Table 3.4 indicate that these samples were highly contaminated with Pb, reflecting the history of lead mining in the Mendip Hills. Due to the high metal content of the samples, they had to be submitted to a series of dilution steps before measurement of the analytical signals.

Table 3.5 shows the lead content of Iraqi sediment and soil was not elevated, however, the lead level may arise from the deposition from leaded gasoline used in vehicles.

Due to the difficulty of separation of the roots of vegetation samples from adhering soils, the analyses were carried out on the green part of the plant samples listed in Table 3.6. The results in Table 3.6 indicate that the Elodea canadensis species is highly contaminated with lead.

ii) Sequential Extraction

The results obtained from the sequential extraction of copper on Caradon native sediment, Caradon secondary rock and Luckett sediment are shown in Tables 3.7 - 3.9 respectively. The prime observation is that the total copper (acid digest) value is higher than the total from the sequential extractions, this may be due to sample loss in the sequential extraction scheme, probably as a result of the number of steps involved. Loss of sample was found to be a source of error in this study, resulting from the "bubbling" effect produced when H_2O_2 was added to samples of high organic content such as the Adit Bridge No. 8 sediment. The second suggestion is that the irreproducible results are due to the natural degree of variation in metal concentrations resulting from inhomogeneities in the sample. The third observation is that the chemical extractant affects more than one geochemical phase, i.e. the processes are not selective. For example, the copper content of the residual fraction in Caradon native sediment and Caradon secondary rock was 9,100 and 29,000 μg/g respectively by using sequential extraction while with direct extraction was found 17,420 and 53,100 μg/g respectively. The problem was also noticed with other fractions, copper levels extracted from the organic fraction in Caradon secondary rock using sequential and direct extraction was found to be 10,625 and 15,500 μg/g respectively. The ratio between the sequential to direct extraction of copper (II) in the residual fraction of Caradon native sediment and Caradon secondary rock was found to be 0.31232 and 0.3280 respectively, this indicates that the same systematic error occurs in these samples during the preparation of samples for the analysis.

Most investigations (29,30) have reported that the copper is predominantly in the organic phase due to its ability to coordinate with organic matter. In the present study, it was found that most of

the copper (96.87%) in Caradon native sediment and (70.38%) in Caradon secondary rock was associated with the residual fraction. In contrast, the copper in the Luckett sediment was mainly present in the Fe-Mn oxide phase.

The association in all three cases is not unexpected, reflecting the mineralogical background to the Caradon rocks. Certainly the Caradon native sediment probably has not had sufficient time of exposure (in the above ground mine dumps) to become altered to a major extent. The area here consists generally of a brecciated siliceous rock, while it is occasionally highly chloritic with pyrite, chalcopyrite, chalcocite and small amounts of cassiterite (31). For the Caradon secondary rock, a greater distribution was anticipated largely because of the nature of formation of the material. The species was prepared by deposition of copper from water solution onto a basic rock e.g. limestone. As for the Luckett sediment, because of the nature of the material which was prepared from a complicated mineral processing system, a high level in the residual phase was not expected. Because of the dissolution of extraction procedures used, high concentrations within the Fe-Mn oxide phase were anticipated. In the Luckett system, the levels of iron and manganese caused many difficulties for the mining/processing company, eventually leading to the closure of the processing site. The distribution of copper in the Caradon native sediment, Caradon secondary rock and Luckett sediment are shown diagrammatically in Figures 3.27 - 3.29.

The results obtained from acid digestion (HNO_3) of Restronguet Creek No. 3, Adit No. 8 and Adit Bridge No. 8 sediments are shown in Tables 3.10 - 3.12 respectively. The results indicate that these sediments contain appreciable quantities of iron but also contain Ca, Mn, Cu, Zn, Cd and Pb. The level of nickel was not sufficiently high to

FIG. 3.27 DISTRIBUTION OF COPPER IN CARADON NATIVE SEDIMENT

A = Exchangeable

B = Carbonate

C = Fe -Mn oxide

D = Organic

E = Residual

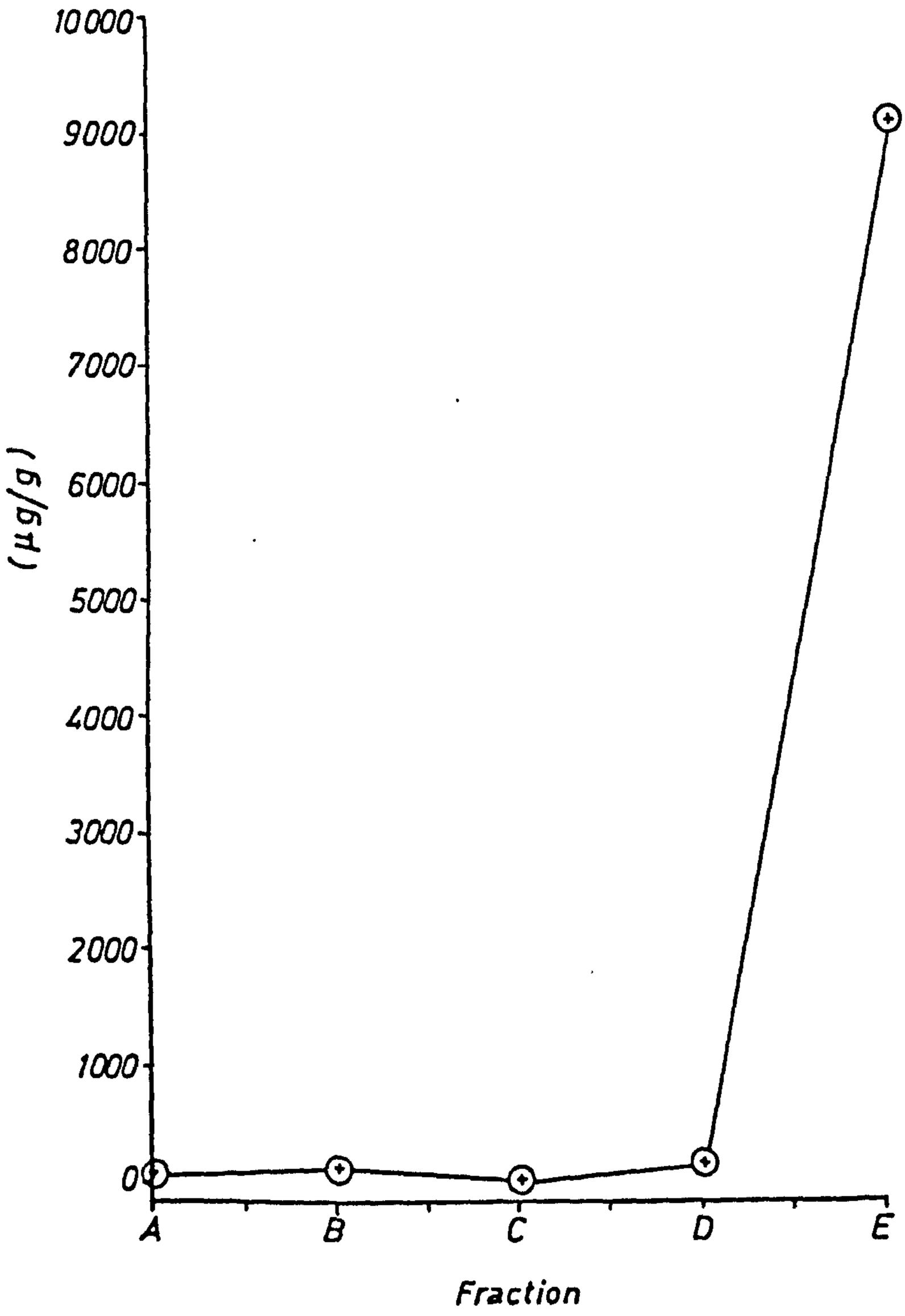

FIG. 3.28 DISTRIBUTION OF COPPER IN CARADON SECONDARY ROCK

A = Exchangeable

B = Carbonate

C = Fe -Mn oxide

D = Organic

E = Residual

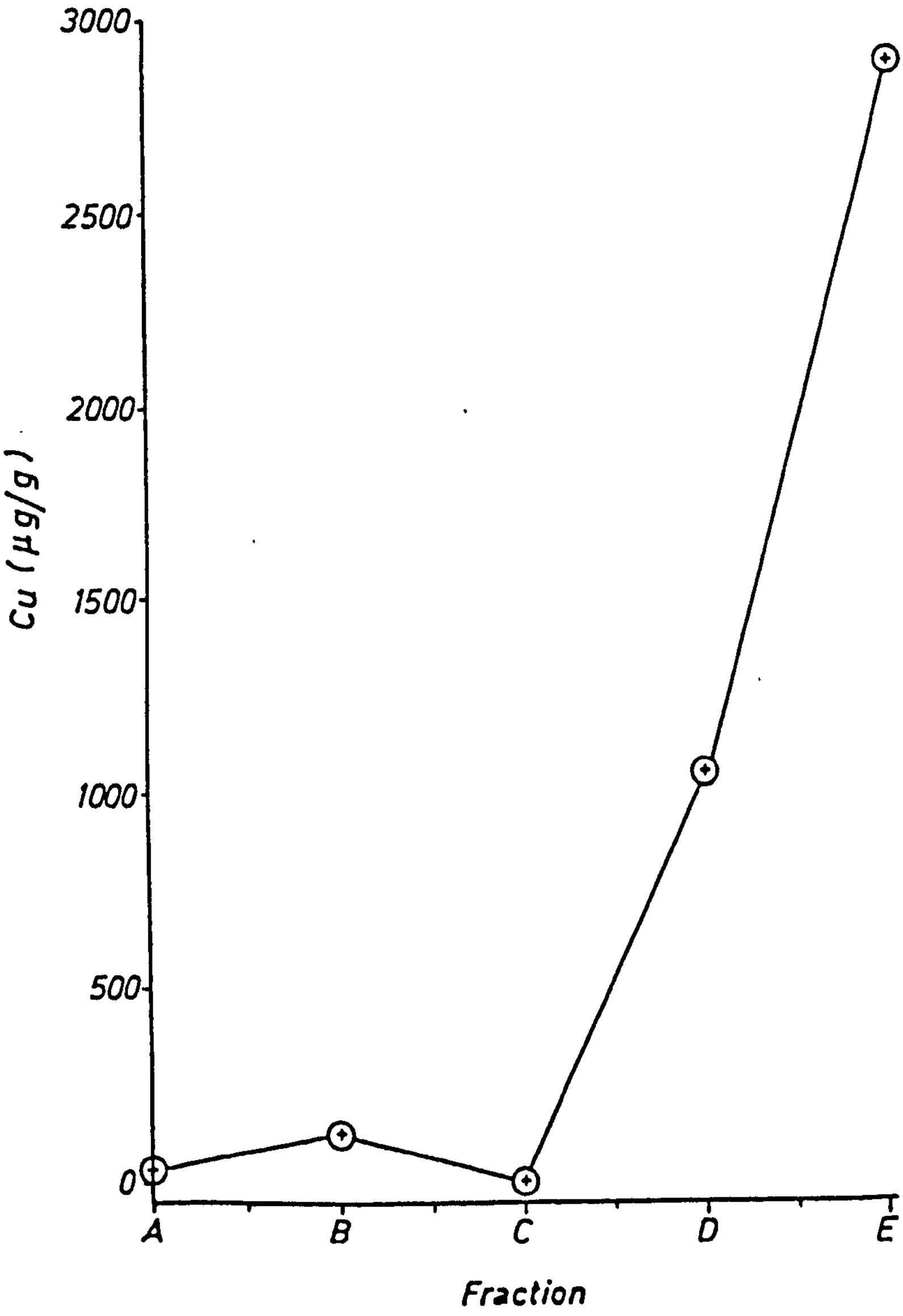

FIG 3.29 DISTRIBUTION OF COPPER IN DRAIN LUCKETT SEDIMENT

A = Exchangeable

B = Carbonate

C = Fe -Mn oxide

D = Organic

E = Residual

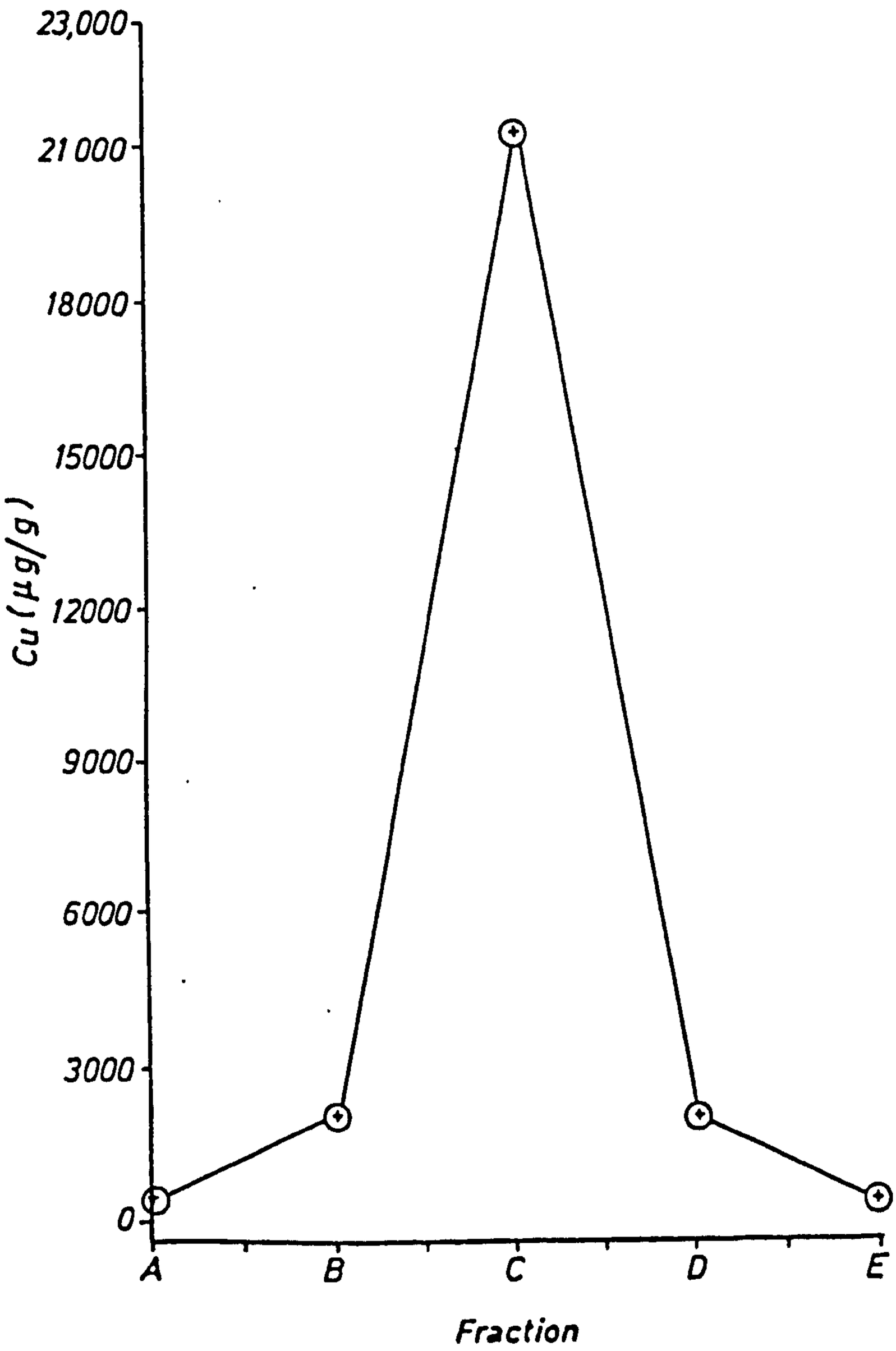

be determined by FAAS. The level of these metals obtained by acid digestion was compared with the total concentration of metals obtained by using the Tessier et alia scheme. The results in Tables 3.10 - 3.12 indicate that the level of metals obtained by acid digestion are higher than the total concentration obtained by the Tessier et alia scheme, except for the zinc and copper in Adit No. 8 and copper in Adit Bridge No. 8. Tables 3.10 - 3.12 list the results for the eight metals associated in the five fractions of each sediment. The percentage association of each metal with the different fraction of each sediment is shown below :-

Table 3.10 : Restronguet Creek No. 3 (listed in order of magnitude)

Calcium : Exchangeable (30.9%), Fe-Mn oxides (30.5%), organic (28.3%), residual (8.4%) and carbonate (1.7%)

Manganese : Residual (46.3%), Fe-Mn oxides (36.7%), organic (11.7%) and exchangeable (5.1%)

Iron : Residual (54.3%), Fe-Mn oxides (24.7%) and organic (20.8%)

Copper : Residual (51.6%), organic (34.4%), Fe-Mn oxides (11.3%) and carbonate (2.5%)

Zinc : Residual (70.1%), Organic (15.3%), Fe-Mn oxides (9.9%), exchangeable (2.8%) and carbonate (1.6%)

Cadmium : Exchangeable (88.2%)

Lead : Fe-Mn oxides (47.4%), residual (40.6%), carbonate (8.2%), organic (2.4%) and exchangeable (1.2%)

Table 3.11 : Adit No. 8 Sediment

Calcium : Carbonate (33.48%), exchangeable (28.1%), organic (26.9%), residual (6.6%) and Fe-Mn oxides (4.7%)

Manganese : Carbonate (30.6%), Fe-Mn oxides (28.4%), exchangeable (21.8%), organic (13.3%) and residual (5.6%)

Iron : Residual (70.1%), Fe-Mn oxides (15.7%), organic (13.7%) and carbonate (0.28%)

Copper : Organic (57.1%) and residual (42.8%)

Zinc : Fe-Mn oxides (27.4%), residual (27.1%), organic (24.9%), carbonate (13%) and exchangeable (7.3%)

Lead : Fe-Mn oxides (52.5%) and organic (47.5%)

Table 3.12 : Adit Bridge No. 8 Sediment

Calcium : Organic (19.7%), carbonate (17.0%), exchangeable (11.5%), Fe-Mn oxides (5.1%) and residual (0.53%)

Manganese : Fe-Mn oxides (55.9%), exchangeable (37.5%), residual (6.1%), carbonate (0.42%) and organic (0.14%)

Iron : Fe-Mn oxides (55.9%), residual (41.7%), organic (1.83%), carbonate (0.33%) and exchangeable (0.06%)

Copper : Organic (52.4%), carbonate (35.5%), residual (5.8%), Fe-Mn oxides (4.9%) and exchangeable (1.3%)

Zinc : Fe-Mn oxides (80.8%), carbonate (12.3%), exchangeable (3.5%), organic (2.6%), residual (0.59%)

Lead : Fe-Mn oxides (64.2%), exchangeable (21.(%), carbonate (13.7%)

In the sequential extraction scheme used it is easy to envisage mobility and bioavailability decreases approximately in the order of extraction procedure from the readily available to unavailable. For instance, the pH 7 for the first extraction is representative of the pH of natural waters. Metal occurring in the carbonate can be considered moderately available, while the metal involved in the organic and residual phases is of very limited availability.

In general the bioavailability of the metals listed in Tables 3.10 - 3.12 follows the orders :-

Cd > Ca > Pb > Mn > Fe > Zn > Cu (Restronguet Creek No. 3 sediment)

Mn > Ca > Zn > Pb > Fe > Cu (Adit No. 8 sediment)

Pb > Zn > Mn > Fe > Cu > Ca (Adit Bridge No. 8 sediment)

These sequences indicate that :-

1. Cadmium is very available while copper is not available in Restronguet Creek No. 3. Harrison et alia (13) found the same sequence in street dusts and this situation may explain the easy uptake of cadmium from soil by plants.

2. Manganese is available while copper is not available in the Adit No. 8 sediment.

3. The lead adsorbed on the Adit Bridge No. 8 sediment is available while calcium is not available; an unexpected result in view of the availability of calcium in the other two sediments.

The distribution of each metal in each sediment is shown diagrammatically in Figures 3.30 - 3.47.

FIG. 3.30 DISTRIBUTION OF CALCIUM IN RESTRONGUET CREEK No.3 SEDIMENT

A = Exchangeable

B = Carbonate

C = Fe -Mn oxide

D = Organic

E = Residual

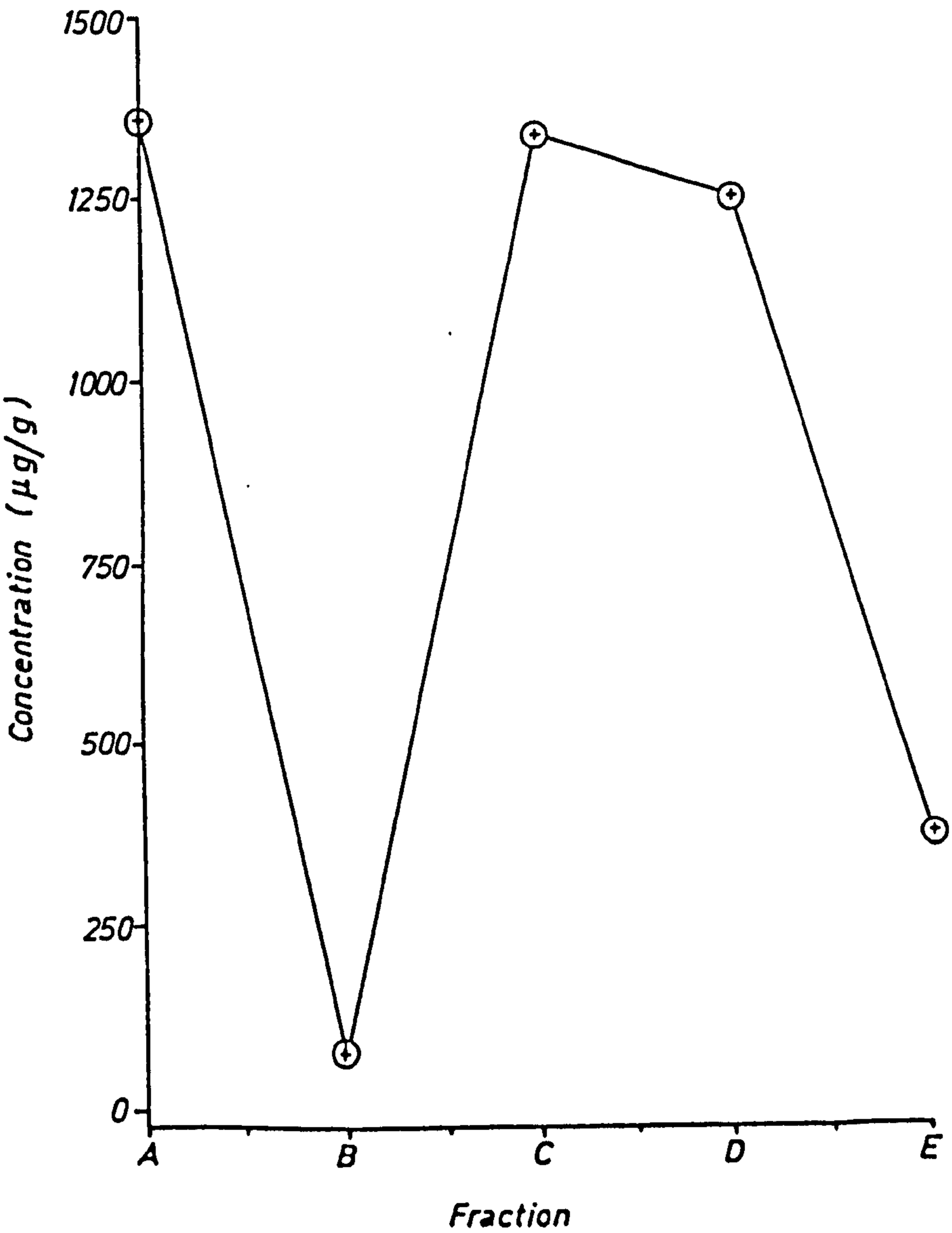

FIG. 3.31 DISTRIBUTION OF MANGANESE IN RESTRONGUET CREEK No.3 SEDIMENT

A = Exchangeable

B = Carbonate

C = Fe -Mn oxide

D = Organic

E = Residual

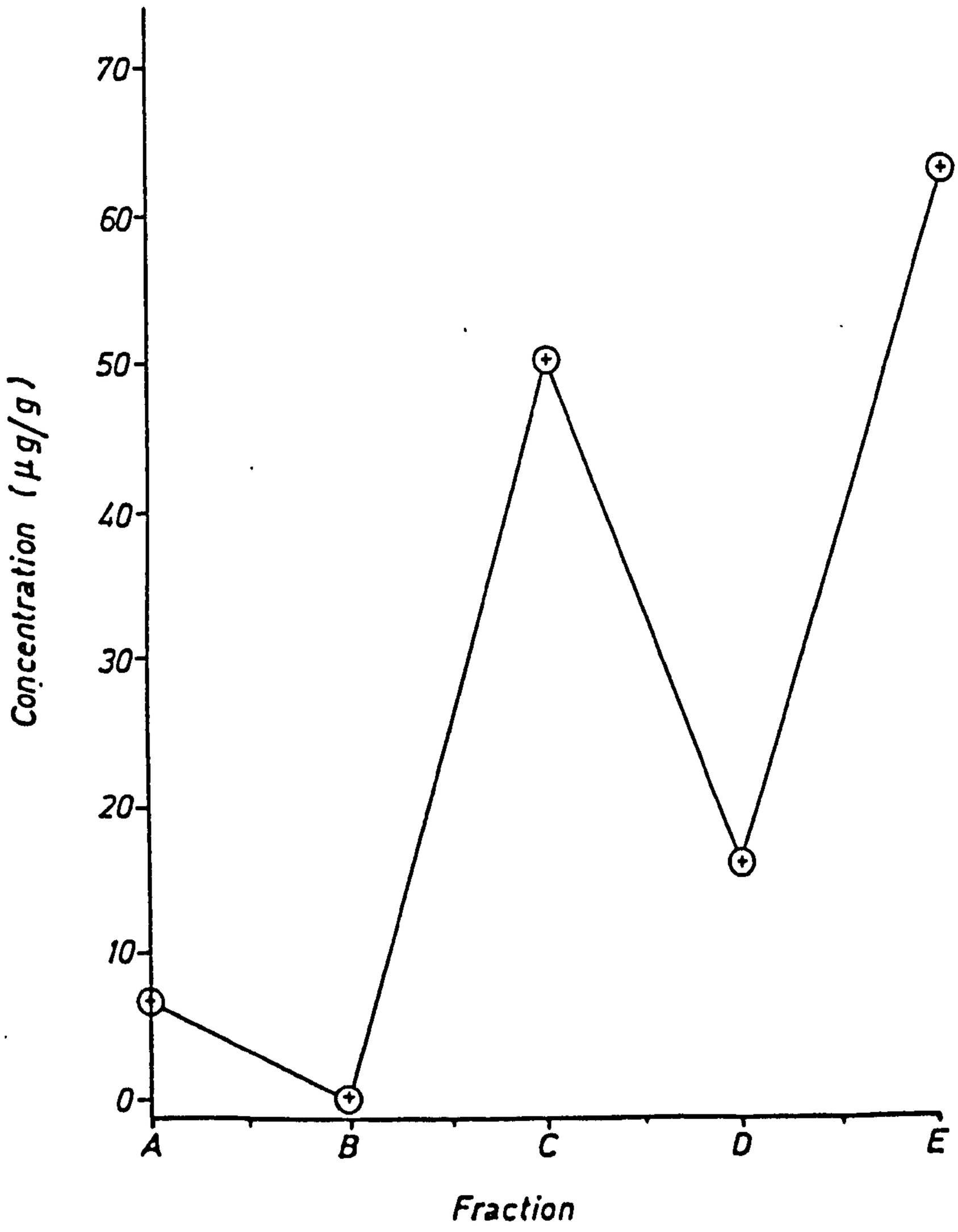

FIG. 3.32 DISTRIBUTION OF IRON IN RESTRONGUET CREEK No.3 SEDIMENT

A = Exchangeable

B = Carbonate

C = Fe -Mn oxide

D = Organic

E = Residual

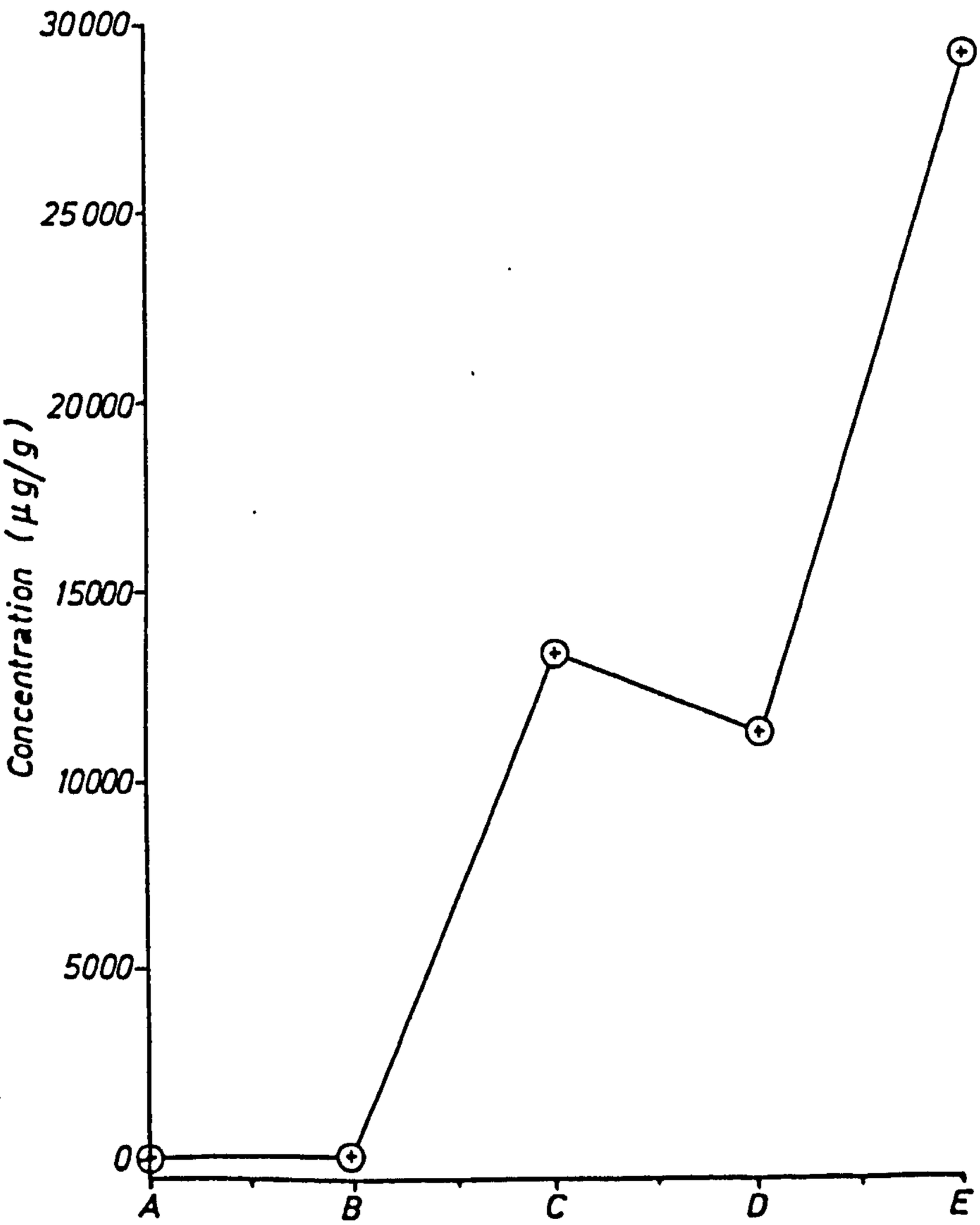

FIG. 3.33 DISTRIBUTION OF COPPER IN RESTRONGUET CREEK No.3 SEDIMENT

A = Exchangeable

B = Carbonate

C = Fe -Mn oxide

D = Organic

E = Residual

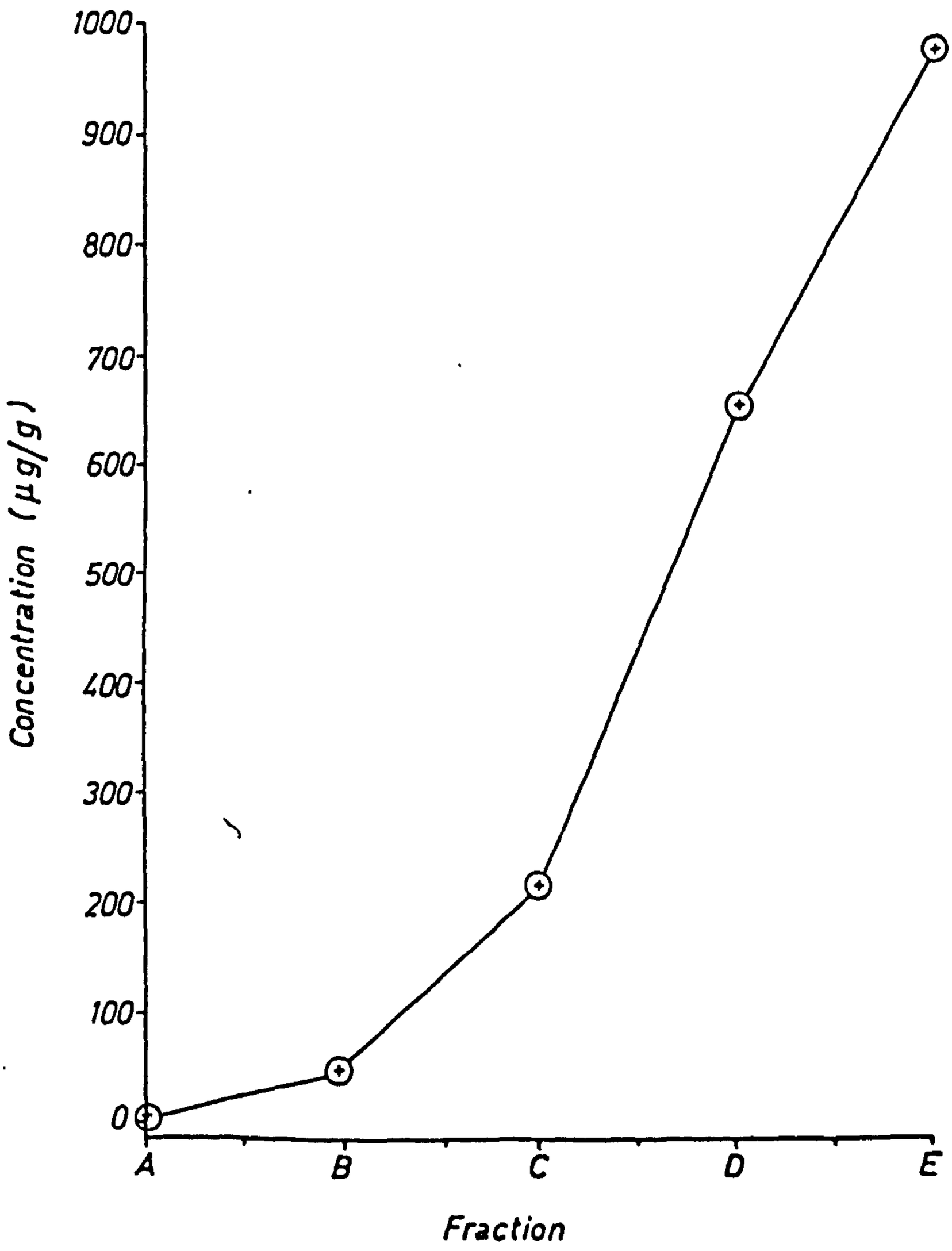

FIG. 3.34 DISTRIBUTION OF ZINC IN RESTRONGUET CREEK No. 3 SEDIMENT

A = Exchangeable

B = Carbonate

C = Fe -Mn oxide

D = Organic

E = Residual

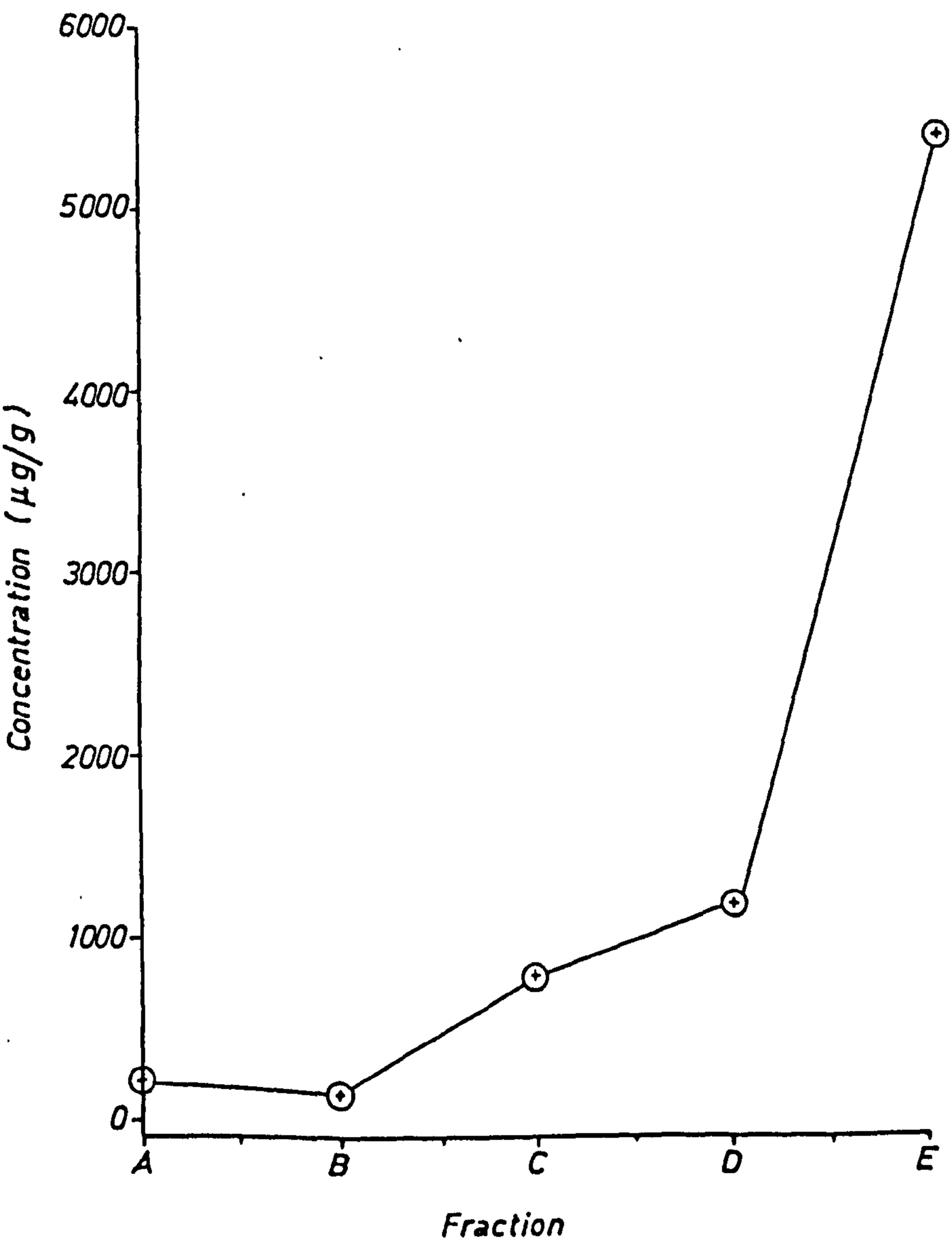

FIG. 3.35 DISTRIBUTION OF LEAD IN RESTRONGUET CREEK No. 3 SEDIMENT

A = Exchangeable

B = Carbonate

C = Fe -Mn oxide

D = Organic

E = Residual

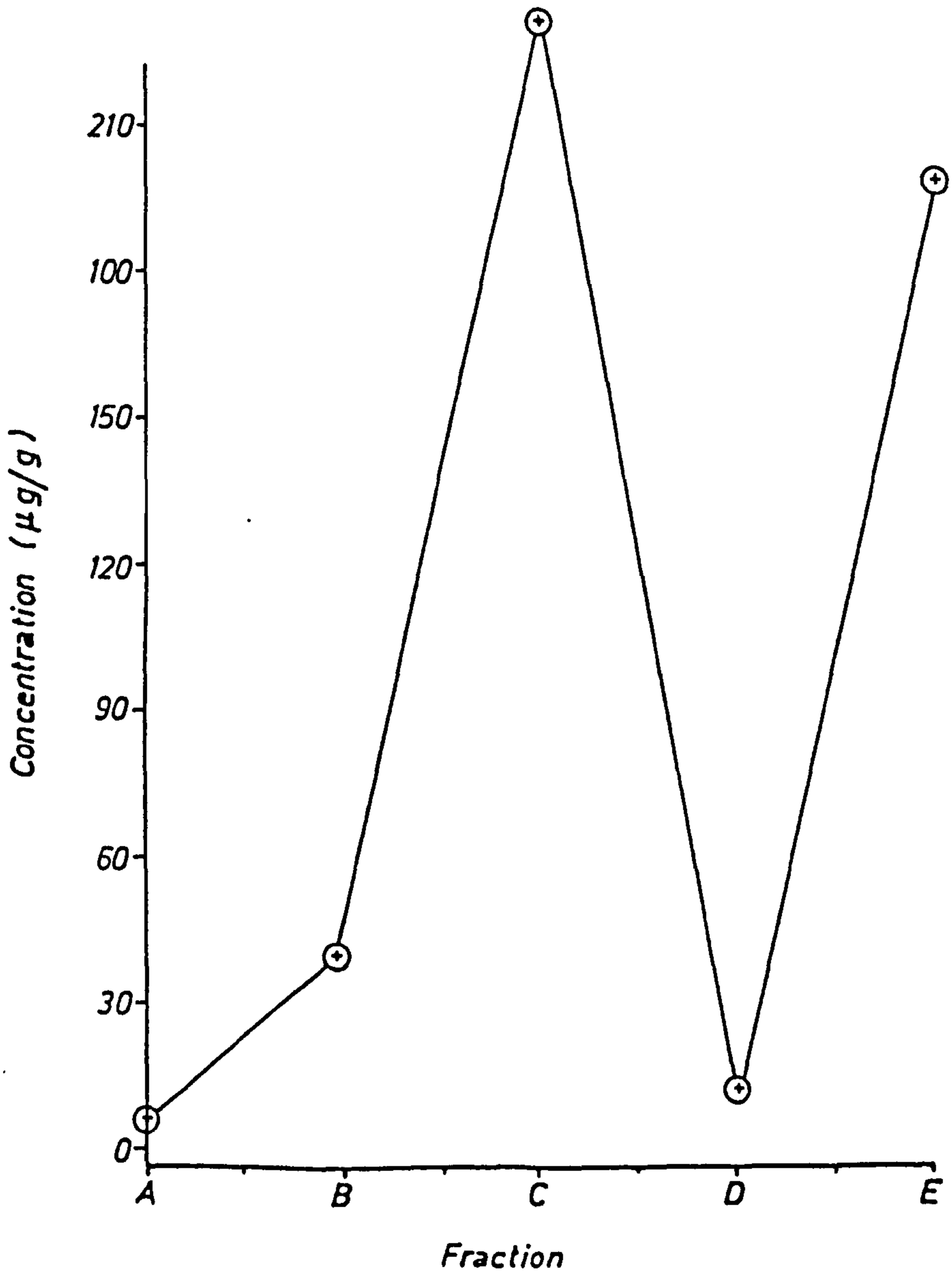

FIG. 3.36 DISTRIBUTION OF CALCIUM IN ADIT No. 8 SEDIMENT

A = Exchangeable

B = Carbonate

C = Fe -Mn oxide

D = Organic

E = Residual

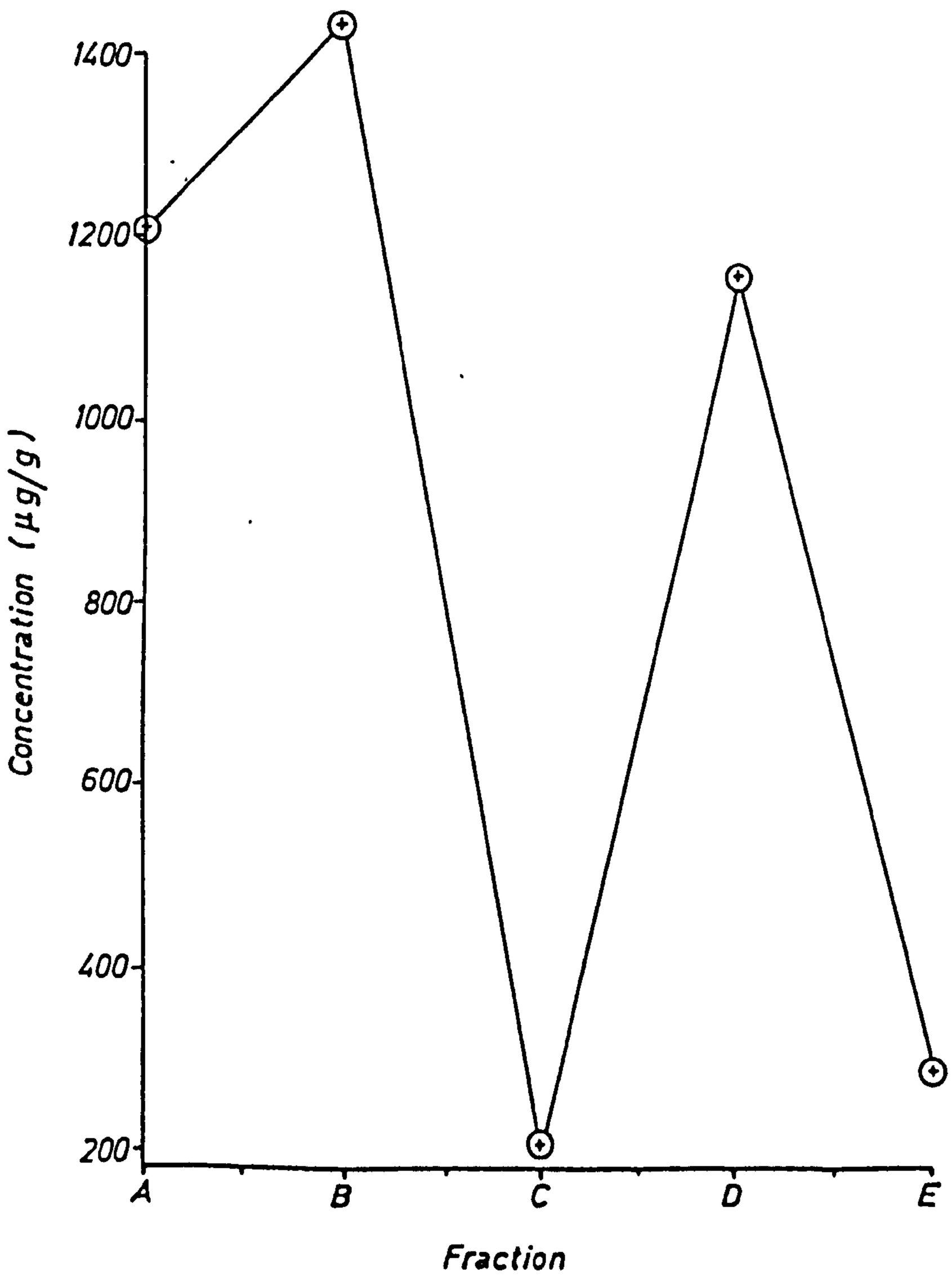

FIG. 3.37 DISTRIBUTION OF MANGANESE IN ADIT No. 8 SEDIMENT

A = Exchangeable

B = Carbonate

C = Fe -Mn oxide

D = Organic

E = Residual

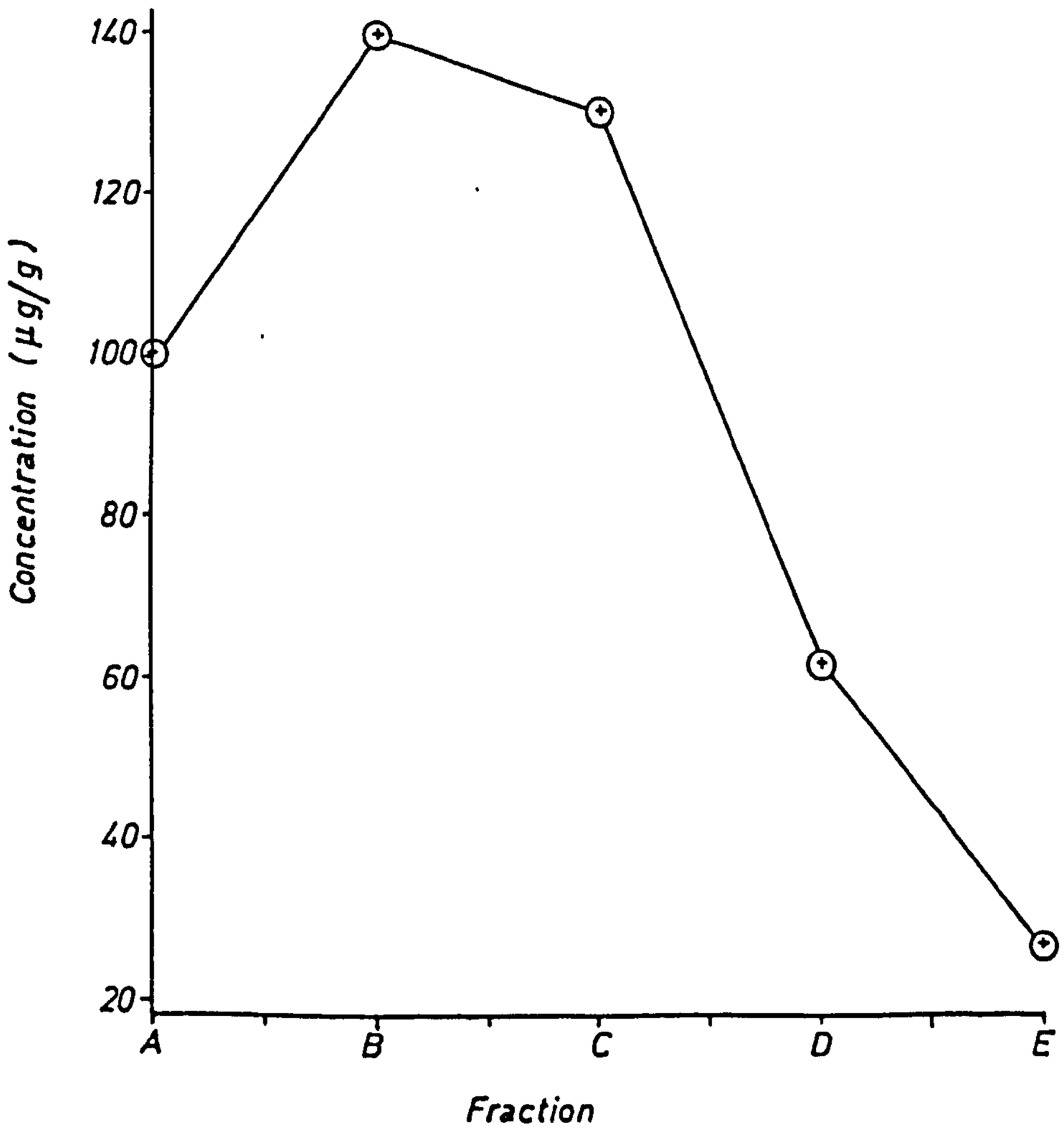

FIG. 3.38 DISTRIBUTION OF IRON ADIT No. 8 SEDIMENT

A = Exchangeable

B = Carbonate

C = Fe -Mn oxide

D = Organic

E = Residual

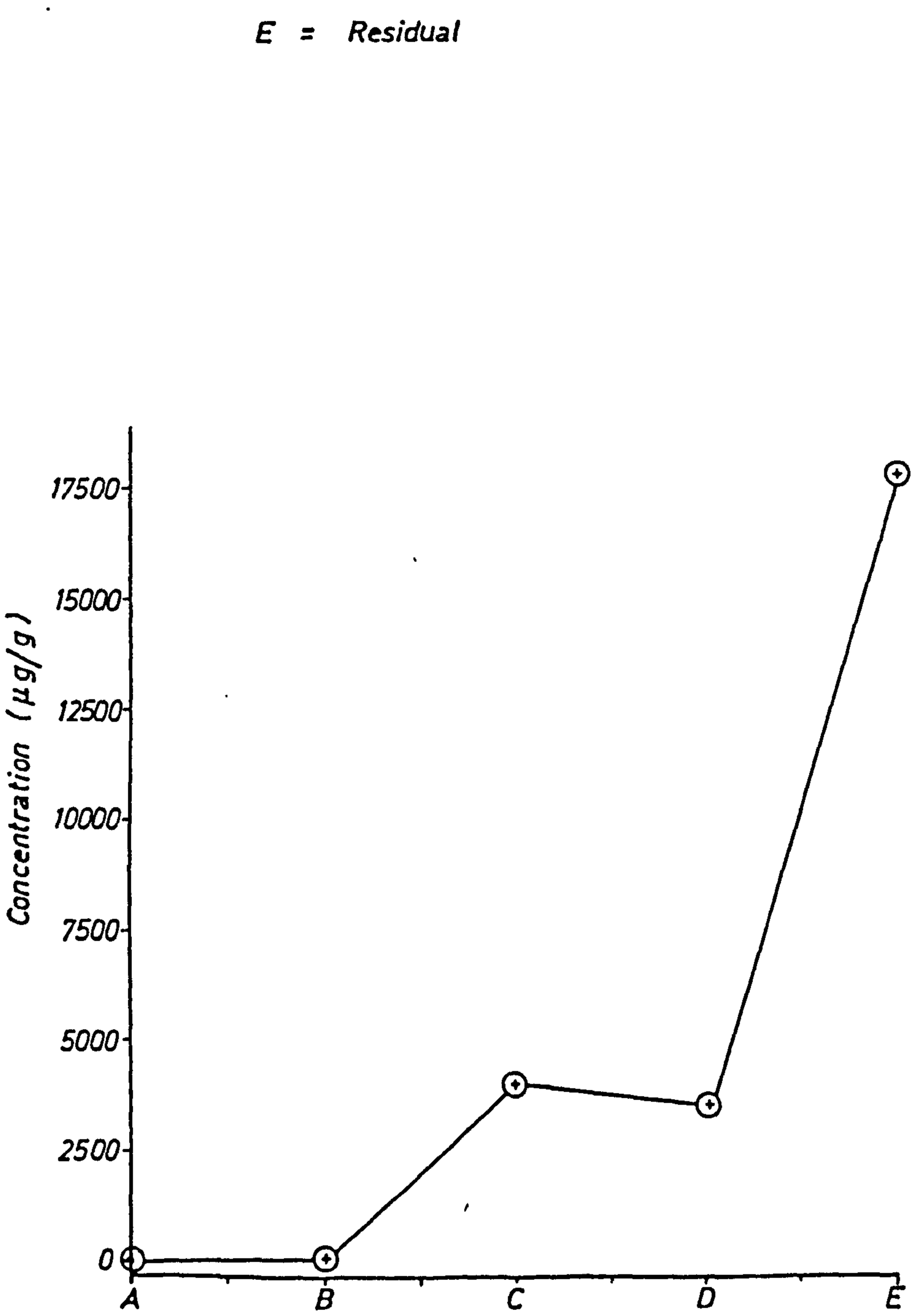

FIG. 3.39 DISTRIBUTION OF COPPER IN ADIT No.8 SEDIMENT

A = Exchangeable

B = Carbonate

C = Fe -Mn oxide

D = Organic

E = Residual

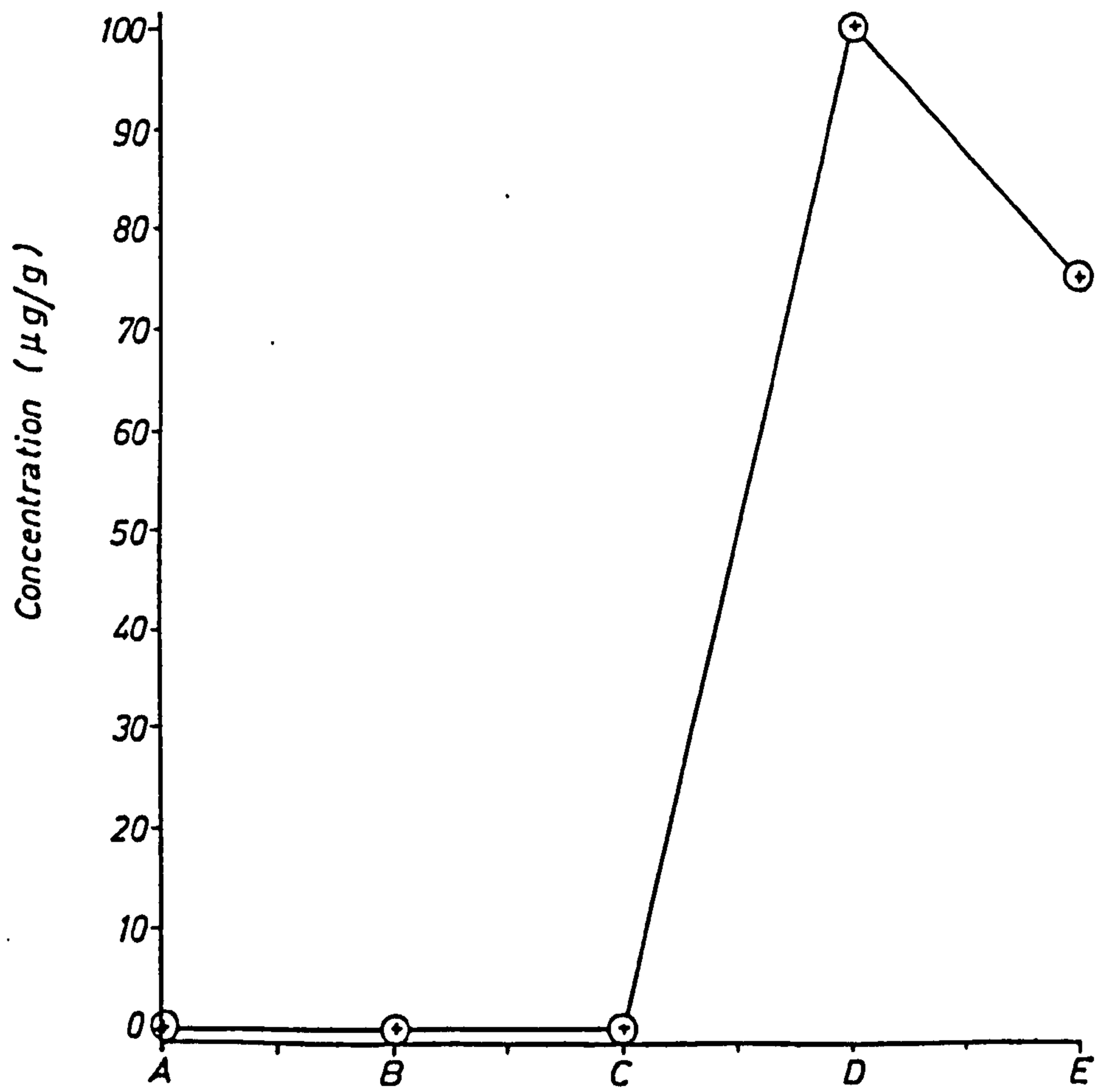

FIG.3.40 DISTRIBUTION OF ZINC IN ADIT No. 8 SEDIMENT

A = Exchangeable

B = Carbonate

C = Fe -Mn oxide

D = Organic

E = Residual

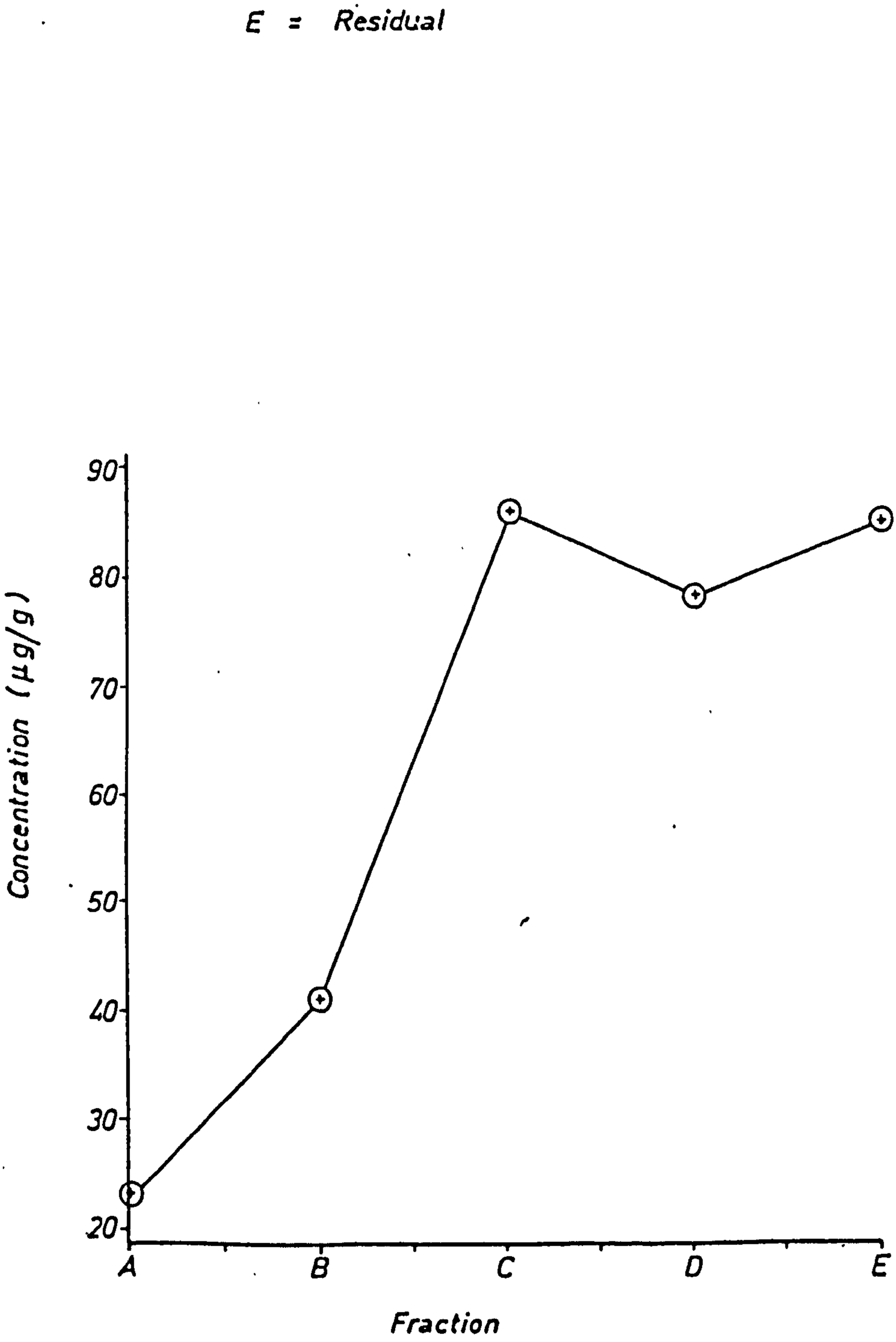

FIG. 3.41 DISTRIBUTION OF LEAD IN ADIT No.8 SEDIMENT

A = Exchangeable

B = Carbonate

C = Fe -Mn oxide

D = Organic

E = Residual

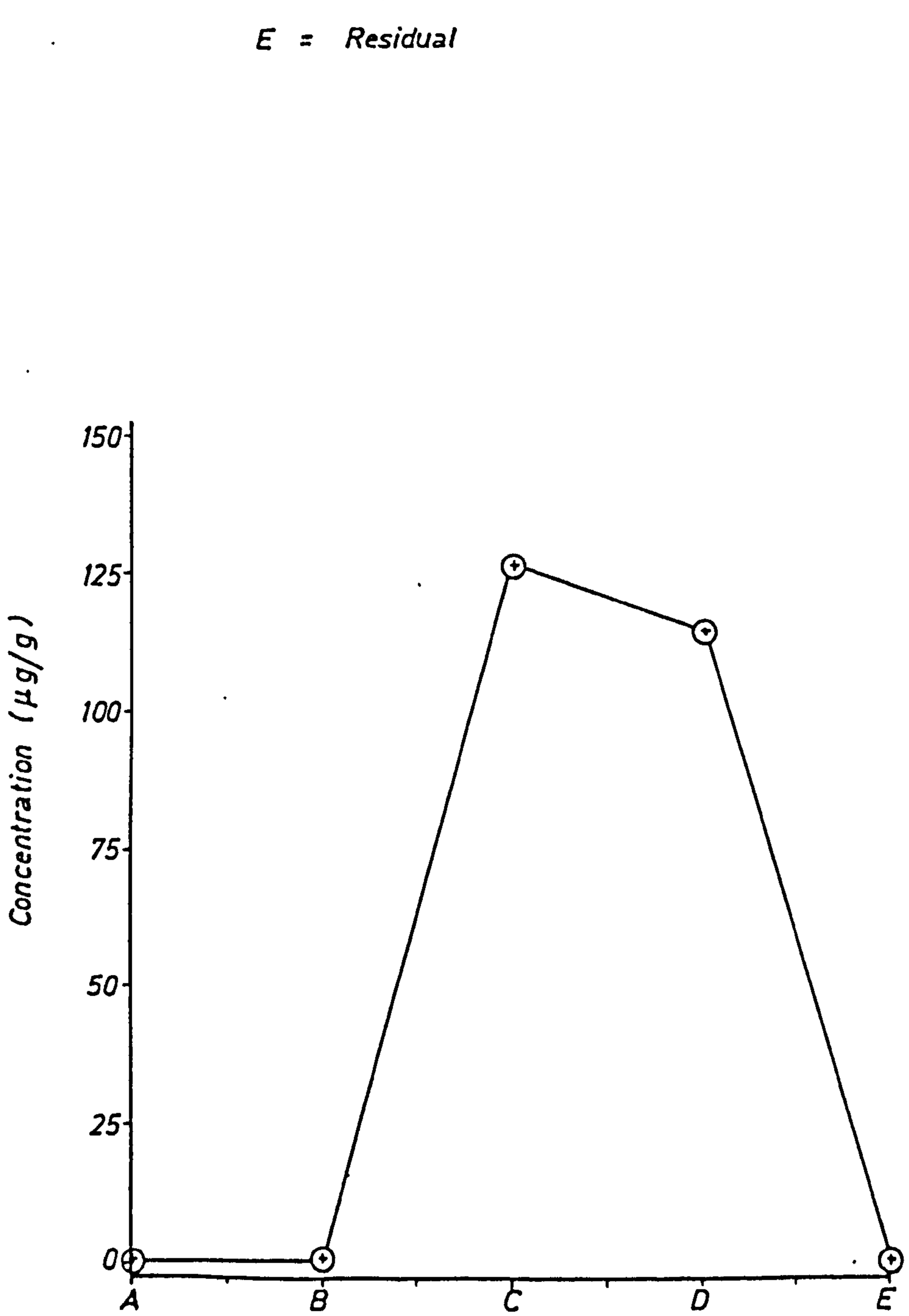

FIG. 3.42 DISTRIBUTION OF CALCIUM IN ADIT BRIDGE No.8 SEDIMENT

A = Exchangeable

B = Carbonate

C = Fe -Mn oxide

D = Organic

E = Residual

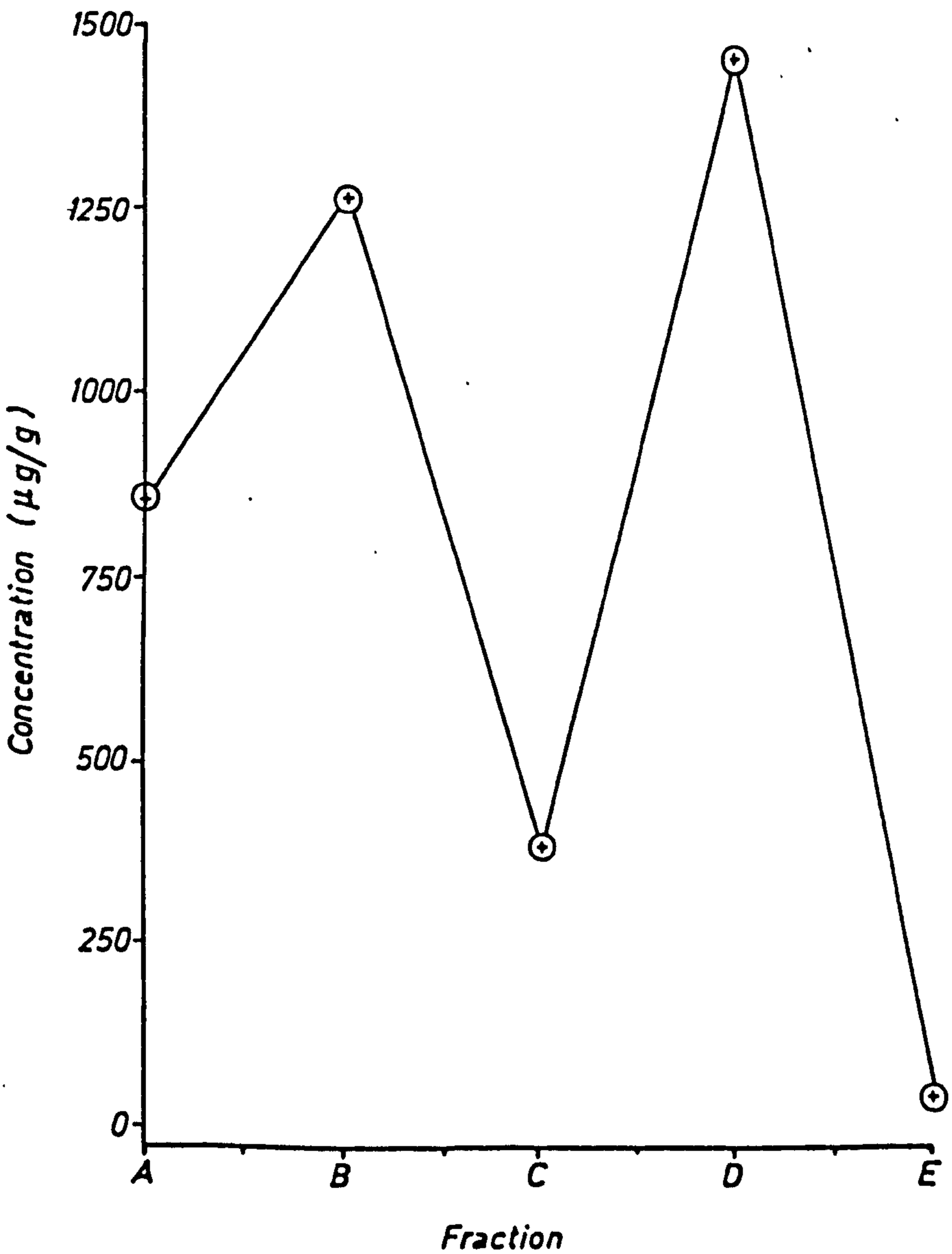

FIG. 3.43 DISTRIBUTION OF MANGANESE IN ADIT BRIDGE No.8 SEDIMENT

A = Exchangeable

B = Carbonate

C = Fe -Mn oxide

D = Organic

E = Residual

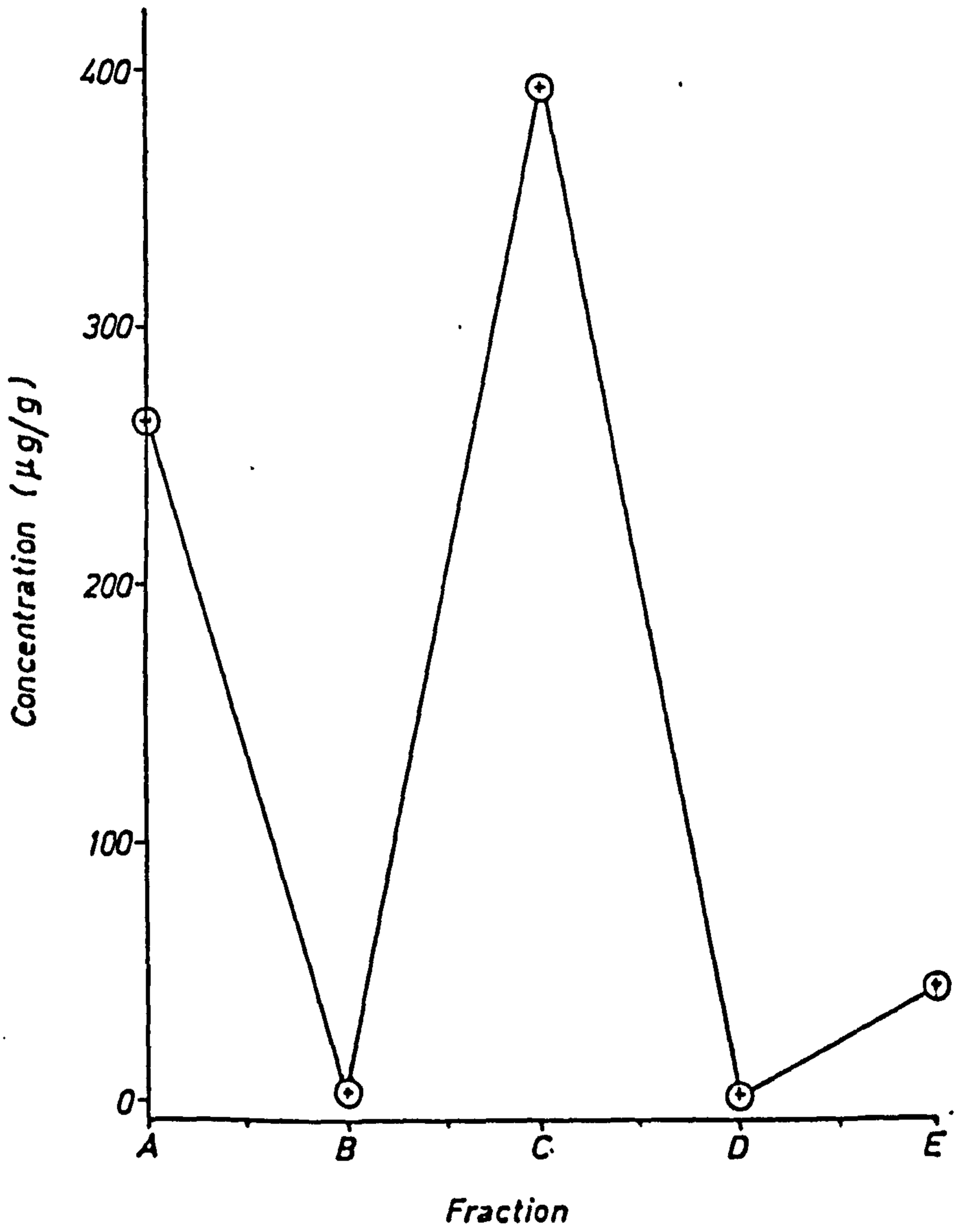

FIG. 3.44 DISTRIBUTION OF IRON IN ADIT BRIDGE No.8 SEDIMENT

A = Exchangeable

B = Carbonate

C = Fe - Mn oxide

D = Organic

E = Residual

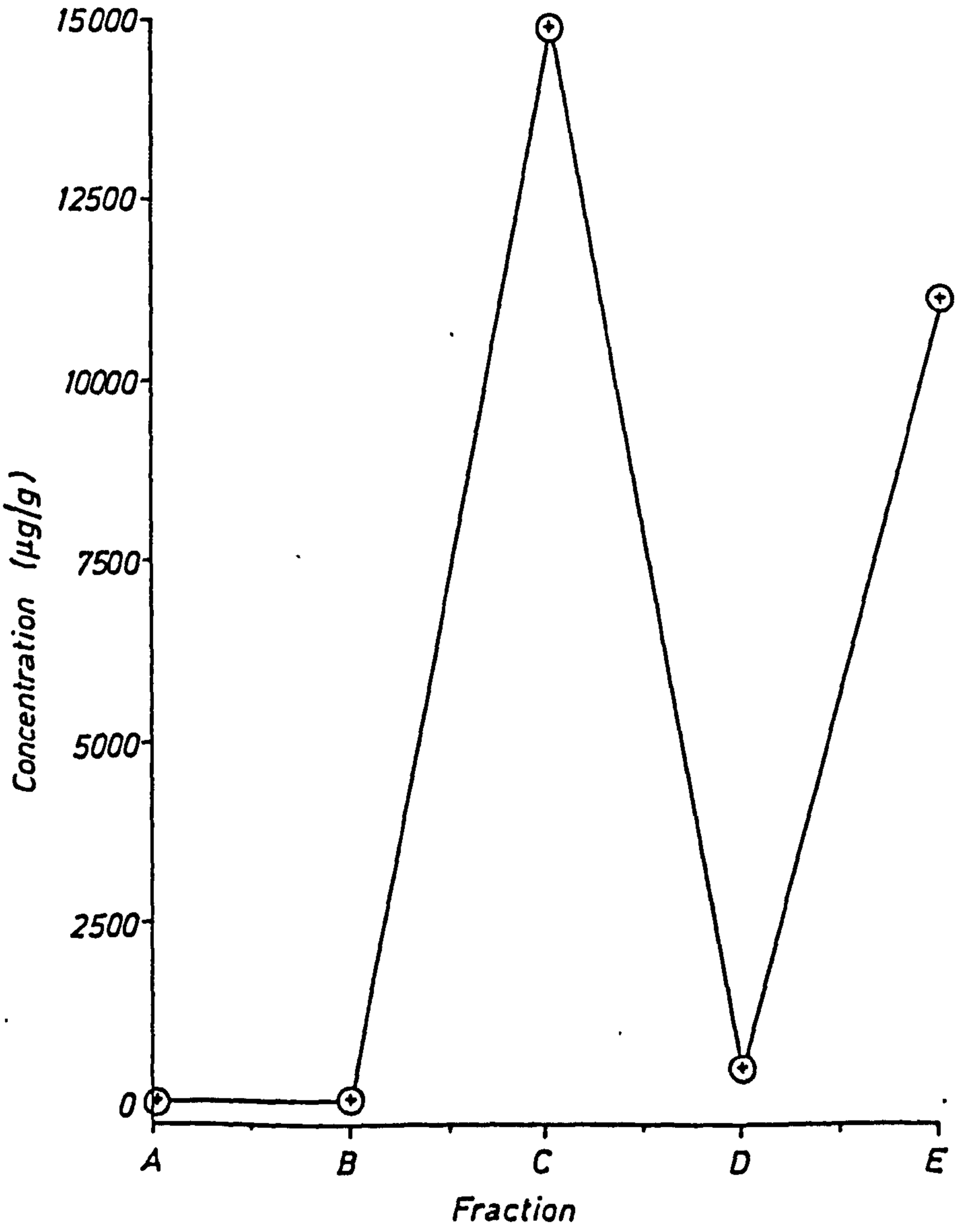

FIG. 3.45 DISTRIBUTION OF COPPER IN ADIT BRIDGE No.8 SEDIMENT

A = Exchangeable

B = Carbonate

C = Fe -Mn oxide

D = Organic

E = Residual

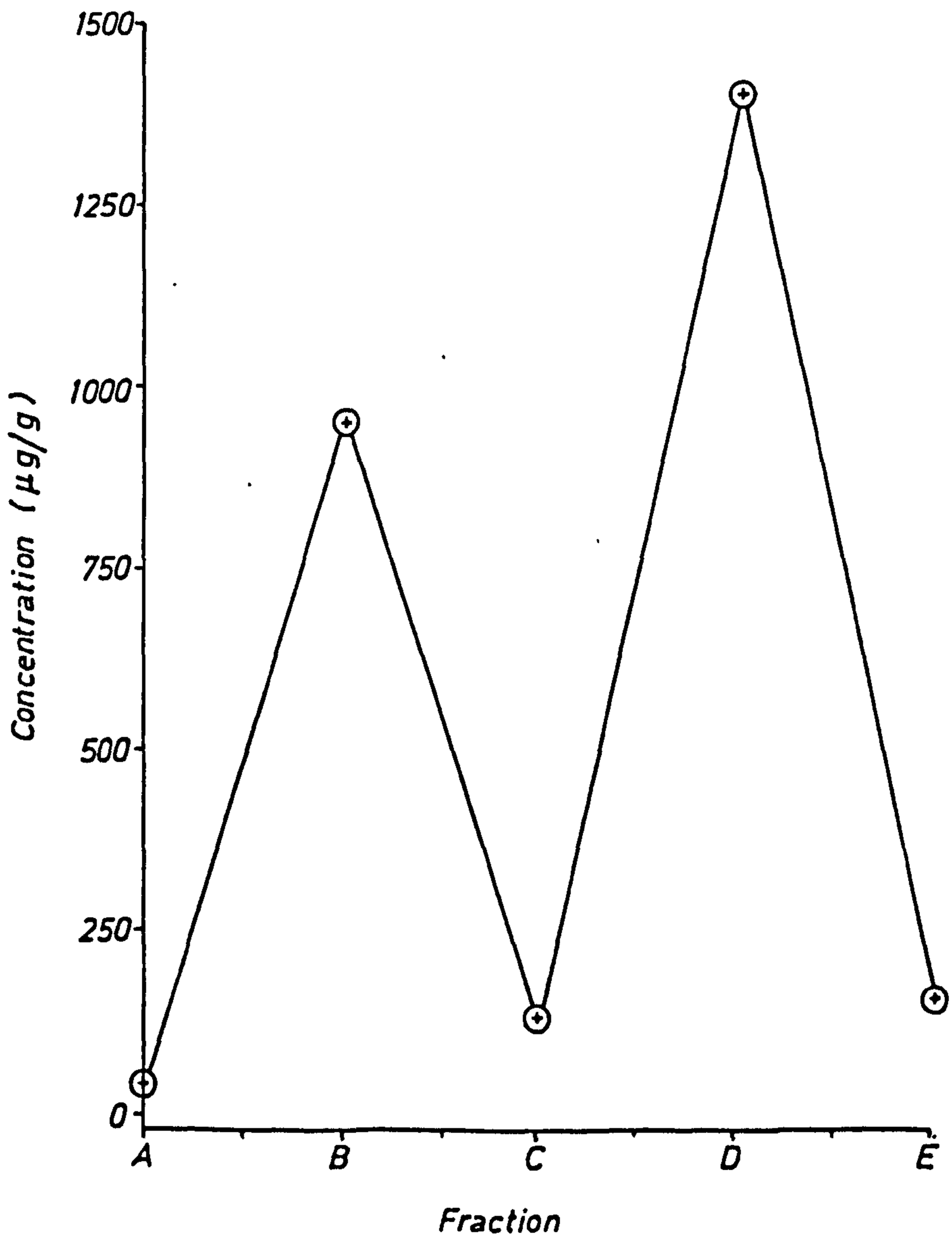

FIG. 3.46 DISTRIBUTION OF ZINC IN ADIT BRIDGE No. 8 SEDIMENT

A = Exchangeable

B = Carbonate

C = Fe -Mn oxide

D = Organic

E = Residual

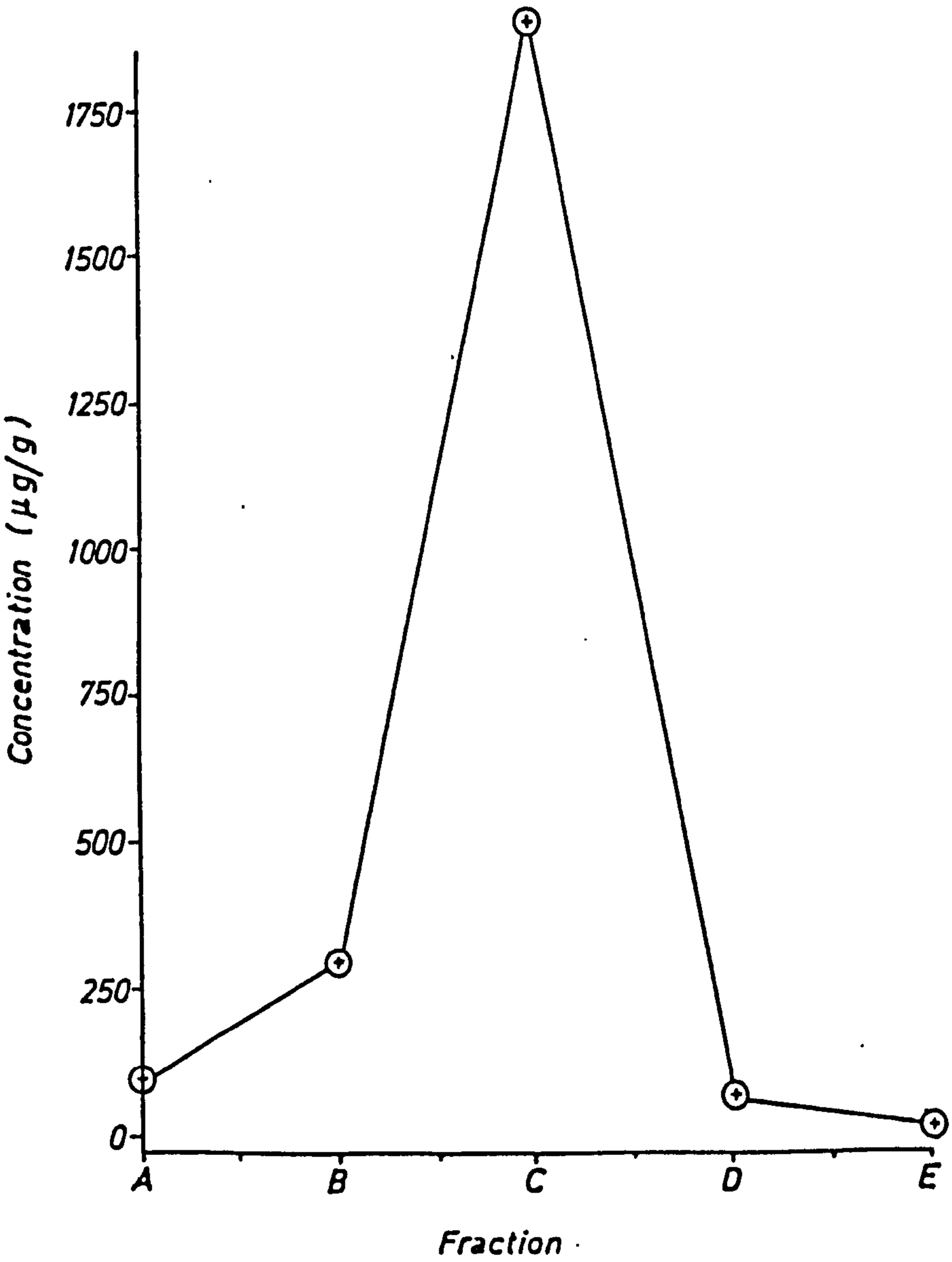

FIG. 3.47 DISTRIBUTION OF LEAD IN ADIT BRIDGE No.8 SEDIMENT

A = Exchangeable

B = Carbonate

C = Fe -Mn oxide,

D = Organic

E = Residual

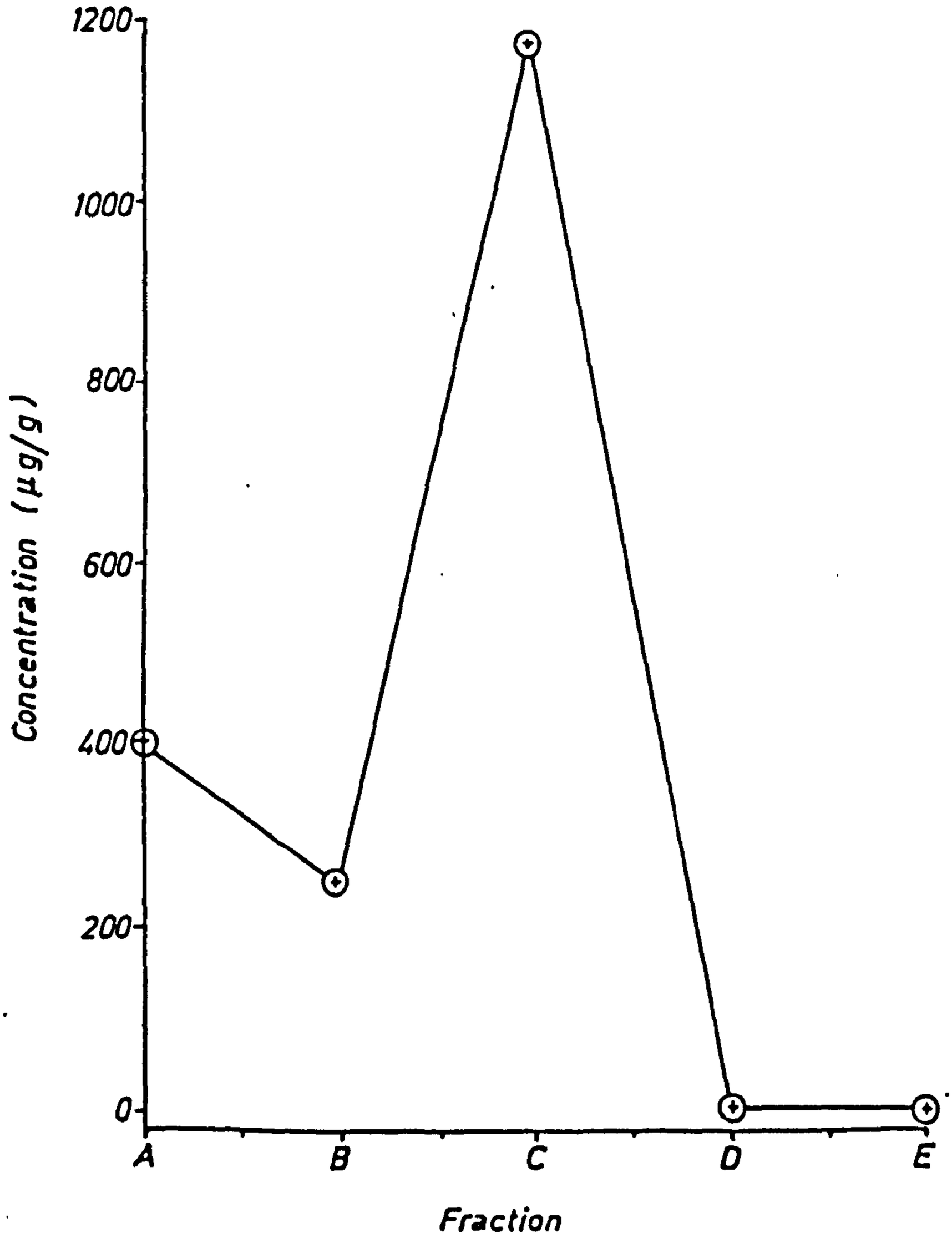

Figures 3.14 - 3.17 indicate four distinguishable Fe phases :-

1. Gel-like material (G)
2. Hairy spheres (Hs)
3. Sheet-like crystal (Sh)
4. Acicular crystal (Ac)

The metals Cu, Zn and Pb appear to be associated with the Fe phases. Spectra are given in Figures 3.17 - 3.20 which show a change between treated and untreated samples while little change was observed between the samples treated with chemical extractants used in the Tessier et alia scheme, maybe EPMA was not sensitive enough to detect alterations in the extracted materials.

The results in Table 3.13 indicate the total, inorganic and organic carbon of the sediments. The organic content of the sediment plays an important role in controlling the concentration of heavy metals. It was expected that for those sediments containing high organic carbon content, a high proportion of metal would be extracted into the organic fraction of the sediment (using the Tessier scheme). This fraction may arise due to the coordination of metal with organic matter, in particular humic and fulvic acid as follows (32) :-

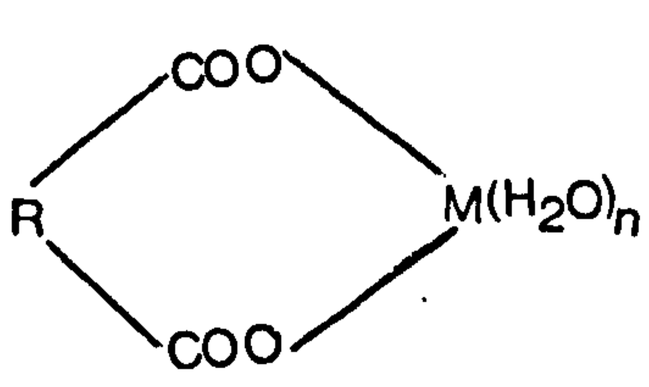

or

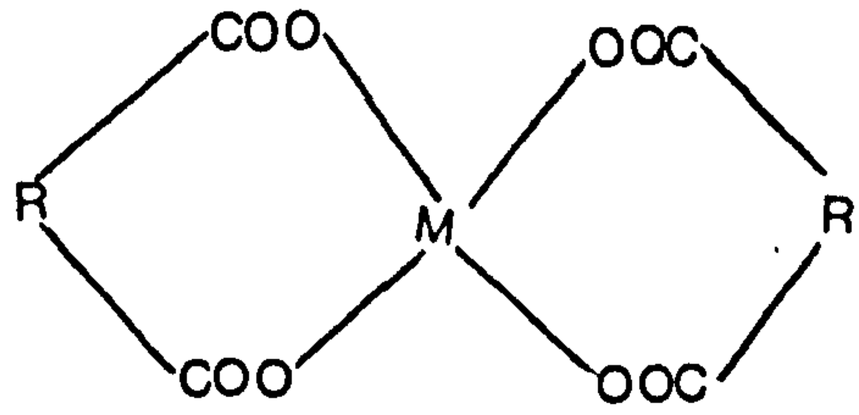

In fact, the results in Table 3.19 were not sufficient to elucidate the relationship between organic carbon and concentration of heavy metals using the stepwise regression procedure and deviated from that expected. However, the level of copper (II) associated with the three sediments' organic fraction was particularly high, reflecting the affinity of copper (II) ion for humic/fulvic materials. But further sediments should be examined where the levels of organic materials (particularly those derived from plant materials) are high, so as to chelate/complex the majority of the metal present.

Table 3.19 : Heavy Metal Extracted (%) in the Organic Fraction using the Tessier Scheme and Organic Carbon Content of the Sediments

Restronguet Creek No. 3 Sediment

Ca	Mn	Fe	Ni	Cu	Zn	Cd	Pb	% C
28.3	11.7	20.8	N.D.	34.4	15.3	N.D.	N.D.	0.38

Adit No. 8 Sediment

Ca	Mn	Fe	Ni	Cu	Zn	Cd	Pb	% C
26.9	13.3	13.7	N.D.	57.1	24.9	N.D.	47.5	0.40

Adit Bridge No. 8 Sediment

Ca	Mn	Fe	Ni	Cu	Zn	Cd	Pb	% C
19.7	0.14	1.83	N.D.	52.2	2.6	N.D.	N.D.	4.93

3.4 REFERENCES

1. Florence. T.M., Talanta, 29, 345 (1982).
2. O'Shea. T.A. and Mancy. K.H., Anal. Chem., 48. 1603 (1976).
3. Florence. T.M., Anal. Proc., 20, 552 (1983).
4. Batley, G.E. and Florence, T.M., Anal. Letters, 9, 379 (1976).
5. Florence, T.M., Anal. Chim. Acta, 141, 73 (1982).
6. Laxen, D.P.H. and Harrison, R.M., Sci. Total Environ., 19, 59 (1981).
7. Laxen, D.P.H. and Chander, I.M., Anal. Chem., 54, 1350 (1982).
8. Batley, G.E. and Farrar, Y.J., Anal. Chim. Acta, 99, 283 (1978).
9. O'Shea, T.A., Anodic Stripping Voltammetric Study of the Competitive Interactions between Trace Metals and the Alkaline Earths for Complexing Ligands in Aquatic Environments, Ph.D. Thesis, University of Michigan (1972).
10. Florence, T.M. and Batley, G.E. Talanta, 22, 201 (1975).
11. Buffle, J., Trends Anal. Chem., 1, 90 (1981).
12. Turner, D.R. and Whitfield, M., Electroanal. Chem., 103, 61 (1979).
13. Harrison, R.M., Laxen, D.P.H. and Wilson, S.J., Environ. Sci. Technol., 15, 1378 (1981).
14. Fraser, J.L. and Lum, K.R., Environ. Sci. Technol., 17, 52 (1983).
15. Lindau, C.W. and Hossner, L.R., J. Environ. Qual., 11, 540 (1982).
16. Tessier, A., Campbell, P.G.C. and Bisson, M., Anal. Chem., 51, 844 (1979).
17. Gupta, S.K. and Chen, K.Y., Environ. Letters, 10, 129 (1975).
18. Chester, R., Kudoja, W.M., Thomas, A. and Towner, J., Environ. Pollut., (B), 10, 213 (1985).
19. Engler, R.M., Brannon, J.M., Rose, J. and Bigham, G., A Practical Selective Extraction Procedure for Sediment Characterization, in "Chemistry of Marine Sediments", Yen, T.F. (Ed.), Ann Arbor Science Publishers Inc., p. 163 (1977).

20. Florence, T.M..and Batley, G.E., Talanta, 22, 201 (1975).

21. Florence, T.M. and Batley, G.E., Talanta, 23, 179 (1976).

22. Sinko, I. and Dolezal, J., J. Electroanal. Chem., 25, 299 (1970).

23. Salter, L.J., Heavy Metals in Some Contaminated Waters, M.Sc. Thesis, University of Bristol (1981).

24. Abaychi, J.K. and Douabul, A.A.Z., Water Res., 19, 457 (1985).

25. Abdullah, M.I., El-Rayis, O.A. and Riley, J.P., Anal. Chim. Acta, 84, 363 (1976).

26. Demora, S.J. and Harrison, R.M., Anal. Chim.,Acta, 153, 307 (1983).

27. Riley, J.P. and Taylor, D., Anal. Chim. Acta, 40, 479 (1968).

28. Jordao, C.P., Chemical Availability of Heavy Metals in the Aquatic Environment, Ph.D. Thesis, University of Bristol (1983).

29. Sanchez, I. and Lee, G.F., Water Res., 7, 587 (1973).

30. Bardi, M.A., Aston, S.R., Environ. Pollut., (B), 6, 181 (1983).

31. Dines, H.G., The Metalliferous Mining Region of South-West England, Volume II, published by Her Majesty's Stationery Office, London, p. 591 (1956).

32. Slavev, J., Wold, J. and Pickering, W.F., Talanta, 29, 743 (1982).

CHAPTER 4

THALLIUM : DETERMINATION AND EFFECTS

CONTENTS

4.1 INTRODUCTION

The determination of thallium in environmental samples, normally at very low levels, is limited by instrumental sensitivity, therefore thallium must be preconcentrated and separated from other elements especially lead. However, there are several analytical techniques available for the determination of thallium but great care must be taken with each technique to reduce interference problems.

FAAS is insufficiently sensitive for the determination of thallium without sample preconcentration. Thallium may be removed from matrix elements by complexation with sodium diethyl dithiocarbamate or ammonium pyrrolidinecarbodithioate and thus extracted with MIBK. Although this extraction is not specific for thallium, it has been used by many workers (1-6); due to the suitability of MIBK for AAS determinations. The reduction in the volume from the aqueous solution to a small volume of organic solvent permits the ready preconcentration of thallium.

GFAAS has the necessary sensitivity for thallium determination in environmental samples but the interference problems with this technique are high. The determination of thallium by GFAAS can generate very severe errors if careful attention is not paid to other species that are present during the analysis of sample. For example, thallium (I) nitrate decomposes at 450^{o}C and will be lost during the ashing step while thallium (III) nitrate is converted to thallium (I) nitrate at 145^{o}C and so will also be lost at 450^{o}C; i.e. the nitrate form should not be used in GFAAS. In fact, this is a most important consideration because nitric acid is popular and useful as a sample matrix for most flameless work (7). To avoid this problem a small volume of 1% (v/v) sulphuric acid has been added as a chemical modifier to prevent loss of

thallium during the ashing step (8). Xiao-quan et alia (9) described the application of palladium or platinum in microgram amounts as matrix-modifiers for the determination of thallium when at the ng/cm^3 level in waste water. In the presence of palladium or platinum the ashing temperature for thallium can be raised to 1000^{o}C so as to decompose the halides and thus minimise the interference effects and allow the direct determination of thallium.

Studies (10,11) have reported that very little interference was found in the determination of thallium in perchloric acid when a platform furnace and the addition of 1% (v/v) sulphuric acidwere employed. Thallium (III) is readily extracted into organic solvents as the hydrated and solvated ion pair, $[H(H_2O)_nS_m^+ TlX_4^-]$, where S is a molecule of solvent, X is a halide ion, and n and m are integers dependent upon hydrohalic acid concentration and solvent used (12-15). Table 4.1 gives the percentage extraction of metal bromides into isopropyl ether from hydrobromic acid (12). Table 4.1 indicates that thallium (III) can be separated from other matrix elements, except indium (III), by extraction from 1 M hydrobromic acid in isopropyl ether. The major problem with this extraction is that isopropyl ether tends to form an unstable peroxide (danger of explosion in the laboratory might occur). The ether solvent is not suitable for AAS determinations. In this dissertation, diethyl ether was used as an extractant instead of isopropyl ether while the thallium was determined by a voltammetric method but evaporation of the ether must be carried out. Thallium was determined in geological materials by acid digestion, extraction of thallium (III) either from 0.5 M hydrobromic solution (13) or 3 N hydrochloric solution (16) into MIBK and direct aspiration into GFAAS. As mentioned in Chapter 2, chloride ions severely interfere with AAS determination so that the thallium (III) was back extracted from the

MIBK layer to an aqueous layer with 20% (w/v) ascorbic acid after reducing thallium (III) to thallium (I). From the above explanation, it is clear that thallium must be converted to one form of thallium, usually thallium (III), then AAS can be carried out for total thallium determination. Now, the question to be asked is, is it possible to separate thallium (I) from thallium (III) for speciation studies on environmental samples and which tools must be used? To answer the first part of the question what is needed is information on the level of thallium in environmental samples. The level, which is expected to be low, leads to the conclusion that speciation of thallium (separation of the two oxidation states quantitatively) is possible but not easy. For example, addition of an oxidising agent to the sample gives the total thallium determination, whilst no addition of the oxidising agent gives thallium (I); subtraction of the two determinations gives thallium (III). In fact, at the present time, there has been no reported separation of thallium (I) from thallium (III) in environmental samples, but this may be due to the low level of thallium which requires a very sensitive analytical technique. Batley et alia (17) determined thallium as thallium (III) in sea water but by spiking with added thallium to the sea water. The answer to the second part of the question is to use liquid-liquid extraction (discussed earlier) and ion-exchange procedures. The complex chloro ion $TlCl_4^-$ isolated using a strong anion-exchange resin gives a fairly good selectivity because above a certain chloride concentration range only thallium (III) and a few other trace elements (noble metals) give stable anionic chloro-complexes (1). Thallium (III) is not adsorbed by cation-exchange resins from dilute hydrochloric acid solutions, whereas thallium (I) and the accompanying minor and trace elements are strongly adsorbed (1). It is clear now that thallium (I) can be adsorbed onto a cation-exchange

resin whereas thallium (III) is adsorbed by strong anion-exchange resins. In practice, the analyst has a choice either to :

i) reduce thallium (III) to thallium (I) and use a cation-exchange resin to concentrate thallium while the eluent must be an oxidising agent to convert thallium (I) to thallium (III) which is not absorbed by the resin; or

ii) oxidise thallium (I) to thallium (III), in this case an anion-exchange resin as adsorbent and a reducing agent as eluent must be used.

The latter method was chosen in the present work due to the low level of interferences encountered. Indeed, the anion-exchange method is better than liquid-liquid extraction due to the sample being free from contamination and suitability for AAS and ASV determinations.

Table 4.1 : Percentage Extraction of Metal Bromides into Isopropyl Ether from Hydrobromic Acid Solutions (12)

Phase ratio 1:1

Amount of metal 0.1 mol/L

Element	Extraction, % Molarity of HBr				
	1	2	4	5	6
Cu(II)	0.5			4.2	6.2
Zn(II)	1.3		4.9		3.6
As(III)	3.0		22.8	63.1	72.9
Sb(III)		37.9	14.9	9.0	6.1
Sb(V)				95.4	79.6
Se(IV)	0.3		3.5	18.3	31
Sn(IV)	11.5	45.2	85.4	77.4	45.1
Mo(VI)		0.2	28	25.0	54.1
Fe(III)	< 0.1	1.4	97.1	97.1	94.6
Cd(II)	0.4				0.9
Te(IV)	0.7				2.2
In(III)	15	85.2	99.9	99.4	93.5
Tl(III)	99.9	> 99.9	> 99.9		99.0
Tl(I)*	99.5		97.0	77.3	6.2

* Extraction into diethyl ether

All the other elements, such as Fe(II), Ti(VI), Co(II), Ni(II) and V(IV), are extracted to a negligible extent

Many polarographic determinations of thallium (12,18-20) have been reported. Thallium gives a well-defined wave at approximately -0.45 V (vs. saturated calomel electrode) in most supporting electrolytes (1). Lead is the most commonly encountered interfering ion. Interference by lead is usually eliminated by a suitable electrolyte, or by complexation with EDTA. In fact, polarographic techniques are not sufficiently sensitive for the determination of thallium in most environmental samples, therefore this technique was not studied in the present work.

Although DPASV with HMDE or TFM on RGCE is capable of determining thallium in the nanogram range, both HMDE and TFME suffer from interference problems. Thallous ions do no form complexes readily. Therefore, when using an HMDE, the approach used is to move the reduction potentials of lead and other interfering ions to more cathodic values by the addition of EDTA or a similar suitable electrolyte (21). Thus Zitko et alia (22) selected a 2 M acetate buffer containing 0.2 M EDTA for the distinguishing/determination of thallium and lead in natural waters by ASV; however Florence et alia (17) selected 1 M acetate with 0.2 M EDTA buffer (pH 4.6) for the determination of thallium in natural waters. Temmerman et alia (19) employed a mixture of 0.3 M HAc + 0.3 M NH_4Ac + 0.05 EDTA for the determination of thallium in analytical grade cadmium. Figure 4.1 illustrates the manner in which the resolution of a group of metals may be improved by the choice of the appropriate supporting electrolyte (21). DPASV with TFM on RGCE is sufficiently sensitive for the determination of thallium but cadmium ions interfere markedly with the determination. The interference problem can be removed by addition of 20 µl of Triton X-100. Although the TFME is sensitive for thallium determinations, it is not reliable. Very careful attention must be taken, especially with the treatment of the electrode surface,

FIG. 4.1 EFFECT OF COMPLEX-FORMING ON PEAK POTENTIAL OF THALLIUM, LEAD AND TIN

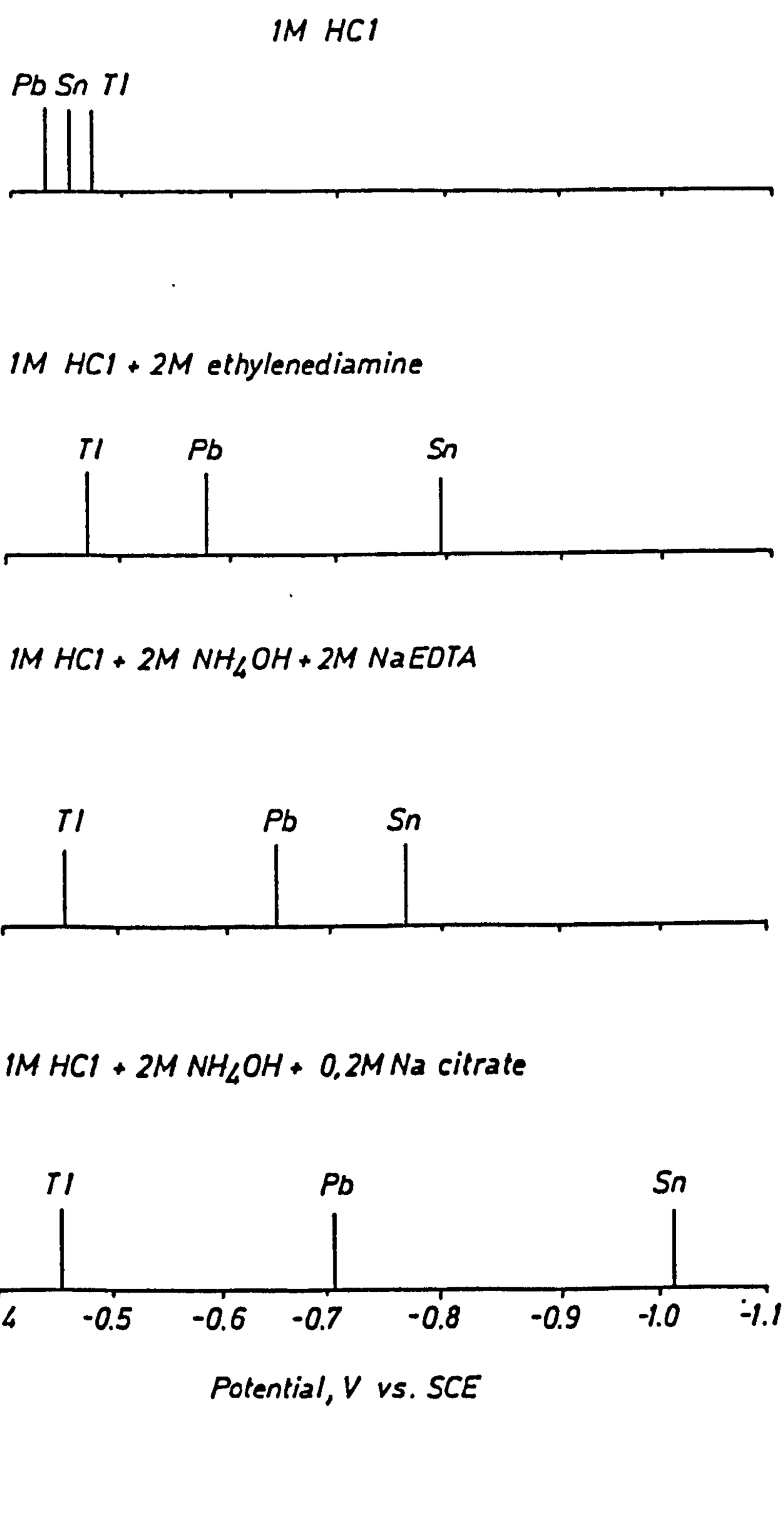

the potential applied, and the storage of electrodes.

However, DPASV with an HMDE is a more reliable technique for the determination of thallium. The next question to be asked is, what is the detection limit of thallium by this technique? The term detection limit is widely used but is a relatively poorly understood termsused to describe the smallest quantity of analyte than can be reliably detected (23). Braun (24) defined the detection limit as $\pm$ 2.5 S where S is the standard deviation of the mean, while +2.5S and -2.5S indicate the upper and lower detection limits respectively. In fact, the detection limit must depend on the calibration function. Therefore, in the present work, the limit of detection of thallium by DPASV with HMDE was calculated by application of the method suggested by Bailey et alia (25). The principle of the method is comparison between two prediction limits for a given concentration. The lower prediction limits were compared with the upper prediction limits on the blank until the lower prediction limit was found which was greater than, or equal to, the upper prediction limit of the blank.

After some deliberation, it was decided to design the experimental work to answer the following questions,(if possible) :

1) What parameters in DPASV using HMDE and TFME give the optimum signal for thallium determination? The observed optimum parameters were applied in the determination of thallium in different samples.

2) Is thallium associated with the smallest particle size of sediments? Most investigations (26,27) have reported that heavy metals are associated with the smaller particle sizes of sediments due to the large surface area, more is adsorbed on the Fe-Mn oxides phase, while high levels of organic materials act as good scavengers for heavy metals. Linton

et alia (28) reported that thallium was associated with the smaller particle sizes of coal fly ash.

3) Does thallium form complexes with humic acid? Several workers (22,29) have reported that the toxicity of thallium is not affected by the presence of humic acids; these studies indicate that thallium does not form a complex with humic acids in natural waters.

4) Is thallium in soil available to plants? If it is, what is the effect on germination of seeds and at which concentration is it toxic to plants?

When studying a particular method for assessing the toxicity it has been shown that the effect upon yield of a potentially harmful element depends on its concentration in the plant tissue (30). This has been established for several metals in plants (31). It was shown that the yield curve (see Figure 1.7) reduces to a straight line when the concentration is plotted in a logarithmic form - one line is horizontal yield plateau and the other a sloping regression line (see Figure 4.2) which meet at the upper critical level, T_C.

FIG. 4.2 YIELD CURVE FOR :–

(A) Essential elements
(B) Non-essential elements
Y_0 Yield unaffected by toxicity
T_{C1} Lower critical level
T_{C2} Upper critical level
TL Lethal concentration

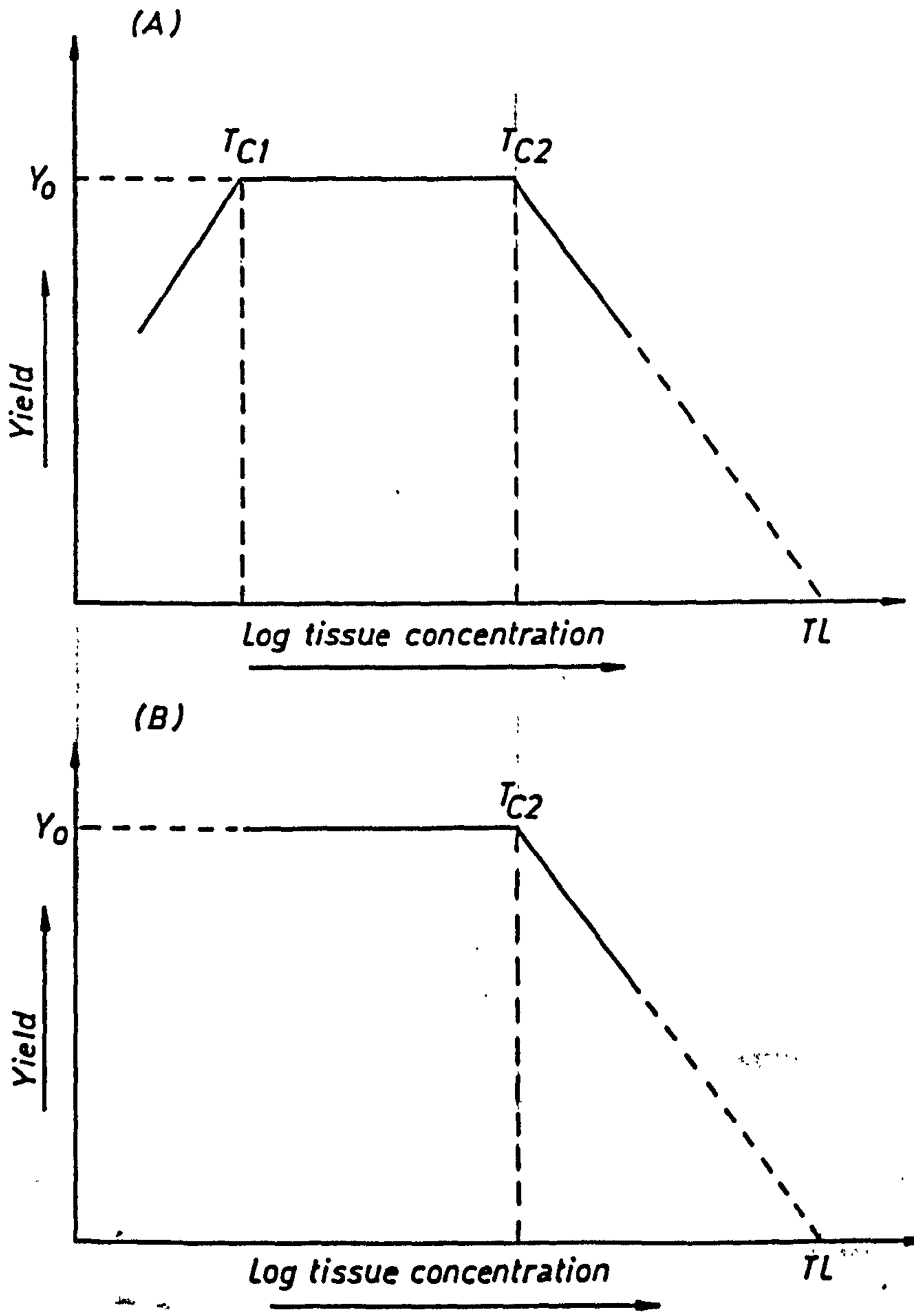

4.2 EXPERIMENTAL AND RESULTS

a) Experimental Preparation

i) Reagents

AnalaR and AristaR reagents were used whenever possible, these were :- nitric acid, acetic acid, thallous nitrate, sodium acetate, ethylenediaminetetra-acetic acid (disodium salt), ascorbic acid, ammonium chloride, 4-methylpentane-2-one, sodium diethyl dithiocarbamate, thallous chloride, thallic nitrate, thallic acetate, hydrochloric acid, aluminium oxide (0.015 um), hydrazine sulphate, sodium sulphite, diethyl ether, hydrobromic acid and bromine.

ii) Preparation of Solutions

Stock solutions containing 1000 ug of the thallium per cm^3 of DDW were prepared by dissolving thallous nitrate (0.5520 g) in DDW and dilution to a final volume of 500 cm^3.

The acetate buffer containing 1 M HAc + 1 M NaAc + 0.01 M EDTA Na_2 electrolyte was prepared by dissolving sodium acetate trihydrate (34.25 g) in DDW (150 cm^3). Glacial acetic acid (14 cm^3) and EDTA Na_2 were added and diluted to 250 cm^3 with DDW.

The 1 M NH_4Cl + 0.1 M citric acid + 0.025 M ascorbic acid electrolyte (pH 2.9) was prepared by dissolving ammonium chloride (26.75 g) and citric acid (10.50 g) in DDW (300 cm^3). Ascorbic acid (2.25 g) was added, the mixture was shaken for 10 minutes and diluted to 500 cm^3 with DDW.

An 0.2 M NH_4Ac electrolyte (pH 7) was prepared by dissolving NH_4Ac (1.5 g) in DDW (100 cm^3).

The citrate buffer (pH 3) was prepared by dissolving citric acid (4.2 g) in DDW (80 cm^3). Sufficient ammonia solution was added to the

citric acid solution until the solution attained the correct pH.

Mercury cathode electrolysis was used for purification of the supporting electrolyte (1 M HAc + 1 M NaAc + 0.01 M EDTA Na_2). The solution was contained in a 3-litre cell designed as in Figure 4.3. A pool of clean mercury encircled a low glass rim in the centre of the cell floor. A magnetic stirrer bar was located on this glass platform. The mercury was negative with respect to the buffer solution. The voltage was increased to -2 V by which metals should be removed from solution. The solution was stirred overnight; the next day the buffer solution was examined by DPASV with HMDE which only yielded a negative peak, probably due to the formation of mercuric-EDTA. Therefore, the electrolytes were used directly without further purification.

b) Determination of Thallium by Polarography and Differential Pulse Anodic Stripping Voltammetry

1) Polarography

Three modes of polarography were used to determine thallium in 1 M HAc + 1 M NaAc + 0.01 M EDTA electrolyte. These included direct current mode (DC), pulse polarography mode (PP) and differential pulse polarography mode (DPP). Background electrolyte (10 cm^3) was placed in a polarographic cell and the polarogram recorded. Known amounts of thallium as $TlNO_3$ (1000 $\mu g/cm^3$) were added as spikes to the background electrolyte to give the concentrations of thallium given in Figures 4.4 - 4.6.

FIG.4.3 MERCURY CATHODE ELECTROLYSIS FOR PURIFICATION OF BACKGROUND ELECTROLYTES

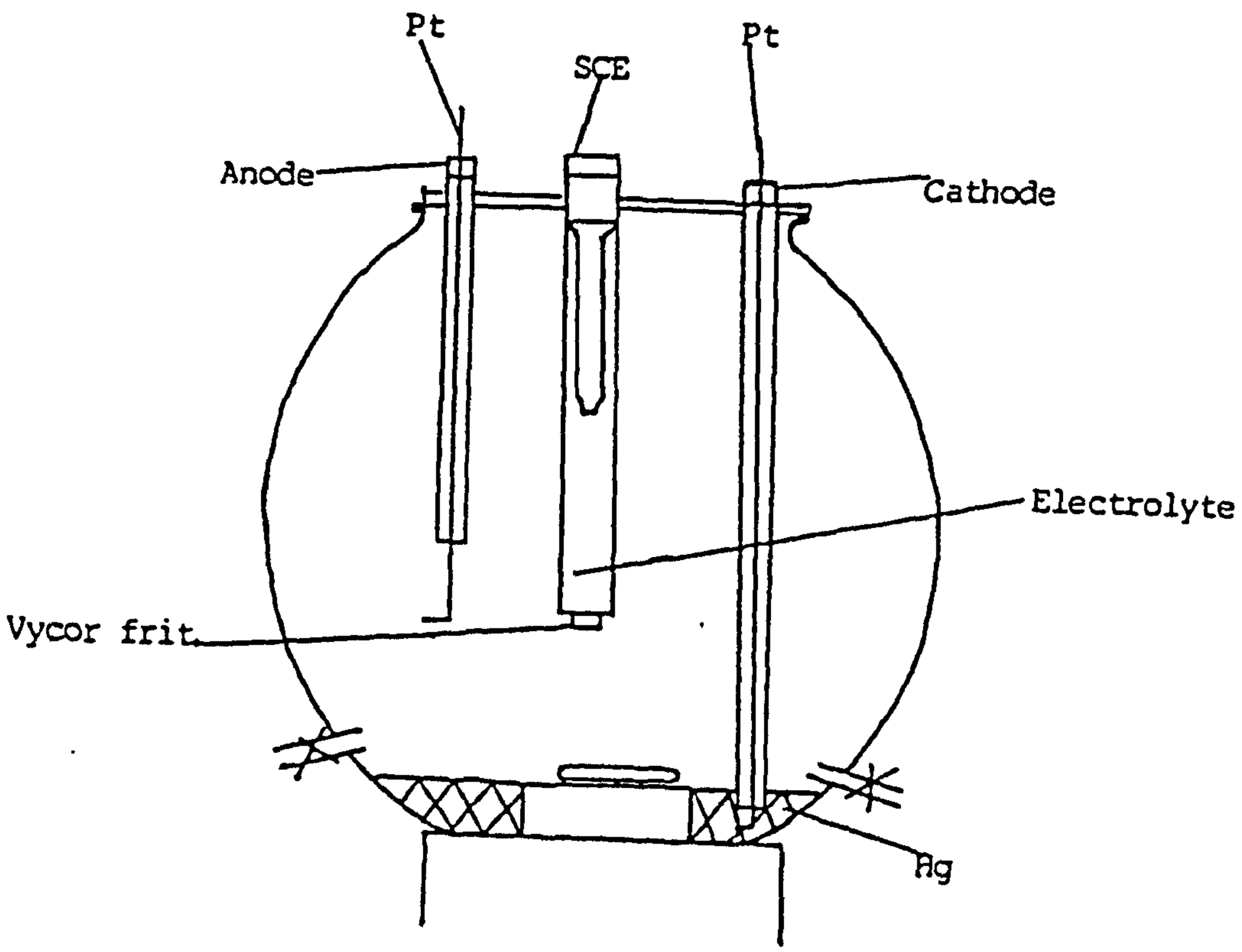

FIG. 4.4 VOLTAMMOGRAM OF THALLIUM BY DC-POLAROGRAPHY

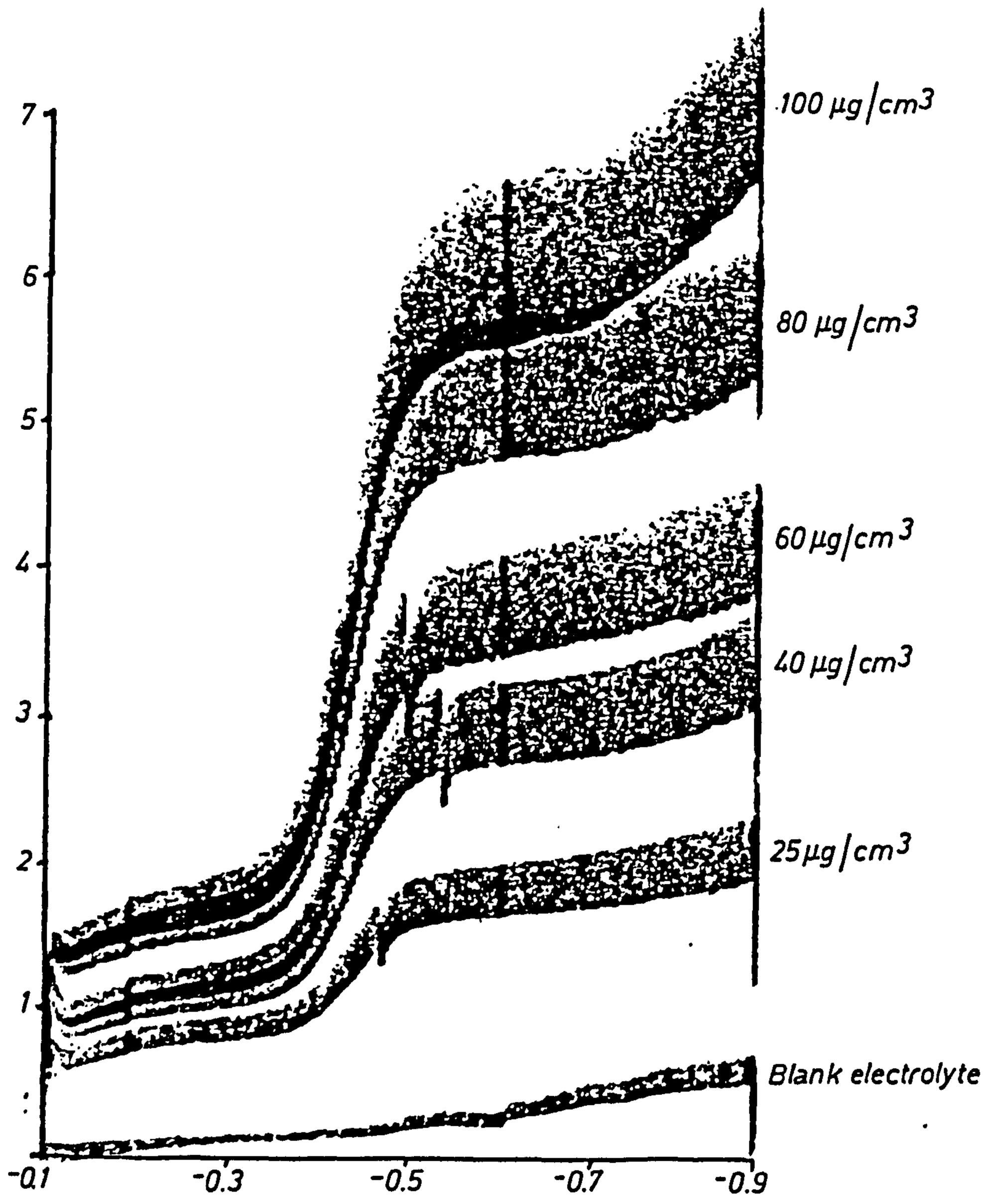

FIG. 4.5 VOLTAMMOGRAM OF THALLIUM BY PULSE - POLARGRAPHY

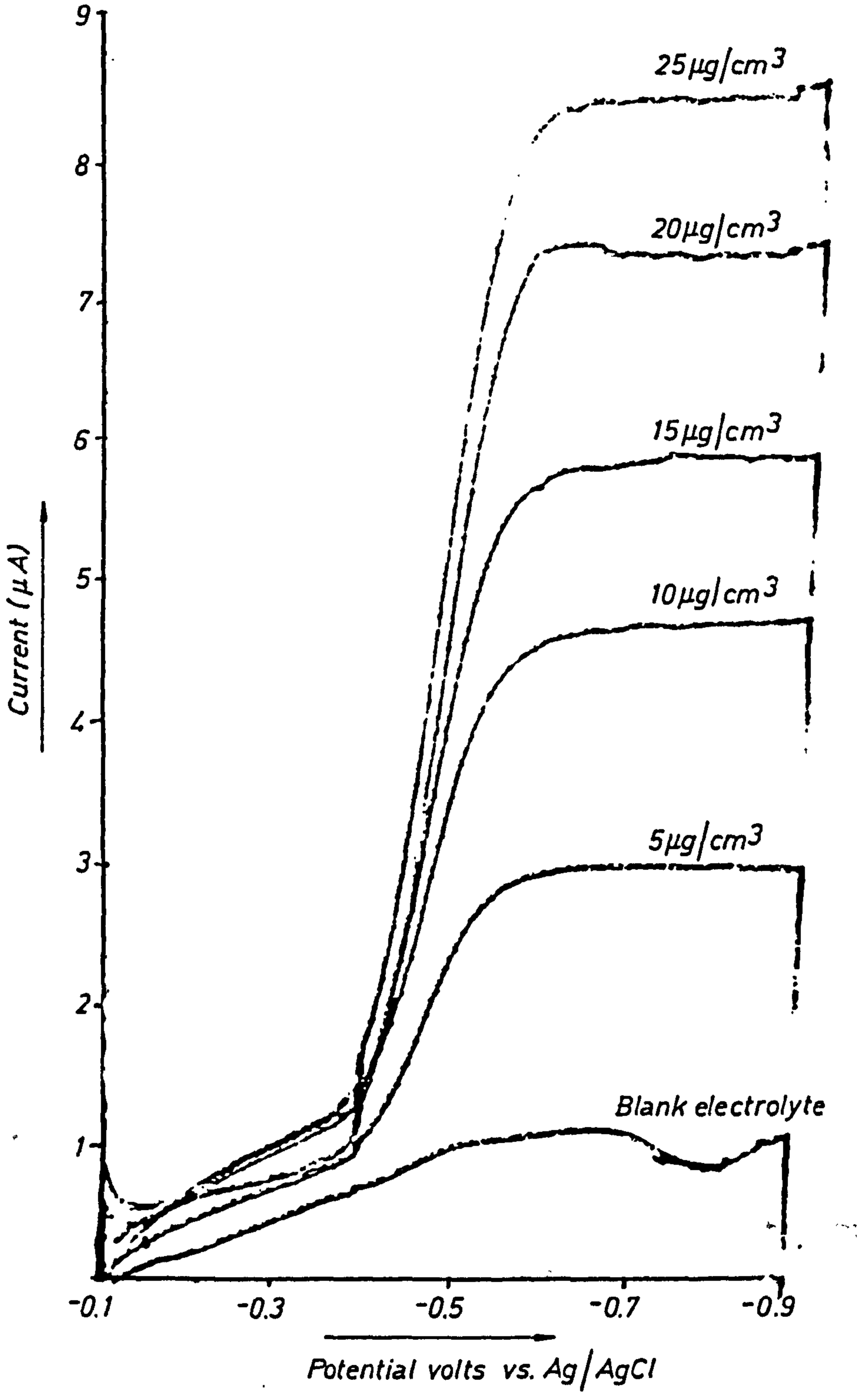

FIG. 4.6 VOLTAMMOGRAM OF THALLIUM BY DIFFERENTIAL PULSE POLARGRAPHY

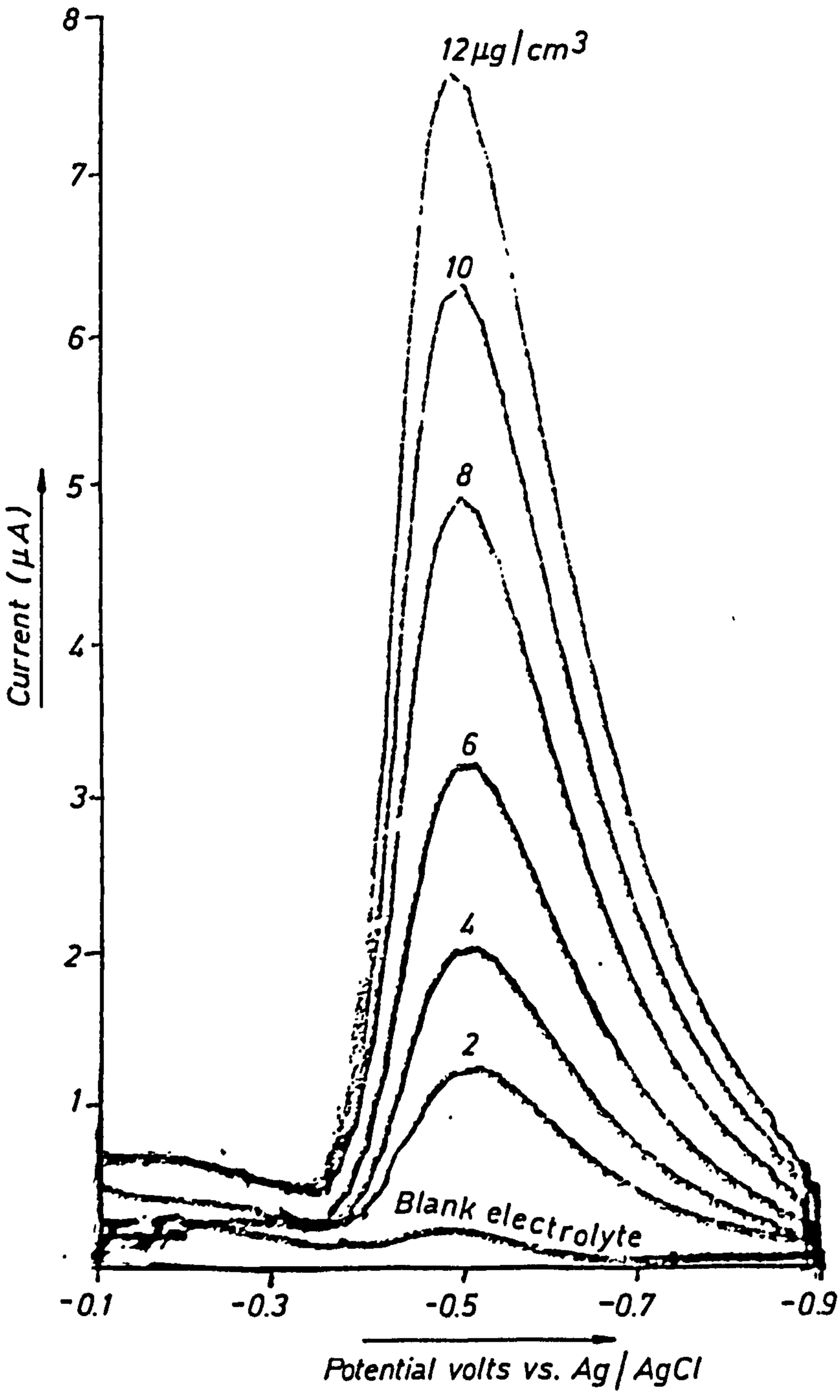

2) DPASV with HMDE

The background electrolyte (1 M HAc + 1 M NaAc + 0.01 M EDTA) (10 cm^3) was placed in a voltammetric cell and deoxygenated by passing purified nitrogen for 5 minutes. The voltammogram was then recorded. Six additions of 20 μl thallium (10 $\mu g/cm^3$) were added and a voltammogram was recorded following each addition. The voltammograms obtained are shown in Figure 4.7.

To investigate the interference of lead and cadmium on thallium peak height using DPASV with the HMDE, the voltammograms of different background electrolytes (10 cm^3) with thallium (400 ng) were recorded Lead or cadmium (20 μl of 10 $\mu g/cm^3$) was added and the voltammogram also recorded. The change in peak height of thallium was examined after each addition of cadmium or lead. The results are listed in Tables 4.2 and 4.3.

Table 4.2 : Effect of Lead on Peak Height (cm) of Thallium at Different Electrolyte Solutions

Electrolyte	A	B	C
Peak height of 40 ppb Tl	6	2	1.6
Peak height of 40 ppb Tl + 40 ng/cm^3 Pb	8	4.8	3.0
Peak height of 40 ppb Tl + 60 ng/cm^3 Pb	10	5.8	3.8

A,B, and C are defined in Table 4.3

FIG. 4.7 VOLTAMMOGRAM OF THALLIUM BY DPASV WITH HMDE

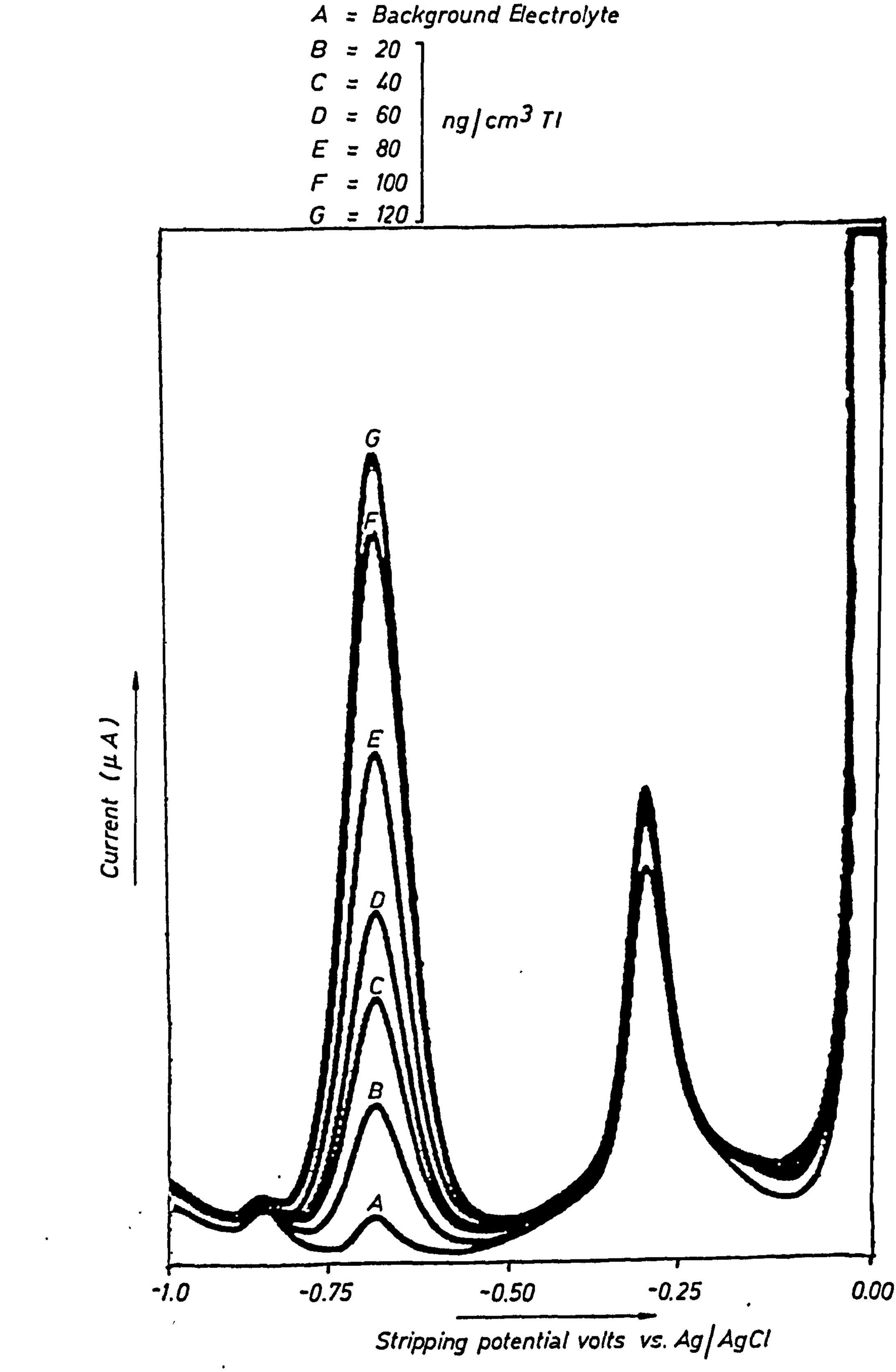

Table 4.3 : Effect of Cadmium on Peak Height (cm) of Thallium at Different Electrolyte Solutions

Electrolyte	A	B	C
Peak height of 40 ppb Tl	6	3.8	3.0
Peak height of 40 ppb Tl + 40 ng/cm^3 Cd	N.C.	N.C.	N.C.
Peak height of 40 ppb Tl + 60 ng/cm^3 Cd	N.C.	N.C.	N.C.
Peak height of 40 ppb Tl + 0.1 μg/cm^3 Cd	N.C.	N.C.	N.C.
Peak height of 40 ppb Tl + 1 μg/cm^3 Cd	N.C.	N.C.	N.C.

A = 10 cm^3 pf 1 M HAc + 1 M NaAc

B = 10 cm^3 of 1 M HAc + 1 M NaAc + 0.01 M EDTA Na_2

C = 10 cm^3 of 0.5 M HAc + 0.5 M HAc + 0.5 M EDTA Na_2

N.C. = No change in peak height.

To study the effect of deposition time on the peak height response of the thallium, a solution of thallium was prepared in DDW and spiked into 10 cm^3 of the electrolyte (1 M HAc + 1 M NaAc + 0.01 M EDTA Na_2) to give a solution of thallium concentration of 60 ng/cm^3. Voltammograms were measured at specific deposition times. After stripping of thallium back to the solution, the electrode was cleaned and the process repeated at a different deposition time with a new solution. The results obtained are presented in Table 4.4.

Table 4.4 : Effect of Deposition Time (sec) on Peak Height (cm) of Thallium at HMDE

Deposition Time (seconds)	Peak Height (cm)
90	8.5
120	10.2
150	11.8
180	13.5
210	17
240	19
270	20
300	23

The effect of pH of different electrolytes on peak height of thallium was also studied. An aliquot (10 cm^3) of each electrolyte solution was placed in a voltammetric cell, spiked with thallium and the voltammogram was recorded. The results are described in Figure 4.8.

An attempt was made to examine the interaction of humic acid with thallium ions. The voltammogram of acetate buffer containing a concentration of thallium (100 ng/cm^3) was recorded. Different amounts of humic acid were added as spikes, each addition being 20 μl of 1% (v/v) humic acid. The voltammograms were recorded and are shown in Figure 4.9.

FIG. 4.8 VOLTAMMOGRAM OF THALLIUM AT DIFFERENT PH's AT AN HMDE

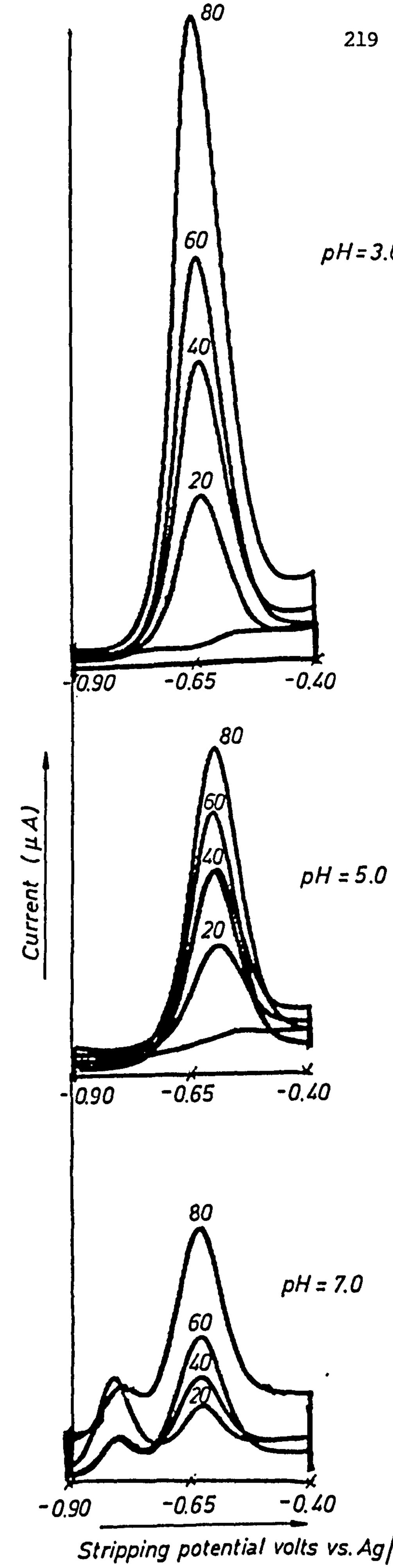

FIG. 4.9 EFFECT OF HUMIC ACID ON THALLIUM PEAK HEIGHT AT HMDE

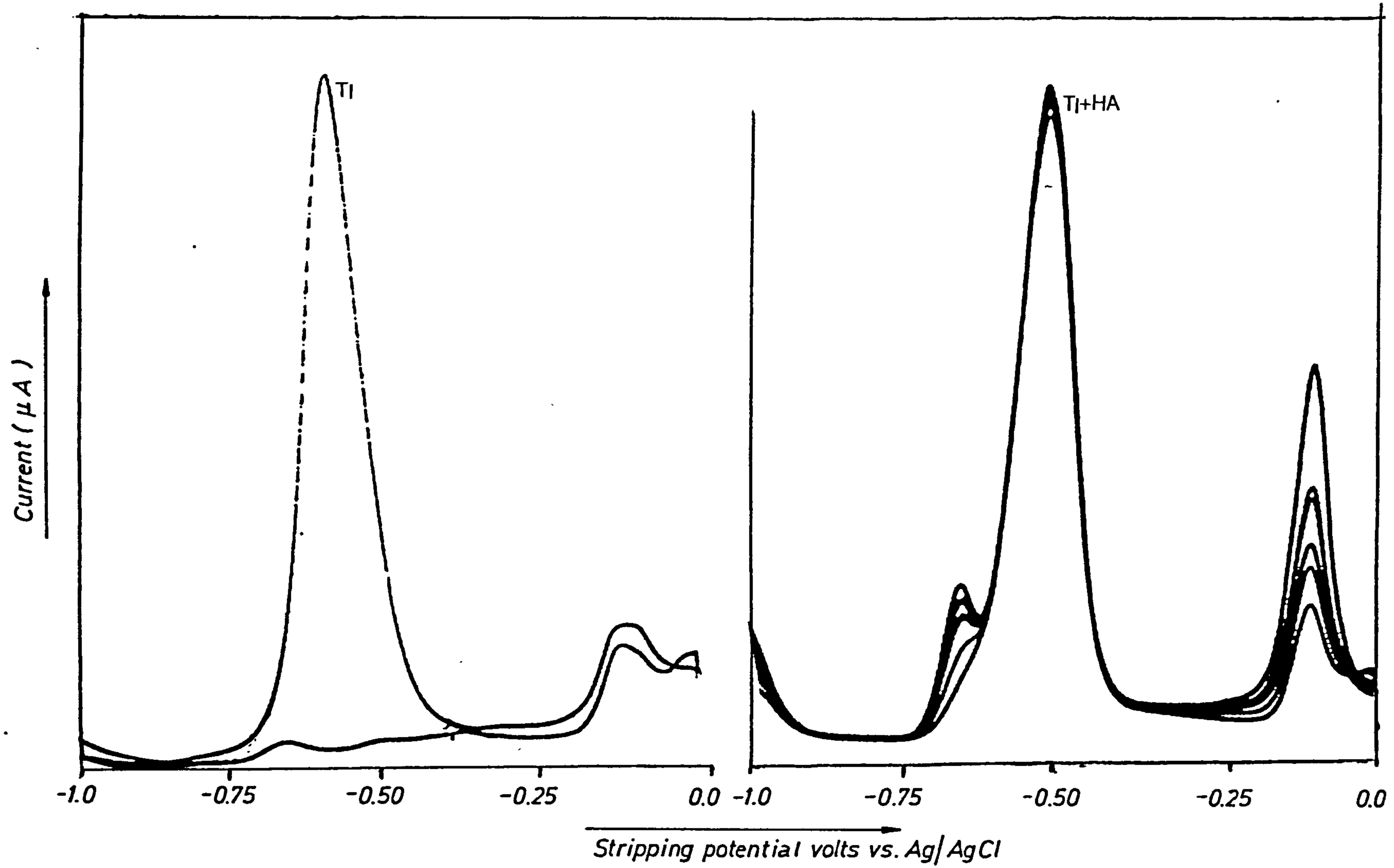

3) DPASV with TFME

The cleaning and preparation of the active electrode surface of an RGC is very important for the determination of thallium. The electrode was cleaned as follows (32) :

i) the electrode tip was polished with aluminium oxide powder using a wet polishing cloth;

ii) the polished front face was rinsed several times with DDW;

iii) the electrode tip was polished on a wet polishing cloth without any aluminium oxide;

iv) the polished face was rinsed several times with DDW.

After polishing the electrode tip, the front face should show a surface as smooth as a mirror. The electrode is ready for use immediately after polishing. The TFM was prepared on RGC by addition of 20 μl of 5×10^{-2} M mercuric nitrate to 20 cm^3 of 1 M NH_4Cl + 0.1 M citric acid + 0.025 M ascorbic acid in the voltammetric cell. The voltammogram was recorded. Next, 20 μl aliquots of thallium (10 $\mu g/cm^3$) were added as a series of spikes and a voltammogram was recorded after each addition. A typical voltammogram is shown in Figure 4.10.

i) Rotation of the electrode

Speeds of rotation between 500-3000 r/min were selected as suitable values. The voltammograms obtained are shown in Figure 4.11.

ii) Modulation Amplitude

Modulation amplitudes between 5 to 50 mv were selected as suitable values for the DP signal. The voltammograms are listed in Figure 4.12.

FIG. 4.10 VOLTAMMOGRAM OF THALLIUM BY DPASV WITH TFME

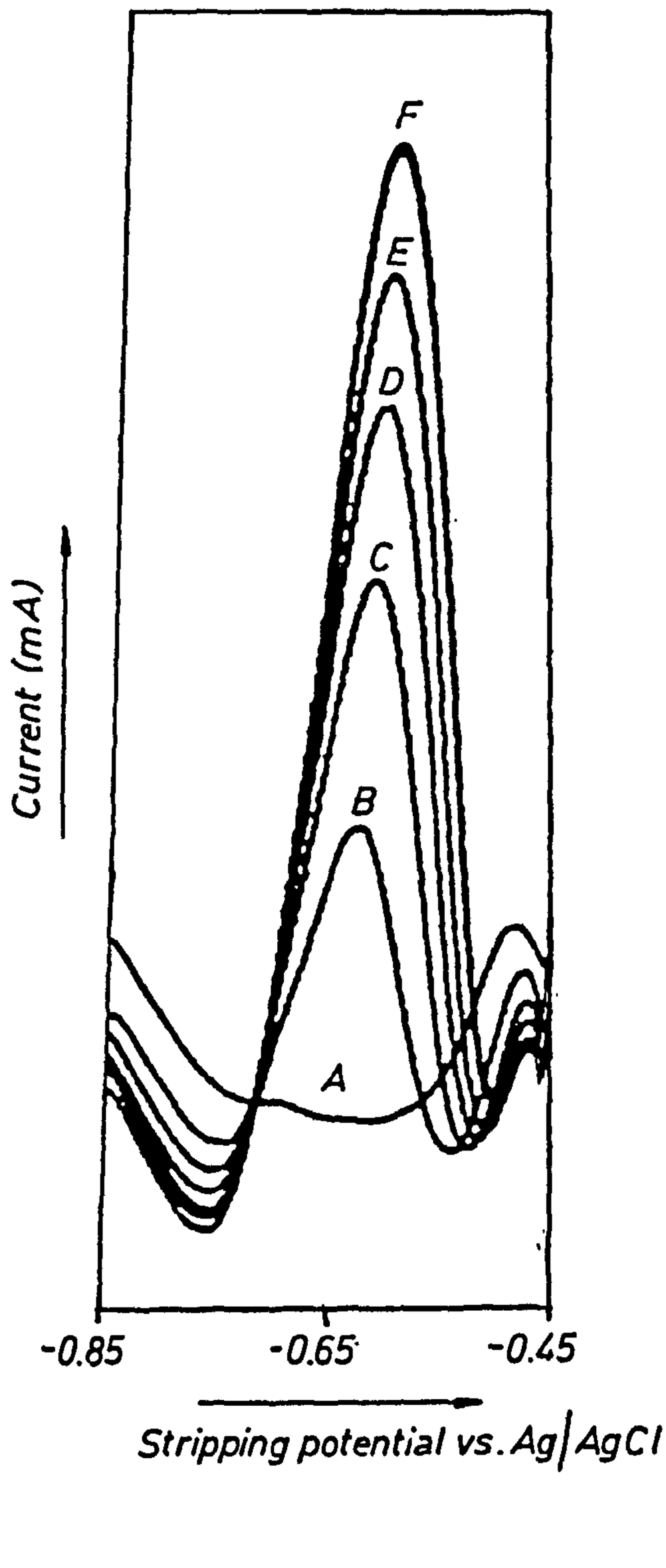

FIG.4.11 EFFECT OF SPEED OF ROTATION OF THE ELECTRODE ON PEAK HEIGHT OF METALS IN BACKGROUND ELECTROLYTE SOLUTION

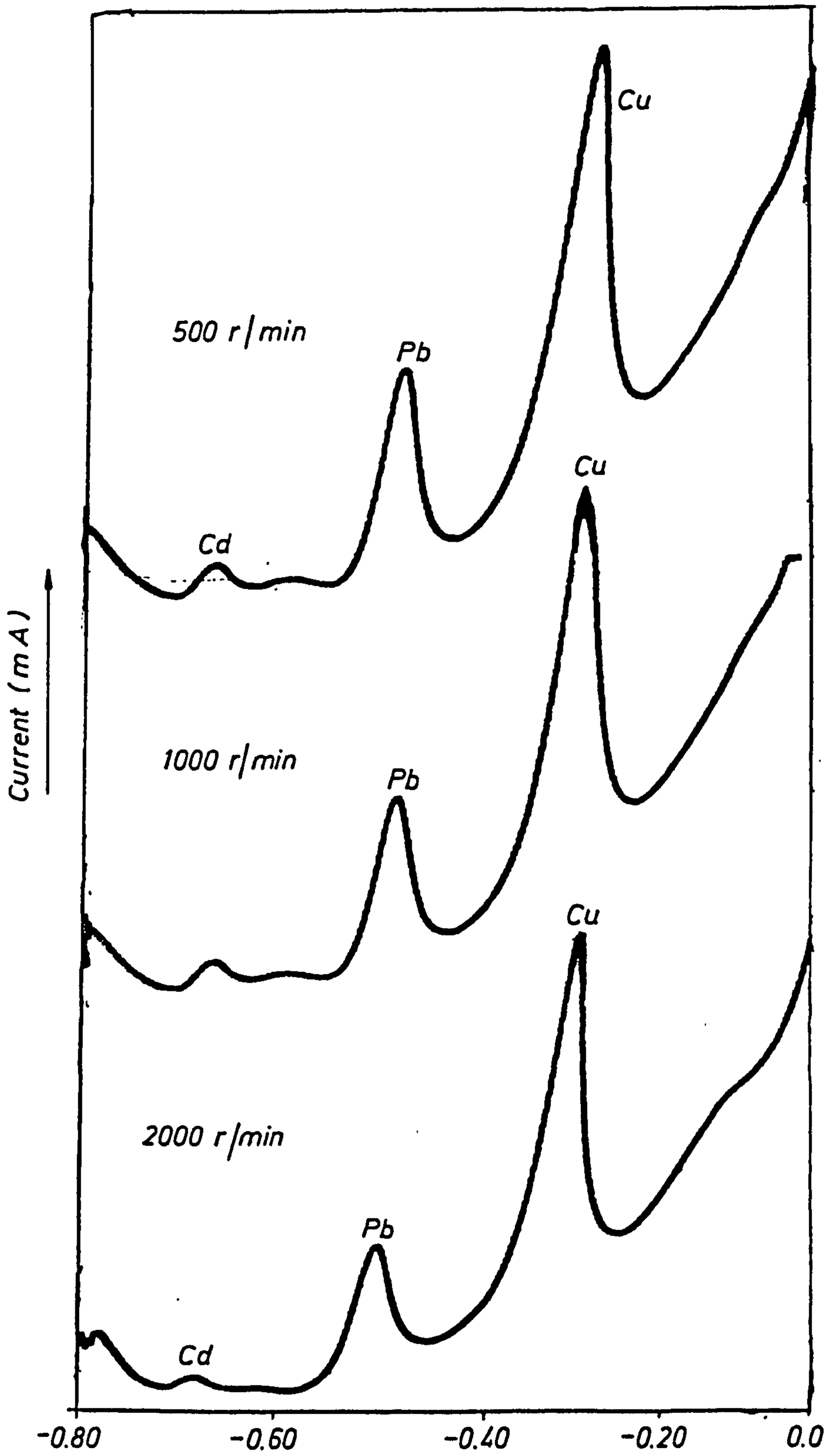

FIG. 4.12 EFFECT OF MODULATION AMPLITUDE ON PEAK HEIGHT OF THALLIUM

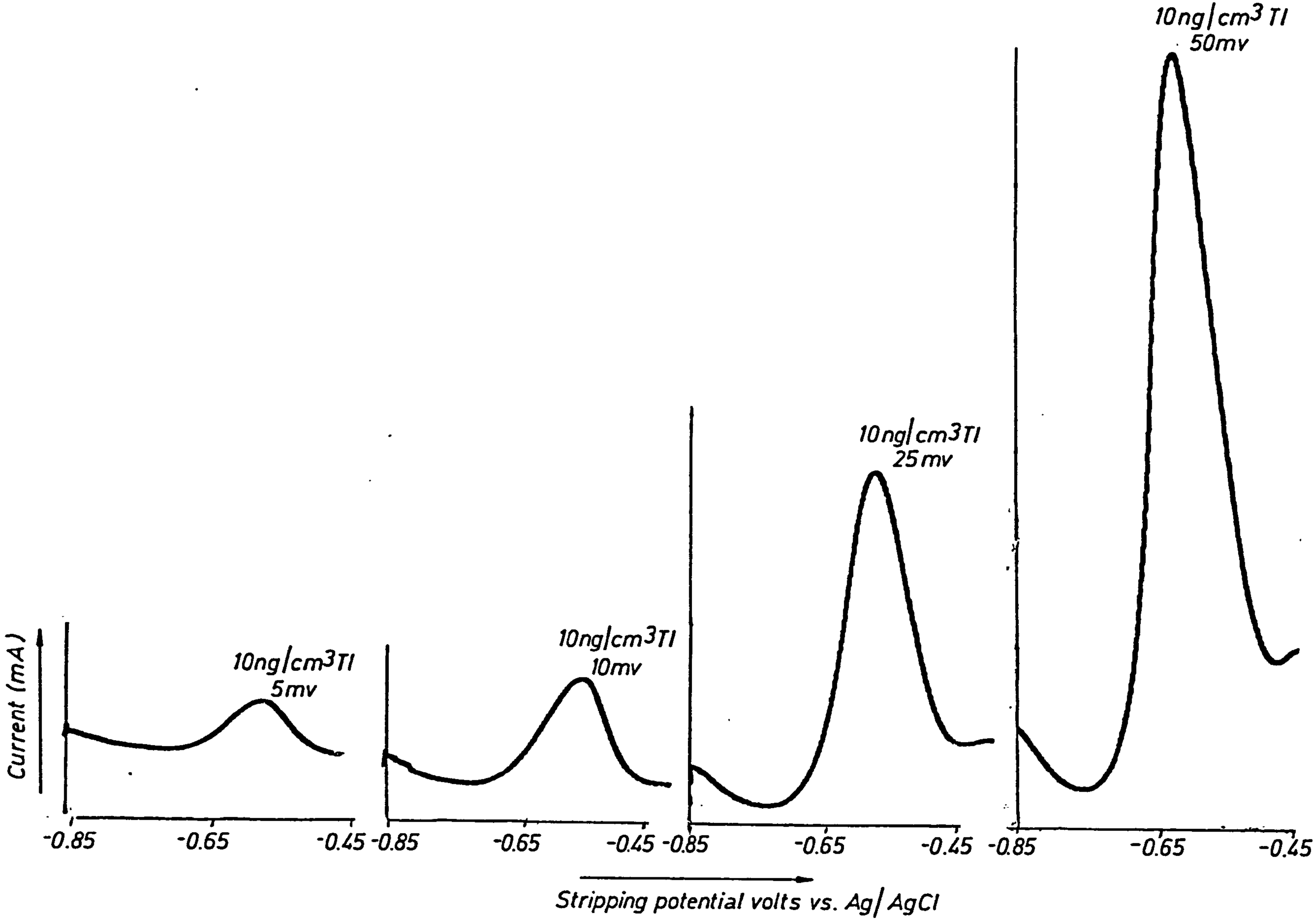

iii) Potential Scan Rate

Scan rates from 2 to 50 mv/sec were selected. The voltammograms are given in Figure 4.13.

iv) Deposition Time

Five pre-electrolysis periods were selected and the results obtained are shown in Table 4.5.

v) pH of Background Electrolytes

Three electrolytes (pH 3, pH 5 and pH 7) were used. The voltammograms are presented in Figure 4.14.

vi) Addition of Triton-X-100

The voltammograms for the background electrolytes were recorded before and after addition of 20 ul of Triton-X-100. The voltammograms are shown in Figure 4.15.

Table 4.5 : Effect of Deposition Time on Peak Height of Thallium at TFME

Peak Height (cm)	Deposition Time (sec)
3	180
4.5	240
5.5	300
6.5	360
6.5	420

FIG. 4.13 EFFECT OF POTENTIAL SCAN RATE ON PEAK HEIGHT OF THALLIUM AT TFME

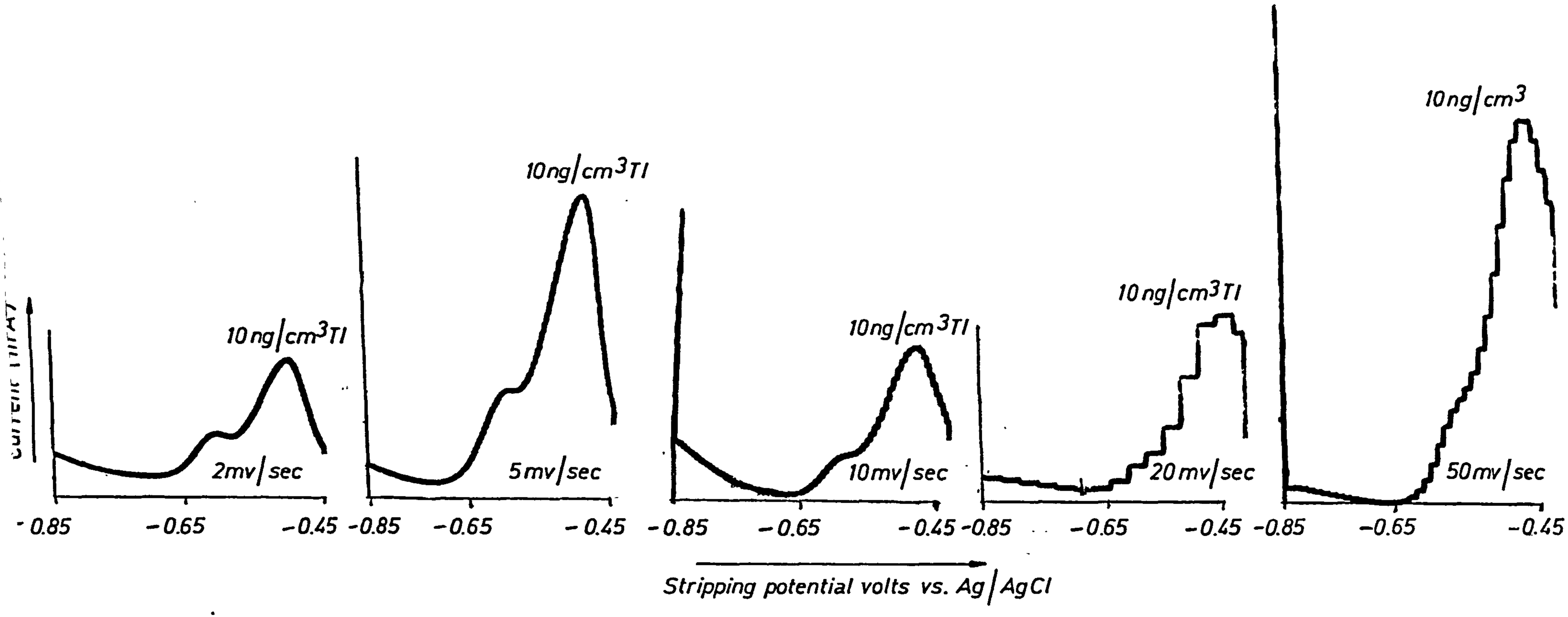

FIG. 4.14 EFFECT OF PH ON PEAK HEIGHT OF THALLIUM AT TFME

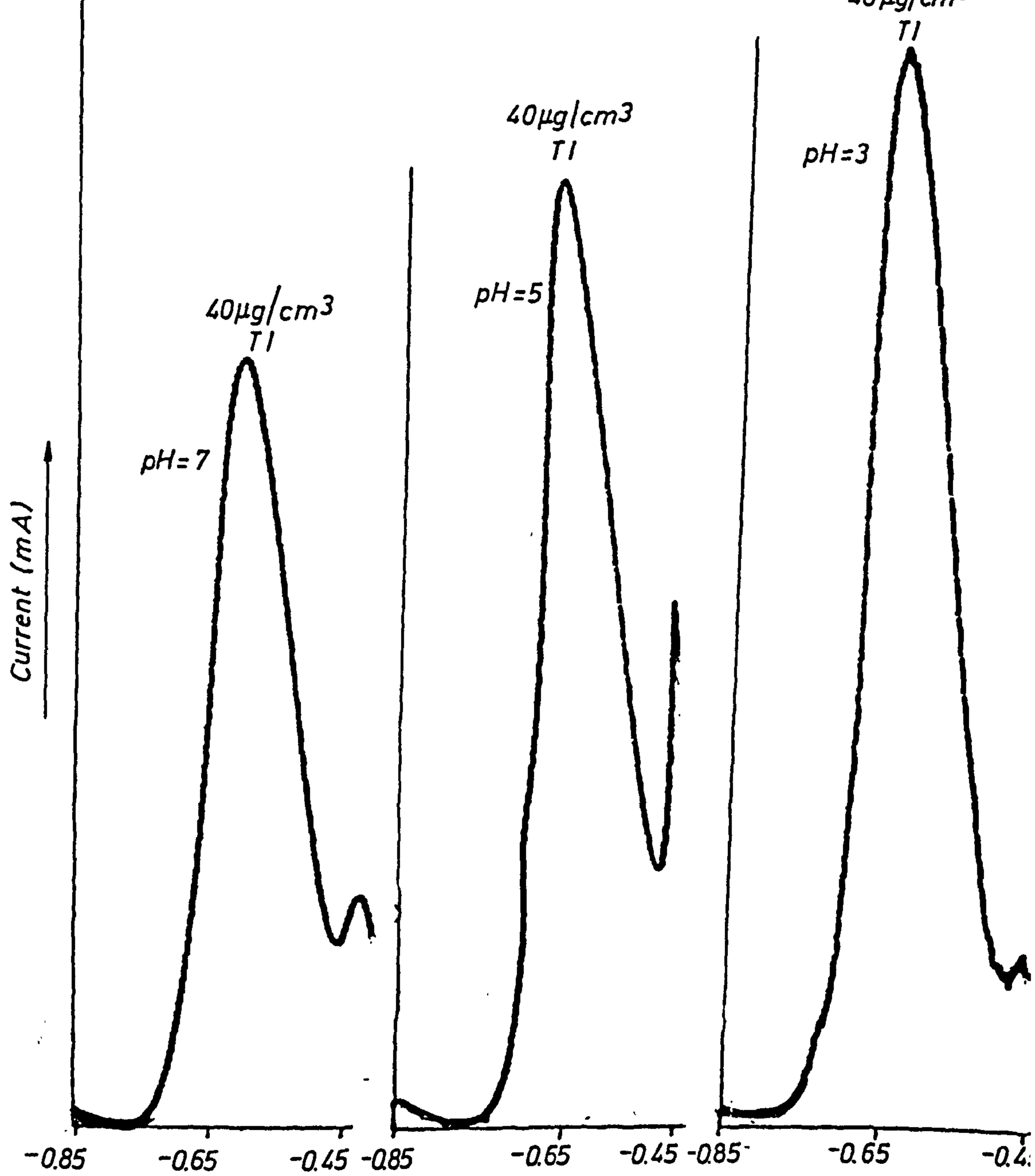

FIG. 4.15 EFFECT OF ADDITION OF TRITON X -100 ON PEAK HEIGHT OF THALLIUM AT TFME

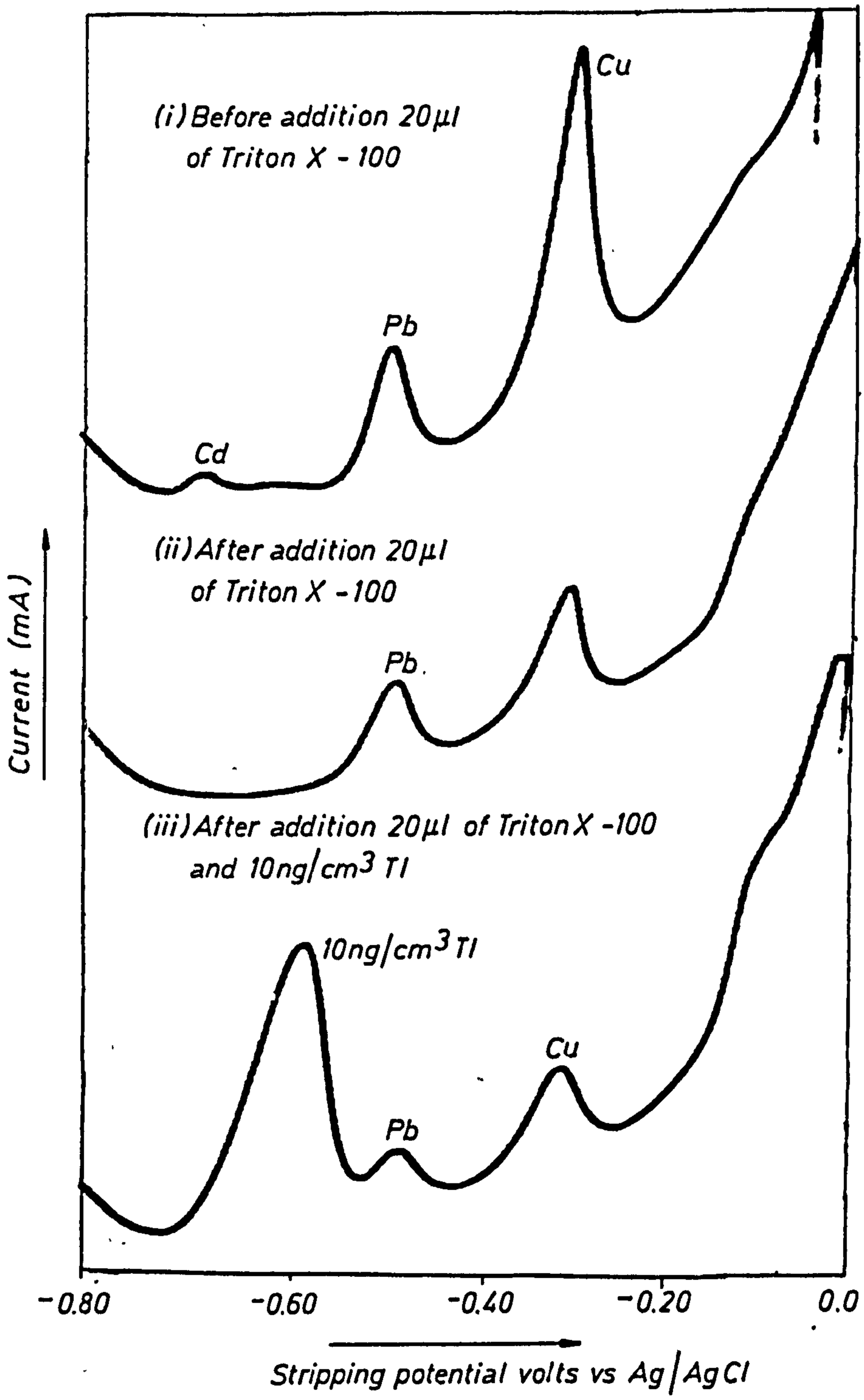

c) Determination of Thallium in Rocks, Sediments, Waters, Soils and Plants

i) Rocks and Sediments

Two procedures were carried out for the determination of thallium in samples after separation from matrix elements. A third procedure was applied for the determination of thallium in galena rock without separation from matrix elements.

1) Procedure A

Full details of the method are given in Figure 4.16. After acid dilution, the method was based on a liquid-liquid extraction of thallium (III) bromide in diethyl ether and the reduction of thallium (III) to thallium (I) by $NH_2.NH_2.H_2SO_4$. Thallium was determined by DPASV with HMDE.

2) Procedure B

Full details of this method are given in Figure 4.17. In this method, thallium was separated from the matrix elements by anion-exchange procedures; the thallium (III) species is reduced to thallium (I) by sodiummetabisulphite which is desorbed from the resin. Thallium was determined as in Procedure A.

A blank was run for each procedure in an attempt to ascertain the level of contamination; fortunately in each blank the level of thallium was not enough to detect by DPASV at HMDE. The thallium in samples was determined by the standard addition method. Other metals (Zn, Cu, Cd, Pb) were also determined in each sample. Each sample (0.5 g) was digested with concentrated HNO_3 (10 cm^3) and heated under an IR lamp until the volume was reduced to 2 cm^3. The sample was cooled and DDW (15 cm^3) was

Figure 4.16 : Procedure A (21)

Place 1 g of sample in a small beaker

↓

Add Br_2 (2 cm^3) and HNO_3 (4 cm^3). Cover and heat gently to expel the bromine

↓

Cool, add HNO_3 (4 cm^3)

↓

Heat again and reduce the volume to 1 cm^3

↓

Add Br_2-HBr mixture (3 cm^3) and wash the cover of the beaker with minimum water

↓

Heat again to expel excess bromine

↓

Cool and filter through Whatman 541 filter paper

↓

*Dilute to 25 cm^3

↓

Transfer the solution to separating funnel

↓

Extract with diethyl ether (10 cm^3)

↑

Shake for 5 minutes

↑

Transfer the aqueous layer to another separating funnel

↑

Extract with diethyl ether (10 cm^3)

↑

Combine the ether layers and discard the aqueous layer

↑

Wash the combined ether layer twice with 1M HBr (10 cm^3)

↑

Run the ether extract into a beaker

↑

Evaporate ether on waterbath (with caution)

↑

Add H_2SO_4 (0.5 cm^3) and heat until white fume

↑

Add HNO_3 (1 cm^3) and heat for 15 minutes

↑

Add 6N H_2SO_4 (2 cm^3) saturated with 1.48×10^{-3} M Na_2SO_4 + 3.8×10^{-4} $NH_2.NH_2.H_2SO_4$ and heat to dryness

↑

Extract the residue with 1 M HAc + 1M NaAc + 0.01M EDTA (10 cm^3)

↑

Determine thallium by DPASV with HMDE

Figure 4.17 : Procedure B (33)

See procedure A for sample decomposition (to step *)

↓

Dilute to 100 cm^3 with 0.5 M HCl

↓

Pass the solution through 11 x 0.5 cm column of 100-200 mesh, Bio-Rad AG1-X8 anion-exchange resin in chloride form at a flow rate of 1-2 cm^3/min

↓

Wash with 2M HNO_3 (100 cm^3) to remove other trace elements

↓

Elute thallium with 1% (w/v) sodium metabisulphite (50 cm^3)

↓

Evaporate the eluate to dryness on a water bath

↓

Extract the residue with 1M HAc + 1M NaAc + 0.01M EDTA (10 cm^3)

↓

Determine thallium by DPASV with HMDE

added. The sample was filtered through Whatman 541 filter paper and diluted to 25 cm^3 with DDW. Zn, Cu, Cd and Pb were determined in the sample by FAAS. The results are presented in Table 4.6.

Table 4.6 : Determination of Zn, Cu, Cd, Tl and Pb in Samples ($\mu g/g$)

Sample	Zn	Cu	Cd	Tl*	Tl**	Pb
Galena	125	1,413	N.D.	0.132	0.020	79,938
Chalcopyrite	5,225	92,513	27	0.082	0.214	434
Sphalerite	40,359	68	113	0.165	0.322	1,360
Mineries Pool Exit Sediment	4,175	30	3	0.290	0.070	13,563

* Tl was separated from matrix elements by liquid-liquid extraction and determined by DPASV with HMDE

** Tl was separated from matrix elements by ion-exchange and determined by DPASV with HMDE

*** Zn, Cu, Cd and Pb were determined by FAAS (after acid digestion)

Figures 4.18 and 4.19 illustrate the voltammograms of thallium in galena extracted by procedures A and B respectively.

An unsuccessful attempt was made to determine the thallium associated with different particle sizes of Caradon stream sediment using procedure A. It was found that thallium was not detected in any fraction.

FIG. 4.18 VOLTAMMOGRAM OF THALLIUM EXTRACTED BY PROCEDURE A

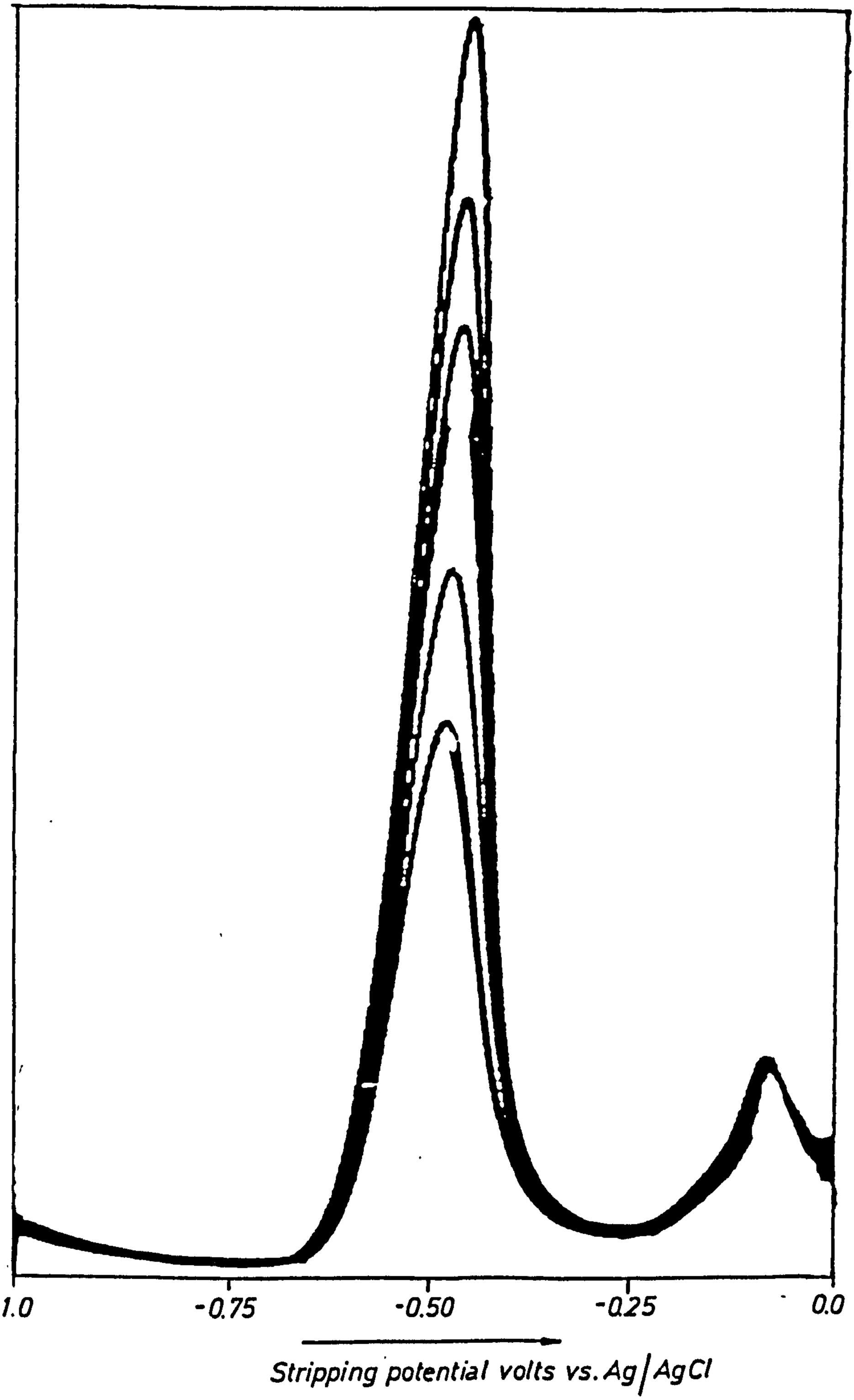

FIG. 4.19 VOLTAMMOGRAM OF THALLIUM EXTRACTED BY PROCEDURE B

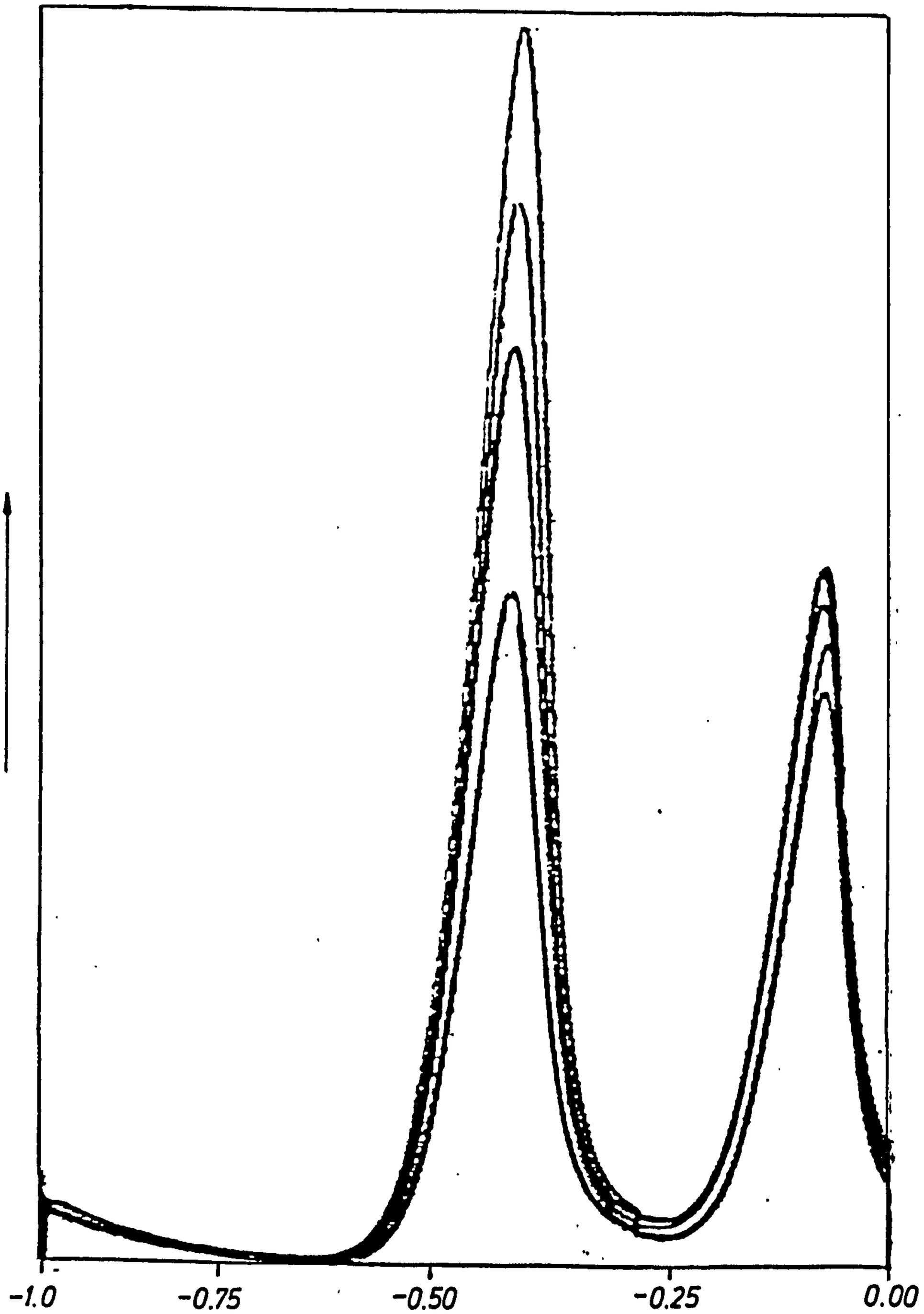

3) Procedure C

Full details of the method are presented in Figure 4.20. The principle of the method is that lead is complexed by tetrabutylammonium chloride (TBAC) and EDTA, and therefore it is not available to interfere with the thallium determination.

A typical voltammogram obtained by this procedure is shown in Figure 4.21. The amount of thallium in the galena sample was found to be 0.46 μg/g.

Figure 4.20 : Procedure C (34)

Place 0.5 g of galena in a small beaker

↓

Digest with HNO_3 (10 cm^3) under an IR lamp until dryness

↓

Cool and add DDW (10 cm^3)

↓

Filter through Whatman 541 filter papers to remove insoluble material

↓

Add 0.2M EDTA (10 cm^3) and 1M tetra-butylammonium chloride (0.25 cm^3)

↓

Adjust the pH of solution to 5 by dropwise addition of 10% (w/v) KOH solution

↓

Complete the volume to 25 cm^3 with 0.25M EDTA

↓

Place the sample (10 cm^3) in volta-mmetric cell and determine thallium by DPASV with HMDE

FIG. 4.21 VOLTAMMOGRAM OF THALLIUM EXTRACTED BY PROCEDURE C

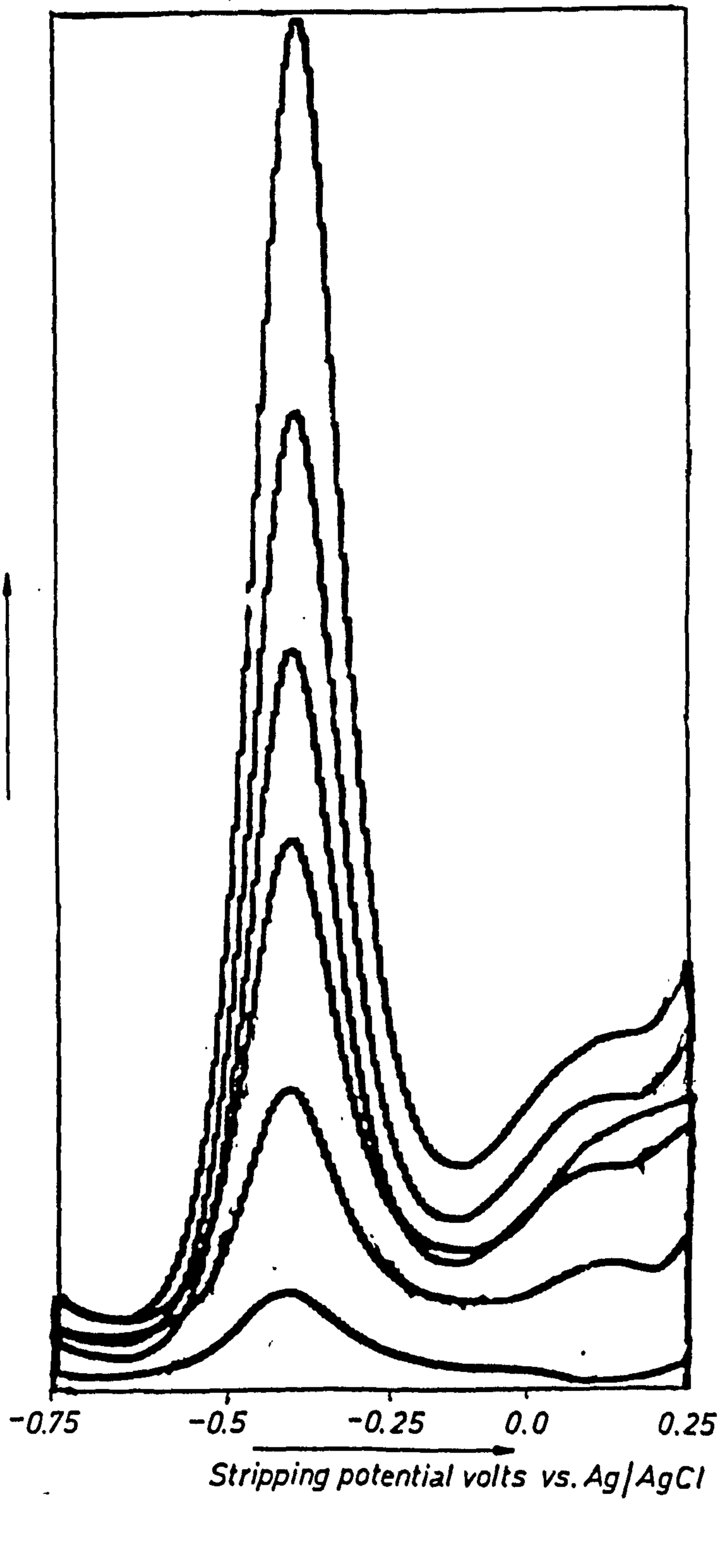

ii) Waters

Thallium was determined in Mendip Hill Waters (see Figure 3.6 for location sites). The procedure used is shown in Figure 4.22. The thallium was determined by DPASV with TFME.

The results obtained are listed in Table 4.7.

Figure 4.23 illustrates the voltammogram of thallium in sample W_2.

An unsuccessful attempt was made to determine thallium in water samples without addition of Br-HBr mixture by the procedure above. It was found that the response for thallium was no different from the blank.

Table 4.7 : Concentration of Thallium in Mendip Hill Waters, Analysis by DPASV with TFME

Sample Site	Thallium (μg/L)
Waldegrave Pool	
W_1	0.28
W_2	0.64
Fair Lady Well	
F_1	0.21
F_2	0.38
F_3	2.62
F_4	1.20

Figure 4.22 : Procedure for Determination of Thallium in Mendip Hill Waters (17)

Add HNO_3 (5 cm^3) to 2.5 litres of sample

↓

Filter, use 0.45 μMillipore filter membrane

↓

Add 4 cm^3 of Br-HBr mixture (1:10) and mix with the sample

↓

Cover the container with a black sheet to exclude dust and light

↓

Allow the sample to pass through 11 x 0.5 cm bed of 100-200 mesh, Bio-Rad AG1-X8 anion-exchange resin in chloride form, and leave it passing overnight at very low flow rate

↓

Wash with DDW (50 cm^3) containing 1 cm^3 of Br-HBr mixture if all the sample has entered the column

↓

Wash with DDW (50 cm^3)

↓

Elute the thallium with 1% (w/v) sodium metabisulphite (50 cm^3)

↓

Evaporate the eluate to dryness in a waterbath

↓

Dissolve the residue in 25 cm^3 of 1M NH_4Cl + 0.1M citric acid + 0.025M ascorbic acid

↓

Place the sample in a voltammetric cell, add 20 μl of 5 x 10^{-2}M $Hg(NO_3)_2$ and 20 μl of Triton X-100

↓

Determine thallium by DPASV with HMDE

FIG. 4.23 VOLTAMMOGRAM OF THALLIUM IN SAMPLE (W_2)

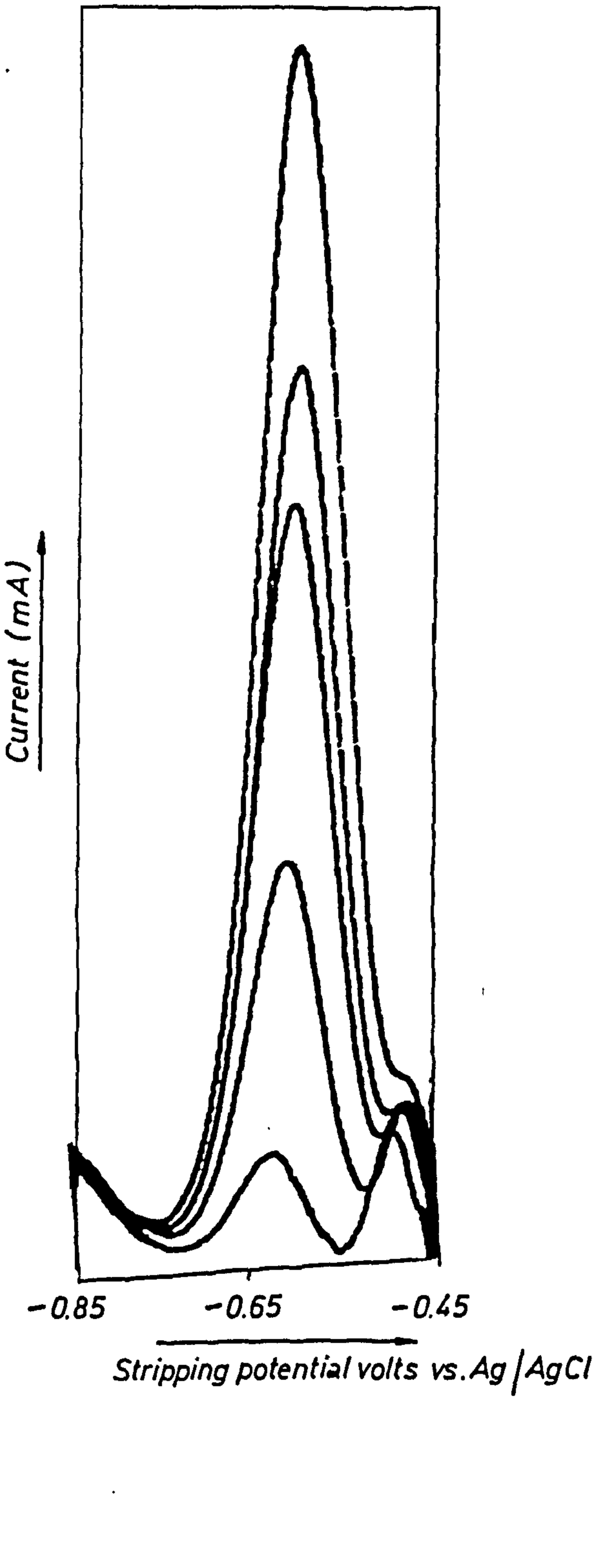

iii) Soils and Plants

Peat (100 g) was shaken with 10, 20, 50, 100 and 200 cm^3 of thallium (1 $\mu g/cm^3$) as thallium (I) nitrate for 12 hours on a mechanical shaker to give concentrations of 0.1, 0.2, 0.5, 1 and 2 $\mu g/g$ of thallium in soil respectively. Seeds of Lolium perenne were grown in these soils for three weeks and a control experiment was also run. After the end of the third week, the plants were separated from the soils, washed and cleaned with DDW and dried between two filter papers. The plants and soils were left in an oven at 55°C overnight and the dry weights were recorded. The samples were digested with concentrated HNO_3 and diluted to 25 cm^3. In soils and plants, the thallium was determined by electrothermal AAS using a Varian-775 instrument and a GTA-95 electrothermal atomiser system. The results obtained are listed in Table 4.8.

Table 4.8 : Thallium (I) nitrate in Peat

Tl added to Peat ($\mu g/g$)	Tl found in Peat ($\mu g/g$)	Recovery %	Tl in plants ($\mu g/g$)
0.0	N.D.	-	N.D.
0.1	N.D.	-	N.D.
0.2	N.D.	-	N.D.
0.5	0.28	56	N.D.
1.0	0.64	64	N.D.
2.0	N.D.	-	N.D.

Different weights of thallium (I) nitrate were ground with silver sand and spread onto known weights of John Innes Soil. Seeds of Lolium perenne were germinated as previously stated and soils and plants were analysed as before. It was observed that the seeds did not germinate roots so the complete plant was analysed. The results obtained are given in Table 4.9.

Table 4.9 : Thallium (I) nitrate in John Innes Soil

Tl added to soil (μg/g)	Tl found in soil (μg/g)	Recovery %	Tl in plants (μg/g)
6.9	0.76	11	N.D.
99.1	9	9	69
370	0.50	0.13	15.8
293	14	4.7	95.8

In order to study the effect of thallium concentration on the germination, the seeds of Lolium perenne were germinated in Petri dishes containing 0.01-0.1 $\mu g/cm^3$ thallium as thallium (I) nitrate and another set of seeds were germinated in 0.01-0.1 $\mu g/cm^3$ thallium as thallium (I) chloride. The seeds were grown for three weeks: control experiments were run containing 0.01 $\mu g/cm^3$ nitrate anion as potassium nitrate for the first set and 0.01 $\mu g/cm^3$ chloride anion as potassium chloride for the second set. The anions were added in order to check that the influence on germination of the seeds was due to the thallium and not the anion. It was observed that at 0.1 $\mu g/cm^3$ thallium, in both sets, seeds germinated shoots but no roots were formed. The germinated seeds were taken from the Petri dishes. The covers from each

of the seeds were removed, the plants were washed twice with DDW and dried at 55°C overnight.

1) Procedure A

The full details of this procedure were described in Figure 4.24; briefly, thallium was complexed with sodium diethyl dithiocarbamate (NDDC) and extracted into methyl isobutyl ketone (MIBK). Aliquots of varying volume ranging from 0.25, 0.75, 1.25, 2.5 to 5 cm^3 of 10 $\mu g/cm^3$ thallium as thallium (I) nitrate were diluted to 25 cm^3 with DDW to give 0.1, 0.3, 0.5, 1.0, 2.0 $\mu g/cm^3$ thallium respectively. Aliquots of 15 cm^3 of each of the standards were treated as in Figure 4.24.

A procedural blank was run throughout the entire procedure in order to ascertain the level of the thallium contamination in the reagents. The determination of the thallium content of the MIBK extracts was carried out using atomic absorption spectrophotometry with the IL-151. However, the procedure adopted was insufficiently sensitive to allow detection let alone determination of the thallium in these samples.

2) Procedure B

The principle of this procedure is that thallium is oxidised to thallium (III) and extracted into MIBK. The details of this method were described in Figure 4.25. Aliquots of 15 cm^3 of each standard as used in Procedure A were used again and treated as in Figure 4.24. A blank was run and a calibration curve constructed. Again this method was insufficiently sensitive to allow for the determination of thallium in plants.

Figure 4.24 : Procedure A (2)

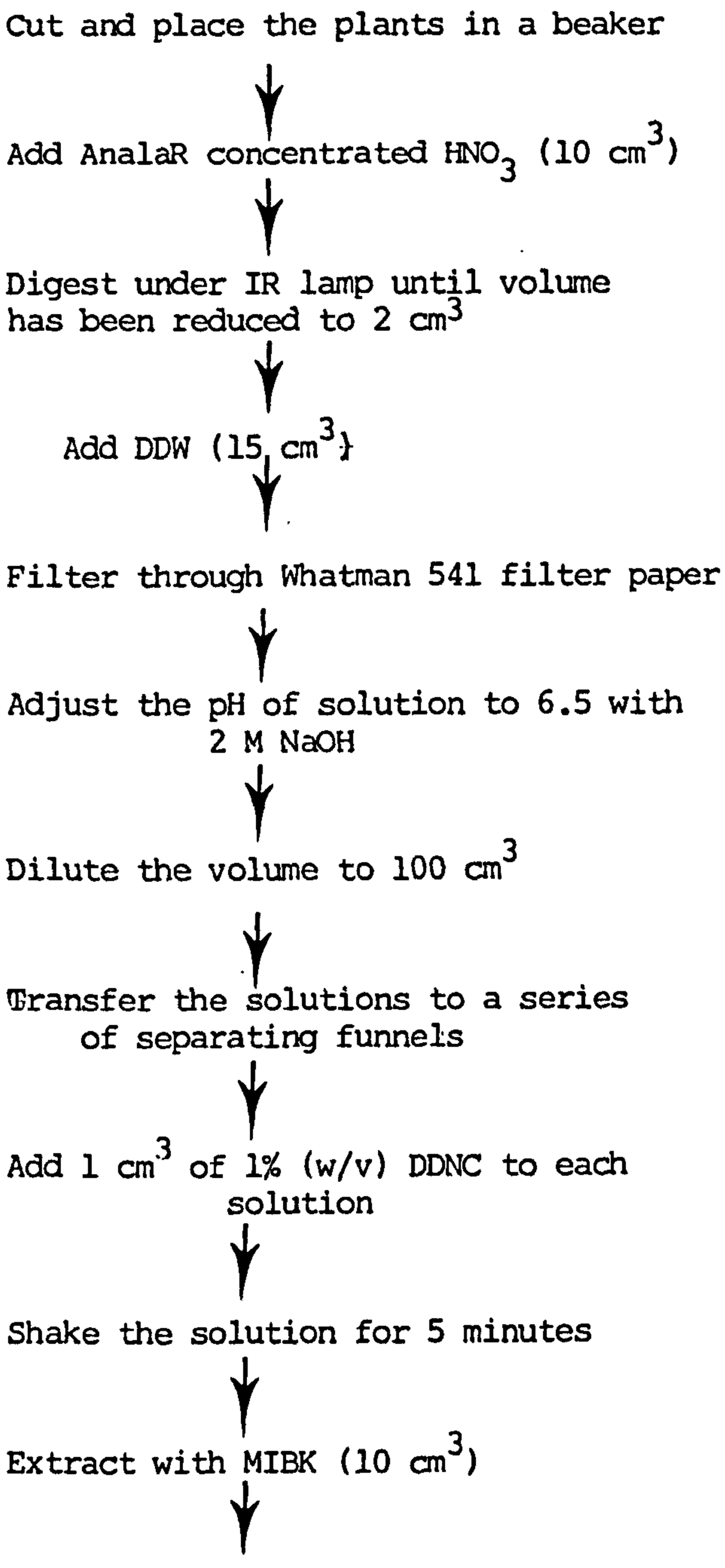

Figure 4.25 : Procedure B (13)

See Figure 4.15 for sample decomposition

↓

Dilute to 25 cm^3 with DDW

↓

Transfer the solutions to a series of separating funnels

↓

Extract with MIBK (10 cm^3)

↓

Shake for 5 minutes

↓

Separate off MIBK layer

↓

Determine the thallium in MIBK layer by FAAS IL-151

3) Procedure C

The procedure is described in detail in Figure 4.26. It was found that this method was suitable for the determination of thallium in plants and the results obtained are given in Table 4.10.

Table 4.10 : Determination of Thallium in Germinated Seeds. Analysis by AAS-775 with GTA-95

Concentration of Thallium in Solution ($\mu g/cm^3$)	Concentration of Thallium in Tissue of Plant ($\mu g/g$)	
Control (0.0)	N.D.	N.D.
0.01	12[a]	12[b]
0.05	21	12
0.06	23	30
0.08	85	34
0.09	97	55
0.10	130	168

a = Thallium fed as $TlNO_3$

b = Thallium fed as TlCl

N.D. = Not detected

Figure 4.26 : Procedure C (35)

Cut and place the plants in a polysulfone tube (Oak Ridge type)

↓

Add AnalaR concentrated HNO_3 (10 cm^3)

↓

Close the tubes and heat in water bath at 40°C for 4 hours

↓

Increase the temperature to 70°C for 4 hours

↓

Release the pressure by opening the tube, then closing it again and heating for 2 hrs

↓

Cool to ambient temperature

↓

Open the tube

↓

Filter through Whatman 541 filter paper

↓

Dilute to 10 cm^3 with DDW

↓

Determine the thallium using the Varian AAS-775 fitted with a GTA-95 furnace

An attempt was made to study the effect of thallium as thallium (I) nitrate on the rate of germination of seeds. Ten seeds of Lolium perenne were placed in Petri dishes containing the previously stated concentrations of thallium. Every day a check was made to observe the percentage of germination. The time (in days) for 50% germination of the seeds in each concentration was recorded. The results are listed in Table 4.11.

Table 4.11 : Effect of Thallium on Rate of Germination of Seeds

Time (days)	Tl concentration ($\mu g/cm^3$) in solution
2	0.0
4	0.01
5	0.05
7	0.06
6	0.08
8	0.09
8	0.10

To study the uptake of thallium by the roots of plants with time, two sets of experiments were carried out. In the first set, 0.1 g of fresh weight roots from Cock's Foot plants were placed in separate beakers. A volume of 25 cm^3 of thallium (5 $\mu g/cm^3$) as thallium (I) nitrate prepared in DDW was added to each beaker. The uptake of the thallium was studied with time. A second set of fresh weight roots (0.1 g) of the above species were also placed in beakers and 25 cm^3 of thallium (5 $\mu g/cm^3$) as thallium (III) nitrate (prepared in 1% (v/v) HNO_3) was added. The

uptake of thallium was studied as above. The roots of the plants were dried and the dry weight recorded. The samples were acid digested and analyses carried out using the Varian AA-775 with GTA-95 for the determination of thallium. The results obtained are presented in Table 4.12.

Lolium perenne which is a relatively hardy species of grass was chosen for studying the critical level of thallium in plants. It is quick growing and hence ideal for this type of study. Lolium seeds were germinated in acid washed silver sand placed in a polyethylene potting tray which had been rinsed with DDW to eliminate any chance of metal contamination of the seedlings. After ten days of development in the sand, the seedlings were transferred to nutrient solutions which contained essential elements for the growth of the plants. The nutrient solution was prepared after the manner of Hoagland and described by Hewitt, and is shown in Table 4.13. The apparatus used for the solution culture of the plant is given in Figure 4.27. The container, or pots, used were the bottom halves of sawn-off Winchester acid or ether bottles and each held one litre. The brown glass of these bottles excluded light from the roots of the plants. Square sheets of expanded polystyrene tiles were cut so that they completely covered the tops of the glass containers and five holes were cut in each polystyrene lid. The germinated seedlings were removed from the sand and their roots washed with DDW. Five seedlings were taken and small strips of sponge wrapped around them at the base of the shoot. Each hole in the polystyrene lid was carefully threaded with the above five seedlings, which were labelled and left to grow in the nutrient solution for one week. Then the roots of plants were cut and the fresh weight of each bunch (five seedlings) were recorded. The experiment was duplicated; $TlNO_3$ and TlCl were added individually to the nutrient

Table 4.12 : Uptake of Thallium (I) and Thallium (III) by Roots with Time. Analysis by Varian AAS-775 with GTA-95

Time (minutes)	Holcus lanatus[a]		Holcus lanatus[b]		Cock's Foot[c]	
	Tl(I)	Tl(III)	Tl(I)	Tl(III)	Tl(I)	Tl(III)
15	124	625	237	159	138	563
30	83	1095	525	131	102	716
60	72	1388	526	216	101	1347
90	61	1320	500	242	95	1320
105	59	964	259	194	43	1120
120	52	386	368	178	25	954

a = species collected from Midger

b = species collected from Hallen

c = species collected from North Road, Bristol

The figures are the concentration of thallium in plant tissues ($\mu g/g$ dry weight)

Table 4.13 : Composition of Hoagland's Nutrient Solution (36) used for Water Culture Experiments with Lolium perenne Seedlings (Full Strength)

Compound	Concentration (g/L)
KNO_3	0.656
$Ca(NO_3)_2.4H_2O$	0.944
$NH_4H_2PO_4$	0.115
$MgSO_4.7H_2O$	0.490
H_3BO_3	0.00286
$MnCl_2.4H_2O$	0.00181
$CuSO_4.5H_2O$	0.0008
$ZnSO_4.7H_2O$	0.0022
H_2MoO_4 ($MoO_3 + H_2O$)	0.0009
$FeSO_4.7H_2O$	0.003
$[CH(OH)COOH]_2$	0.0036

FIG.4.27 PHOTOGRAPHIC REPRESENTATION OF LOLIUM PERRENNE SEEDLING GROWING IN NUTRIENT SOLUTION

solutions and the plants returned to grow for three weeks. Every five days a fresh nutrient solution containing thallium was prepared and the old solution discarded. After the end of the third week, the seedlings were removed from the nutrient solution and each bunch dried between two filter papers. The fresh weight and root length were recorded. The roots and shoots of individual bunches were placed in beakers and left overnight at 50°C. Next day the dry weight of each sample was recorded. Determination of the thallium contents of the acid digested samples was carried out using the Varian AAS775 with GTA-95. The results are listed in Tables 4.14 and 4.15.

An attempt was made to determine the upper critical level of thallium in roots and shoots of Lolium perenne which were collected from the Mendip Hills (see Figure 3.6). The species were treated as previously stated except one plant was placed in each bunch. The results obtained are given in Tables 4.16, 4.17 and 4.18. The yield curves are shown in Figures 4.28 and 4.29.

The uptake of thallium (III) by plants is not well known. An attempt was made to study the uptake of Tl(III) by Lolium perenne seedlings, but the attempt failed. Two observations should be noted :

i) in order to feed Tl(III) solutions suitable for adding to hydroponic cultures, the solution must be prepared and stable in very dilute solutions, preferably in distilled water, without the stabilising effect of excess anions. Regretfully the Tl(III) solution on dilution produced a brown precipitate due to the formation of thallic oxide which was unavailable to the plant.

ii) divalent metals in the nutrient solutions, particularly iron and manganese, were able to reduce the thallium (III) state to the thallium (I) state eg $Tl^{3+} + Fe^{2+} \rightarrow Tl^{+} + Fe^{3+}$ (4.1)

As a consequence of these two difficulties, Tl(III) was not used in the present study. Frankly, this was disappointing because it was intended to try to follow up the germination study using Tl(I) . In this latter case, however, the excess anion, here the NO_3^- ion, appeared to have little effect on germination.

Table 4.14 : Thallium Concentration in Roots and Shoots of Lolium perenne Seedlings (Thallium fed as $TlNO_3$)

Thallium concentration ($\mu g/cm^3$) in nutrient solution	Average Root length (cm) of five plants	Thallium in Root Tissue ($\mu g/g$)	Thallium in Shoot Tissue ($\mu g/g$)	Significance
0.00	20.25 $\pm$ 1.5	N.D.	N.D.	
0.005	19.00 $\pm$ 1.2	1.33	N.D.	NS
0.01	18.4 $\pm$ 1.8	2.36	N.D.	NS
0.1	12.1 $\pm$ 2.3	3.42	0.69	$P < 0.01$
0.5	6.0 $\pm$ 0.7	3.98	1.71	$P < 0.001$
2.0	4.7 $\pm$ 1.3	8.54	4.10	$P < 0.001$

NS = not significant

N.D. = not detected

Table 4.15:: Thallium Concentration in Roots and Shoots of Lolium perenne Seedlings
(Thallium fed as TlCl)

Thallium concentration ($\mu g/cm^3$) in nutrient solution	Average Root Length (cm) of five plants	Thallium in Root Tissue ($\mu g/g$)	Thallium in Shoot Tissue ($\mu g/g$)	Significance
0.000	20.25 $\pm$ 1.5	N.D.	N.D.	
0.005	17.4 $\pm$ 2.6	N.D.	N.D.	NS
0.01	13.7 $\pm$ 1.7	1.35	N.D.	$P < 0.001$
0.1	10.1 $\pm$ 2.9	1.97	N.D.	$P < 0.001$
0.5	8.0 $\pm$ 2.3	2.36	N.D.	$P < 0.001$

Table 4.16 : Thallium Concentration in Roots of Lolium perenne Species

Concentration of thallium ($\mu g/cm^3$) in nutrient solution	Dry weight of plants (mg)	Concentration of thallium (mg/kg) in plant tissue	Log_{10} Concentration of thallium in plant tissue
0.000	37.5	N.D.	—
0.001	31.0	2	0.30
0.005	23.8	2.92	0.46
0.01	13.4	9.0	0.95
0.1	9.5	13.6	1.13
0.5	7.1	22	1.34
1.0	5.9	430	2.63
5.0	3.5	921	2.96
10.0	2.6	1859	3.26

N.D. = Tl < 0.66 mg/kg

Table 4.17 : Thallium Concentration in Shoots of Lolium perenne Species

Concentration of thallium ($\mu g/cm^3$) in nutrient solution	Dry weight of plants (mg)	Concentration of thallium (mg/kg) in plant tissue	Log_{10} Concentration of thallium in plant tissue
0.00	622.6	N.D.	—
0.001	487.3	N.D.	—
0.005	335.4	0.125	-0.90
0.01	292.5	1.00	0.00
0.1	282.5	1.25	0.I0
0.5	226.4	1.99	0.30
1.0	213.7	32	1.50
5.0	175.3	105	2.02
10.0	118.9	244	2.38

N.D. = Tl < 0.040mg/kg

Table 4.18 : Critical Concentration of Thallium in Roots and Shoots of Lolium perenne Seedlings

Critical Concentration and Statistical Information	Roots	Shoots
Y_o (mg)	37.5	622.6
T_c (mg/kg)	1.9	0.056
T_L (mg/kg)	31.6	3.16
Correlation coefficient of regression line	-0.987	-0.936
Regression equation	y = 34.7-21.5x	y = 279-180·x
Standard deviation of y about regression line with (n-2) degrees of freedom	1.757	72.31
r-squared = 97.5 per cent	98.4	81.5
r-squared = 96.7 per cent, adjusted for d.f.	98.0	76.8
SS* due to regression	748.65	92,012
MS = SS/df	748.65	92,012
SS due to residual	12.34	20,916
SS due to total	761.08	112,928

SS* = sum of squares

MS = mean square

FIG. 4.28 YIELD CURVE OF ROOT YIELD PLOTTED AGAINST LOG TISSUE CONCENTRATION IN SUPPLEMENTARY EXPERIMENT TO DETERMINE THALLIUM UPPER CRITICAL LEVEL

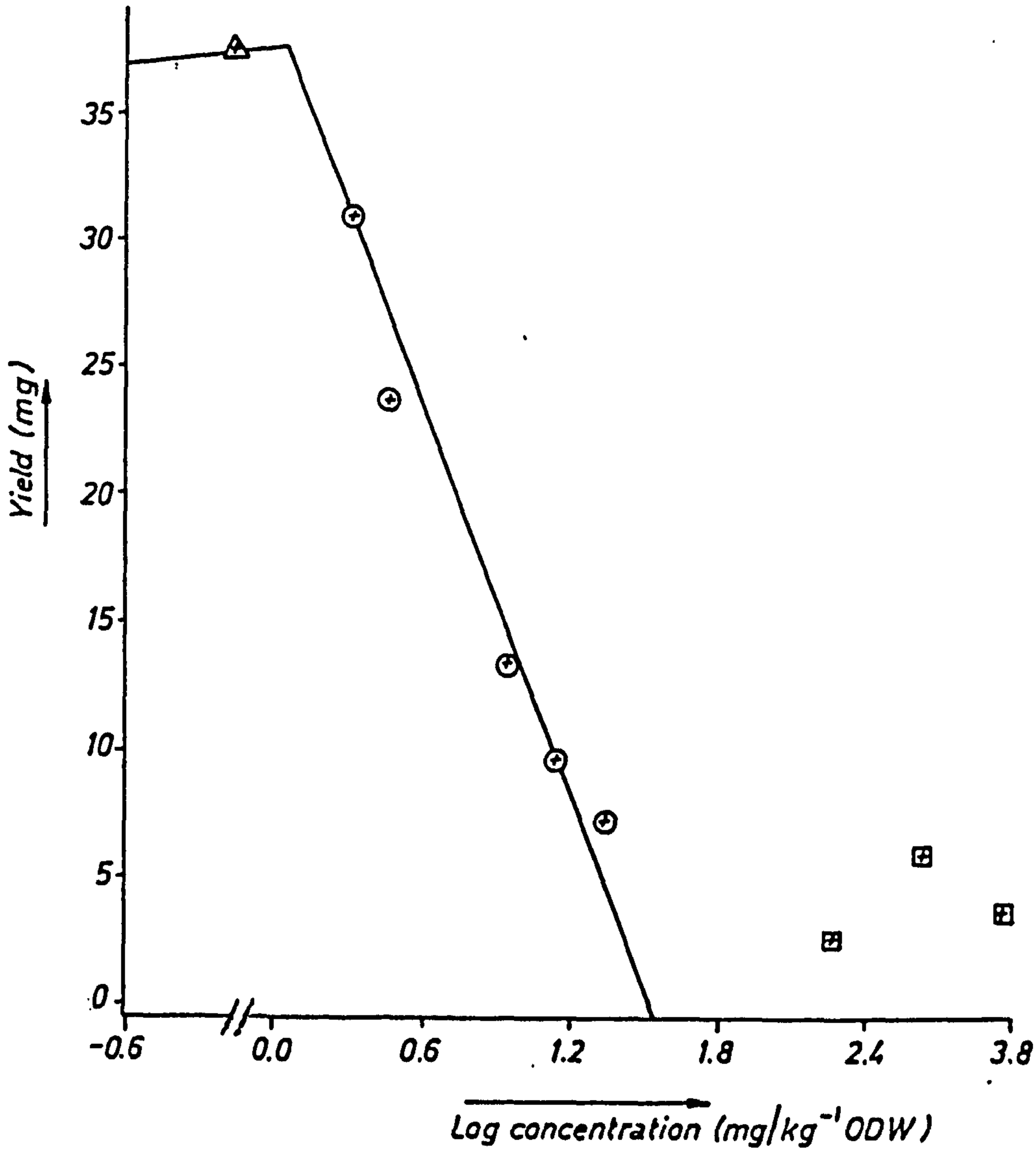

FIG. 4.29 YIELD CURVE OF SHOOT YIELD PLOTTED AGAINST LOG TISSUE CONCENTRATION IN SUPPLEMENTARY EXPERIMENT TO DETERMINE THALLIUM UPPER CRITICAL LEVEL

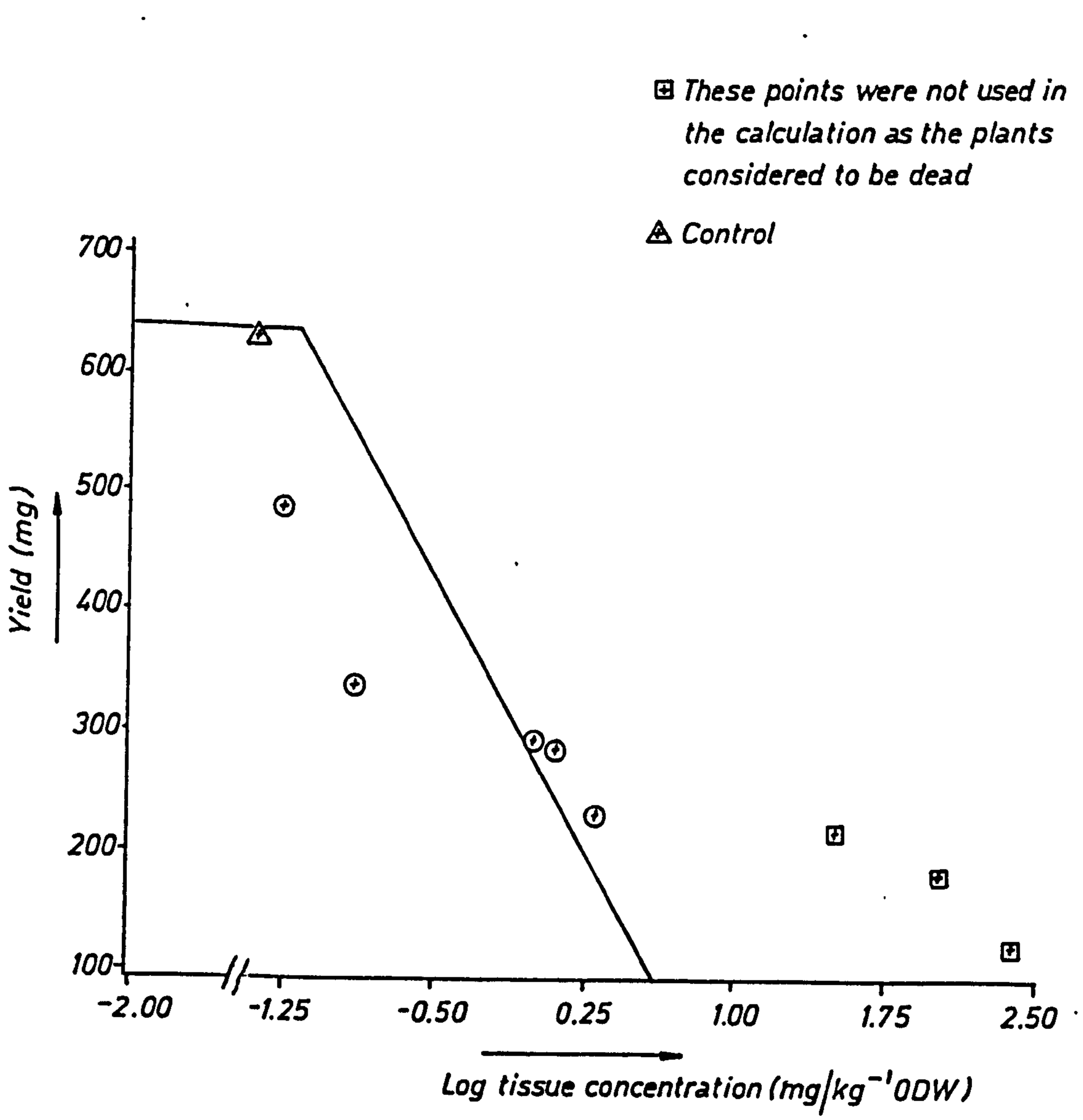

d) Apparatus and Instrumental Parameters

i) Polarography and DPASV

The three modes of polarography (DC, PP, DPP) were used with the PAR 303 SMDE on MDE mode while DPASV was used with HMDE mode. The conditions employed for determination of thallium by DPASV with HMDE and TFME are listed in Tables 4.19 and 4.20 respectively. The standard addition method was applied in both polarographic and voltammetric methods.

Table 4.19 : Conditions for Determination of Thallium by DPASV with HMDE

Electrolyte	=	10 cm^3 of 1 M HAc + 1 M NaAc + 0.01 M EDTA Na_2
Initial potential	=	-1.00 V
Final potential	=	0.00 V
Condition potential	=	0.00 V
Purge time	=	5 minutes
Deposition time	=	180 sec
Working electrode	=	HMDE
Current range	=	5 uA
Potential range	=	3.00 V
Modulation amplitude	=	25 mv
Scan rate	=	5 mv/sec
Reference electrode	=	Ag/AgCl saturated with 3 M KNO_3
Auxiliary electrode	=	Platinum wire
Mode	=	Differential pulse

Table 4.20 : Conditions for Determination of Thallium by DPASV with TFME

Electrolyte	=	20 cm^3 of ammonium chloride + citric acid + ascorbic acid
Initial potential	=	-0.85 V
Final potential	=	-0.45 V
Condition potential	=	0.00 V
Purge time	=	5 minutes
Deposition time	=	300 sec
Equilibration time	=	30 sec
Working electrode	=	TFME
Current range	=	0.1 mA
Reference electrode	=	Ag/AgCl saturated with 3 M KNO_3
Auxiliary electrode	=	Platinum wire
Low pass filter	=	Off

ii) AAS-151L

Typical calibration graphs used for determining thallium by AAS with an air-acetylene flame are shown in Figures 4.30 and 4.31. Figure 4.31 shows the calibration graphs of thallium chelated with NDDC (labelled A) and oxidised to thallium (III) (labelled B) which was extracted into MIBK.

FIG. 4.30 AAS CALIBRATION GRAPH FOR THALLIUM

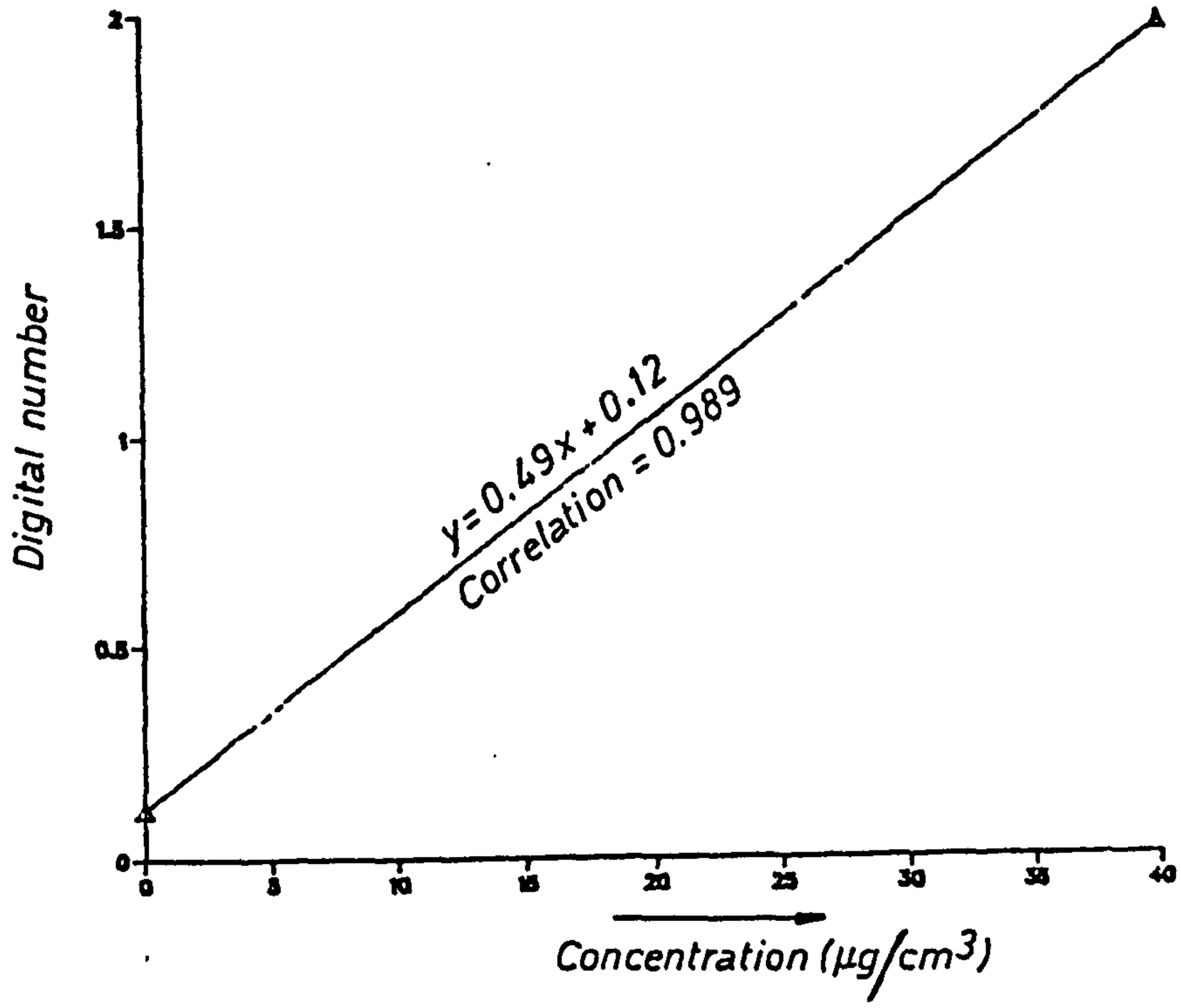

FIG. 4.31 AAS CALIBRATION GRAPH FOR THALLIUM IN MIBK

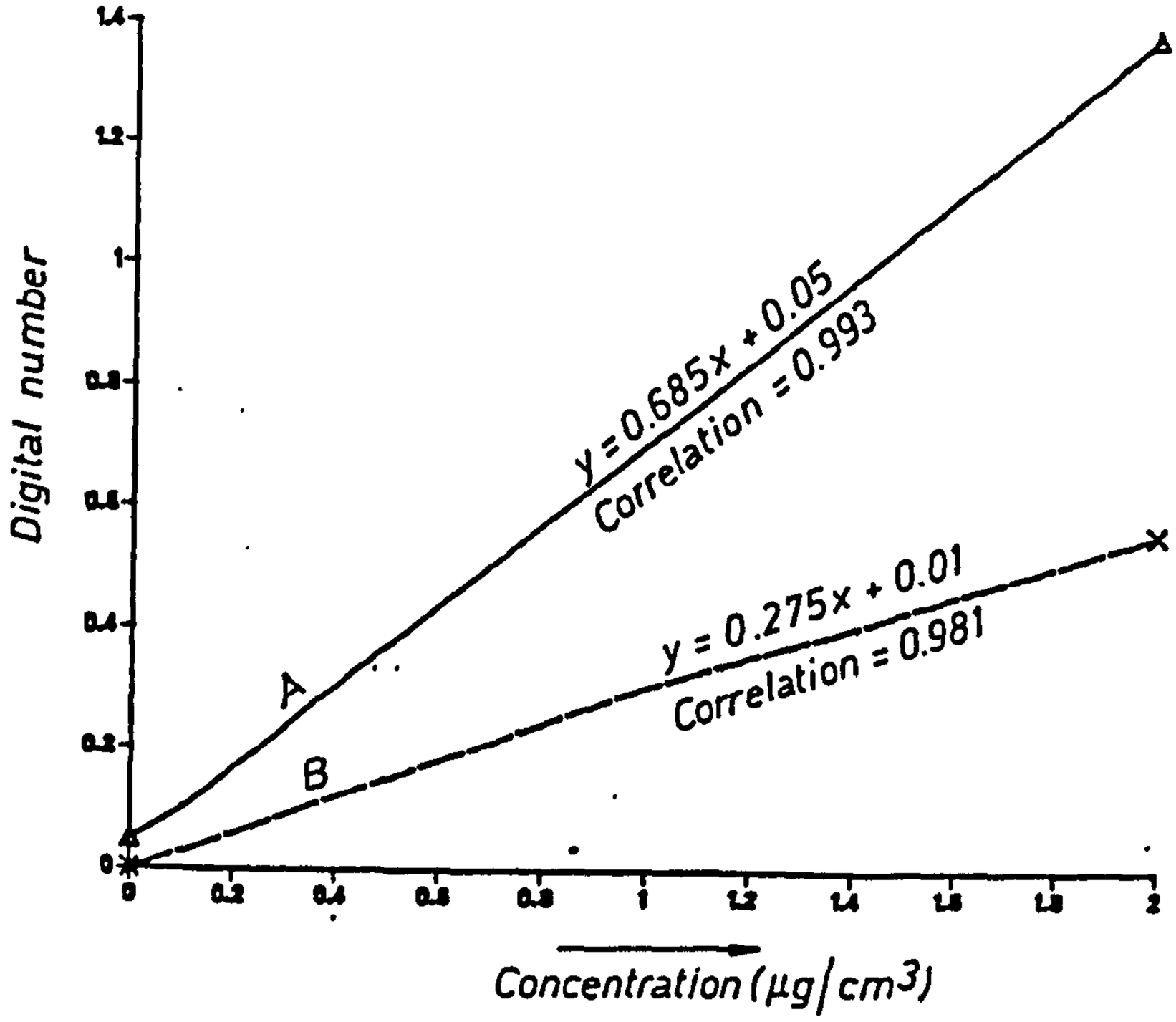

iii) AAS-775 with GTA-95

The instrumental parameters and conditions are given in Table 4.21. The instrument was calibrated with standard solutions on concentration mode. The concentrations of thallium in the samples were compared with the concentration of standard solutions.

Table 4.21 : Determination of Thallium by AAS-775 with GTA-95

Step	Temperature (^{o}C)	Time (sec)	N_2 flow (L/min)	Read
1	75	5.0	3.0	
2	90	6.0	3.0	
3	120	10.0	3.0	
4	200	2.0	3.0	
5	250	5.0	3.0	
6	2200	1.0	0.0	*
7	2200	2.0	0.0	*
8	2200	1.0	3.0	

Wavelength = 277 nm

Spectral bandwidth = 0.5 nm

Lamp current = 3.5 mA

Background correction = ON

Sample injected = 20 μl

* = Read signal

e) Statistical Estimation of Detection Limit of Thallium by DPASV with HMDE

Very small volume spike solutions of thallium were added to the base electrolyte of 1 M HAc + 1 M NaAc + 0.01 M EDTA Na_2 (10 cm^3). The experiment was repeated four times and the method of standard addition was applied.

Symbol

x = concentration of thallium added (ng/cm^3)

y = peak height in cm

Experiment 1		Experiment 2		Experiment 3		Experiment 4	
x	y	x	y	x	y	x	y
5	3	5	2.9	5	3.9	5	3.5
10	5.1	10	5.0	10	5.5	10	5.5
20	7.5	20	7.5	20	7.2	20	7.0
30	10.5	30	11.2	30	9.5	30	10.0
40	13.9	40	12.5	40	13.5	40	13.0
60	17.5	60	18.0	60	19.1	60	20.0

The mean reading of the data was calculated and is shown below:

x	y	$(x-\bar{x})$	$(x-\bar{x})^2$	$(y-\bar{y})$	$(y-\bar{y})^2$	$(x-\bar{x})(y-\bar{y})$
5	3	-26	676	-7	49	182
10	5	-21	441	-5	25	105
20	7	-11	121	-3	9	33
30	10	- 1	1	0	0	0
40	13	9	81	3	9	27
50	16	19	361	6	36	114
60	19	29	841	9	81	261

$$\Sigma(x-\bar{x})(y-\bar{y}) = 722$$

$$\Sigma(x-\bar{x})^2 = 2522$$

$$\Sigma(y-\bar{y})^2 = 209$$

The regression line : $y' = bx' + a'$

$$b' = \frac{[\Sigma(x-\bar{x})(y-\bar{y})]}{[\Sigma(x-\bar{x})^2]}$$

$$b' = \frac{722}{2522} = 0.278$$

$$a' = y' - bx'$$

$$= 10 - 0.278 \times 31$$

$$= 1.382$$

Therefore, the regression line is $y' = 0.278x' + 1.382$. The correlation between the peak height and concentration is measured by the correlation coefficient, r.

$$r = \frac{[\Sigma(x-\bar{x})(y-\bar{y})]}{\sqrt{\Sigma(x-\bar{x})^2 \Sigma(y-\bar{y})^2}}$$

$$r = \frac{722}{\sqrt{2522 \times 209}}$$

$$= 0.994$$

The standard error of the estimate was

$$S_{y,x} = \sqrt{\frac{[\Sigma(y-\bar{y})^2 - b' \Sigma(y-\bar{y})(x-\bar{x})]}{n-2}}$$

$$= \sqrt{\frac{209 - 0.278 \times 722}{28 - 2}}$$

$$= \pm 0.564$$

The prediction limits for area, given a concentration, were calculated by the following equation :

$$y' \pm \left[t_{n-2,\alpha} \; S_{y,x} \sqrt{1 + {}^{1}/n + [(x_p - \bar{x})^2 / \Sigma(x-\bar{x})^2]} \right]$$

Y_{UB}, 99% upper prediction limit on the blank, was calculated by using the positive portion of the above equation as follows :

$$Y_{UB} = y' + \left[t_{n-2,\alpha} \; S_{y,x} \sqrt{1 + {}^{1}/n + [\bar{x}^{-2} / \Sigma(x-\bar{x})^2]} \right]$$

In this work, 99% confidence is selected ($\alpha = 0.01$) and 26 degrees of freedom. The appropriate value for t is 2.479.

$$Y_{UB} = 1.38 + 1.66$$

$$= 3.04$$

Y_L, the 99% lower prediction limit on the expected area at a given concentration, was calculated using the following equation :

$$Y_L = y' - \left[t_{n-2,\alpha} \; S_{y,x} \sqrt{1 + {}^{1}/n + \frac{[(x_p - \bar{x})^2]}{\Sigma(x-\bar{x})^2}} \right]$$

where x_p are values substituted into the above equation.

1) at x = 5

$$Y_L = 2.77 - 1.59$$

$$= 1.18 \text{ i.e. } < Y_{UB}$$

2) at x = 10

$$Y_L = 4.162 - 1.89$$

$$= 2.77 \text{ i.e. } < Y_{UB}$$

3) at x = 20

$$Y_L = 6.942 - 1.455$$

$$= 5.487 \text{ i.e. } > Y_{UB}$$

$$X_{DL} = 20 \text{ ng/cm}^3$$

The peak height corresponding to X_{DL} was referred as Y_Q ,

$$Y_Q = 0.278 \times 20 + 1.382$$

$$= 6.942$$

The detection limit of thallium by DPASV with HMDE was also estimated using the method suggested by Rica et alia (37). The following parameters were obtained by using a computer program which was developed by Chris Scott :-

1) Equation of calibration line

   $y = 2.063 + 0.2781x$

2) Sum of squares of deviation = 11.4079

3) Average distance per point = 0.12062

4) Limits

a) For signal, y(cm)

   i) Upper limit = 6.679

   ii) Lower limit = 4.7962

b) For concentration, C(ng/cm^3)

   i) Upper limit = 17.4991

   ii) Lower limit = 8.6313

All these parameters are shown in Figure 4.32.

FIG. 4.32 ESTIMATION OF DETECTION LIMIT OF THALLIUM BY DPASV WITH HMDE

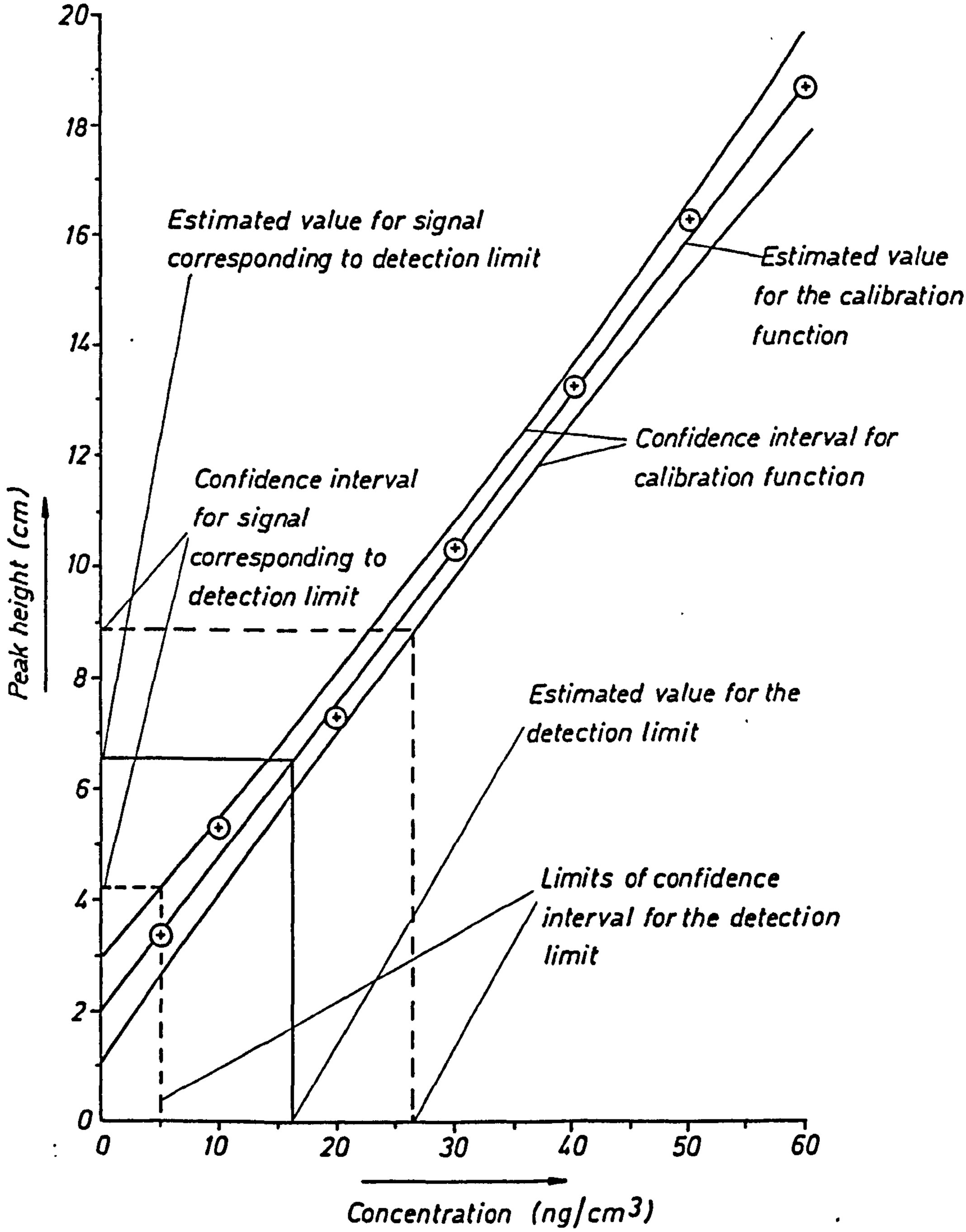

4.3 DISCUSSION

a) Analytical Techniques and Methodology

Figures 4.4 to 4.6 (pp. 212-214) indicate the determination of thallium by polarographic techniques are in order of decreasing sensitivity : DPP > PP ≥ DCP. The sequence is the expected one, being based on the limitations of each of the procedures especially the ability to discriminate between the charging current and the Faradic current (discussed in detail in Chapter 2). Figure 4.33 (p. 270) illustrates the difference in sensitivity between polarographic techniques used for the determination of thallium.

Thallium voltammograms which were obtained by DPASV with HMDE and TFME are shown in Figures 4.7 and 4.9 (pp. 216 and 220) respectively. Although the TFME was more sensitive than the HMDE, many problems were associated with the determination of thallium by TFME (see Chapter 2). Figure 4.34 (p. 271) shows a comparison in sensitivity of DPASV techniques using HMDE and TFME.

Tables 4.2 and 4.3 indicate that lead interferes with thallium while cadmium does not. These Tables also indicate the effect of the addition of EDTA to the background electrolyte. For example, in the presence of lead the peak height of thallium is increased by a factor of 3 greater than that in the acetate buffer without the addition of EDTA. The reason must be the chelation of lead with the EDTA and the resultant shift in the thallium plating potential (discussed earlier in Chapter 2).

The results in Tables 4.4 and 4.5 are presented in Figure 4.35 which shows that the peak height responses of thallium determined by both TFME and HMDE using DPASV were not linearly proportional to the electrodeposition time.

FIG. 4.33 THE DIFFERENCE IN SENSITIVITY OF POLARGRAPHIC TECHNIQUES FOR DETERMINATION OF THALLIUM

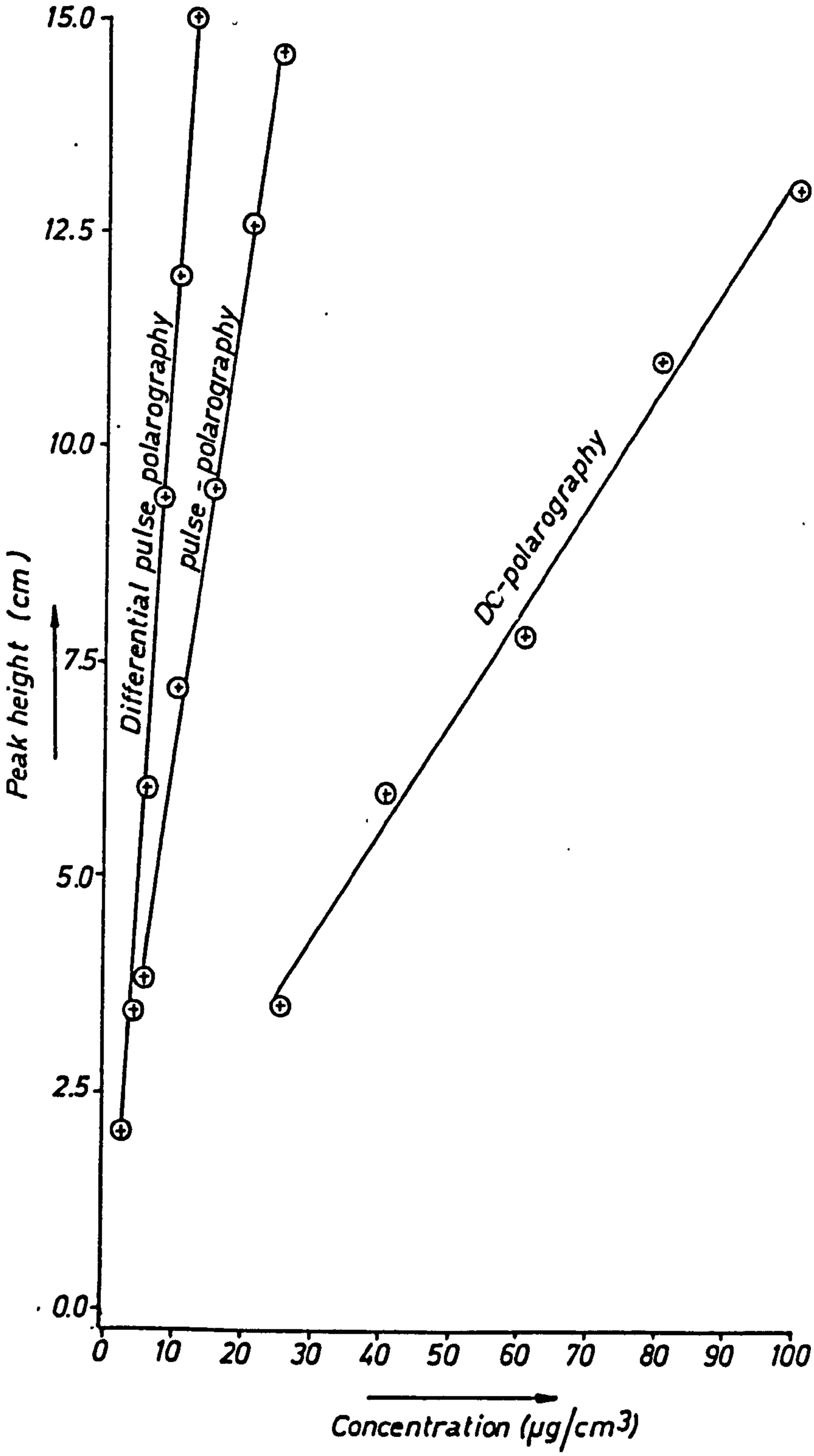

FIG. 4.34 THE DIFFERENCE IN SENSITIVITY OF VOLTAMMETRIC TECHNIQUES FOR DETERMINATION OF THALLIUM

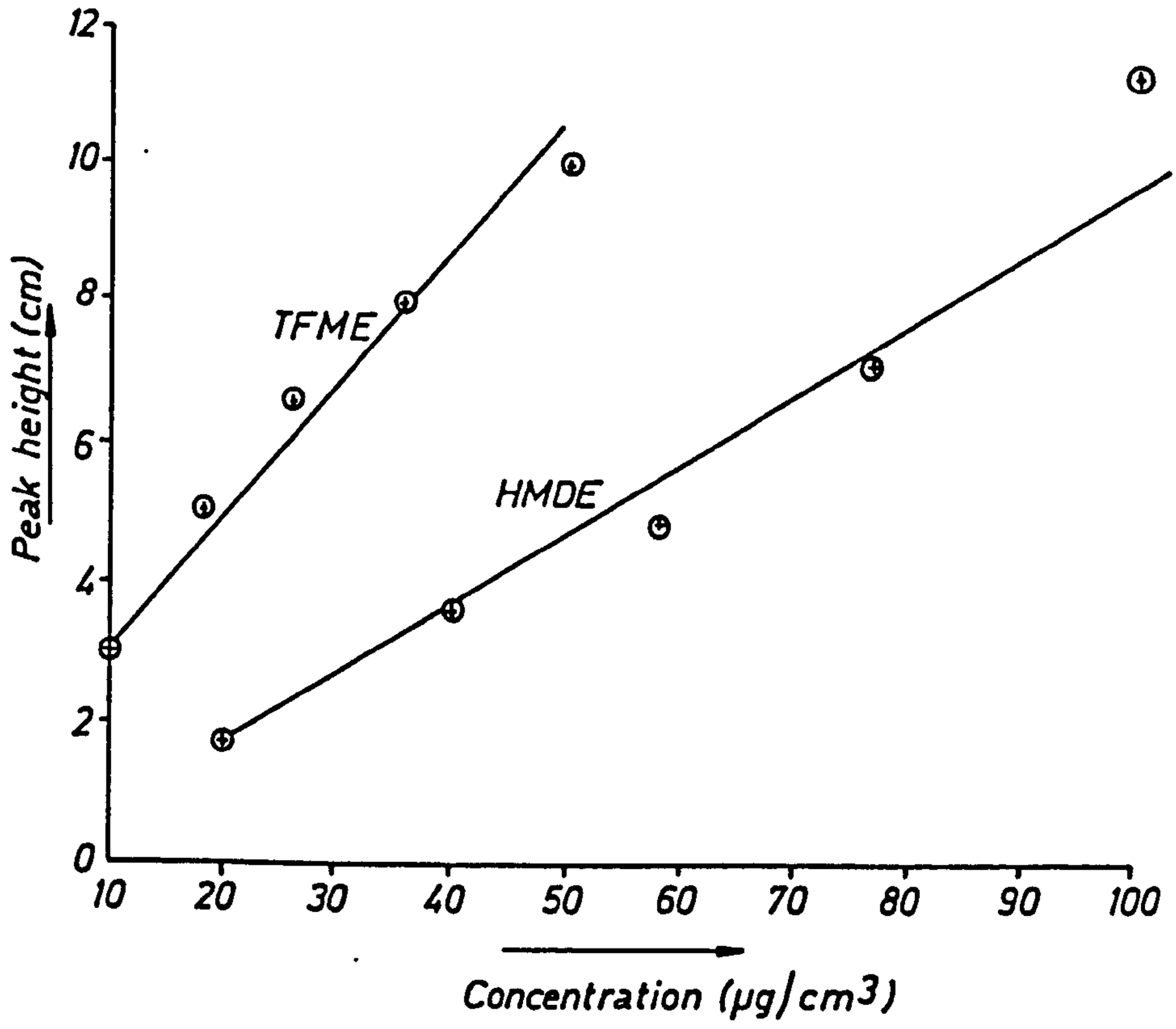

FIG. 4.35 EFFECT OF DEPOSITION TIME ON PEAK HEIGHT OF THALLIUM

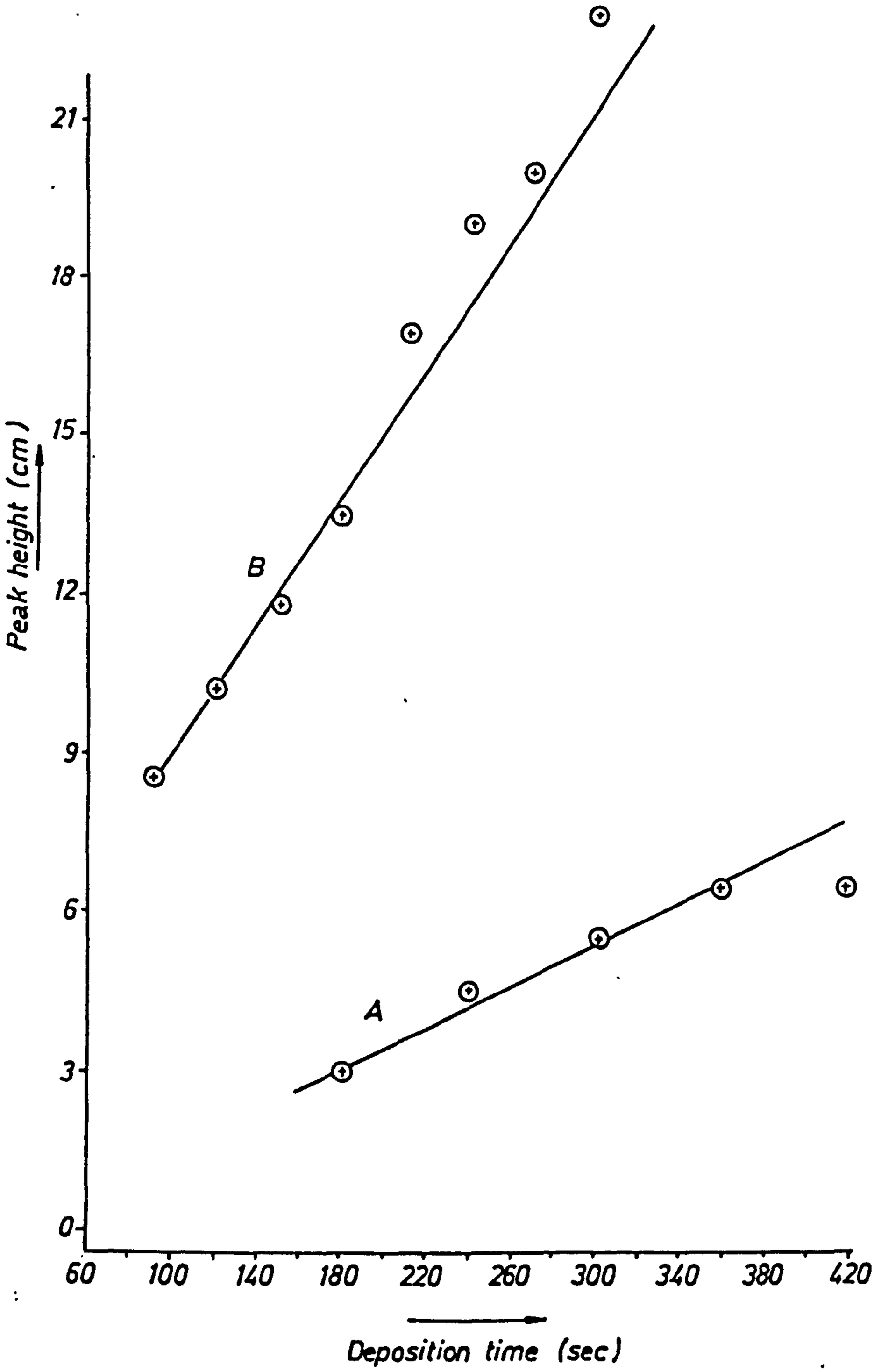

Using the HMDE, the longer deposition times (> 180 secs) leads to a response which is greater than that expected from an extrapolation of the apparently linear response at lower deposition times. It is difficult to offer an explanation for this phenomenon because not only does the peak height response increase but also the broadness (i.e. area) of the peak increases as well. Assuming that the mercury is becoming saturated with thallium leads to a position where the Tl is no longer able to form an amalgam with the mercury and to the plating of thallium as Tl^{o} on the external surface of the drop. When the stripping process is initiated there are almost two forms of Tl associated with the drop; the Tl^{o} which should strip very easily back into solution, the other Tl being present as an amalgam which kinetically may be slower to diffuse back into solution. These two processes could possibly lead to a much broader peak than encountered with shorter deposition times and an increased response in peak height terms from the Tl^{o} species. Obviously much further work has to be carried out to solve this problem although decenvolution methods (as used for resolving overlapping chromatography peaks) may be applicable. These facts agree with Alevata et alia's (38) observation that the peak current of zinc was not linearly proportional to the electrodeposition time.

In the TFME case, the peak height response for Tl at higher deposition times remains linear until a time of 380 seconds is reached. The concentration of the thallium being plated from solution was about half that for the HMDE case and therefore in view of the increased surface area of the electrode such a linear response was expected. At the highest deposition time, 420 seconds, although the shape of the peak remained the same, the response was irreproducible and the point given is the mean of several determinations. Clearly the linearity of this system has also been attained.

The pH of the background electrolyte is very important in the determination of thallium by DPASV with HMDE or TFME. In both HMDE and TFME, the response of thallium decreased as the pH of the background electrolyte increased towards the more alkaline region. This means that the thallium ion is either precipitated from solution or formed a complex which is an electro-inactive species, probably as the $Tl\text{@}H^{+}$ entity which will plate onto the Hg. Figure 4.36 shows the relation between pH of electrolyte solution and peak height for thallium using the HMDE.

Figures 4.30 and 4.31 (p. 262) depict the calibration graphs for thallium by FAAS. Indeed, the sensitivity of the Tl determination by FAAS can be increased markedly by chelation of thallium (I) with DDNC or oxidation of Tl(I) to the corresponding Tl(III) bromide with subsequent extraction of both species into MIBK, followed by aspiration into the flame. Flameless atomic absorption was very sensitive, and a more reliable technique for the determination of thallium than the electroanalytical techniques used. Therefore it was used in this work.

It can be concluded from the techniques which were used for the determination of thallium, that the techniques in order of decreasing sensitivity for thallium were :-

GFAAS > DPASV with TFME > DPASV with HMDE > FASS (chelation with DDNC and extraction with MIBK) > FAAS (oxidised Tl(I) to Tl(III) and extraction with MIBK) > DPP > NPP > FAAS > DCP.

Figure 4.9 indicates that humic acid did not affect the peak height produced by thallium, i.e. humic acid did not form an electro-active complex with thallium. This study agrees with those of Zitko et alia (22) and O'Shea (29). However, it was observed that another peak appeared when humic acid was added and increased with the addition of humic acid; this peak may be due to an electro-active impurity in humic acid.

FIG. 4.36 EFFECT OF pHsON PEAK HEIGHT OF THALLIUM AT HMDE

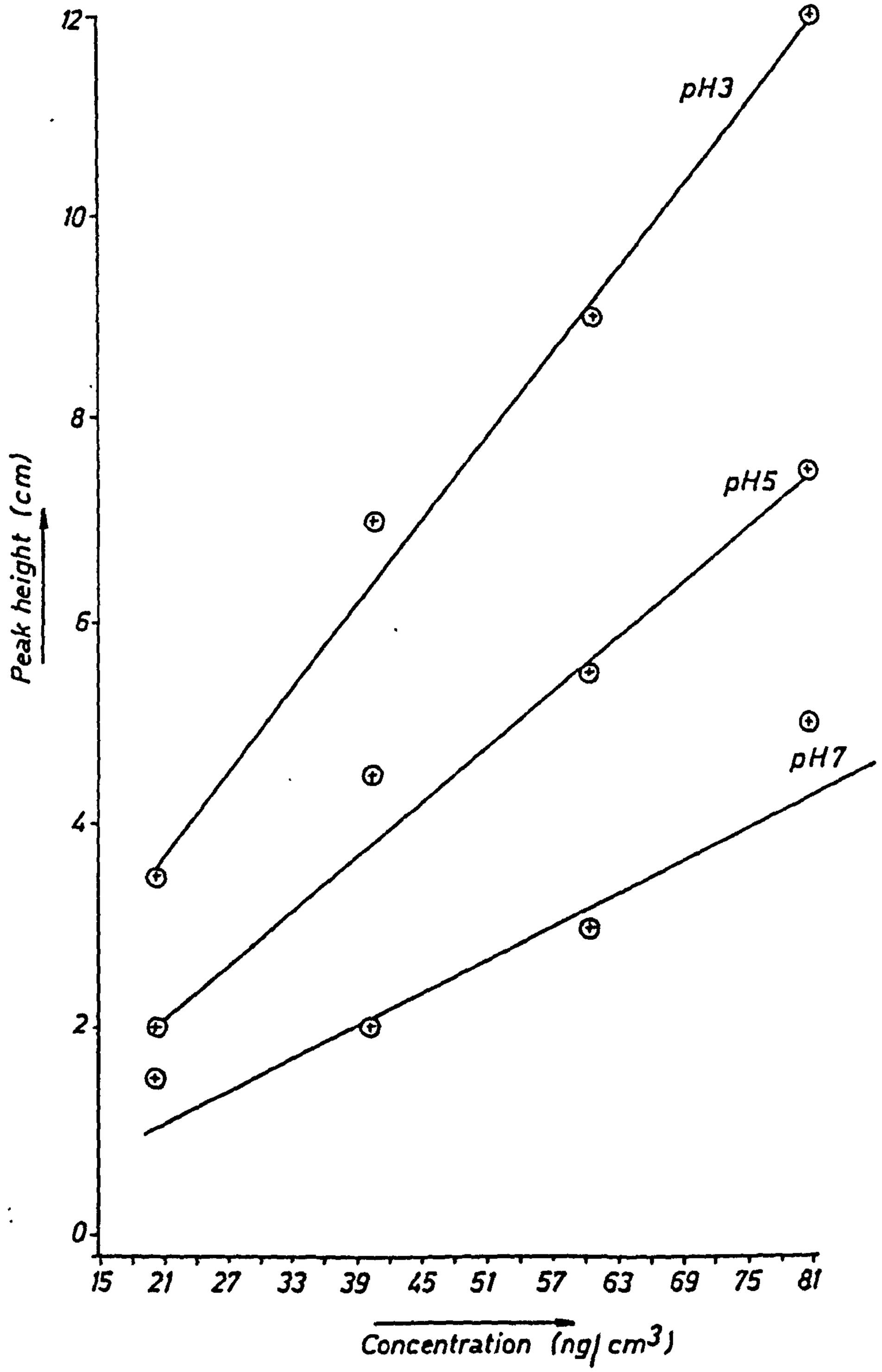

Figure 4.10 illustrates that the speed of rotation of the electrode between 500-2000 rpm does not affect the peak height response of metals in the background electrolyte. A possible explanation of this series of observations is that the solution is sufficiently stirred even at 500 rpm to cause a reasonably constant flux of electroreducible material at the electrode surface. Probably the rate determining step is the rate of transfer from solution to the thin film electrode. The processes involved here are

i) the discharge of Tl^{+} to Tl^{o},

ii) the discharge of Hg^{2+} to Hg^{o}, and

iii) the amalgamation/dissolution of Tl^{o} within the Hg^{o}.

Normally it is assumed that the discharge process is very rapid and hence the critical step is probably step (iii). A comparison should be drawn between the speed of stirring in the TFME case of at least 500 rpm against the same process intthe HMDE situation. In the latter case, the speed of the stirrer is usually less than 100 rpm. Clearly if we had wanted to observe a stirring effect with the TFME, speeds below 500 rpm and possibly less than 100 rpm would be necessary. With the apparatus available this was not possible.

Figures 4.11 and 4.12 indicate that the best modulation amplitude and potential scan rate for determination of thallium by DPASV with TFME are 25 mv and 5 mv/sec respectively. Therefore, these two parameters were selected for future work.

The influence of surfactants, such as Triton X-100, on the anodic stripping voltammetric peak mainly involves change of peak heights and of peak potentials (39). Figure 4.14 illustrates that the peak potential of cadmium is shifted while the peak height of copper is reduced when 20 μl of Triton X-100 was added. The most important feature in this study is the shift of peak potential of cadmium because it is clear that

the peak for thallium occurs at almost the same potential for cadmium, therefore separation of thallium from cadmium must be carried out in the determination of thallium by DPASV with TFME. Brezonik et alia (40) reported that the major disadvantages of addition of a surface active substance which could coat the mercury electrode was a decrease in the rate of metal deposition and therefore a decrease in sensitivity.

The results in Table 4.6 give the level of Zn, Cu, Cd, Tl and Pb in rock samples. Thallium was separated from the matrix elements by two methods (solvent extraction and ion-exchange) and was determined by DPASV with HMDE. The level of thallium in galena and the Mineries Pool exit sediment separated by solvent extraction is higher than ion exchange separation. This suggests that ion exchange removes most of the lead while solvent extraction does not, leading to the positive interference (already noted) in the thallium concentration recorded. Comparison between the levels of thallium in galena determined by these two methods with the levels determined by electrochemical masking of lead (Procedure C) indicates that higher levels of thallium were determined by Procedure C. Probably insufficient tetrabutylammonium chloride was added to mask all the lead in the galena sample and the uncomplexed remainder interfered in the response of the thallium. Although the level of lead in the chalcopyrite and sphalerite ores should not interfere with thallium determination (because it is not as high as in galena ore), differences in the level of thallium were found by using both the solvent extraction and ion exchange procedures. The level of thallium in both cases as determined by the ion exchange method was higher than by solvent extraction. The reason may be contamination or loss of sample because of the many steps used in the two procedures but a more likely explanation is the interference by other metals such as copper or iron from the chalcopyrite or zinc (from the sphalerite). In

the case of ion exchange separation, the Tl^{+} was not adsorbed by the resin, while the M^{2+} ions Cu^{2+} and Pb^{2+} were removed. So a relatively interference free matrix was produced by this process. However, in the solvent extraction case, the M^{2+} ions, particularly the iron, would certainly react with bromine forming extractable iron-bromo complexes. The iron salts resultant from evaporation of the organic solvent may have interfered with the DPASV determination of the Tl.

The concentration of thallium in Mendip Hills waters was found to be very low and the samples were preconcentrated 100 times before the analysis was carried out. The sample (F_3) was found to have a higher thallium concentration than other sample location sites. It is thought that this result is a positive one and not an interference due to lead. If interference was a problem, a much higher level of thallium in sample F_2 would have been expected because it contains much more lead than sample F_3, however this is not the case. It may be due to the pH of water at sample F_3 being different from other location sites (slightly alkaline) and so affecting the solubility of thallium.

b) Toxicity of Thallium to Plants

The results in Tables 4.8 and 4.9 show the recovery of thallium in peat and John Innes soils, which indicate recovery to be very low. The major problem is homogeneity and the distribution of thallium throughout the soil used in the experiment. However, the surprising results are that the levels of thallium in the soil of 99 μg/g and 370 μg/g led to levels in the plants of 69 μg/g and 15.8 μg/g respectively. In fact, it is difficult to relate the concentration of thallium in plants to the concentration of the element in the soil according to these results. Much work on the distribution and effective extraction of thallium from soil samples must be carried out in order to solve this difficulty.

The results in Table 4.10 indicate the accumulation of thallium in germinated seeds. When thallium was fed as $TlNO_3$, the accumulation was different from that when it was fed as TlCl. These results do not agree with Polikarpov (41), who reported that the accumulation of thallium in a green alga, Ulva rigida, does not depend on the nature of anions in solution. The concentration of thallium in germinated seeds increases with the increase in thallium in solution as shown by Table 4.10.

The uptake of thallium by Lolium perenne seedlings is higher when thallium was fed as nitrate than as chloride, the results in Table 4.14 and 4.15 indicate this situation. Because thallium nitrate is more soluble than thallium chloride, therefore, it is probably taken up by the plant more easily.

Thallium (I) nitrate can penetrate the cellulose walls of the seed into the embryo and hence affect the germination. $TlNO_3$ was used to study the effect of thallium on the germination. The result shown in Table 4.11 indicates the level of inhibition of the germination due to thallium (I) nitrate. The results agree with the observations of Dilling (42) who studied the effect of thallium (I) nitrate on the germination of mustard, Sinapsis alba, seeds. The results in Table 4.11 are shown in Figure 4.37. The times to germinate 50% of the seed at concentrations of 0.01 and 0.08 $\mu g/cm^3$ deviate markedly from the curve; this may occur because some of the seeds were already dead.

Both thallium (I) and thallium (III) were taken up by the roots of the Cock's Foot species and the accumulation of thallium (I) is higher than for thallium (III). This fact is illustrated in the results of Table 4.12. These results agree with Logan et alia (43) who reported that thallium (I) accumulated more than thallium (III) in the roots of barley, Hordeum vulgare L. cv. Maris mink. The results in Table 4.12

FIG. 4.37 EFFECT OF THALLIUM ON RATE OF GERMINATION OF LOLIUM PERENNE SEEDS

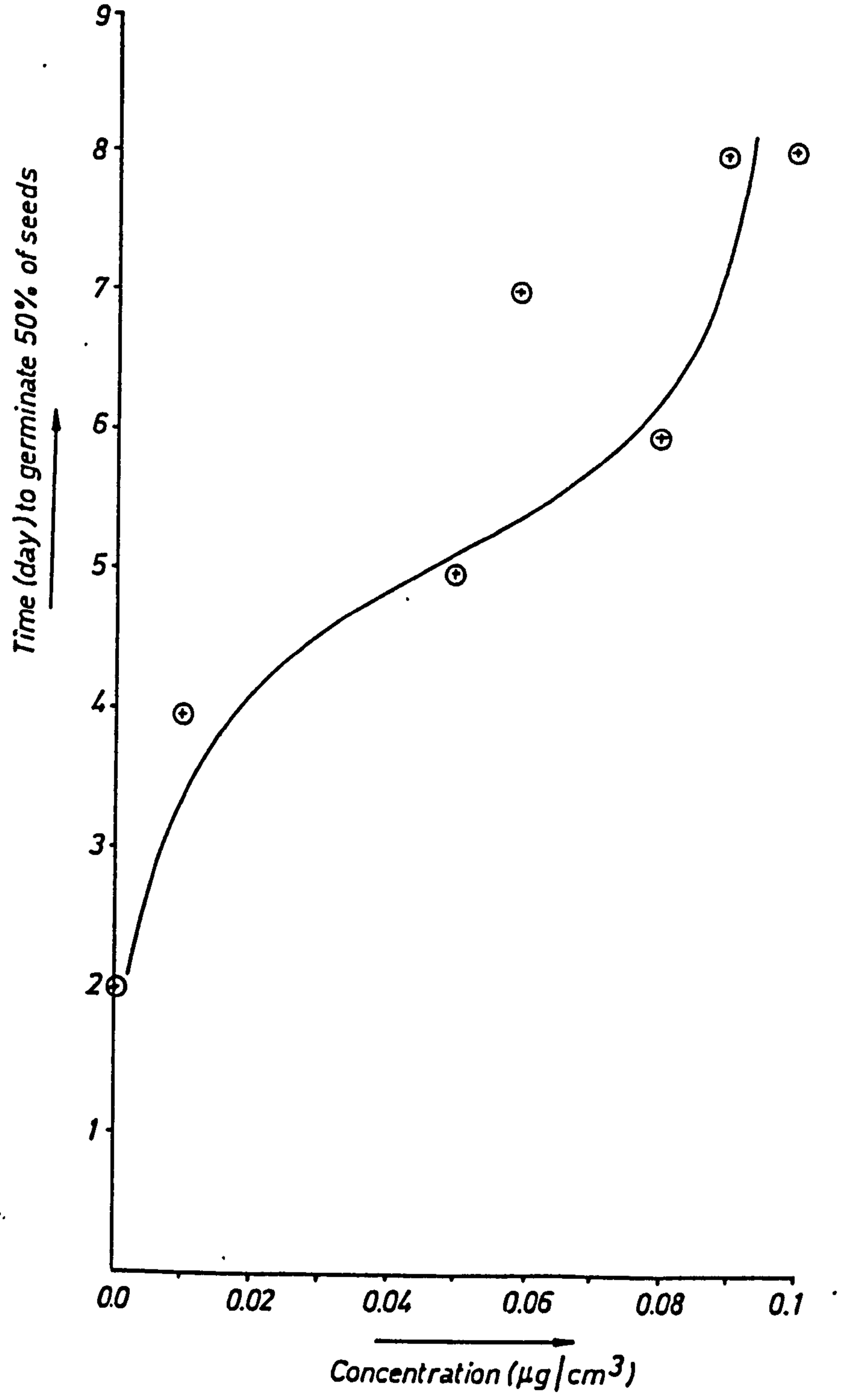

indicate another two observations :-

i) different species accumulate different levels of thallium (I) and thallium (III) but in all species after a specific time (dependent on the species) the level decreases. This may arise because the surface of the root is saturated with the thallium and hence no further thallium can be taken up by the roots;

ii) thallium (III) accumulated to higher levels than thallium (I) in the Holcus species and this does not agree with Logan's study of barley.

To date, it is not known whether the thallium (III) is taken up by plants as the trivalent metal or if it is reduced to thallium (I) on the surface of the root. Thallium (I) may be taken up by the plant in the same mechanism of uptake of potassium due to similar ionic radii and valency.

The critical and lethal concentrations of thallium in Lolium perenne roots were found to be approximately 1.9 and 31.6 mg/kg and in the shoots 0.056 and 3.16 mg/kg respectively. In fact, these results may not be accurate and it may be that the critical level of thallium is less than the figures quoted above. Figures 4.27 and 4.28 illustrate that the yields of the plants were affected by all the concentrations of thallium which were fed to them, therefore it was difficult to determine the unaffected yield (Y_o). The control experiment (see Chapter 5, p.365) was assumed to give Y_o. Perhaps when very low concentrations (< 0.001 $\mu g/cm^3$) of thallium are fed to such plants they might produce an unaffected yield. To estimate the critical level of thallium more reliably, a further series of experiments must be carried out, using extremely dilute solutions of thallium. Probably the feeding time of the experiment may have to be shorter than the three weeks which was used in the present work. Clearly, although we have used an unsatisfactory

experimental design, the toxicity of thallium is very high to such Lolium seedlings. Comparisons with other plants should prove very interesting.

4.4 REFERENCES

1. Zitko, V., Chemistry, Application, Toxicity and Pollution Potential of Thallium, Technical Report, No. 518, (1975), Canada.
2. Berman, E., At. Absorp. News., 6, 57 (1967).
3. Wakid, N.W. and Cortas, N.K., Clin. Chem., 30, 587 (1984).
4. Evans, W.H., Brooke, P.J. and Lucas, B.E., Anal. Chim. Acta, 148, 203 (1983).
5. Liem, I., Kaiser, G. and Sager, M., Anal. Chim. Acta, 158, 179 (1984).
6. Morgan, J.M., McHenry, J.R. and Masten, L.W., Bull. Environ. Contam. Toxicol., 24, 333 (1980).
7. Smith, I.C. and Caroson, B.L., Trace Metals in the Environment, Volume 1, Thallium, Ann Arbor Science Publishers Inc., p. 45 (1977).
8. McKenzie, T., Analytical Data for GTA-95, in "Analytical Methods for Graphite Tube Atomisers", Rothery, E. (Ed.), p. 47 (1982).
9. Xiao-quan, S., Zhe-ming, N. and Li, Z., Talanta, 31, 150 (1984).
10. Slavin, W,, Carnrick, G.R. and Manning, D.C., Anal. Chim. Acta, 138, 103 (1982).
11. Fazakas, J. and Marinescu, D.M., Talanta, 30, 857 (1983).
12. Lee, A.F. and Jones, E.A., The Determination of Thallium and Indium in Sulphide Concentrates, Report No. 2022, National Institute for Metallurgy, South Africa (1979).
13. Elson, C.M. and Albuquerque, C.A.R., Anal. Chim. Acta, 134, 393 (1982).
14. Dean, J.A. and Eskew, J.B., Anal. Letters, 4, 737 (1971).
15. Muralidhar, N., Rangamannar, B. and Krishnan, V.R., Radiochem. Radioanal. Letters, 56, 255 (1982).
16. Ikramuddin, M., At. Spectroscopy, 4, 101 (1983).

17. Batley, G.E. and Florence, T.M., J. Electroanal. Chem., 61, 205 (1975).

18. Hernandez-Mendez, J., Carabias-Martinez, R. and Garcia-Garcia, J.I., Anal. Chem. Acta, 132, 59 (1981).

19. Temmerman, E. and Verbeek, F., J. Electroanal. Chem., 19, 423 (1968).

20. Hoefiich, L.K., Gale, R.J. and Good, M.L., Anal. Chem., 55, 1591 (1983).

21. Lee, A.F., The Application of Anodic Stripping Voltammetry to the Determination of Trace Metals in Standard Reference Materials, Ph.D. Thesis, Rand Afrikaans University (1981).

22. Zitko, V., Carson, W.V. and Carson, W.G., Bull. Environ. Contam. Toxicol., 13, 23 (1975).

23. Watson, K.P., A Comparison of Some Detection Parameters, M.Sc. Thesis, University of Bristol (1985).

24. Braun, R.D., Introduction to Chemical Analysis, McGraw-Hill, New York (1982).

25. Bailey, C.J., Cox, E.A. and Springer, J.A., J. Assoc. Off. Anal. Chem., 61, 1404 (1978).

26. Forstner, U., Metal Concentrations in Freshwater Sediments, Natural Background and Cultural Effects, p. 94, in "Interactions between Sediments and Freshwater". Proceedings of an International Symposium, Amsterdam Sept. 6-10, 1976, Golterman, H.L. (Ed.), Dr. W. Junk - B.V. Publishers (The Hague) (1977).

27. Lau, M.W. and Wong, M.H., Environ. Res., 31, 229 (1983).

28. Linton, R.W., Loh, A. and Natusch, D.F.S., Science, 191, 852 (1976).

29. O'Shea, T.A., Anodic Stripping Voltammetric Study of the Competitive Interactions between Trace Metals and the Alkaline Earths for Complexing Ligands in Aquatic Environments, Ph.D. Thesis, University of Michigan (1972).

30. Beckett, P.H.T. and Davis, R.D., New Phytol., 79, 95 (1977).

31. Morgan, E., The Influence of Heavy Metals upon Tree Growth, Ph.D. Thesis, The Polytechnic of Wäles (1983).

32. Manual of Rotating Disk Electrode Series 628-01, Metrohm Herisau, Switzerland.

33. Calderoni, G. and Ferri, T., Talanta, 29, 371 (1982).

34. Ciszewski, A. and Lukaszewski, Z., Talanta, 30, 11 (1983).

35. William, E.V., J. Food Technol., 13, 267 (1978).

36. Hewitt, E.J., Sand and Water Culture Methods used in the Study of Plant Nutrition, Commonwealth Bureau of Horticulture and Plantation Crops, Tech. Commun., 22 (1966).

37. Liteanu, C. and Rica, I., Statistical Theory and Methodology of Trace Analysis, Published by Ellis Horwood Ltd., Chichester, P. 255 (1980).

38. Alevato, S.D.J. and Rebello, A.D.L., Talanta, 29, 909 (1981).

39. Ciszewski, A. and Lukaszewski, Z., Anal. Chim. Acta, 146, 51 (1983).

40. Brezonik, P.L., Brauner, P.A. and Stumm, W., Water Res., 10, 605 (1976).

41. Polikarpov, G.G., Proc. Symp. Hydrogeochem. and Biogeochem., 1, 356 (1973).

42. Dilling, W.J., Ann. Appl. Biol., 13, 160 (1926).

43. Logan, P.G., Lepp, N.W. and Phipps, D.A., Thallium Uptake by Higher Plants, in "International Conference on Heavy Metals in the Environment", Heidelberg, p. 642 (1983).

CHAPTER 5

ALUMINIUM, SILVER AND LANTHANUM : DETERMINATION, EFFECTS AND FRACTIONATION STUDIES

CONTENTS

5.1 INTRODUCTION

Two types of procedure were used for the determination of aluminium. The first measured all the aluminium in a particular sample, while the other measured only the aluminium in a certain chemical form (such as the simple aquated ion). Atomic absorption techniques constitute the first category while gas liquid chromatography lies in the second (1). Although FAAS is not sufficiently sensitive for the determination of aluminium in environmental samples even when using a high temperature flame such as that of nitrous oxide-acetylene, it has been used for the determination of aluminium in plant tissue (2).

GFAAS has been widely employed for the determination of aluminium in urine and serum using a matrix modification procedure coupled to the L'vov platform (3,4). Aluminium can be reacted with 8-hydroxy quinoline, the resultant aluminium complex being extracted into MIBK. This approach has also been used for the determination of aluminium employing GFAAS (5). Burns et alia (6) determined aluminium in an organoaluminium salt by graphite furnaces, Ta_2O_5 coated or pyrolytically coated. They found that Ta_2O_5 coated tubes gave a greater response for aluminium than the other two furnace materials. Due to the suitability of pyrolytically coated graphite tubes for the determination of aluminium by flameless atomic absorption, this type of tube was used in the present work.

Gas chromatography of aluminium trifluoroacetylacetonate and hexafluoroacetylacetonate has been used for the determination of aluminium in different sample matrices (6-12). Therefore, aluminium trifluoroacetyleactonate was also used later in the present work for the determination of aluminium by gas chromatography.

GFAAS has been widely used for the determination of silver in sewage sludge (13), rainwater (14) and marine sediment (15). Through

the use of $NH_4H_2PO_4$ as a matrix modifier to stabilise the silver at the higher ashing temperature and with optimised furnace parameters, the problems involved in the determination of silver have been eliminated (15). Hosking et alia (16) used furnaces fitted with pyrolytic platforms with a matrix modifier containing nickel, for the measurement of traces of silver in process solutions resulting from the extraction of gold. Silver was determined in ores, concentrates, zinc process solutions and copper metal by GFAAS after separation by extraction of the tribenzylamine-silver bromide complex into MIBK (17,18). Silver in sea water was also determined by GFAAS after coprecipitation of the silver with cobalt (II) pyrrolidinediethiocarbamate, the resultant precipitate being dissolved in concentrated nitric acid (19).

In the voltammetric determination of silver, solid inert electrodes must be used because the oxidation potential of the element is greater than that of mercury. Perone et alia (20) reported the application of stripping analysis to the determination of silver using graphite electrodes while Temmerman et alia (21) used a glassy carbon electrode for the determination of silver in cadmium metal. However, a direct method for the determination of silver in mercury was described by Goldowski et alia (22) using 0.1 M lithium perchlorate solution in acetonitrile as background electrolyte.

Butts et alia (23) reported that lanthanum can be determined by gas chromatography as lanthanum chelate through reaction with mixed ligands (hexafluoroacetylacetonate and tri-n-butylphosphate). In view of this quantitative determination, the mixed ligand systems of lanthanum chelates seem to increase the sensitivity of electron capture detectors. But the major problem is the difficulty in eluting the tri-n-butylphosphate from the detector.

FAAS is insufficiently sensitive for the determination of lanthanum due to the low temperature of the flame, and the high stability of the oxide. Therefore, plasma emission spectrometry was used in this work for the determination of lanthanum in plant tissue. GFAAS is also not suitable for the determination of this metal due to carbide formation so preventing release of free atoms to yield an analytical signal. However, Gupta (24,25) has tried to determine lanthanum and other rare earth elements by GFAAS by lining a tantalum foil inside a pyrolytically coated graphite furnace to prevent formation of carbide. In the present work, a factorial design was carried out to study the effect of flow rate of nitrogen gas, ashing temperature and ashing time on the response of lanthanum by GFAAS using the Gupta method. In a factorial design with n factors, there are n main effects, n(n-1)/2 two-factor interactions and n(n-1)(n-2)/6 three-factor interactions. With three factors (A, B, C), this means that there are 2 x 2 x 2 = 8 possible combinations of factor levels, if each factor contains two levels. Table 5.1 lists the possible combinations of three factors (26) and indicates that each factor has two levels assumed (+) and (-) which measure the higher and lower levels respectively. The number 1 in Table 5.1 is used to indicate that all the factors are at low level. In fact, this design permits the experimenter to evaluate :-

i) the main and the interaction effects between two or more factors

ii) to maximise the response at certain combinations ANOVA can be used to investigate the main and the interaction effects between factors.

To confirm that specific effects are significant, one should optimise values of parameters which are responsible for the effect. Indeed, factorial design is useful in analytical chemistry to obtain the maximum response from an instrument or method which is resultant from the combination of several effects on the analyte.

Table 5.1 : Possible Combinations of 2^3 Factors

Response	A	B	C	Combination
Y_1	-	-	-	1
Y_2	+	-	-	a
Y_3	-	+	-	b
Y_4	-	-	+	c
Y_5	-	+	+	bc
Y_6	+	-	+	ac
Y_7	+	+	-	ab
Y_8	+	+	+	abc

5.2 EXPERIMENTAL AND RESULTS

a) Preparation of Metal Chelates and Determination by GLC

i) Metal Trisacetylacetonates

A solution of aluminium was prepared by dissolving AnalaR aluminium sulphate (6 g) in DDW (40 cm^3) while a similar lanthanum solution was prepared by dissolving lanthanum oxide (1 g) in the minimum amount of 1 N HCl and then adjusting the pH to 5.0. Both solutions were stirred with ammonium acetylacetone to prepare the respective aluminium and lanthanum acetylacetonates. The precipitated metal acetylacetonates were filtered and air-dried. The mass spectra are shown in Figures 5.1 and 5.2 which indicate the molecular weight of these compounds. Stock solutions (1000 $\mu g/cm^3$) of Al and La were prepared by dissolving known amounts of the metal complexes in toluene. Further dilutions were carried out with toluene to produce solutions containing 0.5, 2 and 10 $\mu g/cm^3$ of Al and La. An aliquot (3 μl) of the above standards were injected into the GLC on 5% w/w OV-17 on Chromosorb-W AC-DMCS using a column temperature of 240^{o}C and an ECD detector. Since injections of some 30 ng of chelate had been made, clearly the ECD is not responsive to these acetylacetonate complexes and an electron-attracting group must be introduced into the acetyl-acetone skeleton. One such group is the CF_3 grouping.

ii) Metal Trifluoroacetylacetonates

The mass spectra (Figures 5.3 and 5.4) of these compounds indicated that the HFA as supplied contained more than one compound and was impure. However, the TFA was pure and was used for further investigations. Aluminium nitrate (25 g) and sodium acetate (15 g) were shaken with 0.1 M TFA (250 cm^3) in ethanol for 30 minutes. The

FIG. 5.1 MASS SPECTRUM OF Al $(ACAC)_3$

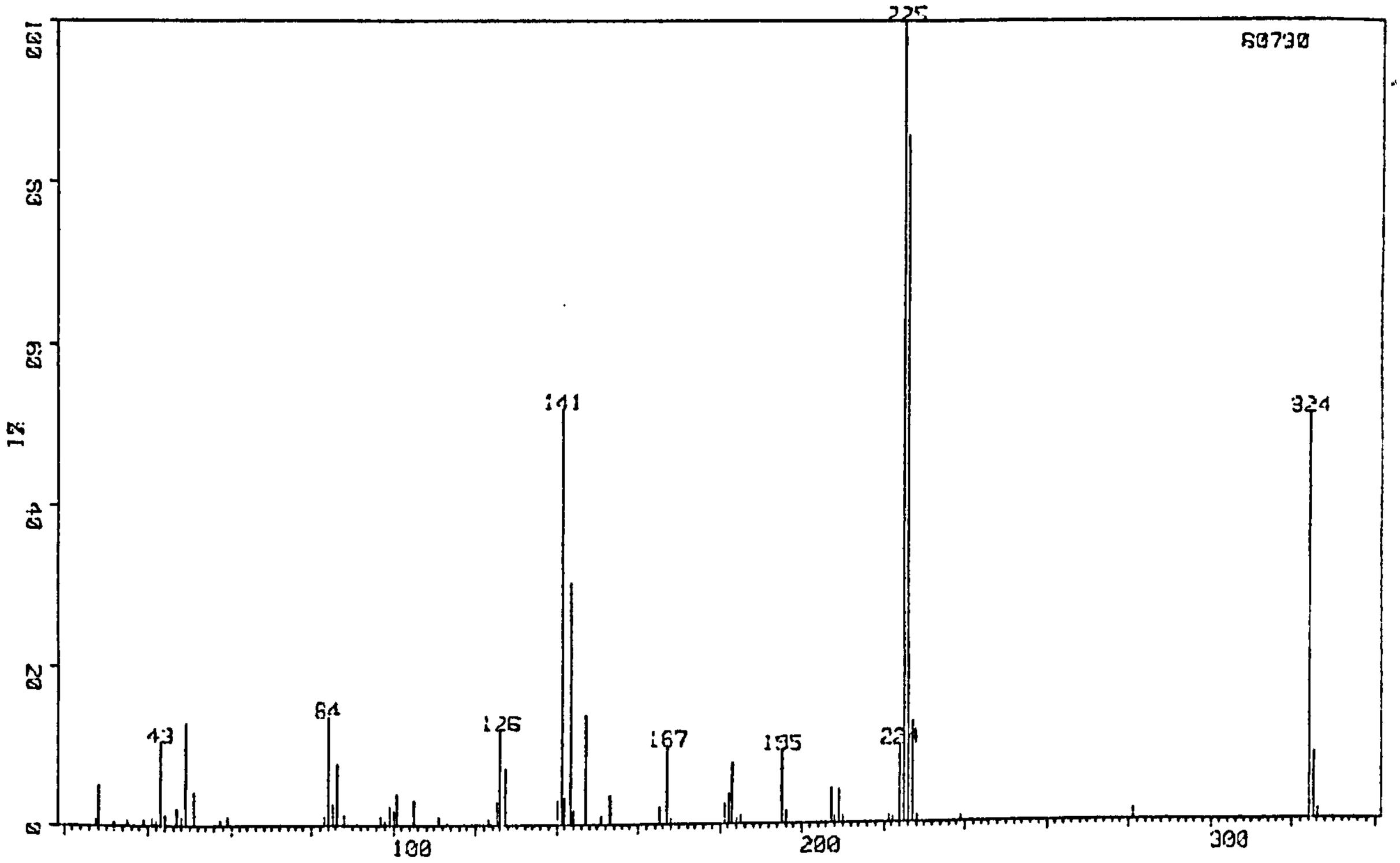

FIG. 5.2 MASS SPECTRUM OF La $(ACAC)_3$

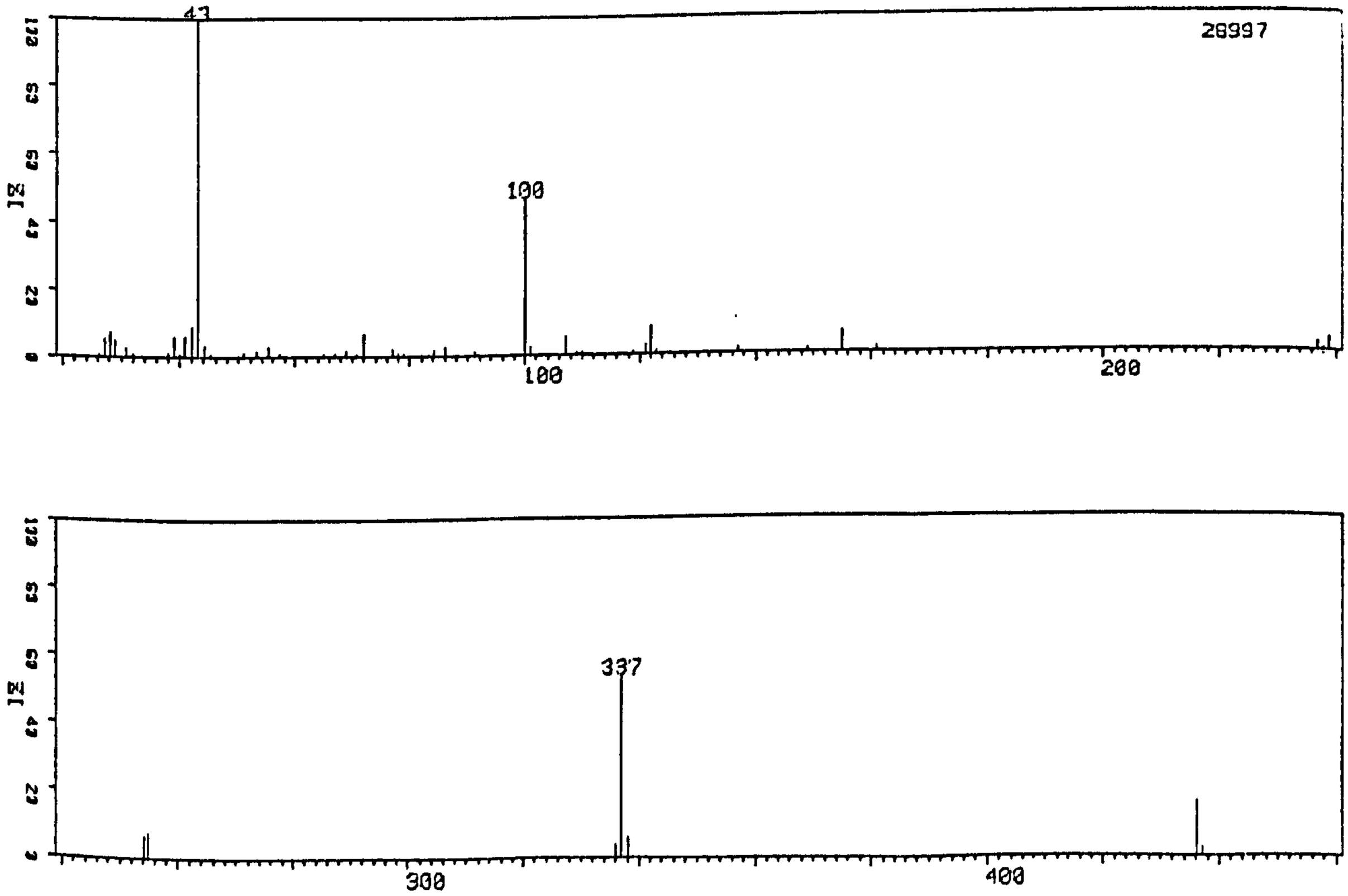

FIG. 5.3 MASS SPECTRUM OF TFA

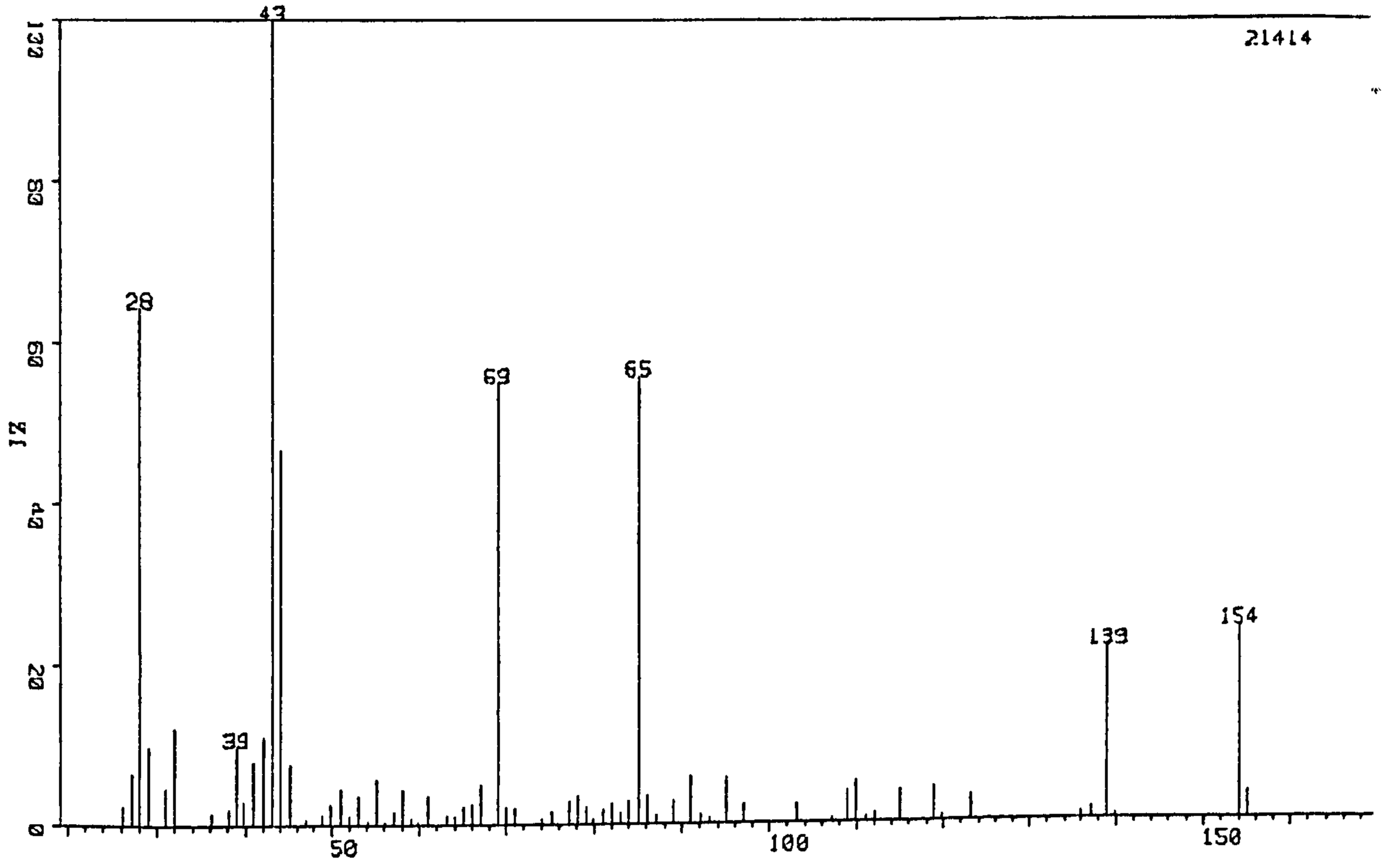

FIG. 5.4 MASS SPECTRUM OF HFA

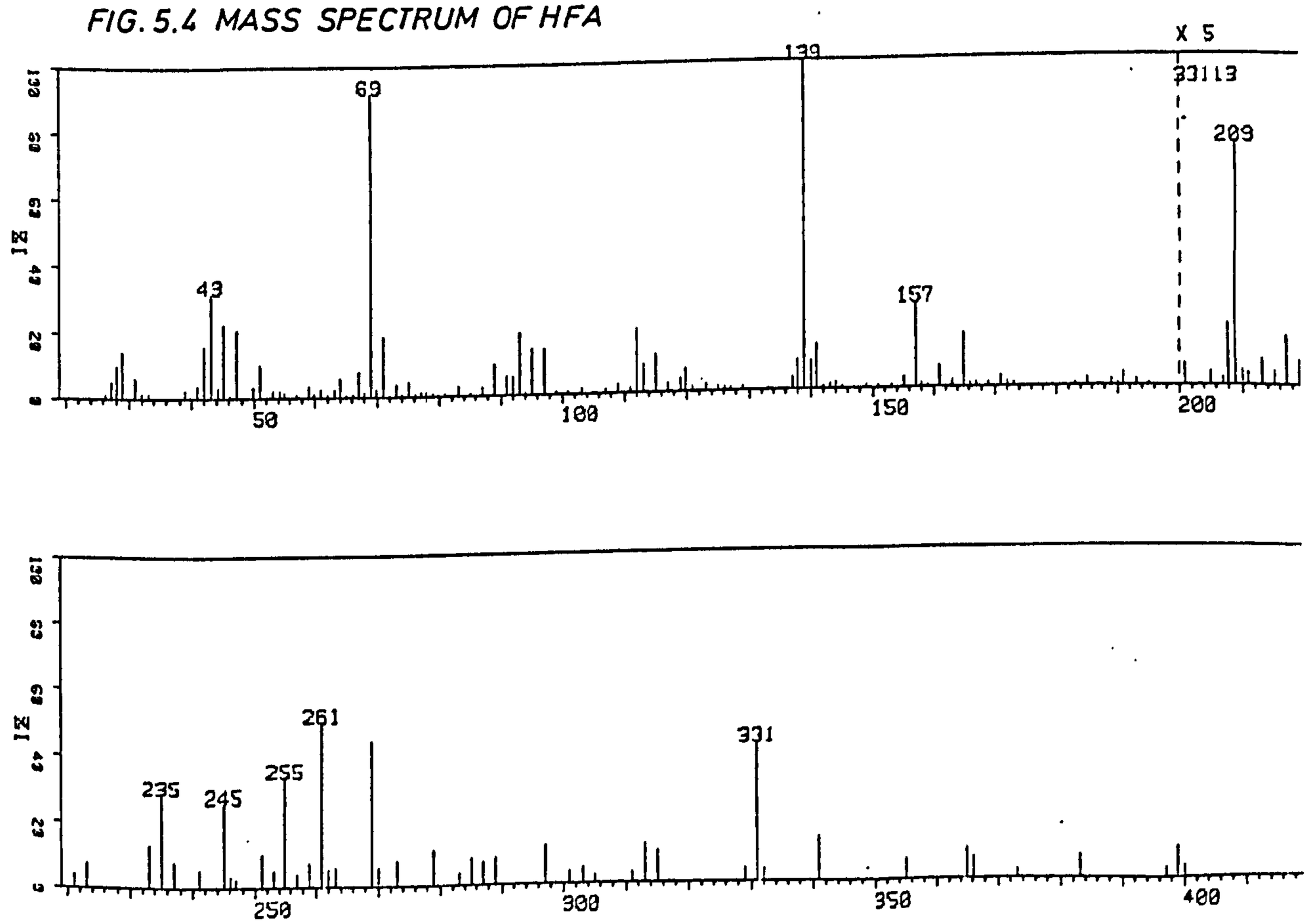

precipitated aluminium trifluoroacetylacetonate was filtered off and the mass spectrum of the solid is illustrated in Figure 5.5.

Ferric chloride (2.7 g) and sodium acetate (5 g) were shaken with TFA (0.048 g) in 20 cm^3 ethanol. The mass spectrum is given in Figure 5.6 showed that the precipitate was $Fe(TFA)_3$.

Stock solutions of aluminium and iron (1000 $\mu g/cm^3$) were prepared individually by dissolving known amounts of the above complexes in toluene. Further dilutions were carried out to prepare standard solutions. No response was observed from the ECD for the iron complex, but it is suggested that the metal complex decomposed on the column, while a good response was obtained for the aluminium complex using the conditions shown in Table 5.2. A typical chromatogram obtained is shown in Figure 5.7. The aluminium complex was also prepared by solvent extraction as follows:-

Aliquots of varying volumes from 10, 35, 60 to 85 cm^3 of a 1.0 $\mu g/cm^3$ of aluminium nitrate were placed in a series of separating funnels, then 15 cm^3 of acetate buffer was added to each funnel followed by 10 cm^3 of 0.1 M TFA in toluene. The organic layer was separated and washed with 6 M NH_4OH (twice) and diluted to 25 cm^3 with toluene. The solutions were analysed by GLC using the conditions given in Table 5.2. The chromatograms produced are shown in Figure 5.8. The GLC calibration graphs for the aluminium complex prepared by the two methods are depicted in Figure 5.9.

Clearly the two methods have widely differing sensitivities. Since the solvent extraction method is much less sensitive than the sensitivity produced from a weighed quantity of pure complex, the solvent extraction reaction has not proceeded to completion, a common fault and unfortunate feature of the derivatisation reactions in the preparation of these metal chelates.

FIG. 5.5 MASS SPECTRUM OF Al (TFA)$_3$

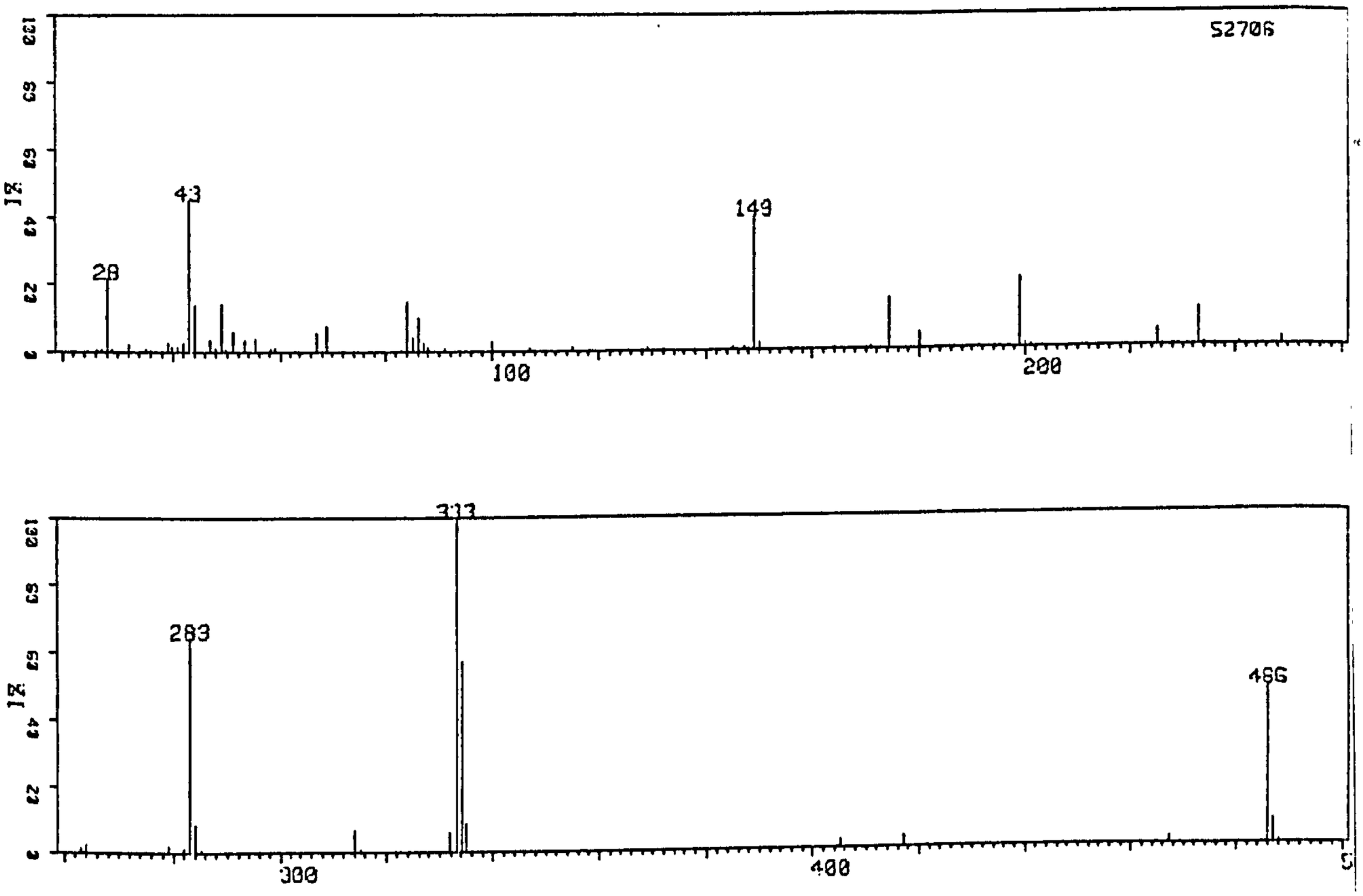

FIG. 5.6. MASS SPECTRUM OF Fe (TFA)$_3$

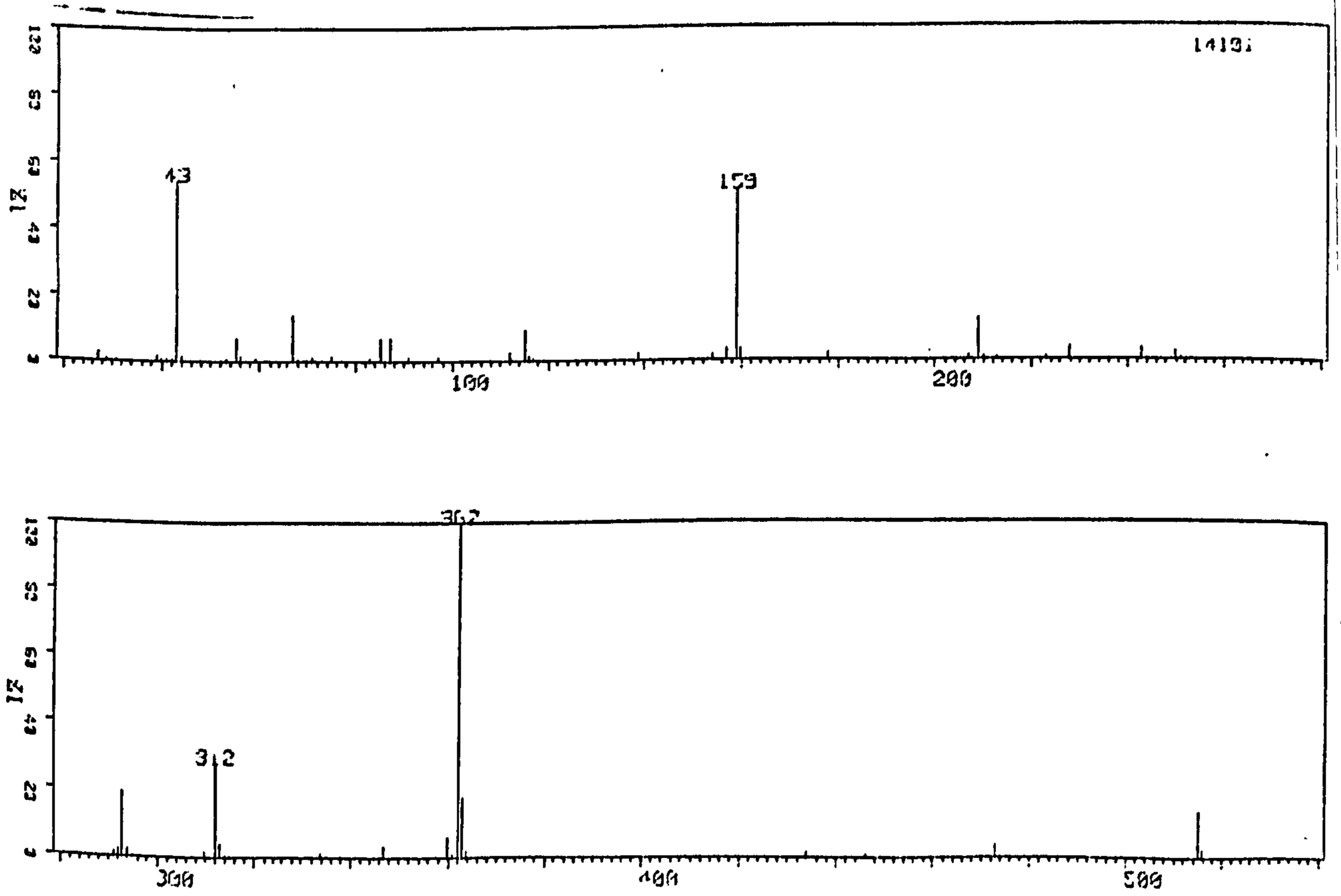

FIG. 5.7 CHROMATOGRAM OF $Al(TFA)_3$ PREPARED ON LARGE SCALE

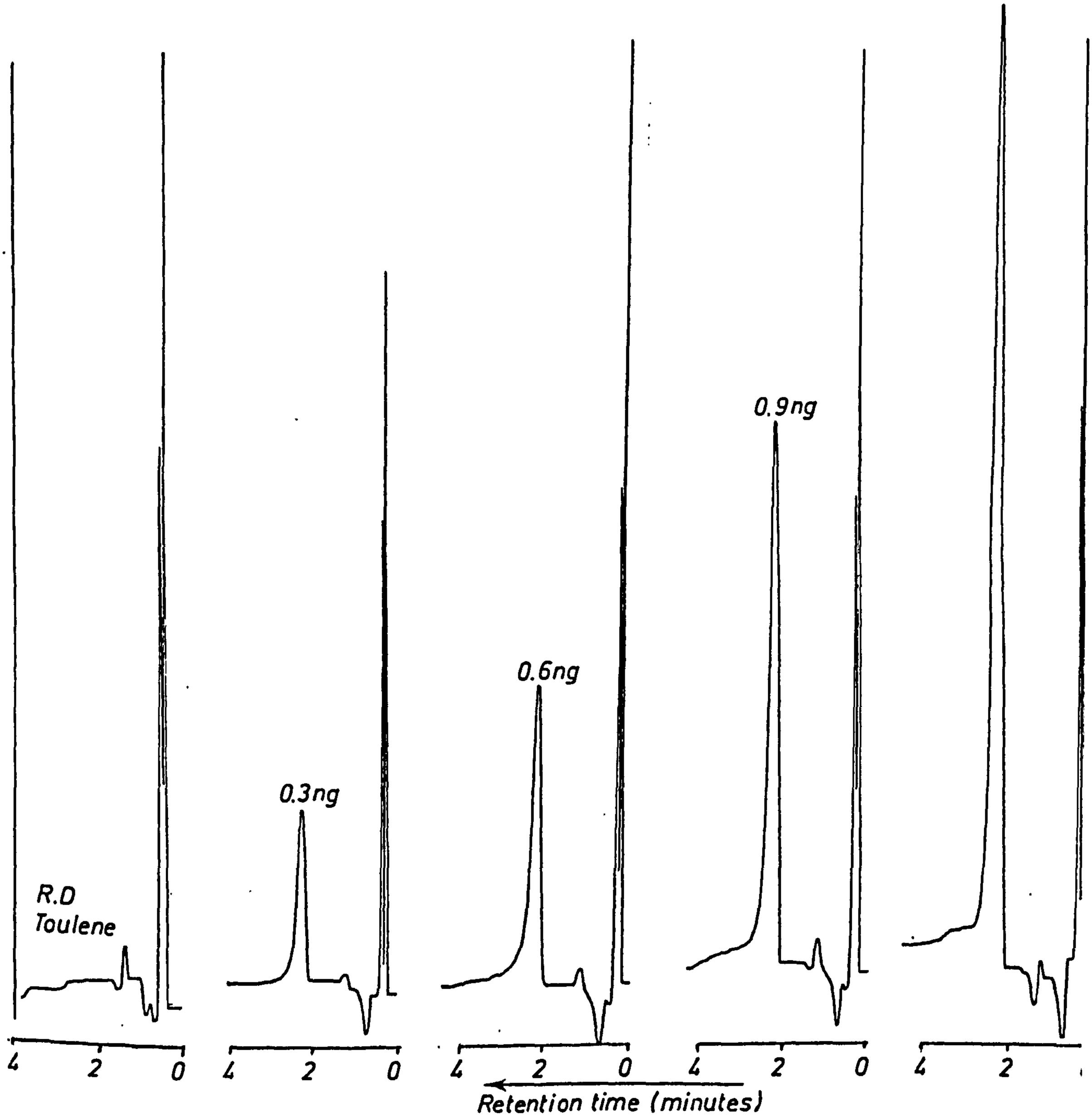

FIG. 5.8 CHROMATOGRAM OF Al (TFA)$_3$ PREPARED BY SOLVENT EXTRACTION METHOD

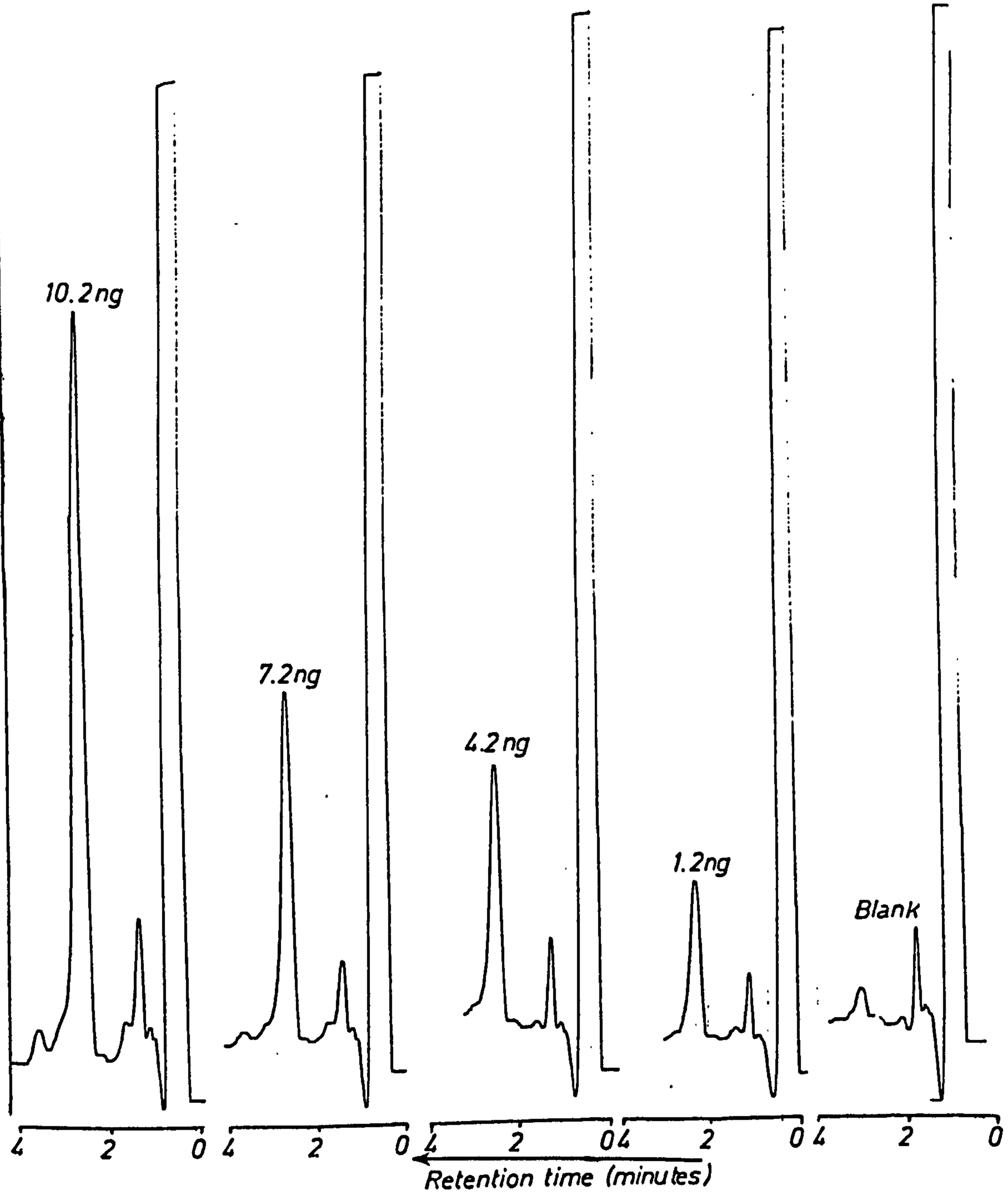

FIG. 5.9 CALIBRATION GRAPHS OF $Al(TFA)_3$ PREPARED BY TWO METHODS

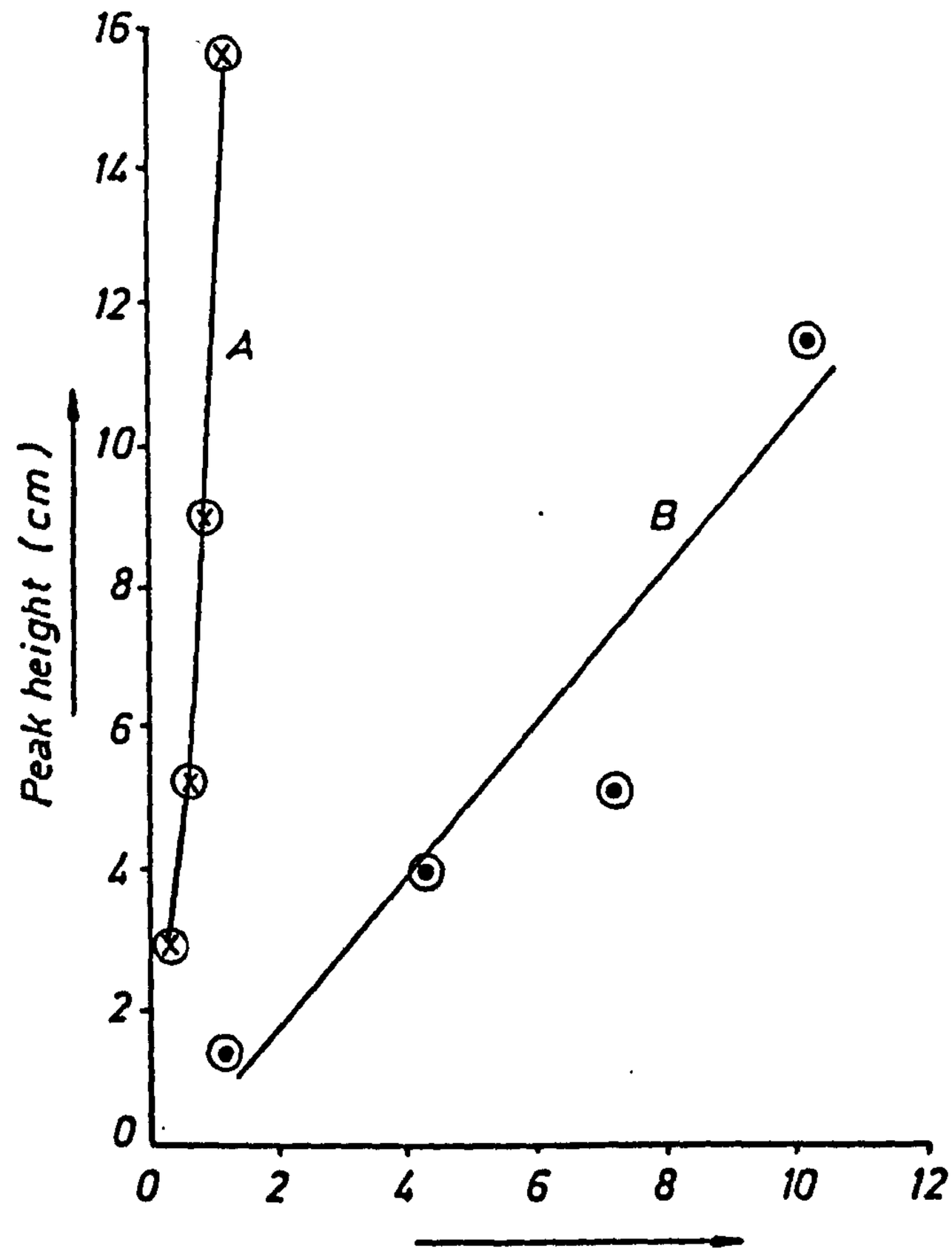

A = prepared $Al(TFA)_3$ on larger scale

B = prepared $Al(TFA)_3$ by solvent extraction method

Table 5.2 : The Gas Liquid Chromatography Conditions used for Determination of Metal Chelates

(a)	Column	A glass column
	(i) Support	Chromosorb WAW
	(ii) Liquid phase	OV-17, 5% w/w
(b)	Temperature	
	(i) Column	150°C
	(ii) Detector	300°C
(c)	Detector	Ni^{63}
(d)	Carrier gas	Nitrogen
	Flow rate	20 cm^3/min
(e)	Purge gas	Nitrogen
	Flow rate	10 cm^3/min
(f)	Total amount injected	3 μl/injection

An attempt was carried out to determine aluminium in Mendip Hills water and tap water in Bristol University by GLC using the solvent extraction method. A water sample (500 cm^3) was placed in a separating funnel, then 50 cm^3 of acetate buffer was added followed by 0.1 M TFA (10 cm^3) in toluene. The organic layer was washed with 6 M NH_4OH (twice) and diluted to 25 cm^3 with toluene. The chromatograms did not show any peaks for aluminium in either sample.

Chromic nitrate nonahydrate (30 g) was shaken with acetate buffer (90 cm^3) and TFA (10 cm^3) for four hours. The precipitate was air-dried and the mass spectrum was recorded and is shown in Figure 5.10.

The same conditions listed in Table 5.2 were used for determination of chromium except that the column temperature was increased to 160°C.

Lanthanum oxide (0.32 g) was dissolved in 1 M HCl and heated to dryness. The residue was dissolved in 1 M HAc + 1 M NaAc solution (20 cm^3). TFA (0.462 g) in 100 cm^3 of cyclohexane was added and the solution stirred overnight. The precipitate was filtered, air-dried and the mass spectrum recorded (see Figure 5.11). Lanthanum solution (100 $\mu g/cm^3$) was prepared by dissolving a known amount of the above metal complex and analysed by GLC under the conditions given in Table 5.2 except the temperature was increased to 240°C. The compound was not eluted through the column.

In order to increase the volatility of lanthanum chelate by removing the hydration water molecules, the metal complex was prepared as follows :-

Lanthanum solution (10 $\mu g/cm^3$) was placed in a separating funnel, then acetate buffer (15 cm^3) was added followed by 10 cm^3 of 0.1 M TFA + 0.07 M TBP in toluene. The solution was shaken for 5 minutes and the organic layer examined by GLC. Unfortunately the excess TBP overloaded the detector which required much cleaning to remove completely, thus no response was seen for this complex.

An attempt was made to separate $Al(TFA)_3$ and $Cr(TFA)_3$, under the conditions these complexes were well separated (see Figure 5.12).

FIG. 5.10 MASS SPECTRUM OF $Cr(TFA)_3$

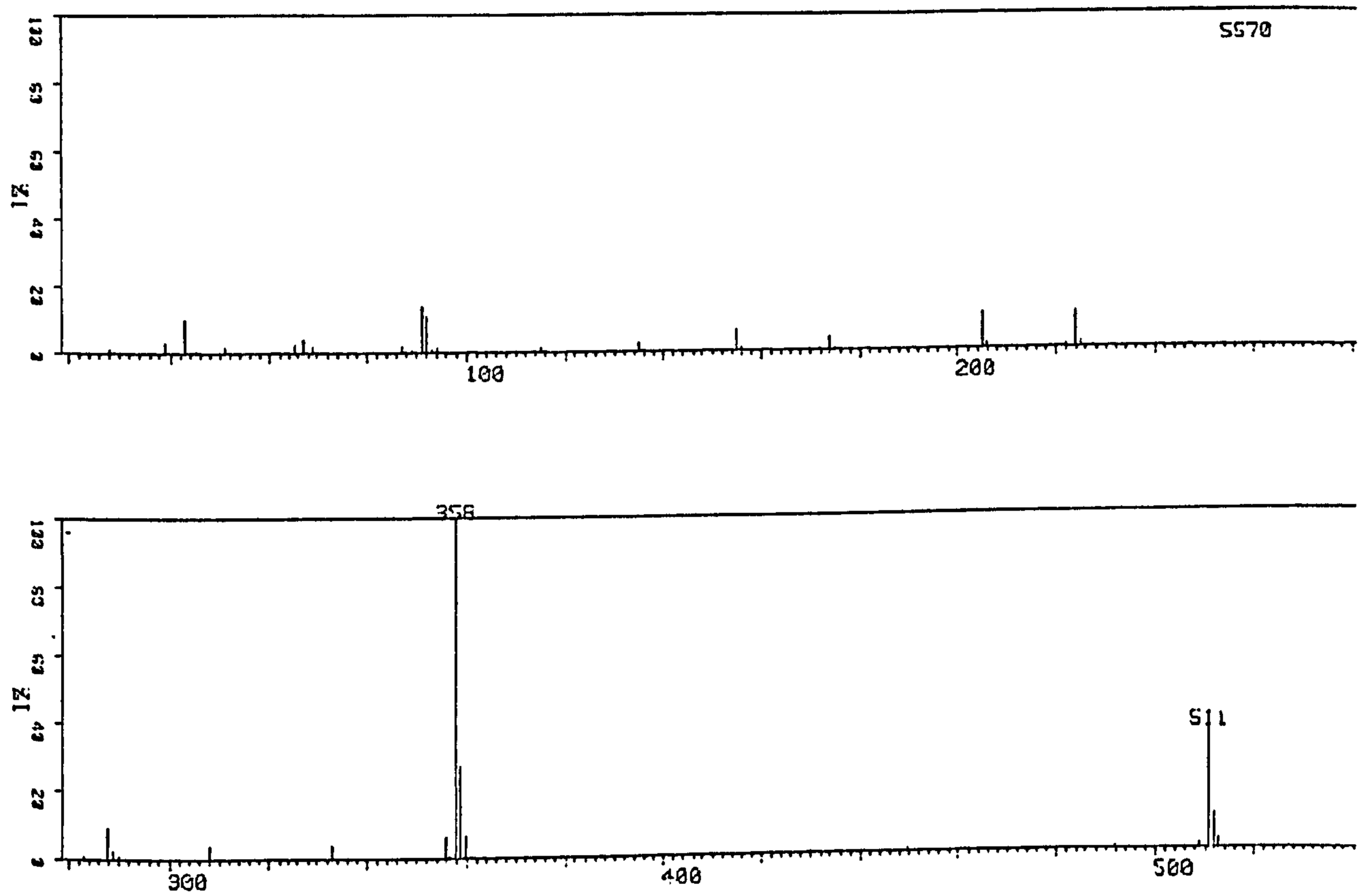

FIG. 5.11 MASS SPECTRUM OF $La(TFA)_3$

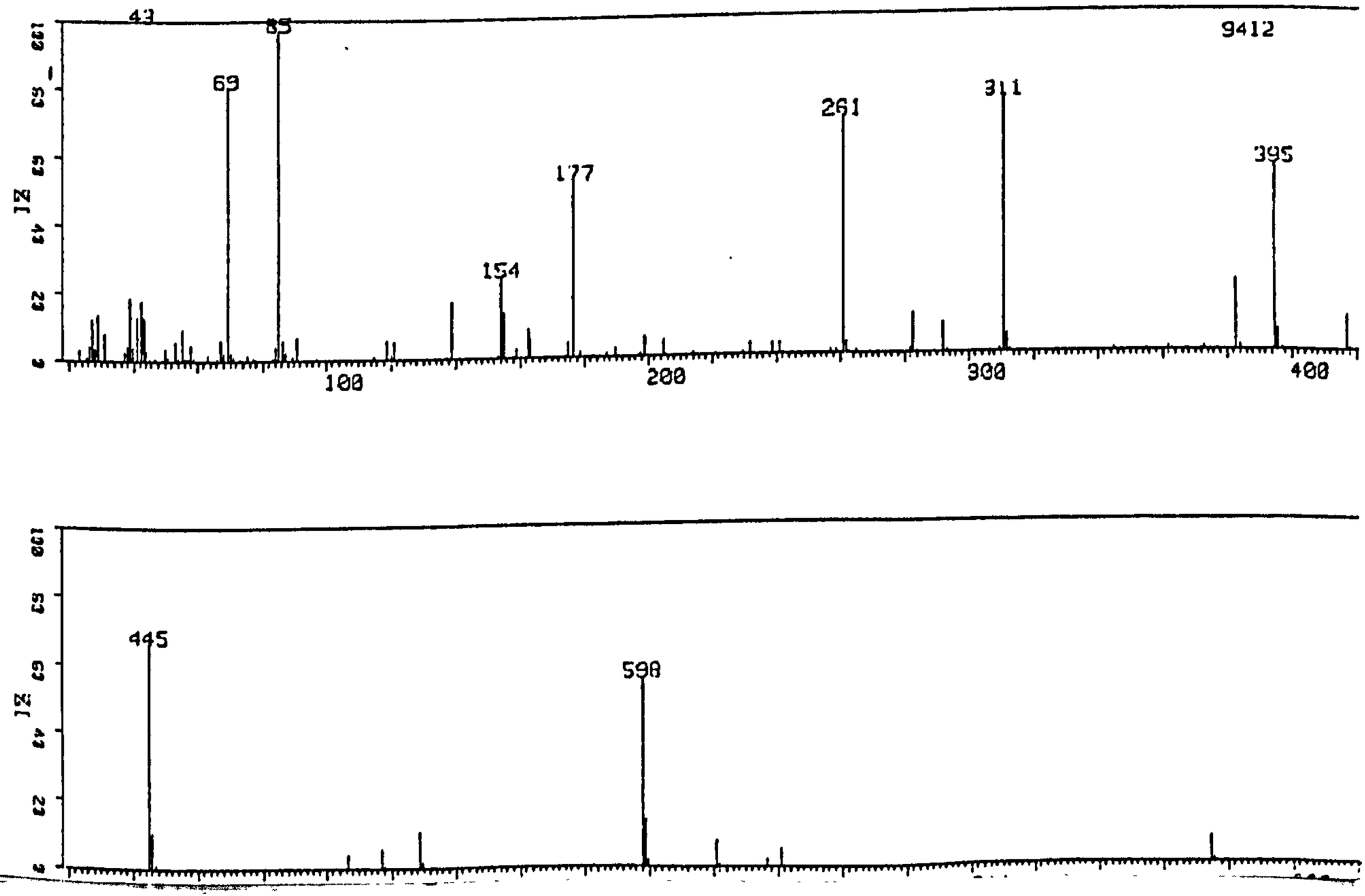

FIG. 5.12 SEPARATION OF ALUMINIUM AND CHROMIUM TRIFLUOROACETYLACETONATES

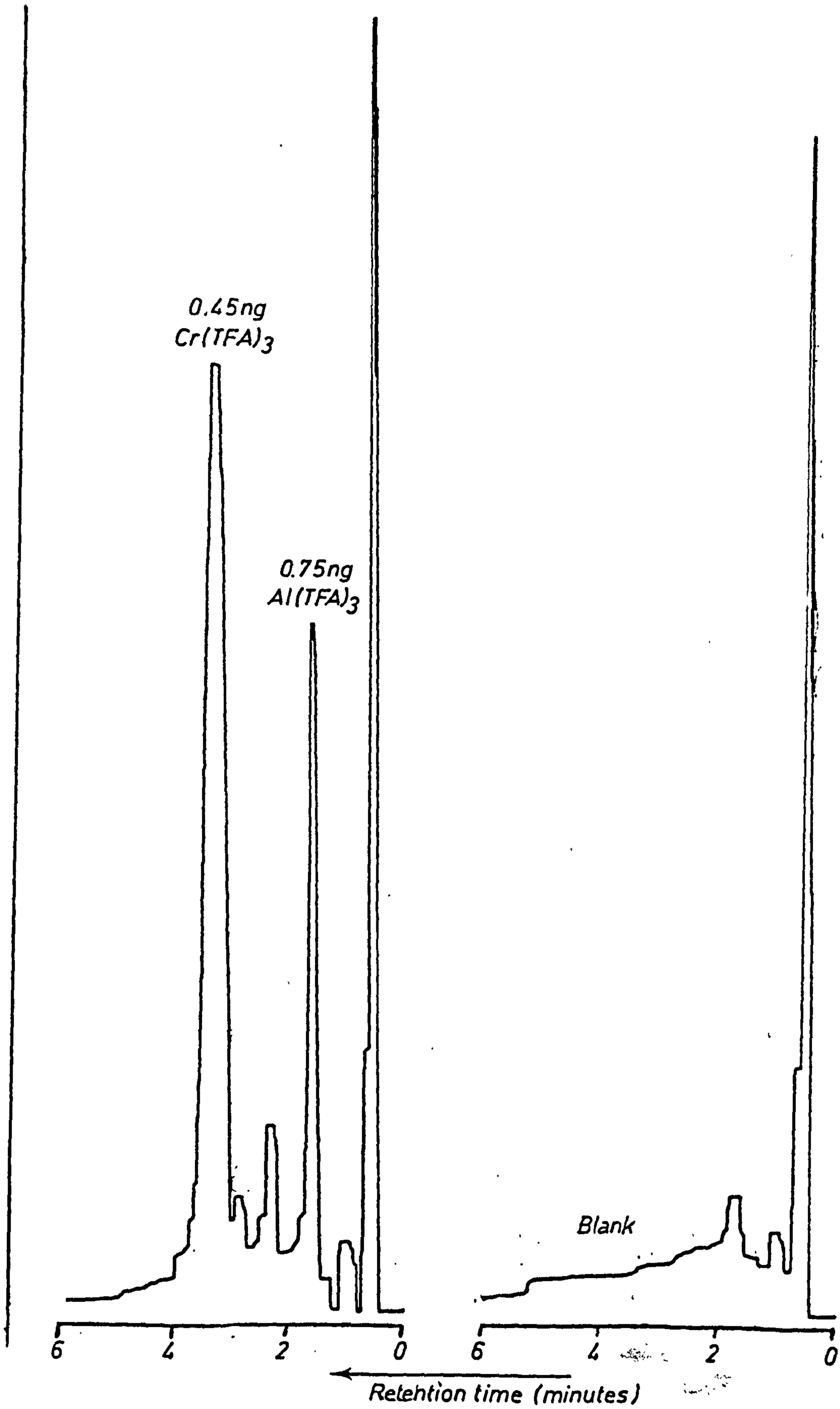

b) Determination of Silver by Direct Current Anodic Stripping Voltammetry

Two background electrolytes were chosen for the determination of silver by this technique, they were 0.1 M KNO_3 + 0.002 M EDTA and 0.2 M NH_4OH + 0.2 M NH_4NO_3. The background electrolyte (25 cm^3) was placed in the voltammetric cell, then the voltammogram was recorded using the instrumental parameters shown in Table 5.3. Aliquots of 20 μl of silver (100$\mu g/cm^3$) were added to the background electrolyte, then the voltammogram was recorded for each addition. Typical voltammograms obtained are shown in Figures 5.13 and 5.14.

The effect of deposition time, modulation amplitude, scan rate and rotation of the electrode on peak height response of silver in both electrolytes was studied. The results obtained are listed in Tables 5.4 to 5.7.

Table 5.3 : Instrumental Parameters for Determination of Silver by DC-ASV

Electrolytes :	0.1 M KNO_3 + 0.002 M EDTA, 0.2 M NH_4OH + 0.2 M NH_4NO_3
Initial potential	: -0.5 V
Final potential	: +0.5 V
Conditional potential	: 0.00 V
Working electrode	: RGCE
Reference electrode	: Ag/AgCl saturated with 3 M KNO_3
Auxiliary electrode	: Platinum wire
Mode	: DC-ASV
Current range	: 2 mA
Purge time	: 5 minutes
Deposition time	: 300 sec
Equilibration time	: 30 sec
Low pass filter	: Off

FIG. 5.13 VOLTAMMOGRAM OF SILVER IN 0.1M KNO_3 +0.002 M EDTA ELECTROLYTE

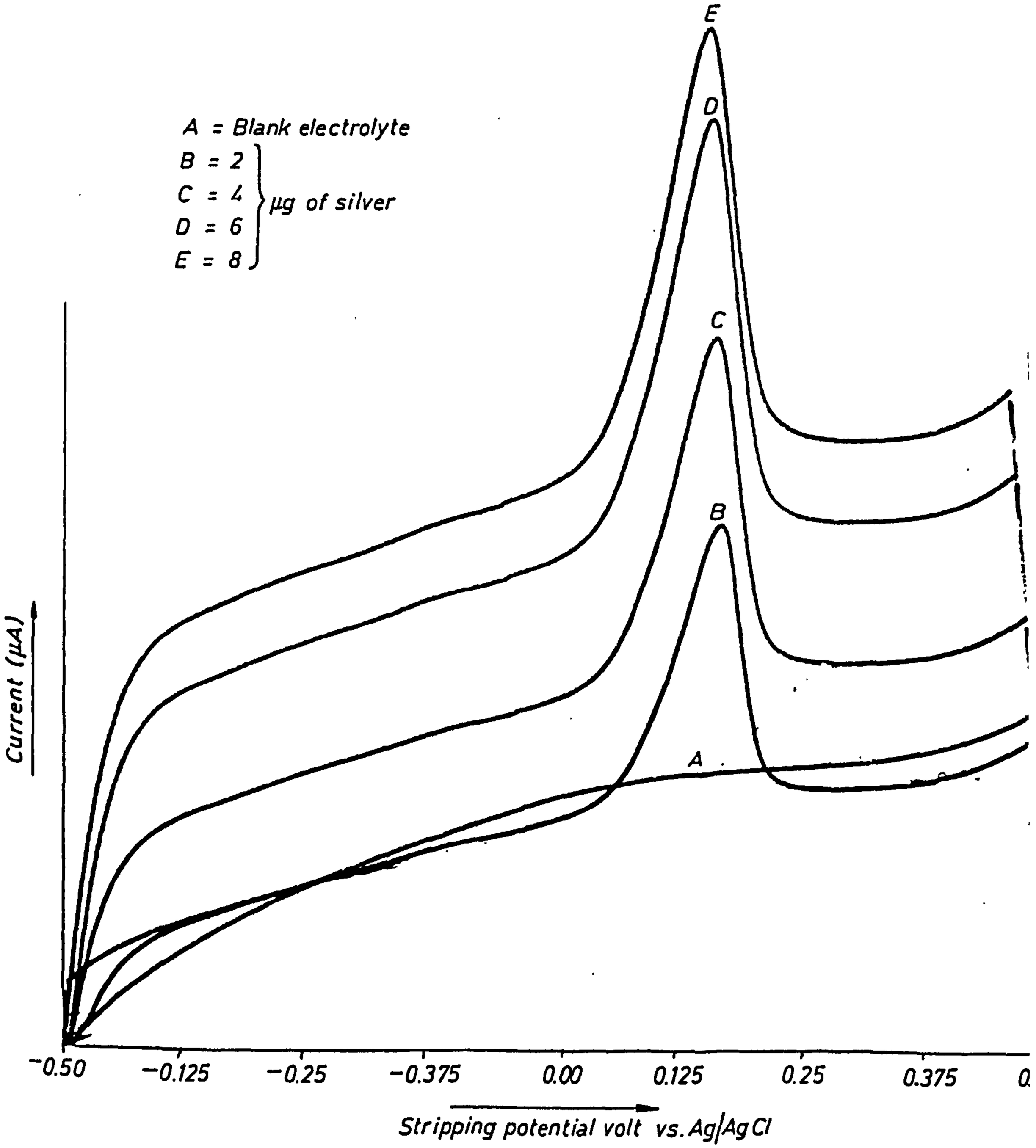

FIG. 5.14 VOLTAMMOGRAM OF SILVER IN 0.2M NH_4OH + 0.2M NH_4NO_3 ELECTROLYTE

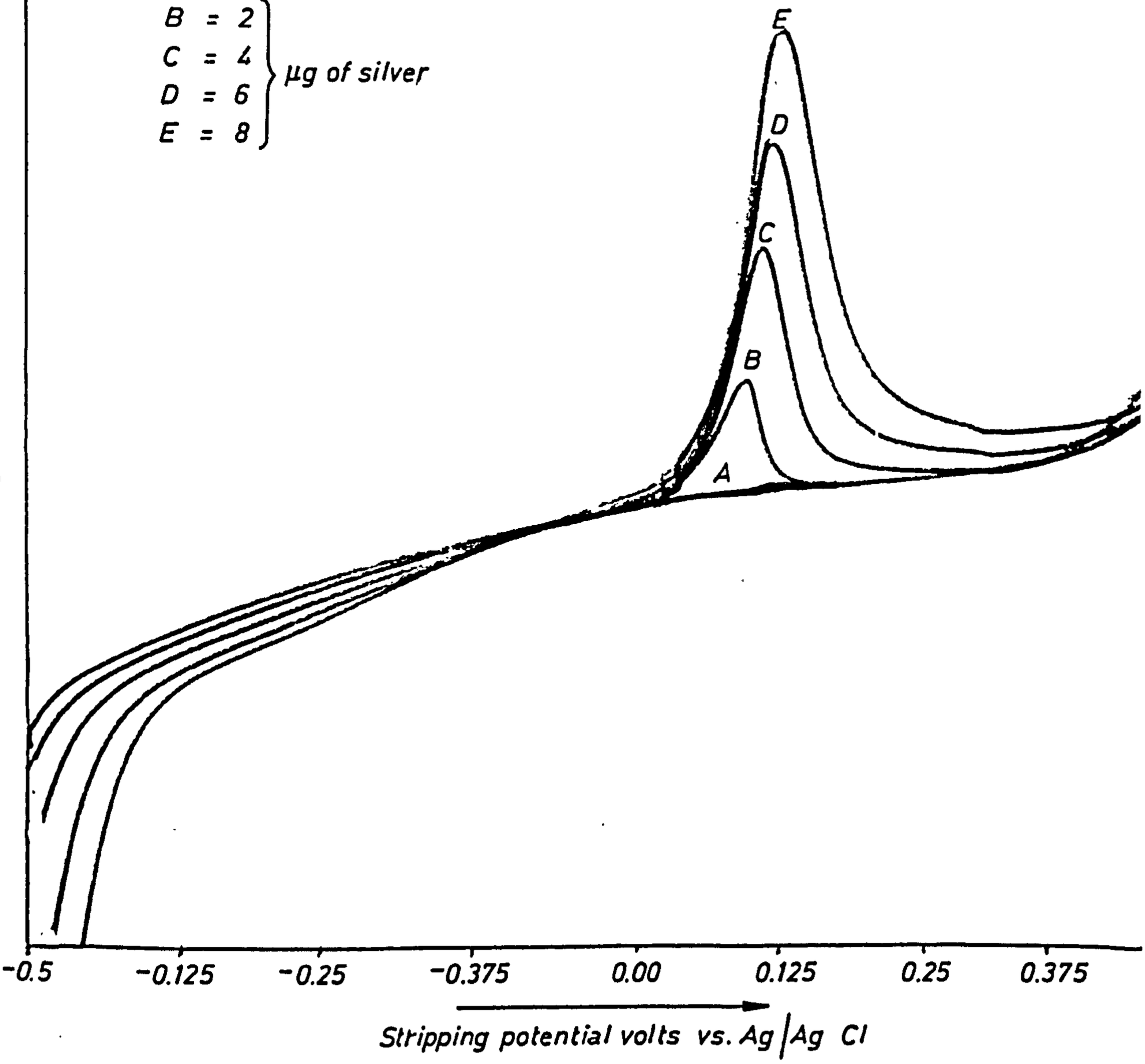

Table 5.4 : Effect of Deposition Time on Peak Height of Silver

Deposition Time (sec)	Peak Height (cm)
50	2.0
100	3.0
150	4.0
200	5.0
250	6.5
300	8.0

* Concentration of silver = 0.32 $\mu g/cm^3$

Electrolyte : 25 cm^3 of 0.1 M KNO_3 + 0.002 M EDTA

Table 5.5 : Effect of Modulation Amplitude on Peak Height of Silver

Modulation Amplitude (mv)	Peak Height (cm)
5	4.5,[a] 4.0[b]
25	5.5, 5.0
50	6.0, 5.5
100	6.0, 5.0

a = 0.1 M KNO_3 + 0.002 M EDTA

b = 0.2 M NH_4OH + 0.2 M NH_4NO_3

Table 5.6 : Effect of Scan Rate on Peak Height of Silver

Scan Rate (mv/sec)	Peak Height (cm)	
2	0[a]	4.0[b]
5	0	4.6
10	0	5.0
20	5.0	
50	5.4	6.0
100	5.0	6.0

a and b were previously stated in Table 5.5

Table 5.7 : Effect of Rotation of Electrode on Peak Height of Silver

Rotation of Electrode (r/min)	Peak Height (cm)	
500	4.5,[a]	2.5[b]
1000	4.5,	3.0
1500	4.5,	6.0
2000	5.0,	7.0

a and b were previously stated in Table 5.5

An unsuccessful attempt was made to determine silver in these electrolytes using DPASV. It was found that the peak position of the silver is shifted to more anodic potentials and overlap occurs between each addition, so it was not possible to obtain quantitative results.

The determination of silver in samples by DC-ASV was carried out on two samples. However, the procedure shown in Figure 5.15 was used for the determination and the results obtained are given in Table 5.8.

Table 5.8 : Silver Concentration in Samples. Analysis by DC-ASV

	Silver (μg/g)
Amalcap*	4,600
Mendipite**	N.D.

* Collected from Dental School, Bristol University

** Collected from Charterhouse (see Figure 5.16)

These figures were the mean of two determinations

Figure 5.15 : Procedure used for Determination of Silver in Samples (27)

Place 0.05 g of sample in a small beaker

↓

Add 10 cm^3 concentrated HNO_3

↓

Heat under IR lamp until the volume is reduced to 2cm^3, then add 10cm^3 DDW. Filter through Whatman 541 filter and dilute to 25cm^3 with DDW

↓

Transfer 10 cm^3 of the above solution into separating funnel and add 10 cm^3 of 0.02M TPPS in chloroform and shak for 10 mins

↓

Separate off the organic layer and add to it 10 cm^3 of 1M NH_4OH, then shake for 10 minutes

↓

Separate off the ammoniacal extract and dilute to 25 cm^3 with 1M NH_4OH

↓

Place the above solution in the voltammetric cell and determine silver by DC-ASV using the conditions listed in Table 5.3

c) Determination of Silver in Soils, Sediments, Rocks and Plants by AAS

Four soil samples (labelled C_1 - C_4) and two plant species (labelled TE and HL) were collected from Charterhouse (see Figure 5.16) on 2nd April 1984 in plastic bags. In addition to these samples, the determination of silver was carried out on other samples using FAAS and GFAAS. In FAAS, the sample was digested with nitric acid and the concentration of silver in the sample was determined using the calibration graph shown in Figure 5.17. In GFAAS, the procedure described in Figure 5.18 was applied and silver determined by AAS-775 with GTA-95 using the conditions given in Table 5.9. The results obtained from both EAAS and GFAAS are shown in Table 5.10.

Table 5.9 : Instrumental Parameters for Determination of Silver by Varian AAS-775 with GTA-95

Stage	Temperature (^oC)	Time (sec)	N_2 flow (L/min)	Read
1	75	5.0	3.0	
2	90	10	3.0	
3	I20	20	3.0	
4	400	10	3.0	
5	400	5.0	3.0	
6	2000	1.0	0.0	*
7	2000	2.0	0.0	*
8	2500	1.0	3.0	

Wavelength = 328 nm Spectral bandwidth = 0.5 nm

Lamp current = 5.0mA Background correction = ON

Sample injected = 20 μl

Chemical matrix modifier = 1 μl of 100 $\mu g/cm^3$ $NH_4H_2PO_4$

* Read Signal

FIG. 5.16 SAMPLE LOCATION SITES NEAR CHARTERHOUSE IN THE MENDIP HILLS

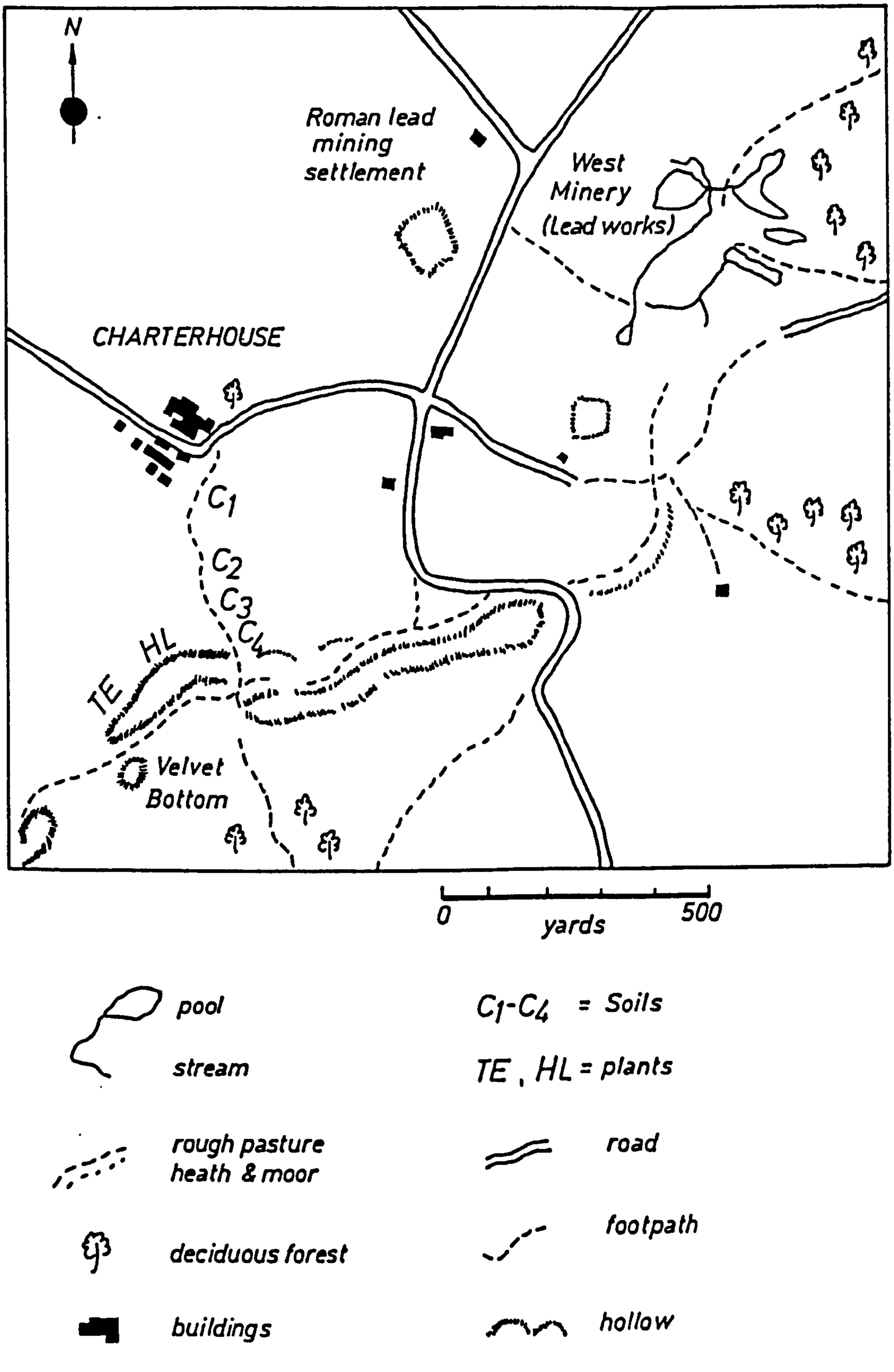

FIG. 5.17 AAS CALIBRATION GRAPH FOR SILVER

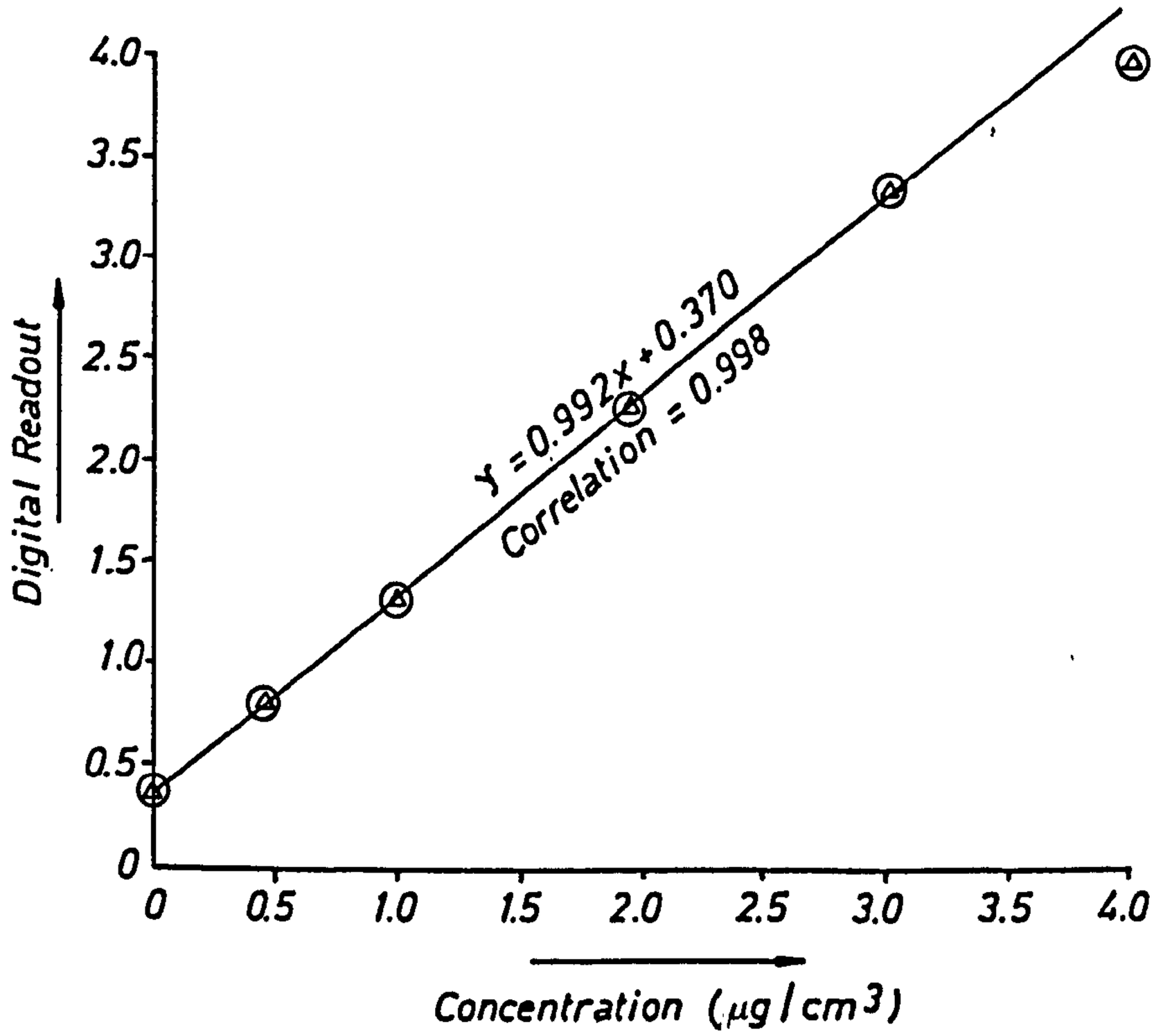

Table 5.10 : Determination of Silver (μg/g) in Samples by FAAS and GFAAS

Sample	FAAS	GFAAS
Soil (Fair Lady Well)	6	7
Soil (Waldegrave Pool)	4	3
Slag No. 1 (Fair Lady Well)	N.D.	N.D.
Slag No. 2 (Fair Lady Well)	N.D.	N.D.
Galena	119	1650
Sphalerite	30	1202
Luckett Soil	6	354
Shipham Soil	N.D.	61
C_1	9.0	23.0
C_2	N.D.	1.54
C_3	N.D.	0.998
C_4	N.D.	N.D.
HL* (root)	N.D.	N.D.
HL (shoot)	N.D.	N.D.
TE** (root)	N.D.	N.D.
TE (shoot)	N.D.	N.D.
Caradon stream sediment	N.D.	N.D.

* : Hieracium pilosella

** Teucrium scorodonia

Figure 5.18 : Procedure for Determination of Silver by GFAAS (15)

Place 1 g of sample in beaker calibrated to 100 cm^3

↓

Add H_2O (5 cm^3) + HNO_3 (5 cm^3) + H_2SO_4 (2 cm^3) and leave the sample for 10 minutes

↓

Heat for two hours at 85-95°C in waterbath

↓

Cool and dilute to 100 cm^3 with DDW

↓

Decant off 30 cm^3 of sample

↓

Determine silver by Varian AAS-775 with GTA-95

d) An Investigation of the Uptake of Silver and Lead by Plants with Time

Five plant species were collected from the Mendip Hills; the determination of silver and lead in soils and plants was carried out by FAAS and the results obtained are presented in Table 5.11.

Each species was separated from the soil and cleaned with DDW, then the species was grown in nutrient solution containing 10 $\mu g/cm^3$ of silver and lead for six days. The species was examined for silver and lead every two days by FAAS and the results obtained are listed in Table 5.12.

Table 5.11 : Concentration of Silver and Lead in Soil-Plant Systems. Analysis by FAAS

Species	Silver (μg/g)	Lead (μg/g)
1) Lolium perenne		
Soil	N.D.	8,425
Root	N.D.	6,182
Shoot	N.D.	798
2) Agrostis tnuis		
Soil	N.D.	59,400
Root	N.D.	4,439
Shoot	N.D.	511
3) Holcus lanatus		
Soil	N.D.	52,513
Root	N.D.	9,255
Shoot	N.D.	1,023
4) Rumex acetosella		
Soil	N.D.	7,293
Root	N.D.	2,290
Shoot	N.D.	186
5) Poa annua		
Soil	N.D.	29,588
Root	N.D.	6,424
Shoot	N.D.	1,421

Table 5.12 : Uptake of Silver and Lead by Plants with Time

Species	Lead (μg/g)			Silver (μg/g)		
	a	b	c	a	b	c
1) Lolium perenne						
Root	17,330	5,927	4,877	2,767	3,004	1,099
Shoot	293	294	935	168	189	48
2) Agrostis tmuis						
Root	9,519	5,653	1,568	3,558	3,411	305
Shoot	2,202	433	1,157	N.D.	363	118
3) Holcus lanatus						
Root	4,568	5,724	1,269	4,227	3,264	2,180
Shoot	1,011	490	497	494	490	157
5) Rumex acetosella						
Root	4,693	4,038	2,866	1,251	1,365	339
Shoot	N.D.	1,222	1,131	654	896	272
5) Poa annua						
Root	20,583	5,625	17,324	3,238	2,063	1,268
Shoot	4,152	720	3,706	858	519	173

a= Metal determined after two days

b= " " " four "

c= " " " six "

e) Determination of Länthanum in Soils, Sediments and Rocks by XRF

For determination of major elements in samples by XRF, glass beads were prepared by the following procedure :

i) Grind the sample and weigh 0.3750 g in a platinum crucible

ii) Add 2.0 g of Spectroflux mixture

iii) Heat the contents of the crucible at 105°C for one hour

iv) Calculate the percentage of volatile material in the sample using the following formula :

$$\% = \frac{W_3 - W_4 \times 100}{0.375} - \frac{W_3 - W_4 \times 100}{2}$$

where W_3 = weight of crucible contents before heating

W_4 = weight of crucible contents after heating

v) Melt the contents of crucible at 1000°C and remove to special disk design

vi) Label the glass beads and analyse by XRF.

Trace lanthanum in the samples was determined by XRF using pellets. Sample (10 g) was placed in a plastic tube, then binder polyvinyl alcohol (0.625 cm^3) was added, followed by 2 glass beads. The sample was homogenised by mechanical agitation using a specially designed mixer. The glass beads were removed and the sample placed between two highly polished stainless steel plattens and pressed in a hydraulic press for 10 minutes at 25 tons pressure. After labelling the edge of the pellet obtained, it was dried at 105°C for 30 minutes. The pellets were then transferred to an oven at 60°C and left for three hours, then the pellets were examined by XRF. The results obtained are given in Table 5.13.

Table 5.13 : Percentage Value of the Major Elements and Trace Lanthanum in Samples. Analysis by XRF

Sample	SiO_2	Al_2O_3	TiO_2	Fe_2O_3	MgO	CaO	Na_2O	K_2O	MnO	P_2O_5	Total	Wt. loss	Lanthanum ($\mu g/g$)
Caradon secondary rock	69.26	8.96	0.15	1.83	0.73	5.12	0.13	2.86	0.03	0.06	89.14	7.560	13
C_4*	49.04	7.39	0.51	4.83	1.16	7.28	0.29	1.46	0.15	0.24	72.35	26.36	32
Waldegrave Pool soil	53.79	6.40	0.43	7.38	1.13	4.75	0.23	1.83	0.12	0.27	76.33	5.66	27
C_3*	59.04	8.51	0.72	6.06	1.25	2.87	0.30	1.93	0.10	0.18	80.97	14.30	28
Fair Lady Well soil	38.57	4.40	0.26	7.38	0.80	10.52	0.21	1.03	0.25	0.36	63.79	22.52	19
Shipham soil	47.81	8.24	0.58	10.55	1.45	0.65	0.74	2.76	0.63	0.21	73.62	18.89	41
Luckett soil	50.31	15.50	0.68	13.19	1.70	0.07	0.80	1.80	0.10	0.11	83.98	7.24	29
Mendipite	73.17	7.74	0.44	2.25	0.73	0.06	0.38	3.42	0.06	0.99	89.25	2.57	28
Sphalerite	74.03	7.69	0.39	3.26	1.67	1.13	0.31	1.45	0.12	0.08	90.13	4.54	18

C_3 and C_4 were soils collected from Charterhouse

f) Determination of Upper Critical Level of Aluminium, Silver and Lanthanum in Lolium perenne Seedlings

The details of this experiment were described in Chapter 4 (p.248) but aluminium, silver and lanthanum were fed to plants individually instead of thallium. Phosphate was deleted from the nutrient solution when lanthanum was fed to the plants to avoid the precipitation of lanthanum phosphate. The pH of the nutrient solution was adjusted to 4 in the situation of aluminium addition to prevent the precipitation of aluminium. All the metals were fed as nitrate salts. Lanthanum was determined by Dc-plasma while aluminium and silver were determined by GFAAS and FAAS respectively. The instrumental parameters used for the determination of aluminium are shown in Table 5.14. The concentration of metals in solution and in plant tissue are listed in Tables 5.15 and 5.16. The upper critical levels of the metals are illustrated in Figures 5.19 - 5.24 and Table 5.17.

Table 5.14 : Instrumental Parameters for the Determination of Aluminium by Varian AAS-775 with GTA-95

Stage	Temperature (^{o}C)	Time (sec)	N_2 flow (L/min)	Read
1	75	5.0	3.0	
2	90	10.0	3.0	
3	120	10.0	3.0	
4	450	10.0	3.0	
5	450	5.0	3.0	
6	2700	1.0	0	*
7	2700	2.0	0	*
8	2700	1.0	3.0	

Lamp current = 7 mA
Wavelength = 309
Sample injected = 20 μl
Spectra bandwidth = 0.5 nm
Background correction = ON
* Read signal

Table 5.15 : Aluminium, Silver and Lanthanum Concentrations in Roots of Lolium perenne Seedlings

Concentration of metals in nutrient solution ($\mu g/cm^3$)			Dry weight (mg)			Concentration of metal in plant tissue (mg/kg)			Log_{10} concentration of metals in plant tissue		
Al	Ag	La	Al	Ag	La	Al	Ag	La	Al	Ag	La
0.00	0.00	0.00	36	18.5	13.5	N.D.	N.D.	N.D.	—	—	—
0.5	0.05	3.0	35.3	17.1	9.9	121	104	354	2.08	2.01	2.54
1.0	0.1	5.0	34.4	13.0	9.5	174	1,023	4,211	2.24	3.00	3.55
2.0	0.25	6.0	28.2	12.5	9.3	191	1,122	6,720	2.28	3.04	3.82
3.0	0.5	8.0	26.0	12.3	8.0	395	1,778	9,506	2.59	3.24	3.97
5.0	1.0	9.0	24.0	12.1	6.0	617	1,820	12,099	2.79	3.26	4.08
10.0	2.0	10.0	16.0	11.7	3.7	2,111	5,624	31,824	3.32	3.75	4.50

N.D. = Al < 0.069 mg/kg; Ag = < 0.0033 mg/kg; La = < 1.85 mg/kg

Table 5.16 : Aluminium, Silver and Lanthanum Concentrations in Shoots of Lolium perenne Seedlings

Concentration of in nutrient solution ($\mu g/cm^3$)			Dry weight (mg)			Concentration of metals in plant tissue (mg/kg)			Log_{10} concentration of metals in plant tissue		
Al	Ag	La	Al	Ag	La	Al	Ag	La	Al	Ag	La
0.00	0.00	0.00	148.4	52.2	67	N.D.	N.D.	N.D.	—	—	—
0.5	0.05	3.0	145	44.9	35	5.0	18	28	0.69	1.25	1.44
1.0	0.1	5.0	144	44.4	31	8.0	110	64	0.90	2.04	1.80
2.0	0.25	6.0	137	29.5	29.3	10.0	439	176	1.0	2.64	2.42
3.0	0.5	8.0	128	23.4	26.5	14.0	465	307	1.14	2.66	2.48
5.0	1.0	9.0	116	19.4	22.1	19.0	565	497	1.27	2.75	2.69
10.0	2.0	10.0	74	15.9	13.5	15.0	646	1,981	1.39	2.81	3.07

N.D. = Al < 0.016 mg/g; Ag < 0.00047 mg/g; La < 0.373 mg/kg

Table 5.17 : Critical Concentrations of Aluminium, Silver and Lanthanum in Roots and Shoots of *Lolium perenne* Seedlings

Critical Concentration & Statistical Information	Root			Shoot		
	Al	Ag	La	Al	Ag	La
Y_o (mg)	36	18.5	10.2	148.4	51.0	33.0
Tc (mg/kg)	141	63.0	3,458	8.0	51.0	126.0
Tl (mg/kg)	1,995	3,981	50,119	70.7	1,000	1,995
Correlation coefficient of regression lines	-0.965	-0.955	-0.925	-0.866	-0.884	-0.996
Regression equations	y=65.9-15.1x	y=53.5-6.86x	y=40-8.1x	y=221-91x	y=72.5-18.2x	y=85-23x
The st. dev. of y about the regression line with (n-2) degrees of freedom	2.089	53.20	0.696	14.96	6.523	0.713
r-squared, per cent	93.2	75	94.6	75.1	78.3	99.3
r-squared, per cent, adjusted for d.f.	91.5	70	91.0	68.8	72.9	98.9
SS* due to regression	238	78	16.95	2694	614	141
ms = SS/df	238	78	16.95	2694	614	141
SS due to residual	17.4	11,322	0.970	895	170	1.01
SS due to total	255	11,400	17.9	3590	784	142

FIG. 5.19 YIELD CURVE OF ROOT YIELD PLOTTED AGAINST LOG TISSUE CONCENTRATION IN SUPPLEMENTARY EXPERIMENT TO DETERMINE Al UPPER CRITICAL LEVEL

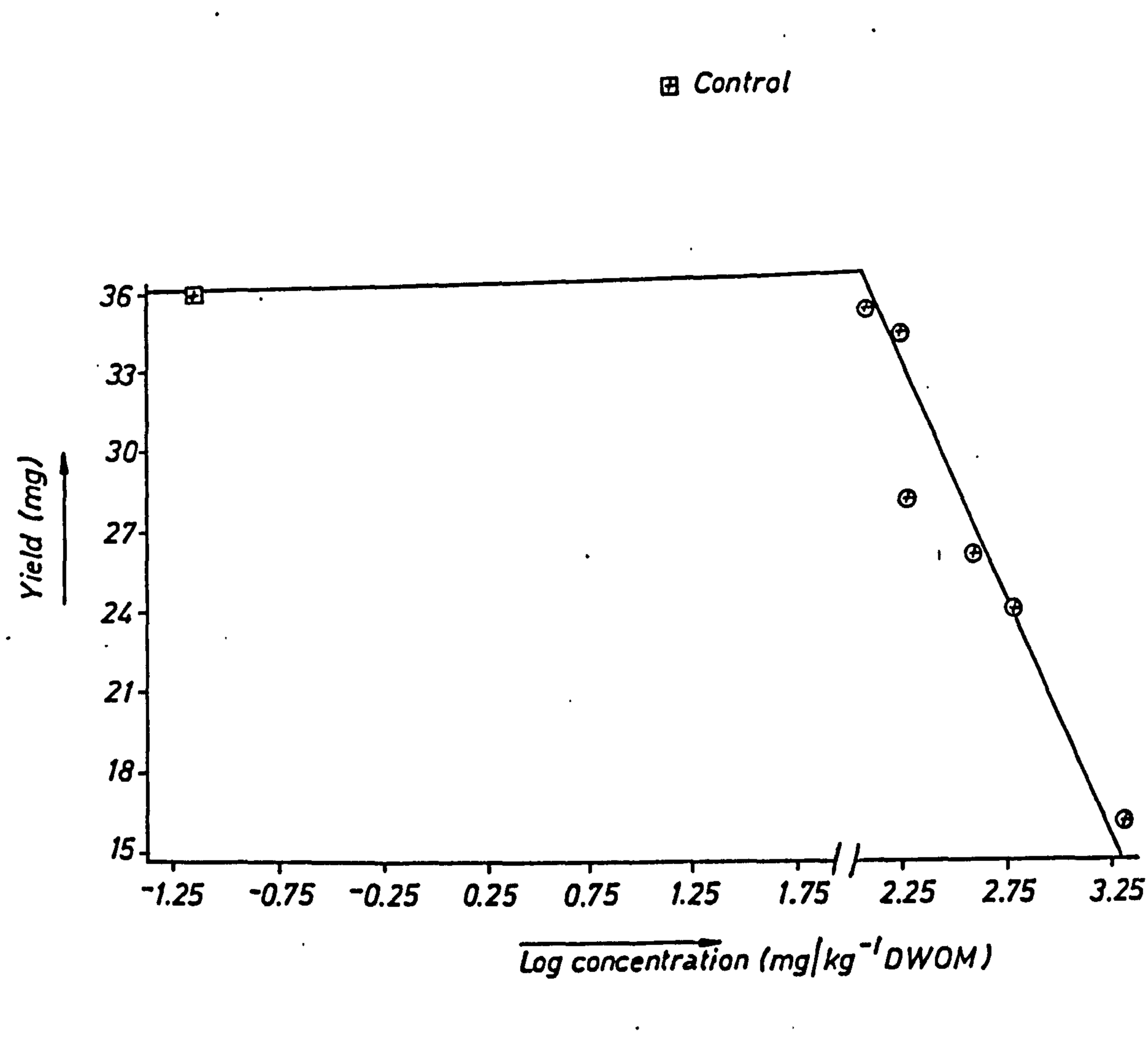

FIG. 5.20 YIELD CURVE OF SHOOT YIELD PLOTTED AGAINST LOG TISSUE CONCENTRATION IN SUPPLEMENTARY EXPERIMENT TO Al UPPER CRITICAL LEVEL

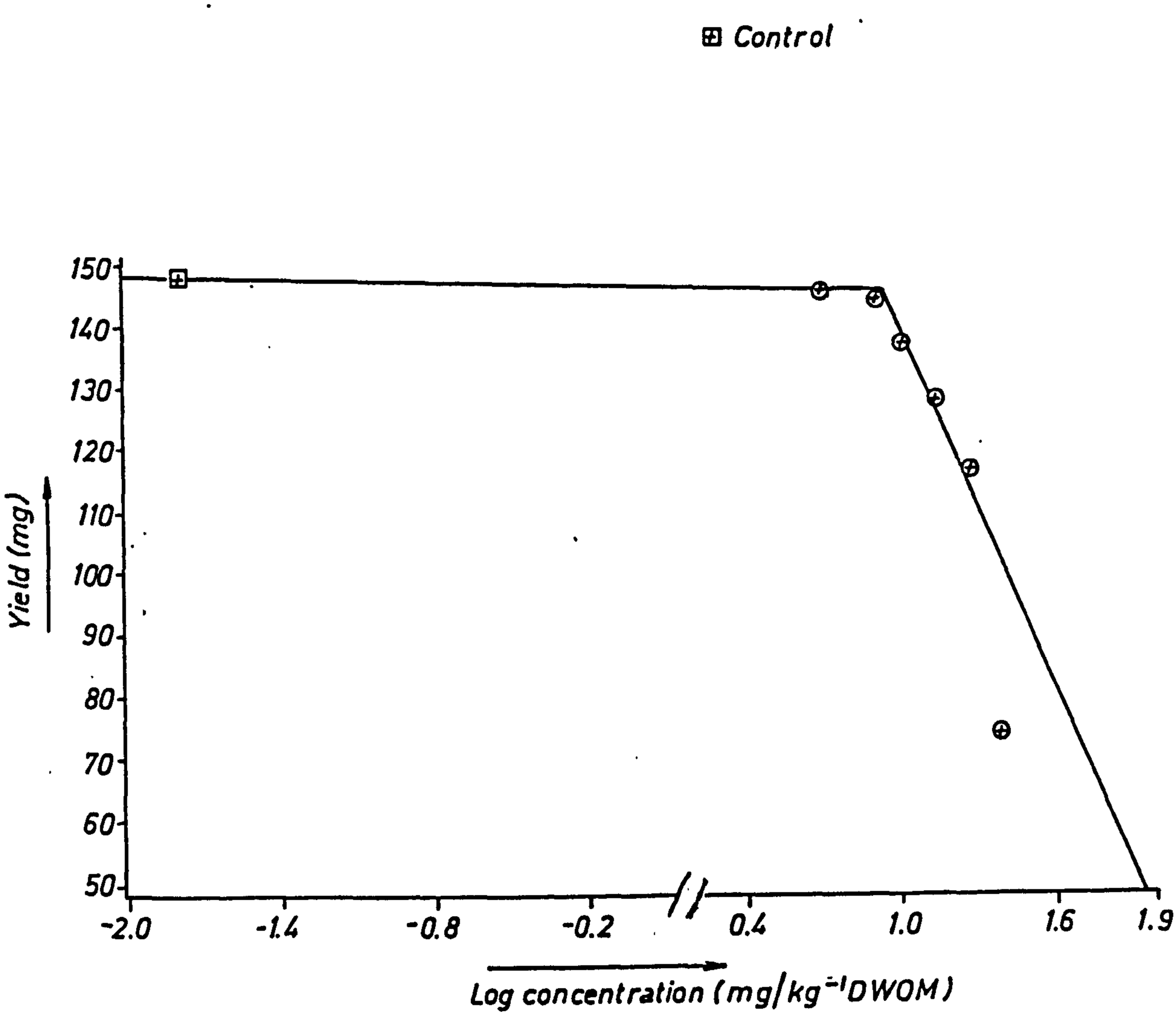

FIG. 5.21 YIELD CURVE OF ROOT YIELD PLOTTED AGAINST LOG TISSUE CONCENTRATION IN SUPPLEMENTARY EXPERIMENT TO DETERMINE Ag UPPER CRITICAL LEVEL

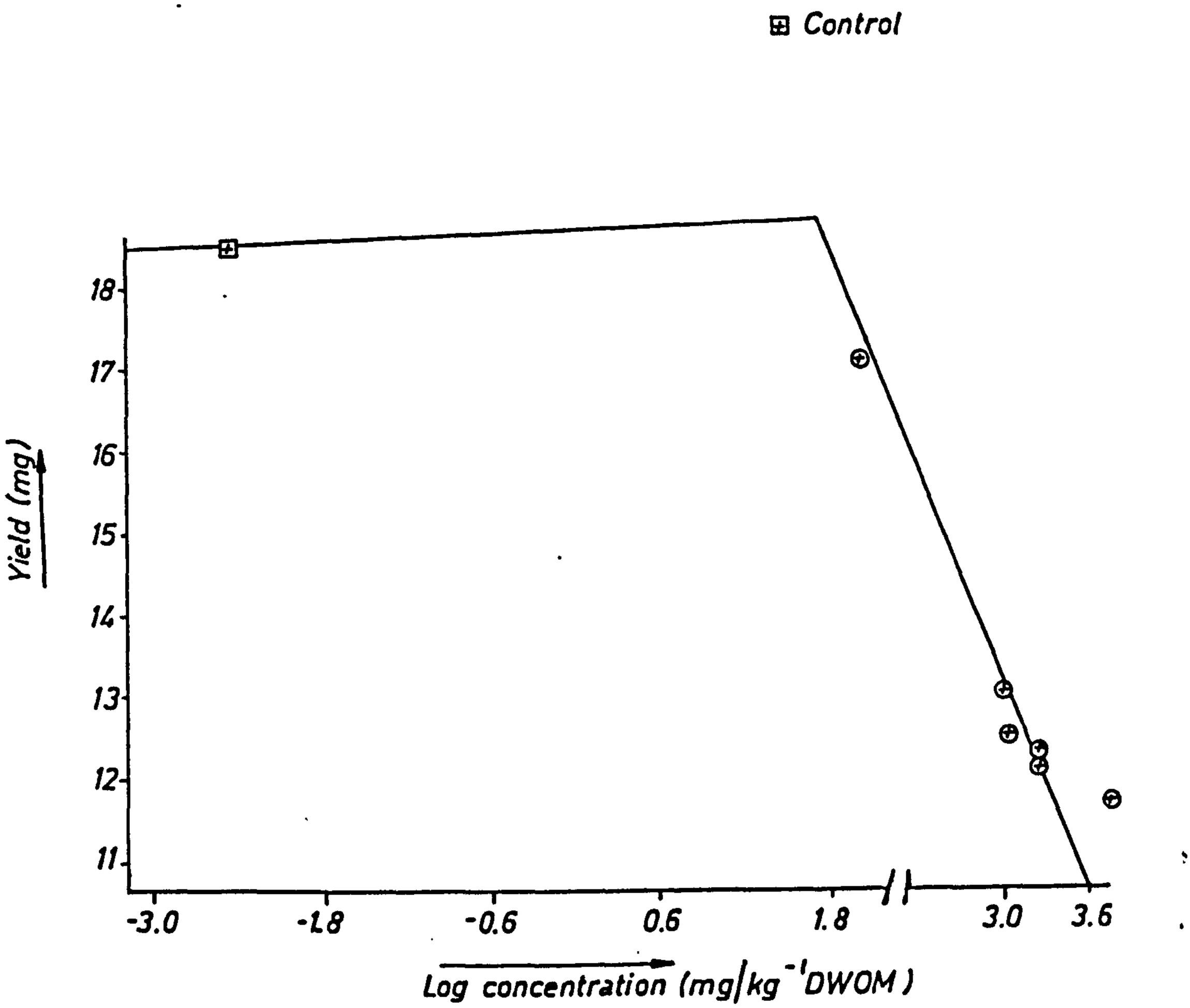

FIG. 5.22 YIELD CURVE OF SHOOT YIELD PLOTTED AGAINST LOG TISSUE CONCENTRATION IN SUPPLEMENTARY EXPERIMENT TO DETERMINE Ag UPPER CRITICAL LEVEL

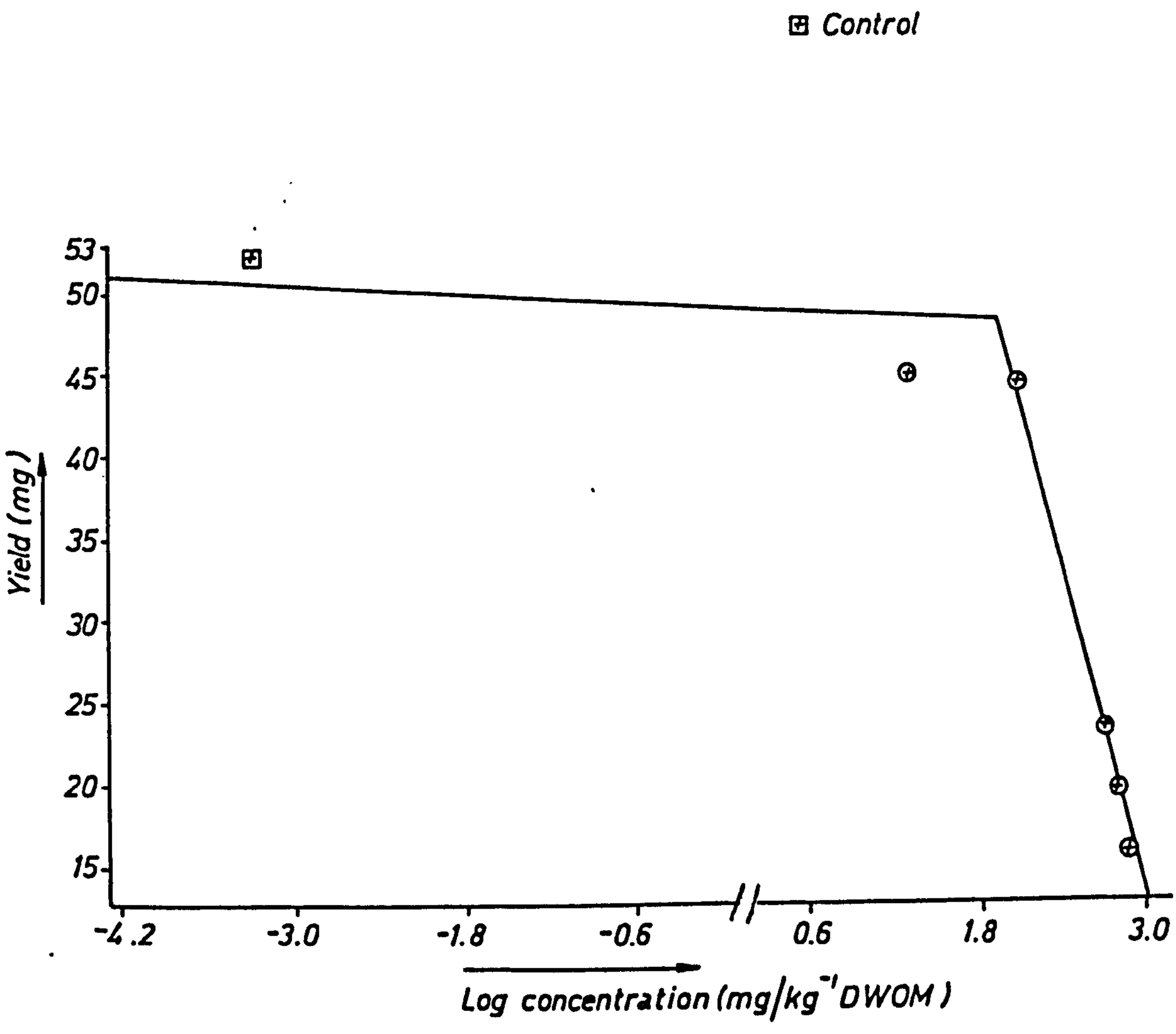

FIG. 5.23 YIELD CURVE OF ROOT YIELD PLOTTED AGAINST LOG TISSUE CONCENTRATION IN SUPPLEMENTARY EXPERIMENT TO DETERMINE La UPPER CRITICAL LEVEL

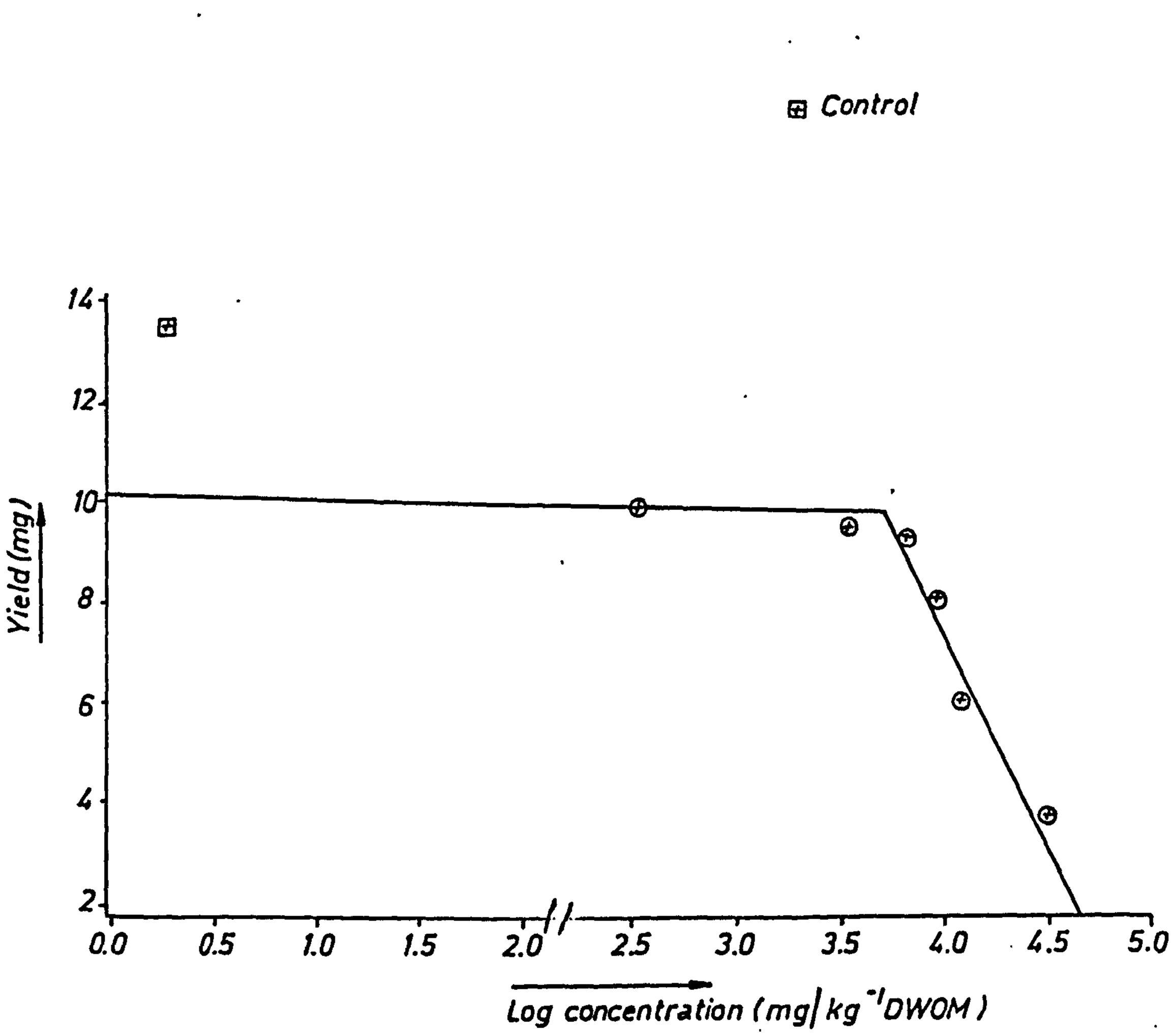

FIG. 5.24 YIELD CURVE OF SHOOT YIELD PLOTTED AGAINST LOG TISSUE CONCENTRATION IN SUPPLEMENTARY EXPERIMENT TO DETERMINE La UPPER CRITICAL LEVEL

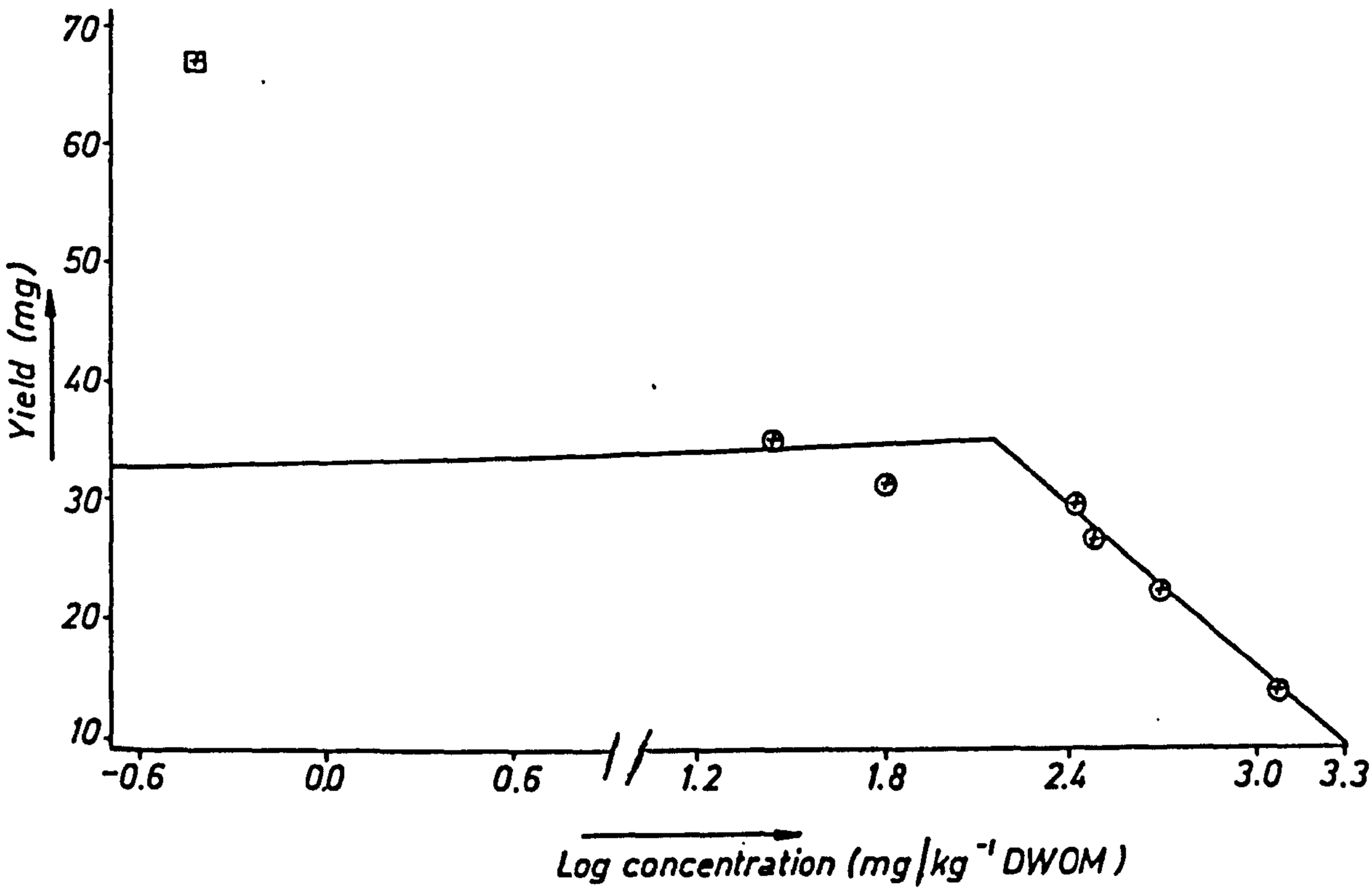

g) Association of Aluminium and Lanthanum in Plants

Aluminium (2 $\mu g/cm^3$) and lanthanum (2 $\mu g/cm^3$) in nutrient solution were fed to Lolium perenne and Holcus lanatus individually. The plants were left to grow for 21 days, then separated into roots and shoots. The Farago et alia (28) extraction procedure was used to study the association of the metals within the plant components. Full details of the procedure are shown in Figure 5.25. The procedure was also applied to a study of the association of aluminium in the SRM orchard leaves (SRM 1571). Aluminium was determined by GFAAS while lanthanum was found by ICP/MS (see Figure 5.26). The results obtained are presented in Tables 5.18 - 5.22.

Figure 5.25 : Scheme for Extraction Procedure

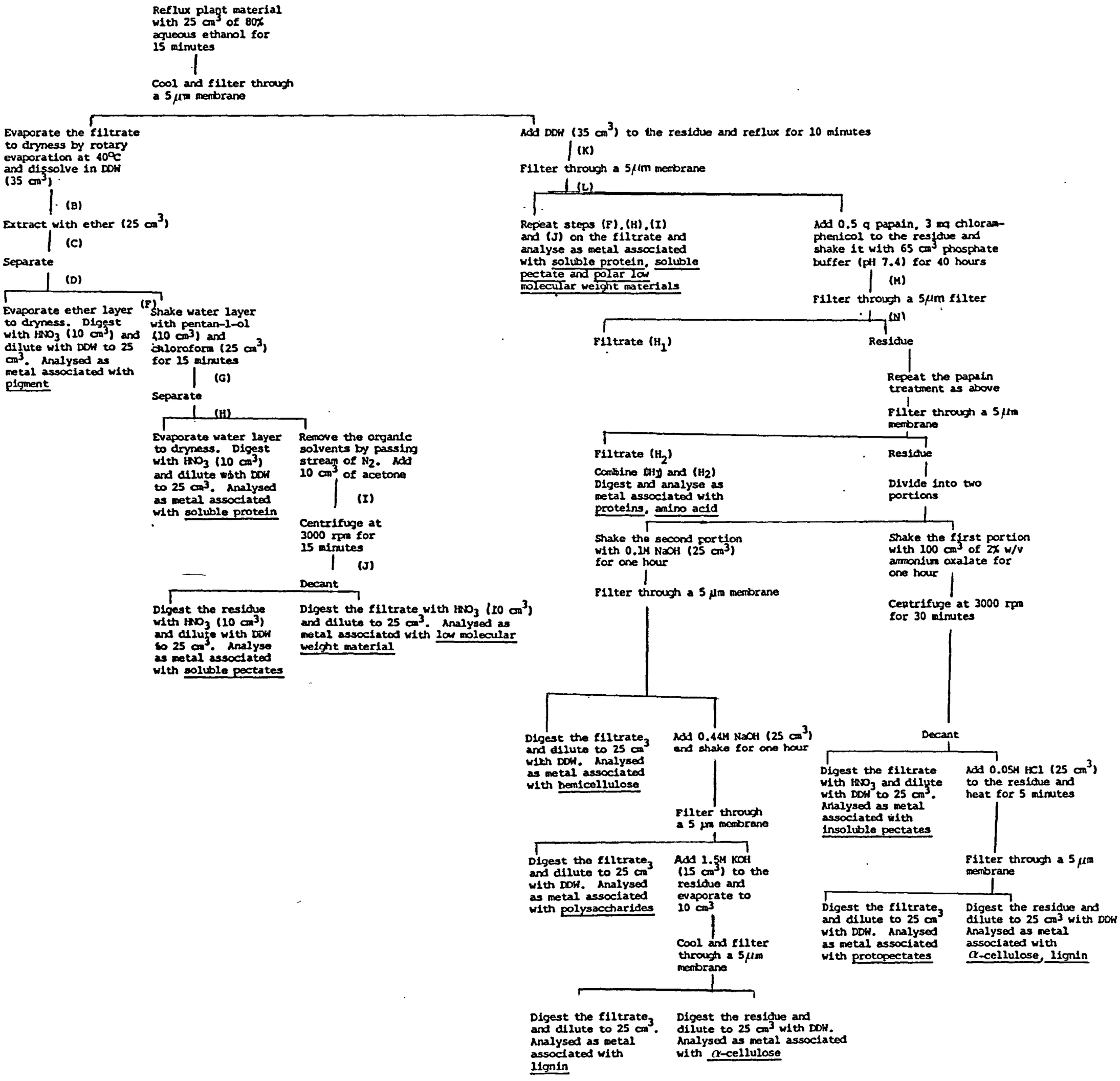

FIG. 5.26 SPECTRA SHOWING LANTHANUM IN SHOOTS AND ROOTS OF LOLIUM PERENNE SEEDLING

a) Shoot

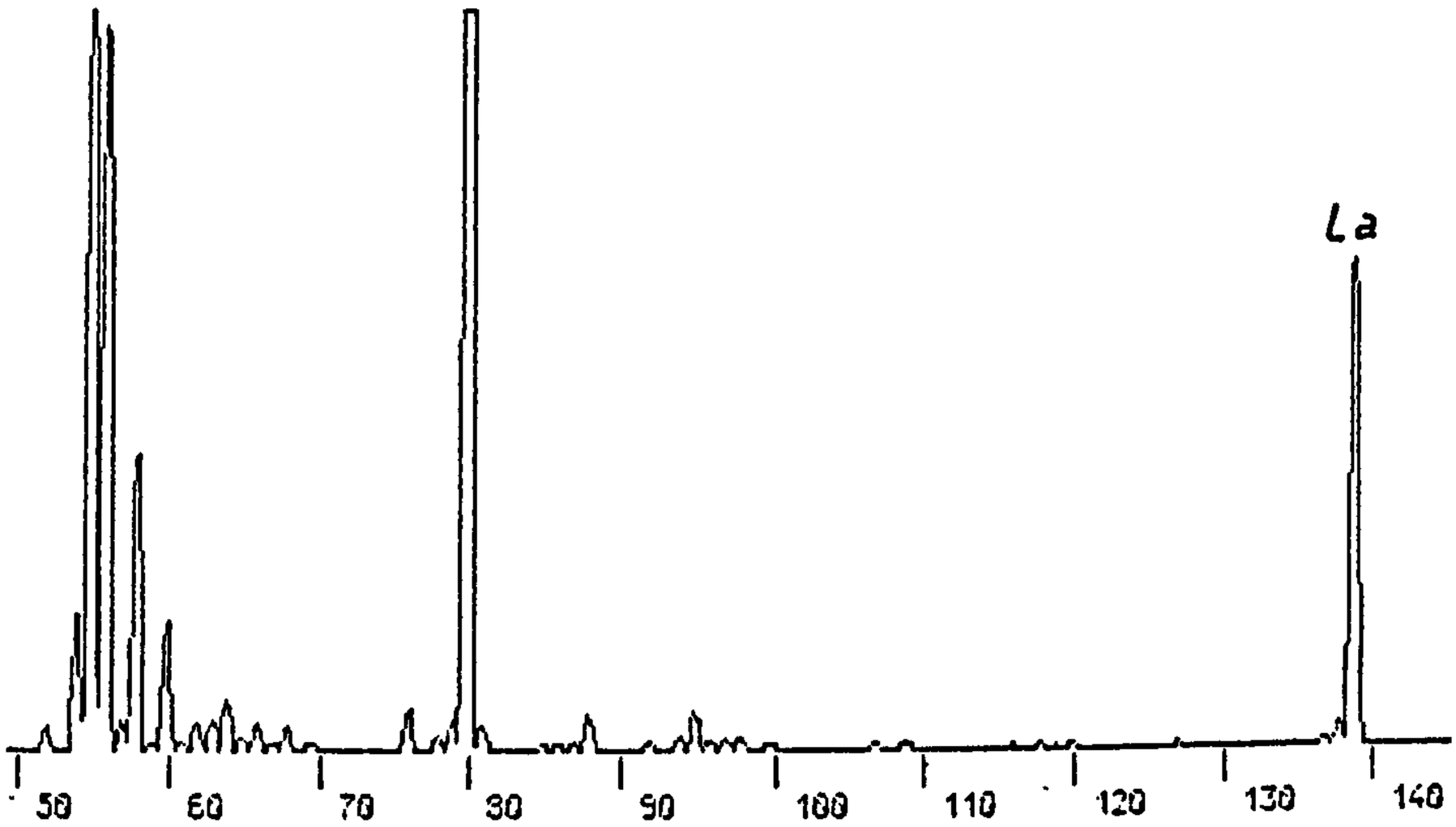

b) Root

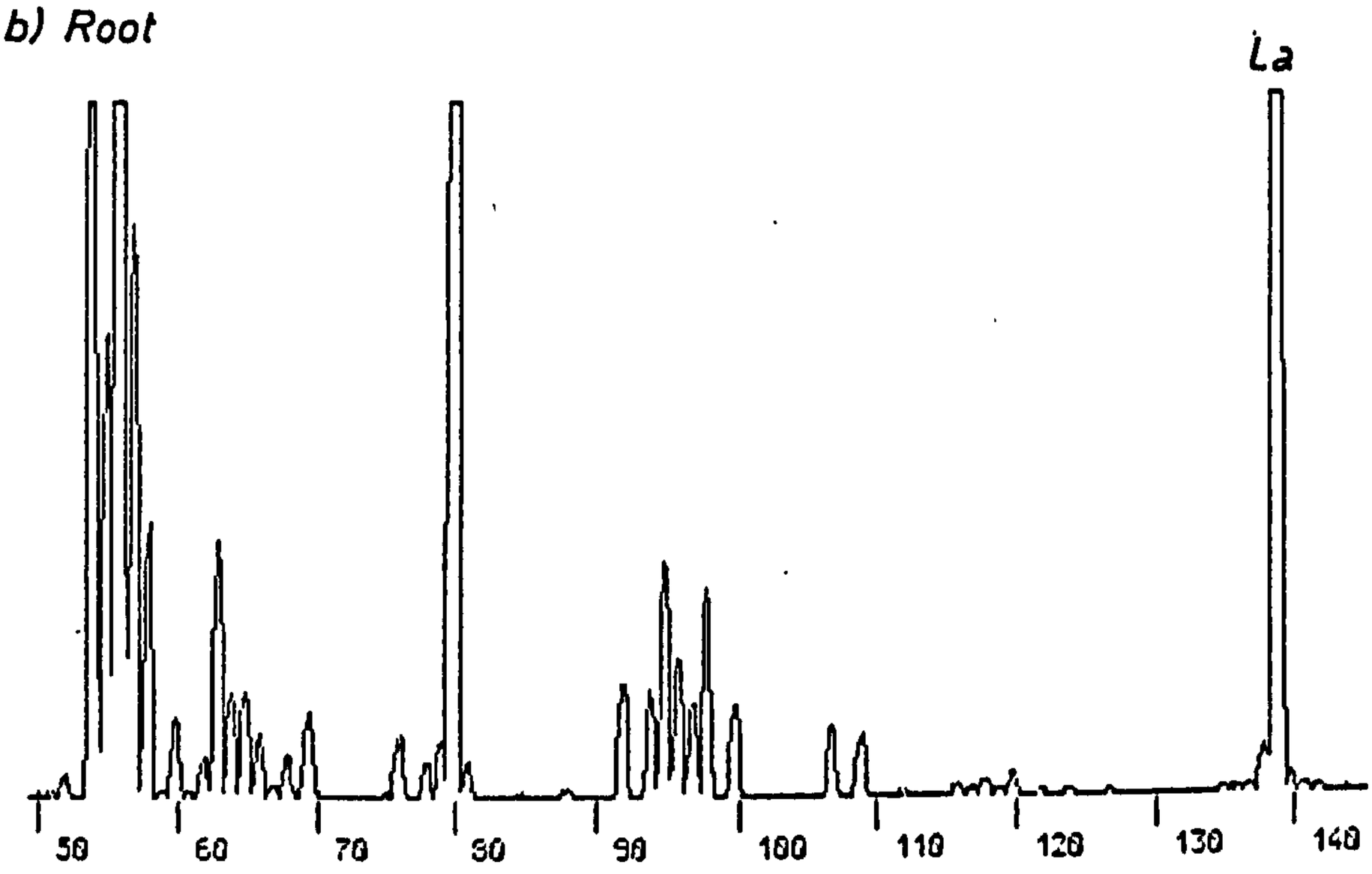

Table 5.18 : Association of Aluminium in Orchard Leaves

(SRM 1571)

Fraction		Concentration (μg/g)	Percentage of total metal
Pigments	(PI)	1.1	0.82
Sol. proteins	(SO)	25	18.69
*Sol. pectates	(SP)	N.D.	-
Low MW materials	(LO)	54.43	40.7
Sol. protein	(SI)	3.9	2.9
Sol. pectates	(SO)	N.D.	-
Polar low MW materials	(PO)	16.4	12.26
Proteins/ amino acids	(HA)	9.9	7.40
Insol. pectates	(IS)	N.D.	-
Protopectates	(PR)	4.5	3.36
α-cellulose, lignin	(CE)	6.0	4.48
Hemicellulose	(HE)	4.9	3.66
Polysaccharides	(PL)	2.8	2.09
Lignin	(LI)	2.9	2.10
α-cellulose	(CI)	1.0	0.74
Total		133.7	-
Total acid digest		98.0	-

* precipitate not formed

Table 5.19 : Association of Aluminium and Lanthanum in Roots of Lolium perenne Seedlings

Fraction		Aluminium		Lanthanum	
		Concentration µg/g	Percentage of total metal	Concentration µg/g	Percentage of total metal
Pigments	(PI)	49.0	4.2	N.D.	-
Sol. proteins	(SO)	N.D.	-	N.D.	-
*Sol. pectates	(SP)	N.D.	-	N.D.	-
Low MW materials	(LO)	7.0	0.60	14	0.53
Sol. protein	(SI)	145	12.5	4	0.15
Sol. pectates	(SO)	N.D.	-	N.D.	-
Polar low MW materials	(PO)	N.D.	-	N.D.	-
Proteins/ amino acids	(HA)	N.D.	-	N.D.	-
Insol. pectates	(IS)	9.0	0.77	227.	8.65
Protopectates	(PR)	13.0	1.12	N.D.	-
α-cellulose, lignin	(CE)	15	1.29	653	24.89
Hemicellulose	(HE)	417	36.1	12	0.45
Polysaccharides	(PL)	324	28.0	49	1.86
Lignin	(LI)	59	5.11	1.0	0.038
α-cellulose	(CI)	115	9.96	1,665	63.47
Total		1,154	-	2,623	-
Total acid digest		1,231	-	2,190	-

* precipitate not formed

Table 5.20 : Association of Aluminium and Lanthanum in Shoots of Lolium perenne Seedlings

Fraction		Aluminium		Lanthanum	
		Concentration µg/g	Percentage of total metal	Concentration µg/g	Percentage of total metal
Pigments	(PI)	9.0	4.39	2	1.52
Sol. proteins	(SO)	6.0	2.92	1.70	1.29
*Sol. pectates	(SP)	N.D.	-	N.D.	-
Low MW materials	(LO)	5.0	2.43	3.60	2.74
Sol. protein	(SI)	27.0	13.17	N.D.	-
Sol. pectates	(SO)	11.0	5.36	N.D.	-
Polar low MW materials	(PO)	N.D.	-	14	10.68
Proteins/ amino acids	(HA)	N.D.	-	N.D.	-
Insol. pectates	(IS)	N.D.	-	23	17.50
Protopectates	(PR)	8.0	3.90	N.D.	-
α-cellulose, lignin	(CE)	14	6.82	17	12.97
Hemicellulose	(HE)	31.0	15.12	0.72	0.54
Polysaccharides	(PL)	22.0	10.73	0.84	0.64
Lignin	(LI)	9.0	4.39	N.D.	-
α-cellulose	(CI)	63	30.73	68	51.90
Total		205	-	131	-
Total acid digest		288	-	127	-

* precipitate not formed

Table 5.21 : Association of Aluminium and Lanthanum in Roots of Holcus lanatus Seedlings

Fraction		Aluminium		Lanthanum	
		Concentration µg/g	Percentage of total metal	Concentration µg/g	Percentage of total metal
Pigments	(PI)	63	3.37	23	0.19
Sol. proteins	(SO)	33	1.77	3.92	0.03
*Sol. pectates	(SP)	N.D.	-	N.D.	-
Low MW materials	(LO)	N.D.	-	36	0.30
Sol. protein	(SI)	164	8.79	28.85	0.24
Sol. pectates	(SO)	N.D.	-	5,804	48.40
Polar low MW materials	(PO)	N.D.	-	N.D.	-
Proteins/ amino acids	(HA)	N.D.	-	N.D.	-
Insol. pectates	(IS)	N.D.	-	N.D.	-
Protopectates	(PR)	109	5.84	N.D.	-
α-cellulose, lignin	(CE)	55	2.95	844	7.04
Hemicellulose	(HE)	313	16.79	151	1.26
Polysaccharides	(PL)	853	45.76	N.D.	-
Lignin	(LI)	152	8.10	N.D.	-
α-cellulose	(CI)	59	3.10	5,092	42.40
Total		1,864	-	11,982	-
Total acid digest		2,340	-	10,866	-

* precipitate not formed

Table 5.22 : Association of Aluminium and Lanthanum in Shoots of Holcus lanatus Seedlings

Fraction		Aluminium		Lanthanum	
		Concentration µg/g	Percentage of total metal	Concentration µg/g	Percentage of total metal
Pigments	(PI)	3.0	1.06	10	2.29
Sol. proteins	(SO)	7.0	2.47	0.73	0.160
*Sol. pectates	(SP)	N.D.	-	N.D.	-
Low MW materials	(LO)	11.0	3.88	N.D.	-
Sol. protein	(SI)	23.0	8.12	1.36	0.31
Sol. pectates	(SO)	N.D.	-	68.0	15.50
Polar low MW materials	(PO)	N.D.	-	N.D.	-
Proteins/ amino acids	(HA)	N.D.	-	N.D.	-
Insol. pectates	(IS)	22.0	7.77	N.D.	-
Protopectates	(PR)	54.0	19.08	3.54	0.81
α-cellulose, lignin	(CE)	42.0	14.84	341	78.21
Hemicellulose	(HE)	43.0	15.19	2.47	0.56
Polysaccharides	(PL)	30.0	10.60	2.66	0.61
Lignin	(LI)	19.0	6.71	0.75	0.170
α-cellulose	(CI)	29.0	10.24	N.D.	-
Total		283	-	436	-
Total acid digest		330	-	355	-

* precipitate not formed

h) Statistical Design for Determination of Lanthanum by Varian AAS-775 with GTA-95

In separate experiments, aliquots (20 μl) in volume of three different concentrations of lanthanum (100, 200, 300 $\mu g/cm^3$) were placed in turn in a furnace fitted to the GTA-95 which was operated at the operating parameters given in Table 5.23. No response was observed for lanthanum, perhaps due to the formation of the extremely stable carbide. The furnace was then lined with tantalum foil as follows (25) :

1) drill a 2 mm hole in a 12 x 14 mm piece of tantalum foil as shown below :-

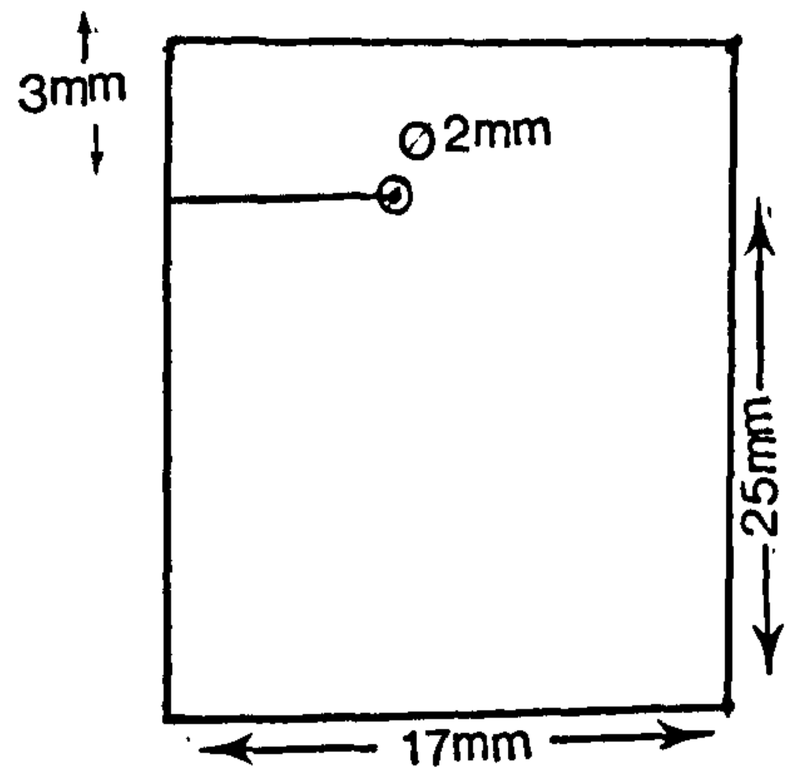

2) wrap the foil on a 4 mm glass rod and insert into the centre of a pyrolytically coated graphite tube so that the hole in both tubes coincides;

3) insert a glass rod (3 mm) into the tube and roll the tantalum foil over the "hump" at the centre of the tube. The tantalum-lined graphite tube was used with GTA-95 and prior to the addition of lanthanum solutions, it was fired twice. Aliquots of 20μl of lanthanum (100 $\mu g/cm^3$) were placed into the tube which was operated at the level of parameters in Table 5.23.

Table 5.23 : Instrumental Parameters for Determination of Lanthanum by Varian AAS-775 with GTA-95

Stage	Temperature (^{o}C)	Time (sec)	N_2 flow (L/min)	Read
1	75	15	3	
2	90	60	3	
3	120	60	3	
4	850	10	3	
5	1800	10	3	
6	1800	10	3	
7	2600	1.3	0	*
8	2600	2.0	0	*
9	2600	1.0	3	

ABS Expansion = 5

Volume of Sample = 20 μl

BC correction = off

Wavelength = 550 nm

Lamp current = 10 mA

* = Read signal

A good response was obtained for lanthanum, and therefore a statistically designed experiment was carried out to investigate the influence of operating parameters of the GTA-95 on the lanthanum signal. The following factors were chosen for the investigation :-

A - the ashing temperature at two levels, A_1 = 1500°C and A_2 = 1800°C

B - the ashing time at B_1 = 5 sec and B_2 = 10 sec

C - the nitrogen flow rate at C_1 = 3 L/min, C_2 = 2 L/min and C_3 = 1 L/min.

The experiment was carried out in triplicate, therefore 3(2 x 2 x 2) = 36 experimental results were obtained, and are shown in Table 5.24. In order to study the interaction between the factors, the results were fitted to a general linear mode (GLM) by using Statistical Analysis Systems (SAS); the information obtained is listed in Table 5.25.

Table 5.24 : Experimental Design and Results for Determination of Lanthanum by Varian AAS-775 with GTA-95

Experiment	Factors			Peak Area (Arbitrary Units)		
1	A_1	B_1	C_1	7.40	7.07	7.80
2	A_1	B_2	C_1	6.05	6.81	5.29
3	A_2	B_1	C_1	5.80	6.09	5.64
4	A_2	B_2	C_1	5.72	5.96	5.49
5	A_1	B_1	C_2	4.14	5.07	2.13
6	A_1	B_2	C_2	5.73	3.24	8.0
7	A_2	B_1	C_2	6.82	6.94	6.70
8	A_2	B_2	C_2	6.05	6.19	5.90
9	A_1	B_1	C_3	5.56	2.90	6.14
10	A_1	B_2	C_3	3.77	2.00	4.60
11	A_2	B_1	C_3	6.44	2.88	5.70
12	A_2	B_2	C_3	5.88	6.37	5.0

+ Each value is the mean of three readings

Table 5.25 : General Linear Model Procedure (GLM)

(a) Model

$$Y = b_o + b_A x + b_B x_B + b_C x_C + b_D x_A x_B + b_E x_A x_C + b_F x_B x_C + b_G x_A x_B x_C$$

(b) Class Level Information

Class	Levels	Values
A	2	A_1 A_2
B	2	B_1 B_2
C	3	C_1 C_2 C_3

Number of observations in data set = 36

(c) Dependent Variables : Y

Source	DF	SS	F-value	PR
Model	11	42.47	2.66	0.021
Error	24	34.80	-	-
Corrected total	35	77.28	-	-
A	1	4.18	2.88	0.102
B	11	0.224	0015	0.697
C	2	12.82	4.42	0.023
A*B	1	0.1860	0.13	0.723
A*C	2	12.348	4.26	0.026
B*C	2	2.665	0.92	0.412
A*B*C	2	10.047	3.46	0.047

5.3 DISCUSSION

a) Mass Spectra of Metal Complexes

Figures 5.1 - 5.6, 5.10 and 5.11 illustrate the molecular weight of the metal complexes and the fragmentation pattern as follows :-

1) $[Al(ACAC)_3]^+$ —(- ACAC)→ $[Al(ACAC)_2]^+$

m/e 324 → m/e 225

m/e 324 —(-2 ACAC)→ $[Al(ACAC)]^+$

m/e 126

m/e 126 —(- $Al(C_3H_4O)$)→ CH_3CO^+

m/e 43

2) $[La(ACAC)_3]^+$ —(- ACAC)→ $[La(ACAC)_2]^+$

m/e 436 → m/e 337

m/e 436 —(-$[La(ACAC)_2]^+$)→ $C_5H_7O_2^+$

m/e 99

m/e 99 —(-C_3H_4O)→ CH_3CO^+

m/e 43

3) $[C_5H_5O_2F_3]^+ \xrightarrow{-CH_3} [C_4H_2O_2F_3]^+$

m/e 154 → m/e 139

m/e 154 $\xrightarrow{-C_3H_2OF_3}$ CH_3CO^+

m/e 43 $\xrightarrow{-CH_3}$ CO^+

m/e 27

m/e 139 $\xrightarrow{-CF_3}$ $C_3H_2O_2^+$

m/e 70

4) $[C_5H_2O_2F_6]^+ \xrightarrow{-CF_3} [C_4H_2O_2F_3]^+$

m/e 209 → m/e 139

m/e 209 $\xrightarrow{-C_3H_2OF_3}$ CH_3CO^+

m/e 43

m/e 139 $\xrightarrow{-CF_3}$ $C_3H_2O_2^+$

m/e 70

5) $[Al(C_5H_4O_2F_3)_3]^+ \xleftarrow{-C_5H_4O_2F_3} [Al(C_5H_4O_2F_3)_2]^+$

m/e 486 ← m/e 333

m/e 333 $\xrightarrow{-C_4H_2}$ $[Al(C_6H_6O_4F_3)]$

m/e 283

$[Al(C_6H_6O_4F_3)] \xrightarrow{-[Al(C_4H_3O_3F_3)]} CH_3CO^+$

m/e 283 → m/e 43

$CH_3CO^+ \xrightarrow{-CH_3} CO^+$

m/e 43 → m/e 27

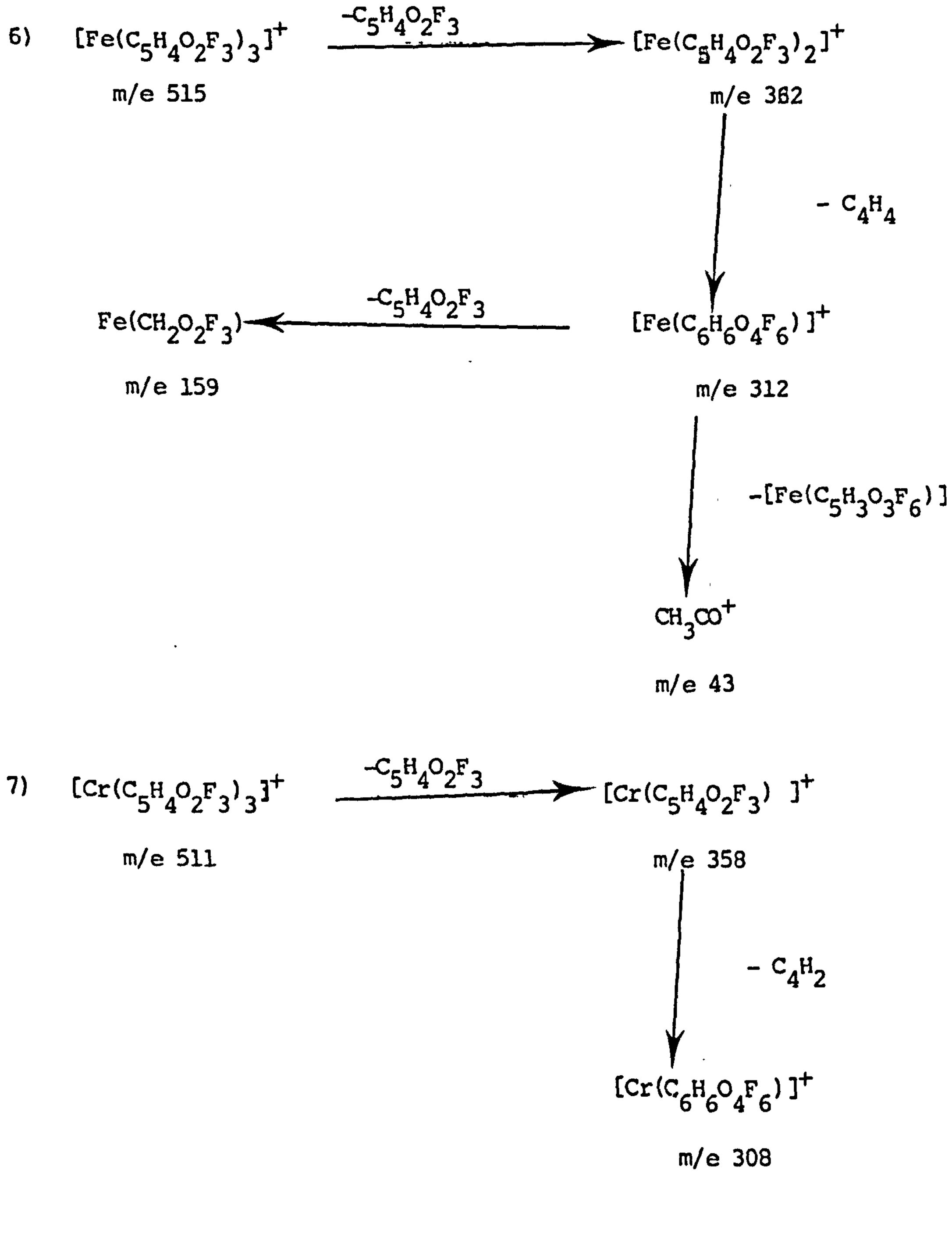
6)
$[Fe(C_5H_4O_2F_3)_3]^+$
m/e 515
$-C_5H_4O_2F_3$
$[Fe(C_5H_4O_2F_3)_2]^+$
m/e 382
$- C_4H_4$
$[Fe(C_6H_6O_4F_6)]^+$
m/e 312
$-C_5H_4O_2F_3$
$Fe(CH_2O_2F_3)$
m/e 159
$-[Fe(C_5H_3O_3F_6)]$
CH_3CO^+
m/e 43
7)
$[Cr(C_5H_4O_2F_3)_3]^+$
m/e 511
$-C_5H_4O_2F_3$
$[Cr(C_5H_4O_2F_3)]^+$
m/e 358
$- C_4H_2$
$[Cr(C_6H_6O_4F_6)]^+$
m/e 308

8) $[La(C_5H_4O_2F_3)_3]^+ \xrightarrow{-C_5H_4O_2F_3} [La(C_5H_4O_2F_3)_2]^+$

m/e 598

m/e 445

$\downarrow -C_4H_4$

$[La(C_6H_6O_4F_6)]^+$

m/e 395

$\downarrow -La(CH_2O_2F_3)$

$C_5H_4O_2F_3 \xrightarrow{-CF_3} C_4H_4O_2 \xrightarrow{-CH_3} C_3HO_2$

m/e 153 m/e 85 m/e 70

b) Determination of Metals by GLC

The ECD did not respond to aluminium and lanthanum acetylacetonates, even when 30 ng of each metal was injected into the GLC, probably because these compounds did not contain an electron capturing functional group and so no response was expected.

Figure 5.7 shows the chromatogram of the prepared $Al(TFA)_3$ which dissolved in toluene while Figure 5.8 illustrates the chromatogram of $Al(TFA)_3$ prepared by solvent extraction. In fact, the low response obtained for the complex prepared in the second method may arise from the experimental conditions not producing a 100% yield of the complex. Figure 5.9 demonstrates the difference in response of ECD for $Al(TFA)_3$ prepared by the two methods. Aluminium in water samples was not detected; this indicates that the aluminium is precipitated from the samples almost certainly due to the alkaline pH of the solution.

One of the problems encountered with the determination of chromium by GLC was the lack of a symmetrical shape for the chromium trifluoro-acetylacetonate peak. The conditions were adjusted to try to obtain a symmetrical peak shape by increasing the column temperature to 160°C. At this temperature, chromium can be separated from aluminium (see Figure 5.12), and gives a greater response. The unsymmetrical peak shape of the chromium at the lower column temperature is probably due to partial resolution of the two possible isomers formed by this tris-bidentate complex.

Iron and lanthanum trifluoroacetylacetonates did not give any response, even by ECD, perhaps due to the complexes not being thermally stable at the column temperature, or maybe the selected experimental conditions were not suitable for the determination of these complexes by GLC.

c) Determination of Silver by DC-ASV and AAS

Figures 5.13 and 5.14 illustrate the peak current of silver in 0.1 M KNO_3 + 0.002 EDTA and 0.2 M NH_4OH + 0.2 M NH_4NO_3 respectively. The formation of $[Ag(NH_3)_2]^+$ in the second electrolyte may affect the deposition of silver on the electrode and hence account for the lower peak current than in the case of the first electrolyte. Figure 5.27 demonstrates the difference in peak current for silver in both electrolytes.

The results in Table 5.4 are shown diagrammatically in Figure 5.28 which indicates that the peak current of silver does not increase linearly with deposition time (the same observation was made with thallium). This observation was discussed earlier with respect to thallium (see Chapter 4). Figures 5.29 - 5.31 depict the results obtained in Tables 5.5 - 5.7, which show the effect of modulation

FIG. 5.27 DC-ASV CALIBRATION GRAPHS FOR SILVER
(A) in 0.1M KNO_3 + 0.002M EDTA ELECTROLYTE
(B) in 0.2M NH_4OH + 0.2M NH_4NO_3 ELECTROLYTE

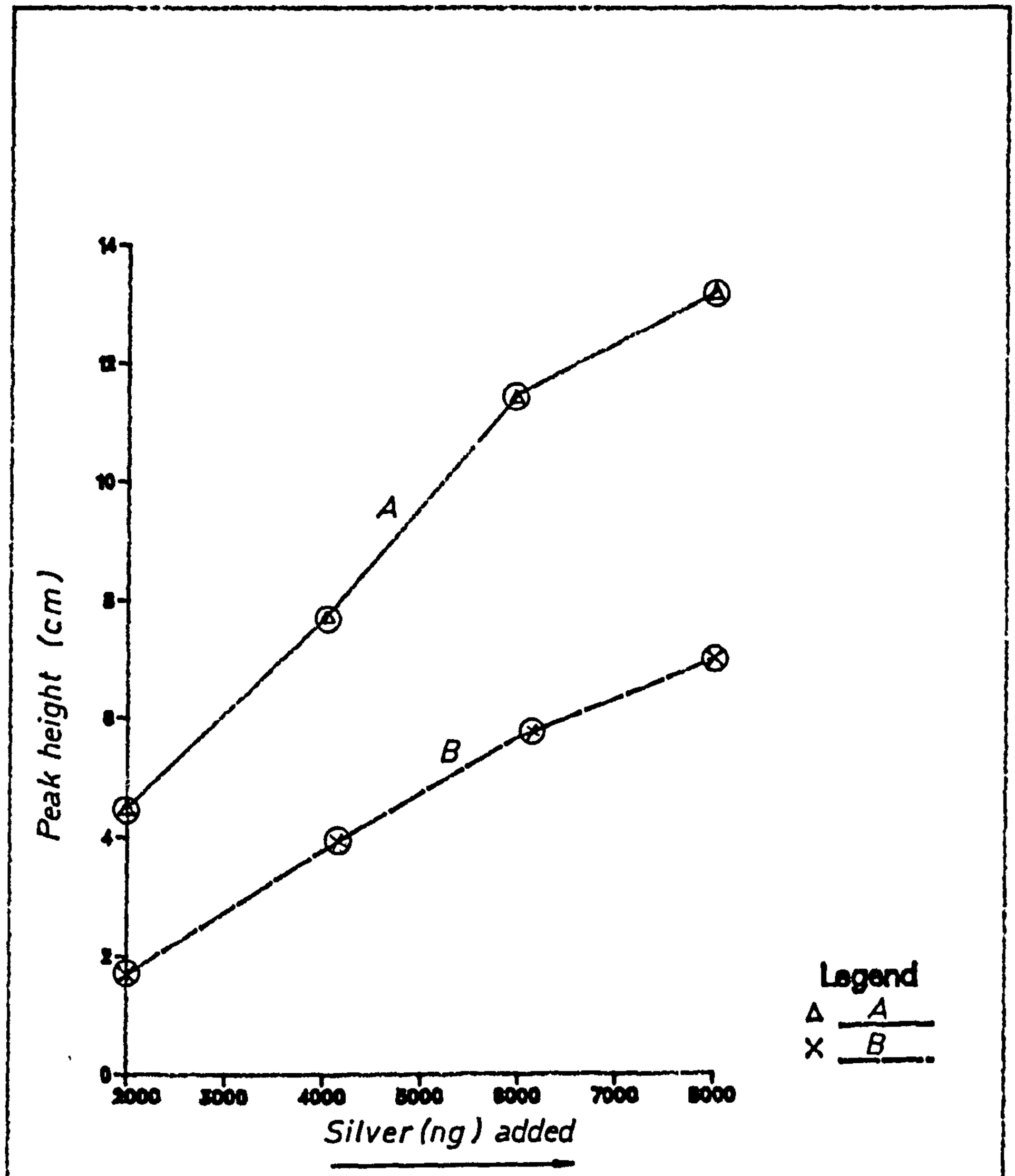

FIG. 5.28 EFFECT OF DEPOSITION TIME ON PEAK HEIGHT OF SILVER IN 0.1M KNO_3 + 0.002M EDTA ELECTROLYTE

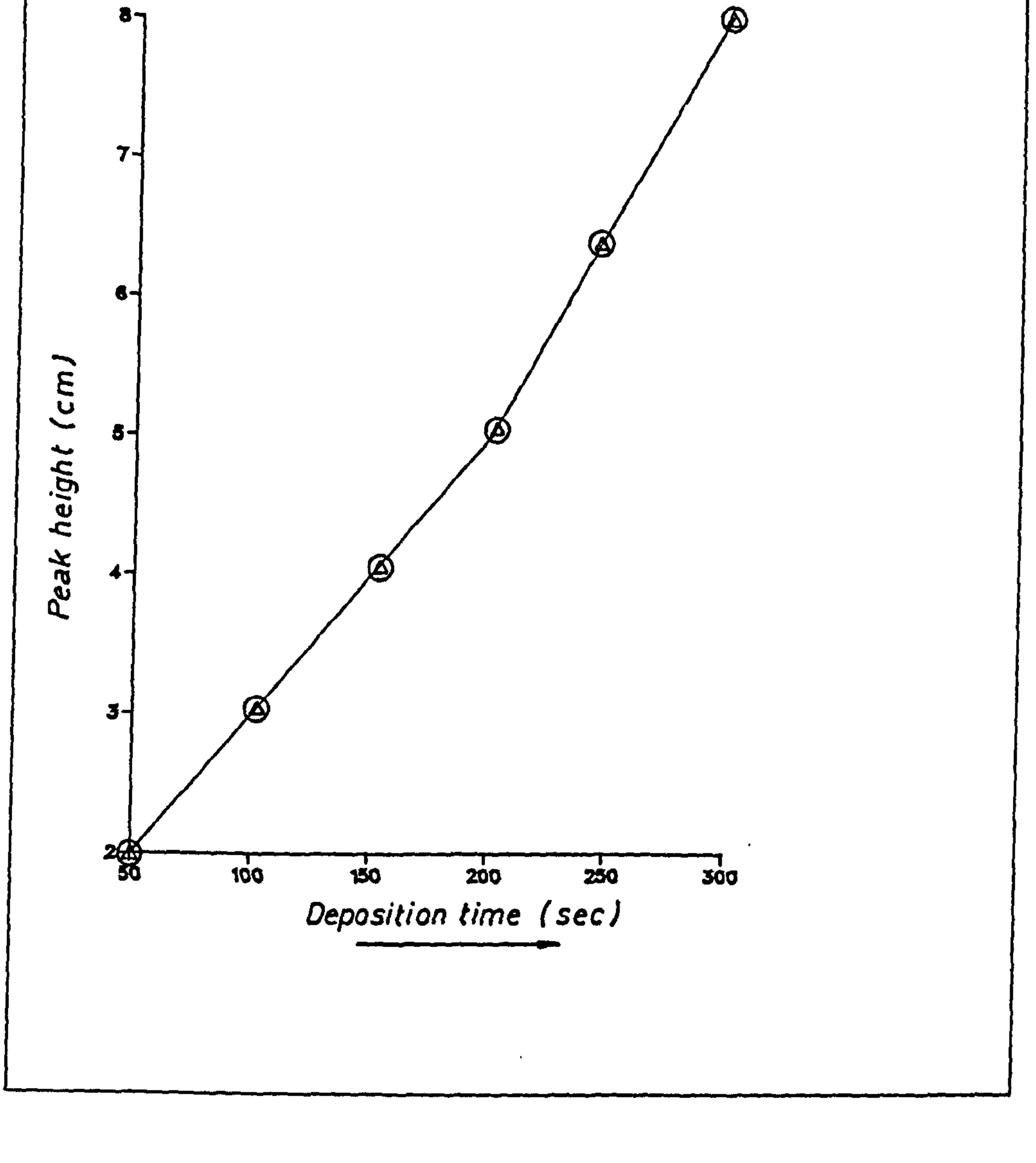

FIG. 5.29 EFFECT OF MODULATION AMPLITUDE ON PEAK HEIGHT OF SILVER IN :—(A) 0.1M KNO_3 +0.002M EDTA Electrolyte (B) 0.2M NH_4OH+0.2 NH_4NO_3 Electrolyte

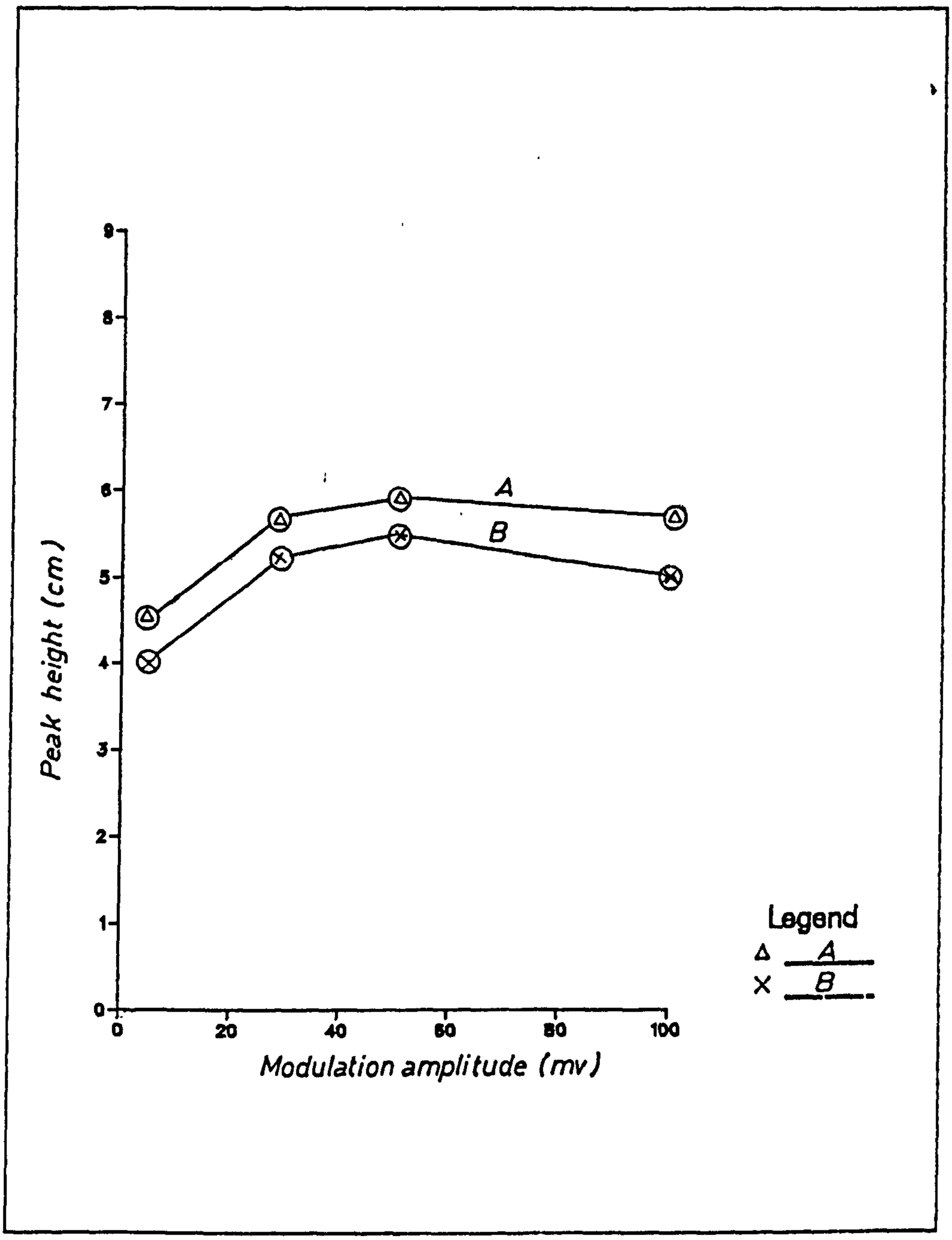

FIG. 5.30 EFFECT OF SCAN RATE ON PEAK HEIGHT OF SILVER IN :—
(A) 0.1M KNO_3 + 0.002M EDTA Electrolyte
(B) 0.2M NH_4OH + 0.2M NH_4NO_3 Electrolyte

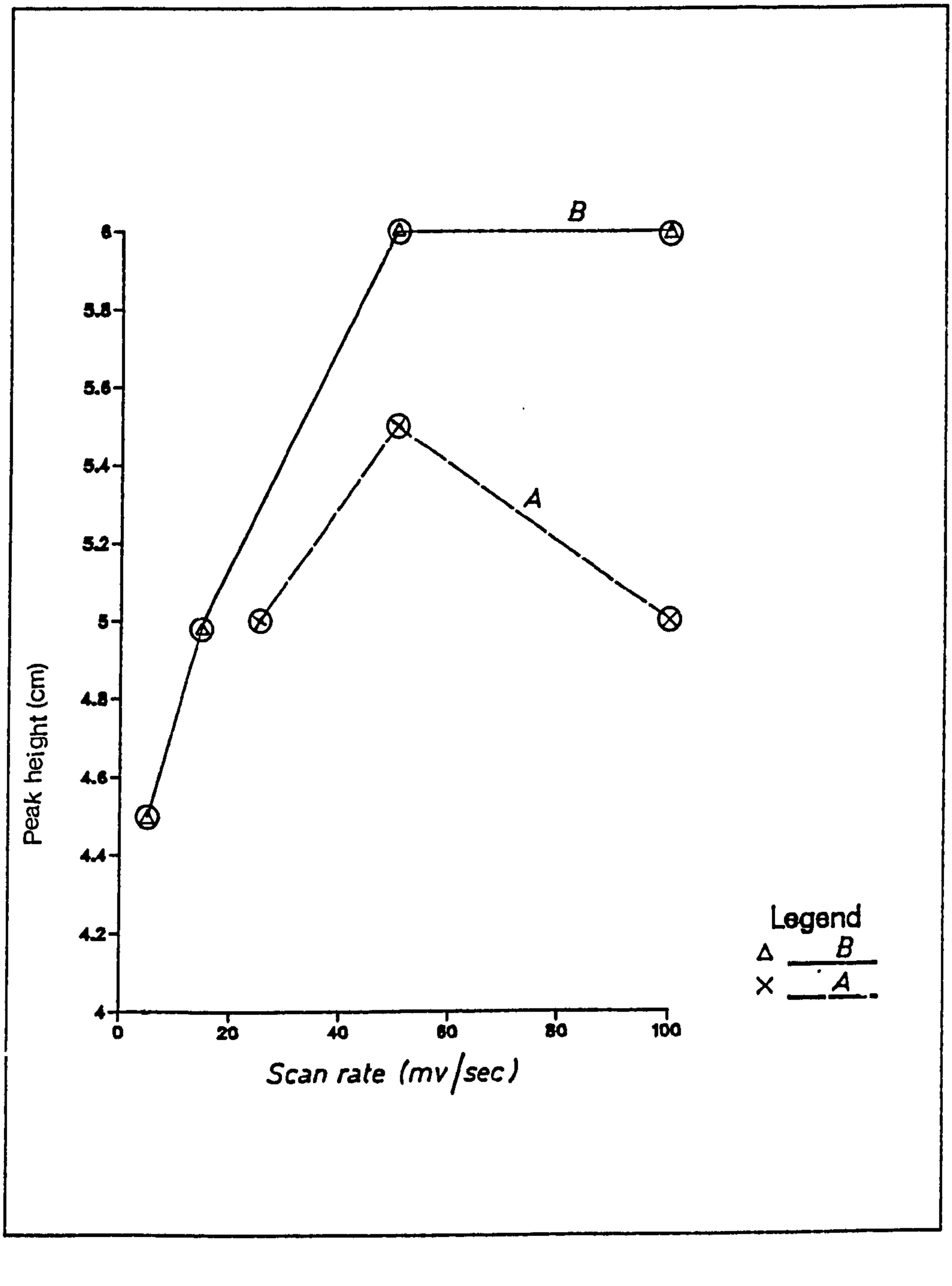

FIG. 5.31 EFFECT OF ROTATION OF THE ELECTRODE ON PEAK HEIGHT OF SILVER IN:-(A) 0.1M KNO_3 +0.002M EDTA Electrolyte (B) 0.2M NH_4OH +0.2M NH_4NO_3 Electrolyte

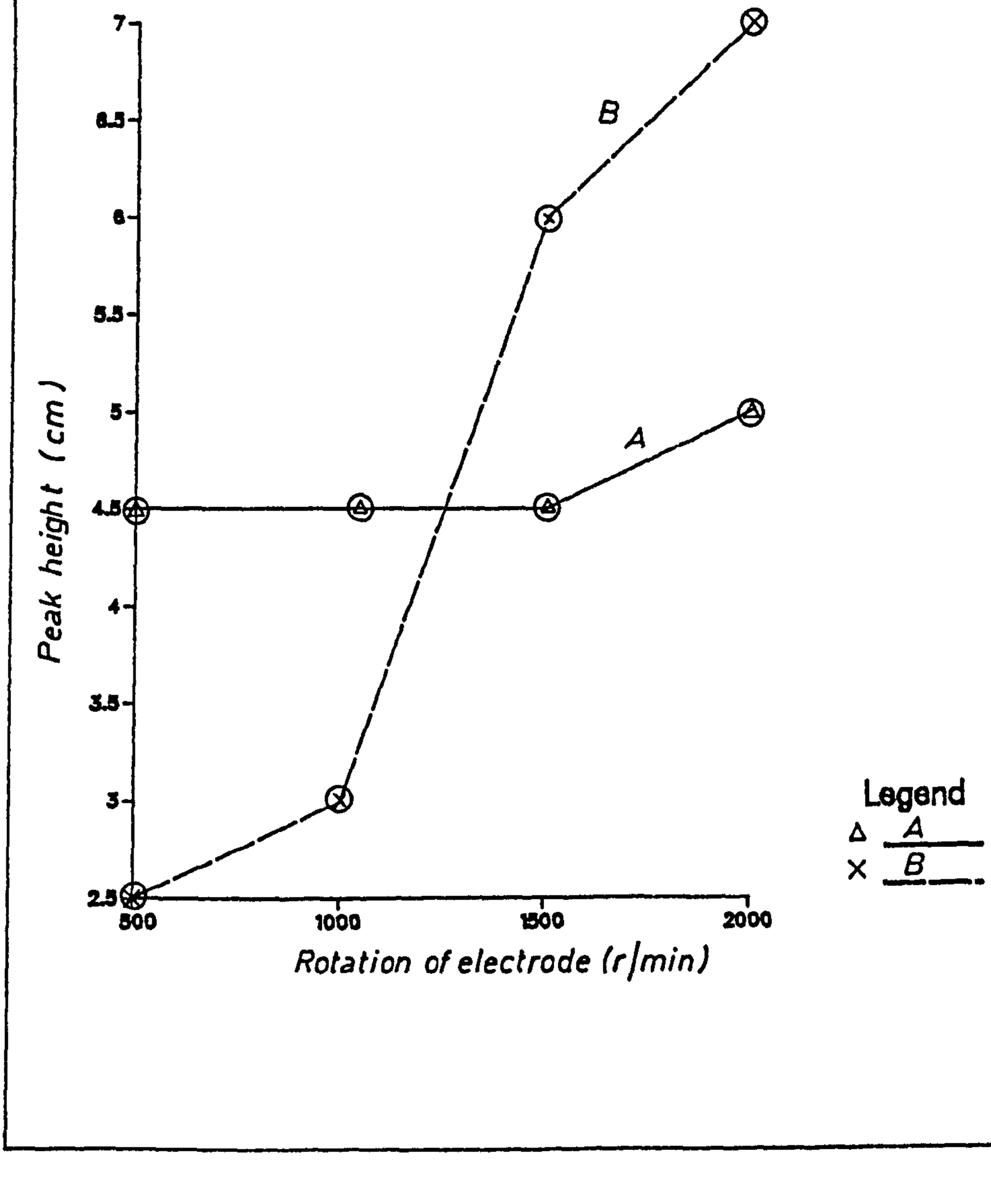

amplitude, scan rate and rotation of electrode, respectively, on the peak current of silver in both electrolytes. In most cases, higher peak currents were formed in the case of 0.1 M KNO_3 + 0.002 M EDTA rather than in the 0.2 M NH_4OH + 0.2 M NH_4NO_3 electrolyte. Silver in the amalcap alloy (see Table 5.8) was determined by DC-ASV and found to be 4,600 μg/g, while by AAS determination it was 37,800 μg/g. Clearly these two values should be of the same order. The major difference in the two must be due to a systematic error in the tributylphosphine oxide extraction/back extraction system. The original reference source (27) makes no mention of the adjustment of pH in these extractions and possibly the extraction of the Ag from the original diluted HNO_3 solution was not quantitative. The AAS result is clearly the most reliable.

The results in Table 5.10 indicate the level of silver in soils, sediments, rock and plants determined by FAAS and GFAAS. It was found that the level of silver determined by GFAAS was higher than in FAAS for the same sample. The inhomogeneity of the sample and the different procedures used with each technique may be responsible for the difference in level of silver in each sample. The GFAAS method was a much more rigorous dissolution procedure. The results in Table 5.11 indicate the level of silver and lead in soil-plant systems. The level of silver was not high enough to be detected by FAAS while the level of lead is very high, which reflects the mining history of the Mendip Hills. The small particle size of the soil made it difficult to separate from the roots of the plants, which may explain the high levels of lead detected in the roots of the plants.

Silver and lead were taken up by plants and the maximum accumulation was observed on the first day (see Table 5.12). However, the level of the metals in plant tissues decreased from the second day onwards.

The plants either grew and so diluted the metal taken up, or the root surface is saturated with the metal. Therefore, the level of metal in these plant tissues decreased after being fed the metals. The dilution of metals by plants can be clearly delineated from the yield of the plants and the amount of metals in the plants (see Table 5.26).

It was observed that the plant species died after a specific time (dependent on the species) as follows :-

Species	Time (in days)
Poa annua	4
Agrostis tenuis	5
Lolium perenne	6
Rumex acetosella	7
Holcus lanatus	8

From the above observations the resistance of the species to silver and lead was in the following order :- Holcus lanatus > Rumex acetosella > Lolium perenne > Agrostis enuis > Poa annua. The results in Table 5.12 are shown in Figures 5.32 - 5.39 which illustrate the uptake of lead and silver in roots and shoots of the above species. The metals were accumulated in roots to much higher levels than in the shoots, i.e., the species may localise the metals in the roots and so decrease their toxicities. Figure 5.33 demonstrates that lead was taken up by Poa annua roots, a higher level of lead in the roots being found after six days of feeding rather than after four days of feeding. The same situation was observed with shoots of Agrostis enuis and Lolium perenne seedlings. These observations are shown to be due to a reduction in biomass which leads to an effective concentration of the metals.

Table 5.26 : Yield of Plants per Treatment

Species	Dry Weight (g)
L. perenne	
Root	0.0281,[a] 0.0624,[b] 0.1581[c]
Shoot	0.0845, 0.0994, 0.0291
H. lanatus	
Root	0.0143, 0.0252, 0.0320
Shoot	0.0539, 0.0873, 0.0951
R. acetosella	
Root	0.0341, 0.1273, 0.1416
Shoot	0.0253, 0.0530, 0.0651
A. tnuis	
Root	0.0078, 0.0203, 0.0405
Shoot	0.0235, 0.0571, 0.0142
P. annua	
Root	0.0150, 0.0252, 0.0059
Shoot	0.0233, 0.0375, 0.0136

a, b and c as defined in Table 5.12.

FIG.5.32 UPTAKE OF LEAD BY ROOTS OF:—
(A) LOLIUM PERENNE (B) AGROSTIS TENUIS
(C) HOLCUS LANATUS

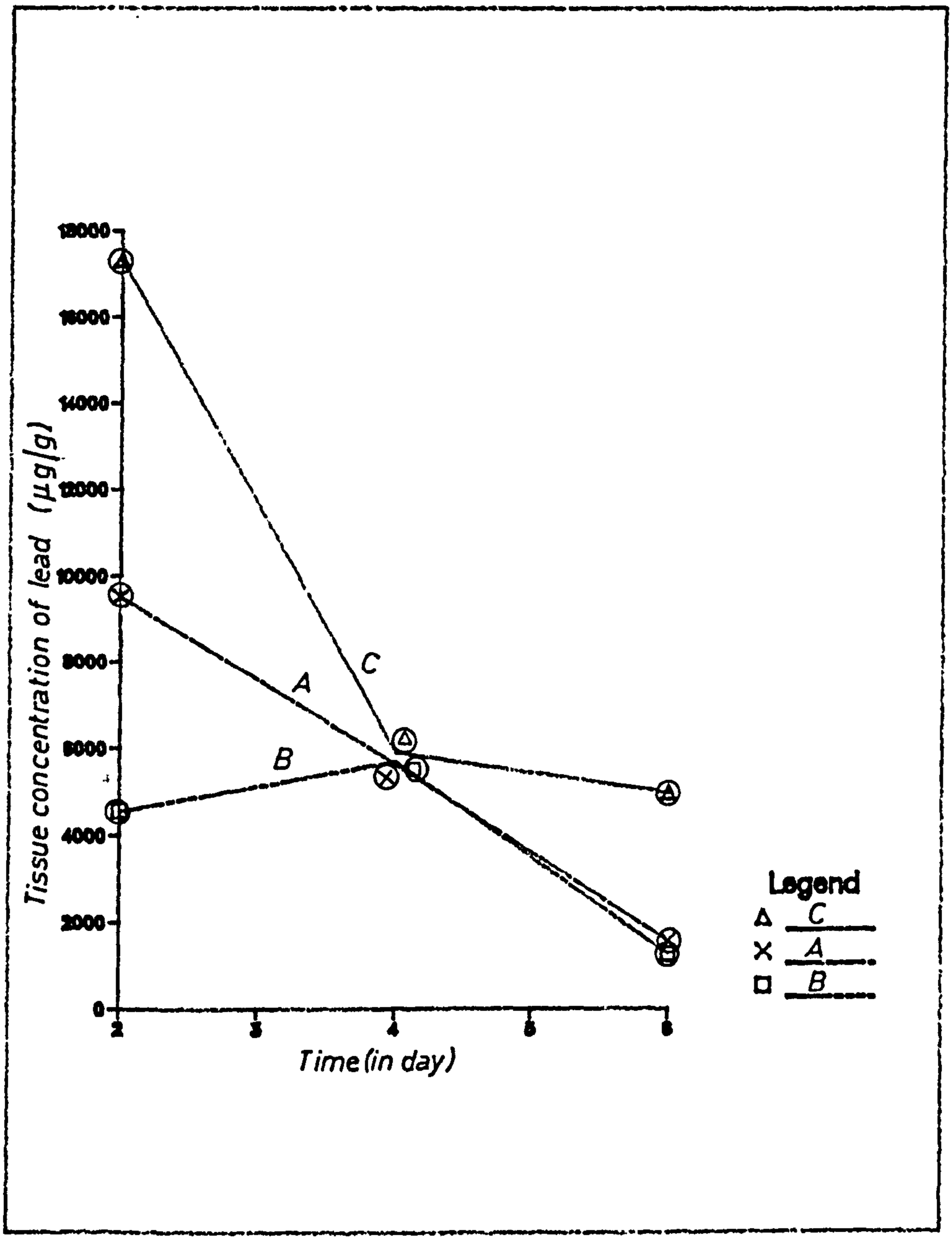

FIG. 5.33 UPTAKE OF LEAD BY ROOTS OF :—
(A) RUMEX ACETOSELLA
(B) POA ANNUA

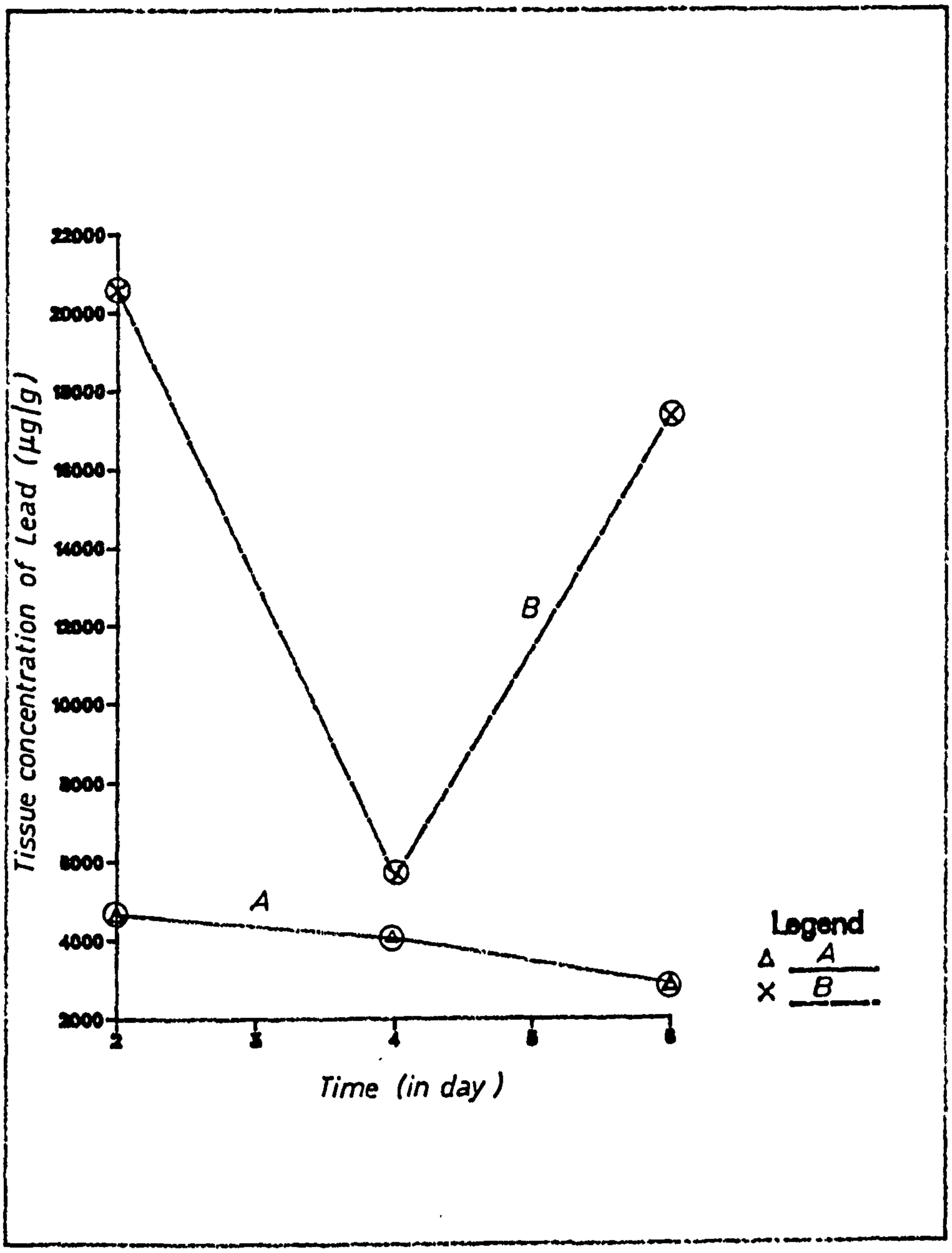

FIG. 5.34 UPTAKE OF LEAD BY SHOOTS OF:—
(A) AGROSTIS TENUIS (B) HOLCUS LANATUS
(C) LOLIUM PERENNE

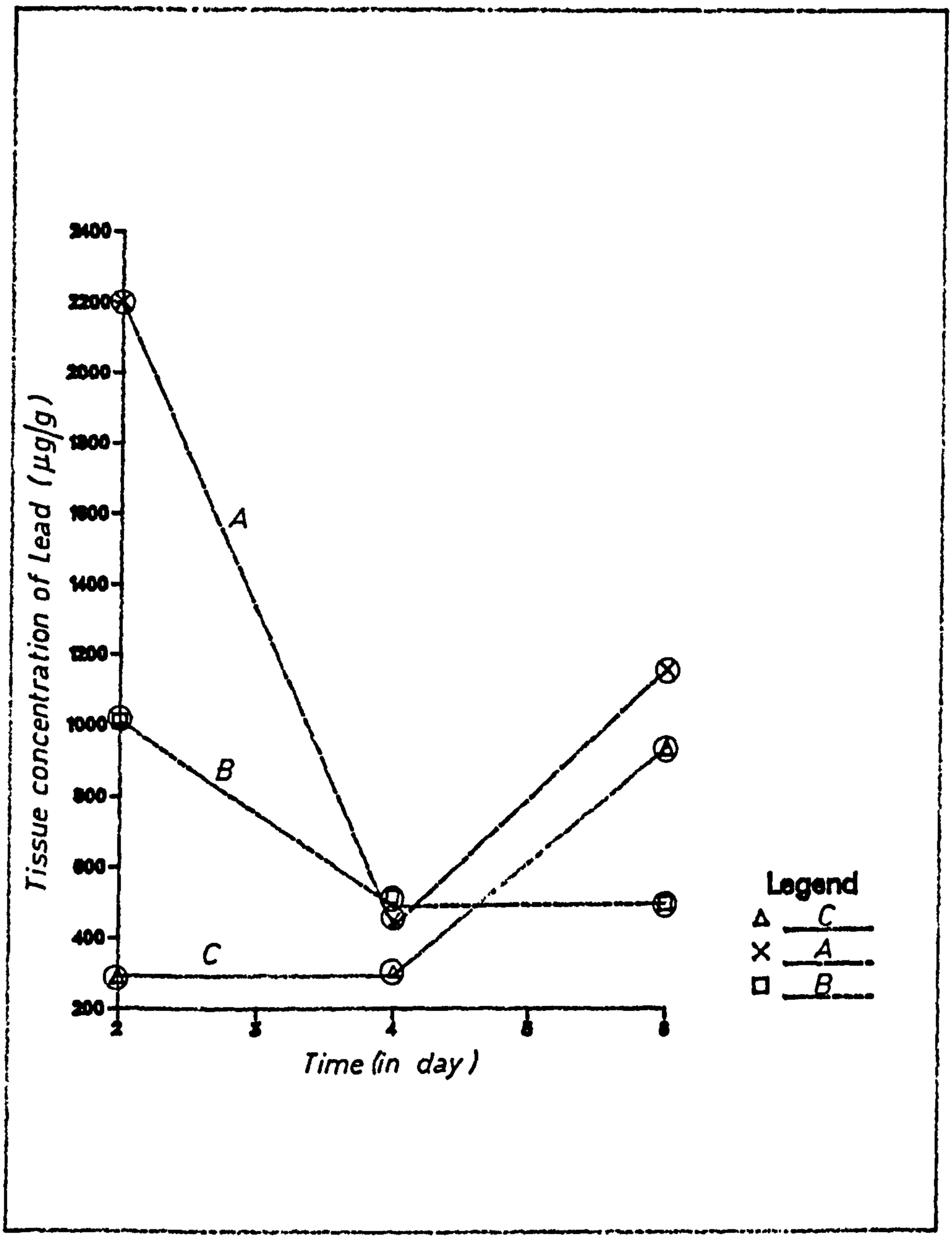

FIG. 5.35 UPTAKE OF LEAD BY SHOOTS OF:—
(A) RUMEX ACETOSELLA (B) POA ANNUA

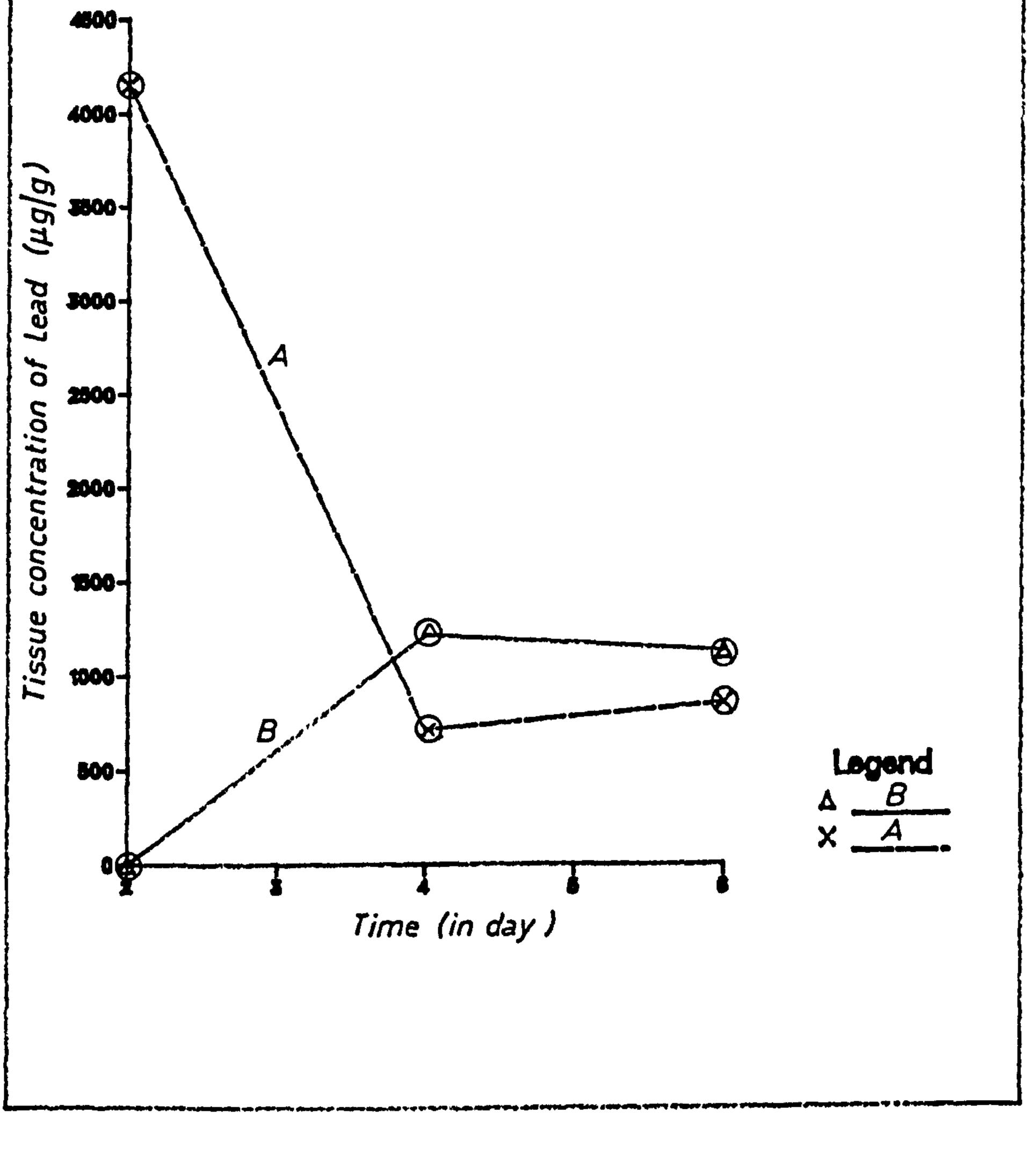

FIG. 5.36 UPTAKE OF SILVER BY ROOTS OF: —
(A) HOLCUS LANATUS (B) AGROSTIS TENUIS
(C) LOLIUM PERENNE

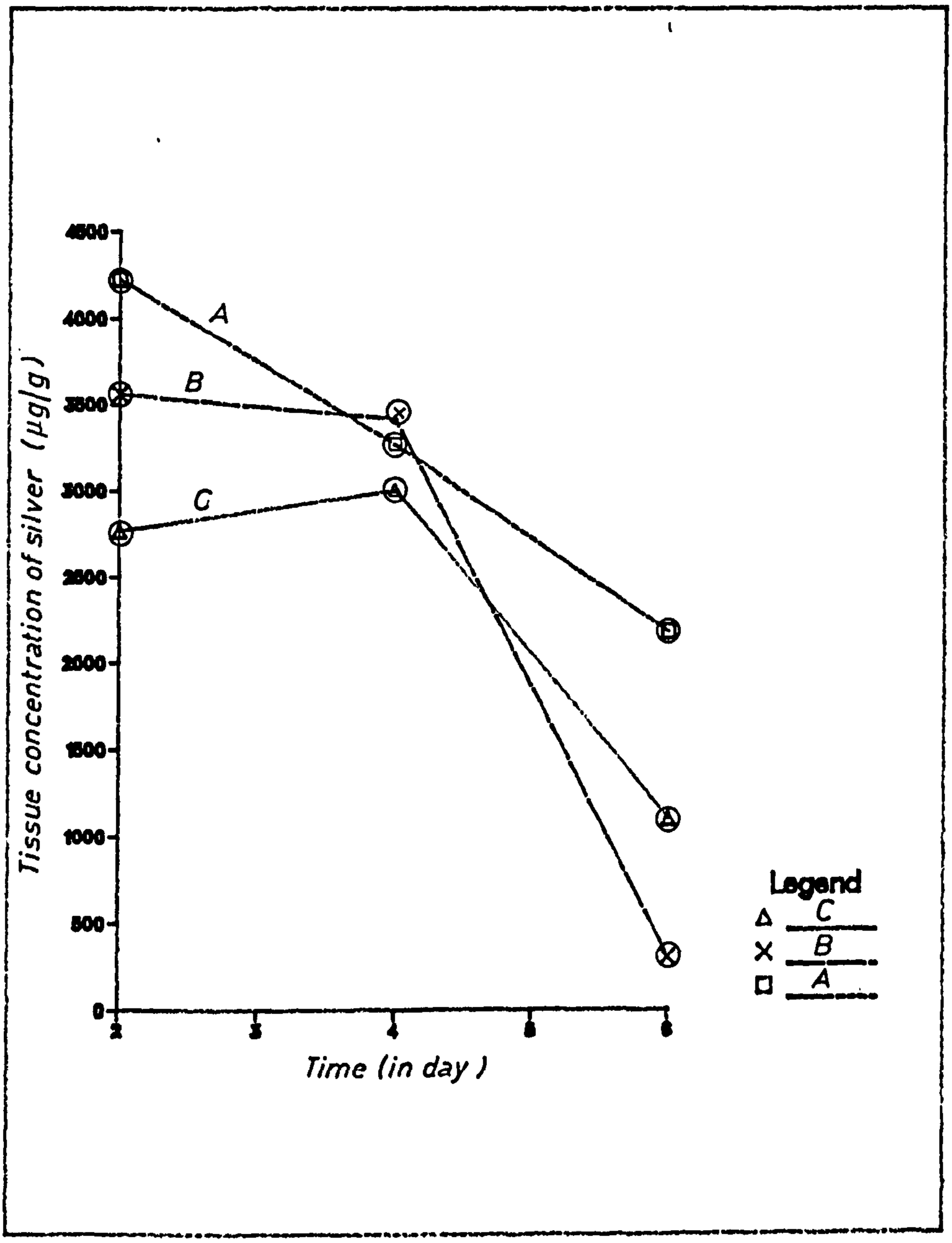

FIG. 5.37 UPTAKE OF SILVER BY ROOTS OF:—
(A) POA ANNUA (B) RUMEX ACETOSELLA

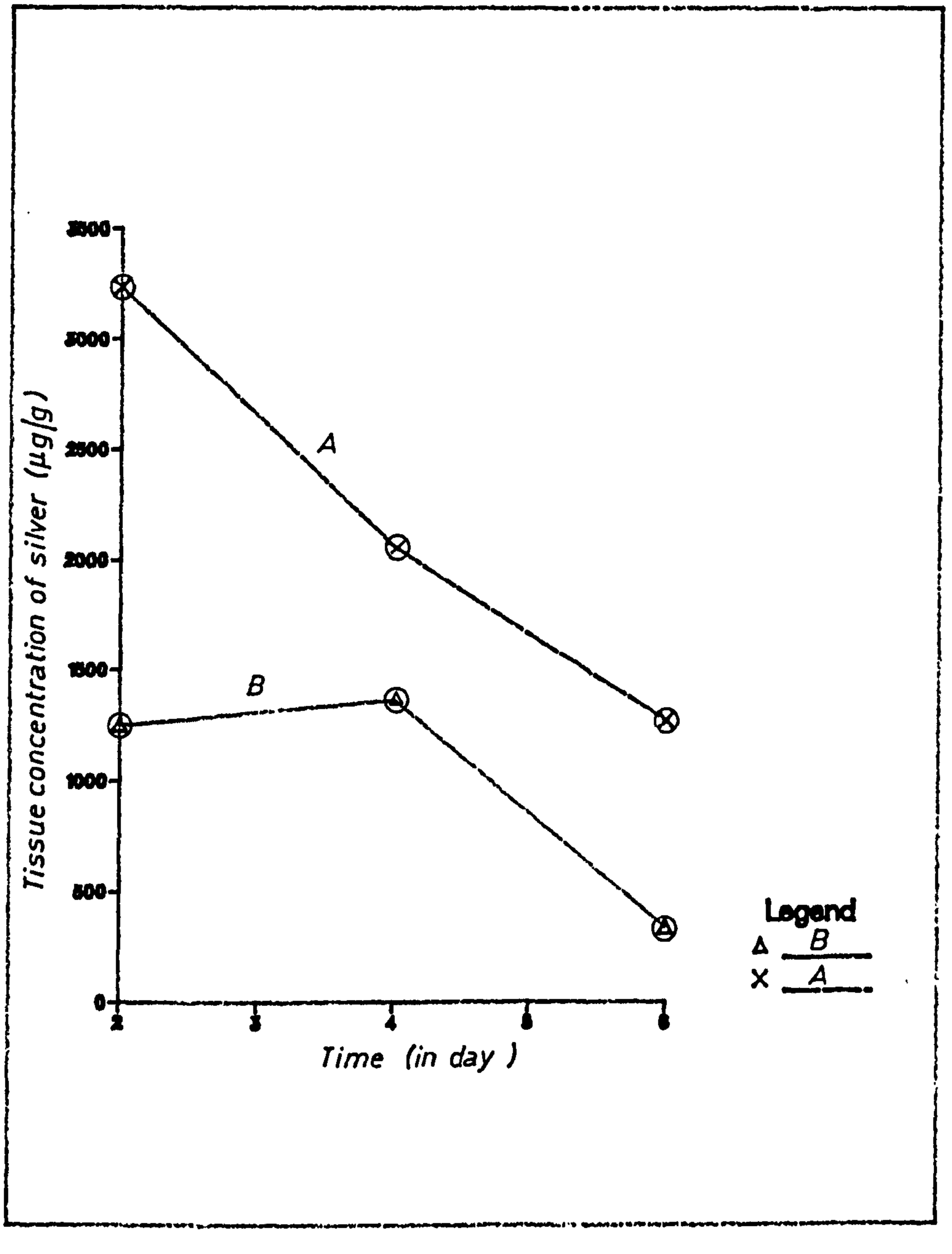

FIG. 5.38 UPTAKE OF SILVER BY SHOOTS OF:—
(A) HOLCUS LANATUS (B) LOLIUM PERENNE .
(C)AGROSTIS TNUIS

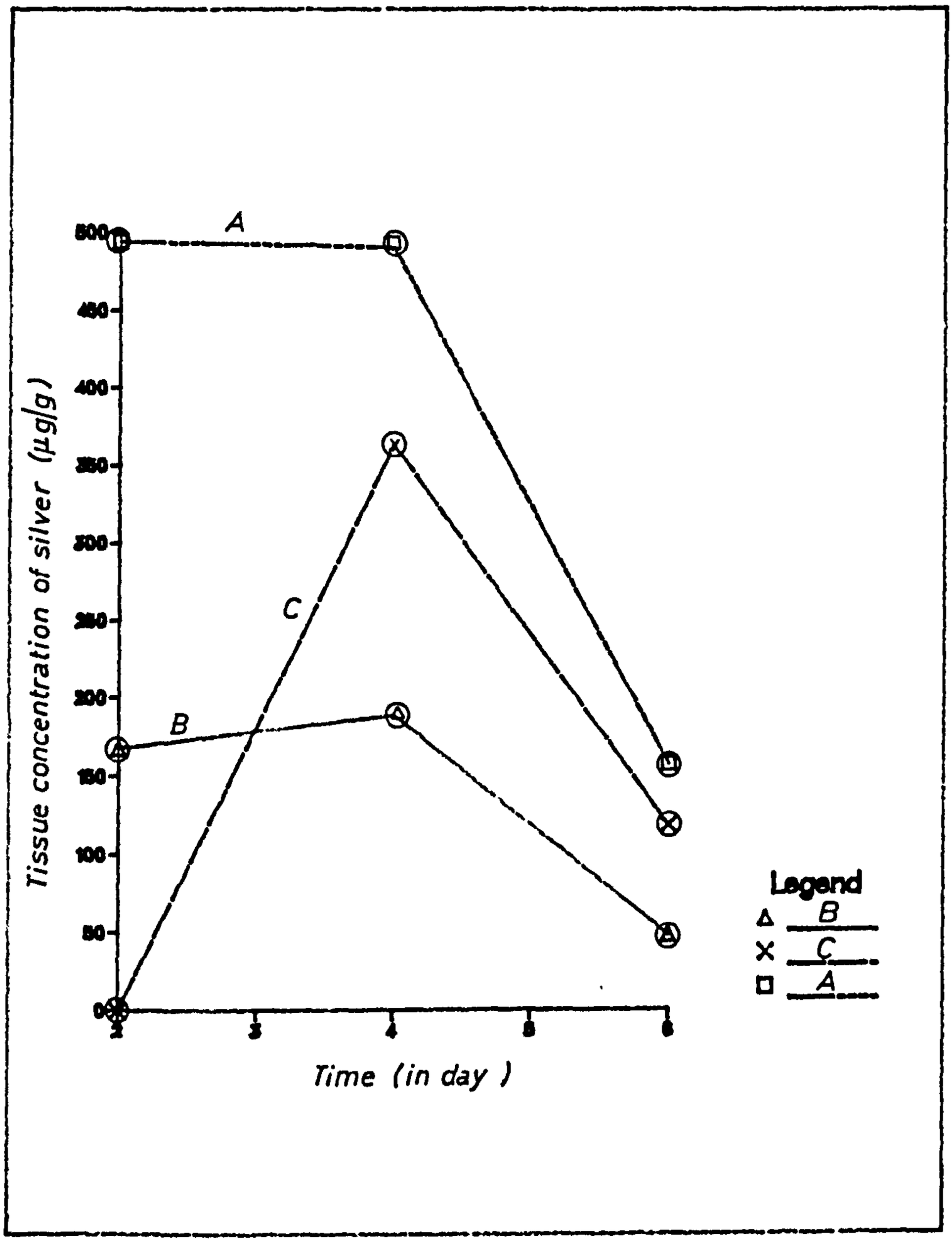

FIG. 5.39 UPTAKE OF SILVER BY SHOOTS OF:—
(A) POA ANNUA (B) RUMEX ACETOSELLA

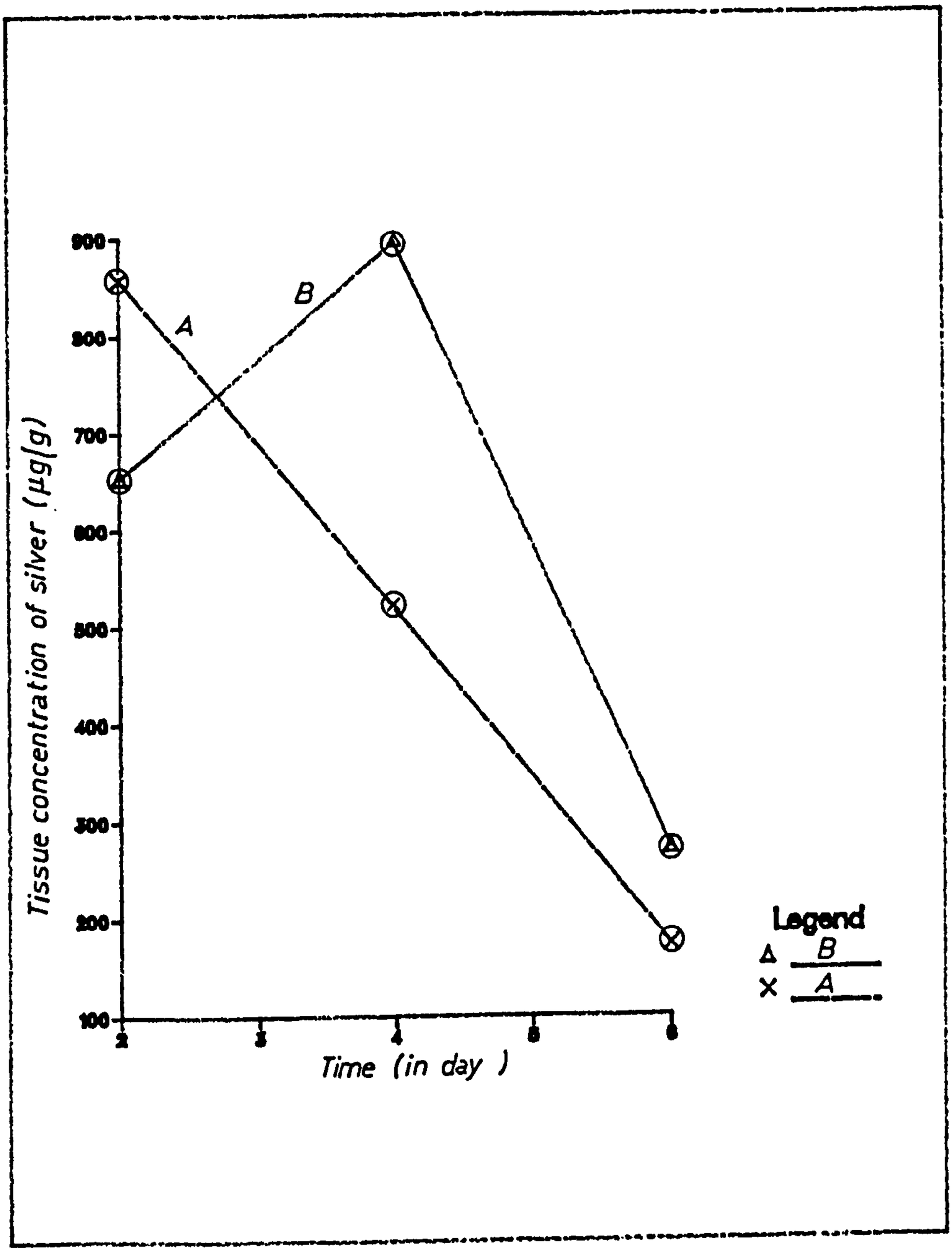

d) Determination of Lanthanum in Samples by AAS, XRF, DC-Plasma and ICP/MS

It is extremely difficult to determine lanthanum in samples by the readily available techniques such as AAS or colorimetry, however, coated graphite tubes lined with tantalum foil and used with flameless atomic absorption improve the signal of lanthanum by AAS. Although the signal was improved using the foil, it was irreproducible. From the results in Table 5.24 it is obvious that $A_1\ B_1\ C_1$, $A_1\ B_2\ C_1$ and $A_2\ B_1\ C_2$ are good combinations, and they give the highest responses. Further optimisation can then be carried out by performing another factorial experiment in the provisional optimal area and choosing narrower levels between A_1 and A_2; between B_1 and B_2; between C_1 and C_2. The results obtained from applying the GLM program are shown in Table 5.25 which indicates the effects on the response :-

1) A change in factor C produces larger effects in the response than factors A or B, since for C (PR > 0.023), for A (PR > 0.102) and for B (PR > 0.697).

2) The effects due to the interaction between two factors are A*B (PR > 0.723), A*C (PR > 0.0262) and B*C (PR > 0.4125), i.e. the interactions between ashing temperature and nitrogen flow are significant.

3) The effect due to interactions between three factors A*B*C (PR > 0.0477) is significant.

However, the statistical design offered a great advantage in optimising the lanthanum signal by using a graphite tube coated with tantalum foil. The major problem was that after 20 measurements the foil cracked and some small pieces of it were scattered in the beam of light from the HCL, and so irreproducible results were obtained.

Clearly although the advantage of the tantalum foil has been demonstrated, many problems remain to be solved. The cracking of the foil means that a more ductile metal than tantalum is required to meet the strain of the repeated rapid heating and cooling cycles during the analysis cycle.

The major elements and trace lanthanum in solid samples were determined by XRF (see Table 5.13). The level of lanthanum in different samples varied between 13-41 μg/g and this is in general agreement with the level of lanthanum found in sedimentary rocks (29).

Indeed, lanthanum is accumulated in plants to a high level in suitable circumstances, but it is not detected by AAS. Dc-plasma and ICP/MS are the most suitable techniques for the determination of lanthanum in acid digested plant tissues. In fact, ICP/MS was designed to be more sensitive and reliable than the Dc-plasma, but in practice it was vice versa. In the case of ICP/MS, the system was so unreliable that the technique required calibration after every two measurements while the Dc-plasma was reliable and stable over a long term.

e) Toxicity of Metal to Plants

The results in Table 5.17 indicate that the toxicity of these metals decreases in the following order :-

Ag > Al > La (in roots)

Al > Ag > La (in shoots)

However, when these results are combined with the toxicity of thallium the order becomes :-

Tl > Ag > Ag > La (in roots)

Tl > Al > Ag > La (in shoots)

The difficulty of obtaining an unaffected yield was discussed in

Chapter 4, p. 281. Any concentration of the metals studied, except for lanthanum, affected the yield of the plants and so no point was obtained on the horizontal line, therefore the estimation of an unaffected yield (Y_o) was not accurate. This confirms the difficulties encountered in confirming the toxicity of thallium described in Chapter 4. The level of metals in the control experiment was not detected by the analytical technique used, but the level of such metals was estimated by using 10 times the detection limits for the procedure and the value was fitted to the horizontal line in the T_c calculation.

It was also observed that some experimental points deviated markedly from the regression line, which as a consequence decreased the correlation coefficient. Because the plants were heavily contaminated with metals, a low quality relationship between the uptake of metals and the yield of plants ensues.

The results shown in Figures 5.19 - 5.24 (pp. 323-328) for tissue concentration confirm the general form of the yield curve for very toxic elements (see Figure 4.2, p. 208). The concentration of the element in the nutrient solution retards the growth of the plant to a very marked extent. In general, the critical level of Al, Ag, La and Tl in the roots of Lolium perenne was found to be higher than in the shoots. From these results it can be concluded that the roots have the ability to concentrate metals and store them while surviving. Obviously Al, Ag and Tl are very toxic elements to the Lolium perenne species and the original concentration range chosen was too high to produce completely reliable figures for critical levels of Al, Ag and Tl in these plants. Furthermore, the experiments should be repeated several times over an extended period, so that an estimation of the average critical level for each element in plants can be obtained.

It appears that Benkhayal (30) has experienced the same problems, as found in the present work, for the determination of silver in Holcus

lanatus species. Davis et alia (31) have determined the critical level of Cu, Zn and Ni in barley species with success. However, these elements are not as toxic, as for example thallium, and therefore it was possible to plan a suitable feeding programme, because they do have a relatively easily determined background levels in the roots and shoots.

From the point of view of toxicity, the determination of accurate figures for the critical levels of Al, Ag and Tl in plants is difficult and requires very careful planning.

Aluminium and lanthanum are both trivalent metals, The question to be asked is, "Why is aluminium more toxic to plants than lanthanum, while the latter metal was accumulated more than the former?" (See Tables 5.15 and 5.16). The results in Tables 5.18 - 5.22 were aimed at investigating this observation. Unfortunately, the level of aluminium in Orchard leaves (SRM 1571) is not known, therefore it was difficult to check the accuracy of the procedure used for the above investigation. However, some difference in the determined levels of aluminium and lanthanum in the acid digested sample and the lengthy extraction procedure was expected. The difference may occur due to the many steps present in the procedure and so either sample loss (decrease in the level) or contamination occurs (increase in the level). In the scheme for extraction of aluminium and lanthanum from plants (see Figure 5.25), the ethanol extract was further fractionated using DDW, ether, chloroform/ n-pentanol and acetone.

The extract was initially mixed with DDW and ether-separation of the pigments was achieved. The DDW extract was mixed with chloroform/ n-pentanol; proteins soluble in such organic solvents, i.e. proteins containing a high proportion of valine, leucine, isoleucine, phenylalanine, tryptophan are partitioned in the chloroform fraction, leaving the more polar plant components such as organic acids in the DDW phase. The

pectins are obtained from this solution by precipitation with acetone. In fact, the precipitation was not observed in this work. The water layer contains low molecular weight materials such as amino acids. The insoluble pectate was isolated by treating with ammonium oxalate to convert to soluble ammonium pectate. Lignin was extracted by hydrolysing cellulose by 1.5 M KOH, leaving lignin as the residue (32,33).

The results in Tables 5.18 - 5.22 are represented in Figures 5.40 - 5.48, The major associations of aluminium and lanthanum within the plant compȯnents are as follows :-

1) Lolium perenne

	Al	Fraction	La	Fraction
Root	36.1%	hemicellulose	63.47%	α-cellulose
Shoot	30.7%	α-cellulose	51.9%	α-cellulose

2) Holcus lanatus

	Al	Fraction	La	Fraction
Root	45.76%	polysaccharide	48.4%	Sol. pectates
Shoot	19.08%	protopectates	78.2%	α-cellulose

It is clear from this data that a higher percentage of lanthanum was associated with the cell wall materials than aluminium, perhaps this is responsible for lanthanum ion inactivation. Aluminium is associated with all plant components, probably explaining the element's higher toxicity.

FIG. 5.40 DISTRIBUTION OF ALUMINIUM IN ORCHARD LEAVES (SRM 1571)

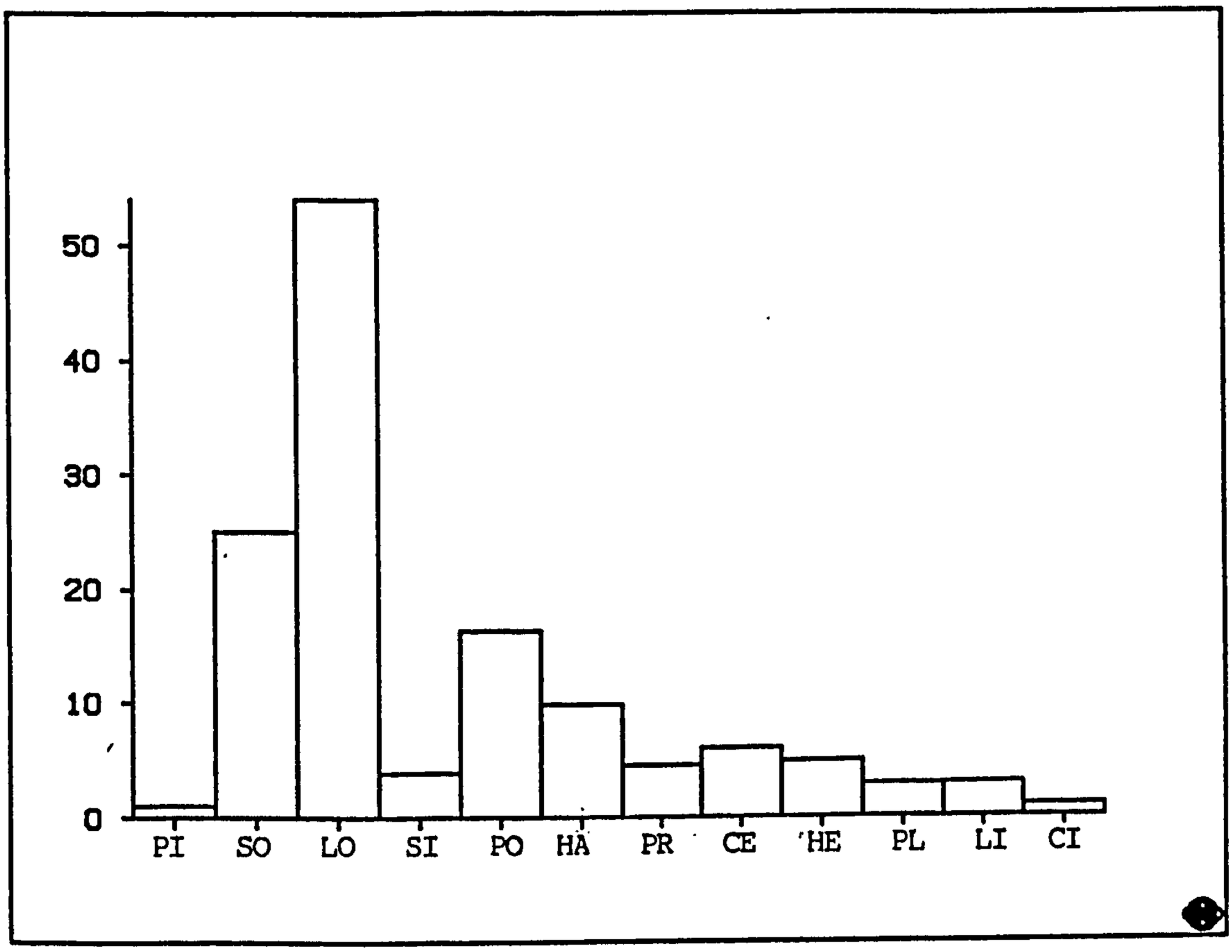

FIG. 5.41 DISTRIBUTION OF ALUMINIUM IN ROOTS OF LOLIUM PERENNE SEEDLING

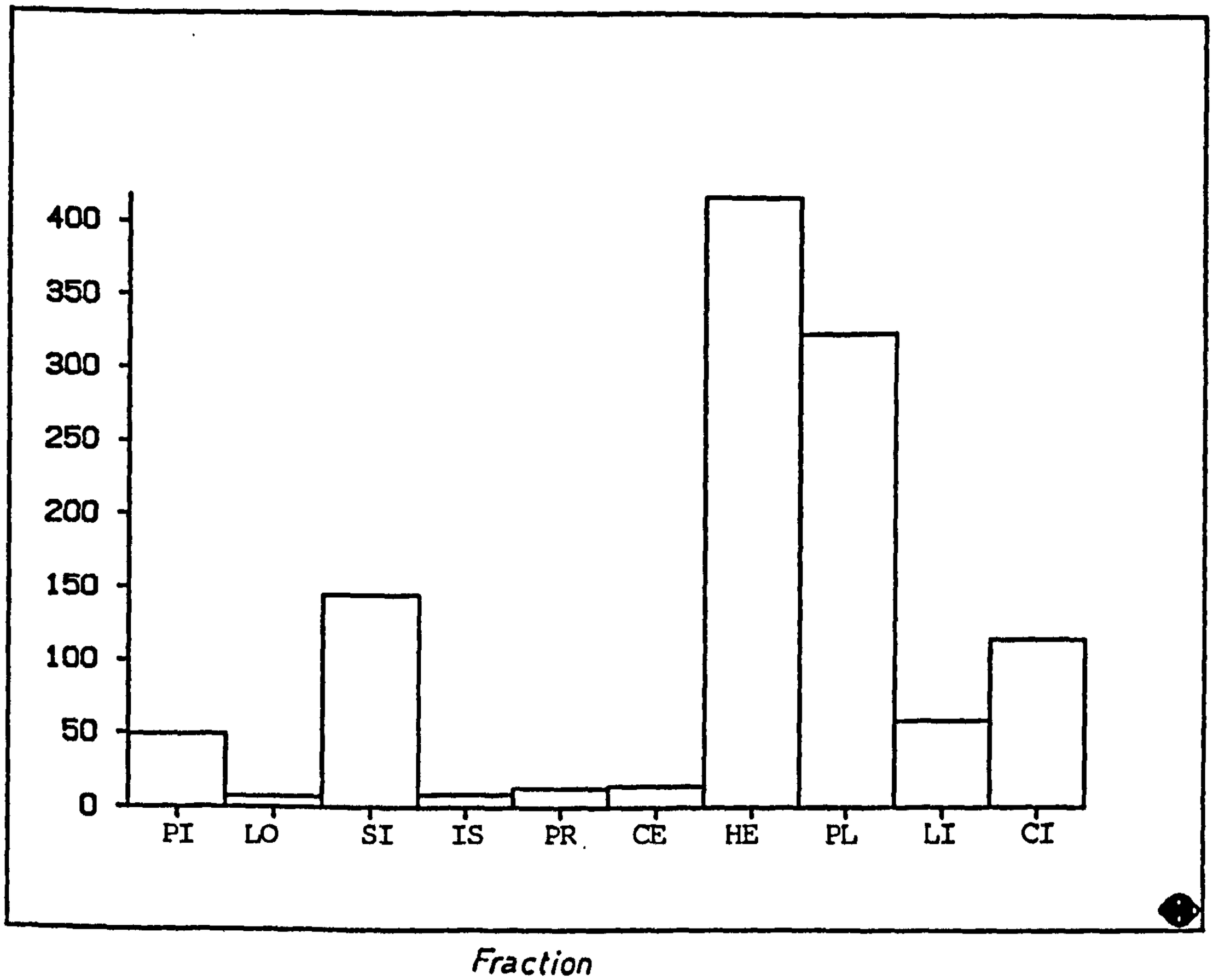

FIG. 5.42 DISTRIBUTION OF ALUMINIUM IN SHOOTS OF LOLIUM PERENNE SEEDLING

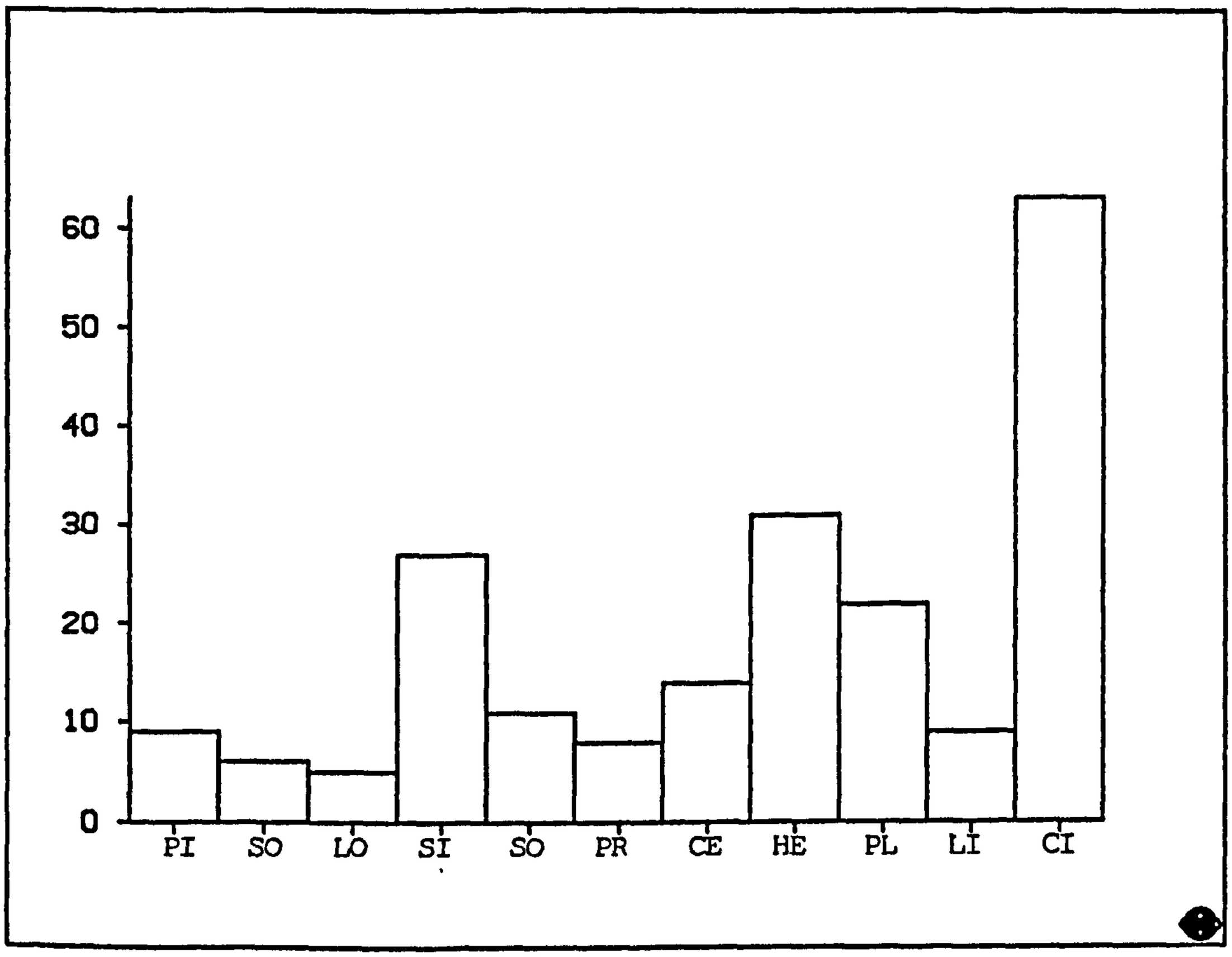

FIG. 5.43 DISTRIBUTION OF ALUMINIUM IN ROOTS OF HOLCUS LANATUS SEEDLING

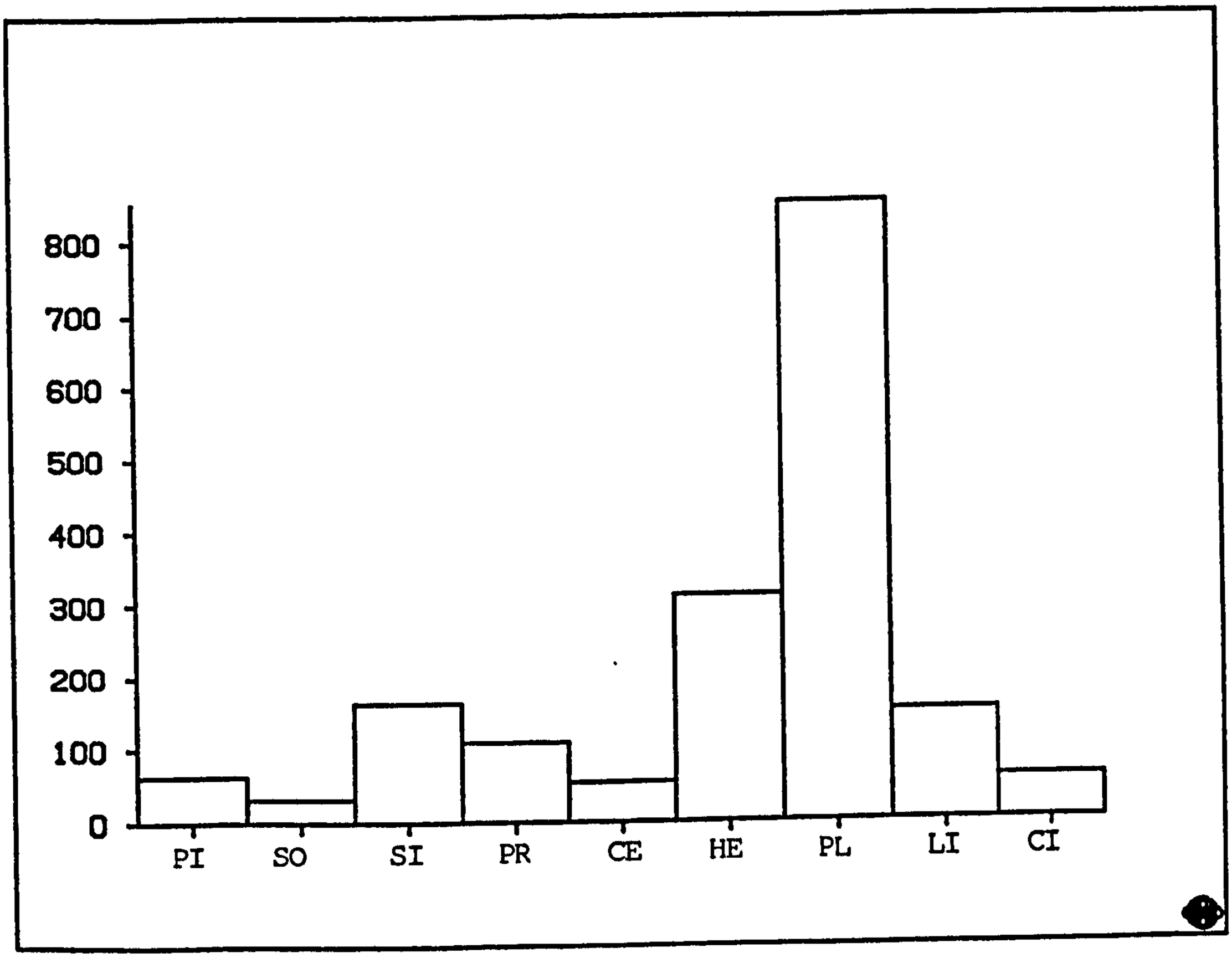

FIG. 5.44 DISTRIBUTION OF ALUMINIUM IN SHOOTS OF HOLCUS LANATUS SEEDLING

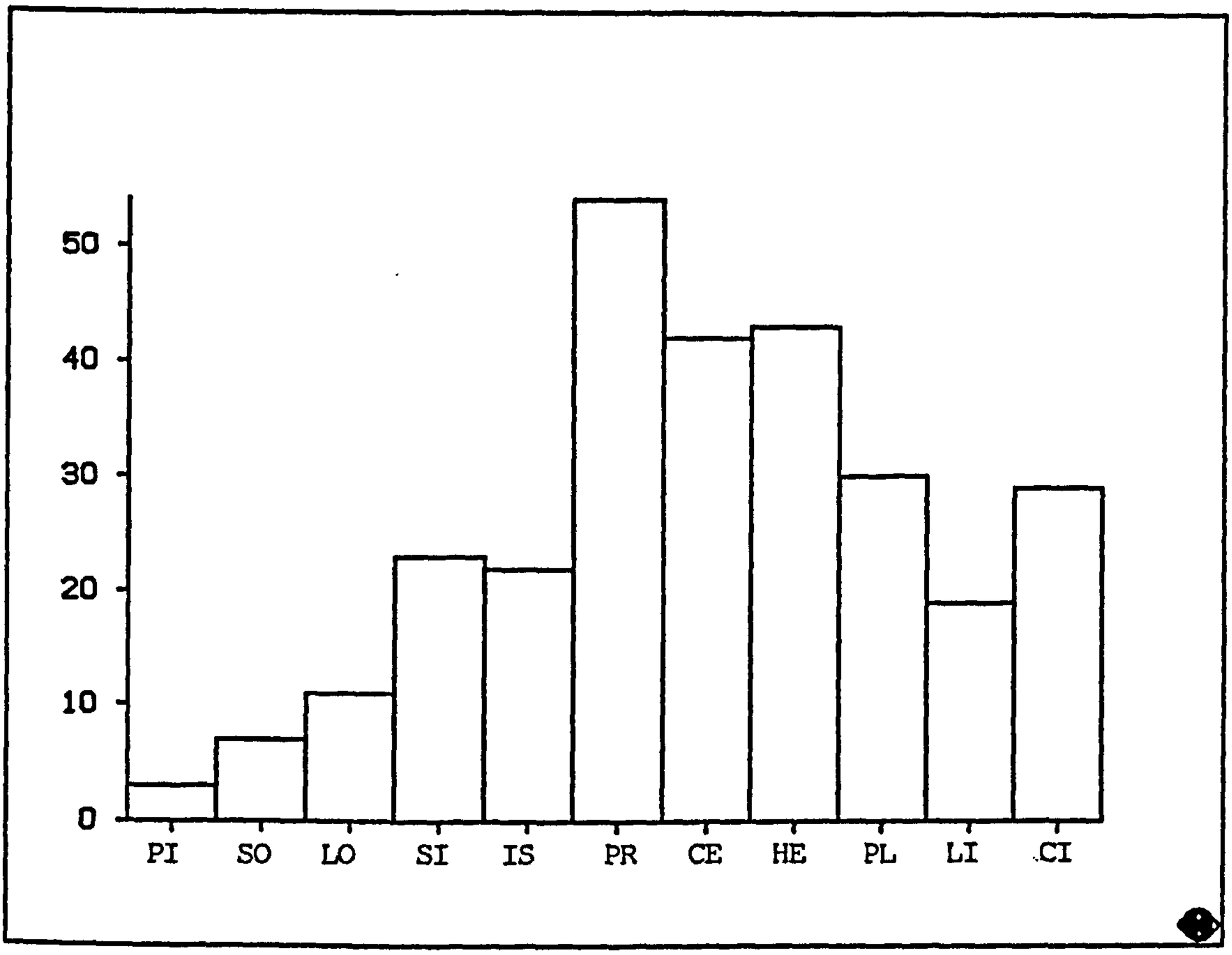

FIG. 5.45 DISTRIBUTION OF LANTHANUM IN ROOTS OF LOLIUM PERENNE SEEDLING

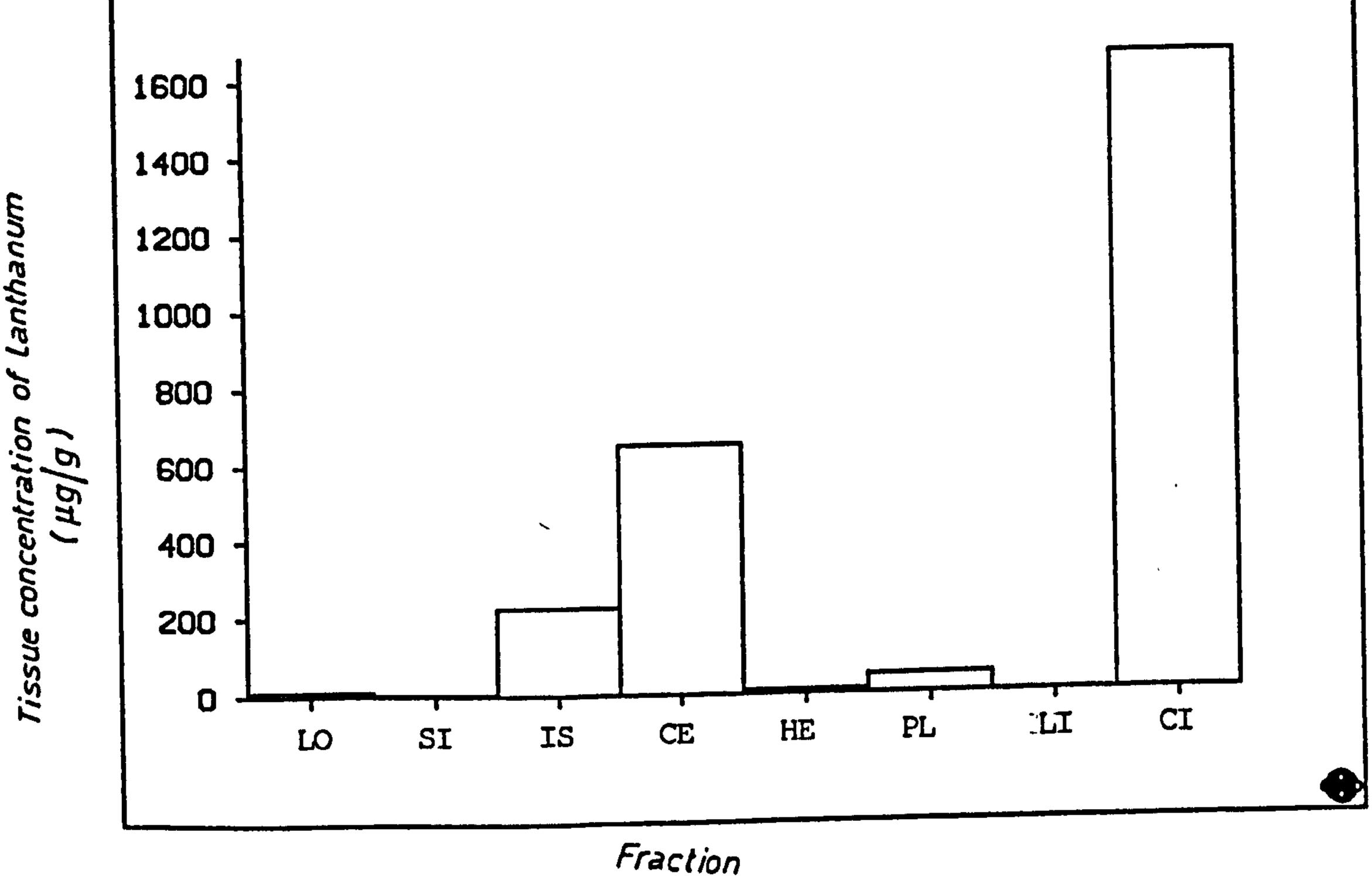

FIG. 5.46 DISTRIBUTION OF LANTHANUM IN SHOOTS OF LOLIUM PERENNE SEEDLING

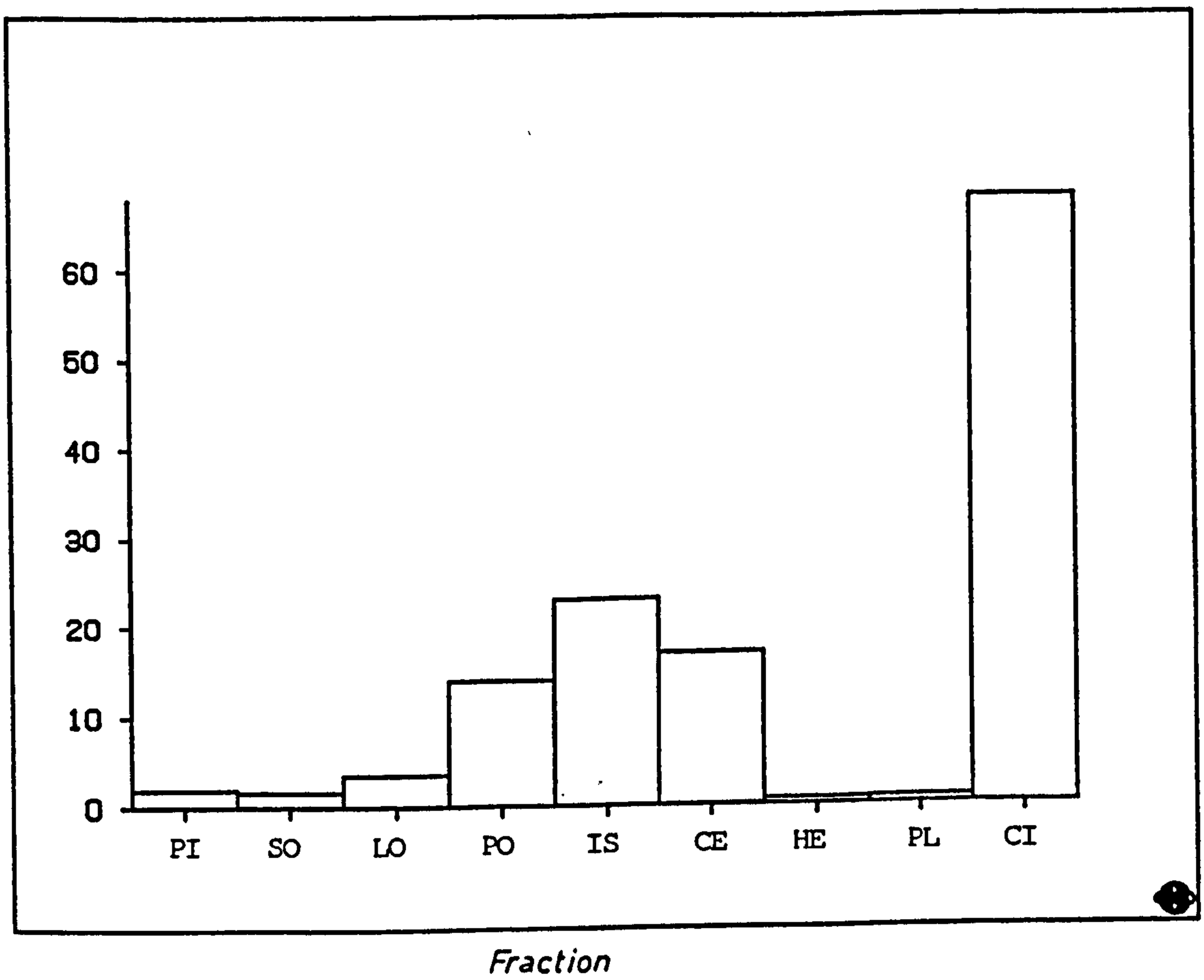

FIG. 5.47 DISTRIBUTION OF LANTHANUM IN ROOTS OF HOLCUS LANATUS SEEDLING

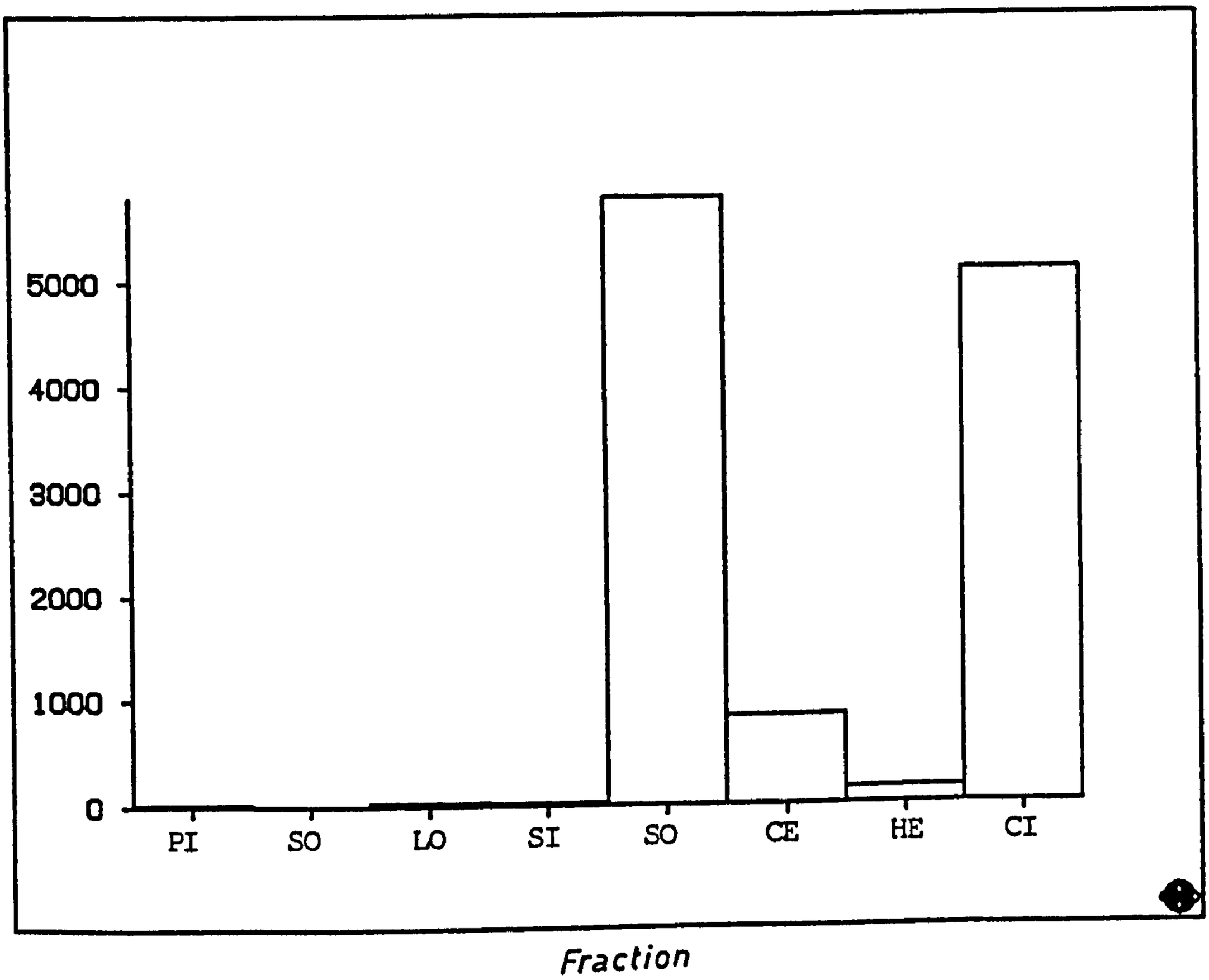

FIG. 5.48 DISTRIBUTION OF LANTHANUM IN SHOOTS OF HOLCUS LANATUS SEEDLING

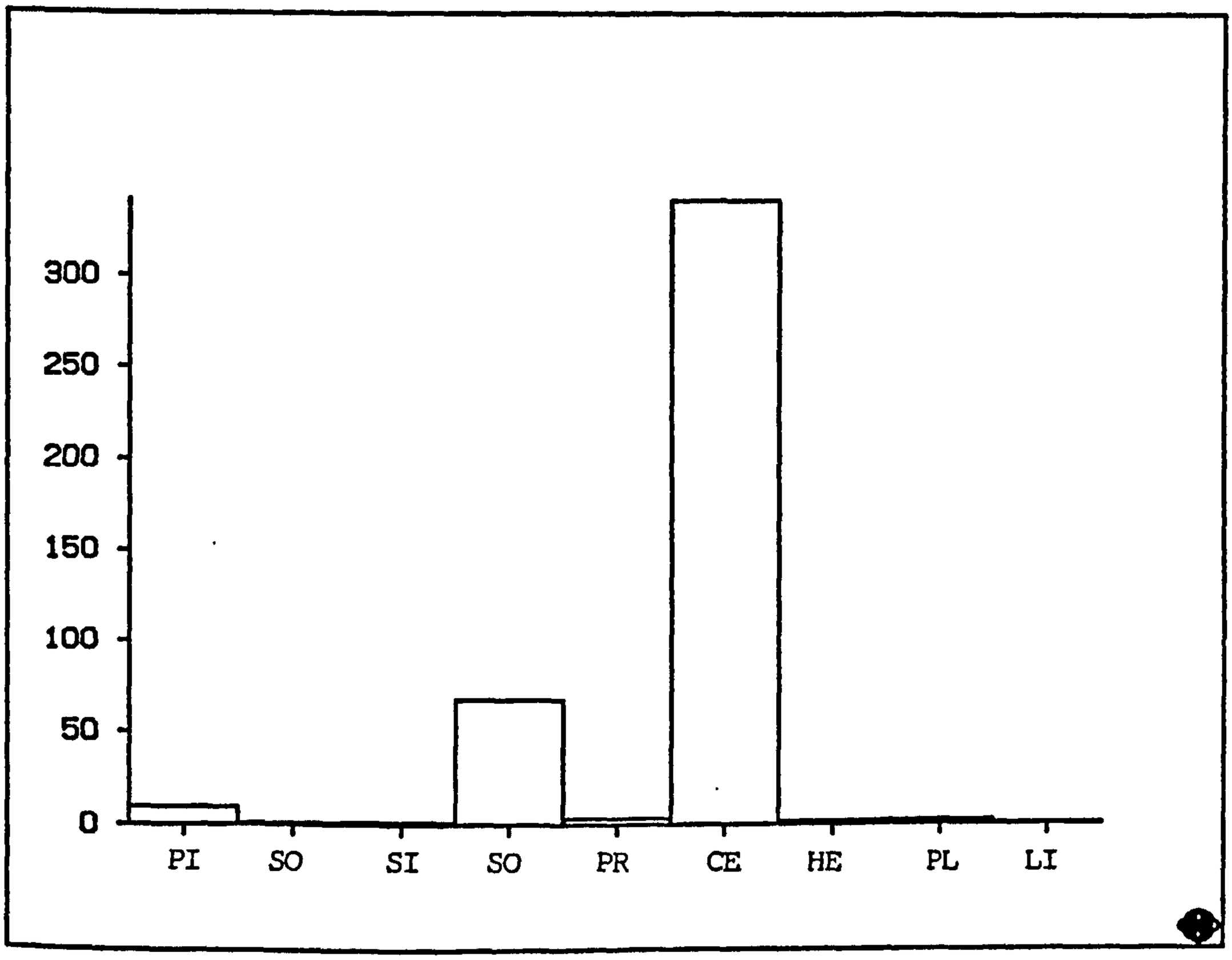

Possibly the aluminium is incorporated into the cell walls as bridge-structures between functional groups containing oxygen in the cell wall fraction (34), as follows :-

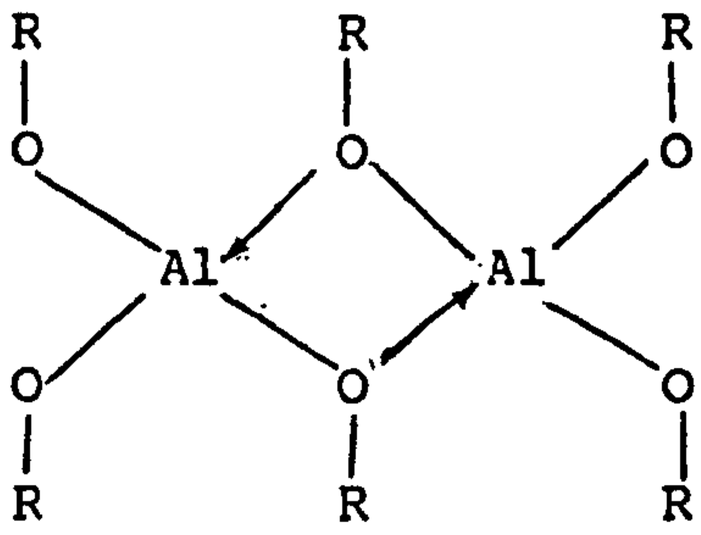

Interaction between aluminium and phosphorus may occur in the roots of the plant. Matsumoto et alia (35) reported that aluminium inhibits the genetic DNA synthesis in roots; this may indicate that the element is associated with nucleic acids, leading to inhibition of cell division (36). At the present time, the binding site of DNA with aluminium is not known. The nature and precise location of the phosphorus and aluminium held in plant roots remains uncertain. Bollard (37) has suggested that both the aluminium and phosphorus are located in the root cells in a complex binding situation. However, there is still no clear understanding of the binding of aluminium or lanthanum with plant components. Further investigation of the interaction between the metals and oxygen, nitrogen, phosphorus or sulphur may lead to a better understanding of the ways in which the metals bind to plant components. From the evidence presented in this work, there are indications that aluminium and lanthanum are associated in a different manner with plant components. Aluminium was taken up by the plant and probably reduced the level of calcium in the plant (39); the question to be asked is, "does lanthanum exhibit the same effect?" Response surface experiments (see Chapter 6), must be run to investigate the relationship between

aluminium and calcium on the one hand and lanthanum and calcium on the other. Then a conclusion may be possible to the question of whether aluminium or lanthanum replaces the calcium in plant components.

Comparable solvent extraction experiments by Farago et alia (28) have shown that much of the copper in the Cu-tolerant Armeria maritima is associated with the pectates and other carbohydrates in the roots. Presumably the unpaired electrons in the donor atom (oxygen) in the carbohydrate coordinate to the copper rather than the unpaired electron in the nitrogen or sulphur of the amino acid. Oehme (38) reported that metal ion binds with the sulfhydryl groups and to a lesser degree with the amino, phosphate, carboxylate and hydroxyl of enzymes. More stable complexes are formed with the sulphur and nitrogen than with the oxygen. Randall (39) found that most of the cadmium present (some 67%) in the root of Holcus lanatus was associated with the protein-amino acid fractions, while little cadmium was found in the α-cellulose (8%). However, the majority of the zinc (43%) in the roots of Holcus lanatus was present in the cell wall fraction, while for zinc in shoots of the same species some 67% was associated with cellulose. In the present work, it was found that most of the aluminium and lanthanum in Lolium perenne and Holcus lanatus was associated with the carbohydrate fraction. There is a well established preference of nitrogen and sulphur donors for soft metals such as Ag^{+}, Tl^{+}, while preferential complexation of oxygen ligands occurs to hard metals such as Al(III) and Cr(III) (see Table 1.5). In fact, this type of coordination between aluminium and oxygen ligands may be responsible for the association of aluminium with the carbohydrate component of the cell wall of the plants. Further studies are required on the molecular structures of the cell wall materials which appear to confer the observed specificity for metal binding. Moreover, accumulation by root cell walls is an important feature of metal tolerance.

5.4 REFERENCES

1. Burrows, W.D., CRC Crit. Rev. Environ. Control, 7, 167 (1977).
2. David, D.J., Commun. In Soil Sci. and Plant Analysis, 11, 189 (1980).
3. Leung, F.Y. and Henderson, A.R., At. Spectro., 4, 1 (1983).
4. Bettinelli, M., Baroni, U., Fontana, F. and Poisetti, P., Analyst, 110, 19 (1985).
5. Lindahl, P.C., Voight, K.C., Bishop, A.M., Lafon, G.M. and Huang, W.L., At. Spectro., 5, 137 (1984).
6. Burns, D.T., Dadgar, D., Harriott, M., McBride, K. and Swindall, W.J., Analyst, 109, 1613 (1984).
7. Genty, C., Hollin, C., Malherbe, P. and Schott, R., Anal. Chem., 43, 235 (1971).
8. Lee, M.L. and Burrell, D.C., Anal. Chim. Acta, 66, 245 (1973).
9. Belcher, R., Jenkins, C.R., Stephen, W.I. and Uden, P.C., Talanta, 17, 455 (1970).
10. Morie, G.P. and Sweet, T.R., Anal. Chim. Acta, 34, 314 (1966).
11. Scribner, W.G., Treat, W.J. and Weis, J.D., Anal. Chem., 37, 1136 (1965).
12. Moshier, R.W. and Schwarberg, J.E,, Talanta, 13, 445 (1966).
13. Sterritt, R.M. and Lester, J.N., Analyst, 105, 616 (1980).
14. Rattonetti, A., Anal. Chem., 46, 739 (1974).
15. Bloom, N., At. Spectro., 4, 204 (1983).
16. Hosking, J.W. and Robert, R.V.D., S. Afr. J. Chem., 37, 129 (1984).
17. Donaldson, E.M., Talanta, 31, 443 (1984).
18. Donaldson, E.M., Talanta, 29, 1069 (1982).
19. Bloom, N.S.,and Crecelius, E.A., Anal. Chim. Acta, 156, 139 (1984).
20. Perone, S.P., Anal. Chem., 35, 2091 (1963).
21. Temmerman, E. and Verbeek, F., Anal. Chim. Acta, 58, 263 (1972).

22. Glodowski, S. and Kublik, Z., Anal. Chim. Acta, 156, 61 (1984).

23. Butts, W.C. and Banks, C.V., Anal. Chem., 42, 133 (1970).

24. Gupta, J.G.S., Talanta, 32, 1 (1985).

25. Gupta, J.G.S., Talanta, 31, 1053 (1984).

26. Miller, J.C. and Miller, J.N., Statistics for Analytical Chemistry, Ellis Horwood Limited, Chichester, p. 153 (1984).

27. Lee, A.F., The Application of Anodic Stripping Voltammetry to the Determination of Trace Elements in Standard Reference Materials, Ph.D. Thesis, Rand Afrikaans University, p. 339 (1981).

28. Farago, M.E., Mullen, W.A., Cole, M.M. and Smith, R.F., Environ. Pollut. (A), 21, 225 (1980).

29. Taylor, S.R., Geochimica et Cosmochimica Acta, 28, 1273 (1964).

30. Benkhayal, A.A., Silver as a Pollutant, M.Sc. Thesis, University of Bristol, p. 70 (1983).

31. Beckett, P.H.T. and Davis, R.D., New Phytol., 79, 95 (1977).

32. Freeman, R.D., Determination of Total Carbohydrate Fraction of Extracted Wood : Pentosans and Miscellaneous Hexosans in Wood, Chap. 17, p. 629, in "Wood Chemistry", Wise, L.E. (Ed.), Reinhold Publishing Corp. (New York),(1944).

33. Phillip, M., The Chemistry of Lignin, Chap. 3, p. 318, in "Wood Chemistry", Wise, L.E., (Ed.), Reinhold Publishing Corp. (New York) (1944).

34. Woolhouse, H.W., Toxicity and Tolerance in the Responses of Plants to Metals, in "Encyclopedia of Plant Physiology", Lange, O.L., Nobel, P.S., Osmond, C.B. and Ziegler, H., (Eds.), 12C, p. 245 (1983).

35. Matsumoto, H., Hirasawa, E., Torikai, H. and Takahashi, E., Plant and Cell Physiol., 17, 127 (1976).

36. Matsumoto, H., Morimura, S. and Takahashi, E., Plant and Cell Physiol., 18, 987 (1977).

37. Bollard, E.G., Involvement of Unusual Elements in Plant Growth and Nutrition, in "Encyclopedia of Plant Physiology", Lauchli, A. and Bieleski, R.L. (Eds.), 15B, 695 (1983).

38. Oehme, F.W., Mechanics of Heavy Metal Inorganic Toxicities, in "Toxicity of Heavy Metals in the Environment", Oehme, F.W. (Ed.), p. 69 (1978), Marcel Dekker, Inc., New York.

39. Randall, L., Fractionation of Heavy Metals in Natural Samples, Ph.D. Thesis, University of Bristol, p. 409 (1984).

CHAPTER 6

RESPONSE SURFACE METHODOLOGY (RSM)

Contents

6.1 INTRODUCTION

Response Surface Methodology (RSM) was initially developed and described by Box and Wilson (1) in 1951. RSM is a technique used in studying the relationships between one or more measured responses on the one hand and a number of input factors on the other (1-4). However, the response surface for more than two factors is difficult to visualise, but it can be approached by plotting two factors at a time while holding the other factors constant (5,6). Therefore, the response surface can be represented in three dimensions showing the relationship between the response and the levels of two factors (7,8).

a) Response Functions and Fitting Model to Data

The relation between response R and two factors x_1 and x_2 or more may be represented by a surface called the response surface :

$$R = \emptyset \ (x_1, x_2, \ldots\ldots x_K) \qquad [6.1]$$

A model of such a surface was described in Figure 6.1. The possible form of the true function $\emptyset$ is a polynomial which satisfies the relationship between the response R and the K important variables x_1, x_2, ... x_K (4). The most common polynomials are :

i) first order polynomial

$$R = B_o + B_1x_1 + B_2x_2 + \ldots\ldots + B_Kx_K \qquad [6.2]$$

ii) second order polynomial

$$R = B_o + B_1x_1 + B_2x_2 + \ldots\ldots B_Kx_K + B_{12}x_1x_2 + \ldots\ldots + B_{K-1}x_{K-1}x_K + B_{11}x_1^2 + B_{22}x_2^2 + \ldots\ldots + B_{KK}x_K^2 \qquad [6.3]$$

iii) third order polynomial

$$R = B_o + B_1x_1 + B_2x_2 + B_{11}x_1^2 + B_{22}x_2^2 + B_{12}x_1x_2 + B_{111}x_1^3 + B_{222}x_1^3 + B_{112}x_1^2x_2 + B_{122}x_1x_2^2 \qquad [6.4]$$

FIG. 6.1 RESPONSE SURFACE FOR TWO FACTORS

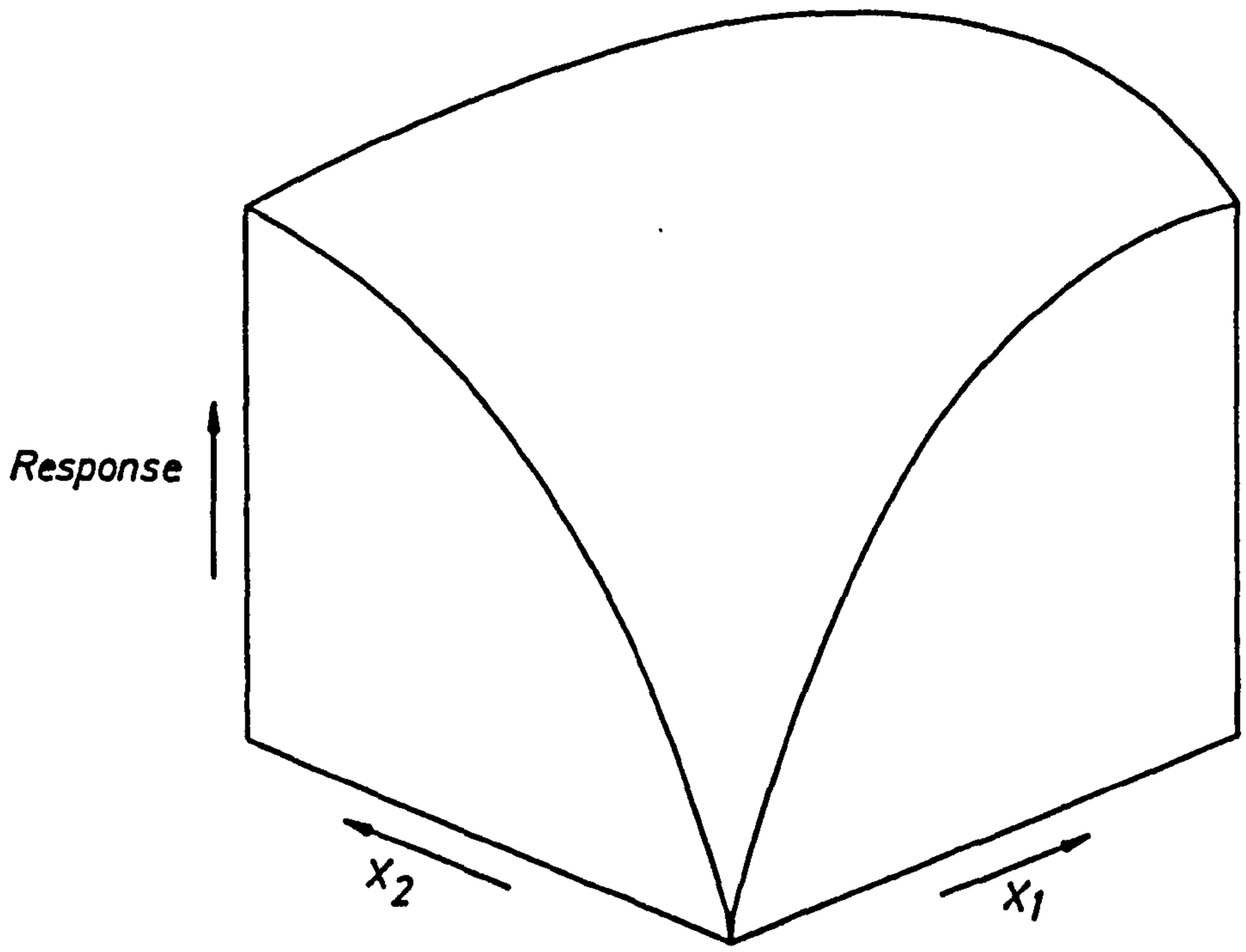

The coefficients B_o, B_1, B_2, B_{11}, B_{22}, B_{12}, B_{111}, B_{222}, B_{112} and B_{122} are parameters to be estimated from the data. Table 6.1 gives the number of coefficients in different degrees of polynomial (1).

Table 6.1 : Number of Coefficients with Different Degrees of Polynomial

Number of Factors	Degree of Polynomial			
	First	Second	Third	Fourth
2	3	6	10	15
3	4	10	20	35
4	5	15	35	70
5	6	21	56	126

Indeed, the precise nature of the response surface is not known but it is approximated by fitting the polynomial of the Kth degree (9) to the data.

For K equal to 2 and 3 the first order polynomial and second order polynomial were illustrated in the equations below :

For K = 2

$$R = B_o + B_1x_1 + B_2x_2 \qquad [6.5]$$

$$R = B_o + B_1x_1 + B_2x_2 + B_{12}x_1x_2 + B_{11}x_1^2 + B_{22}x_2^2 \qquad [6.6]$$

For K = 3

$$R = B_o + B_1x_1 + B_2x_2 + B_3x_3 \qquad [6.7]$$

$$R = B_o + B_1x_1 + B_2x_2 + B_3x_3 + B_{12}x_1x_2 + B_{13}x_1x_3 + B_{23}x_2x_3 + B_{11}x_1^2 + B_{22}x_2^2 + B_{33}x_3^2 \qquad [6.8]$$

where the parameters :-

B_o = intercept

B_1, B_2, B_3 = linear

B_{11}, B_{22}, B_{33} = quadratic

B_{12}, B_{13}, B_{23} = interaction.

For the purpose of fitting a polynomial equation three considerations must be kept in mind :

i) the assumption being that a polynomial of the degree assumed can adequately represent the surface in the region examined. The error of estimated points on the fitted surface should be very small (1).

ii) the biases in the estimated coefficients, which might occur if the assumed equation were representationally inadequate, should be small.

iii) the number N of experimental points needed to determine L constants cannot be less than L, it should exceed this number (1,3).

The first degree equation represents a plane, if the degree of fit is inadequate, then a second degree equation should be used. Analysis of the fitted second degree equation might indicate certain features of the surface requiring further study. If the second degree equation is a poor fit, then steps should be taken to fit a third degree equation. The latter polynomial is quite complicated. The goodness of the fitted polynomial can be examined by estimation. The term "lack of fit" is a component which measures the deviations of the responses from the fitted surfaces and experimental errors which are calculated from the replicated points at the centre (14,15) of the polynomial. In the present work, all the coefficient parameters of the fitted polynomial and "lack of fit" were determined by computational methods (10,11). There are basically four types of surfaces which the second order polynomial can

represent (1,4) :-

i) if B_{11} and B_{22} are of the same sign, the shape of surface is similar to Figure 6.2a. In this particular case B_{11} and B_{22} are both negative and the centre of the system is a maximum. However, if they are positive, the surface is a minimum.

ii) when B_{11} and B_{22} are of opposite sign, the shape of the surface is described by Figure 6.2b. The surface is called a saddle point or minimax.

iii) when B_{22} is zero, Figure 6.2c describes the shape of the surface which is called a stationary ridge surface.

iv) if B_{22} is zero and the centre of the systems were at infinity, the resultant shape of the surface is a rising ridge system which is represented by Figure 6.2d.

b) Applications of RSM

The purpose of this Chapter was to investigate the extent to which recently reported research in environmental chemistry is concerned with problems which appear to involve the idea of response surface. A typical RSM study begins with a definition of the problem :-

(1) which responses are to be measured

(2) how they are to be measured

(3) which variables are to be studied

(4) over what ranges they are to be explored.

In particular (3,12), attention must be paid to :-

i) performing statistically designed experiments

ii) estimating the coefficients in the response surface equation

iii) checking the adequacy of the equation

iv) studing the response surface in the region of interest.

FIG. 6.2 FUNDAMENTAL AND LIMITING SURFACE GENERATED BY SECOND ORDER POLYNOMIAL IN TWO DIMENSIONS

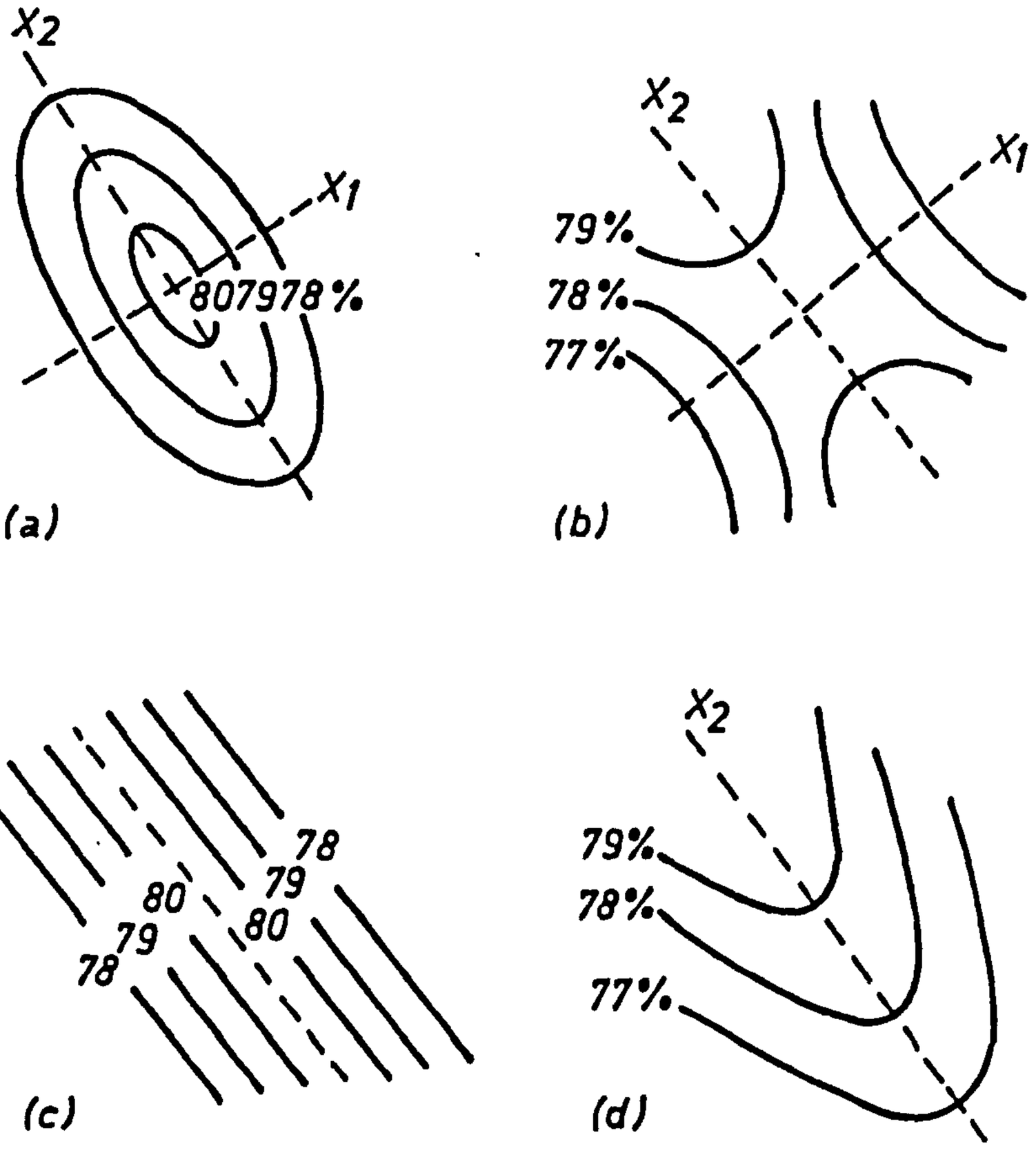

The application of RSM in the field of chemistry has been known for a long time. Thus the following applications have been discussed :-

1) the improvement in the yield of product D in the reaction

   A + B + C ⟶ D + B + C + other products (13).

2) studying the effect of complexing agents on the yield of a certain antibiotic, by fitting a second order model for both cost and yield responses (14).

3) an important application of RSM was to investigate the relationships between copper, iron and molybdenum in the growth and nutrition of lettuce (15,16).

4) RSM has been used to study the precipitation of the dihydrate of calcium hydrogen orthophosphate, $CaHPO_4.2H_2O$ at constant temperature and varying concentrations of calcium chloride and ammonium phosphate (17).

5) From an analytical chemist's point of view, such measured responses could be separation and analysis time. The relationships between the controlled factors in GLC (flow rate, temperature and stationary phase) and the measured response was examined by Morgan et alia (18).

The response surface approach assumes that experimental data can be fitted adequately by a second-order polynomial.

c) Advantages of RSM

RSM has been used to answer questions of different types, as follows (3) :-

i) how is a particular response affected by a given set of input variables over some specified region of interest?

ii) what setting, if any, of the input will give a product simultaneously satisfying desired specifications?

iii) what values of the inputs will yield a maximum for specific response, and what is the response surface like close to the maximum?

RSM has other advantages, which are discussed below :-

i) several responses may be evaluated simultaneously when more than one factor is used;

ii) reducing the time spent in evaluating results;

iii) it can elucidate factor interactions and effects not clearly apparent in the original data from a visual inspection;

iv) for systems involving a large number of factors, the experiment can be designed to estimate the model parameters efficiently with a minimum number of experiments. The response approach can help the experimenter to determine the optimal level for factors and to predict responses within the limits of the experimental region. Therefore, knowledge of the response in the region of the optimum makes it possible to assign which factors must be controlled (1).

6.2 EXPERIMENTAL AND RESULTS

a) Experimental Design : General Criteria

The design of an experiment plays an important role in the investigation of any response relationships. The experimental design may be defined as the combination of each factor level in any set of trials corresponding to points in the space (15).

In general, the factorial design trials for a three-level factorial design is equal to 3^K, where K is equal to a number of factors. Therefore, for K equal to 2, 3 and 4, the number of trials are 9, 27 and 81 respectively. Designs for four factors are generally unsatisfactory, because of the large number of experiments involved. In such cases, a composite design system is more suitable. In the latter, design consists of 2^K factorial and $2K+1$ treatment combinations. In this design for 2, 3 and 4 x-variables, the experiments required are 9, 15 and 25 treatments respectively as compared with 9, 27 and 81 in the 3^K series. Composite designs can be fitted to second-order response surfaces; this starts with a 2^K factorial to which a linear response surface is fitted. Treatment combinations $2K+1$ are added to create a central composite design. The design utilises the results of the initial 2^K experiment and the $2K+1$ treatment combination to which a quadratic surface is fitted (4). In order to introduce rotability to the composite design, the distance (α) between the centre of the composite design and points in the design must be $2^{K/4}$. The value of α is $2^{(K-1)/4}$ with half replication in the case of K = 5 and 6 to keep the design rotatable. The estimated response in the composite rotatable design at a given point have a value which is dependent only on the distance of that point from the centre of the design and not on the direction (see Figure 6.3). This type of design depicts a response surface with a small number of

FIG. 6.3 CENTRAL COMPOSITE ROTATABLE DESIGN IN THREE X VARIABLES WITH FIVE LEVELS

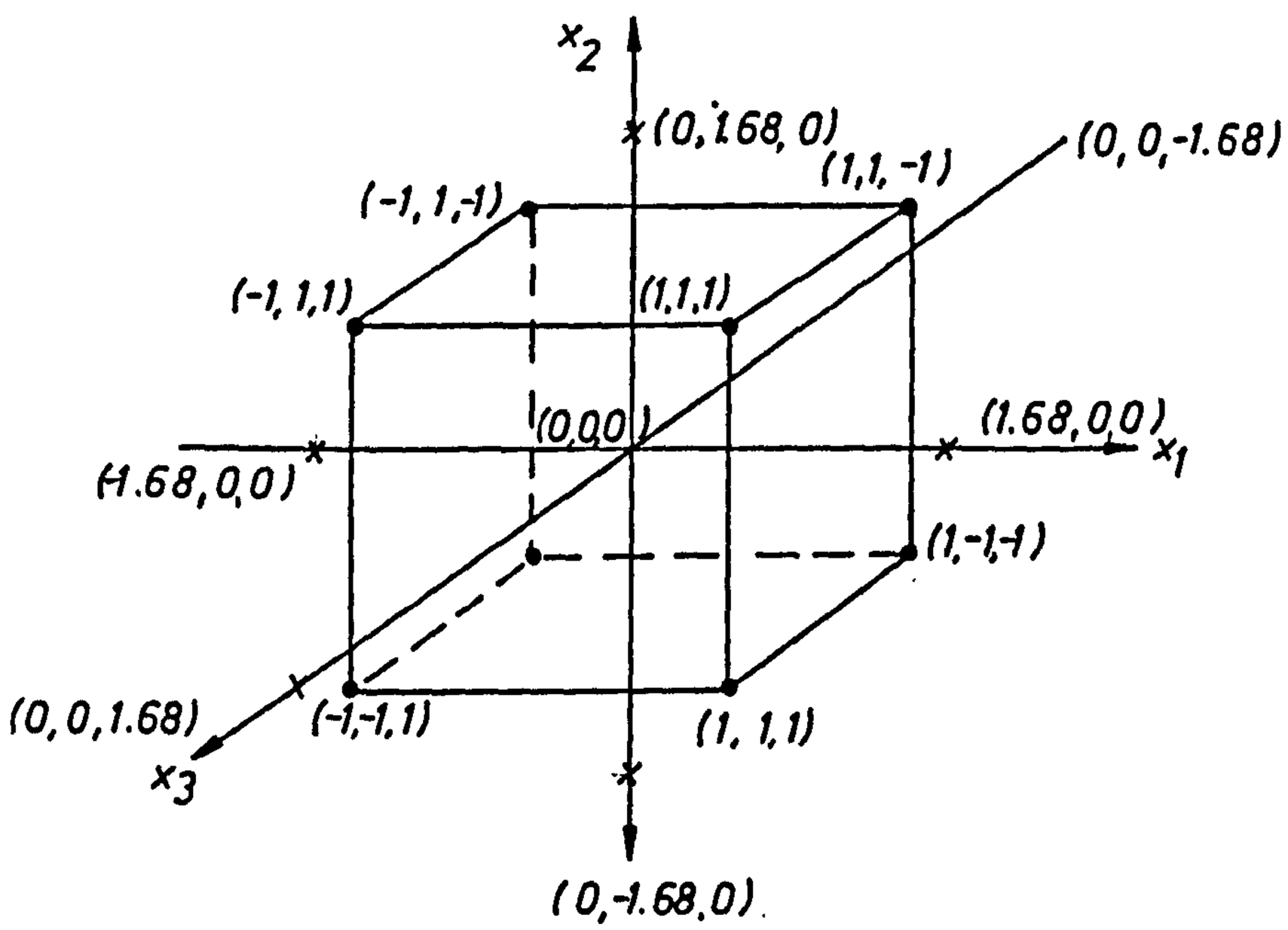

experiments. Therefore, the design was used in the present work.

However, three points must be kept in mind when choosing the experimental design :-

i) what factors should be varied?

ii) in what manner the factors should be varied

iii) by how much should each factor be varied.

b) The Use of RSM to Study Metals Released from Sediments

Restronguet Creek No. 3 (0.5 g) and Adit Bridge No. 8 (0.5 g) sediments were shaken separately with 50 cm^3 of acetate buffer solutions (at different pHs) at different times to investigate the possible influence of pH and time simultaneously with metals released from the sediments. Table 6.2 gives the ratio between acid and salt solutions which were used to prepare the buffer solutions (19).

A 5^2 factorial design was used (see Figure 6.4). The coded values representing the pH and time levels were chosen such that -1.68 to 1.68 were the minimum and maximum values respectively (see Table 6.3). The pH and time were on a logarithmic scale and related to the coded values according to the equation below :-

$$\log (V) = a + bx \qquad [6.9]$$

where V is the variable, either pH or time, a, b are constants, and x is the coded value.

By putting the maximum and minimum values of pH and time in equation 6.9, it was a simple matter to determine the values of a and b and hence the intermediate pH and time values. Table 6.4 shows the coded values with their corresponding pH and time values. In fitting a second-order polynomial to the data, the log scale of pH and time were related to the measured response. The released Ca, Mn, Fe, Cu, Zn and

Pb in each trial of sediments were determined by FAAS. Some samples had metal concentrations which were too low to be detected using the FAAS; their metal concentrations were determined using GFAAS which offers a far greater sensitivity. The results obtained are listed in Tables 6.5 and 6.6. The data were fitted to a second-order polynomial (see Equation 6.6) and analysed by SAS and Minitab packages; the results are presented in Tables 6.7 - 6.10. In each experiment, although there are some 25 data points, this number is insufficient for drawing a 3-D surface, a random picture otherwise being obtained. Therefore, an additional 400 data points were generated using the second-order polynomial equation via a computer program. The extra data now allows a meaningful 3-D surface to be produced. The diagram of the 3-D and contour surfaces which are produced by GINO (Appendix 1) and SAS (Appendix 2) are shown in Figures 6.5 to 6.28.(see page 429 onwards)•

Table 6.2 : Preparation of Buffer Solution (ratio between acid and salt volumes)

pH	0.2M HAc : 0.2M NH_4OAc	0.1M ClAc : 0.1M NH_4OAc
1.99		9 : 1
2.57		5 : 5
3.74	9 : 1	
5.43	1.5 : 8.5	
6.99	0 : 10	

FIG. 6.4 FACTORIAL DESIGN IN TWO X-VARIABLES WITH FIVE LEVELS

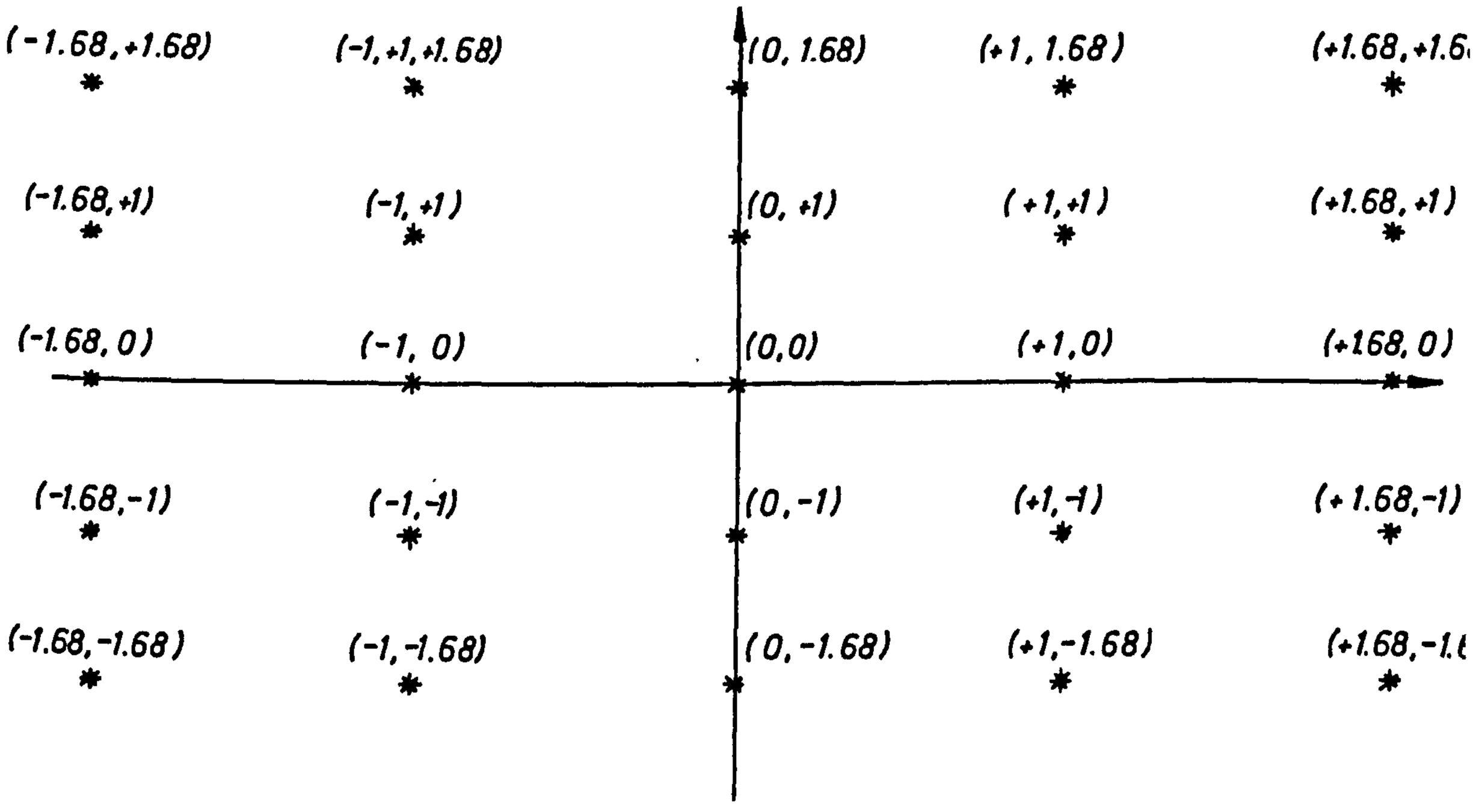

Table 6.3 : Experimental Design 5^2 Factorial

Trials	x_1 (Time)	x_2 (pH)
1	-1.68	-1.68
2	-1.00	-1.68
3	0.00	-1.68
4	1.00	-1.68
5	1.68	-1.68
6	-1.68	-1.00
7	-1.00	-1.00
8	0.00	-1.00
9	1.00	-1.00
10	1.68	-1.00
11	-1.68	0.00
12	-1.00	0.00
13	0.00	0.00
14	1.00	0.00
15	1.68	0.00
16	-1.68	1.00
17	-1.00	1.00
18	0.00	1.00
19	1.00	1.00
20	1.68	1.00
21	-1.68	1.68
22	-1.00	1.68
23	0.00	1.68
24	1.00	1.68
25	1.68	1.68

Table 6.4 : The Coded Values with their Corresponding pH and Time Values

Coded Values	pH Value	Time (hours)
-1.68	1.99	0.5
-1.00	2.57	1.26
0.00	3.74	4.99
+1.00	5.43	19.68
+1.68	6.99	50.00

Table 6.5 : Concentration of Ca, Mn, Fe, Cu, Zn and Pb in Restronguet Creek No. 3 Sediment Released from the Sediment at Different pHs and Times

Trial	Factors				Concentration ($\mu g/g$)					
A	B	C	D	E	Ca	Mn	Fe	Cu	Zn	Pb
1	-1.68	0.50	-1.68	1.99	2045	22	597	135	435	21
2	-1.00	1.26	-1.68	1.99	2747	28	892	213	493	31
3	0.00	4.99	-1.68	1.99	2590	25	1305	207	481	31
4	1.00	19.68	-1.68	1.99	4080	40	2373	237	528	45
5	1.68	50.00	-1.68	1.99	4103	63	2723	276	544	121
6	-1.68	0.50	-1.00	2.57	1874	21	529	147	451	22
7	-1.00	1.26	-1.00	2.57	2451	25	695	152	451	25
8	0.00	4.99	-1.00	2.57	1924	20	291	187	500	70
9	1.00	19.68	-1.00	2.57	2613	20	308	164	490	70
10	1.68	50.00	-1.00	2.57	2290	23	331	209	488	73
11	-1.68	0.50	0.00	3.74	1718	14	271	115	430	20
12	-1.00	1.26	0.00	3.74	1937	20	354	132	460	26
13	0.00	4.99	0.00	3.74	2201	16	600	152	473	24
14	1.00	19.68	0.00	3.74	2729	23	1070	220	559	33
15	1.68	50.00	0.00	3.74	2420	30	1417	257	526	48
16	-1.68	0.50	1.00	5.43	1590	18	140	126	380	20
17	-1.00	1.26	1.00	5.43	1530	14	53	52	295	25
18	0.00	4.99	1.00	5.43	1624	17	22	94	418	27
19	1.00	19.68	1.00	5.43	2000	18	17	142	476	29
20	1.68	50.00	1.00	5.43	1700	20	47	181	478	63
21	-1.68	0.50	1.68	6.99	1431	19	13	52	61	25
22	-1.00	1.26	1.68	6.99	1534	10	13	58	74	22
23	0.00	4.99	1.68	6.99	1481	11	14	57	81	26
24	1.00	19.68	1.68	6.99	1758	13	13	66	252	22
25	1.68	50.00	1.68	6.99	1319	13	14	46	146	24

A = Treatments; B = Coded Time ; C = Actual Time (hour);
D = Coded pH ; E = Actual pH.

Table 6.6 : Concentration of Ca, Mn, Fe, Cu, Zn and Pb in Adit Bridge No.8 Sediment Released from the Sediment at Different pH and Times

Trial Factors					Concentration (μg/g)					
A	B	C	D	E	Ca	Mn	Fe	Cu	Zn	Pb
1	-1.68	0.50	-1.68	1.99	984	490	184	60	260	722
2	-1.00	1.26	-1.68	1.99	1087	560	134	64	151	320
3	0.00	4.99	-1.68	1.99	890	580	454	58	146	206
4	1.00	19.68	-1.68	1.99	809	720	809	75	260	180
5	1.68	50.00	-1.68	1.99	626	780	1348	60	169	713
6	-1.68	0.50	-1.00	2.57	1243	490	68	48	109	131
7	-1.00	1.26	-1.00	2.57	1051	770	368	64	164	490
8	0.00	4.99	-1.00	2.57	10021	620	34	54	151	250
9	1.00	19.68	-1.00	2.57	903	570	50	55	197	211
10	1.68	50.00	-1.00	2.57	706	640	22	58	159	197
11	-1.68	0.50	0.00	3.74	1029	470	42	50	122	159
12	-1.00	1.26	0.00	3.74	1105	460	76	52	164	97
13	0.00	4.99	0.00	3.74	935	530	408	59	141	112
14	1.00	19.68	0.00	3.74	1042	680	494	64	229	18
15	1.68	50.00	0.00	3.74	478	650	752	63	150	244
16	-1.68	0.50	1.00	5.43	1002	470	202	60	106	22
17	-1.00	1.26	1.00	5.43	1213	420	32	52	79	41
18	0.00	4.99	1.00	5.43	1069	484	57	53	104	145
19	1.00	19.68	1.00	5.43	908	518	30	60	141	150
20	1.68	50.00	1.00	5.43	689	560	99	57	249	192
21	-1.68	0.50	1.68	6.99	975	197	15	50	38	22
22	-1.00	1.26	1.68	6.99	1029	225	23	55	42	25
23	0.00	4.99	1.68	6.99	1051	450	17	56	51	28
24	1.00	19.68	1.68	6.99	1213	520	25	57	169	28
25	1.68	50.00	1.68	6.99	859	350	20	57	18	25

A,B,C,D,E, were defined in Table 6.5

Table 6.7 : Response Surface (Log. Scales) for Concentrations of Ca, Mn, Fe, Cu, Zn and Pb in Restronguet Creek No. 3 Sediment Released from the Sediment at Different pHs and Times. Analysis of Data by : a) SAS, b) Minitab

a) SAS

	Ca	Mn	Fe	Cu	Zn	Pb
1. Coefficient						
B_0	2060	16.57	395	156	503	26.3
prob	0.0001	0.0001	0.0485	0.0001	0.0001	0.0009
B_1	-424	3.433	178	23	32	14
prob	0.0001	0.0251	0.0234	0.0002	0.003	0.0001
B_2	-28	-5.94	-413	-14	-91	-14
prob	0.6692	0.567	0.0001	0.0001	0.0001	0.0001
B_{11}	-140	1.884	20.54	5.5	-2	4
prob	0.0080	0.006	0.8009	0.3352	0.881	0.206
B_{22}	86.00	1.337	99.60	-12	-67	-2
prob	0.2025	0.1156	0.2156	0.048	0.001	0.475
B_{12}	-140	-1.90	-135.48	-6.42	7.1	-7
prob	0.0080	0.0032	0.0321	0.1307	0.3839	0.003
2. Regression						
linear (SS)	8690635	1801	7647357	86539	355545	14367
prob	0.0001	0.0001	0.0001	0.0001	0.0001	0.0001
quadratic (SS)	253045	161	348983	5241	138885	533
prob	0.3988	0.562	0.4348	0.0921	0.0001	0.347
cross product (SS)	1149258	211	1072778	2413	2975	2670
prob	0.0080	0.0561	0.0321	0.1307	0.3839	0.003
total (SS)	10092939	2175	9069119	94194	497376	17571
prob	0.0001	0.0004	0.0002	0.0001	0.0001	0.0001
3. Residual						
lack of fit (SS)	2490272	32166	3761286	1837	71163	4530
prob	1.000	0.561	0.3616	1.000	1.00	1.000
pure error (SS)	0.00	0	47740	0	0	0
total error (SS)	2490272	2942	3809026	1837	71163	4530
4. Solution	Saddle point	Saddle point	Saddle point	Saddle point	Maxi-mum	Saddle point

Table 6.7 (continued)

b) Minitab

	Ca	Mn	Fe	Cu	Zn	Pb
1. Coefficient						
B_0	2060	16.57	396	155	503	26
B_1	217	3.43	178.5	23	33	14
B_2	-424	-5.94	-413	-41	-91	-14
B_{11}	-28	1.884	20.54	5.5	-2	3.6
B_{22}	86	1.337	99.61	-12	-67	-2.01
B_{12}	-140	-1.900	-135.4	-7	7	-6.76
2. R-squared (%)	80.2	73.9	70.4	84	87	79.50
R-squared adjusted for d.f. (%)	75.0	67.1	62.6	79	84	74.1
3. Regression						
linear (SS)	8690634	1801	7647356	86539	355545	14367
quadratic (SS)	253045	161	348983	5241	138856	533
cross product (SS)	1149257	211	1072778	2413	2975	2670
total regress (SS)	10092937	2175	9069117	94194	497376	17572
4. Residual	2490272	767	3809026	18372	71162	4531
5. Total (SS)	12583208	2942	12878143	112566	568538	22102

Table 6.8 : Response Surface (Log. Scales) for Concentrations of Ca, Mn, Fe, Cu, Zn and Pb in Adit Bridge No. 8 Sediment Released from the Sediment at Different pHs and Times. Analysis of Data by : a) SAS, b) Minitab

a) SAS

	Ca	Mn	Fe	Cu	Zn	Pb
1. Coefficient						
B_0	1044	590	132	57	161	82
prob	0.0001	0.0001	0.2658	0.0001	0.0001	0.2142
B_1	-98	53	98	2	18	-0.337
prob	0.0001	0.0007	0.033	0.0455	0.0571	0.9893
B_2	31.5	-78	-132	-2	-36	-115
prob	0.1020	0.0001	0.006	0.0508	0.0006	0.0001
B_{11}	-62	-12	34	-0.5196	-0.1826	35.25
prob	0.0066	0.435	0.481	0.5861	0.9847	0.2087
B_{22}	4	-29	22	0.9171	-13.89	29.05
prob	0.846	0.0618	0.6451	0.3405	0.1643	0.2833
B_{12}	29	0.6387	-73	$-3x10^{-3}$	9.6735	11.8619
prob	0.067	0.9524	0.0484	0.9960	0.1842	0.5545
2. Regression						
linear (SS)	407791	337794	1032344	254	61159	505695
prob	0.0001	0.0001	0.0042	0.0257	0.0008	0.0005
quadratic (SS)	120051	29841	51745	34.68	6031	62722
prob	0.0224	0.1288	0.6848	0.542	0.3706	0.2556
cross product (SS)	48207	24	310140	$7x10^{-4}$	5471	7725
prob	0.0678	0.9524	0.0480	0.9960	0.1842	0.5545
total (SS)	576049	367658	1394228	279.95	72662	576142
prob	0.0002	0.0001	0.0120	0.1189	).0042	0.0033
3. Residual						
lack of fit (SS)	244131	123931	1324532	522	54750	383294
prob	1.00	1.000	1.000	1.00	1.000	1.000
pure error (SS)	0.00	0	0	0	0	0
total error (SS)	244131	123931	1324532	522	54750	383294
4. Solution	Saddle point	Maxi-mum	Saddle point	Saddle point	Saddle point	Maxi-mum

Table 6.8 (continued)

b) Minitab

	Ca	Mn	Fe	Cu	Zn	Pb
1. Coefficient						
B_0	1044	590	131	57	161	82
B_1	-98	53	98	2	18	-5
B_2	32	-78	-132	-2	-36	-118
B_{11}	-62	-12	34	-0.46	-0.18	31
B_{22}	4	-29	22	0.98	-14	31
B_{12}	29	0.64	-73	-0.120	10	9.0
2. R-squared (%)	70	75	51	32	57	60.4
R-squared adjusted for d.f. (%)	62	68	38	14	46	50.0
3. Regression						
linear (SS)	407791	337794	1032994	218	84400	530049
quadratic (SS)	120651	29831	51586	36	6030	59797
cross product (SS)	48207	24	31060	0.84	5471	4764
total regress (SS)	576049	367658	1395190	256	72662	595609
4. Residual	244131	123931	1324865	545	54750	390573
5. Total (SS)	820180	491589	2720055	801	127411	86182

c) The Use of RSM to Study Metal Uptake by Plants

Two plant species were used to study the uptake of metals by plants; these were Lolium perenne and Cock's Foot. The species were grown in Hoagland's solution with a double concentration of phosphate for one week. Then the roots of the species were cut and grown in Hoagland's solution without phosphate to prevent precipitation of any metal phosphate.

Four experiments were run, as follows :-

Experiment Number	Species	Metal Ions Added to Nutrient Solution
1	Cock's Foot	La^{3+}, Pb^{2+}, Tl^{+}
2	Cock's Foot	La^{3+}, Pb^{2+}, Ag^{+}
3	Lolium perenne	Al^{3+}, Pb^{2+}, Tl^{+}
4	Lolium perenne	Al^{3+}, Pb^{2+}, Ag^{+}

The metals were added as metal nitrates and the addition was on a logarithmic scale on a level as shown in Table 6.9.

Table 6.9 : The Coded Values with Corresponding Levels of Al, Ag, La Tl and Pb

Coded Value	Concentration of Metals ($\mu g/cm^3$)				
	Al	Ag	La	Tl	Pb
-1.68	$5x10^{-4}$	$2x10^{-4}$	$2.5x10^{-3}$	$1x10^{-4}$	$5x10^{-4}$
-1.00	$3.22x10^{-3}$	$1.28x10^{-3}$	0.0161	$6.4x10^{-4}$	$3.2x10^{-3}$
0.00	0.55	0.02	0.250	0.01	0.05
+1.00	0.755	0.3	3.876	0.155	0.775
+1.68	5.000	2.00	25	1.0	5.000

A composite rotatable design with three variables was used (see Table 6.10). The roots and shoots of plants were digested with concentrated HNO_3 and examined for metals. Lanthanum was determined in plant tissue using Dc-plasma, while aluminium and silver were determined by GFAAS. The other metals in the plant tissue were determined by FAAS. Some samples had metal concentrations which were too low to be detected using the FAAS; therefore GFAAS was used for the determination. The results obtained are given in Tables 6.11 to 6.18. The data were fitted to second-order polynomials (see equation 6.8) and analysed by SAS and the Minitab packages. The results are presented in Tables 6.19 to 6.22. The 3-D plots of measured responses with two metals were drawn up by SAS and GINO packages while the other metal was kept constant. The diagrams obtained are shown in Figures 6.29 to 6.64 (see page 466 onwards).

Table 6.10 : Composite Rotatable Design

Trials		x_1	x_2	x_3
2^3 2 factorial	1	-1	-1	-1
	2	+1	-1	-1
	3	-1	+1	-1
	4	+1	+1	-1
	5	-1	-1	+1
	6	+1	-1	+1
	7	-1	+1	+1
	8	+1	+1	+1
Additional points to form a central composite design	9	+1.68	0	0
	10	-1.68	0	0
	11	0	+1.68	0
	12	0	-1.68	0
	13	0	0	+1.68
	14	0	0	-1.68
Central point	15	0	0	0
	16	0	0	0
	17	0	0	0
	18	0	0	0
	19	0	0	0
	20	0	0	0

Table 6.11 : Tissue Concentrations of La, Pb, Tl, Cu, Zn, Fe, Mg and Mn in Roots of Cock's Foot Seedlings

Trials	Independent variables			Dependent variables									
	x_1(La)	x_2(Pb)	x_3(Tl)	La	Pb	Tl	Cu	Zn	Fe	Mg	Mn	DWOM	R.L*
1	-1	-1	-1	381	520	2.0	3333	612	15000	26984	555	0.0063	2.04
2	+1	-1	-1	2736	305	3.5	2722	527	10000	2444	750	0.009	1.70
3	-1	+1	-1	412	6392	1.0	600	109	6571	3428	250	0.0357	0.46
4	+1	+1	-1	974	841	144	2978	1617	5000	19117	2128	0.0068	2.16
5	-1	-1	+1	1957	1110	3.0	79	154	3157	3092	585	0.0387	3.50
6	+1	-1	+1	3030	935	44	880	251	5194	2500	934	0.0231	4.50
7	-1	+1	+1	261	2186	69	426	684	4195	5375	111	0.0651	9.16
8	+1	+1	+1	3867	1830	73	80	115	7933	4482	81	0.0375	1.34
9	+1.68	0	0	4138	94	13	103	152	6534	4741	112	0.0290	0.82
10	-1.68	0	0	304	842	12	477	372	3630	2826	184	0.1150	16.18
11	0	+1.68	0	1274	5520	5	5312	3771	10937	7812	4464	0.0084	0.56
12	0	-1.68	0	1331	57	15	306	93	5562	4000	118	0.0402	3.78
13	0	0	+1.68	385	196	58	159	42	1850	2240	58	0.0779	0.94
14	0	0	-1.68	522	308	2	52	167	2254	1964	125	0.1638	13.10
15	0	0	0	1384	892	14	811	30	6000	3166	157	0.0302	9.30
16	0	0	0	1152	1013	10	197	96	11912	3500	175	0.0408	10.10
17	0	0	0	1102	643	11	183	45	4177	3285	300	0.0767	15.20
18	0	0	0	1692	872	13	170	538	6206	6250	81	0.0594	13.80
19	0	0	0	1159	682	10	165	211	1171	7500	537	0.0414	11.80
20	0	0	0	860	846	15	181	231	7314	5724	104	0.0605	10.80

R.L. = Root length (cm)

DWOM = Dry weight of plant per treatment (g)

* significant from control

Concentration of Metal = μg/g per dry weight of plant

Table 6.12 : Tissue Concentrations of La, Pb, Tl, Cu, Zn, Fe, Mg and Mn in Shoots of Cock's Foot Seedlings

Trials	Independent variables			Dependent variables								
	x_1(La)	x_2(Pb)	x_3(Tl)	La	Pb	Tl	Cu	Zn	Fe	Mg	Mn	DWOM
1	-1	-1	-1	16	54	0.085	20	26	165	100	45	0.14314
2	+1	-1	-1	277	17	0.290	11	12	105	81	18	0.17202
3	-1	+1	-1	18	591	2.33	26	33	206	108	45	0.12553
4	+1	+1	-1	14	43	1.77	16	22	119	63	38	0.20485
5	-1	-1	+1	378	270	0.260	13	31	116	87	32	0.16496
6	+1	-1	+1	593	61	0.297	15	19	237	136	31	0.09365
7	-1	+1	+1	12	391	0.517	17	29	116	57	17	0.11698
8	+1	+1	+1	518	405	0.410	25	17	193	111	42	0.10978
9	+1.68	0	0	1057	26	1.890	6	26	257	110	38	0.18057
10	-1.68	0	0	9.0	30	3.35	24	22	130	78	66	0.17057
11	0	+1.68	0	18	1410	0.2663	23	21	135	76	45	0.1708
12	0	-1.68	0	96	10	1.030	23	32	119	59	39	0.20261
13	0	0	+1.68	113	59	2.797	20	14	244	132	43	0.08605
14	0	0	-1.68	102	39	0.5103	19	53	122	66	52	0.19713
15	0	0	0	153	54	2.54	22	19	211	134	44	0.10434
16	0	0	0	92	58	1.269	27	24	154	83	35	0.16181
17	0	0	0	7	0.0	0.625	26	35	130	75	37	0.19473
18	0	0	0	85	34	2.083	45	23	167	146	52	0.21009
19	0	0	0	77	30	2.895	52	23	130	82	38	0.17034
20	0	0	0	88	35	1.1651	22	42	130	87	32	0.18495

DWOM = Dry weight of plant per treatment (g)

Concentration of metal = $\mu g/g$ per dry weight of plant

Table 6.13 : Tissue Concentrations of La, Pb, Ag, Cu, Zn, Fe, Mg and Mn in Roots of Cock's Foot Seedlings

Trials	Independent variables			Dependent variables									
	x_1(La)	x_2(Pb)	x_3(Ag)	La	Pb	Ag	Cu	Zn	Fe	Mg	Mn.	DWOM	R.L
1	-1	-1	-1	439	17	20	62	59	373	194	12	0.6128	22.4*
2	+1	-1	-1	995	53	9	65	33	229	180	31	0.2852	22.4
3	-1	+1	-1	165	1957	125	15	151	491	461	9	0.1469	16.50
4	+1	+1	-1	69	18	719	625	104	5250	3250	14	0.4095	17.30
5	-1	-1	+1	202	1534	31	168	570	600	350	27	0.2296	18.60
6	+1	-1	+1	948	214	224	240	229	727	545	33	0.2440	22.50
7	-1	+1	+1	29	960	821	49	154	1000	541	19	0.3621	18.60
8	+1	+1	+1	1626	430	257	35	94	500	498	35	0.1636	14.50
9	+1.68	0	0	3911	100	130	30	33	1187	812	11	0.2264	5.5
10	-1.68	0	0	112	184	190	142	119	1666	1000	41	0.1334	18.50
11	0	+1.68	0	300	905	66	100	210	1804	902	125	0.1269	2.50
12	0	-1.68	0	192	67	77	153	230	468	562	17	0.3130	19
13	0	0	+1.68	186	54	1075	45	89	548	433	22	0.0469	1.50
14	0	0	-1.68	307	116	12	67	97	774	419	45	0.2940	14.5
15	0	0	0	352	173	67	65	56	758	448	53	0.3005	12
16	0	0	0	650	432	100	50	85	700	441	40	0.2968	10.50
17	0	0	0	543	412	45	59	70	745	423	41	0.2873	18
18	0	0	0	454	345	80	58	100	785	399	39	0.4215	13
19	0	0	0	378	239	87	60	85	714	350	40	0.1906	12.5
20	0	0	0	456	198	105	67	97	745	412	35	0.2988	15

DWOM = Dry weight of plant per treatment (g)

R.L. = root length (cm)

* = significant from control

Concentration of metals = μg/g per dry weight of plants

Table 6.14 : Tissue Concentrations of La, Pb, Ag, Cu, Zn, Fe, Mg and Mn in Shoots of Cock's Foot Seedlings

Trials	Independent variables			Dependent variables								
	x_1(La)	x_2(Pb)	x_3(Ag)	La	Pb	Ag	Cu	Zn	Fe	Mg	Mn	DWOM
1	-1	-1	-1	31	4	1	7	19	62	63	38	1.880
2	+1	-1	-1	327	123	2	14	67	31	138	41	0.9397
3	-1	+1	-1	19	288	7	52	55	296	123	33	1.0899
4	+1	+1	-1	12	33	3	10	28	120	159	53	1.0981
5	-1	-1	+1	305	8	11	4	26	178	118	32	1.1823
6	+1	-1	+1	521	22	15	4	31	103	152	54	0.8528
7	-1	+1	+1	3	206	2	7	26	155	129	41	1.1644
8	+1	+1	+1	308	12	4	8	42	137	183	47	0.7168
9	+1.68	0	0	1460	3	6	15	41	223	208	32	0.6715
10	-1.68	0	0	22	11	5	42	46	269	212	125	0.6693
11	0	+1.68	0	39	315	3	20	27	85	109	43	0.4215
12	0	-1.68	0	49	18	2	5	37	45	105	41	1.280
13	0	0	+1.68	13	23	25	10	17	50	180	22	0.2150
14	0	0	-1.68	37	5	1	8	22	96	866	43	0.7639
15	0	0	0	35	17	0.5	14	41	109	702	46	0.8977
16	0	0	0	25	15	0.87	25	50	110	799	44	1.2346
17	0	0	0	44	18	1.20	35	23	112	879	35	0.93450
18	0	0	0	25	22	0.6	41	19	115	745	40	1.03410
19	0	0	0	30	14	0.9	15	45	105	725	41	0.94520
20	0	0	0	28	16	1.0	12	60	130	699	32	0.80230

DWOM = Dry weight of plants per treatment (g)

Concentration of metals = μg/g per dry weight of plants

Table 6.15 : Tissue Concentrations of Al, Pb, Tl and Fe in Roots of Lolium perenne Seedlings

Trials	Independent variables			Dependent variables					
	x_1(Al)	x_2(Pb)	x_3(Tl)	Al	Pb	Tl	Fe	DWOM	R.L
1	-1	-1	-1	83	747	100	1889	0.2159	18.86*
2	+1	-1	-1	126	59	91	1063	0.4198	21.36
3	-1	+1	-1	61	91	190	1855	0.2170	20.50
4	+1	+1	-1	413	2703	150	876	0.5019	22.20
5	-1	-1	+1	20	291	210	1357	0.3083	20.90
6	+1	-1	+1	703	90	180	1581	0.2334	16.20
7	-1	+1	+1	98	9003	120	3673	0.1148	12.80
8	+1	+1	+1	1329	429	100	1376	0.1563	8.900
9	+1.68	0	0	3792	1147	20	1627	0.0603	3.00
10	-1.68	0	0	40	956	70	829	0.2145	19.00
11	0	+1.68	0	534	2261	60	955	0.0387	1.500
12	0	-1.68	0	63	3065	880	827	0.5300	21.40
13	0	0	+1.68	1010	1612	1050	5788	0.0619	7.70
14	0	0	-1.68	19	198	5	656	0.6113	24.20
15	0	0	0	421	361	60	1401	0.2026	24.80
16	0	0	0	314	169	40	920	0.1728	25.20
17	0	0	0	247	344	50	688	0.6024	25.80
18	0	0	0	136	29	10	207	0.5994	26.0
19	0	0	0	153	417	70	1474	0.2887	25.62
20	0	0	0	33	512	50	782	0.5314	24.40

DWOM = Dry weight of plant per treatment (g)

R.L. = Root length (cm)

* = significant from control

Concentration of metals = µg/g per dry weight of plant

Table 6.16 : Tissue Concentrations of Al, Pb, Tl and Fe in Shoots of Lolium perenne Seedlings

Trials	Independent variables			Dependent variables				
	x_1(Al)	x_2(Pb)	x_3(Tl)	Al	Pb	Tl	Fe	DWOM
1	-1	-1	-1	11	17	10.80	284	0.6623
2	+1	-1	-1	13	5	10.80	148	1.9612
3	-1	+1	-1	8	206	10.47	133	0.6241
4	+1	+1	-1	31	0.35	30.52	134	1.5382
5	-1	-1	+1	8	19	5.80	422	1.5271
6	+1	-1	+1	16	2.0	41	141	0.9713
7	-1	+1	+1	104	320	30	245	0.6531
8	+1	+1	+1	6	150	2	119	0.7180
9	+1.68	0	0	93	10	6.30	280	0.3210
10	-1.68	0	0	56	7	3.50	110	1.0773
11	0	+1.68	0	12	4209	1.20	222	0.1278
12	0	-1.68	0	43	238	9	408	0.8827
13	0	0	+1.68	16	44	161	622	0.4013
14	0	0	-1.68	41	13	0.50	134	1.8151
15	0	0	0	40	14	2.0	191	0.5986
16	0	0	0	86	15	3.0	51	0.5196
17	0	0	0	20	22	5.0	97	1.7984
18	0	0	0	40	8	1.50	151	1.5980
19	0	0	0	33	33	2.0	95	0.6834
20	0	0	0	9	5	1.30	100	1.5622

DWOM = Dry weight of plant per treatment (g)

Concentration of metals = µg/g per dry weight of plant

Table 6.17 : Tissue Concentration of Al, Pb, Ag and Fe in Roots of *Lolium perenne* Seedlings

Trials	Independent variables			Dependent variables					
	x_1(Al)	x_2(Pb)	x_3(Ag)	Al	Pb	Ag	Fe	DWOM	R.L
									*
1	-1	-1	-1	23	123	25	988	0.3761	26.4
2	+1	-1	-1	52	109	55	1110	0.3535	21.52
3	-1	+1	-1	23	4563	51	1375	0.2645	21.0
4	+1	+1	-1	63	219	814	524	0.1357	8.0
5	-1	-1	+1	35	192	277	988	0.4425	16.8
6	+1	-1	+1	65	3124	397	1204	0.3029	12.20
7	-1	+1	+1	32	474	1048	2403	0.1523	4.60
8	+1	+1	+1	14	461	38	1154	0.3306	11.80
9	+1.68	0	0	83	2186	23	938	0.4282	14.80
10	-1.68	0	0	8	161	21	463	0.8677	25.80
11	0	+1.68	0	42	2507	438	536	0.7508	20.80
12	0	-1.68	0	10	12	13	455	0.8726	24.60
13	0	0	+1.68	14	196	14	659	0.6010	20.60
14	0	0	-1.68	39	7353	639	2201	0.1799	13.40
15	0	0	0	16	303	39	1154	0.4776	23.40
16	0	0	0	14	121	35	350	0.1369	24.60
17	0	0	0	19	123	27	366	0.5337	26.40
18	0	0	0	13	150	39	402	0.6574	23.80
19	0	0	0	16	118	2.0	435	0.8656	25.0
20	0	0	0	18	83	14	268	0.3574	26.90

R.L. = Root length

DWOM = Dry weight of plant per treatment (g)

* = significant from control

Concentration of metals = μg/g per treatment of plant

Table 6.18 : Tissue Concentrations of Al, Pb, Ag and Fe in Shoots of Lolium perenne Seedlings

Trials	Independent variables			Dependent variables				
	x_1(Al)	x_2(Pb)	x_3(Ag)	Al	Pb	Ag	Fe	DWOM
1	-1	-1	-1	9	4	0.50	82	1.0961
2	+1	-1	-1	10	4	0.45	87	1.087
3	-1	+1	-1	6	121	5.0	82	0.9008
4	+1	+1	-1	41	35	9.8	97	0.7410
5	-1	-1	+1	7	95	2.0	50	1.1652
6	+1	-1	+1	4	14	35.0	305	0.8868
7	-1	+1	+1	10	153	4.0	143	0.7251
8	+1	+1	+1	4	106	0.50	48	0.92471
9	+1.68	0	0	9	23	12.0	52	1.3430
10	-1.68	0	0	5	7	0.39	36	1.5828
11	0	+1.68	0	4	232	1.50	50	1.7152
12	0	-1.68	0	15	0.8	0.50	23	1.2870
13	0	0	+1.68	13	8.0	7.0	36	1.47870
14	0	0	-1.68	12	3.2	3.0	60	0.7550
15	0	0	0	2	8.0	0.39	56	1.1451
16	0	0	0	23	0.89	2.0	25	1.5322
17	0	0	0	5	2.0	3.0	41	1.8812
18	0	0	0	5	2.0	2.0	56	1.3292
19	0	0	0	5	4.2	2.0	42	1.5265
20	0	0	0	5	6.0	4.0	31	1.5621

DWOM = Dry weight of plants per treatment (g)

Concentration of metals = $\mu g/g$ per dry weight of plants

Table 6.19: Response Surface for La, Pb, Tl, Cu, Zn, Fe, Mg and Mn taken up by Root and Shoot of Cock's Foot Seedlings. . Analysis of Data by i) SAS; ii) Minitab

a) Root

i) SAS

	La	Pb	Tl	Cu	Zn	Fe	Mg	Mn	DWOM	R.L
1. Coefficient										
B_0	1143.26	863	10.055	243	187	5274	4427	216.06	0.06831	12.0
prob	0.0001	0.6650	0.256	0.3132	0.0429	0.0758	0.0873	0.3940	0.0008	0.0001
B_1	10.035	-308	10.76	-320	911	1960	-980	-172	0.0116	1.007
prob	0.9483	0.8447	0.1351	0.1080	0.1713	0.3748	0.608	0.3907	0.3290	0.2285
B_2	-259	-2830	10.398	1106.2	54	-3639	-4729	-738	0.0253	2.8313
prob	0.1164	0.0946	0.1475	0.0001	0.5824	0.1154	0.0286	0.003	0.0503	0.0048
B_3	281	-171	1.438	-167	-77	611	-2051	160	-0.004	0.8951
prob	0.0912	0.9131	0.8324	0.3788	0.9056	0.7780	0.2937	0.420	0.5955	0.2806
B_{11}	881.53	-749	16.27	2.65	-19	2699	1476	-75.7	-0.0155	-3.775
prob	0.001	0.5898	0.0188	0.9870	0.8632	0.1755	0.3846	0.6620	0.1595	0.0003
B_{22}	-257	3580	4.050	995	66	2137	1727	684	-0.0054	-1.1923
prob	0.0809	0.0238	0.5017	0.0001	0.4014	0.2754	0.3125	0.0023	0.6179	0.1142
B_{33}	-232	-1045	13.971	52.617	31	1449	948	-78	-0.0046	-3.3217
prob	0.1094	0.4551	0.0371	0.7478	0.2091	0.4519	0.5723	0.6504	0.5565	0.0007
B_{12}	-760	-864	41.515	336	108	9323	3024	49	0.0093	1.359
prob	0.0046	0.6931	0.0011	0.2111	0.6737	0.0097	0.2662	0.8570	0.5594	0.2406
B_{13}	-520	1714	-34.76	-297	-69	-8142	-1670	-91.5	0.00045	-1.09
prob	0.0322	0.4389	0.0036	0.2652	0.4737	0.0194	0.530	0.738	0.9877	0.9223
B_{23}	328	-85	-24.76	433	35	-6776	3435	-91.55	-0.0101	0.451
prob	0.1474	0.9690	0.0371	0.1157	0.5618	0.0432	0.2106	0.7385	0.5297	0.6875
2. Regression										
linear (SS)	1285057	91265292	2021	1841467	102311	763008001	38436251	8529767	$8x10^{-3}$	138
prob	0.2327	0.1350	0.3061	0.0003	0.5482	0.0212	0.0636	0.0085	0.1923	0.0094
quadratic (SS)	14366916	231850134	3607	1450197	107509	67180043	73863844	7150931	$4x10^{-3}$	362
prob	0.0002	0.0007	0.1234	0.0008	0.5290	0.7226	0.6044	0.0149	0.4201	0.0003
cross product (SS)	7199861	20723148	13879	3059002	91473	759480949	187663215	544389	$1x10^{-3}$	15
prob	0.0029	0.0003	0.0029	0.0966	0.5906	0.0215	0.2431	0.7296	0.8683	0.5584
total regress (SS)	22851833	344828574	19508	35975653	301294	1589668993	646363309	161215087	0.0139	515
prob	0.0006	0.0056	0.0147	0.0004	0.6739	0.0305	0.1703	0.0154	0.4614	0.0014
3. Residual										
lack of fit (SS)	1717490	262117738	4787	3297042	277154	422327983	354954756	3971756	0.0024	41.76
prob	0.1030	0.0001	0.0001	0.0041	0.1709	0.0121	0.0014	0.0002	0.08651	0.1715
pure error (SS)	824815	324864	111.42	3795974	179195	74880554	27658620	154153	0.01212	27.0
total error (SS)	2542306	262442602	4899	3676639	456350	497208537	382613375	4125909	0.1459	68.83
4. Solution	Saddle point	Saddle point	Saddle point	Saddle point	Saddle point	Saddle point	Saddle point	Saddle point	Saddle point	Saddle point

Table 6.19 (continued)

ii) Minitab

	La	Pb	Tl	Cu	Zn	Fe	Mg	Mn	DWOM	R.L
1. Coefficient										
B_0	1143.3	863	10.005	242.7	188	5269	4418	216.6	0.068	12.00
B_1	10.0	-308	10.768	-326	111	-2038	-1117	-165.4	0.0116	1.007
B_2	-2519.4	-2831	10.399	-1113	54	3737	-5211	-710.6	0.0253	2.8313
B_3	281.9	-172	1.439	-141	-77	912	-1867	152.9	-0.004	0.8951
B_{11}	881.5	-749	16.274	6.1	-19	2739	1546	-79.4	-0.0155	-3.7752
B_{22}	-257	3580	4.051	999	66	2177	1301	709.8	-0.0054	-1.1923
B_{33}	-232.6	-1045	13.971	28	31	1168	948	-82.4	-0.0046	-3.3217
B_{12}	-760.6	-864	41.516	324	108	9190	2790	61.5	0.0093	1.359
B_{13}	-520.5	1714	-34.76	-285	-69	-8010	-1437	-316	0.00045	-0.109
B_{23}	328.7	-85	-24.77	445	35	-6644	3669	-103.7	-0.0101	0.451
2. R-squared (%)	90	56	79	90	43	75	64	81.0	48	88
R-squared adjusted for d.f. (%)	81.0	17	61	81	-8	53	31	63.9	1.5	77
3. Regression										
linear (SS)	1285057	91265292	2021	1841467	102311	763008001	85958644	8529767	0.0024	48
quadratic (SS)	14366916	231850134	3607	1450197	1107509	73863844	77373638	7140931	0.08651	27
cross product (SS)	7199861	20723148	13879	3059002	91473	187663215	66513950	544389	0.01458	75
total regress (SS)	22851830	343838536	19509	360833483	341060	1591895240	681511878	16341255	0.01370	515.516
4. Residual (SS)	2542306	262442588	4899	3845858	451612	521598285	383079183	3838621	0.01475	68.837
5. Total (SS)	25394136	606291119	24408	39929341	792673	2113493502	1064591065	20179876	0.028455	584.35

Table 6.19 (continued)

b) Shoot

i) SAS

	La	Pb	Ag	Cu	Zn	Fe	Mg	Mn	DWOM
1. Coefficient									
B_0	91.91	40.3	78.50	34.74	28.53	149.96	96.28	41.72	0.1567
prob	0.1564	0.7422	0.2166	0.0001	0.0001	0.0001	0.0001	0.0001	0.0001
B_1	-75.74	42.52	-0.54	1.658	-2.449	-24.71	-7.123	-1.99	0.0169
prob	0.1393	0.6623	0.9912	0.6587	0.4073	0.0728	0.4389	0.5623	0.1783
B_2	-16.94	-120.55	0.33	1.933	-0.045	15.10	4.140	3.905	$2x10^{-5}$
prob	0.7269	0.2309	0.9945	0.6071	0.9877	0.2487	0.6495	0.2689	0.9989
B_3	59.47	0.46	-0.10	-1.294	3.703	-18.904	-11.230	-4.01	$4x10^{-3}$
prob	0.2359	0.9962	0.9985	0.7297	0.2201	0.1554	0.2367	0.2570	0.7162
B_{11}	212.48	29.82	-26.66	-7.052	-2.269	20.88	4.072	-2.661	-0.0132
prob	0.0004	0.7266	0.5339	0.0517	0.3825	0.0825	0.6108	0.3845	0.2249
B_{22}	-61.75	208.57	-26.43	-4.218	-2.269	-11.89	-7.797	2.831	$8x10^{-3}$
prob	0.1664	0.0306	0.5374	0.2161	0.3825	0.2971	0.3382	0.3562	0.4136
B_{33}	-29.5	-34.31	-26.39	-4.927	-1.737	5.47	-1.242	-2.302	0.01272
prob	0.4920	0.6877	0.5380	0.1540	0.5002	0.6241	0.8759	0.4076	2442
B_{12}	-172.25	-54.6	-0.28	1.837	-1.268	-12.95	-13.61	4.00	0.03013
prob	0.0250	0.6860	0.9970	0.7236	0.7500	0.4662	0.2929	0.8744	0.0931
B_{13}	-38.25	146.3	0.28	0.913	7.036	-2.30	-1.39	-0.75	$8x10^{-3}$
prob	0.5717	0.2904	0.9967	0.8602	0.1034	0.8958	0.9919	0.3251	0.6227
B_{23}	80.25	-49.4	-0.22	-2.337	-0.964	2.70	4.11	-7.75	0.0145
prob	0.2480	0.7140	0.9974	0.6534	0.8111	0.8775	0.744	0.1249	0.3944
2. Regression									
linear (SS)	60554	701534	249	113	133	16425	2956	342.8	0.00218
prob	0.5153	0.5805	0.997	0.8567	0.6933	0.0694	0.383	0.4661	0.7062
quadratic (SS)	806045	713704	26992	1247	130	9654	1168	354	0.00626
prob	0.0018	0.1301	0.7818	0.094	0.7003	0.1940	0.7250	0.452	0.3085
cross product (SS)	235462	182100	1.46	62	339	1189	1254	391	0.00551
prob	0.0728	0.6243	1.000	0.933	0.3379	0.8708	0.7037	0.4126	0.3581
total regress (SS)	1102062	1101147	27243	1417	603	27268	5378	1088.62	0.0139
prob	0.0101	0.3749	0.9980	0.4582	0.6627	0.1895	0.7092	0.5114	0.4864
3. Residual									
lack of fit (SS)	237163	994766	53.6	232	50.9	10954	2987	850.6	0.00343
prob	0.0003	0.0001	1.00	0.880	0.982	0.1304	0.5761	0.0957	0.7801
pure error (SS)	11107	2153	248365	1247	843.7	6004	5730	391.71	0.011
total error (SS)	248270	996919	248419	1480	894.6	16959	8717	1242	0.0152
4. Solution	Saddle point	Saddle point	Saddle point	Maxi-mum	Saddle point	Saddle point	Saddle point	Saddle point	Saddle point

SS = sum of squares

Table 6.19 (continued)

ii) Minitab

	La	Pb	Tl	Cu	Zn	Fe	Mg	Mn	DWOM
1. Coefficient									
B_0	91.91	40.3	78.50	34.74	28.53	149.96	96.28	41.72	0.1567
B_1	-75.74	42.52	-0.54	1.658	-2.449	-24.71	-7.123	-1.99	0.0169
B_2	-16.94	-120.55	0.33	1.933	-0.045	15.10	4.140	3.905	$2x10^{-5}$
B_3	59.47	0.46	-0.10	-1.294	3.703	-18.94	-11.230	-4.01	$-4x10^{-3}$
B_{11}	212.48	29.82	-26.66	-7.052	-2.269	20.88	4.072	-2.661	-0.0132
B_{22}	-61.75	208.57	-26.43	-4.218	-2.269	-11.89	-7.797	2.831	$8x10^{-3}$
B_{33}	-29.51	-34.31	-26.39	-4.927	-1.737	5.47	-1.242	-2.307	0.01272
B_{12}	-172.25	-54.6	-0.28	1.837	-1.268	-12.95	-13.61	4.00	0.03013
B_{13}	-38.25	146.3	0.28	0.913	7.036	-2.30	-1.39	-0.75	$-8x10^{-3}$
B_{23}	80.25	-49.4	-0.22	-2.377	-0.964	2.70	4.11	-7.75	-0.0145
2. R-squared (%)	81.6	52	9.9	48.9	40.3	61	38	46	47
R-squared adjusted for d.f. (%)	65.1	9.7	-71	3.0	13.5	27	-17	-1.3	0.8
3. Regression									
linear (SS)	60554	701534	249	113	133	16425	2956	342	
quadratic (SS)	806045	713804	26992	1247	130	9654	1168	354	
cross product (SS)	235462	182100	1.46	62	339	1189	1254	391	
total regress (SS)	1102062	1101147	27244	1417	603	27269	5379	1088	0.013968
4. Residual (SS)	248271	996920	248419	1480	894	16959	8718	1242	0.015259
5. Total (SS)	1350332	2098066	275663	2897	1497	44228	14096	2330	0.029227

Table 6.20 : Response Surface for La, Pb, Ag, Cu, Zn, Fe, Mg and Mn taken up by Root and Shoot of Cock's Foot Seedlings. Analysis of Data by i) SAS; ii) Minitab

a) Root

i) SAS

	La	Pb	Ag	Cu	Zn	Fe	Mg	Mn	DWOM	R.L
1. Coefficient										
B_0	335	160.43	58.46	57.59	81.61	736.51	416	42.04	0.29512	13.2
prob	0.1270	0.2550	0.1142	0.2438	0.0274	0.0497	0.0859	0.0023	0.0002	0.0006
B_1	692.74	-63.183	-85.71	36.12	-59.98	-429.6	-233	1.436	-0.03318	-2.064
prob	0.0004	0.4902	0.0095	0.2690	0.0170	0.0783	0.1382	0.838	0.3411	0.3089
B_2	-18.21	438.76	12.483	6.59	-16.24	-189.34	-127	13.150	-0.0704	-2.535
prob	0.8943	0.0006	0.6510	0.8351	0.4569	0.4078	0.3991	0.084	0.0597	0.2173
B_3	48.86	-149.73	260.19	-22.13	35.66	396.07	221	-1.366	-0.0374	-1.603
prob	0.8943	0.1204	0.0001	0.4897	0.1201	0.1008	0.1591	0.846	0.2862	0.426
B_{11}	532	74.67	38.74	23.51	1.33	272.32	197	-9.961	-0.01615	1.325
prob	0.8950	0.4054	0.1300	0.4525	0.9495	0.2311	0.194	0.1677	0.6285	0.467
B_{22}	-93.105	196.559	7.386	37.86	52.35	80.824	135	5.982	$-1x10^{-3}$	0.882
prob	0.4913	0.0453	0.7598	0.2367	0.0284	0.7130	0.3620	0.392	0.9533	0.625
B_{33}	-92.92	54.482	I74.79	12.88	7.35	1.1048	-43	-7.304	$-1x10^{-2}$	-0.0915
prob	0.4921	0.5404	0.0001	0.6775	0.7267	0.9960	0.7708	0.3009	0.5605	0.959
B_{12}	24.75	-148.125	-30.89	63.87	57.35	534.5	320	-0.75	0.0471	0.8204
prob	0.891	0.2274	0.4248	0.1440	0.0623	0.0914	0.1220	0.935	0.3023	0.4795
B_{13}	235	6.625	-131.147	-68.12	-66	-623.5	-328	-0.5	-0.0148	0.479
prob	0.2077	0.9553	0.0054	0.1219	0.0368	0.0544	0.6012	0.9567	0.7385	0.8607
B_{23}	213	-282.87	10.147	105.89	64.25	-620.5	-399	1.5	0.0492	-0.229
prob	0.2500	0.0339	0.7902	0.0253	0.0411	0.0533	0.0613	0.8706	0.2829	0.9330
2. Regression										
linear (SS)	6585120	2987219	1098768	25076	70045	5148682	1635663	2413	0.1019	177.11
prob	0.0034	0.0030	0.0001	0.646	0.0445	0.1086	0.1943	0.3433	0.1441	0.3083
quadratic (SS)	4634977	612799	426343	27074	39674	1121363	826813	2834	0.0084	32.33
prob	0.0111	0.1896	0.0002	0.5762	0.1510	0.6471	0.4495	0.2819	0.9032	0.8598
cross product (SS)	811446	816025	103996	159444	94322	8478185	2955333	24.5	0.0389	2.829
prob	0.3907	0.1134	0.0336	0.0391	0.0199	0.0340	0.0605	0.997	0.4917	0.9953
total regress (SS)	12031543	4416044	1629108	211595	204042	14748229	5417808	5272	0.1492	212.27
prob	0.0069	0.0127	0.0001	0.1845	0.001	0.0848	0.1327	0.5518	0.4372	0.8115
3. Residual										
lack of fit (SS)	2432798	1059657	79529	58714	2565	6547259	2873753	6254	0.1235	391.91
prob	0.0001	0.0001	0.0001	0.0004	0.0006	1.00	0.0001	0.0007	0.0599	0.0029
pure error (SS)	6944	1840	478	178	1386	4666	2137	185	0.0269	39.80
total error (SS)	2439742	1061497	80008	129958	60101	6551925	2875890	6440	0.1504	431.71
4. Solution	Saddle point	Saddle point	Saddle point	Saddle point	Saddle point	Saddle point	Saddle point	Saddle point	Saddle point	Saddle point

Table 6.20 (continued)

ii) Minitab

	La	Pb	Ag	Cu	Zn	Fe	Mg	Mn	DWOM	R.L
1. Coefficient										
B_0	335	160.4	58.46	57.59	81.61	736.5	416	42.05	0.2473	13.207
B_1	693	-63.18	-85.72	36.12	-59.98	-429.7	-233	1.436	-0.033	-2.064
B_2	-18.2	438.76	12.48	6.59	-16.24	-189.3	-127	13.151	-0.0705	-2.535
B_3	49	-149.74	260.20	-22.13	35.66	396	220	-1.366	-0.0374	-1.603
B_{11}	532	74.68	38.74	23.51	1.33	272	196	-9.961	$1x10^{-4}$	1.326
B_{22}	-93	196.56	7.39	37.86	52.35	80.8	135	5.982	0.0143	0.480
B_{33}	-93	54.48	174.80	12.88	7.35	1.1	-42.4	-7.304	$-3x10^{-3}$	-0.092
B_{12}	25	148.1	-30.90	63.87	57.50	534.5	320	-0.750	0.0471	-0.616
B_{13}	235	6.6	-131.15	-68.12	-66.00	-623.5	-327	-0.50	-0.0148	0.480
B_{23}	213	-282.9	10?15	-105.87	-64.25	-620.7	-399	1.50	0.0492	0.230
2. R-squared (%)	83	80.6	95.3	62.0	77	69.2	65	45	39.2	33.0
R-squared adjusted for d.f. (%)	68	63.2	91.1	27	56	41.6	34	4.5	15.6	27.4
3. Regression										
linear (SS)	6585119	2987218	450369	25076	70045	5148681	1635663	2412	0.1018	175
quadratic (SS)	4634977	612800	1098768	27074	39674	1121364	626813	2835.5	$1.92x10^{3}$	32.12
cross product (SS)	811445	816025	79871	159444	94322	4027317	2957332	24.5	0.0403	4.88
total regress (SS)	12031541	4416043	1629108	211585	204042	14748227	5417808	5272	0.1441	212
4. Residual (SS)	2439741	1061497	80009	129959	60101	6551925	2875890	6440	0.2237	431
5. Total (SS)	14471282	5477539	1709117	31554	264144	21300152	8293698	11712	0.3679	643

Table 6.20 (continued)

b) Shoot

i) SAS

	La	Pb	Ag	Cu	Zn	Fe	Mg	Mn	DWOM
1. Coefficient									
B_0	34.31	16.277	0.892	40.07	114	107.36	762	39.88	0.959119
prob	0.6071	0.4226	0.6330	0.0001	0.0001	0.0001	0.0001	0.0002	0.0001
B_1	279.36	-27.80	1.5155	-5.596	-0.50	-15.05	6.616	-1.021	-0.11265
prob	0.0001	0.0569	0.2361	0.2068	0.6324	0.0189	0.877	0.847	0.2602
B_2	-19.99	60.899	0.3429	2.067	2.58	51.462	4.963	-14.95	-0.150929
prob	0.6512	0.0008	0.7813	0.6453	0.2954	0.0001	0.9081	0.0161	0.1409
B_3	8.917	-8.776	3.1748	-4.793	-12	5.754	-72.66	3.425	-0.1599
prob	0.8392	0.5125	0.0247	0.2735	0.1053	0.3030	0.1138	0.5251	0.1211
B_{11}	231.53	1.0386	1.2801	-6.50	-30	28.555	-219	0.1717	-9×10^{-3}
prob	0.0002	0.9359	0.3003	0.1395	0.0001	0.0002	0.0003	0.9716	0.9203
B_{22}	-15.417	57.550	0.2171	-5.30	-23	27.49	-255	12.395	0.054
prob	0.7200	0.0010	0.8567	0.220	0.0013	0.0002	0.0001	0.0252	0.5669
B_{33}	-22.148	3.5188	3.9374	-9.70	-20	-18.390	-108	-3.9028	-0.073
prob	0.6079	0.7856	0.0072	0.0383	0.0033	0.0036	0.0240	0.4269	0.4425
B_{12}	-26.75	-72.75	-0.875	6.37	-13	-18.115	0.125	3.4822	0.1038
prob	0.6434	0.0015	0.5896	0.2220	0.2470	0.0002	0.9982	0.6343	0.4194
B_{13}	29	-5.5	1.125	4.87	-5	31.6149	-5.37	-1.751	0.0193
prob	0.6160	0.7512	0.4901	0.0468	1.000	0.0019	0.923	0.8116	0.8782
B_{23}	-23.15	-0.75	-3.375	4.62	-3.20	-44.135	-2.37	-2.7519	0.0597
prob	0.6838	0.9654	0.0571	0.0468	0.7938	0.0002	0.998	0.7084	0.6385
2. Regression									
linear (SS)	1071423	62207	170.48	815.93	1575	38293	72978	2658.28	0.832
prob	0.0006	0.0033	0.0892	0.3831	0.263	0.0001	0.0001	0.0918	0.1412
quadratic (SS)	816441	47932	235	2044	20150	28553.9	1552684	2534.65	0.1338
prob	0.0017	0.0080	0.0420	0.0926	0.0002	0.0001	0.0001	0.1013	0.7785
cross product (SS)	16870	42587	107	699	536	26160	276	91.99	0.11773
prob	0.8776	0.0117	0.2082	0.445	0.6742	0.0001	0.9996	0.9591	0.8082
total regress (SS)	1904735	152727	513	3559	22262	93007	1625938	5284.93	1.0844
prob	0.0013	0.0021	0.0569	0.2250	0.0023	0.0001	0.0020	0.1689	0.5007
3. Residual									
lack of fit (SS)	250920	22748	197	1151.75	3018	2565	215779	2525.72	1.1066
prob	0.0002	0.0001	0.0001	0.5365	0.0202	0.0060	0.0157	0.023	0.0118
pure error (SS)	266	40	0.3681	1255	382	222	24196	591.33	0.1089
total error (SS)	251193	22788	197.36	2407	3399	2787	239975	3117.06	1.2156
4. Solution	Saddle point	Saddle point	Saddle point	Saddle point	Maxi-mum	Saddle point	Maxi-mum	Saddle point	Saddle point

SS = sum of squares

Table 6.20 (continued)

ii) Minitab

	La	Pb	Ag	Cu	Zn	Fe	Mg	Mn	DWOM
1. Coefficient									
B_0	34.32	16.28	0.884	40.07	114	108.39	762.15	40.199	0.9591
B_1	279.36	-27.81	1.516	-5.596	-0.50	-33.02	6.62	4.391	-0.1126
B_2	-19.99	60.90	0.343	2.067	2.58	33.50	4.92	-9.391	-0.151
B_3	8.92	-8.78	3.175	-4.793	-12	12.43	-72.66	-1.560	-0.159
B_{11}	231	1.04	1.283	-6.50	-30	22.068	-219	-1.783	$-9x10^{-3}$
B_{22}	-15.42	57.55	0.220	-5.30	-23	21.005	4255	10.440	0.0543
B_{33}	-22.15	3.52	3.940	-9.70	-20	-24.87	-108	-5.858	-0.0735
B_{12}	-26.75	-72.75	-0.875	-6.37	-13	-48.75	0.12	-5.750	0.1038
B_{13}	29.00	-5.50	1.125	4.87	-5	43.00	-5.37	6.750	0.0194
B_{23}	-23.50	-0.75	-3.375	-4.62	-3.20	-32.75	-2.37	5.750	0.0597
2. R-squared (%)	88.3	87	72.2	59	87	90.7	87.1	50	47
R-squared adjusted for d.f. (%)	77.9	75	47.3	22	76	81.3	75.6	5.0	0.4
3. Regression									
linear (SS)	1071422	62208	169	816	1575	33348	72977	1539	0.832
quadratic (SS)	816442	47933	235	2044	20150	26057	1552684	2322	0.1338
cross product (SS)	16870	42587	109	699	536	39077	277	895	0.11773
total regress (SS)	1904734	152728	513	3559	22262	98482	1625938	4756	1.0845
4. Residual (SS)	251194	22789	197	2414	3584	10152	239976	4752	1.2161
5. Total (SS)	2155928	175517	710	5930	29173	10863	1865914	9509	2.3006

Table 6.21 : Response Surface for Al, Pb, Tl and Fe taken up by Roots and Shoots of Lolium perenne Seedlings. Analysis of Data by i) SAS, ii) Minitab

a) Root

i) SAS

	Al	Pb	Tl	Fe	DWOM	R.L
1. Coefficient						
B_0	237.34	303.35	54.1	916	0.3986	25.11
prob	0.3933	0.6112	0.6295	0.0504	0.0004	0.0001
B_1	573.57	-832.121	-4.62	-115	-0.0136	-2.48
prob	0.0088	0.0553	0.9503	0.6819	0.7884	0.0828
B_2	71.4	356.49	-93.71	224	-0.1025	-3.58
prob	0.6945	0.3748	0.2236	0.4304	0.0651	0.0193
B_3	287.13	982.97	125.66	730	-0.078	-3.63
prob	0.1351	0.023	0.1125	0.0235	0.1419	0.0188
B_{11}	474.98	277	-47.98	85	-0.086	-3.86
prob	0.0202	0.4762	0.5109	0.7558	0.1087	0.0118
B_{22}	-98.10	848	102.60	-34	-0.035	-3.76
prob	0.5813	0.0468	0.1757	0.9006	0.5044	0.0146
B_{33}	-21.575	225	122.97	792	-0.016	-2.07
prob	0.9027	0.5609	0.1112	0.0140	0.7637	0.1243
B_{12}	107.125	-634	-2.62	-334	0.024	0.000
prob	0.6523	0.2345	0.9783	0.3715	0.7108	1.00
B_{13}	189.80	-1337	-0.13	-34	-0.065	-1.60
prob	0.4296	0.0236	0.9990	0.9271	0.3347	0.3641
B_{23}	54.875	883	-39.87	282	-0.044	-2.235
prob	0.8168	0.1086	0.6814	0.4335	0.5096	0.2136
2. Regression						
linear (SS)	5683551	24366275	335559	8147060	0.23128	437
prob	0.0312	0.0403	0.2570	0.1052	0.1389	0.0106
quadratic (SS)	3589949	11095993	404024	9190180	0.11321	403
prob	0.0939	0.2036	0.1949	0.0817	0.3839	0.0135
cross product (SS)	404316	23761237	12775	1582541	0.0546	60.44
prob	0.8132	0.0429	0.9798	0.6801	0.6632	0.4795
total regress (SS)	9677816	59223505	752359	18920680	0.39910	901.87
prob	0.0825	0.0393	0.4003	0.1379	0.3322	0.0147
3. Residual						
lack of fit (SS)	4160344	19943003	709711	9089845	0.1212	225
prob	0.0004	0.0001	0.0001	0.0191	0.752	0.0001
pure error (SS)	96437	154721	2133	1119130	0.2134	1.912
total error (SS)	4256782	20097724	711844	10208975	0.3346	226.912
4. Solution	Saddle point	Saddle point	Saddle point	Saddle point	Saddle point	Maximum

SS = sum of squares

Table 6.21 (continued)

ii) Minitab

	Al	Pb	Tl	Fe	DWOM	R.L
1. Coefficient						
B_0	237.3	303	54.1	916	0.3986	25.11
B_1	573.6	-832.1	-4.62	-115	-0.0136	-2.48
B_2	71.4	356.5	-93.71	224	-0.1025	-3.58
B_3	787.1	983	125.66	730	-0.078	-3.63
B_{11}	475	276.9	-47.98	85	-0.086	-3.86
B_{22}	-98.1	847.9	102.60	-34	-0.035	-3.70
B_{33}	-21.6	225	122.97	792	-0.016	-2.07
B_{12}	107.1	-634	-2.62	-334	0.024	0.00
B_{13}	189.9	-1337.4	-0.13	-34	-0.065	-1.60
B_{23}	54.9	882.9	-39.87	292	-0.044	-2.235
2. R-squared (%)	69	74	51	65	55	80
R-squared adjusted for d.f. (%)	42	51	7	33	15	62
3. Regression						
linear (SS)	5683551	24366275	33559	8147060	0.23128	437
quadratic (SS)	3589949	11095993	404024	9191080	0.11321	403
cross product (SS)	404316	2371237	12775	1582541	0.0546	60
total regress (SS)	9677814	59223498	752360	18920677	0.404	904
4. Residual (SS)	4256781	20097723	711845	10208974	0.322	226
5. Total (SS)	13934596	79321221	1464204	29129652	0.726	1130

Table 6.21 (continued)

b) Shoot

i) SAS

	Al	Pb	Tl	Fe	DWOM
1. Coefficient					
B_0	38.64	39.90	2.86	117.60	0.907
prob	0.0135	0.9887	0.7805	0.0880	0.0006
B_1	-3.57	-26.6	-1.314	23.42	0.0315
prob	0.6850	0.8984	0.8466	0.5832	0.840
B_2	0.214	538.1	-4.209	-7.36	-0.2110
prob	0.9806	0.0241	0.5392	0.8621	0.1947
B_3	5.497	20.30	24.50	34.58	-0.239
prob	0.5356	0.9221	0.0042	0.4220	0.1456
B_{11}	8.862	-153.1	0.7519	0.8735	0.5966
prob	0.3135	0.4563	0.7519	0.8735	0.5966
B_{22}	-7.790	631.7	-2.119	49.09	-0.078
prob	0.3729	0.0095	0.7519	0.2506	0.3359
B_{33}	-7.436	-146	24.68	71.42	0.1351
prob	0.3941	0.4769	0.0034	0.1064	0.6742
B_{12}	-10.62	-43.30	-5.43	36.50	0.0295
prob	0.3648	0.873	0.5434	0.514	0.8847
B_{13}	-14.37	3.80	-1.663	-34	-0.338
prob	0.2279	0.9887	0.8514	0.5426	0.1191
B_{23}	8.87	33.1	-4.29	-4.25	-0.083
prob	0.4461	0.9030	0.6303	0.9388	0.6834
2. Regression					
linear (SS)	588	3965772	8409	24542	1.404
prob	0.8970	0.1330	0.0271	0.7891	0.2766
quadratic (SS)	3046	6926048	9236	99200	0.4897
prob	0.4269	0.0383	0.0208	0.2939	0.6786
cross product (SS)	3186	23893	406	20050	0.9763
prob	0.4087	0.9975	0.8760	0.8337	0.4185
total regress (SS)	6820	10915714	18052	143793	2.8703
prob	0.6573	0.1225	0.0365	0.7086	0.4870
3. Residual					
lack of fit (SS)	6516	5604083	5973	220676	1.4376
prob	0.2560	0.0001	0.0001	).0032	0.5725
pure error (SS)	3502	515	7.180	12113	1.7070
total error (SS)	10018.05	5604598	5980.18	232789	3.144
4. Solution	Saddle point	Saddle point	Saddle point	Saddle point	Saddle point

SS = sum of squares

Table 6.21 (continued)

ii) Minitab

	Al	Pb	Tl	Fe	DWOM
1. Coefficient					
B_0	38.64	39.9	2.86	117.60	0.907
B_1	-3.57	-26.6	-1.314	23.42	0.0315
B_2	0.214	538.1	-4.209	-7.36	-0.2110
B_3	5.497	20.3	24.50	34.58	-0.239
B_{11}	8.862	-153.1	-2.119	6.58	-0.009
B_{22}	-7.790	631.7	-2.119	49.09	-0.078
B_{33}	-7.436	-146	24.68	71.42	0.1351
B_{12}	-10.62	-43.3	-5.43	36.50	0.0295
B_{13}	-14.37	3.8	-1.663	-34	-0.338
B_{23}	8.87	33.1	-4.29	-4.25	-0.083
2. R-squared (%)	40.5	66	75	38	50
R-squared adjusted for d.f. (%)	13.0	35	52	17	5
3. Regression					
linear (SS)	588	3965772	8409	24542	1.404
quadratic (SS)	3046	6926048	9236	99200	0.4897
cross product (SS)	3186	23893	406	20050	0.9763
total regress (SS)	6820	10915712	18168	143794	2.76
4. Residual (SS)	10018	5604597	6037	232789	2.73
5. Total (SS)	16838	16520310	24205	376583	5.508

Table 6.22 : Response Surface for Al, Pb, Ag and Fe taken up by Roots and Shoots of Lolium perenne Seedlings. Analysis of Data by : i) SAS, ii) Minitab

a) Root

i) SAS

	Al	Pb	Ag	Fe	DWOM	R.L
1. Coefficient						
B_0	15.844	185	21.6	485	0.9313	26.28
prob	0.0622	0.7583	0.8615	0.040	0.0001	0.0001
B_1	11.066	147	-89	-2.6	-0.017	-1.677
prob	0.0517	0.7118	0.290	0.9850	0.8477	0.3703
B_2	-3.316	469	65	164	-0.0135	-1.488
prob	0.5231	0.253	0.4350	0.2589	0.8823	0.4246
B_3	-0.073	-926	63	-130	0.0141	-2.713
prob	0.9886	0.038	0.4430	0.365	0.8763	0.1600
B_{11}	11.439	142	270	140	-0.160	-2.418
prob	0.0412	0.7154	0.7410	0.317	0.0908	0.1952
B_{22}	4.530	172	99	67	-0.102	-2.276
prob	0.3755	0.6583	0.2349	0.623	0.2589	0.2205
B_{33}	4.707	1063	133	399	-0.252	-4.296
prob	0.3578	0.0183	0.120	0.0135	0.0150	0.0333
B_{12}	-4.625	-922	-43	-305	0.0263	0.460
prob	0.4958	0.0984	0.6870	0.1182	0.8231	0.8477
B_{13}	-7.125	897	-204	-38	0.023	2.560
prob	0.3018	0.1066	0.0794	0.8355	0.8408	0.2985
B_{23}	-8.125	-879	-53	196	0.0085	0.790
prob	0.2427	0.1130	0.6240	0.2986	0.9436	0.7240
2. Regression						
linear (SS)	1821	14999650	222073	593287	0.0092	169
prob	0.2158	0.1246	0.4993	0.5329	0.9929	0.330
quadratic (SS)	2204	16317885	359425	2434780	1.246	364
prob	0.1579	0.1056	0.3076	0.0713	0.0439	0.0959
cross product (SS)	1105	19416864	370753	1060295	0.0106	59
prob	0.4029	0.0728	0.2958	0.3022	0.9913	0.7216
total regress (SS)	15131	50734399	952253	4088361	1.26681	592
prob	0.2193	0.0652	0.3830	0.1896	0.3327	0.2648
3. Residual						
lack of fit (SS)	3399	20446489	873326	2007852	0.544	384
prob	0.0001	0.0001	0.0001	0.0867	0.4797	0.0228
pure error (SS)	26	20491	1140	535720	0.5181	51
total error (SS)	3425	20476980	874466	2543573	1.063	435
4. Solution	Saddle point	Saddle point	Saddle point	Saddle point	Maxi-mum	Maxi-mum

SS = sum of squares

Table 6.22 (continued)

ii) Minitab

	Al	Pb	Ag	Fe	DWOM	R.L
1. Coefficient						
B_0	15.844	185	21.6	485	0.9313	26.28
B_1	11.066	147	-89	-2.6	-0.017	-1.677
B_2	-3.316	410	65	164	-0.0135	-1.488
B_3	-0.073	-926	63	-130	0.0141	-2.713
B_{11}	11.439	142	27	140	-0.160	-2.418
B_{22}	4.530	172	99	67	-0.102	-2.276
B_{33}	4.707	1063	133	399	-0.252	-4.296
B_{12}	-4.625	-922	-43	-305	0.0263	0.460
B_{13}	-7.125	897	-204	-38	0.023	2.560
B_{23}	-8.125	-879	-53	196	0.0085	0.790
2. R-squared (%)	60	71	52	61	54	57
R-squared adjusted for d.f. (%)	24	45	9.0	27	13	19
3. Regression						
linear (SS)	1821	14999650	222073	593287	0.0092	169
quadratic (SS)	2204	16317885	359425	2434780	1.246	364
cross product (SS)	1105	19416864	370753	1060295	0.010	59
total regress (SS)	5131	50734394	952253	4088361	1.26	593
4. Residual (SS)	3426	20479679	874466	2543537	1.06	435
5. Total (SS)	8557	71211374	182671966	6631934	2.32	1028

Table 6.22 (continued)

b) Shoot

i) SAS

	Al	Pb	Ag	Fe	DWOM
1. Coefficient					
B_0	7.447	3.240	2.284	37	2.347
prob	0.0392	0.6698	0.423	0.1343	0.0001
B_1	-2.512	-4.919	-3.233	6.07	0.014
prob	0.2559	0.3319	0.1053	0.7641	0.9451
B_2	-4.066	59.10	2.897	-12.65	-0.077
prob	0.0797	0.0001	0.1417	0.4903	0.7143
B_3	2.102	6.747	1.743	20.64	0.0179
prob	0.3371	0.1921	0.3598	0.2536	0.9322
B_{11}	0.156	7.805	2.092	14.55	-0.42
prob	0.9404	0.1271	0.2645	0.3641	0.0620
B_{22}	1.041	43.75	0.213	11.90	-0.229
prob	0.6193	0.0001	0.9068	0.4524	0.2778
B_{33}	2.104	4.475	1.206	16	-0.54
prob	0.3247	0.3618	0.5110	0.3224	0.0218
B_{12}	3.875	-6.50	-2.337	-39	0.040
prob	0.1851	0.3265	0.2645	0.0827	0.8818
B_{13}	-5.625	-5.250	-5.40	21	0.0113
prob	0.0657	0.4241	0.0460	0.2981	0.9673
B_{23}	-3.125	0.250	2.825	-26	0.017
prob	0.2777	0.9691	0.2611	0.2230	0.9496
2. Regression					
linear (SS)	372	48611	299	7371	0.0889
prob	0.165	0.0001	0.1495	0.5776	0.9837
quadratic (SS)	74	27674	78	7747	6.49
prob	0.7455	0.0001	0.6449	0.5587	0.0484
cross product (SS)	451	559	341	23476	0.0168
prob	0.1156	0.6373	0.1168	0.1506	0.9986
total regress (SS)	897	76845	717	38595	6.596
prob	0.2148	0.0001	0.1931	0.3842	0.3542
3. Residual					
lack of fit (SS)	297	3137	442	34711	1.449
prob	0.4973	0.0001	0.0002	0.0004	0.8714
pure error (SS)	295	38	8	803	4.306
total error (SS)	593	3175	450	35514	4.756
4. Solution	Saddle point	Minimum	Saddle point	Saddle point	Maximum

SS = sum of squares

Table 6.22 (continued)

ii) Minitab

	Al	Pb	Ag	Fe	DWOM
1. Coefficient					
B_0	7.477	3.240	2.284	37	2.347
B_1	-2.512	-4.919	-3.233	6.07	0.014
B_2	-4.066	59.101	2.897	-12.65	-0.077
B_3	2.102	6.747	1.743	20.64	0.0179
B_{11}	0.156	7.805	2.092	14.55	-0.420
B_{22}	1.041	43.73	0.213	11.90	-0.229
B_{33}	2.104	4.475	1.206	16	-0.540
B_{12}	3.875	-6.50	-2.377	-39	-0.040
B_{13}	-5.625	-5.250	-5.400	21	0.0113
B_{23}	-3.125	0.250	2.825	-26	0.0174
2. R-squared (%)	60	96	61	49	53
R-squared adjusted for d.f. (%)	30	90	50	35	15
3. Regression					
linear (SS)	372	48611	299	7371	0.0889
quadratic (SS)	74	27674	78	7747	6.49
cross product (SS)	451	559	341	23476	0.0168
total regress (SS)	897.32	76822	717	36667	6.59
4. Residual (SS)	529.88	3175	450	36826	5.75
5. Total (SS)	1490	79998	1167	73493	12.35

6.3 DISCUSSION

a) Metal Released from Sediments

The results in Tables 6.5 and 6.6 show the metal released from Restronguet Creek No. 3 and Adit Bridge No. 8 sediments respectively when using acetate buffers. The highest percentage extraction of metal when compared to total acid digestion was found at pH 1.99. The sequence was as follows :-

Ca (76%) > Pb (24%) > Mn (20.3%) > Cu (8.4%) > Fe (4.2%) > Zn (1.8%) (for Restronguest Creek No. 3) and Cu (89.2%) > Mn (80.6%) > Ca (51.6%) > Pb (30%) > Zn (17.8%) > Fe (4.56%) (for Adit Bridge No. 8).

The chemical associations of the above metals within the sediments are shown in Tables 3.10 (p. 147) and 3.12 (p. 148) respectively. The results in Tables 3.10 and 3.12 explain the different percentages of extraction of the same metal in the two samples above. Just to take one example, 70% of the zinc in Restronguet Creek No. 3 was associated with the residual phase of the sediment whilst only 0.59% of the metal in Adit Bridge No. 8 was associated with the residual phase. Reference to Tables 3.10 and 3.12 will illustrate several similar examples.

Trace metal studies (20,21) of sediments often include a chemical leaching or attack of the solid phase with selected reagents such as EDTA, NH_4Cl, $MgCl_2$, $NH_4C_2O_4$, 25% v/v CH_3COOH, 25% v/v CH_3COOH + $NH_2.OH.HCl$, even HNO_3 and aqua regia. The release process for metals in sediments is primarily a function of pH with differing dependences for individual elements, however, the sample type can also play an important role in release mechanisms. Trefry et alia (20) have used phthalate buffers from pH values of 2.2 to 6.0 to release Cd, Cu, Fe, Mn, Pb and Zn from two Gulf of Mexico sediment samples. However, in view of possible matrix interference during AAS determination, this type of buffer solution

was avoided during the present work. Therefore, acetate buffers (NH_4Ac + HAc or ClAc) with pH values of 1.99 to 6.99 were used. In general, the results presented by these workers (20) are in agreement with the results presented here. The results in Tables 6.5 and 6.6 indicate that the level of extracted metal increases with a decrease in pH and increase in time, i.e. the release process for metal in sediments is a function of pH and time. The increase in the level of extracted metal may be due either to:-

i) the release of metal from organic ligands (capable of chelation) which are adsorbed onto the residual phase surface;

ii) the competitive desorption of metals adsorbed directly onto the sediment surface by the action of hydrogen ions;

iii) the gradual dissolution of such adsorptive species as hydrous oxides, particularly Fe and Mn species, so releasing metal ions into solution. The latter process is an important factor in the present situation because much metal is associated with hydrous oxides (cf. Tables 3.10 and 3.12).

It is best to discuss the release process for each metal in the sediments individually.

Calcium

Figures 6.5 and 6.6 depict the 3-D and contour plots of the response surface for calcium released from Restronguet Creek No. 3 sediment. The figures indicate that the highest level of extracted calcium is associated with lowest pH and longest time. Calcium in Adit Bridge No. 8 sediment appears to exhibit a different release process from that in the Restronguet Creek No. 3 sediment. Figures 6.7 and 6.8 illustrate that the level of extracted calcium decreased with longer times of extraction with approximately no change in release throughout the pH range.

FIG. 6.5 RESPONSE SURFACE OF CALCIUM RELEASED FROM RESTRONGUET CREEK No.3 SEDIMENT

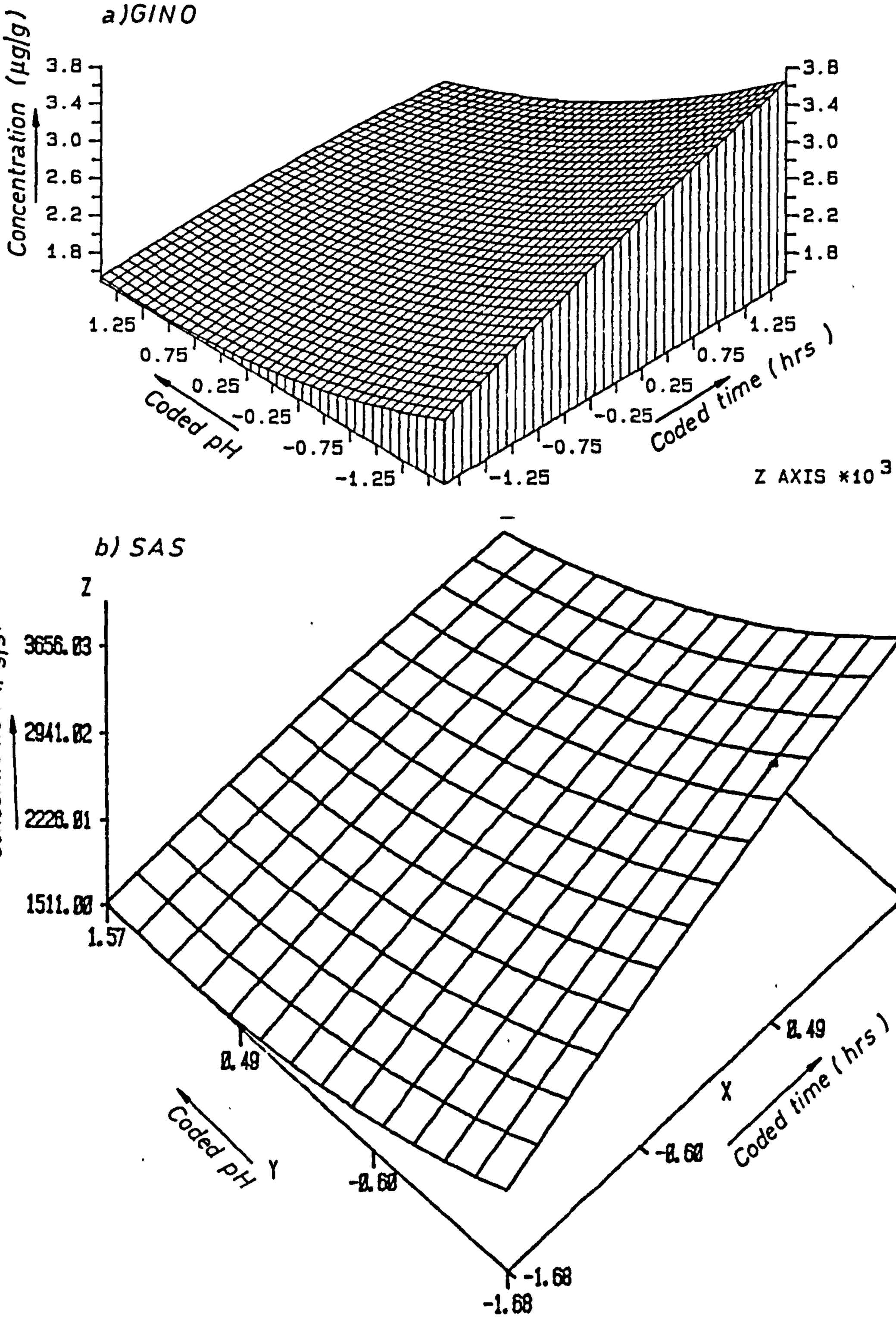

FIG. 6.6 CONTOUR PLOT OF RESPONSE SURFACE FOR CALCIUM RELEASED FROM RESTRONGUET CREEK No. 3 SEDIMENT

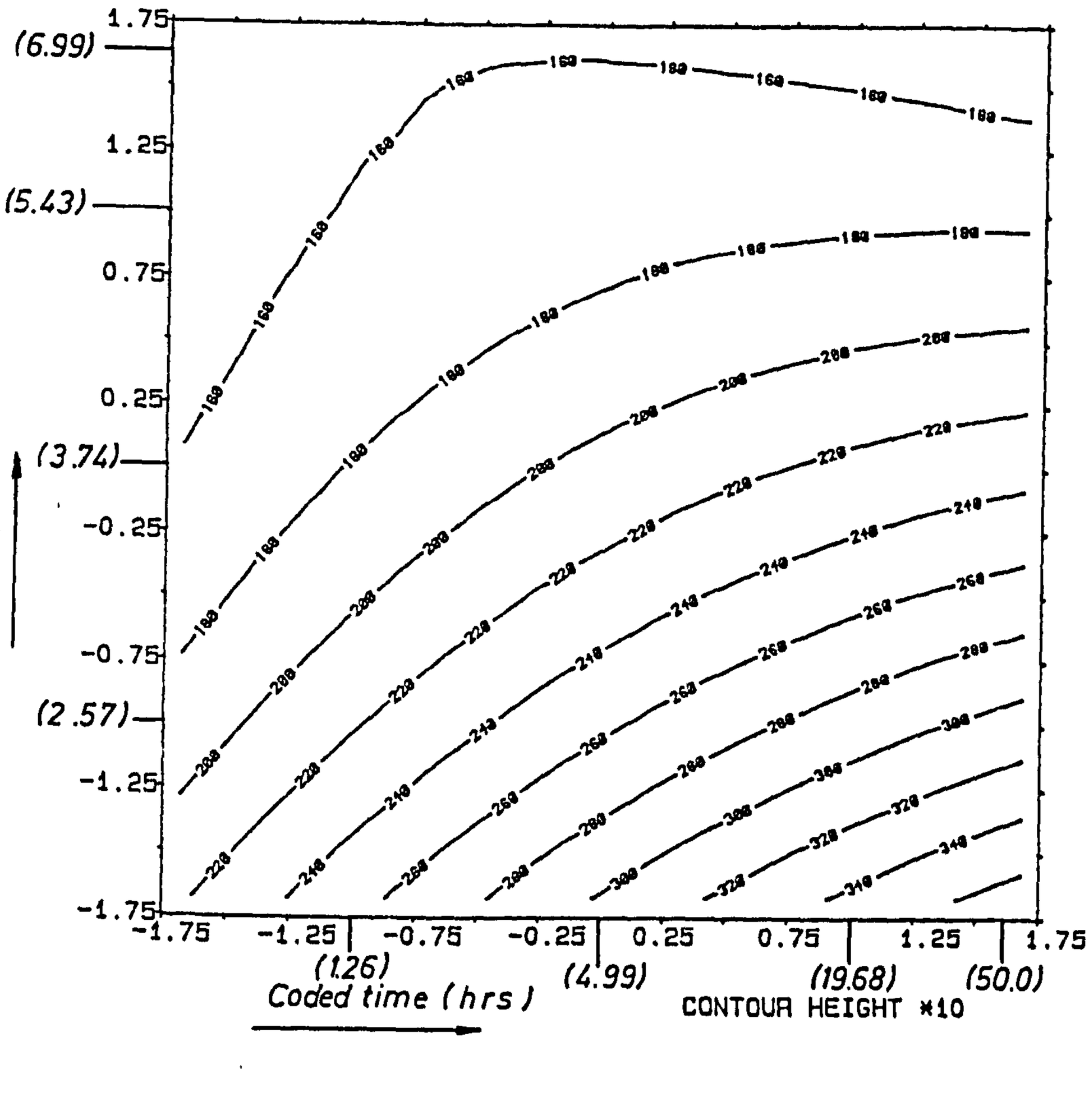

FIG. 6.7 RESPONSE SURFACE FOR CALCIUM RELEASED FROM ADIT BRIDGE No. 8 SEDIMENT

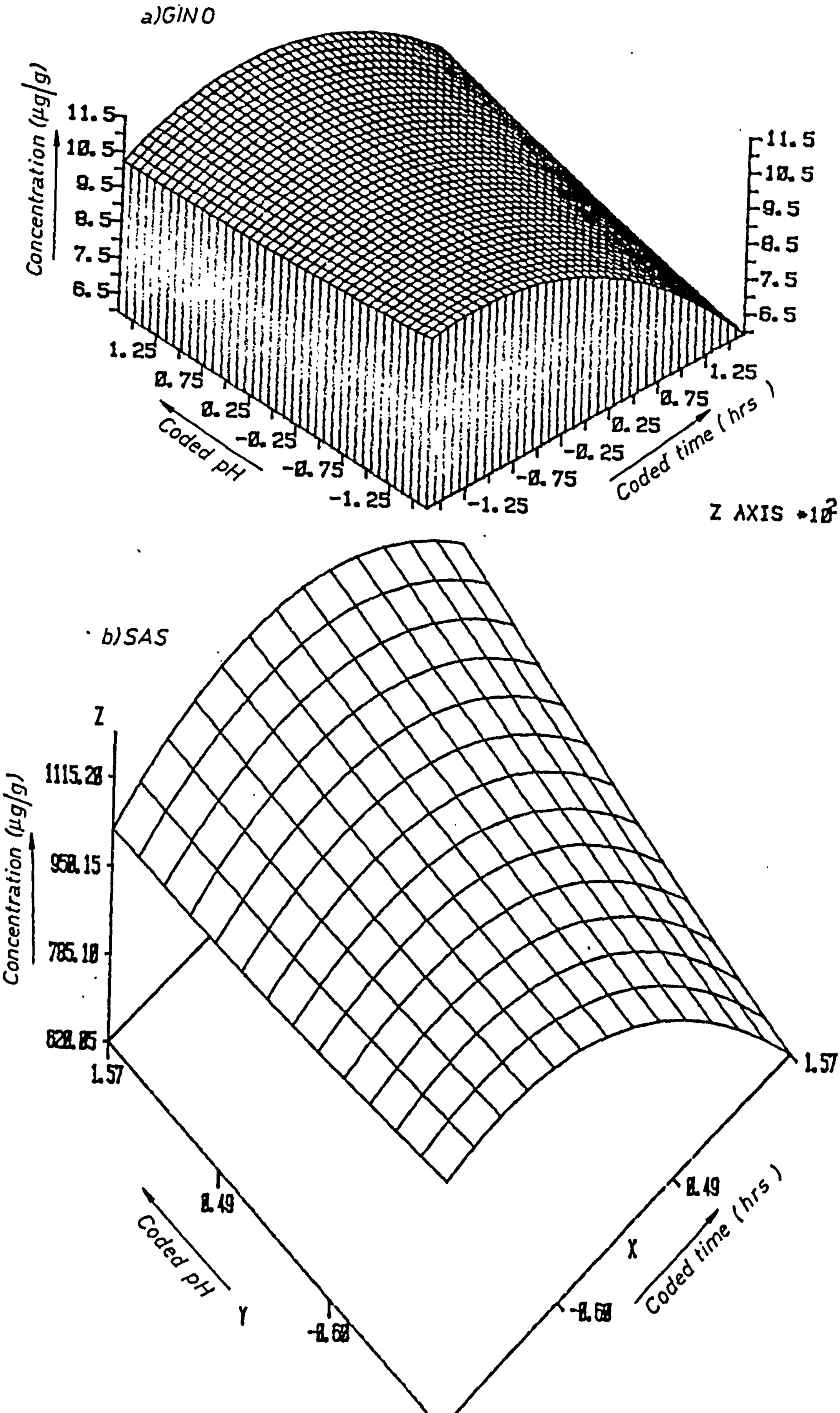

FIG. 6.8 CONTOUR PLOT OF RESPONSE SURFACE FOR CALCIUM RELEASED FROM RESTRONGUET CREEK No.3 SEDIMENT

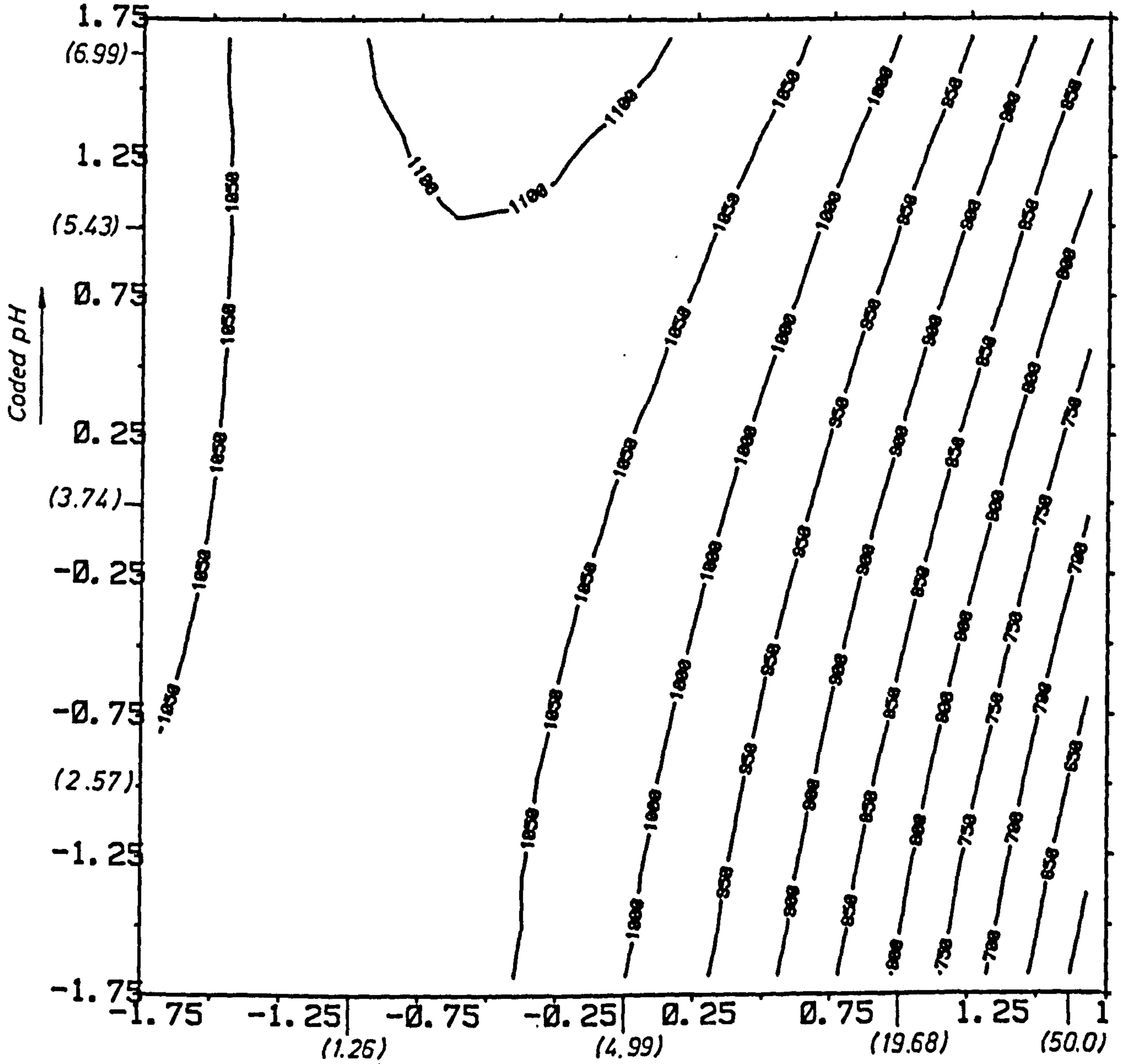

Probably calcium is released at highest pH but readsorbed on the sediment. The possibility of metal being released from a certain phase of a sediment during weak extraction procedures and then being readsorbed by the sediment on other phases has been reported by Batley et alia (22). Readsorption has also been used to explain an apparent loss of metal at different pHs from chemical extracts (22). Thus, in half an hour, 35% of the leachable Fe and 70-80% of Cd, Cu, Mn, Pb and Zn were removed from the Gulf of Mexico sediments using phthalate buffers but after 12 hours the release process for metals from such sediments become much slower (20). Therefore, shorter extraction time and lower pH ranges may give more useful information concerning the release process for calcium in the Adit Bridge No. 8 sediment.

Manganese

Figures 6.9 to 6.12 illustrate that the release process for manganese in Restronguet Creek No. 3 and Adit Bridge No. 8 sediments shows similar behaviour (the extracted level of the metal increases with decrease in pH and increase in time). The response surface obtained for manganese from Restronguet Creek No. 3 sediment is different from the surface obtained for the metal in the Adit Bridge No. 8 sediment. This difference may arise due to the different chemical association of the element within the sediments. For Restronguet Creek a large proportion of the manganese is associated with the residual phase, while the remainder is mainly in the Fe-Mn fraction.

However, for the Adit No. 8 sample, much manganese (37.5%) is present in the exchangeable form and should be readily available at acid pHs.

FIG. 6.9 RESPONSE SURFACE FOR MANGANESE RELEASED FROM RESTRONGUET CREEK No.3 SEDIMENT

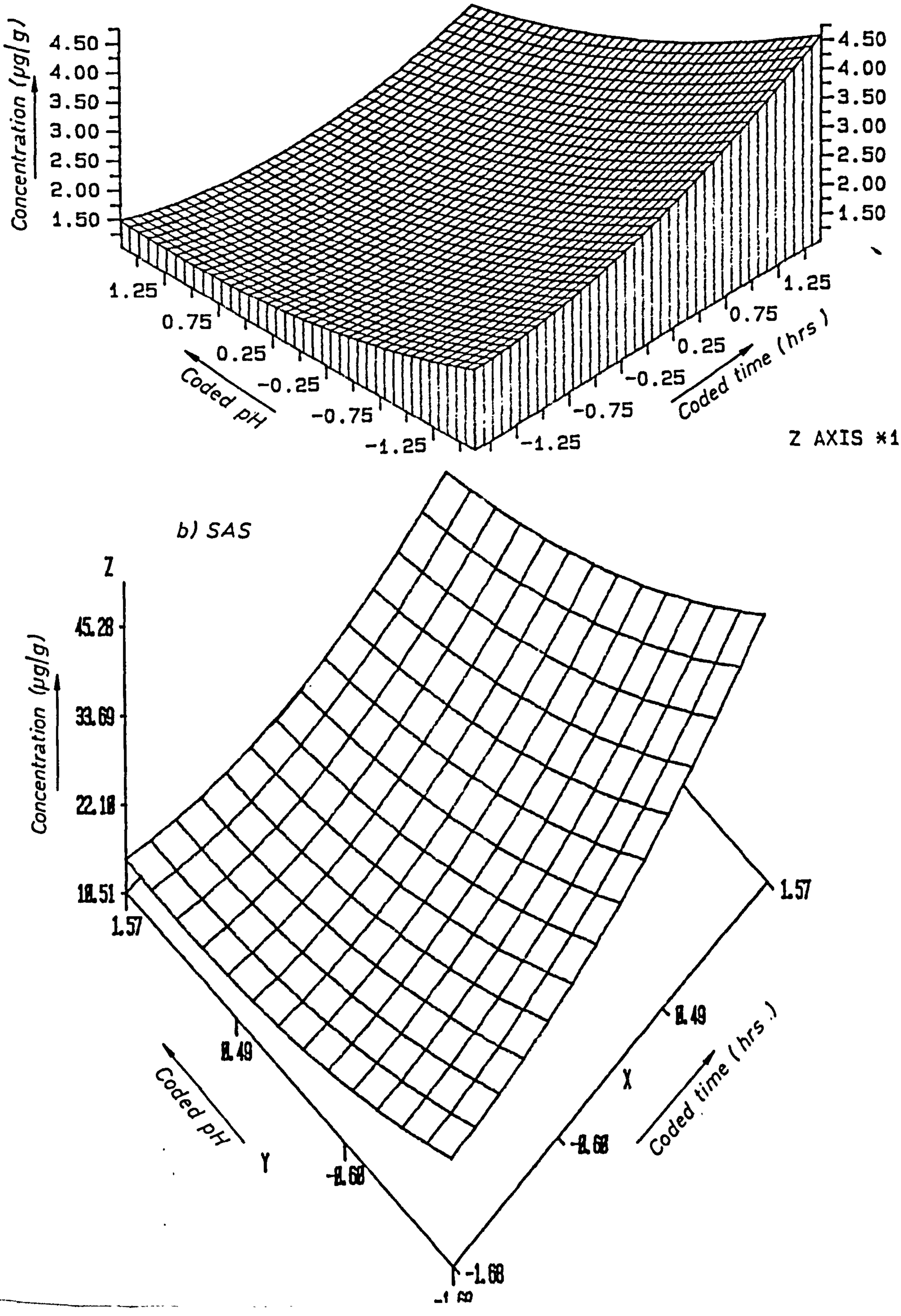

FIG. 6.10 CONTOUR PLOT OF RESPONSE SURFACE FOR MANGANESE RELEASED FROM RESTRONGUET CREEK No. 3 SEDIMENT

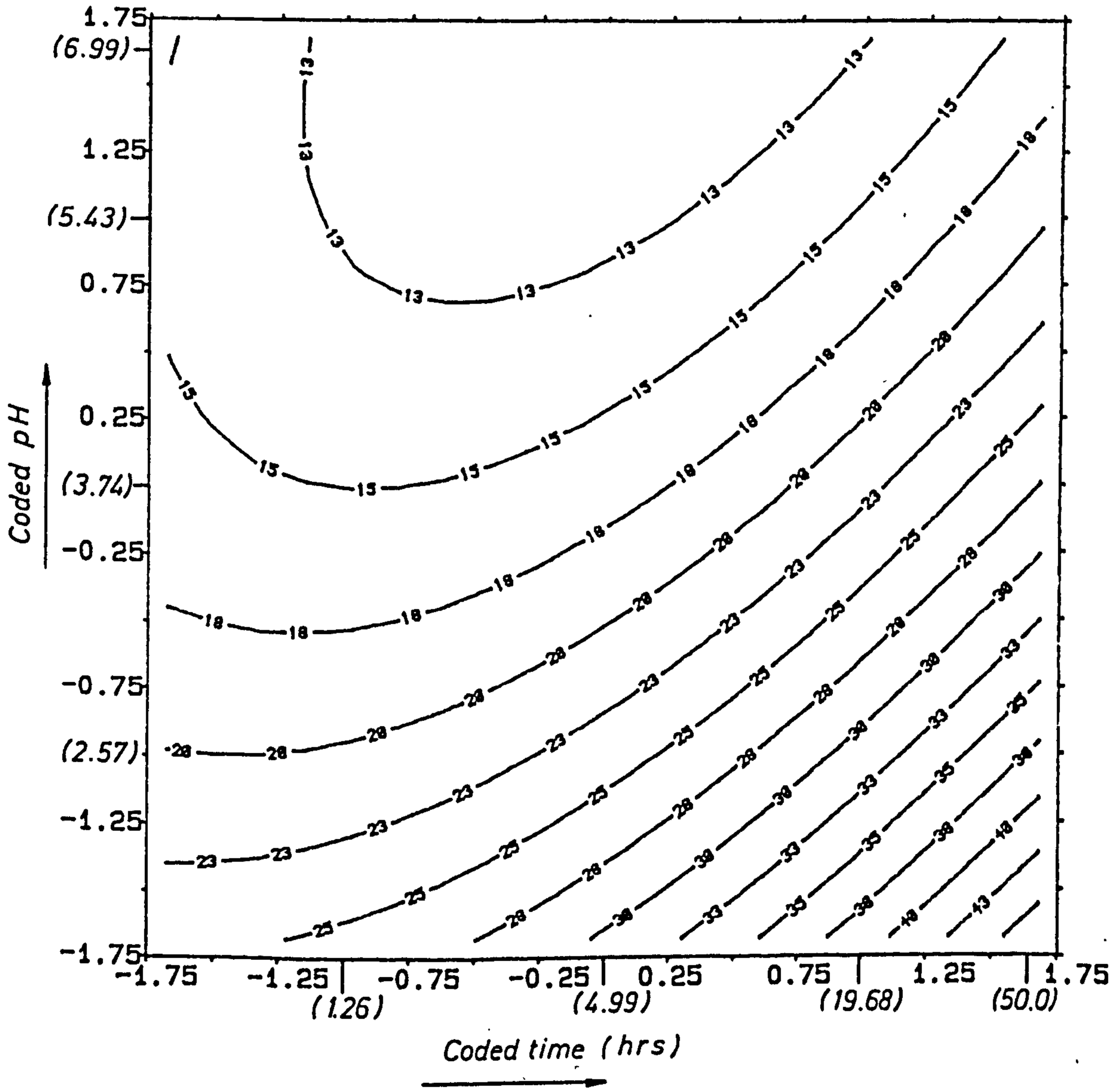

FIG. 6.11 RESPONSE SURFACE FOR MANGANESE RELEASED FROM ADIT BRIDGE No. 8

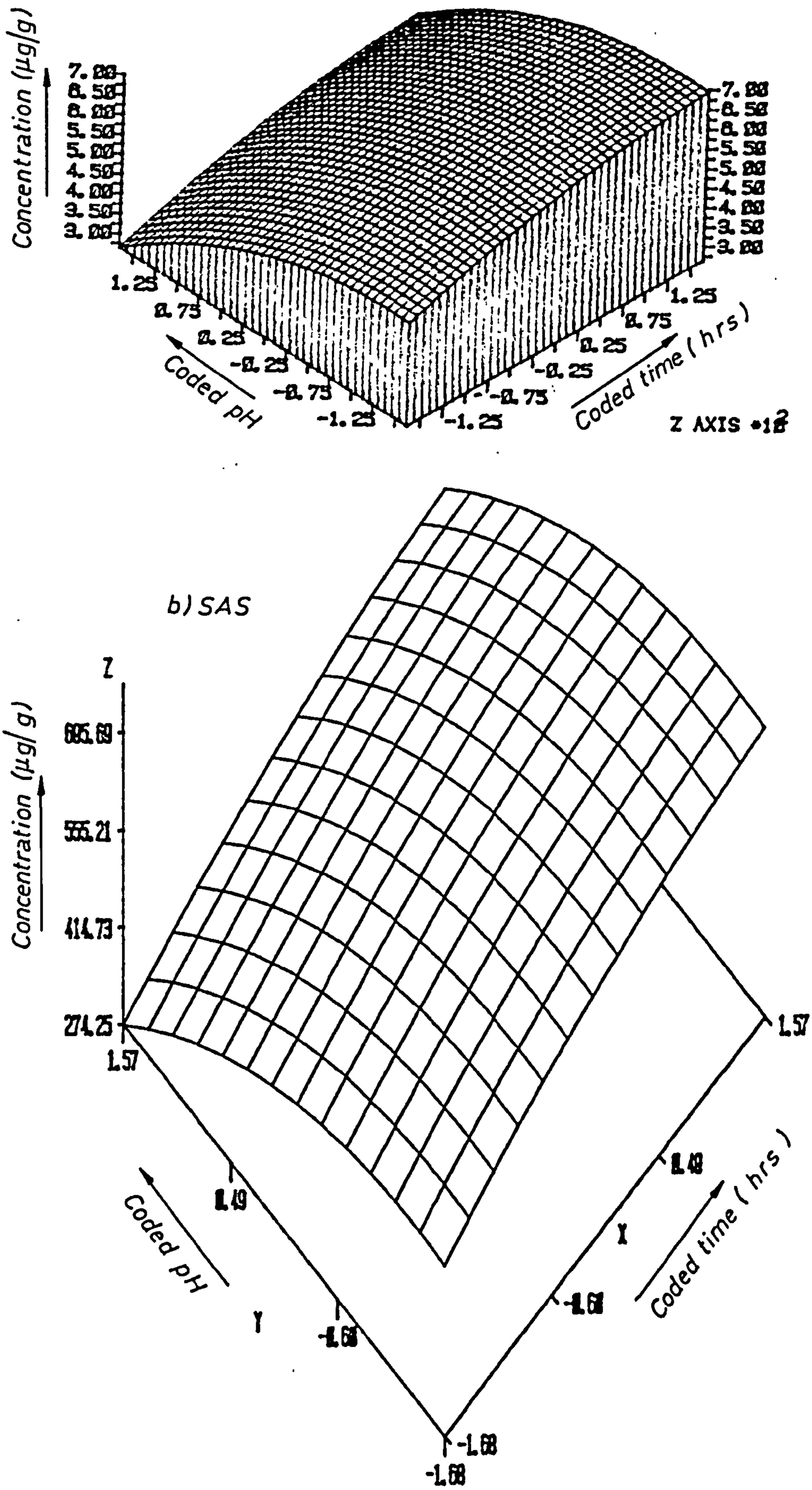

FIG. 6.12 CONTOUR PLOT OF RESPONSE SURFACE FOR MANGANESE RELEASED FROM ADIT BRIDGE No. 8 SEDIMENT

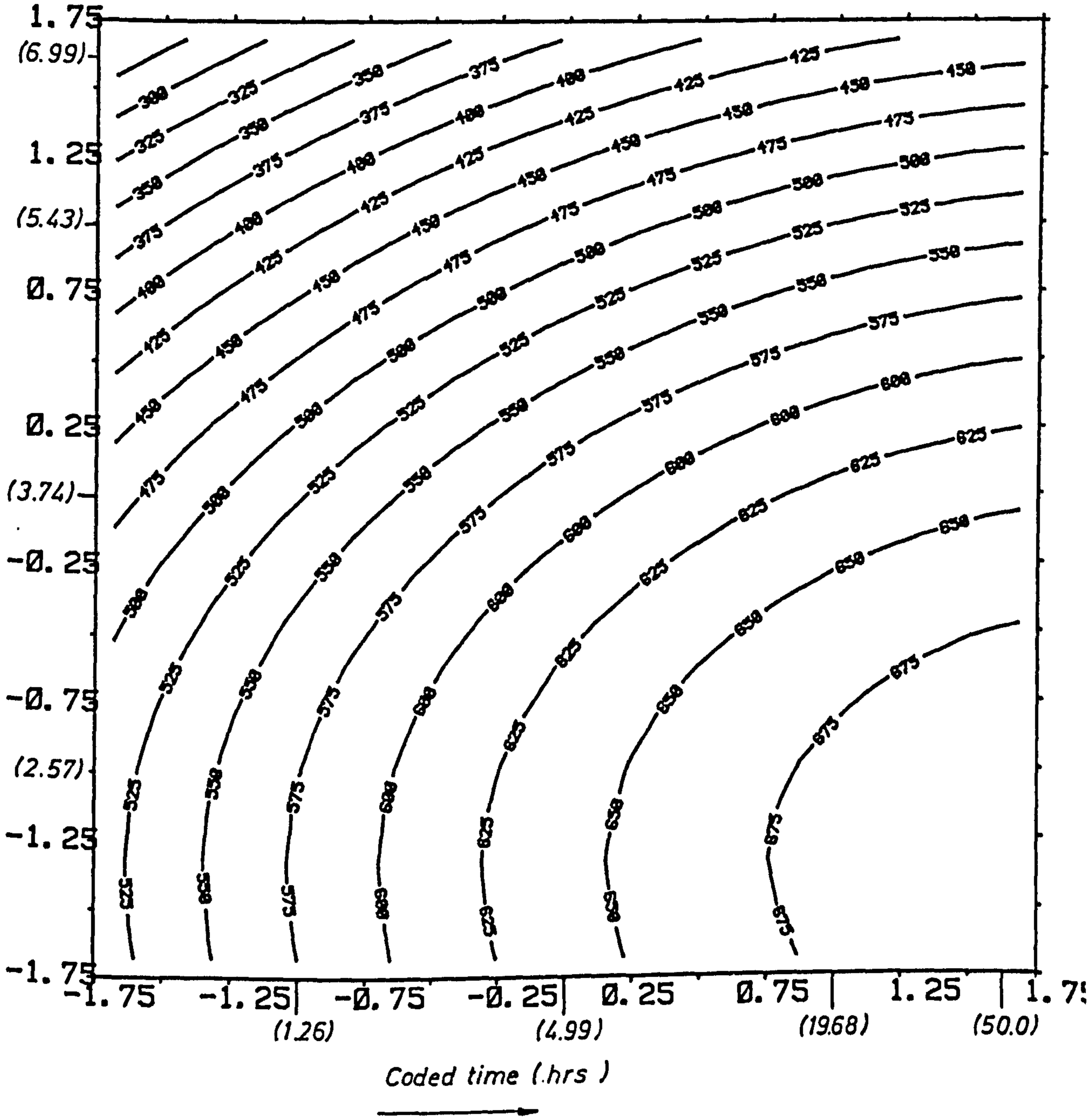

Iron

The same form of response was obtained for iron in both sediments (see Figures 6.13 to 6.16). In this case, the iron was associated with the same geochemical phases, in the hydrous oxide and residual portion of the sediments.

Copper

Figures 6.17 and 6.18 show the surface response for copper released from Restronguet Creek No. 3 sediment. The surface indicates that the level of extracted copper increases with time. At the coded pH 0.0 (actual pH 5.43), a maximum level of extracted copper was observed. A possible explanation of the shape of this surface is that, of all the elements,copper is the one most likely to be bound with the organic fraction of the sediment, principally as chelated compounds. If in these complexes the copper is strongly bound, then a kinetic factor (i.e. a time delay) will be observed in the release of Cu from these complexes, possibly due to steric effects as the complexes unwind and decompose. Support for this concept is afforded from the Tessier scheme where much of the Cu (35%) is associated with the organic phase. The response surface for copper in Adit Bridge No. 8 sediment (Figures 6.19 and 6.20) demonstrates that the level of extracted copper also increased with the decrease in pH and increase in time. However, in this case much of the copper is present in the carbonate phase and will be released on treatment with very dilute acids.

FIG. 6.13 RESPONSE SURFACE FOR IRON RELEASED FROM RESTRONGUET CREEK No. 3 SEDIMENT

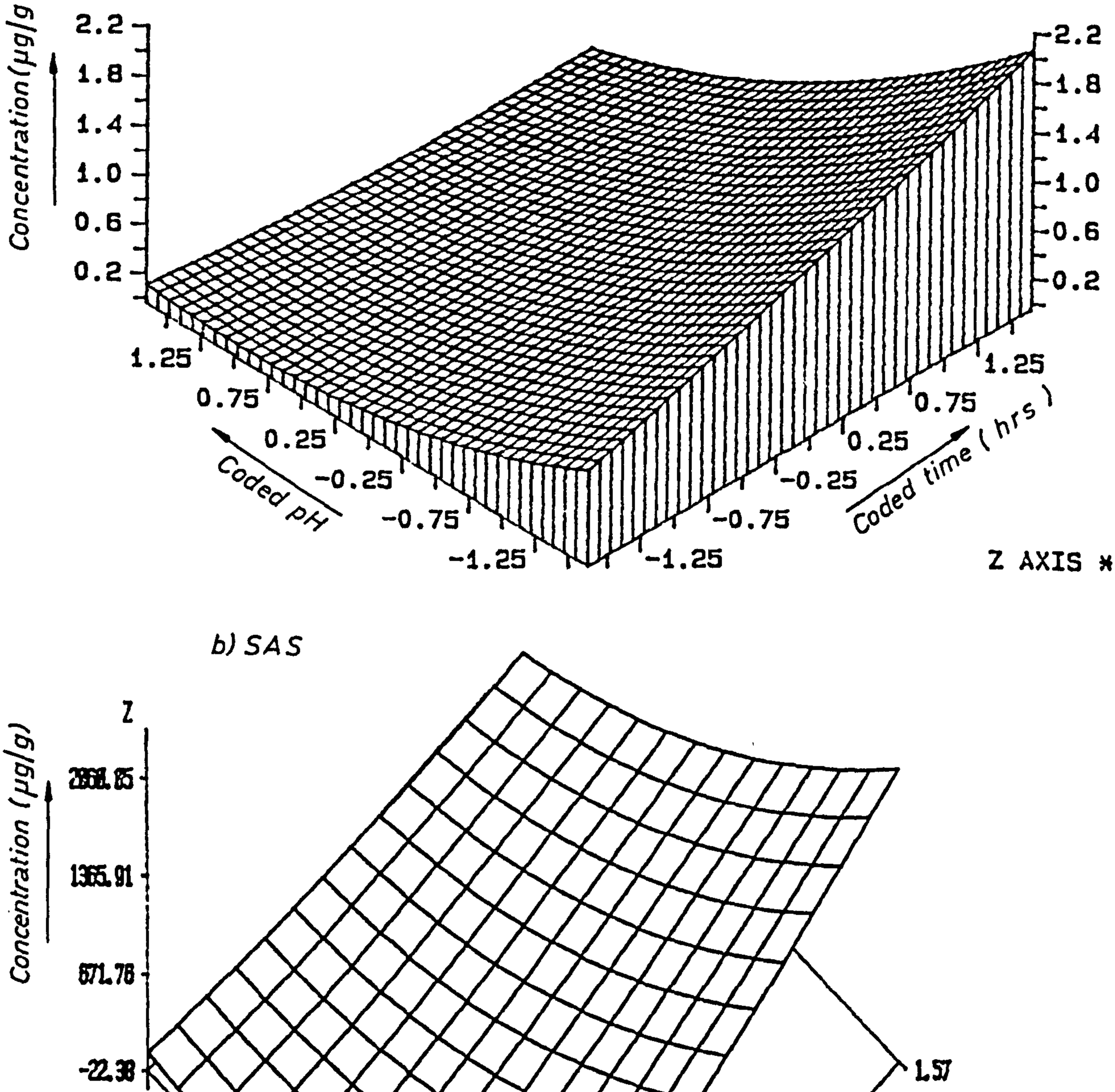

FIG. 6.14 CONTOUR PLOT OF RESPONSE SURFACE FOR IRON RELEASED FROM RESTRONGUET CREEK No. 3 SEDIMENT

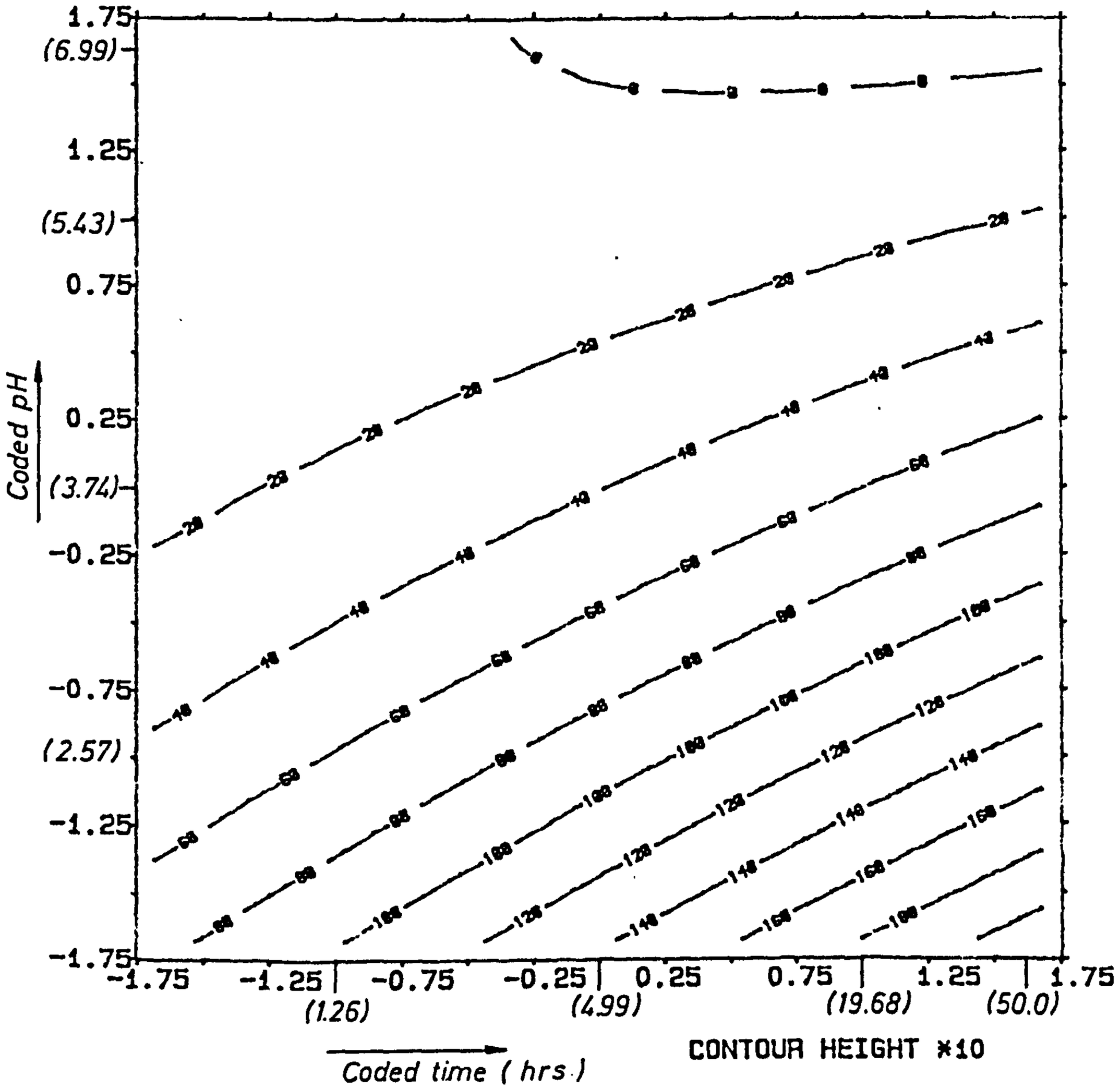

FIG. 6.15 3-D PLOT FOR RESPONSE SURFACE FOR IRON RELEASED FROM ADIT BRIDGE No.8 SEDIMENT

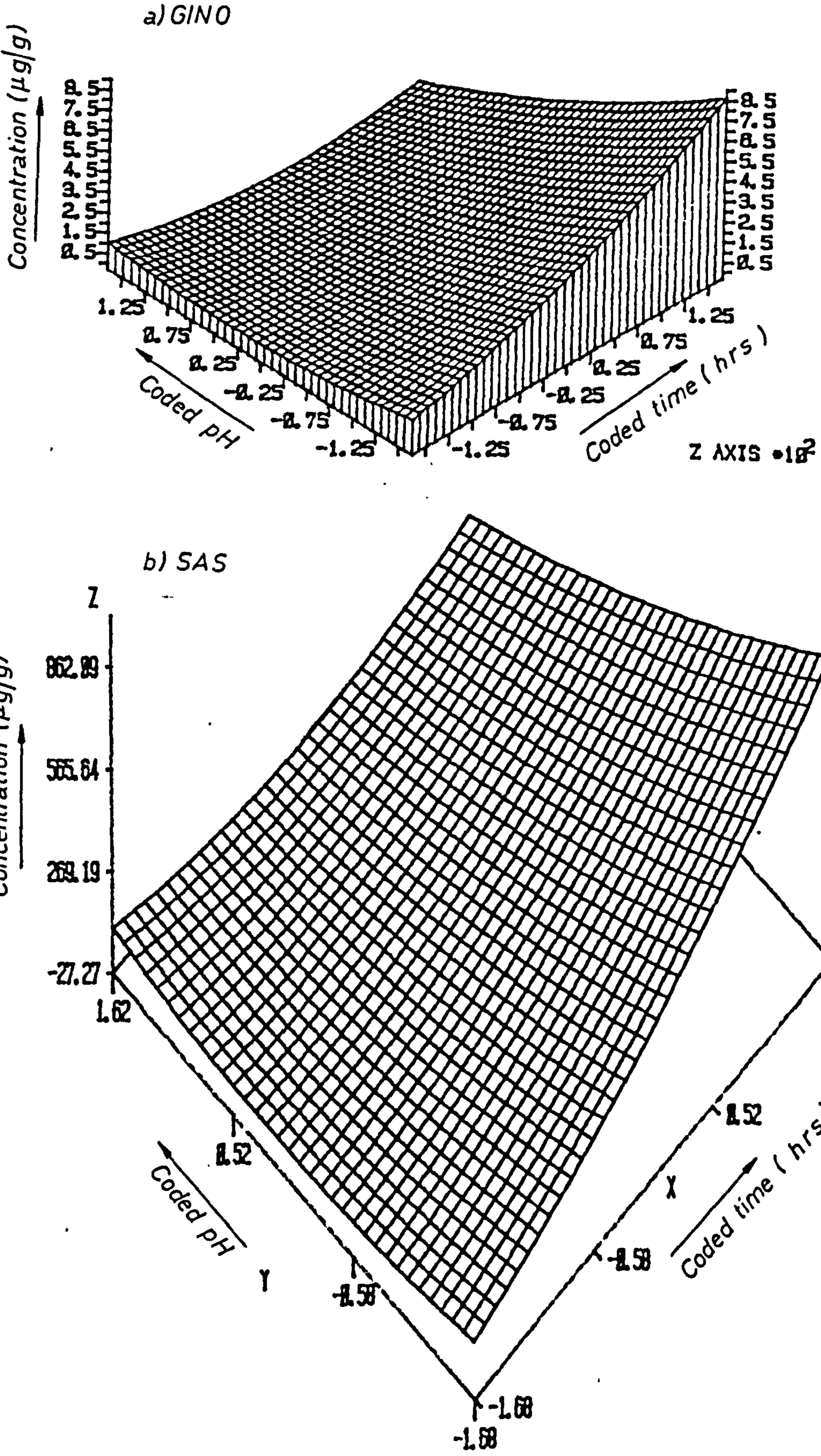

FIG. 6.16 CONTOUR PLOT OF RESPONSE SURFACE FOR IRON RELEASED FROM ADIT BRIDGE No.8 SEDIMENT

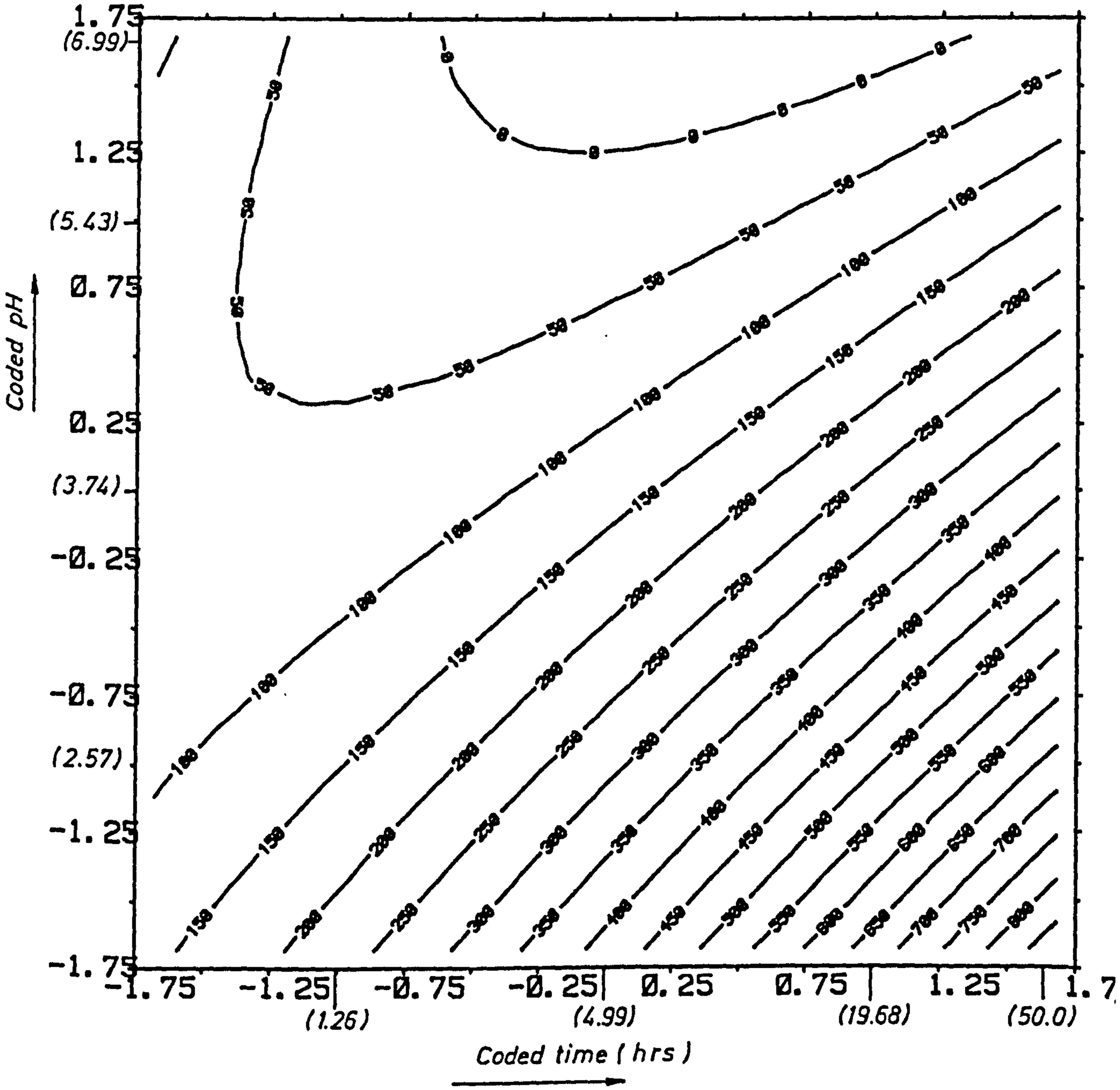

FIG. 6.17 RESPONSE SURFACE FOR COPPER RELEASED FROM RESTRONGUET CREEK No. 3 SEDIMENT

a) GINO

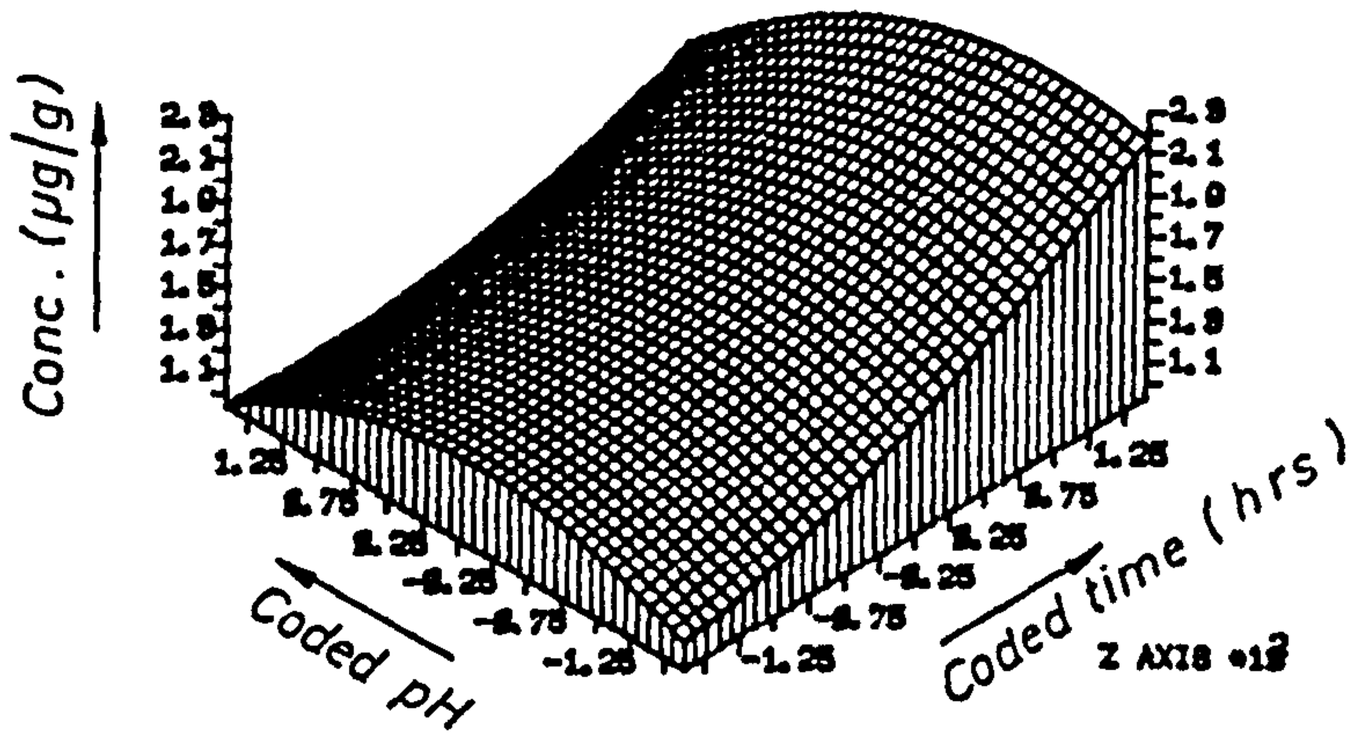

b) SAS

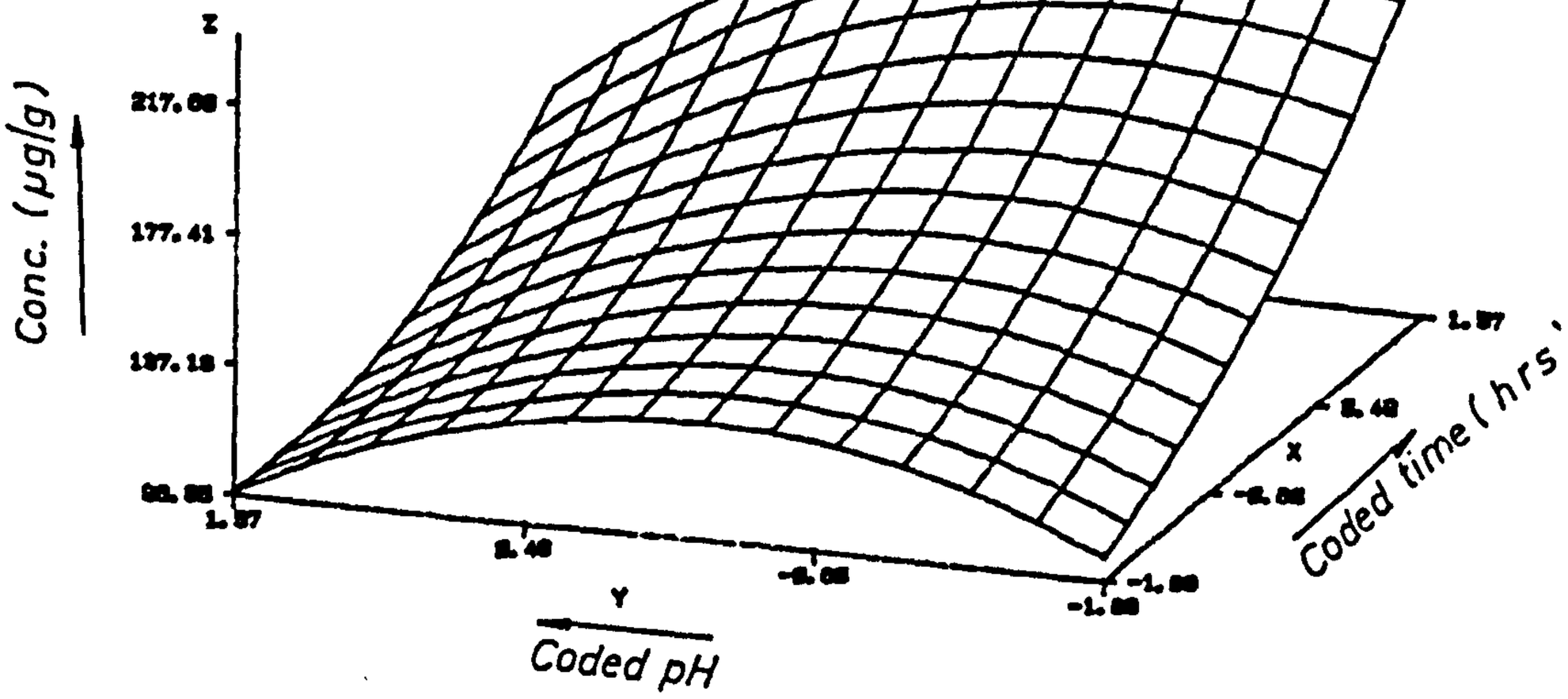

FIG. 6.18 CONTOUR PLOT FOR COPPER RELEASED FROM RESTRONGUET CREEK No 3 SEDIMENT

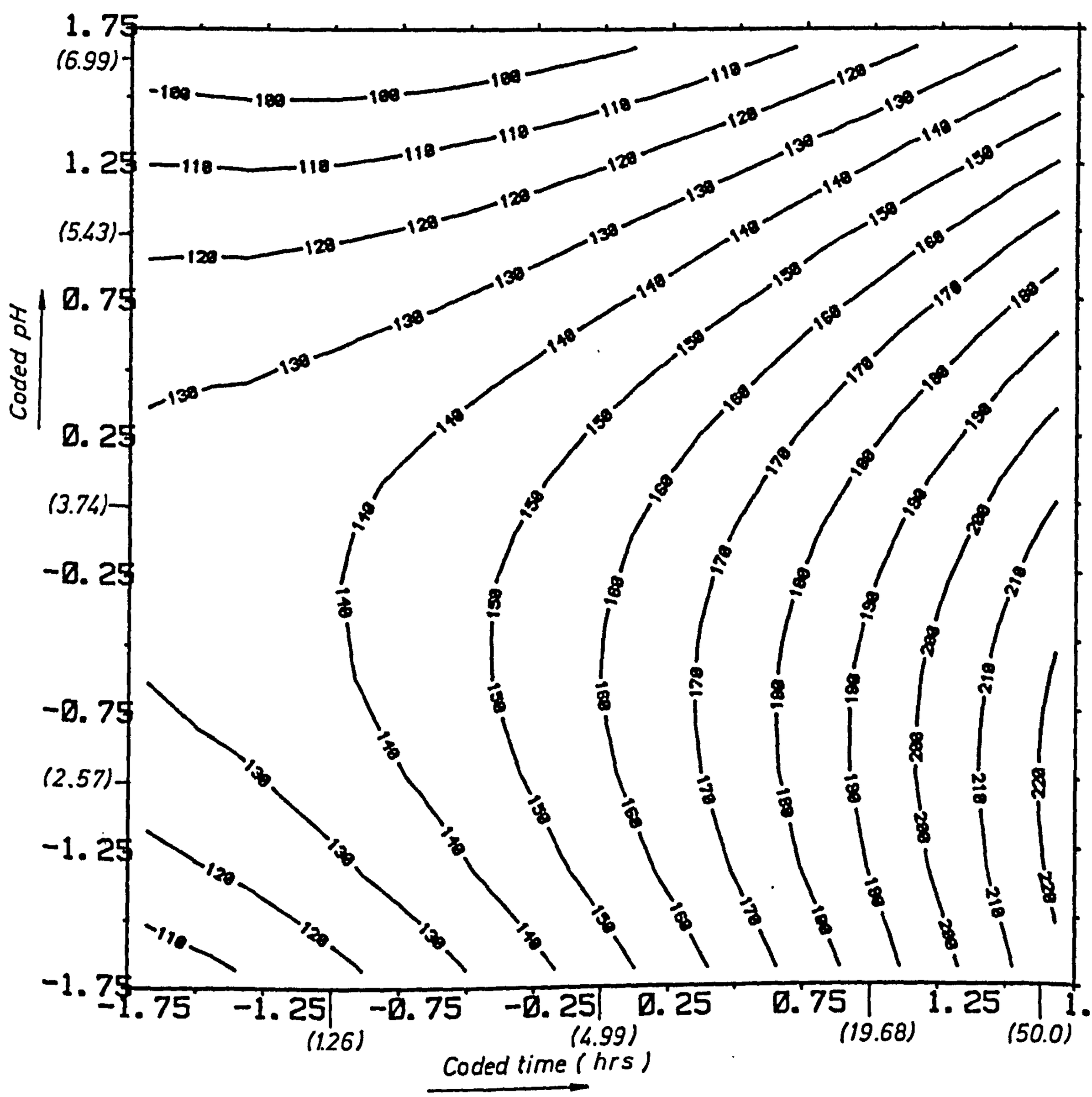

FIG. 6.19 RESPONSE SURFACE FOR COPPER RELEASED FROM ADIT BRIDGE No.8 SEDIMENT

a) GINO

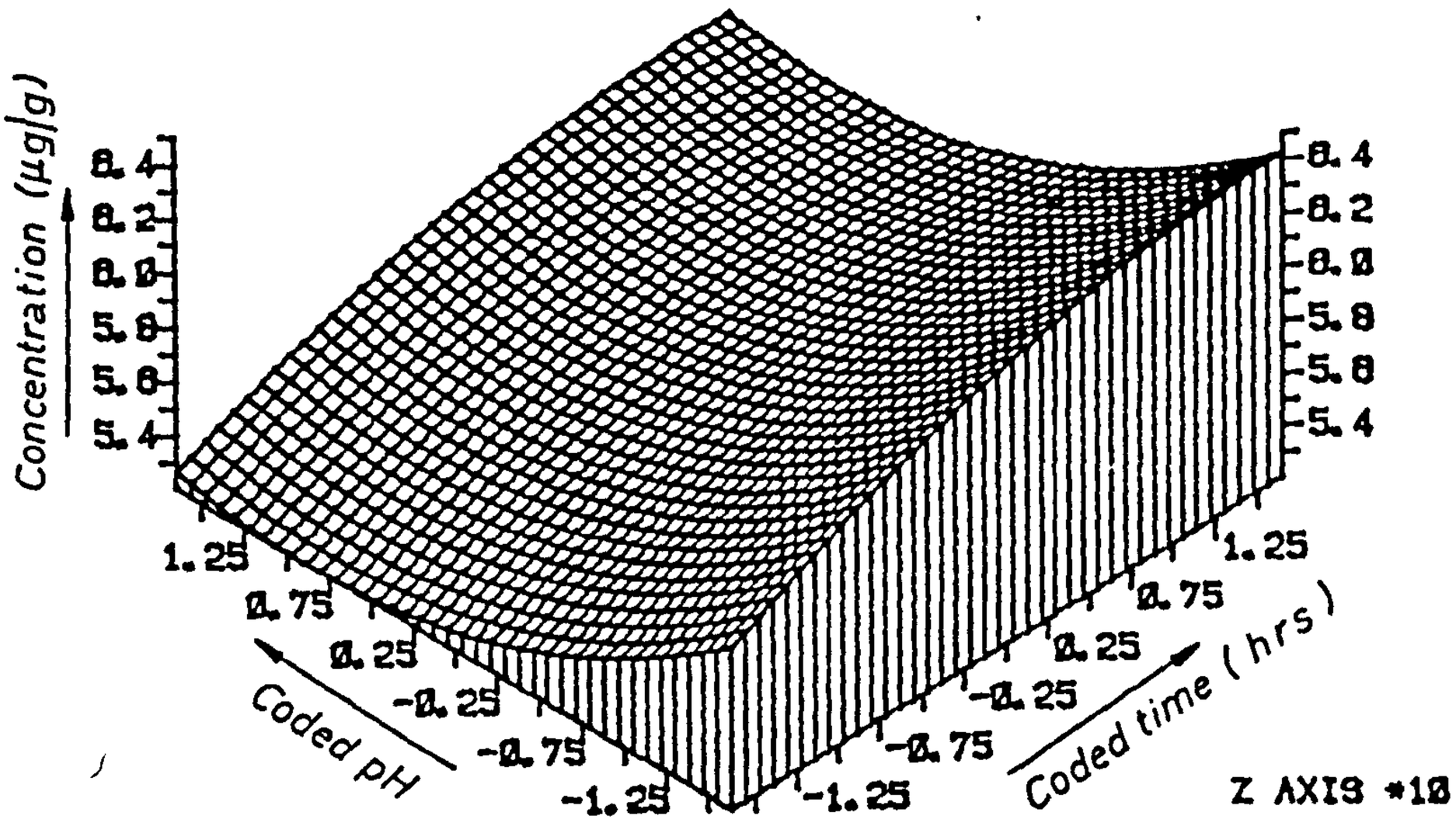

b) SAS

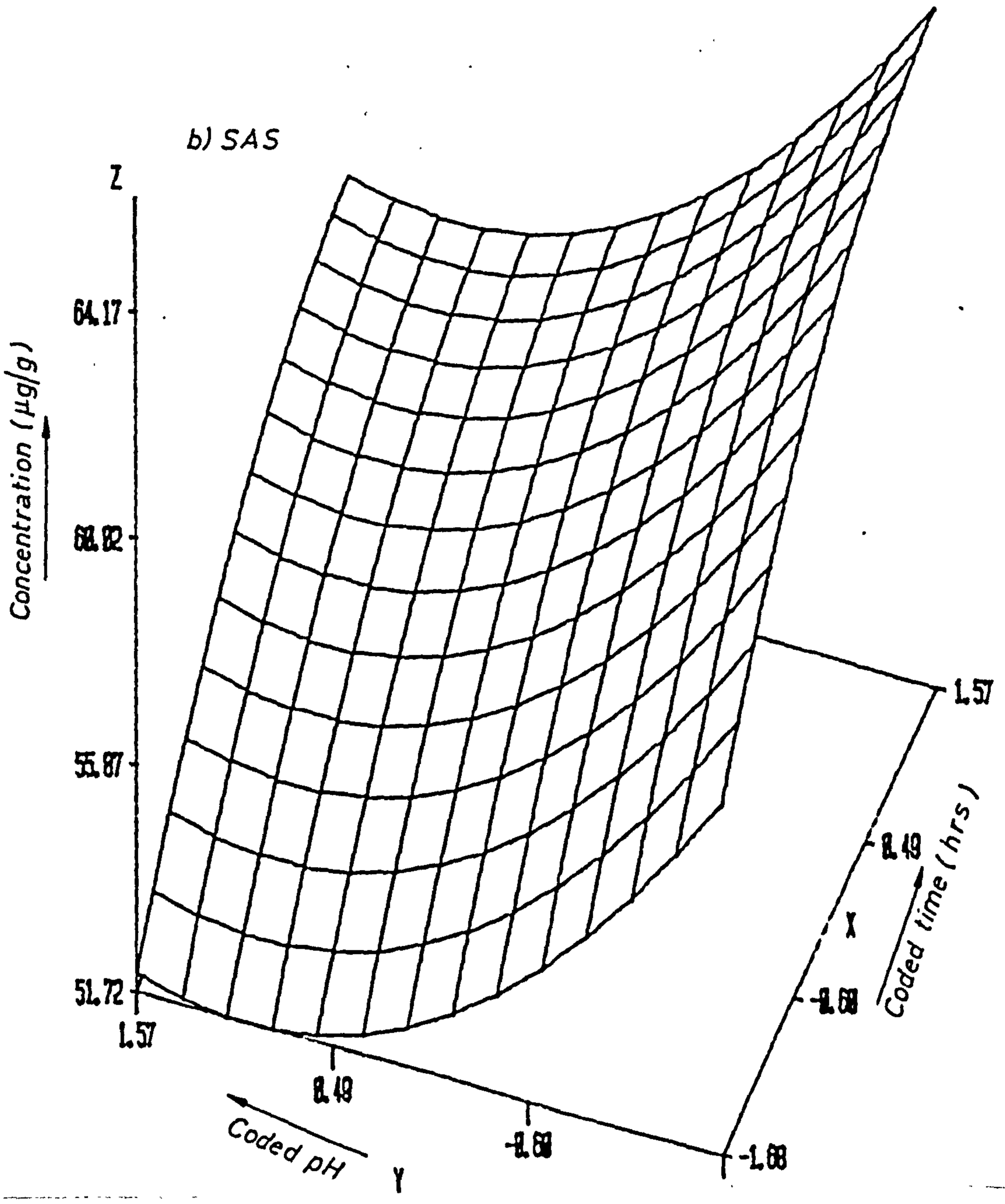

FIG. 6.20 CONTOUR PLOT OF COPPER RELEASED FROM ADIT BRIDGE
No. 8 SEDIMENT

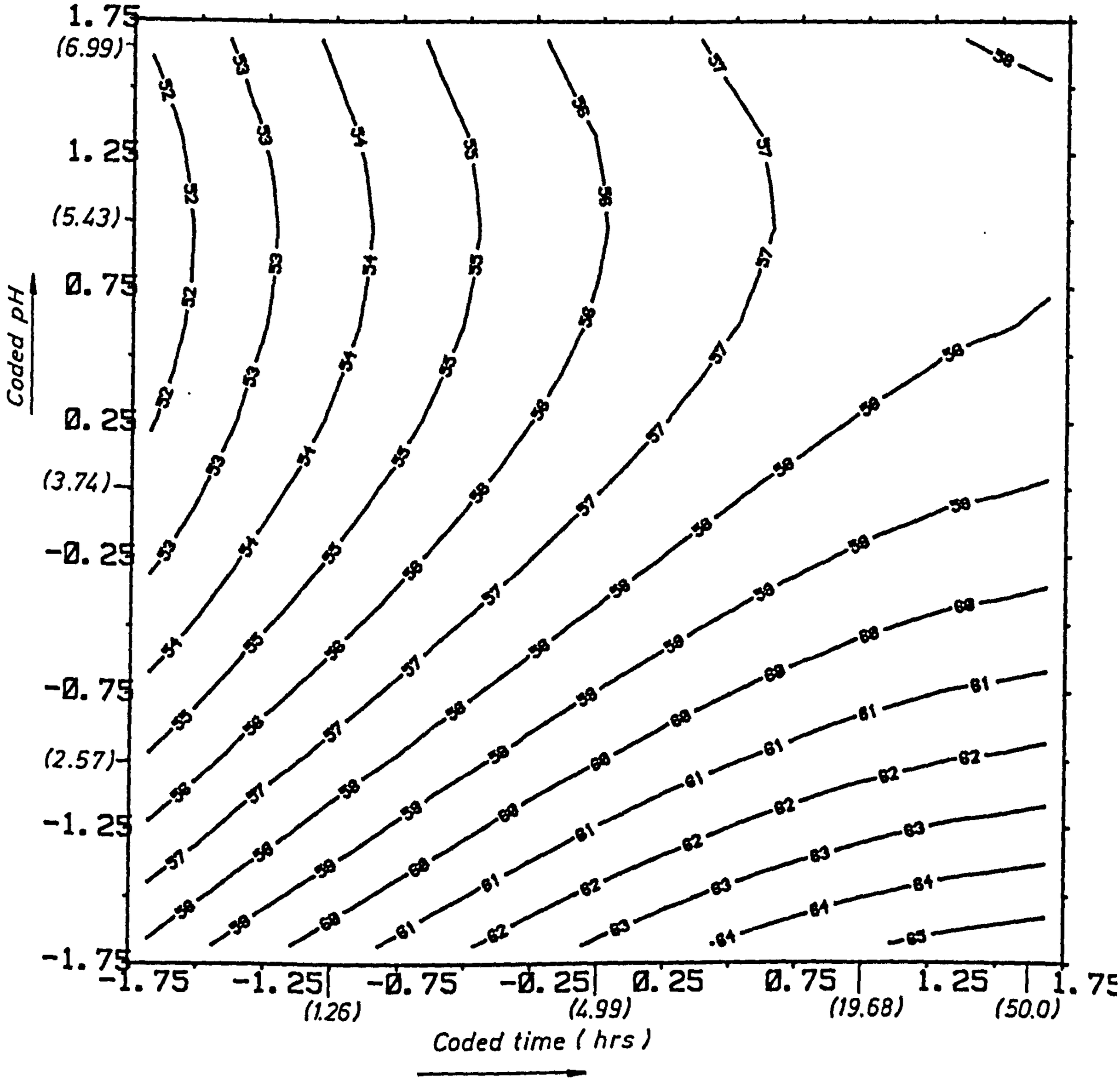

Zinc

Figures 6.21 to 6.24 show the surface response for the release of zinc from Restronguet Creek No. 3 and Adit Bridge No. 8 sediments. At the coded pH -1 (actual pH 2.57) a maximum level of extracted zinc in the Restronguet Creek No. 3 sediment was also observed (the problem was discussed earlier). The surface for zinc in the Adit Bridge No. 8 sediment indicates that the level of extracted zinc increases with decreasing pH and increased time.

Lead

The surface responses obtained for lead in Restronguet Creek No. 3 and Adit Bridge No. 8 sediments are shown in Figures 6.25 to 6.28. The level of extracted lead from Adit Bridge No. 8 sediment increased with decreased pH and increased time. The levels of extracted lead from Restronguet Creek No. 3 does not follow the same surface response as for the Adit Bridge No. 8 sediment.

The difference between the two response surfaces may be due to the adsorption of lead into the Fe-Mn oxide phase, which has a much greater concentration in the Restronguet Creek sample than the Adit No. 8 specimen. The desorption of metal ions adsorbed on hydrous oxides (23-25) followed by the reaction of metal ions with humic acids or other organic particulates may be responsible for soluble metal losses. These organic-metal materials may then be adsorbed onto the surface of the remaining sediment phases.

Green *et alia* (26) have reported that cupric ions bind to humic acid even at pHs as low as 1.35.

FIG 6.21 RESPONSE SURFACE FOR ZINC RELEASED FROM RESTRONGUET CREEK No.3 SEDIMENT

a) GINO

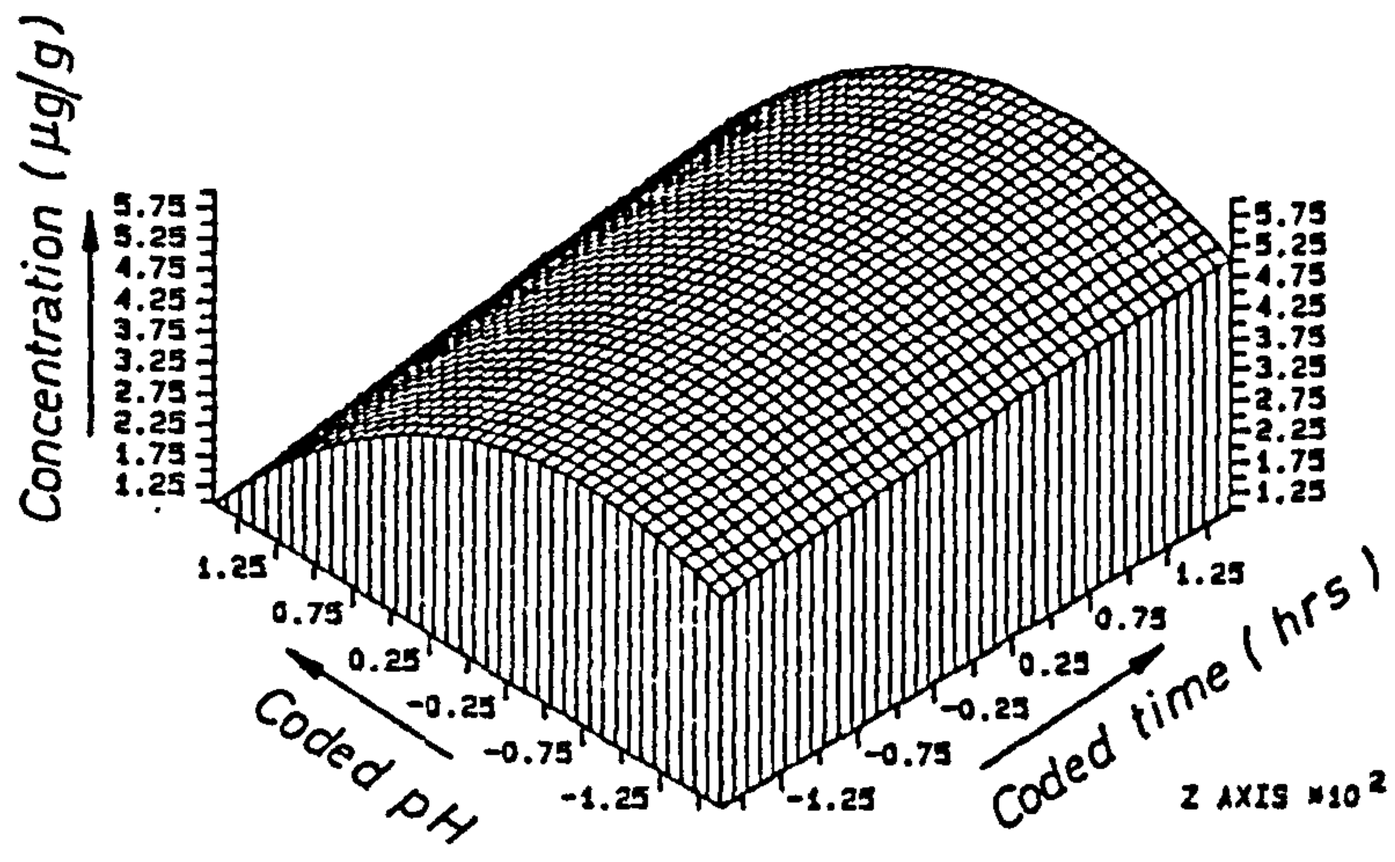

b) SAS

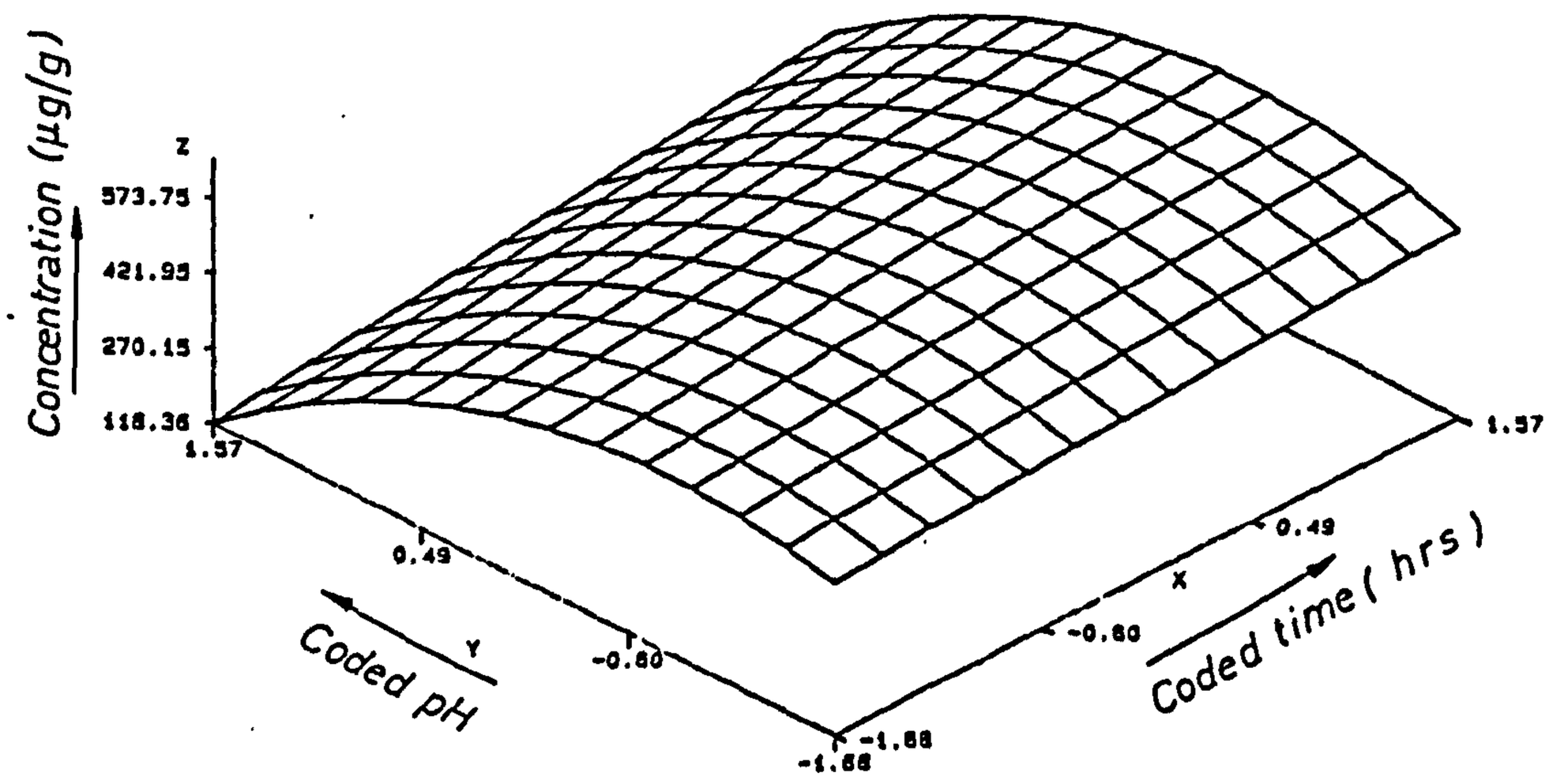

FIG. 6.22 CONTOUR PLOT OF RESPONSE SURFACE FOR ZINC RELEASED FROM RESTRONGUET CREEK No.3 SEDIMENT

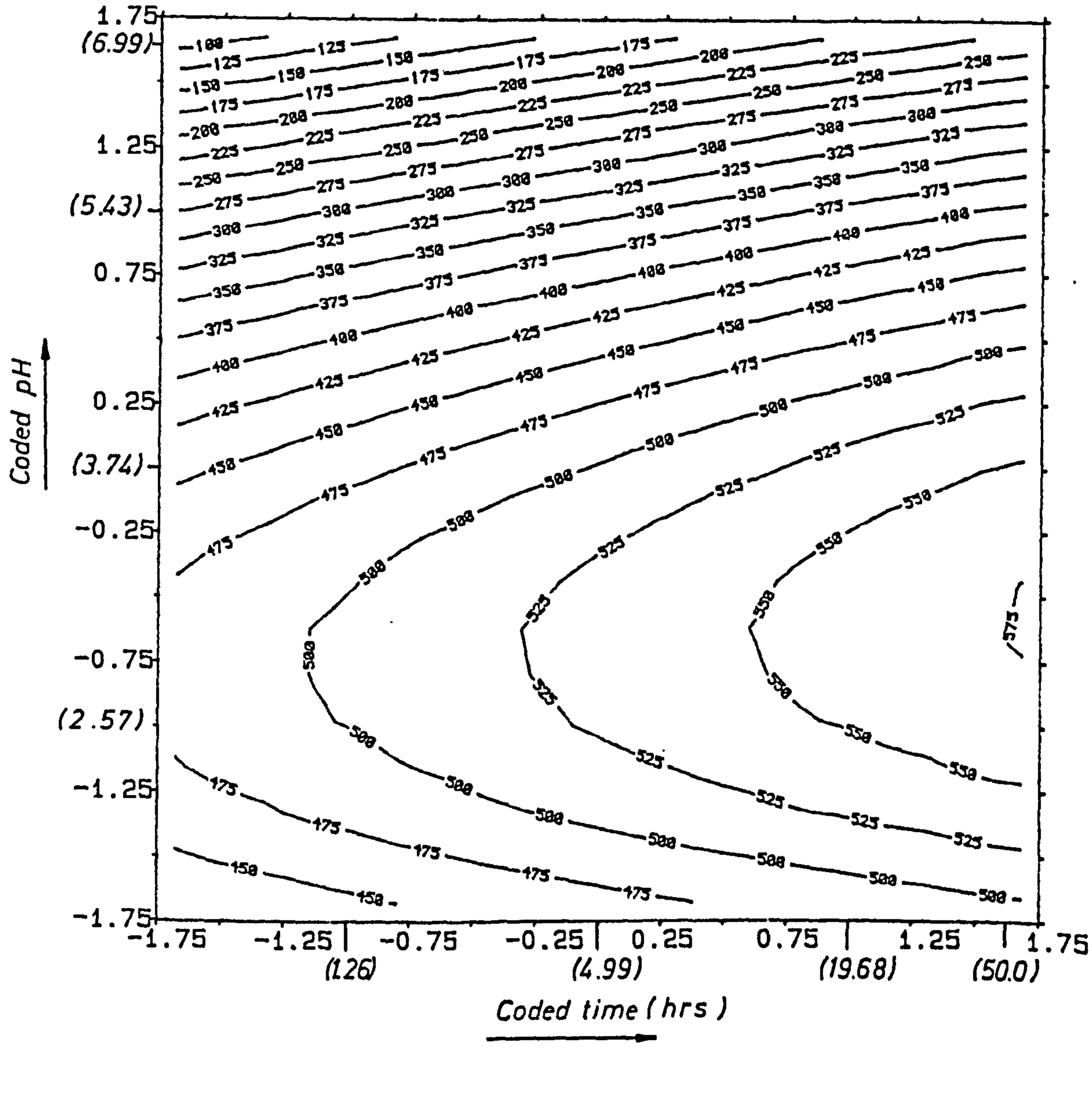

FIG. 6.23 RESPONSE SURFACE FOR ZINC RELEASED FROM ADIT BRIDGE No.8 SEDIMENT

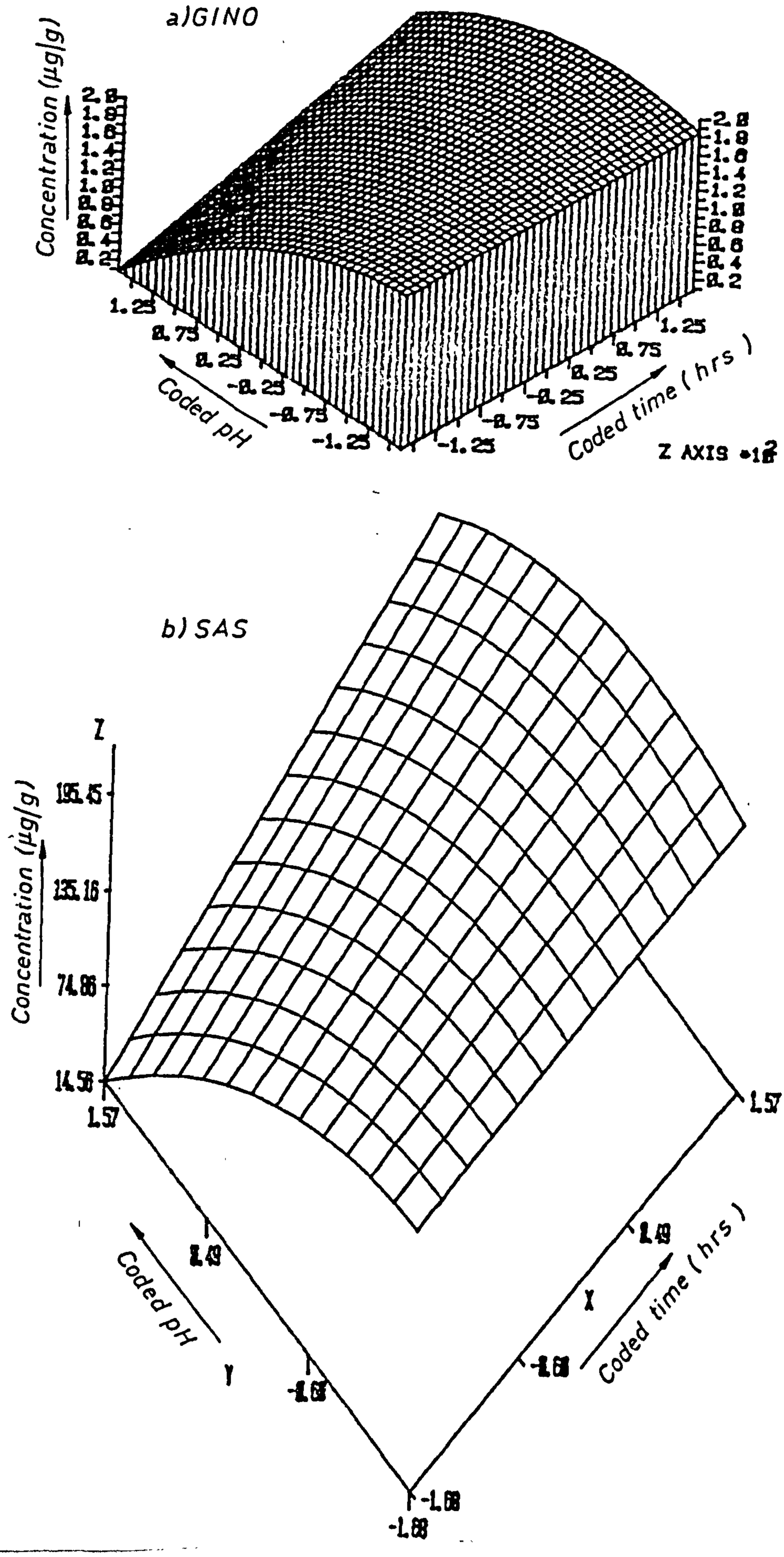

FIG. 6.24 CONTOUR PLOT OF RESPONSE SURFACE FOR ZINC RELEASED FROM ADIT BRIDGE No.8 SEDIMENT

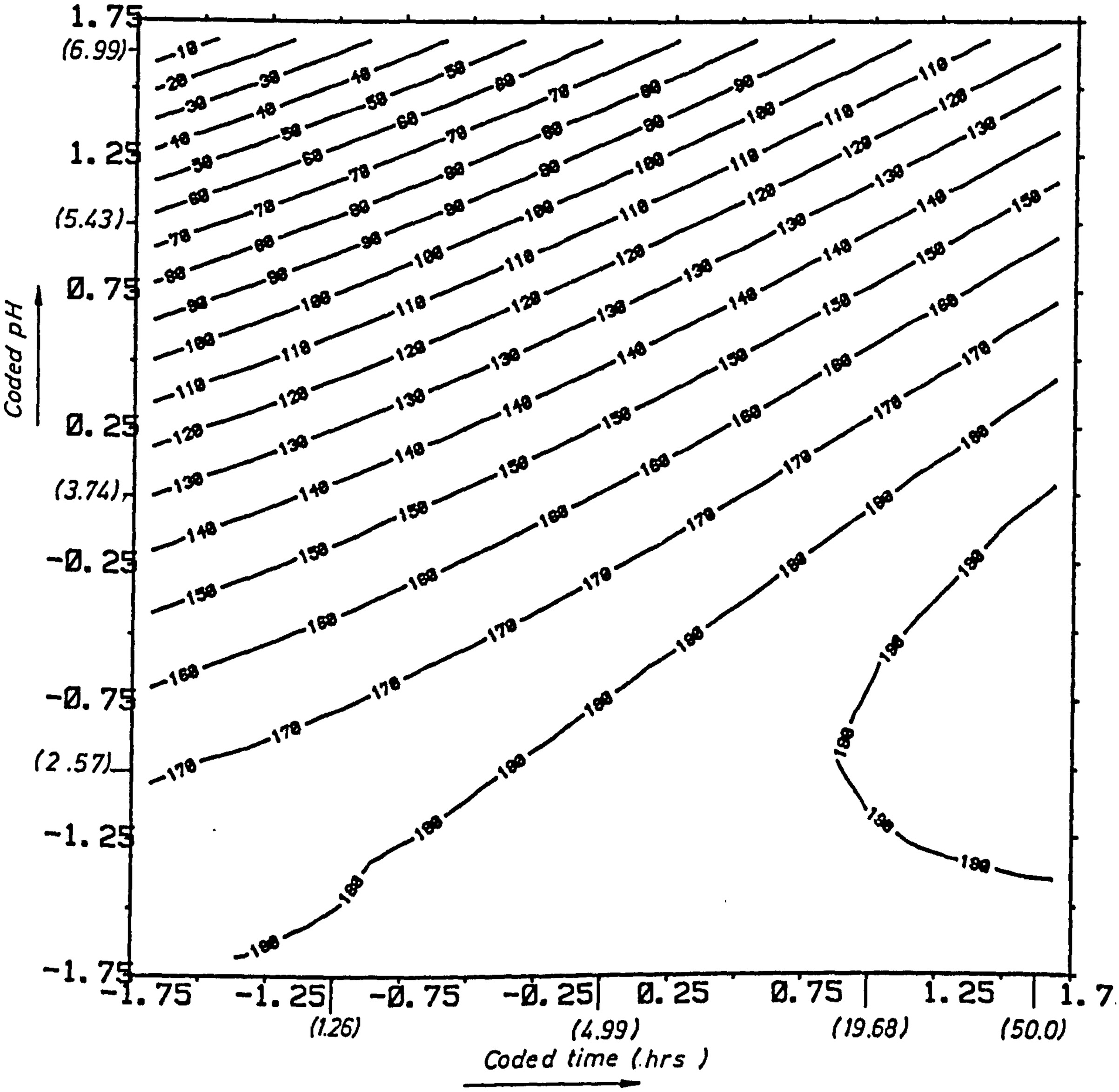

FIG. 6.25 RESPONSE SURFACE FOR LEAD RELEASED FROM RESTRONGUET CREEK No. 3 SEDIMENT

a) GINO

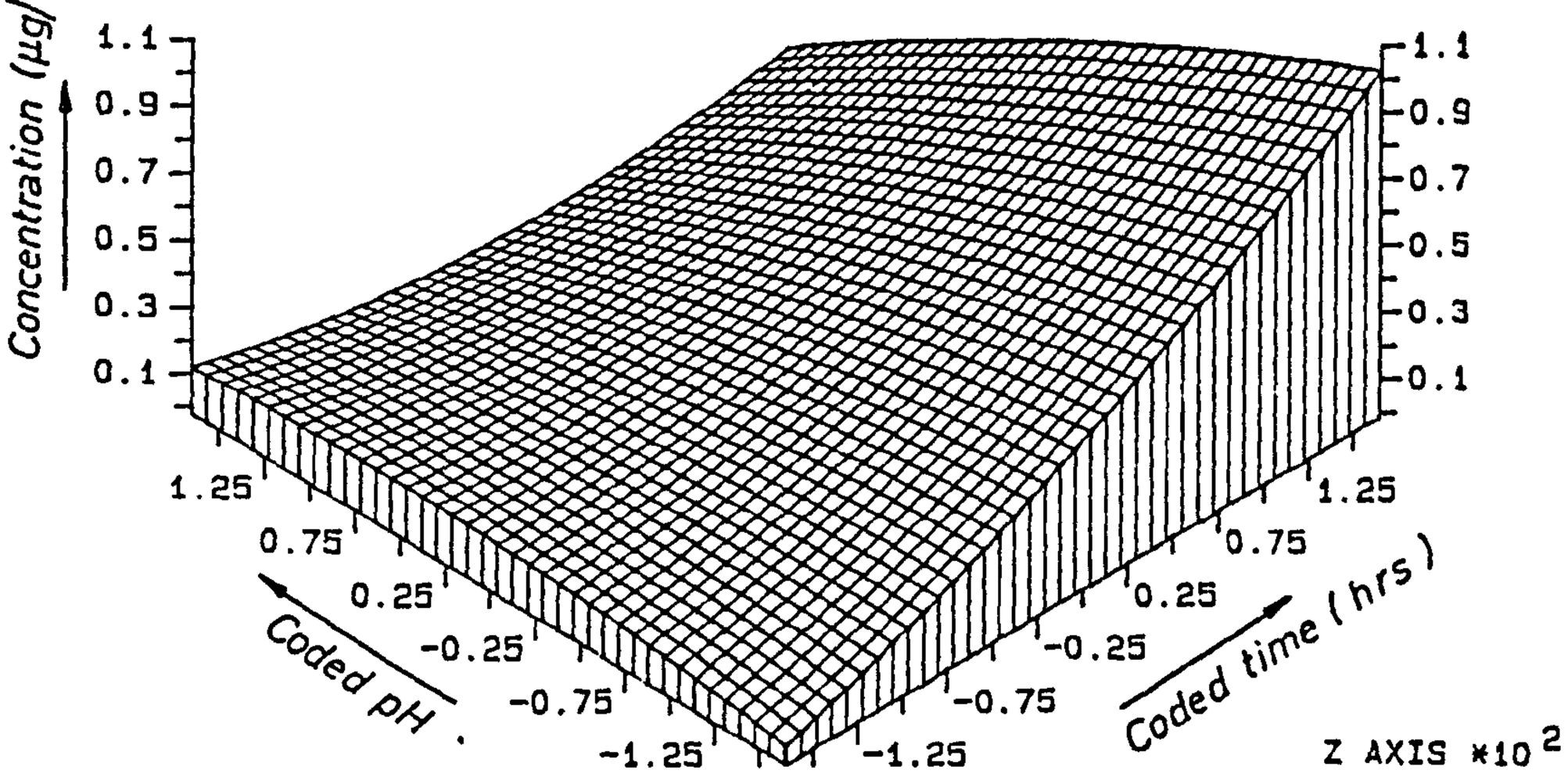

b) SAS

FIG. 6.26 CONTOUR PLOT OF RESPONSE SURFACE FOR LEAD RELEASED FROM RESTRONGUET CREEK No.3 SEDIMENT

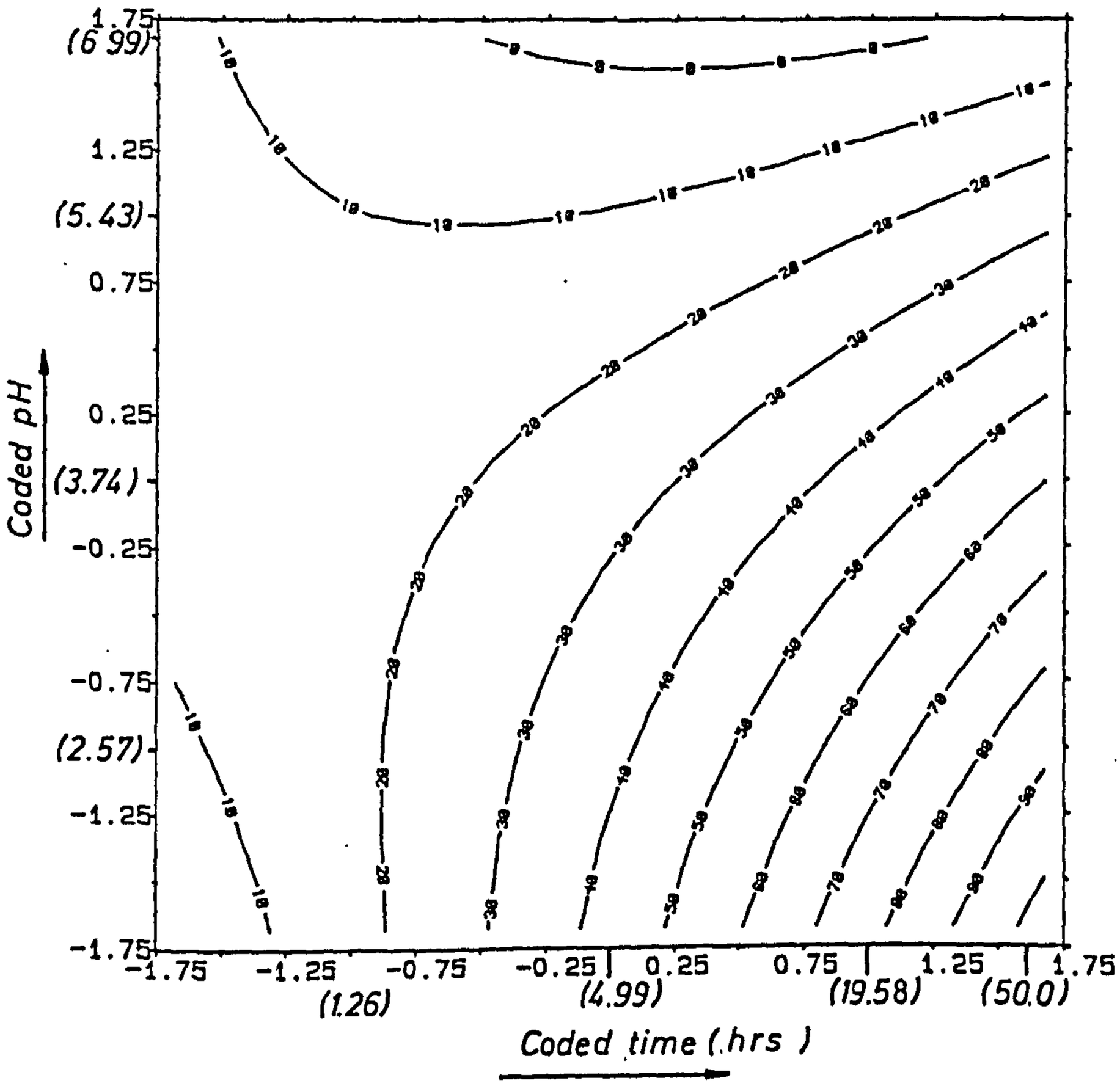

FIG. 6.27 RESPONSE SURFACE FOR LEAD RELEASED FROM ADIT BRIDGE No.8 SEDIMENT

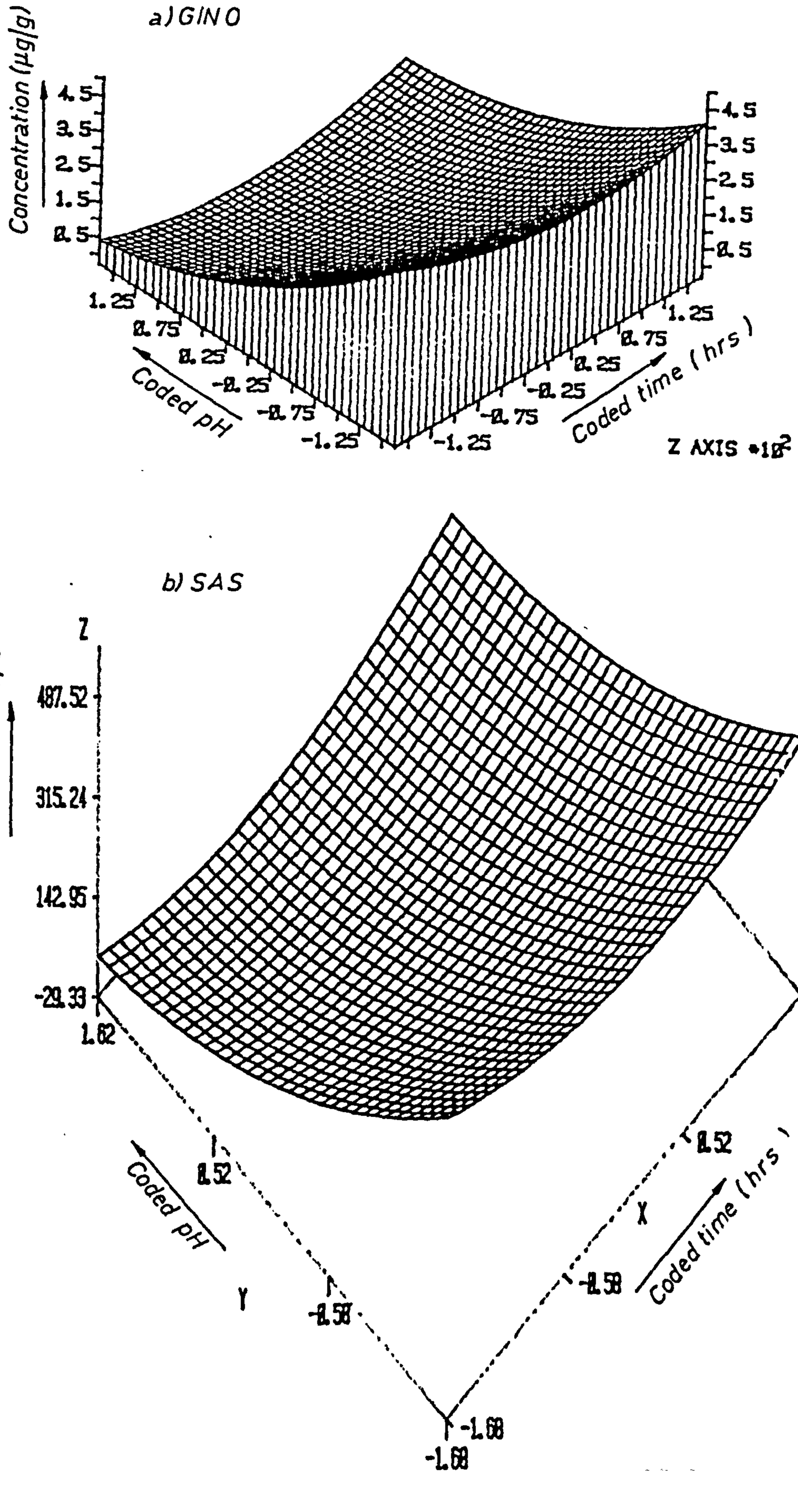

FIG. 6.28 CONTOUR PLOT OF RESPONSE SURFACE FOR LEAD RELEASED FROM ADIT BRIDGE No. 8 SEDIMENT

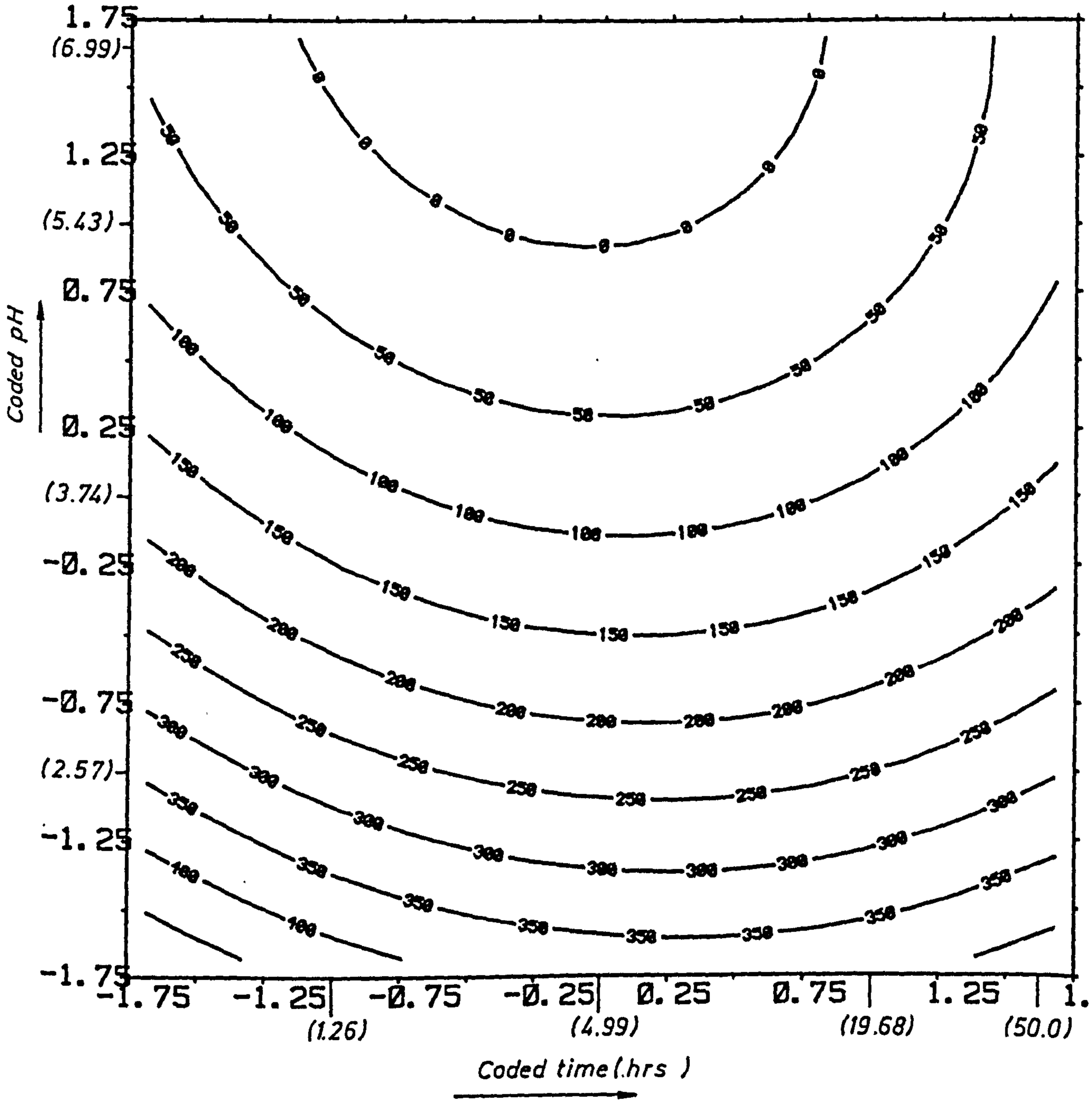

The evidence presented in this work indicates that pH and time are very important factors in investigating the release processes for metals from sediments. The observed amounts of metal released from the sediments are given in Tables 6.5 and 6.6. The regression coefficients for the response surfaces of metal released from the sediments and ANOVA are shown in Tables 6.7 and 6.8. These coefficients were used in the equations which describe the response surfaces for metal released from sediments. For example, the equation for the amount of calcium released from the Adit Bridge No. 8 sediment as a function of pH and time is :-

$$y = 1044 - 98x_1 + 31.5x_2 - 62x_1^2 + 4x_2^2 - 29x_1x_2$$

where x_1 = coded value of time

x_2 = coded value of pH

Both parameters are on a log scale.

The ANOVA (Tables 6.7 and 6.8) showed that linear coefficients and quadratics were obtained from the system. The mean square for lack of fit is a measure of the failure of second-order polynomial equations to predict the observed results. An estimation of the effect of pH and time on the amount of metal released from Restronguet Creek No. 3 and Adit Bridge No. 8 sediments may be made by comparison of the magnitudes of the coefficient (B_{12}) which form the sequence :-

Restronguet Creek No. 3 Sediment

Zn > Mn > Cu > Pb > Fe > Ca

Adit Bridge No. 8 Sediment

Ca > Zn > Cu > Pb > Mn > Fe

The coefficient B_o represents the estimated amount of metal released from sediment at the centre of the design pattern at $x_1 = 0$ and $x_2 = 0$. Taking the partial derivative with respect to x_1, then :-

$$\frac{\delta y}{\delta x_1} = B_1 + 2B_{11}x_1 + B_{12}x_2$$

This equation shows how the change in amount of metal released from sediment per unit change in x_1 depends on x_1 and x_2. It is apparent that B_1 is the slope of the surface in the x_1 direction at the centre of the design pattern. Taking the second partial differential with respect to x_1 :

$$\frac{\delta^2 y}{\delta x_1^2} = 2B_{11}$$

which indicates that B_{11} is related directly to how rapidly the slope in the x_1 direction is changing, thus, B_{11} is a measure of curvature. Next taking the mixed partial derivative for the amount of metal released from the sediment with respect to x_1 and x_2

$$\frac{\delta^2 y}{\delta x_1 \delta x_2} = B_{12}$$

Thus B_{12} shows by how much the x_1 effects change with x_2; that is, B_{12} measures the interaction of x_1 and x_2. The equations for the quantity for each metal released from the sediment may be solved to obtain points in terms of x_1 and x_2 which correspond to the maximum quantity of metals released from the sediment. This can be done by taking the first partial derivatives of the equations with respect to x_1 and x_2, setting them equal to zero and then solving the two equations simultaneously. Fortunately all the previous equations can be solved by computational methods (see Appendix 6.2). The values obtained for the solution of these equations are given in Table 6.23. Under the conditions of this experiment, the optimum pH and time values were higher than are generally used in this type of experiments (20).

Table 6.23 : Levels of Time and pH used in the Experiment Estimated to Produce Maximum Amount of Metal Released from Sediments

a) Restronguet Creek No. 3 Sediment

Metal	Coded Value of x		Actual Value of x		Estimated am Amount of Metal (μg/g)
	x_1	x_2	x_1	x_2	
Ca	-0.6717	1.856	1.98	7.44	1,583
Mn	-1.9521	-1.205	0.33	2.39	53
Fe	-2.0127	0.7075	0.30	4.86	69
Cu	-2.7073	-1.0319	0.11	2.55	146
Zn	1.819	-0.1335	60.49	3.65	675
Pb	-1.9729	-0.063	0.32	3.65	13

b) Adit Bridge No. 3 Sediment

Metal	Coded Value of x		Actual Value of x		Estimated Amount of Metal (μg/g)
	x_1	x_2	x_1	x_2	
Ca	-0.9321	-0.59218	1.35	3.08	1,080
Mn	2.260	-1.3288	111	2.28	701
Fe	-1.875	0.8720	0.36	5.16	1,405
Cu	1.7428	0.9668	54.35	5.35	57
Zn	-1.6720	-1.8755	0.48	1.86	179
Pb	-0.340	2.0518	3.04	8.00	36

x_1 = Time (in hours)

x_2 = pH

A detailed examination of the data in Table 6.23 is not possible, since some of the coefficients reported are obviously in error: for example, the value of pH 8.00 being the best pH to leach lead from a sample. Clearly the fit of the surface and the consequent extrapolation outside the surface boundary conditions must invalidate any conclusions which may be drawn.

In general for the range of pH values quoted in Table 6.23, none or very little of the residual phase metals would be expected to dissolve in the solution. Thus with the pH values given, decomposition of the phases from exchangeable to organic inclusive must be taking place.

Any examination of the data in Table 6.23 seems to indicate that for calcium, iron and possibly manganese the conditions for optimum yield are satisfactory for both sediments.

However, for the other three elements, Cu, Pb and Zn, there are anomalies in the interpretation of the data. Thus, the optimum yield of Cu from the Restronguet Creek appears to be satisfactory by the two values of 0.11 hours and pH 2.55. But this is in direct contrast to the values of 54.35 hours and pH 5.35 for the Adit No. 8 sediment. Indeed in this latter sediment some 35% of Cu is in the carbonate phase and should be readily available to dissolution. It appears that examination of data in Table 6.6 shows that a relatively constant amount of copper dissolves almost immediately even at pH 6, probably from the exchangeable form, but nothing else, leading to a plane type surface. In the Restronguet Creek sediment the figures are much more varied, leading to a much more clearly defined surface.

Turning to zinc, here the roles are reversed; the parameters for the Adit sediment are reasonable with 0.48 hours and pH 1.86. Such values are in line with those expected from a consideration of the fact that 80% of the zinc is bound to the Fe-Mn hydrous oxide phase. However,

for the Restronguet Creek, the majority of the zinc is in the residual phase (70%), and therefore a very long time is expected to cause its dissolution but not at the pH 3.65 quoted.

Finally for lead, clearly it is rather immobile, some 13 $\mu g/g$ being released from Restronguet Creek sediment and 36 $\mu g/g$ from the Adit Bridge. Therefore, although the values of 0.32 hours and pH 3.65 appear satisfactory (for the Restronguet Creek sediment), the corresponding values for the Adit sediment of 3.04 hours and pH 8.00 are clearly in error.

The validity of the response surface methodology has been demonstrated although difficulties of interpretation possibly due to kinetic factors and the inhomogeneity of the sample remain. Much further work remains to be carried out in this area but the surfaces obtained show that the technique of experimental design clearly has much further potential.

b) Interactive Effects of Metals on Plants

To study the interactive effects of elements upon plant growth there are two major questions to be considered (27). How far does the presence of one of these elements :-

1) in the solution around the roots of the test crop modify the uptake of other elements and their translocation to the shoots?

2) in the tissue of the shoot modify the toxicity of the other elements in the same tissues?

In general, the results in Tables 6.11 and 6.12 indicate that the levels of essential metals such as Cu, Zn, Fe, Mg and Mn in the roots of Cock's Foot seedlings when fed thallium was higher than when the silver was employed. Although the nutrient solution contained lanthanum and lead in the two sets of experiments, silver may cause more interference effects than thallium particularly with divalent heavy metals through precipitation reactions, consequently decreasing the level taken up by the plant. The results in Table 6.13 and 6.14 illustrate that silver has a significant effect on the translocation of magnesium and manganese from the roots to the shoots of the plant, i.e. in some treatments the same level of manganese or magnesium was found in the roots and shoots. In one or two cases the concentrations were even higher in the shoots than in the roots. Heavy metal interactions are often merely suspected but there is little 'hard evidence' to support these suspicions. Copper decreases the absorption of zinc and its translocation from the roots to the shoots. Brar et alia (28) reported that zinc and copper co-ordinated to N and S groups of amino acids. So it seems that copper by competing with zinc for the binding sites of amino acids may affect the translocation of zinc within the plant. Brar et alia (29) also reported that by increasing the iron concentration

the zinc uptake by plants was reduced. Wallace et alia (30) reported that nickel decreased the level of manganese in the shoots while it increased the levels of cobalt and zinc in the shoots. Silver has a greater affinity to chelate with the sulfhydryl group present in some amino acids than other divalent heavy metals (see Table 6.24). So competition between such metals as lead and zinc for the binding sites of the sulphur-amino acids can affect their translocation and uptake by Cock's Foot seedlings which were used in the present work.

Tables 6.15 to 6.18 indicate that Lolium perenne seedlings also accumulated more metals in the roots than in the shoots. The plants were grown in a nutrient solution containing aluminium and lead; when silver was added to the solution the level of iron in the plants was less than the level when thallium was employed.

Table 6.24 : Stability Constant Values for Some Metals with S-Methylcysteine at 25°C (31)

Metal Ion	Equilibrium	Log K
Ag^{+}	ML/M.L.	5.25
Zn^{2+}	ML/M.L.	4.46
Pb^{2+}	ML/M.L.	4.43
Cd^{2+}	ML/M.L.	3.77

A similar observation was made when using the Cock's Foot species, i.e. silver has similar effects in the two species. It is more useful to discuss the interactive effects of metals on the plant responses (e.g. root length, dry weight of plant and metal concentrations of plant tissue) by taking each species individually.

1) Cock's Foot Seedlings

The observed plant responses for the roots and shoots are given in Tables 6.11 to 6.14. The equation [6.8] represents the response surfaces of plant response. The regression coefficients of the surfaces are shown in Tables 6.19 and 6.20.

a) Interactive Effects of La and Pb on Copper in Plant Tissues

Figure 6.29 illustrates the effects of La and Pb solution levels on copper in the roots when the Tl level is held constant at coded value 0 (0.01 $\mu g/cm^3$). The surface indicates that when Pb is present in the nutrient solution in very low concentrations (less than a coded level of -1.00 which is equivalent to 3.2×10^{-3} $\mu g/cm^3$) higher levels of copper are taken up than when the lead is increased in the nutrient solution. However, the nutrient solution also contained lanthanum but the shape of the surface indicates that the level of lanthanum does not affect the uptake of copper. Thus it can be concluded that lead interacted with the copper uptake while lanthanum does not do so. Figures 6.30a and 6.30b demonstrate the effect of lead and lanthanum on copper uptake when the Tl level is constant at the coded values of -1.68 (1×10^{-4} $\mu g/cm^3$) and 1.68 (1 $\mu g/cm^3$) respectively. The surfaces also illustrate that the copper uptake increased at low levels of lead while the uptake decreased for the higher levels of lead. In general, it can be concluded that lead has a negative interaction with copper taken up by the roots of Cock's Foot seedlings.

Since the interactive effects of the metals on the root response (root length, dry weight and metals in roots) was dependent on the particular level of the third metal present (even though it was held constant at a set level), it was decided to examine the surface responses for the roots for any two metals, but at three constant levels for the third

FIG. 6.29 RESPONSE SURFACE FOR COPPER TAKEN UP BY ROOTS OF COCKS FOOT SEEDLING AT CODED TI = 0

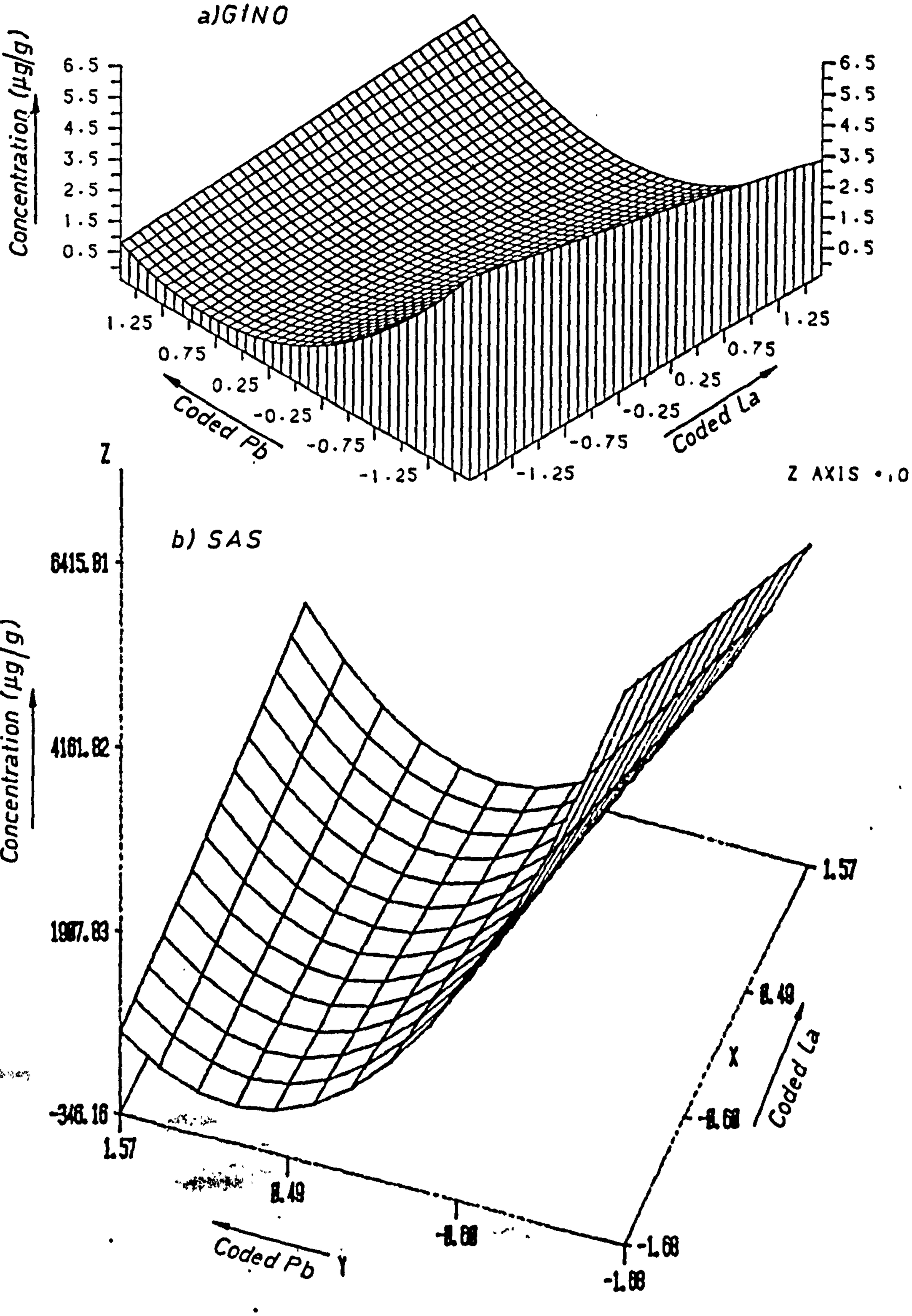

FIG. 6.30 RESPONSE SURFACE FOR COPPER TAKEN UP BY ROOTS OF COCKS FOOT SEEDLING

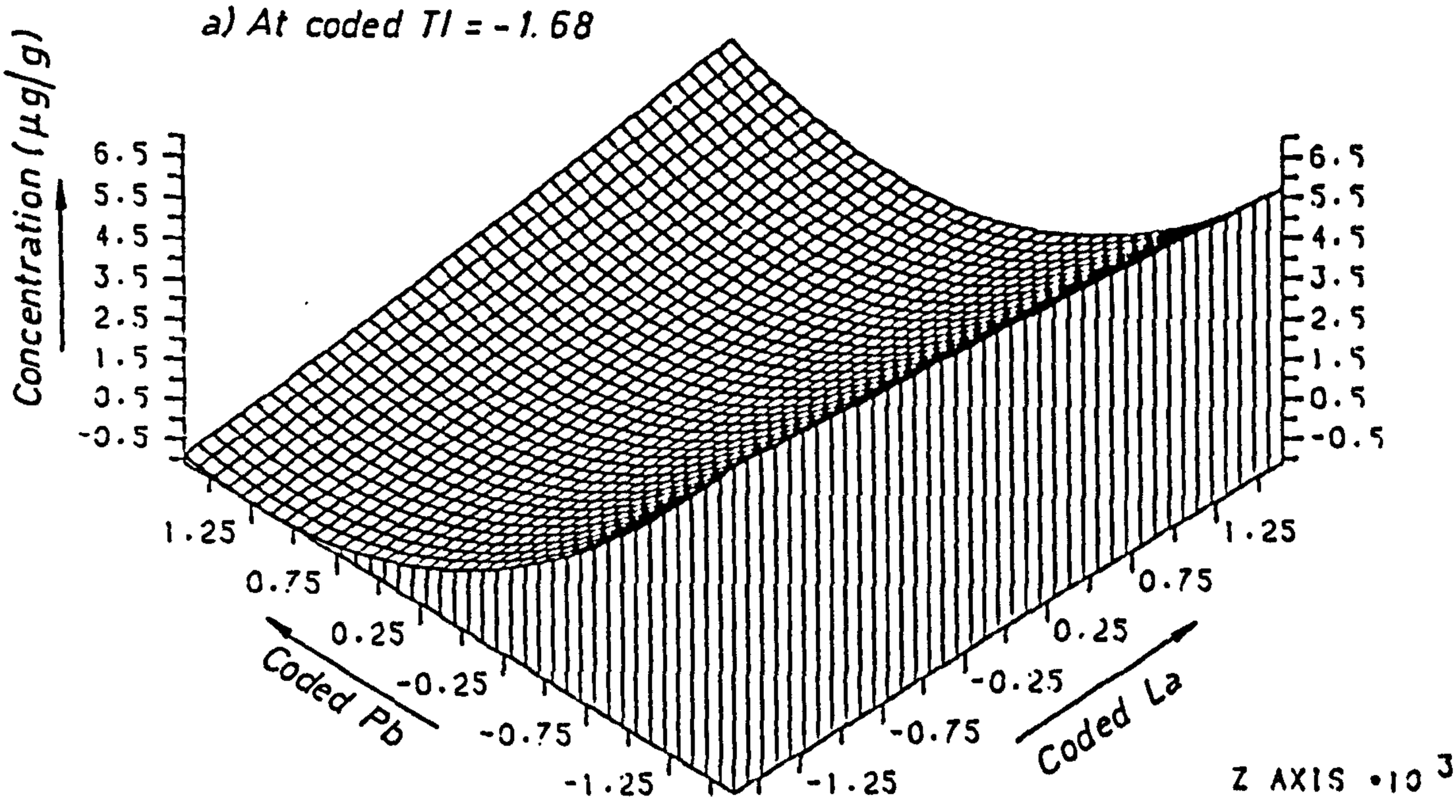

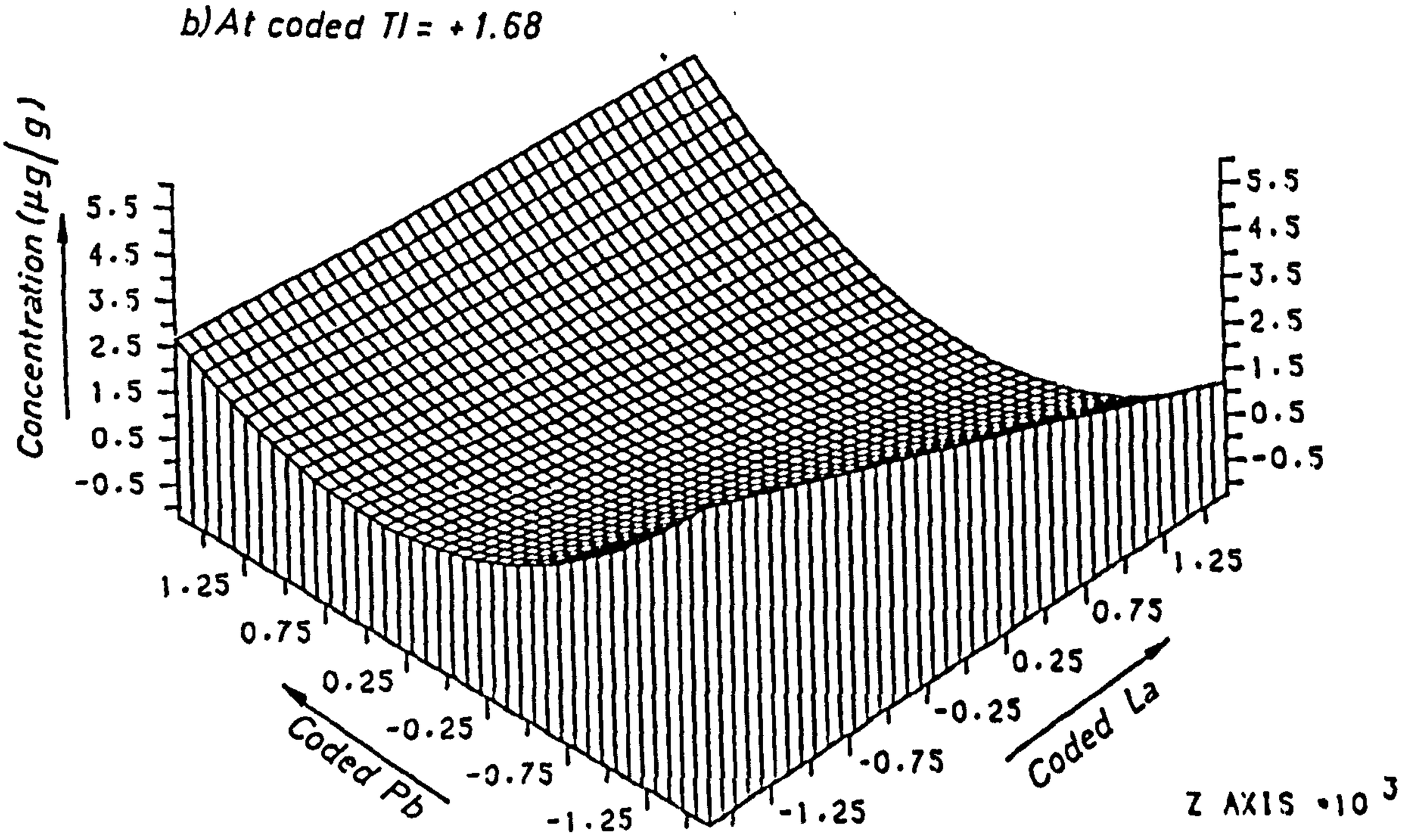

metal (namely, -1.68, 0 and 1.68), so that three surfaces could be obtained from any one particular system. Thus for one species, Cock's Foot, all response surfaces possible for the roots have been determined and are reproduced. For the other species, only the more interesting surfaces have been produced, although the respective regression equations have been calculated. In order to limit the number of surfaces for the shoots, only one of the three possible surfaces generated at each level will be presented within this dissertation. To provide a meaningful comparison, the coded value 0 was chosen as the reference point.

Figure 6.31 illustrates the interactive effects of La and Pb in the nutrient solution on copper in shoots at a Tl coded level of 0. The surface indicates that both lanthanum (> 0.25 $\mu g/cm^3$) and lead (> 0.05 $\mu g/cm^3$) decreased the level of copper in shoots. Chaudhry et alia (32) reported that zinc may depress the Cu concentration in plant tops by dilution of absorbed Cu through promotion of plant growth. Probably, lanthanum behaved as zinc and so reduced the copper content of the shoots. Lead showed negative interaction with the copper content of roots, perhaps it decreased the Cu content of the shoots by inhibiting its translocation from the roots to the shoots.

b) Interactive Effects of La and Pb on Iron in Plant Tissues

Figure 6.32 illustrates the interactive effects of La and Pb on iron in roots at a coded level of Tl = 0. At high levels of lead and lanthanum, the iron uptake was reduced. From Figures 6.29 and 6.32, it is observed that lanthanum and lead in the nutrient solution at a Tl level of 0 have different interactive effects on the copper and iron taken up by the plant. Figures 6.33a and 6.33b demonstrate the interactive effects of La and Pb on iron in the roots but at Tl levels of 1.68 (1 $\mu g/cm^3$) and-1.68 (1 x 10^{-4} $\mu g/cm^3$) respectively. The latter

FIG. 6.31 RESPONSE SURFACE FOR COPPER TAKEN UP BY SHOOTS OF COCKS FOOT SEEDLING AT CODED TI=0

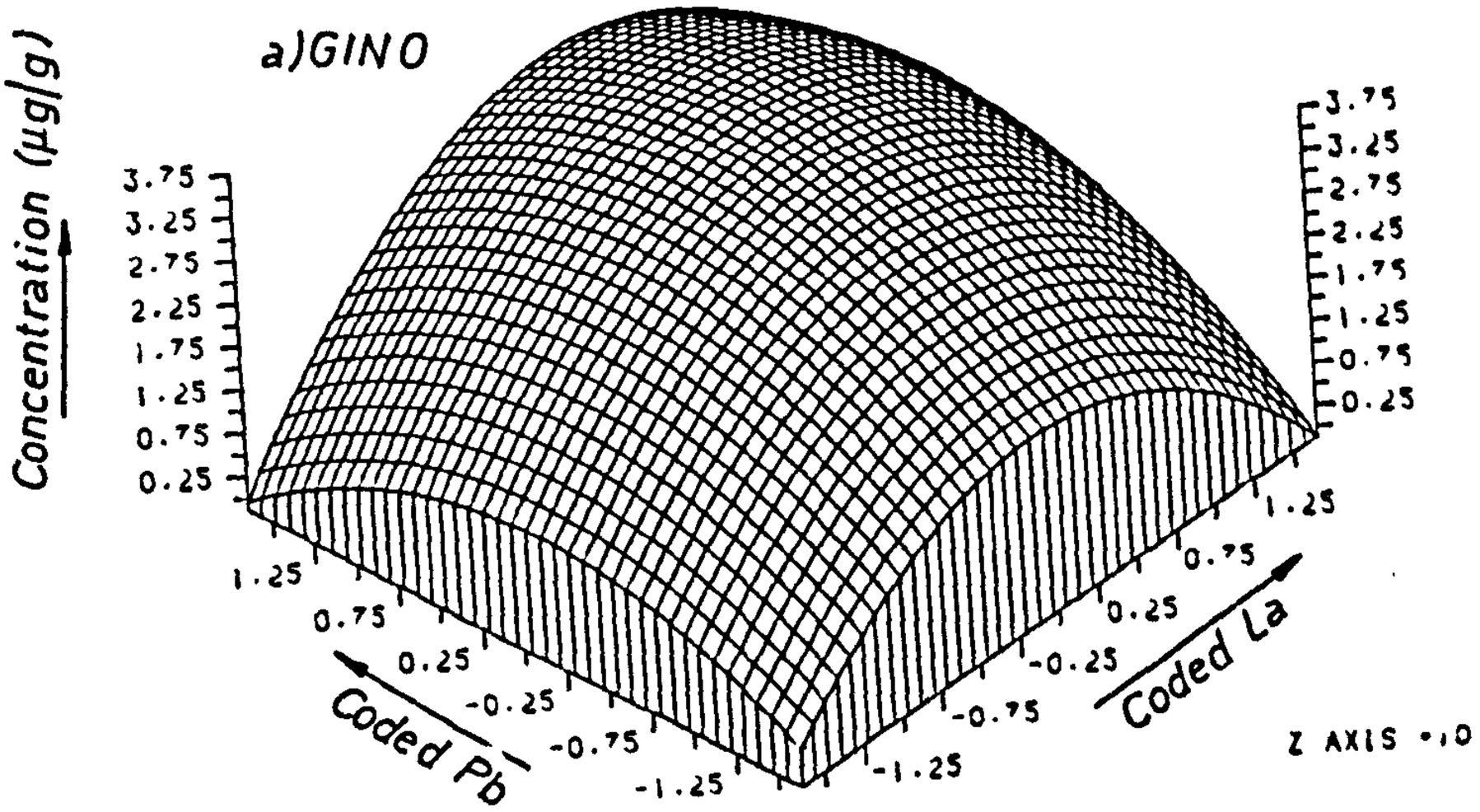

FIG. 6.32 RESPONSE SURFACE FOR IRON TAKEN UP BY ROOTS OF COCKS FOOT SEEDLING AT CODED TI = 0

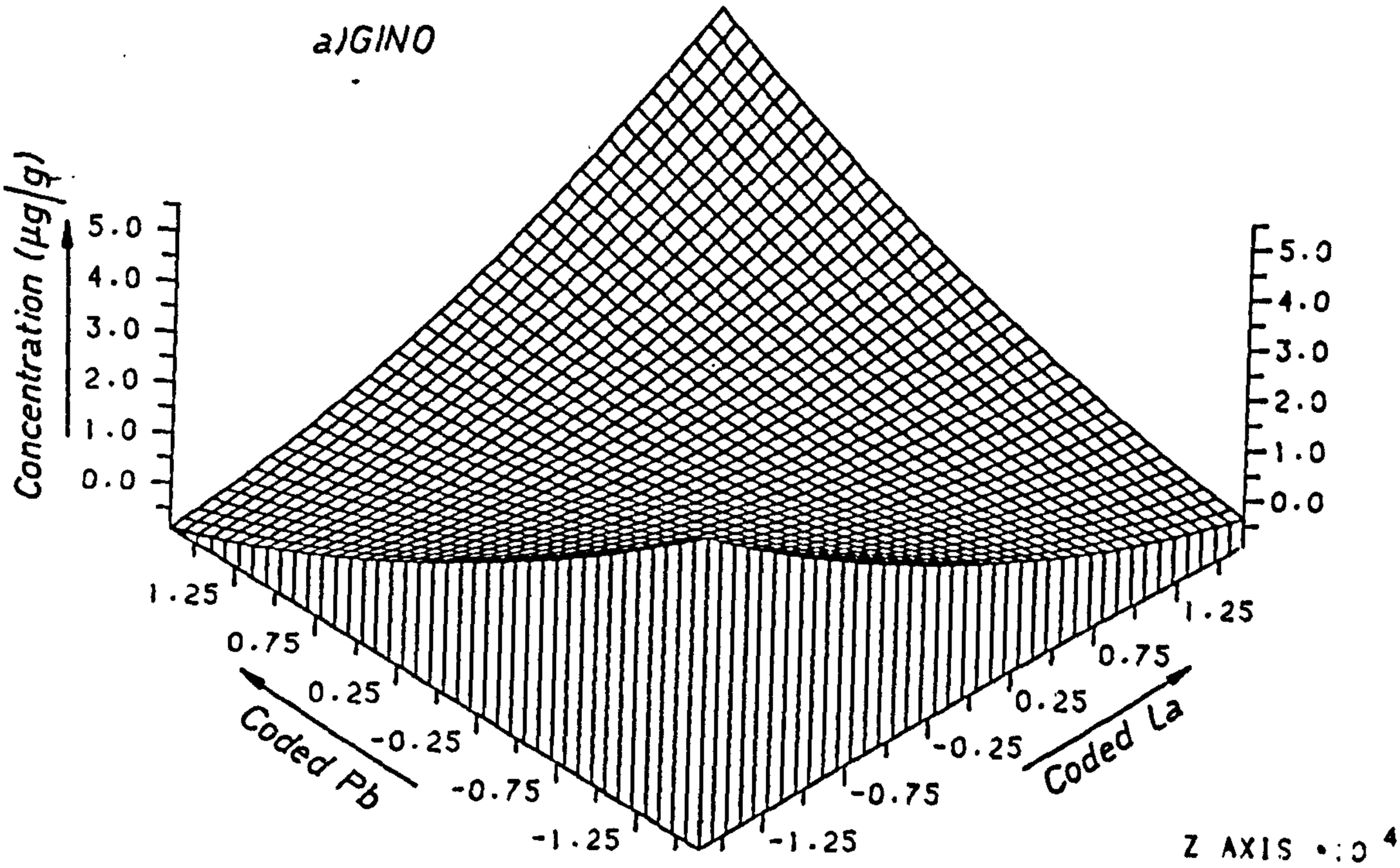

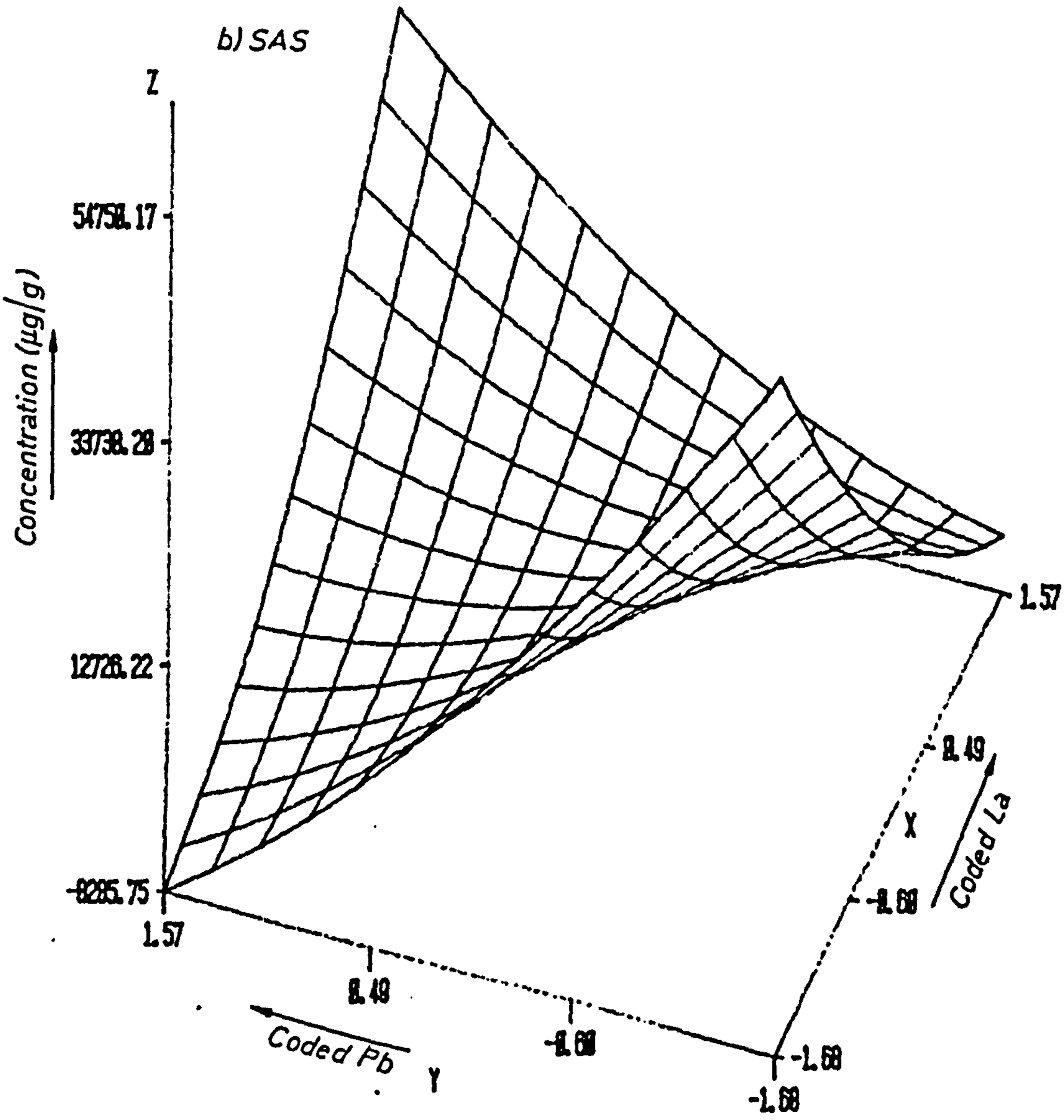

FIG. 6.33 RESPONSE SURFACE FOR IRON TAKEN UP BY ROOTS OF COCKS FOOT SEEDLING

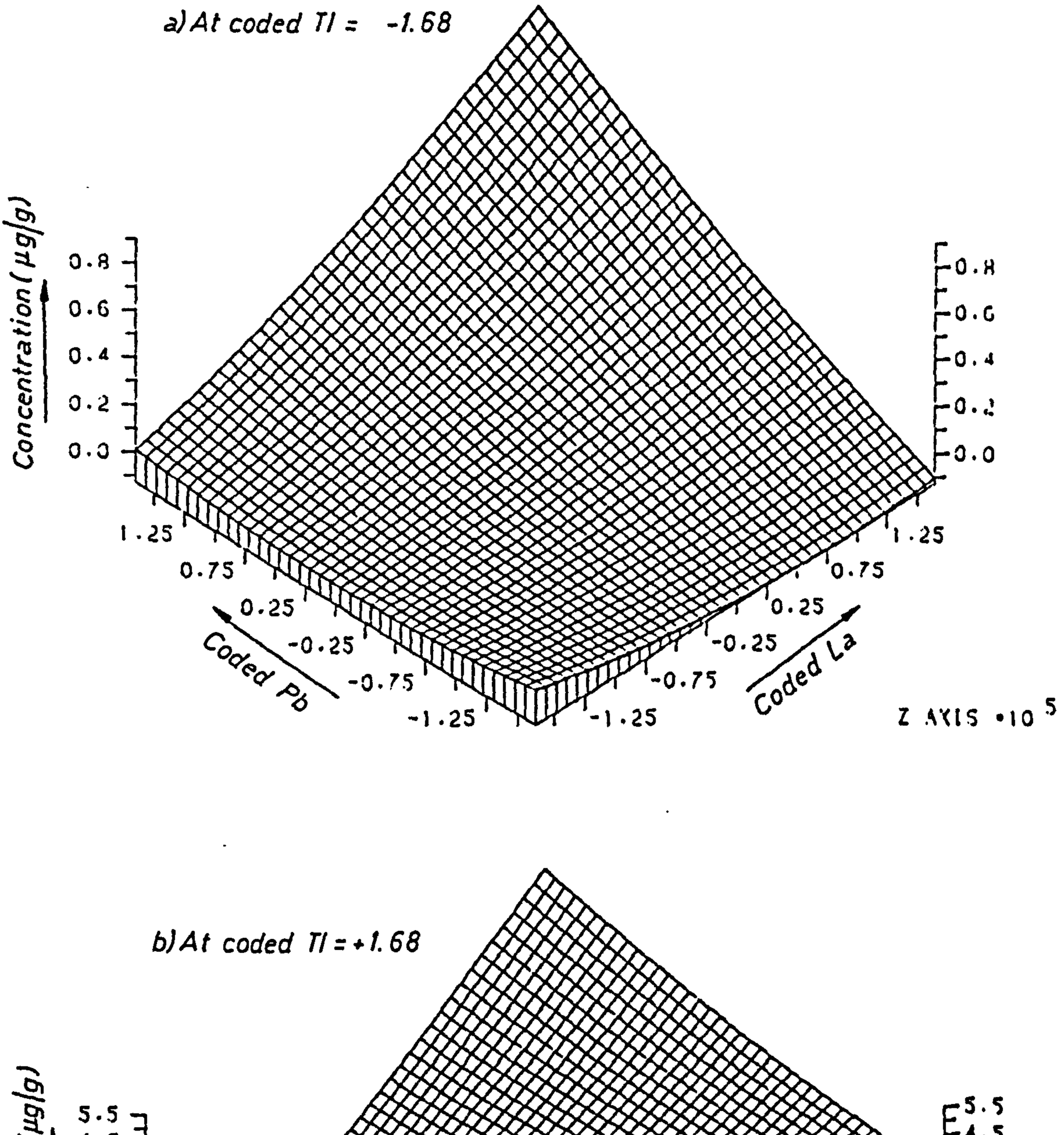

figures are different in shape from Figure 6.32, since the surfaces are quite different, thus Tl may control the interaction between La and Pb. Figure 6.33a indicates that at low levels of La (> 0.0161 $\mu g/cm^3$), only a little iron was taken up by the plant while the uptake decreases linearly with the increased level of lead in the nutrient solution. Figure 6.34 depicts the interactive effects of La and Pb on iron in shoots at the Tl level of 0. The surface exhibits a different shape from that generated for the roots. However, Figure 6.34 indicates that while the level of iron in the shoots increased with an increased level of lead, a much more complicated response was shown by lanthanum which seems to pass through a definite minimum.

c) Interactive Effects of La and Tl on Magnesium in Plant Tissues

Figure 6.35 shows the interactive effects of La and Tl solution levels on magnesium levels with the roots when the Pb level is constant at a coded value of 0, while Figure 6.36a and 6.36b depict the effects when the Pb levels are -1.68 and 1.68 respectively. The surfaces (Figures 6.35 and 6.36a) indicate the increase of the uptake of magnesium with increase in Tl and La in the nutrient solution. Figure 6.36b illustrates that the uptake of magnesium is very low at low levels of La and Pb, less than 2.5×10^{-3} and 5×10^{-4} $\mu g/cm^3$ respectively. The three generated surfaces for magnesium uptake are different with the different levels of lead. Therefore, lead must control the interaction effects of La and Tl on magnesium uptake by the roots.

Figure 6.37 illustrates the effect of La and Tl solution levels on magnesium in the shoots when the Pb level is held constant at a coded value of 0. The surface is particularly flat and there is almost no interaction between these particular elements. Thus it appears that the translocation of magnesium into the shoots is almost independent

FIG. 6.34 RESPONSE SURFACE FOR IRON TAKEN UP BY SHOOTS OF COCKS FOOT SEEDLING AT CODED TI=0

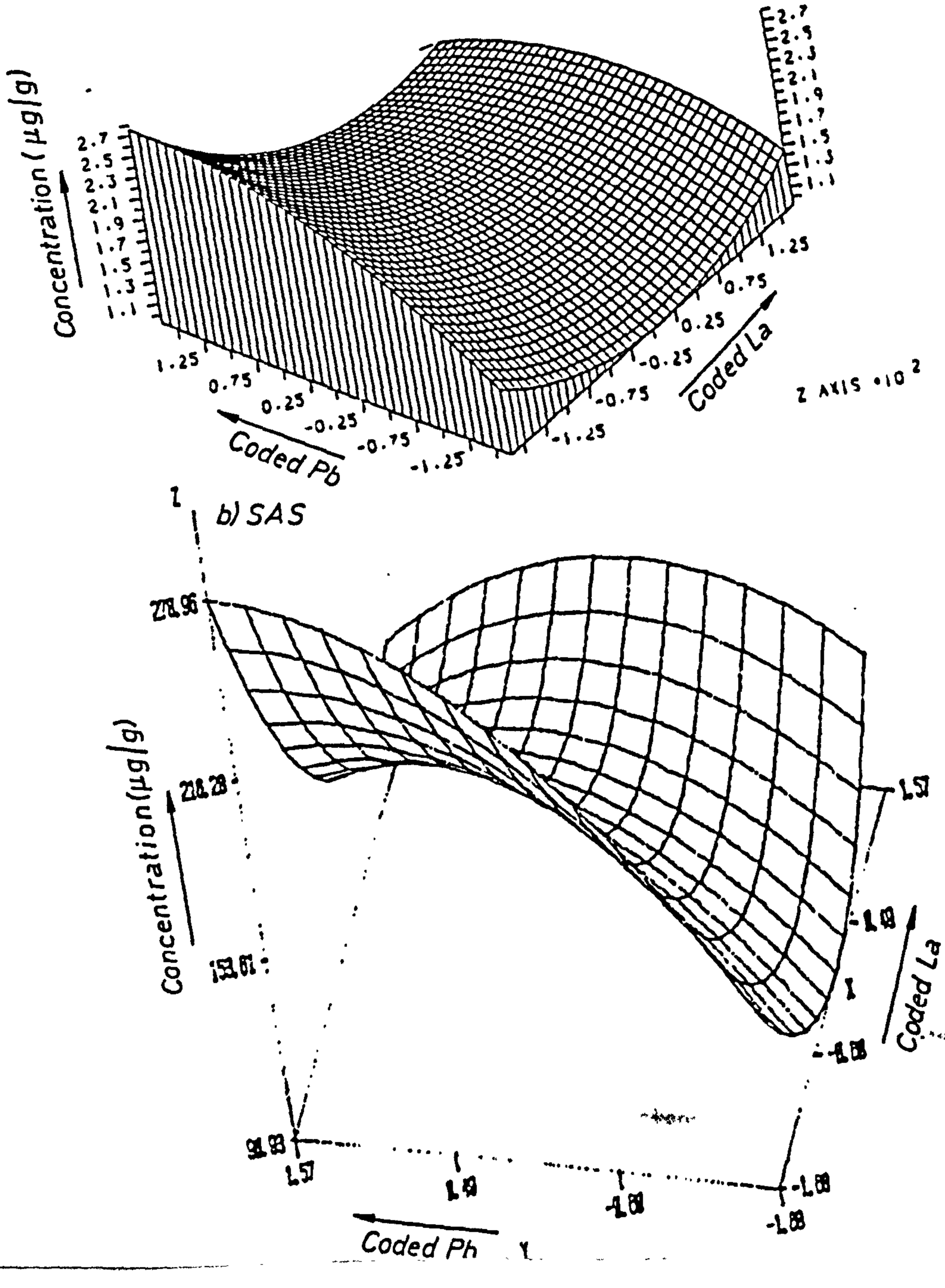

FIG. 6.35 RESPONSE SURFACE FOR MAGNESIUM TAKEN UP BY ROOTS OF COCKS FOOT SEEDLING AT CODED Pb = 0

a) GINO

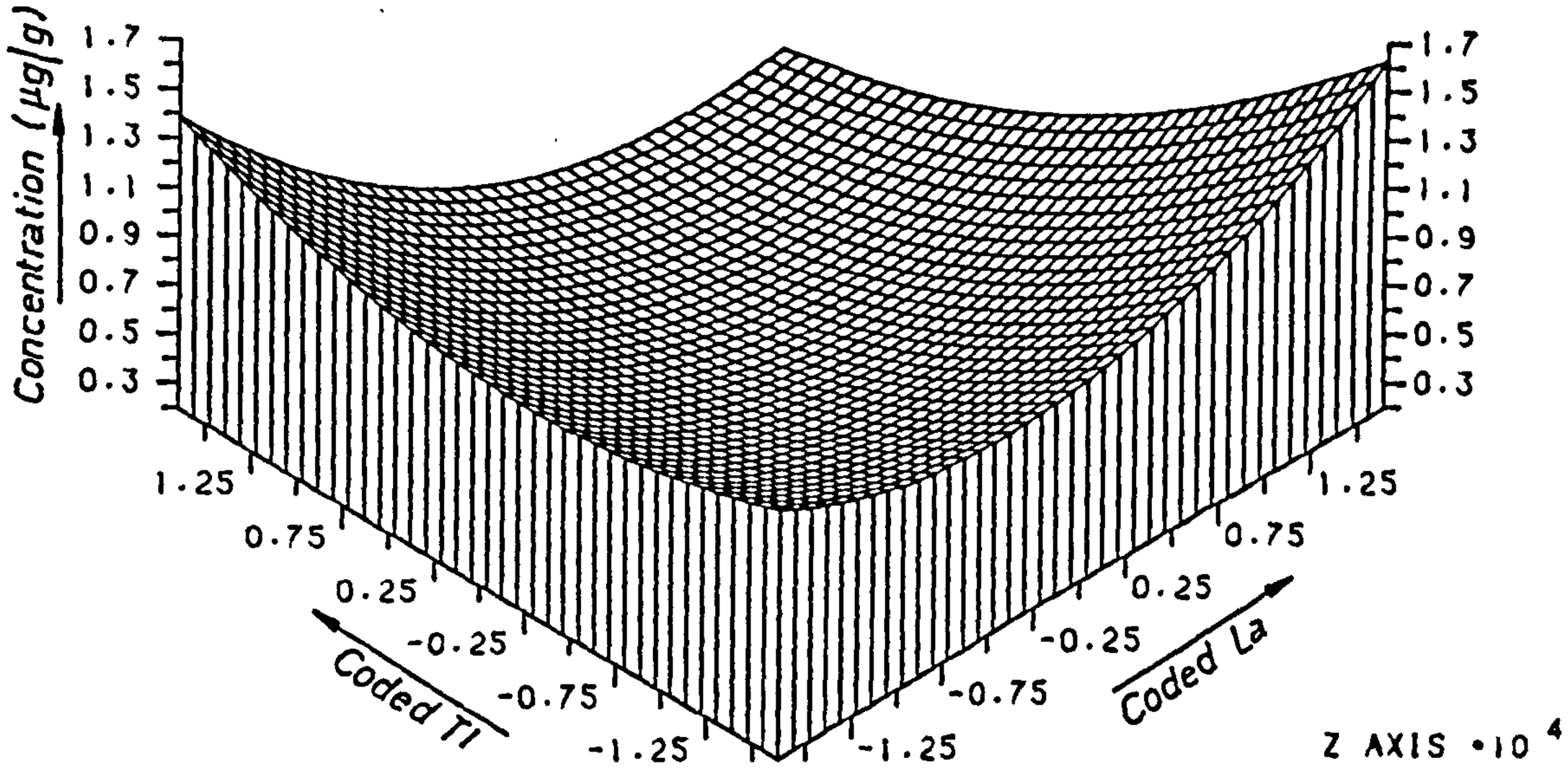

b) SAS

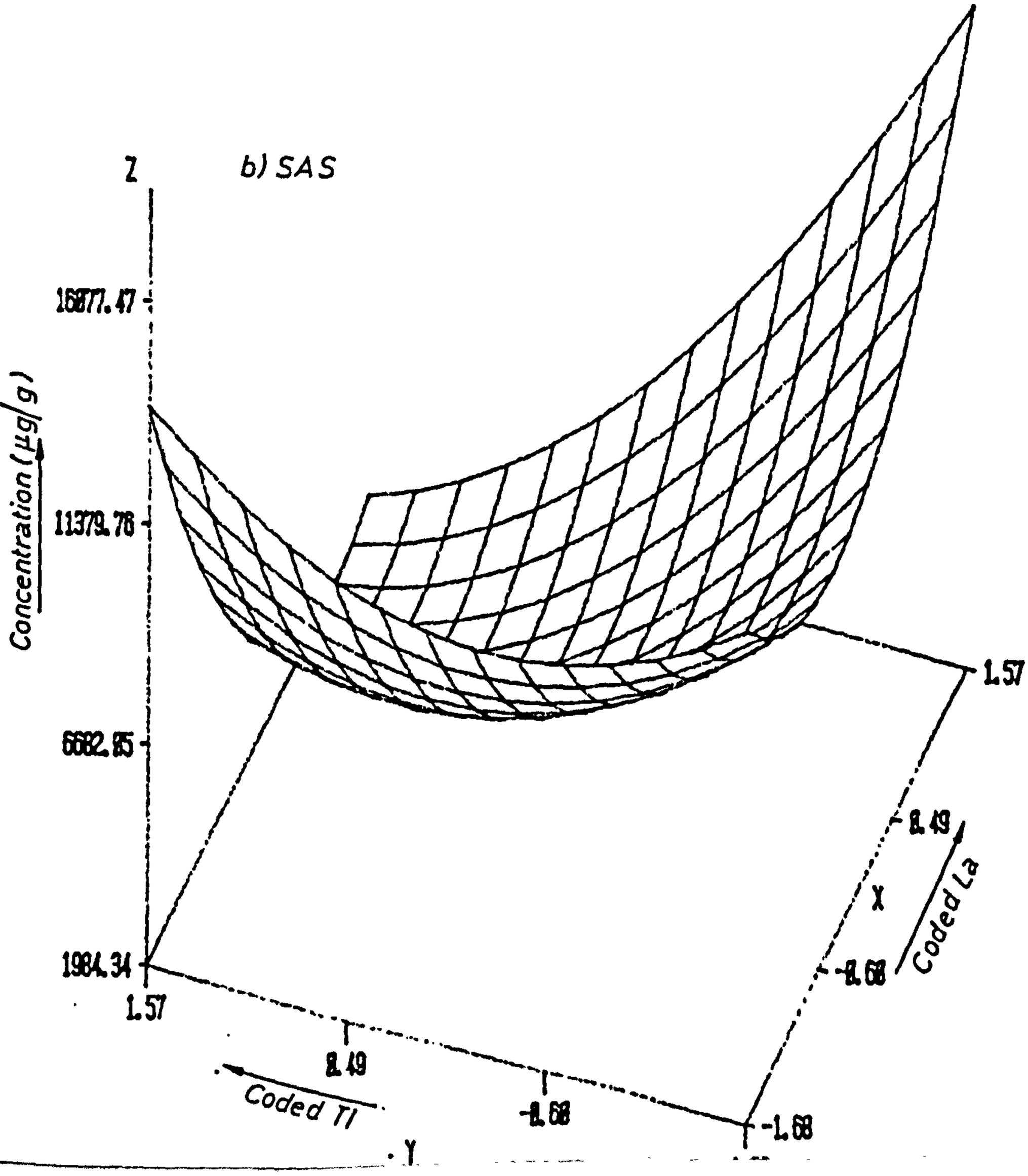

FIG. 6.36 RESPONSE SURFACE FOR MAGNESIUM TAKEN UP BY ROOTS OF COCKS FOOT SEEDLING

a) At coded Pb = -1.68

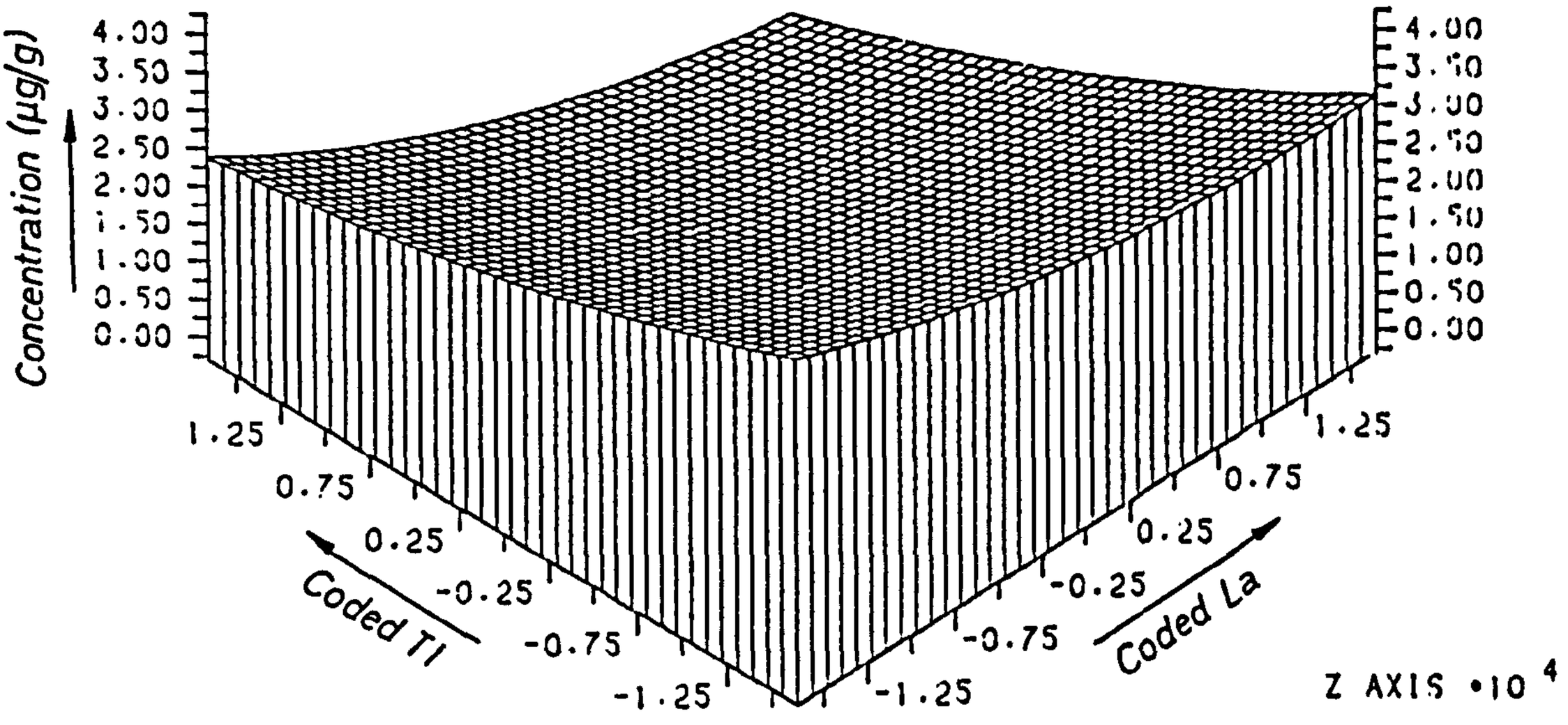

b) At coded Pb = +1.68

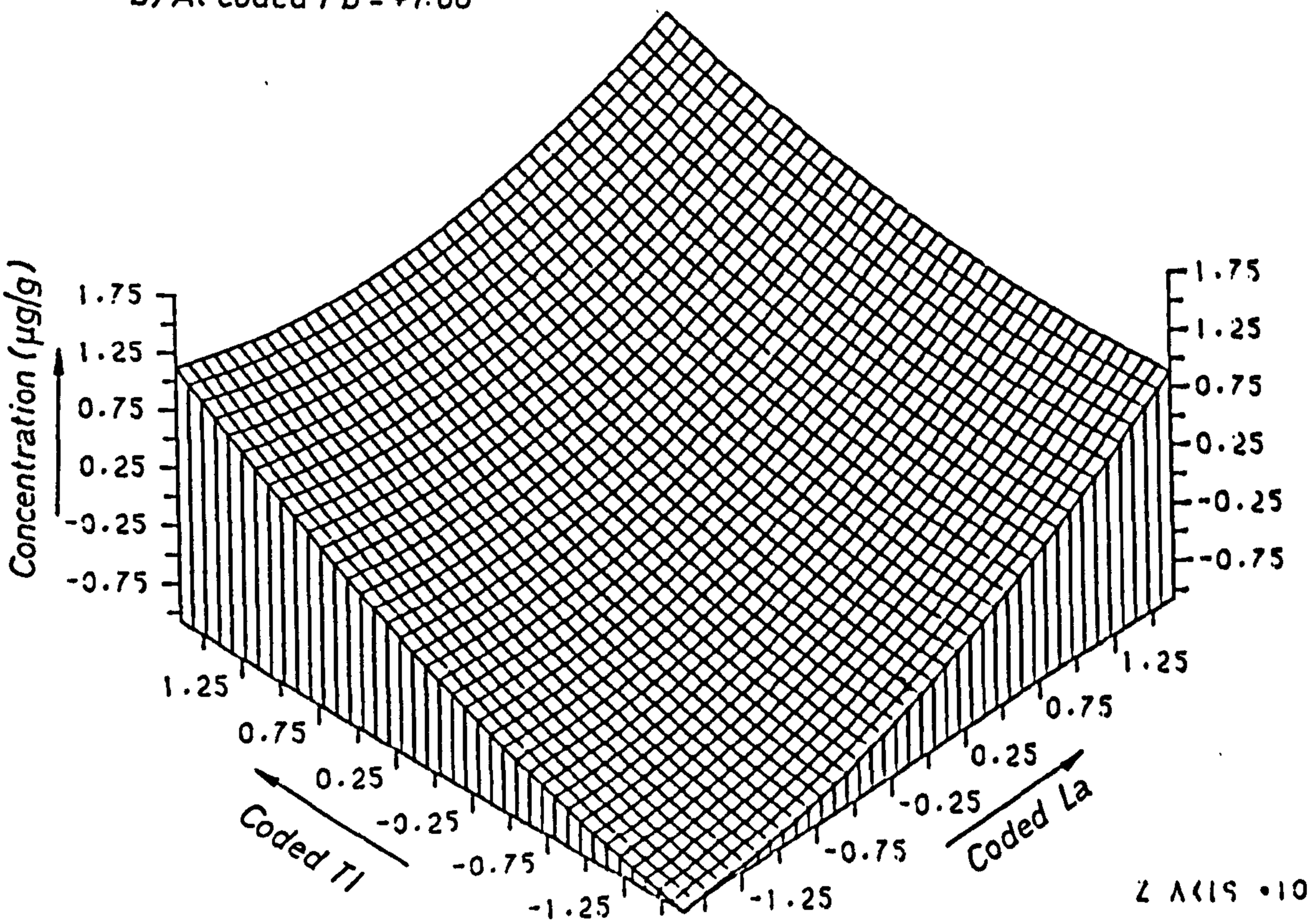

FIG. 6.37 RESPONSE SURFACE FOR MAGNESIUM TAKEN UP BY SHOOTS OF COCKS FOOT SEEDLING AT CODED Pb = 0

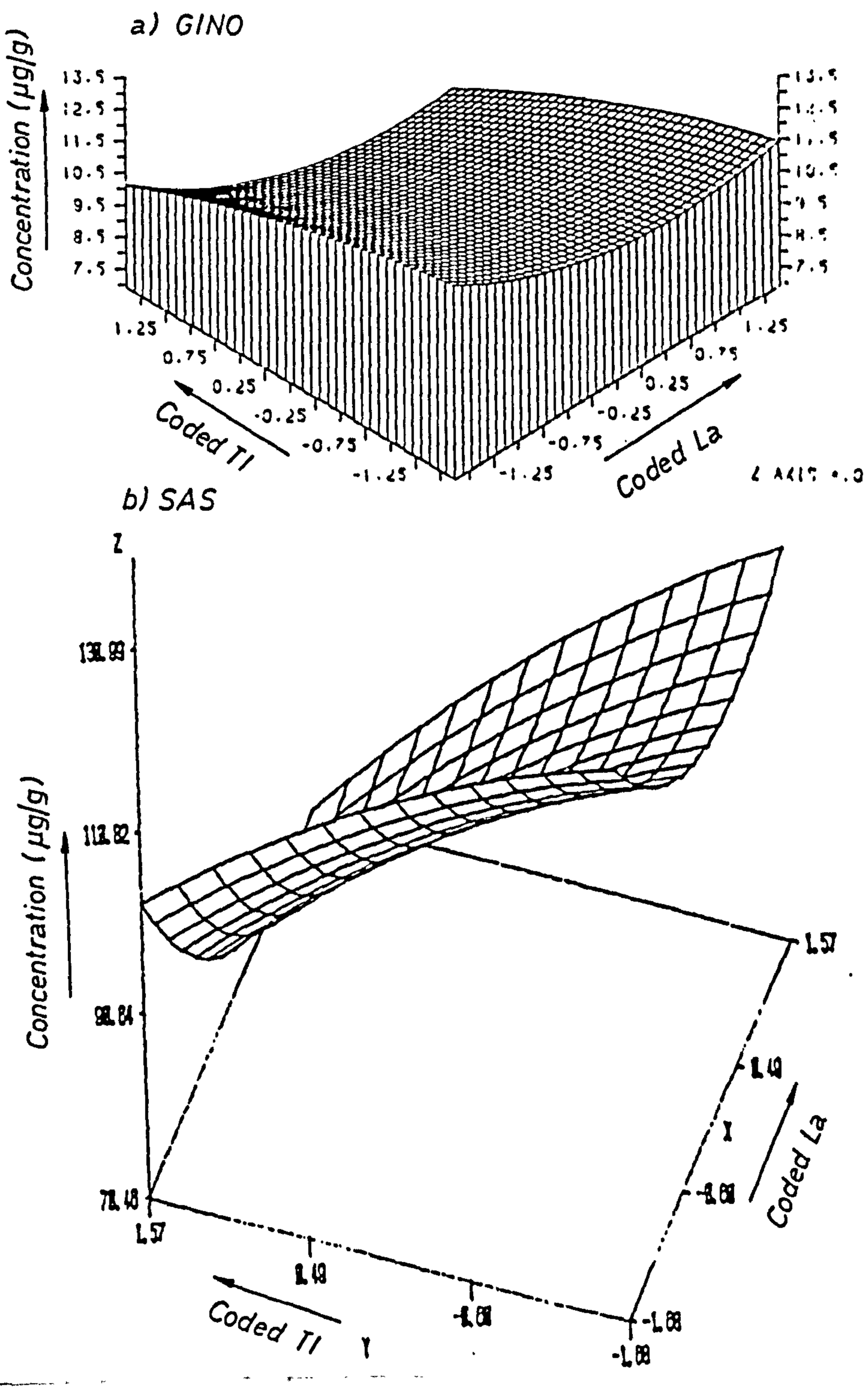

of the lanthanum and thallium concentrations, which is in direct conflict with the effect seen for the roots, except at very low levels of lead.

d) Interactive Effects of Pb and Ag on Iron in Plant Tissues

Figure 6.38 demonstrates the interactive effects of Pb and Ag solution levels on iron uptake by roots when the La level is constant at a coded value of 0. The surface indicates that the iron uptake decreases at high levels of silver (> 0.02 $\mu g/cm^3$) and lead (> 3.2 x 10^{-3} $\mu g/cm^3$). When the surface is compared with Figure 6.32, the surfaces seem different and suggest different interactive effects of Pb and Ag from that of La and Pb on iron uptake. Figure 6.39a and 6.39b illustrate the effects of Pb and Ag on iron uptake at La coded levels of -1.68 (2.5 x 10^{-3} $\mu g/cm^3$) and 1.68 (25 $\mu g/cm^3$) respectively. Figure 6.39a shows that uptake of iron increased with an increase in the level of silver while it decreased with an increase in Pb in the nutrient solution. At an La level of +1.68 (25 $\mu g/cm^3$) the uptake of iron increased with increased levels of silver and lead in the nutrient solution. Figure 6.40 demonstrates the interactive effects of Pb and Ag solution levels on iron in shoots when the La level is constant at a coded value of 0. Clearly an increase in the level of lead has little effect on the translocation of iron to the shoots from the roots, but in contrast the level of silver in the solution has a dramatic effect. The iron uptake increases markedly by a factor of a thousand, so perhaps the plant is trying to detoxify the effect of the silver by increasing the level of an essential metal such as iron.

FIG. 6.38 RESPONSE SURFACE FOR IRON TAKEN UP BY ROOTS OF COCKS FOOT SEEDLING AT CODED La = 0

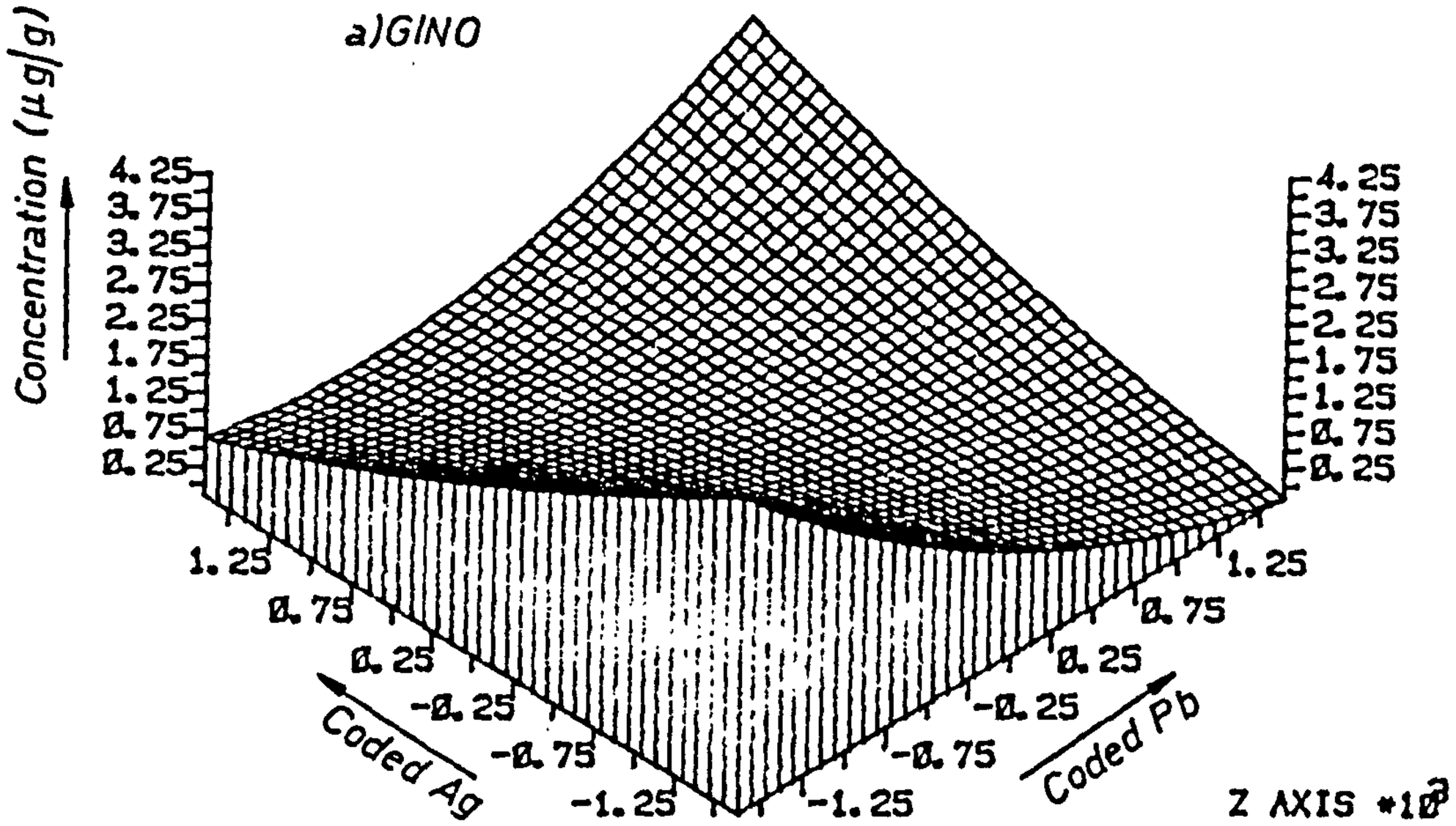

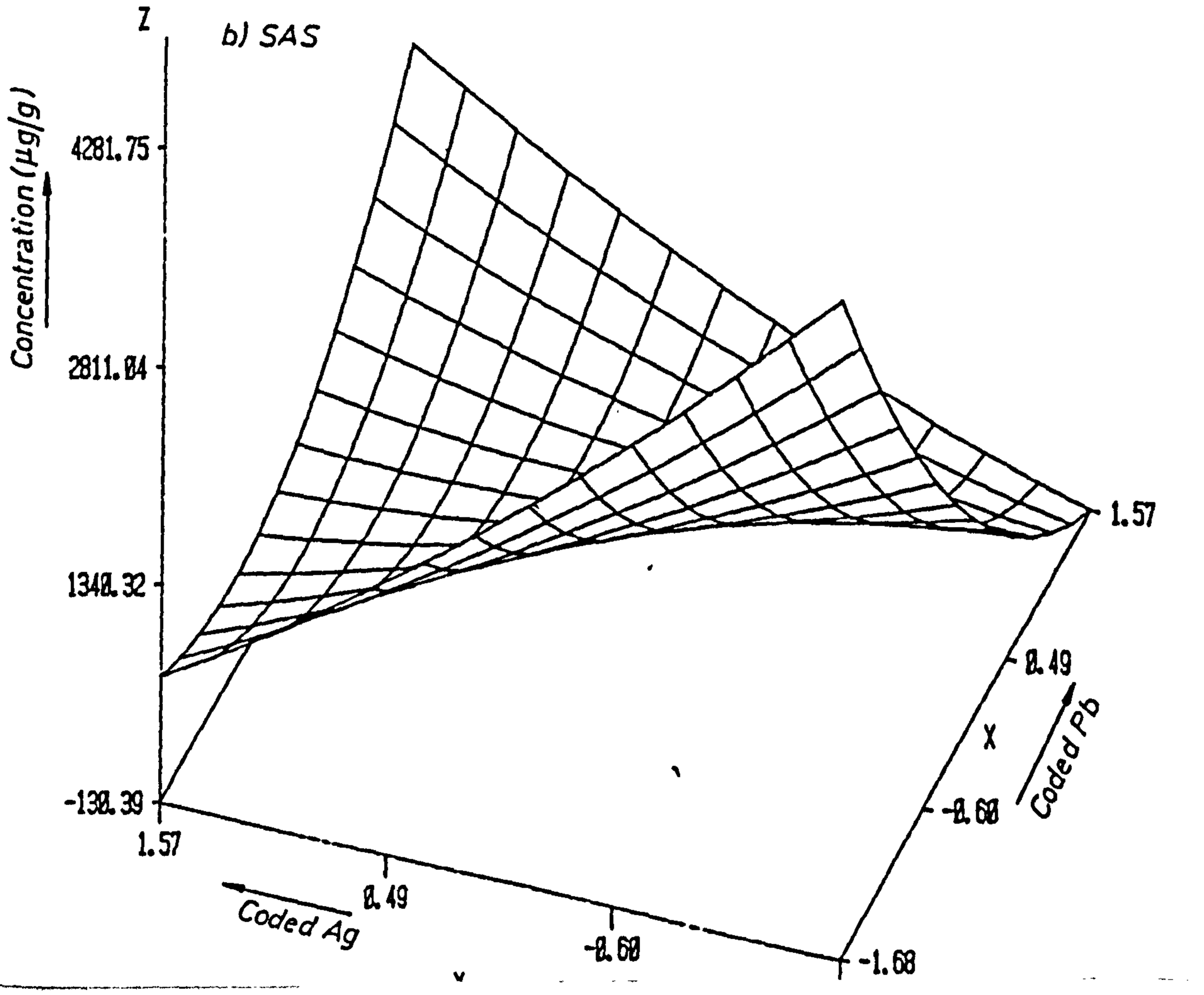

FIG. 6.39 RESPONSE SURFACE FOR IRON TAKEN UP BY ROOTS OF COCKS FOOT SEEDLING

a) At coded La = -1.68

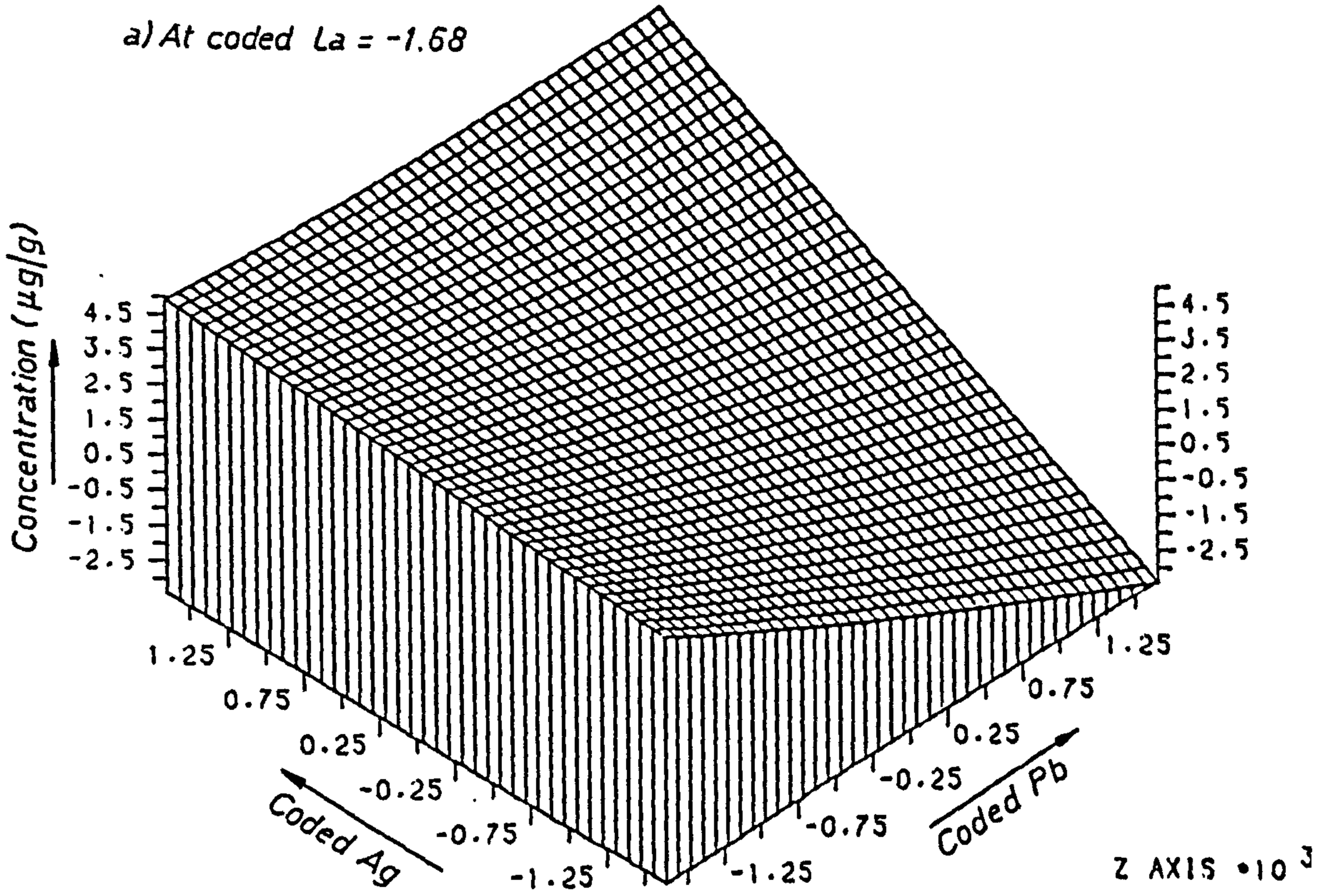

b) At coded La = +1.68

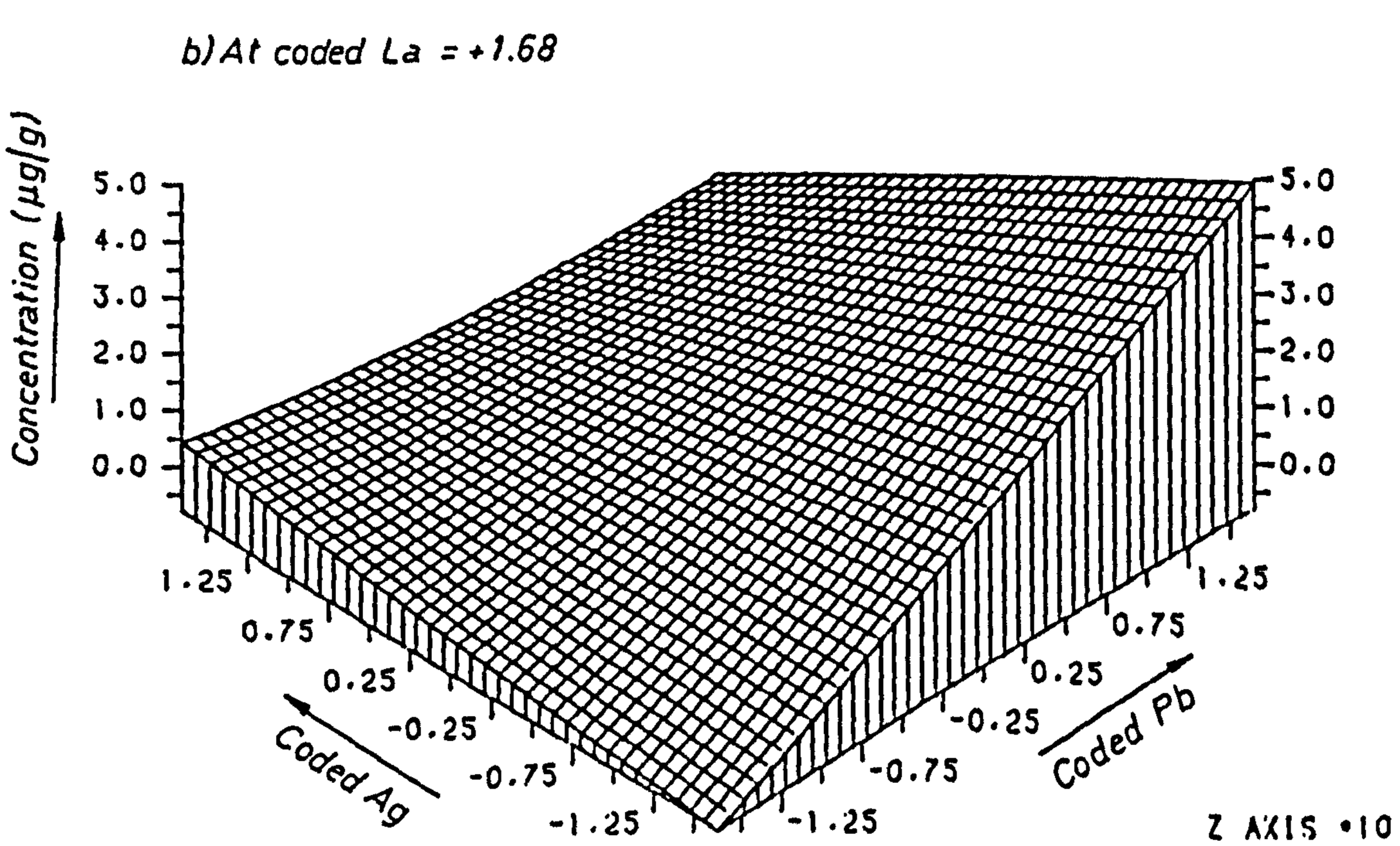

FIG. 6.40 RESPONSE SURFACE FOR IRON TAKEN UP BY SHOOTS OF COCKS FOOT SEEDLING AT CODED La = 0

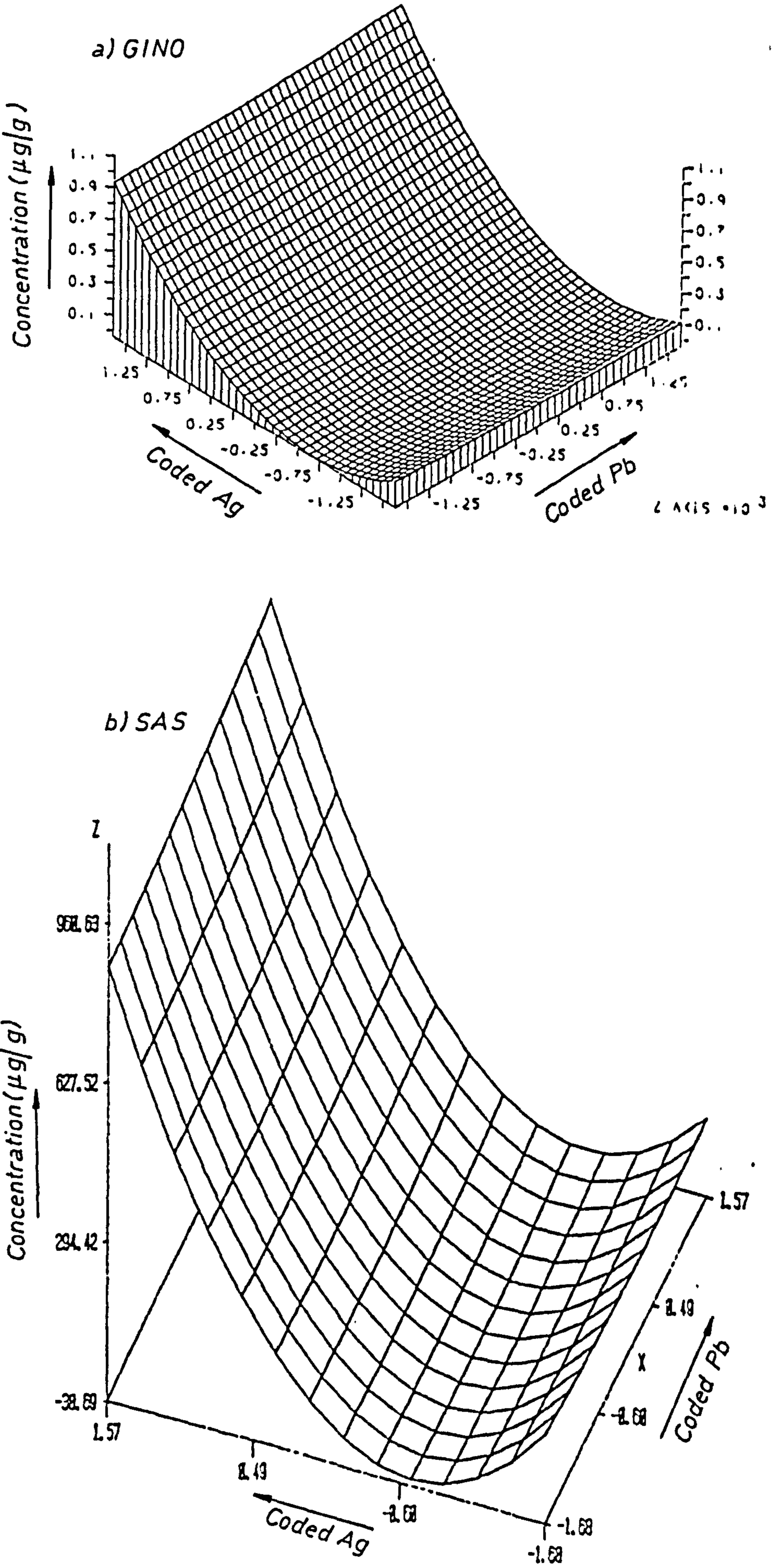

e) Interactive Effects of Pb and Tl on Manganese in Plant Tissues

Figure 6.41 represents the interactive effects of Pb and Tl solution levels on manganese in the roots when the La level is constant at a coded value of 0 (0.250 $\mu g/cm^3$). In fact, the surface produced by the SAS package (see Figure 6.37a) indicates a critical point, at which there is no uptake of manganese when the level of lead in the nutrient solution is between 3.2×10^{-3} to 5×10^{-2} $\mu g/cm^3$, while manganese is taken up by the plant when the concentration of lead is lower than 3.2×10^{-3} or greater than 5×10^{-2} $\mu g/cm^3$. However, Figure 6.41 indicates that the uptake of manganese increases linearly by about a factor of 2.7 with increase in concentration of thallium. Figures 6.42a and 6.42b illustrate the interactive effects of Pb and Tl on manganese uptake at coded levels of La of -1.68 (25×10^{-4} $\mu g/cm^3$) and 1.68 (25 $\mu g/cm^3$) respectively. The three surfaces suggest that Pb has a significant effect on the uptake of manganese while thallium has only a slight effect.

Figure 6.43 illustrates the interactive effects of Pb and Tl solution levels on manganese in the shoots when the coded La level is held constant. The level of manganese rises in the shoots as the levels of lead and thallium are raised. It appears that lead has a greater effect than thallium. However, when the level of lead is greater than 0.05 $\mu g/cm^3$ in addition to a level of thallium greater than 0.01 $\mu g/cm^3$ the level of manganese is suddenly decreased. Clearly these two toxic metals combine to prevent transport of the manganese to the shoots above a critical level. Further work should be carried out in the region of the change of direction of the envelope to establish the geometry of the area.

FIG. 6.41 RESPONSE SURFACE FOR MANGANESE TAKEN UP BY ROOTS OF COCKS FOOT SEEDLING AT CODED La = 0

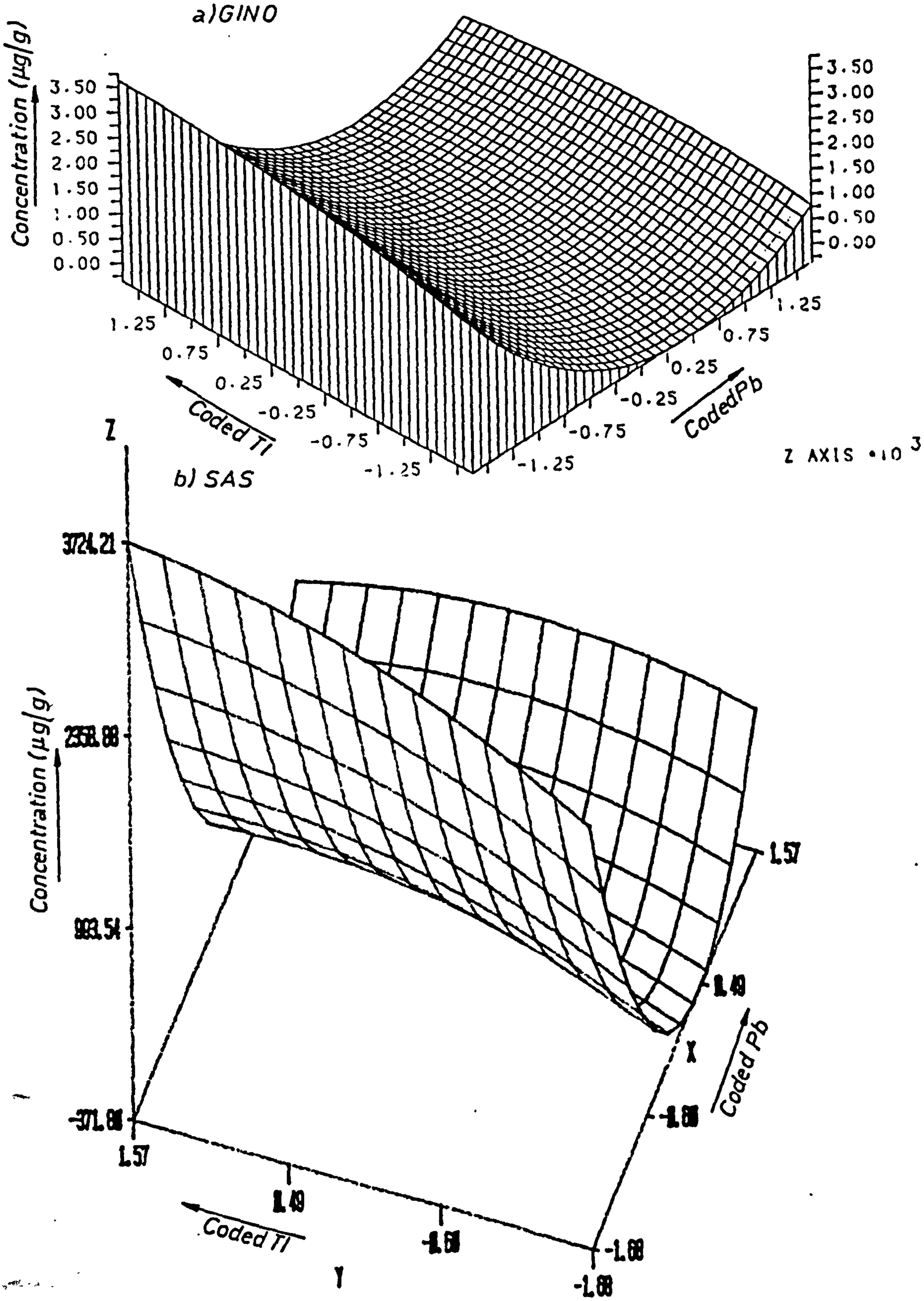

FIG. 6.42 RESPONSE SURFACE FOR MANGANESE TAKEN UP BY ROOTS OF COCKS FOOT SEEDLING

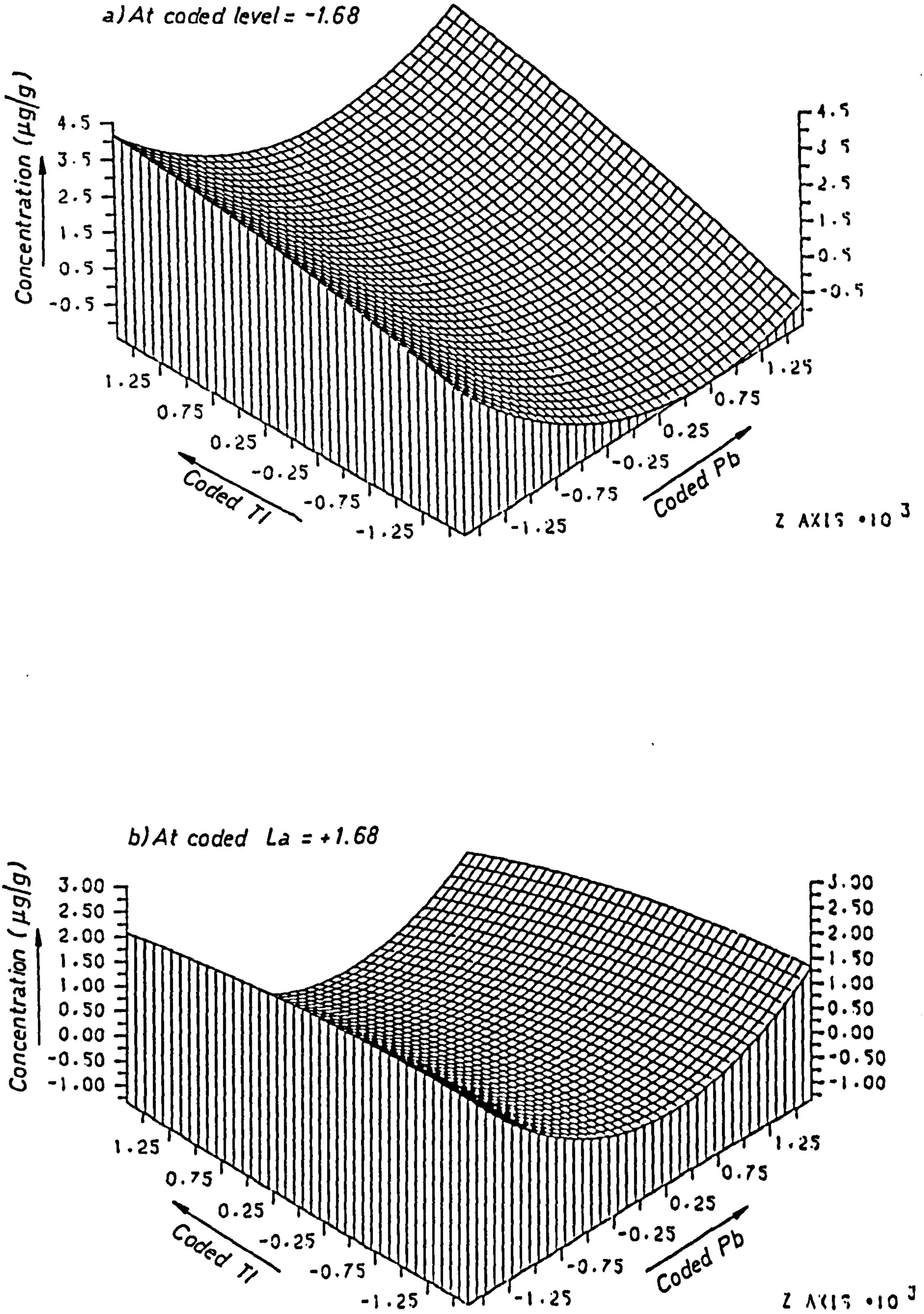

FIG. 6.43 RESPONSE SURFACE FOR MANGANESE TAKEN UP BY SHOOTS OF COCKS FOOT AT CODED La = 0

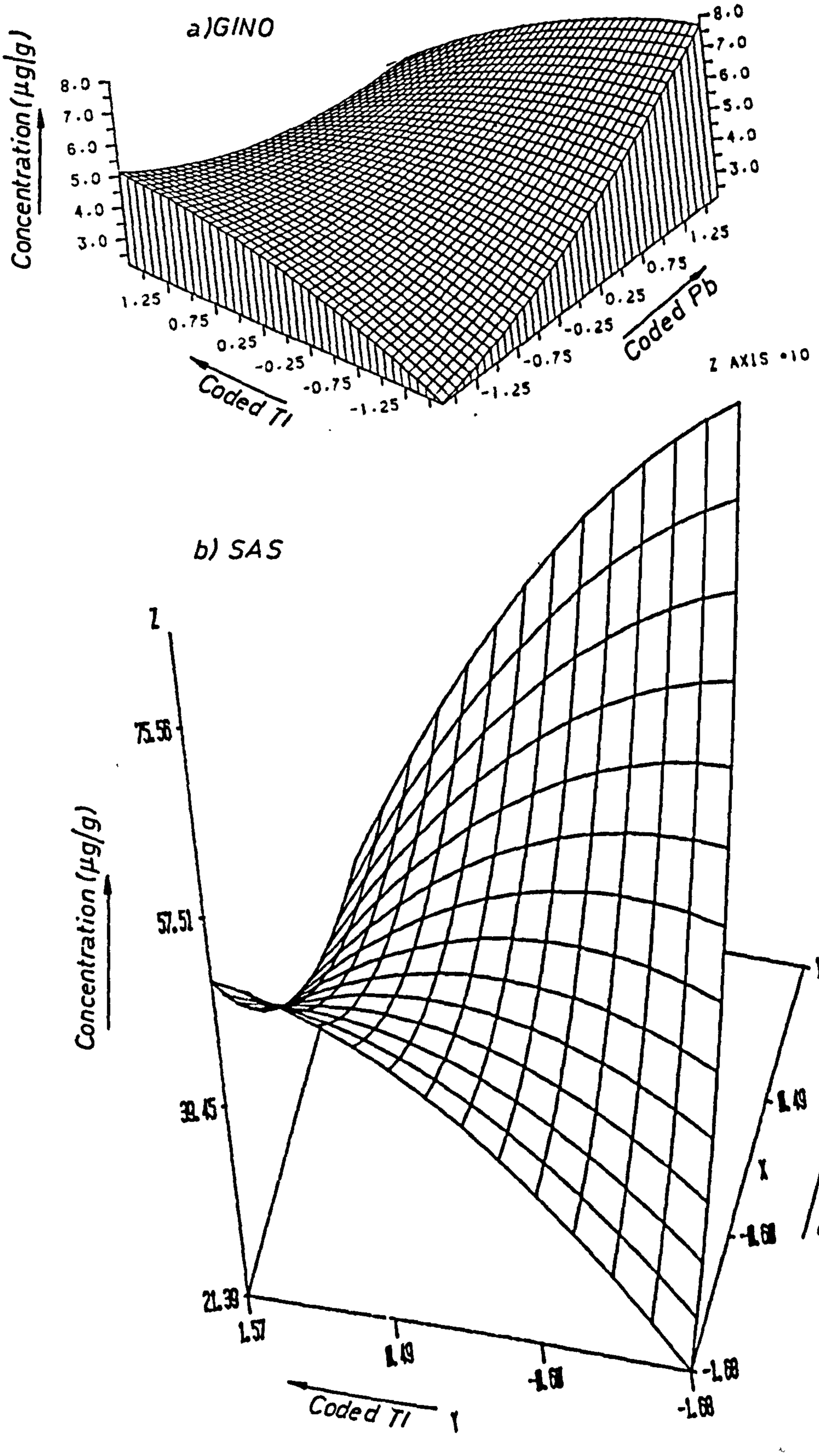

f) Interactive Effects of La and Pb on Zn in Plant Tissues

Figure 6.44 depicts the interactive effects of La and Pb on zinc uptake by the roots when the level of thallium is held constant at coded value 0. The surface indicates that high levels of lead (> 0.05 $\mu g/cm^3$) decreased the uptake of zinc while the level of lanthanum showed no effect on the zinc uptake. Probably competition for the root binding sites between zinc and lead affects the uptake of the metals. At low levels of lead (< 3.2×10^{-3} $\mu g/cm^3$), zinc has the priority of uptake by the roots. Another explanation is that both metals are coordinated to -SH groups in the amino acids (see Table 6.24). Competition may take place between the metals for chelation to such groups. The level of zinc in the shoots increased with the increased concentration of lead in the nutrient solution (see Figure 6.45). This indicates that lead increased the translocation from roots to shoots, probably because of saturation of the roots with lead. Therefore, the plant translocated zinc to the shoots. Lanthanum also exhibits a similar effect on the level of zinc in the shoots.

g) Interactive Effects of Pb and Ag on Mg in Plant Tissues

It was expected that both levels of Pb and Ag used in the experiment would decrease the uptake of magnesium in the roots. In fact, the surface (Figure 6.46) indicates that the level of magnesium increased with the increased levels of Pb and Ag when the level of lanthanum was held constant at coded value 0. Clearly, the levels of Pb and Ag used in the experiment caused interaction with the magnesium uptake by the roots. The level of magnesium in the shoots was reduced at high concentrations of lanthanum (3.87 $\mu g/cm^3$) and silver (0.02 $\mu g/cm^3$) when the level of lead was held constant at coded value 0 (see Figure 6.47). It was found that most lanthanum in plants was associated with

FIG. 6.44 RESPONSE SURFACE FOR ZINC TAKEN UP BY ROOTS OF COCKS FOOT AT CODED TI = 0

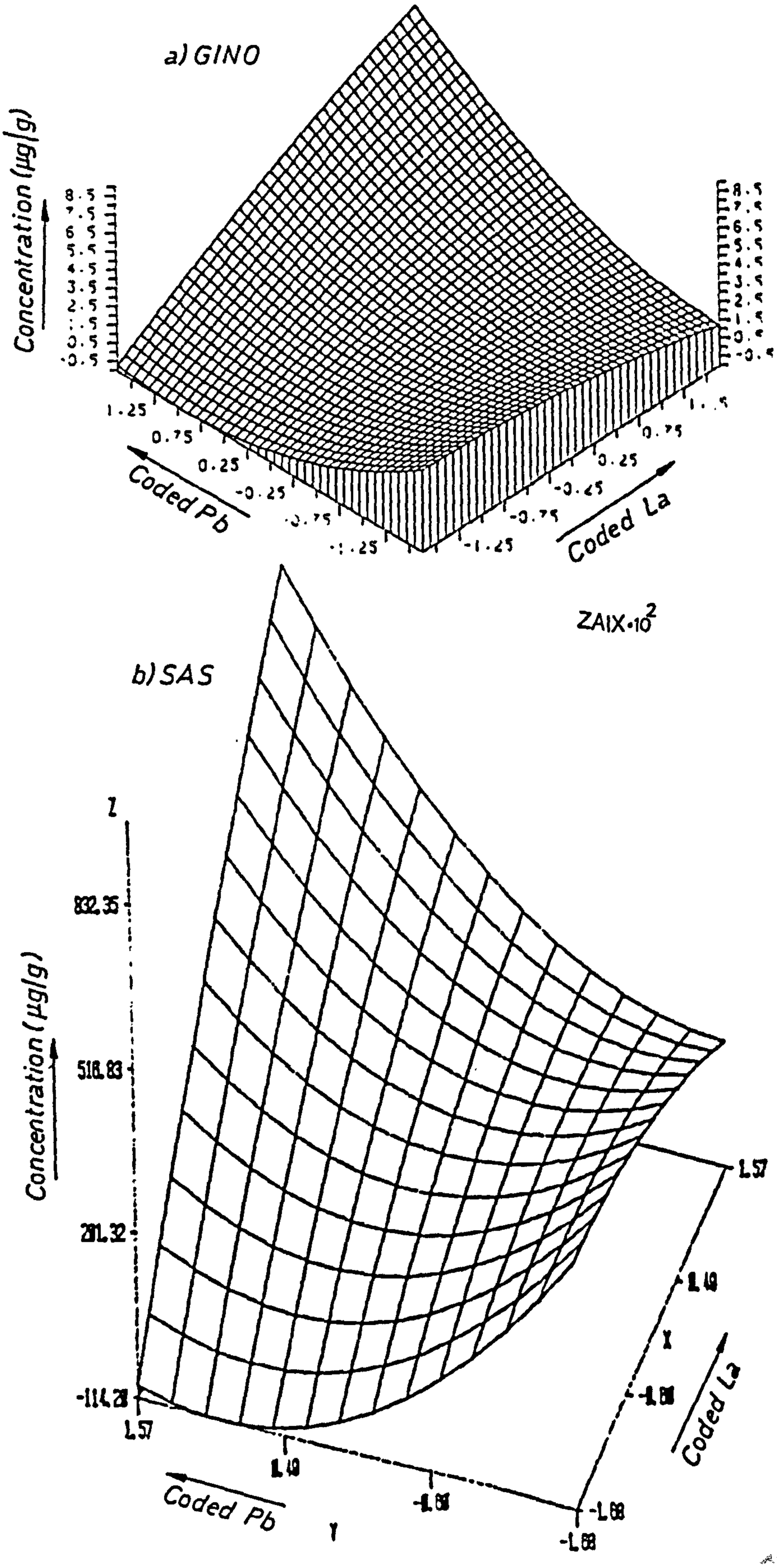

FIG. 6.45 RESPONSE SURFACE FOR ZINC TAKEN UP BY SHOOTS OF COCKS FOOT AT CODED TI=0

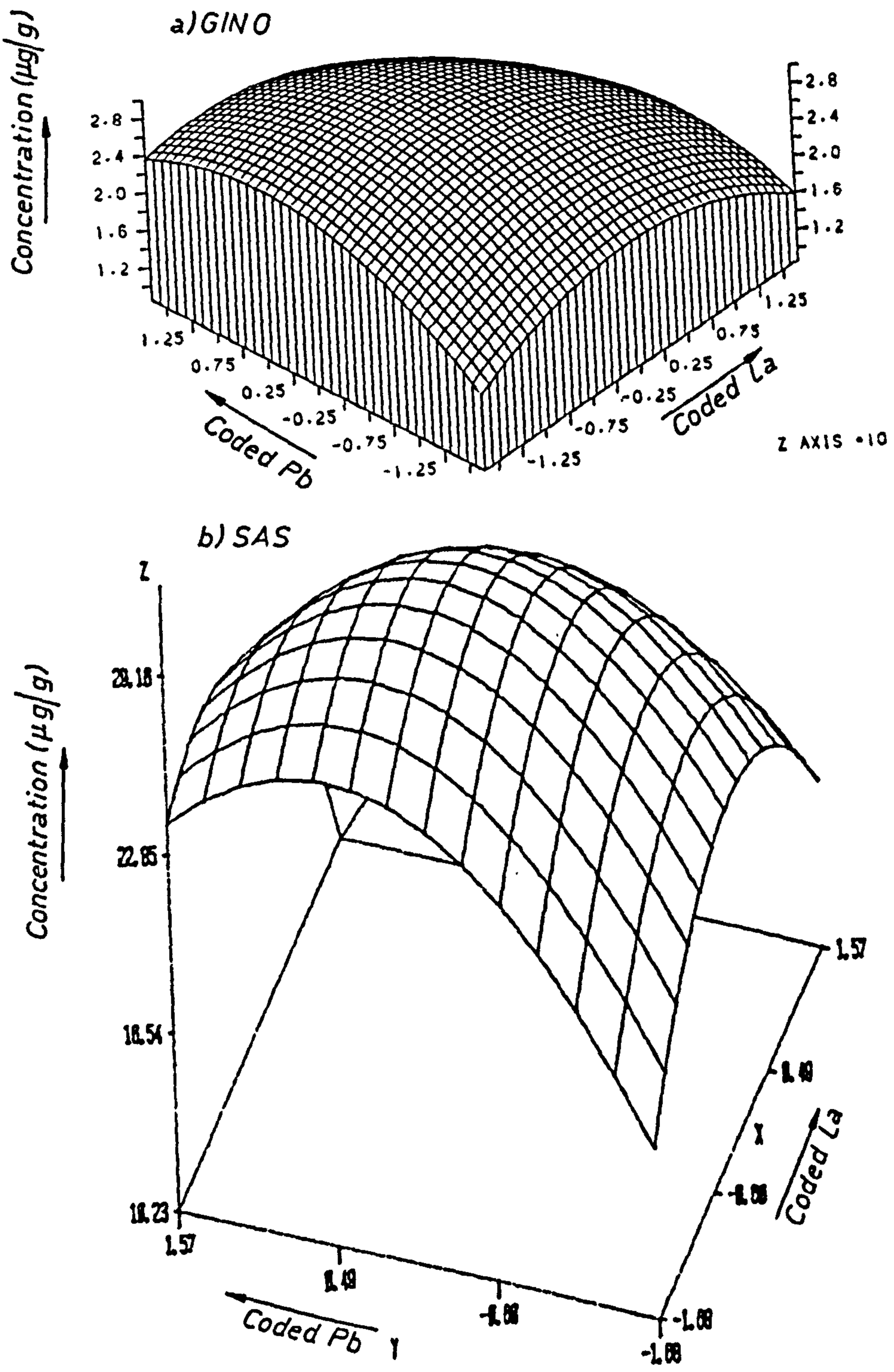

FIG. 6.46 RESPONSE SURFACE FOR MAGNESIUM TAKEN UP BY ROOTS OF COCKS FOOT SEEDLING AT CODED La = 0

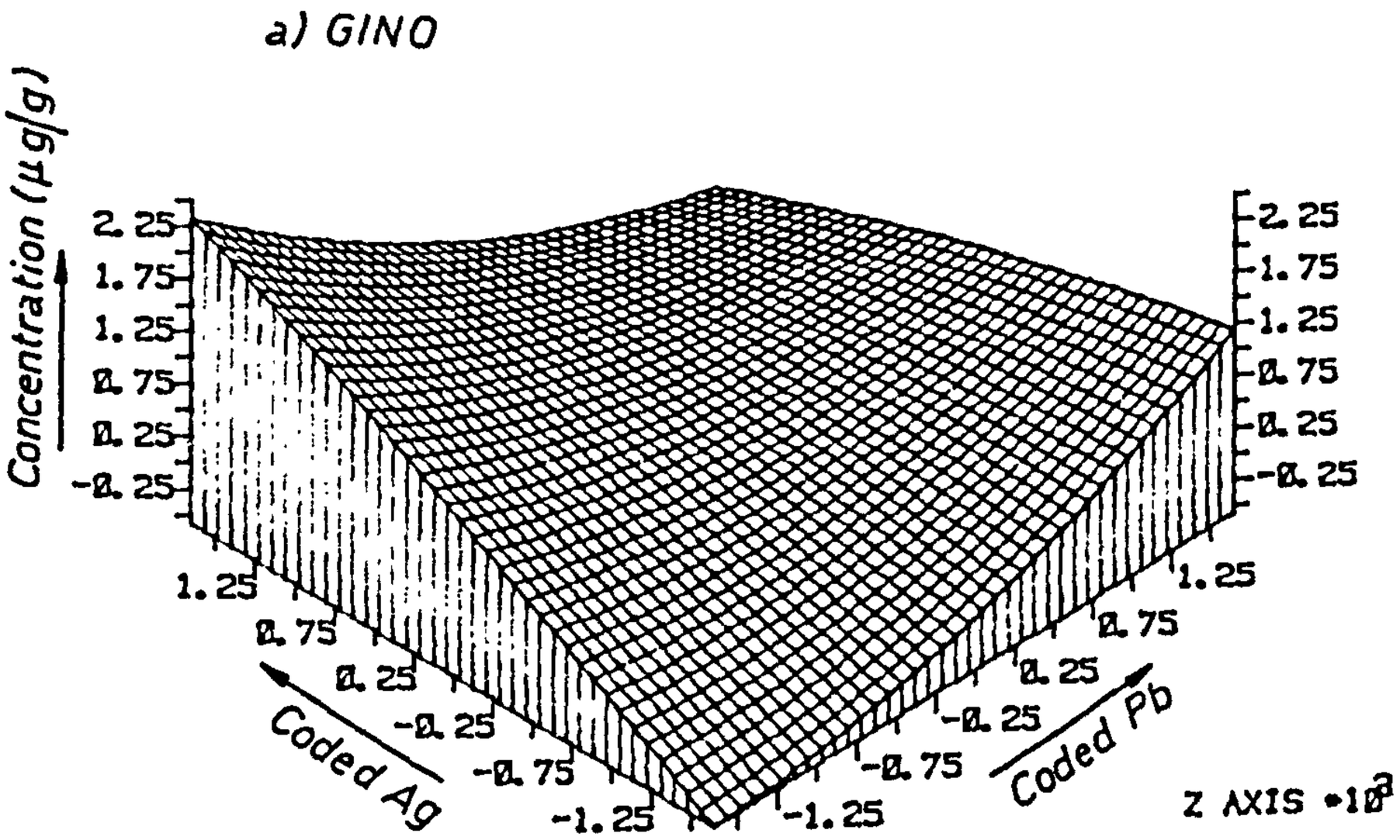

FIG. 6.47 RESPONSE SURFACE FOR MAGNESIUM TAKEN UP BY SHOOTS OF COCKS FOOT SEEDLING AT CODED Pb = 0

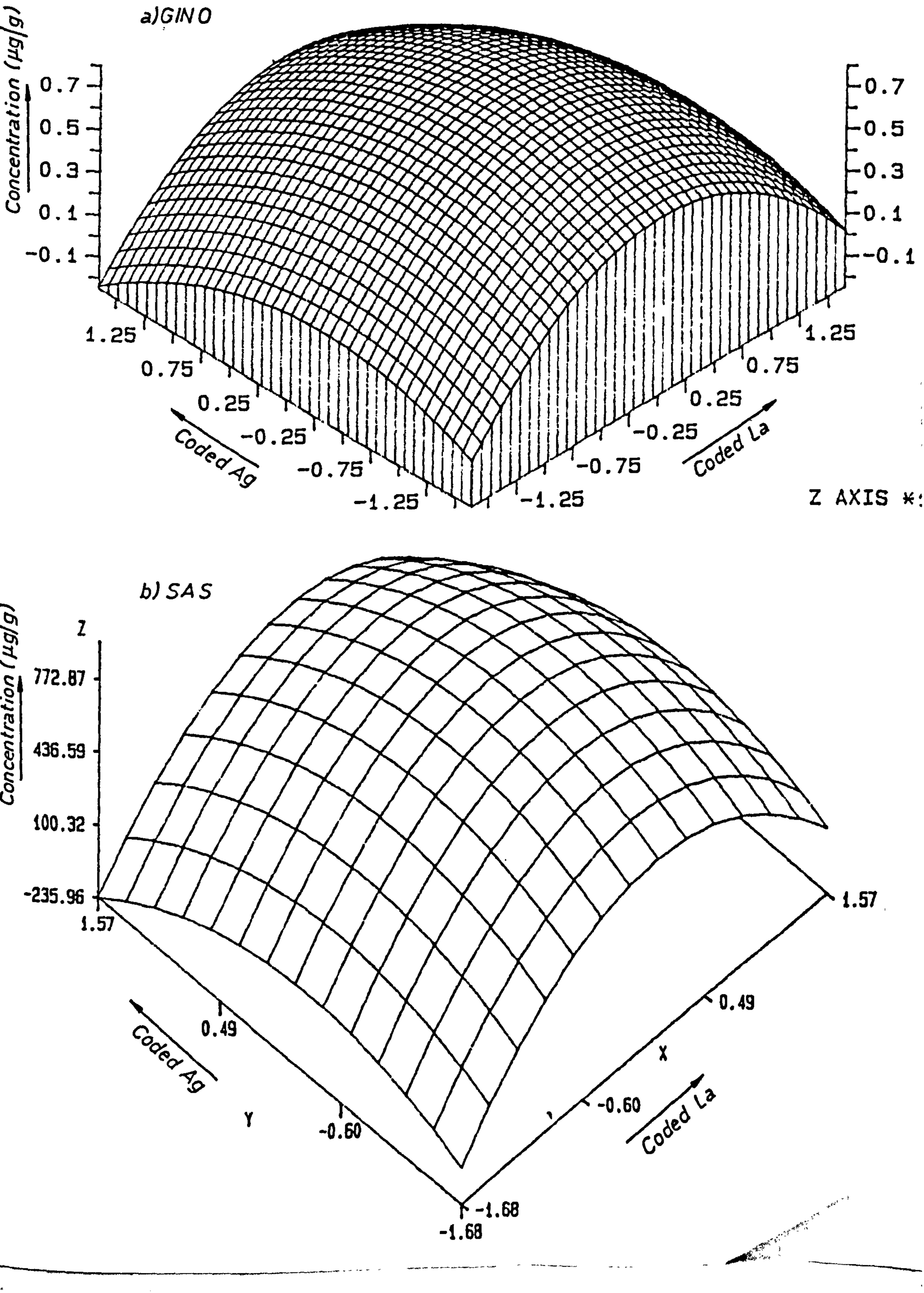

those components containing oxygen groups (see Chapter 5). Therefore, competition between the lanthanum and magnesium may be possible and responsible for the reduction in the level of magnesium in the shoots. Mg and Ag both have the ability to coordinate with N and O groups; again competition between the metals may take place and be responsible for the interactive effect of Ag on the Mg level in these plants.

h) Interactive Effects of La and Ag on Manganese in Plant Tissues

Figure 6.48 illustrates that both levels of lanthanum (> 0.250 $\mu g/cm^3$) and silver (> 0.020 $\mu g/cm^3$) decreased the level of manganese in the roots when the level of lead was held constant at coded value 0. The surface also shows that at low levels of La and Ag in the nutrient solution, the uptake of manganese is low but it increased gradually until the critical level mentioned previously was obtained. This surface for manganese is completely different from Figure 6.49 when thallium was added to the nutrient solution instead of silver (see Figure 6.50). The surface shows that lanthanum has no effect on the manganese uptake when the nutrient solution contained La, Pb and Tl while it has a significant effect when the solution contained La, Pb and Ag. Clearly either Tl or Ag must control the interactive effects of La and Ag on manganese uptake. Figures 6.50, 6.51a and 6.51b depict the interactive effects of La and Pb on manganese in the shoots when the level of thallium is held constant at the levels -1.68, 0 and +1.68 respectively. The three surfaces are quite different, indicating separate interactions between La and Pb on the level of manganese in the shoot at different levels of thallium in the nutrient solution. However, at the level of thallium at coded value 0, lanthanum reduced the level of manganese in the shoots.

FIG. 6.48 RESPONSE SURFACE FOR MANGANESE TAKEN UP BY ROOTS OF COCKS FOOT SEEDLING AT CODED Pb = 0

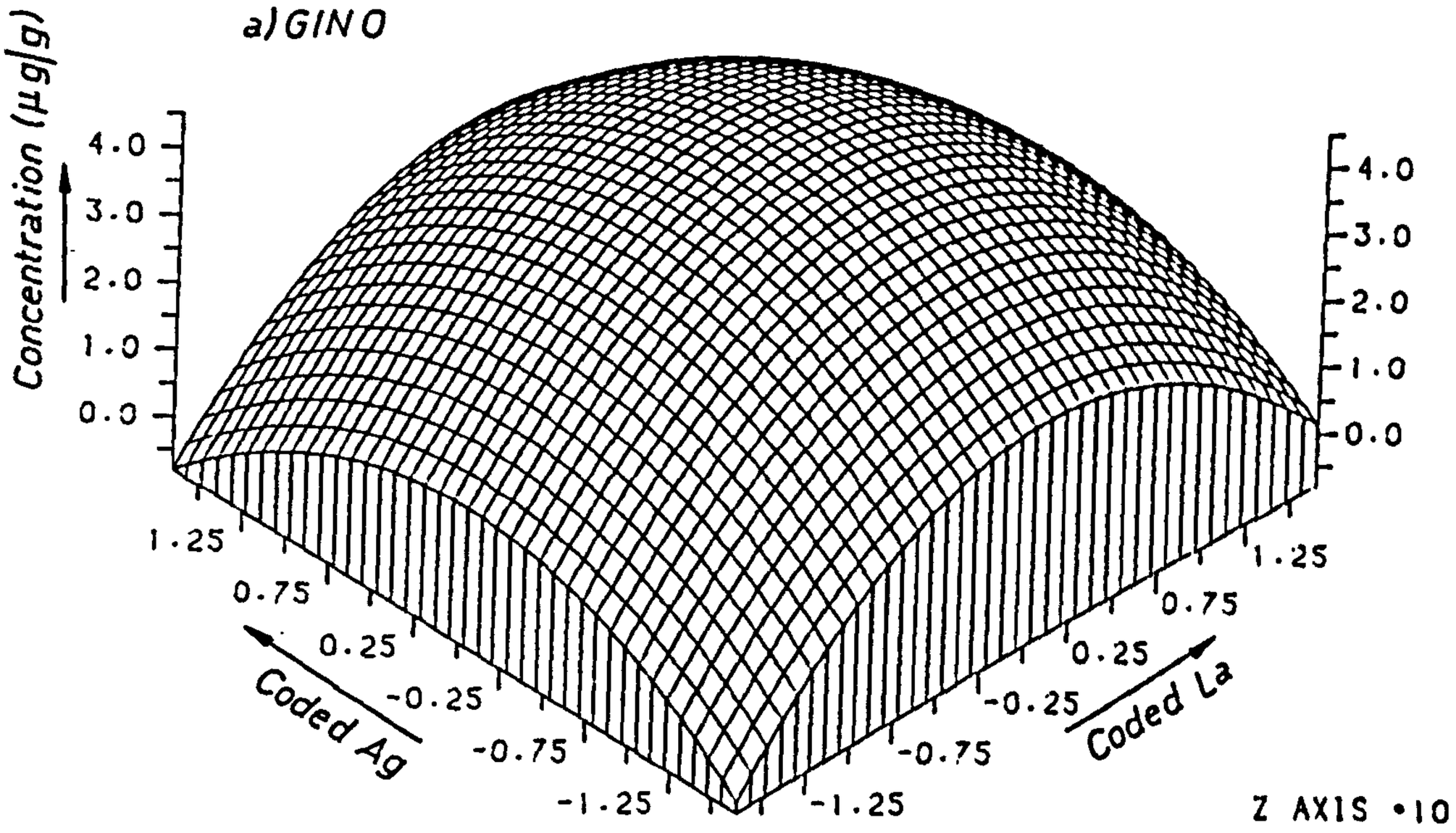

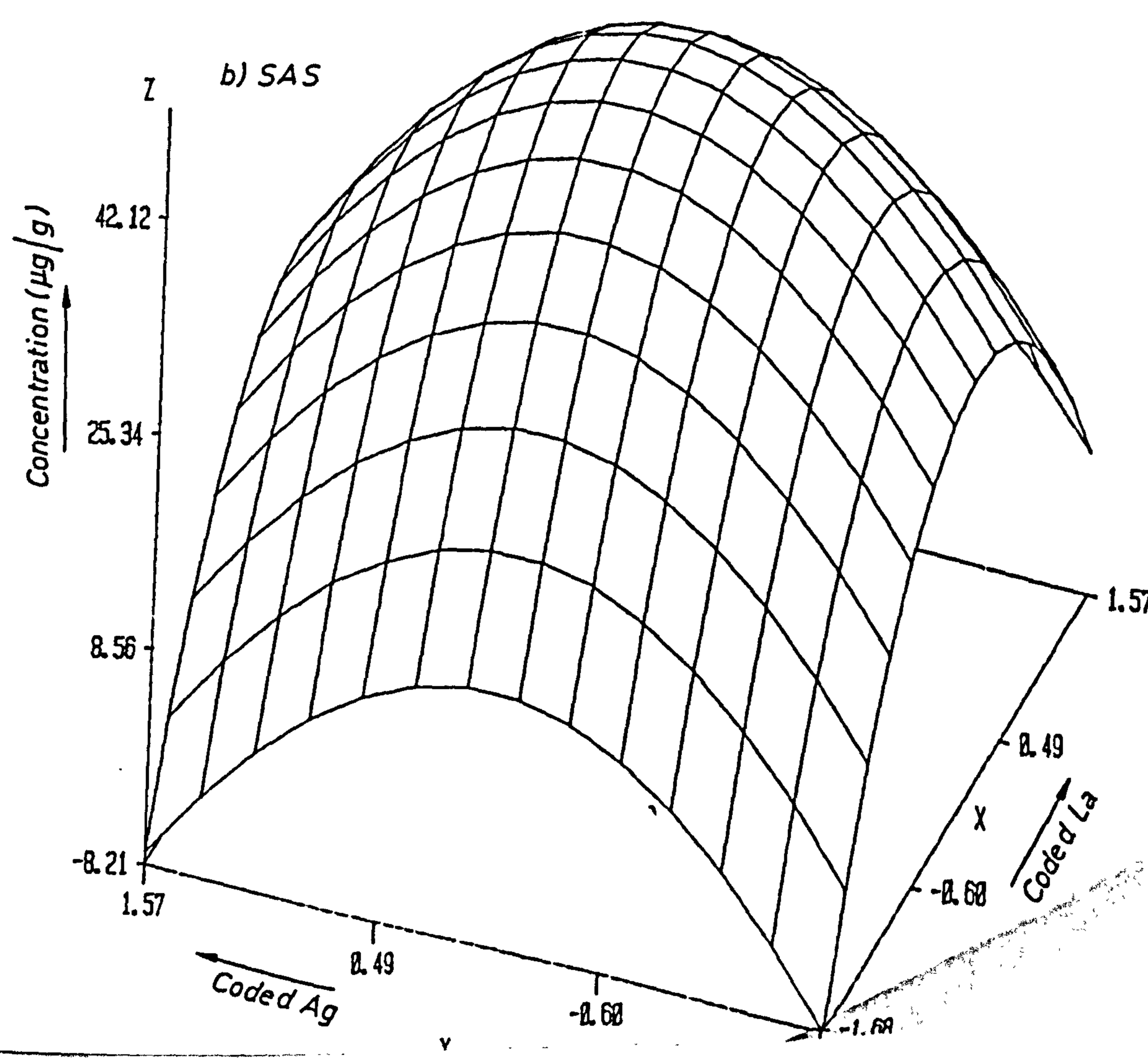

FIG. 6.49 RESPONSE SURFACE FOR MANGANESE TAKEN UP BY ROOTS OF COCKS FOOT SEEDLING AT CODED Pb = 0

a) GINO

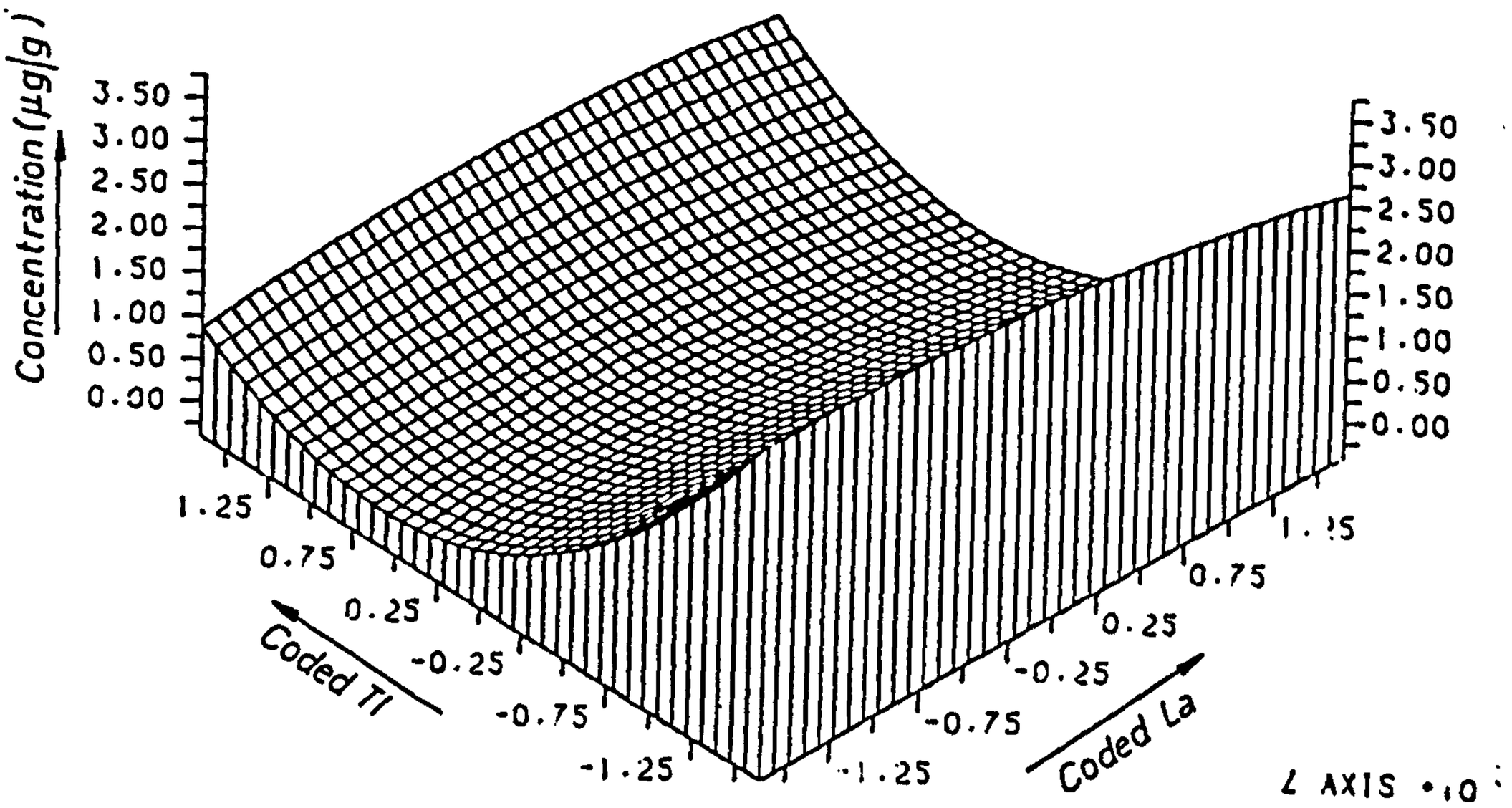

b) SAS

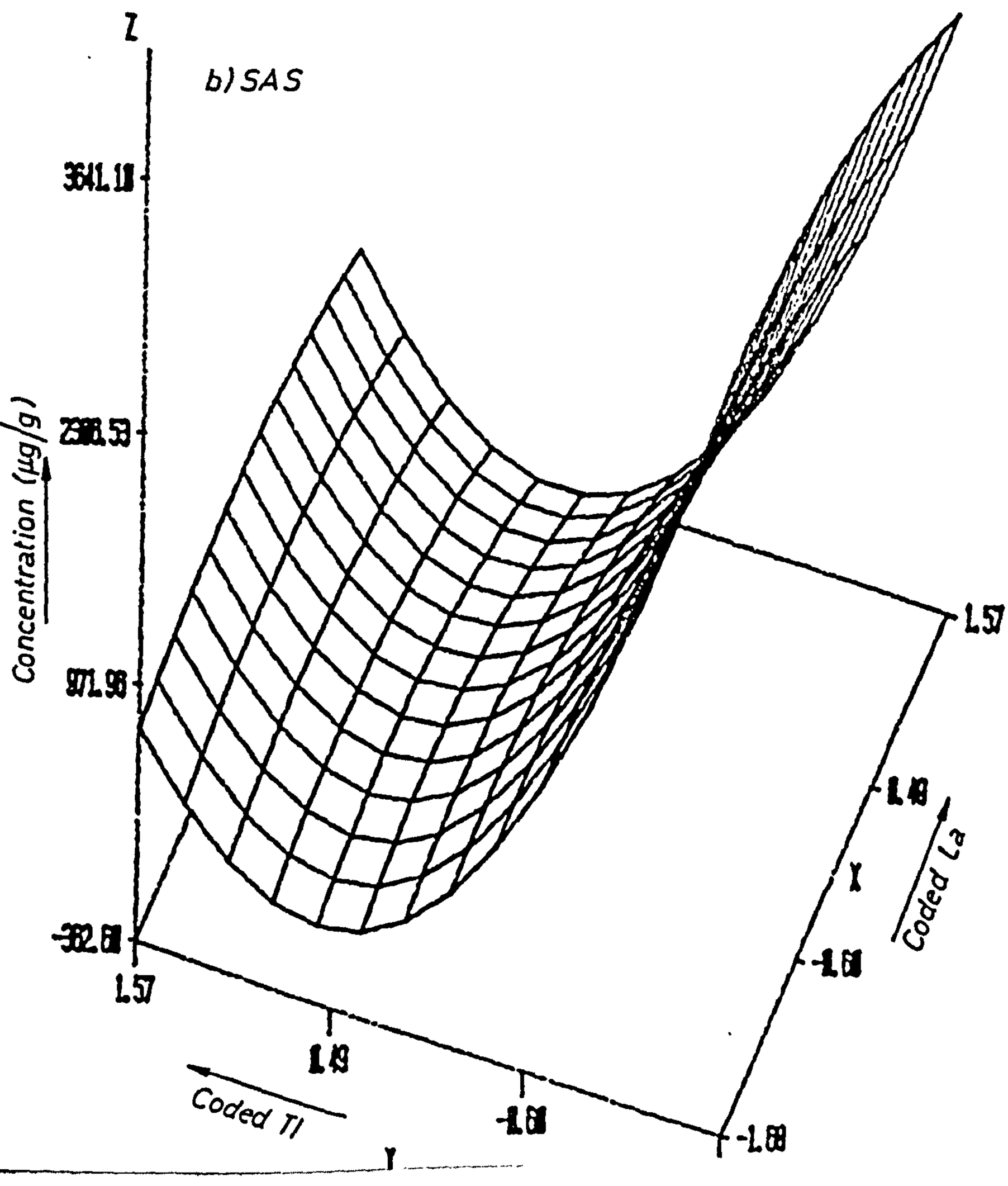

FIG. 6.50 RESPONSE SURFACE FOR MANGANESE TAKEN UP BY SHOOTS OF COCKS FOOT SEEDLING AT CODED TI = 0

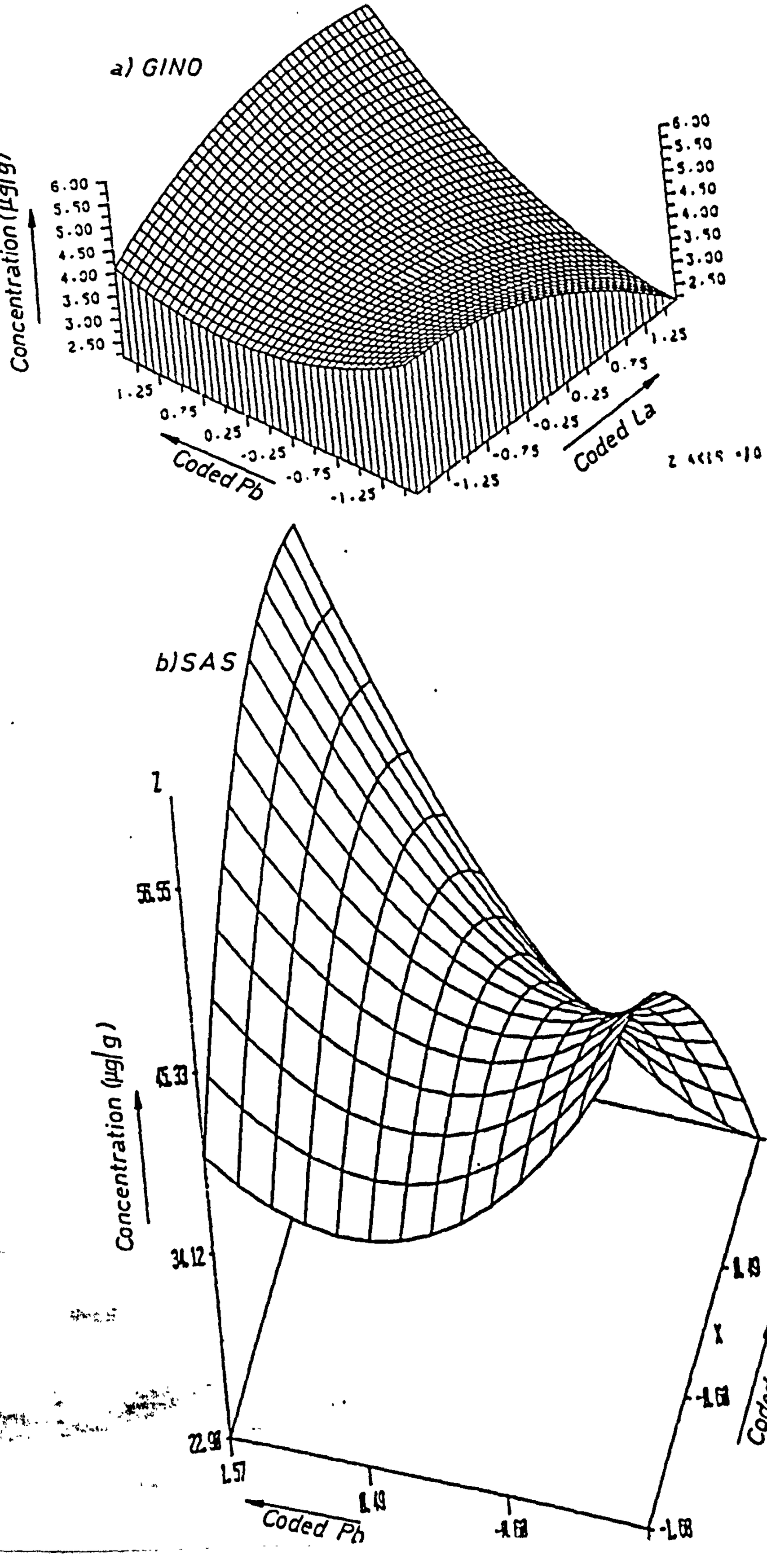

FIG. 6.51 RESPONSE SURFACE FOR MANGANESE TAKEN UP BY SHOOTS OF COCKS FOOT SEEDLING

a) At coded TI = -1.68

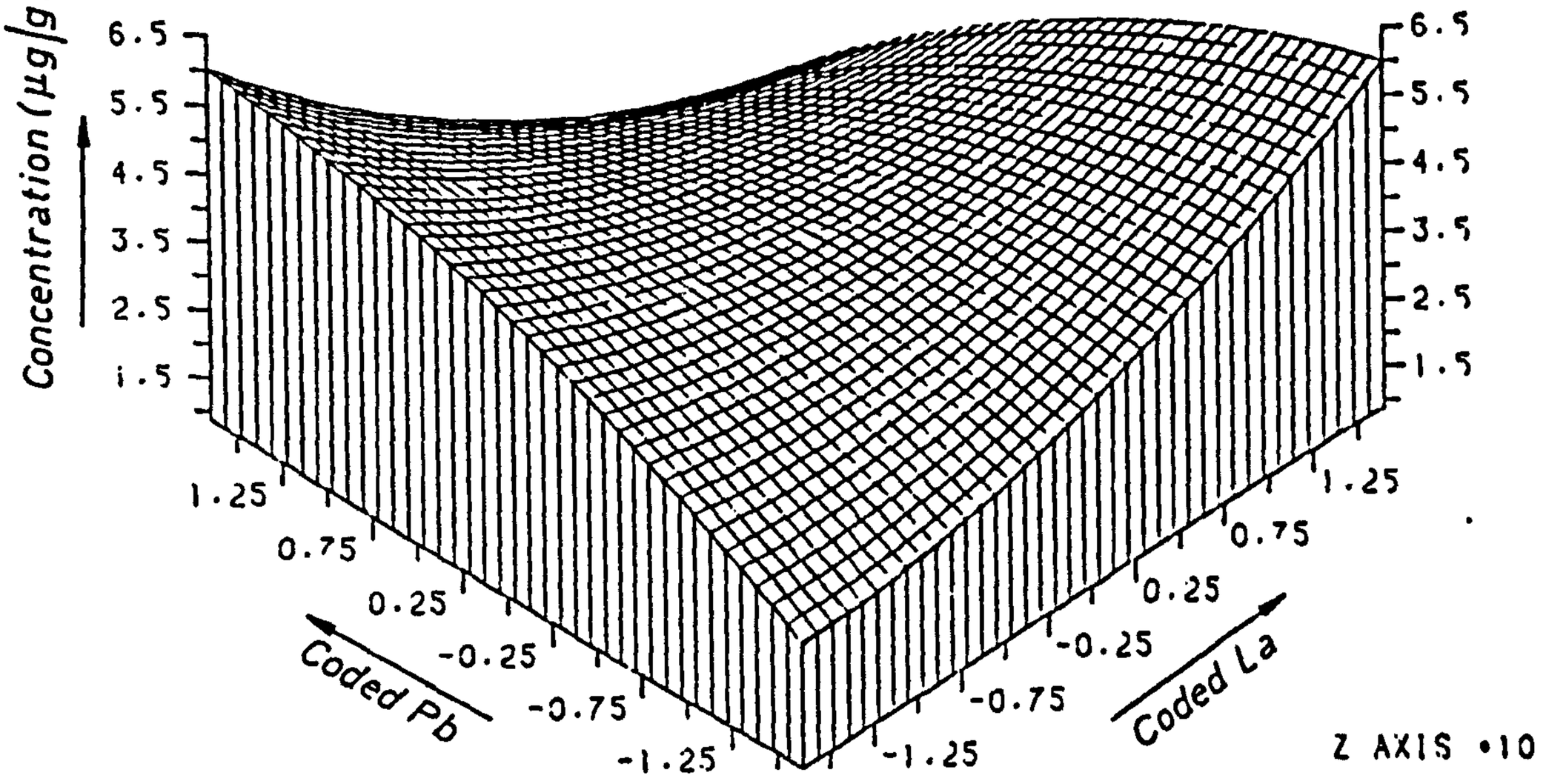

b) At coded TI = +1.68

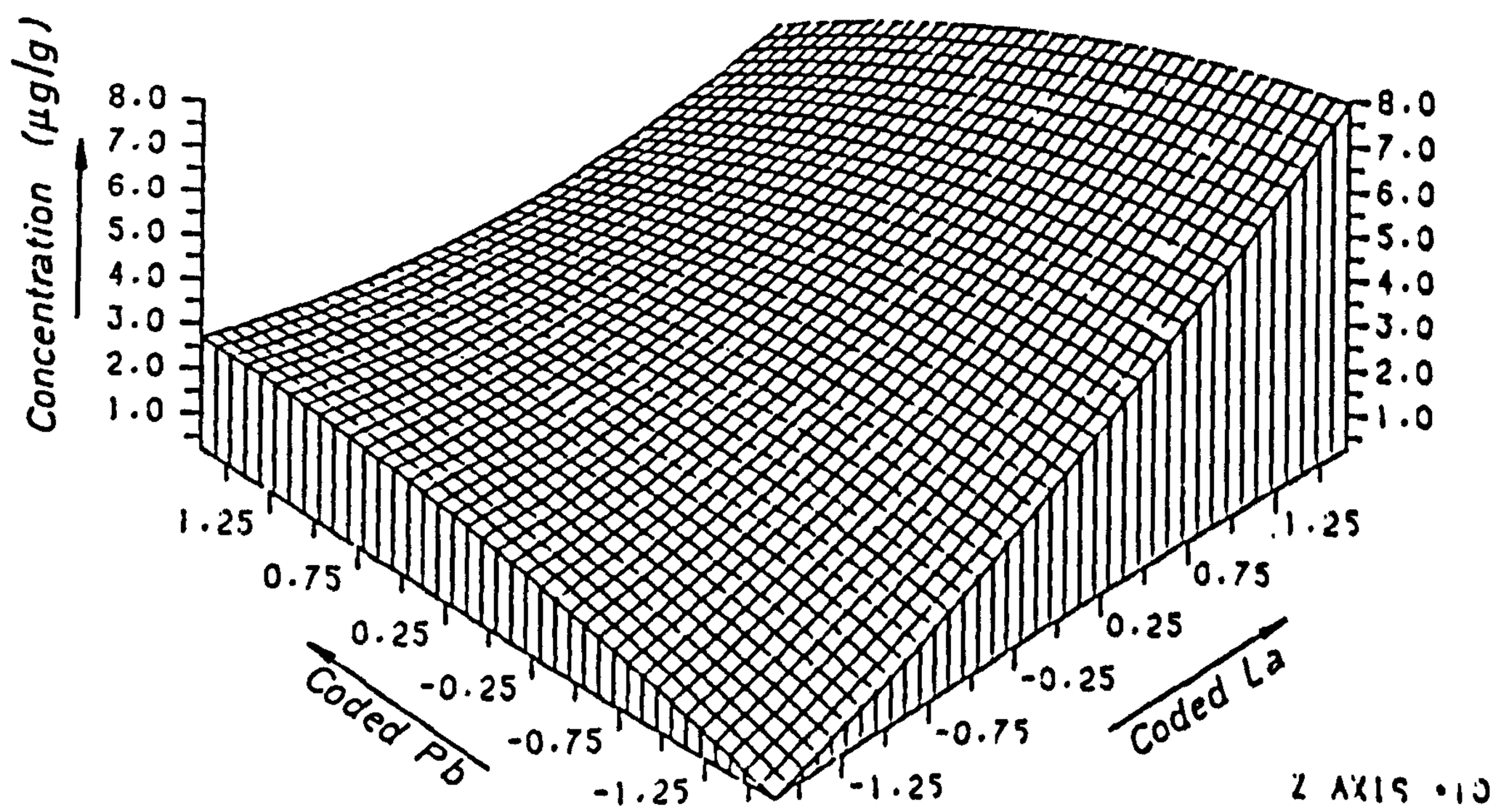

i) Interactive Effects Between La and Pb on Silver in Plant Tissues

Figure 6.52 demonstrates that the level of silver in roots increased with the increased concentration of lead and lanthanum when the level of silver was held constant at coded value 0 (0.02 $\mu g/cm^3$). This is unexpected since there should be direct competition between the silver and lead for chelation sites in the roots. In general, the stability constants for silver-sulphur or silver-nitrogen complexes are a factor of 100 greater than for lead. Therefore, in order for lead to be an effective competitor against silver it must be present in concentrations about 100 times greater than that of silver. The range of lead concentrations is from 5×10^{-4} $\mu g/cm^3$ to 5.0 $\mu g/cm^3$. At the lower Pb levels, obviously it cannot compete with silver; what is unexpected is the increase in Ag concentration when the lead level is 5.00 $\mu g/cm^3$, that it is in excess of Ag by a factor of 250.

j) Interactive Effects between Pb and Ag on Lanthanum in Plant Tissues

Figure 6.53 indicates a complicated response, in that at the level of lanthanum is decreased in the roots when either the level of lead or silver is increased when the lanthanum is held constant. However, when the concentration of both silver and lead is increased simultaneously, then the level of lanthanum rapidly increases, reaching a peak at +1.68 Ag, +1.68 Pb. With increasing level of lanthanum in the nutrient solution, the level of lanthanum in the shoots passed through a distinct minimum with respect to lanthanum concentration (0.250 μg La/cm^3) in the shoots, before increasing rapidly as the level of lanthanum in the solution was enhanced further to 25 $\mu g/cm^3$. The critical section of the surface was unexpected. Increased levels of thallium showed only a marginal effect on the lanthanum concentration. The result plane is almost a quadratic in the La concentration solution axis direction (see Figure 6.54).

FIG. 6.52 RESPONSE SURFACE FOR SILVER TAKEN UP BY ROOTS OF COCKS FOOT SEEDLING AT CODED Ag = 0

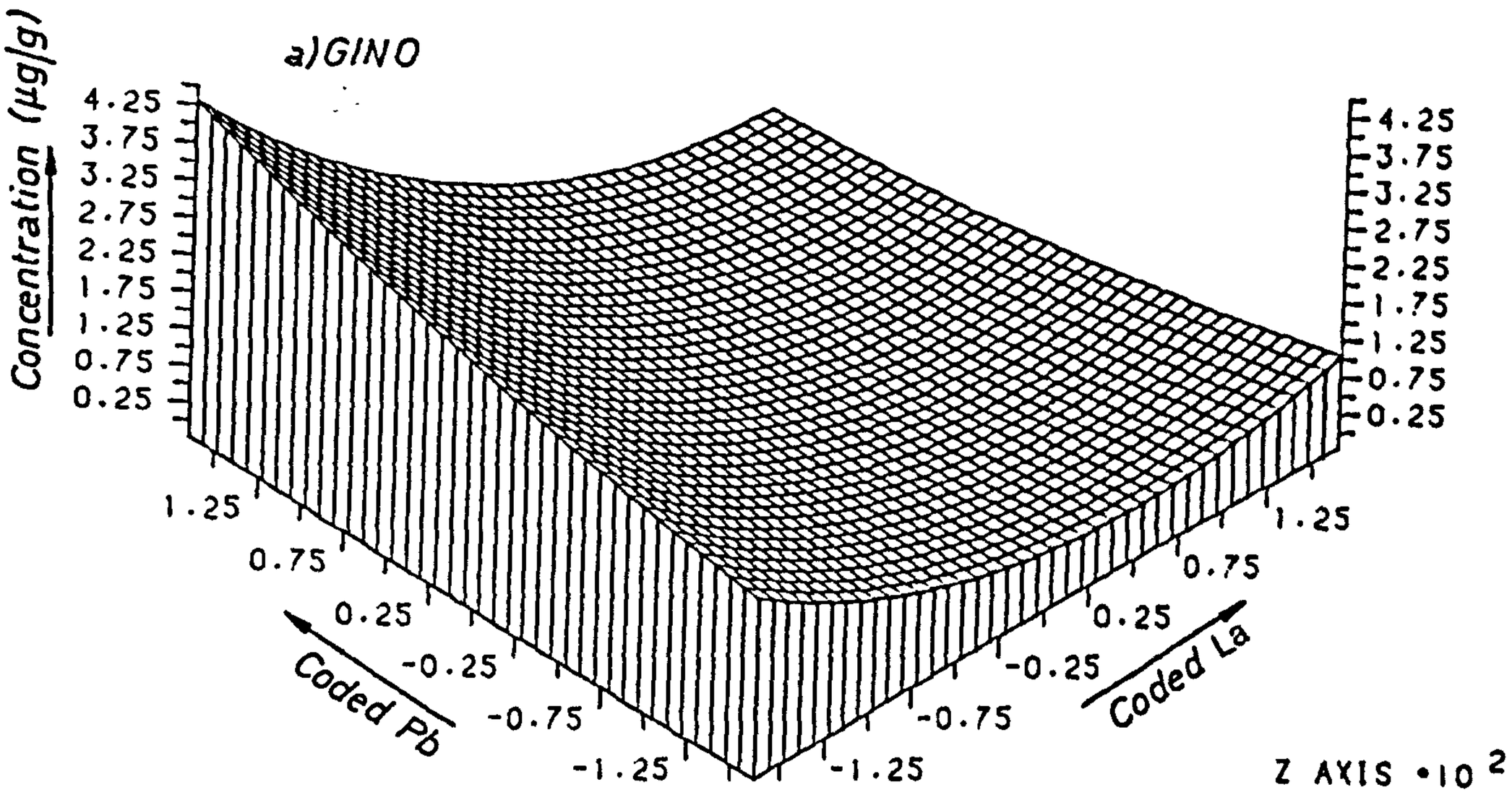

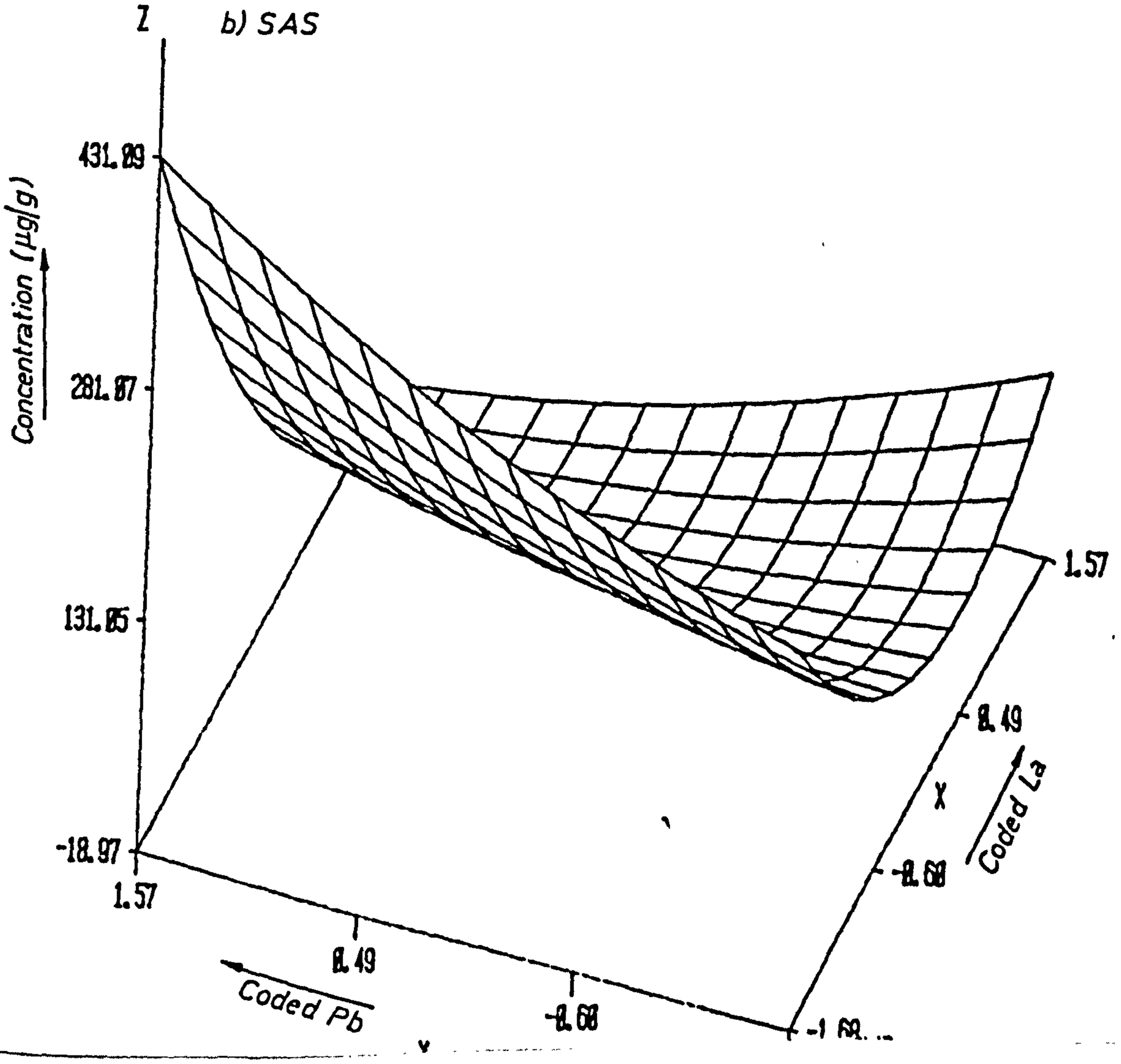

FIG. 6.53 RESPONSE SURFACE FOR LANTHANUM TAKEN UP BY ROOTS OF COCKS FOOT SEEDLING AT CODED La = 0

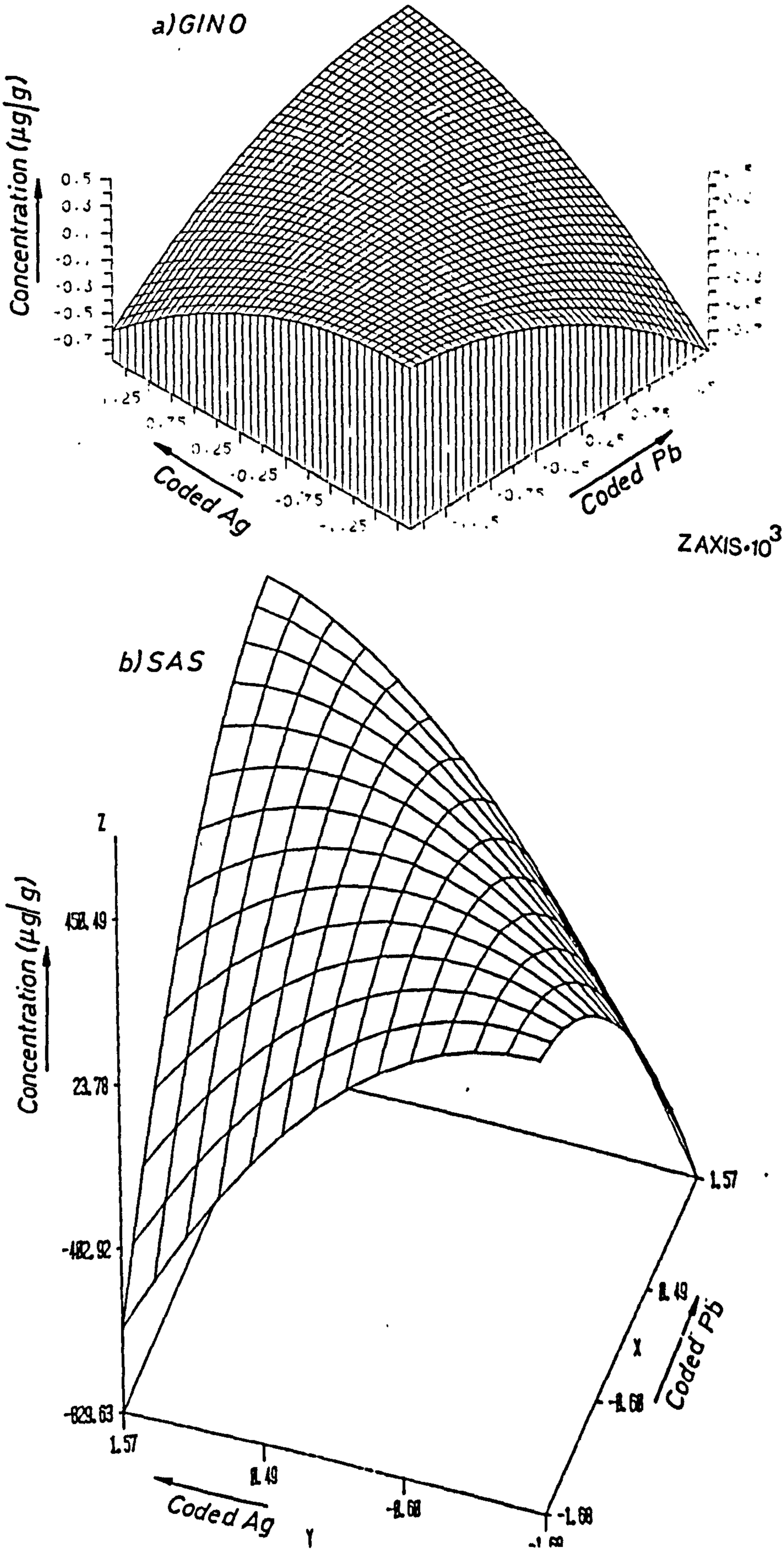

FIG. 6.54 RESPONSE SURFACE FOR LANTHANUM TAKEN UP BY SHOOTS OF COCKS FOOT SEEDLING AT CODED Pb = 0

a) GINO

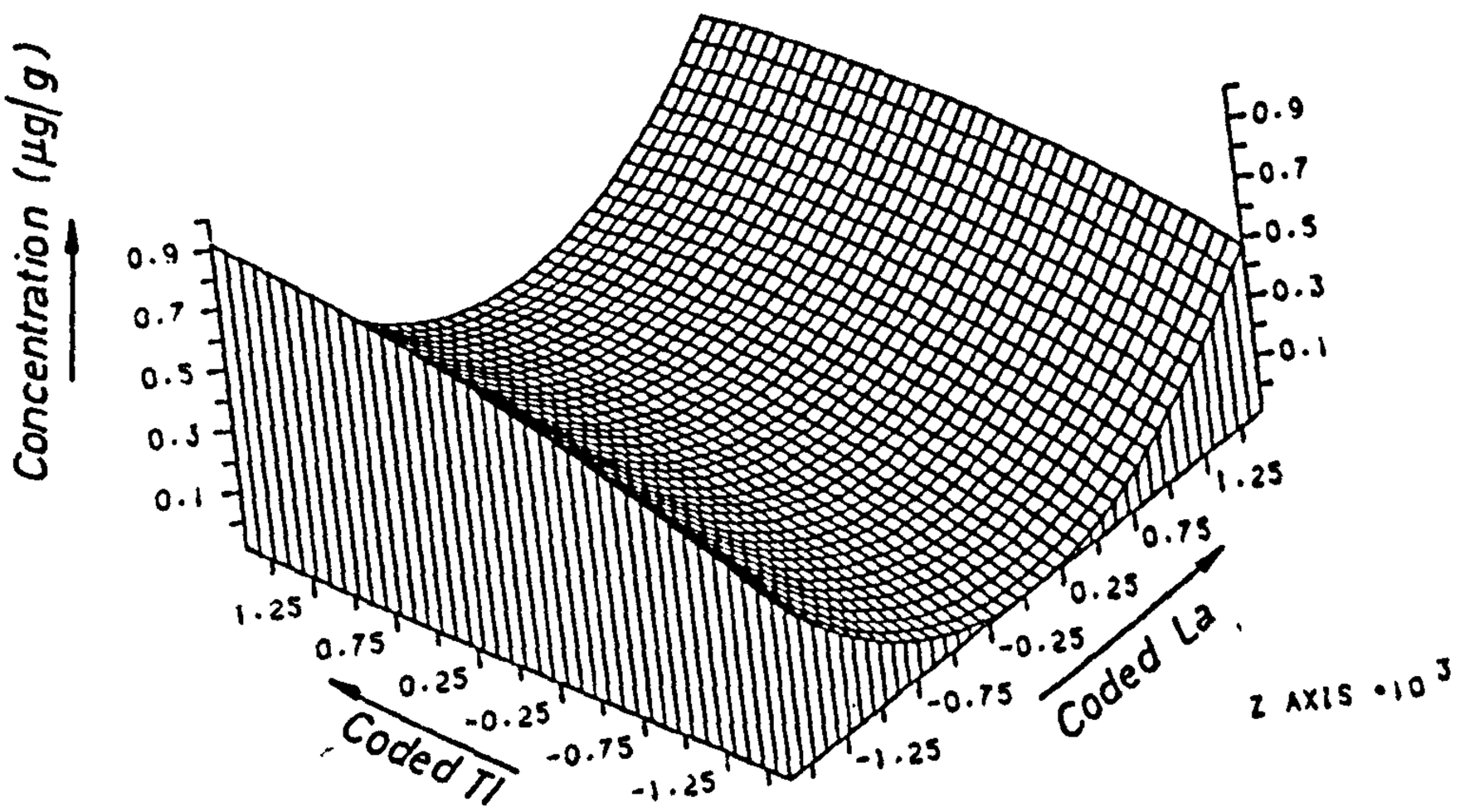

b) SAS

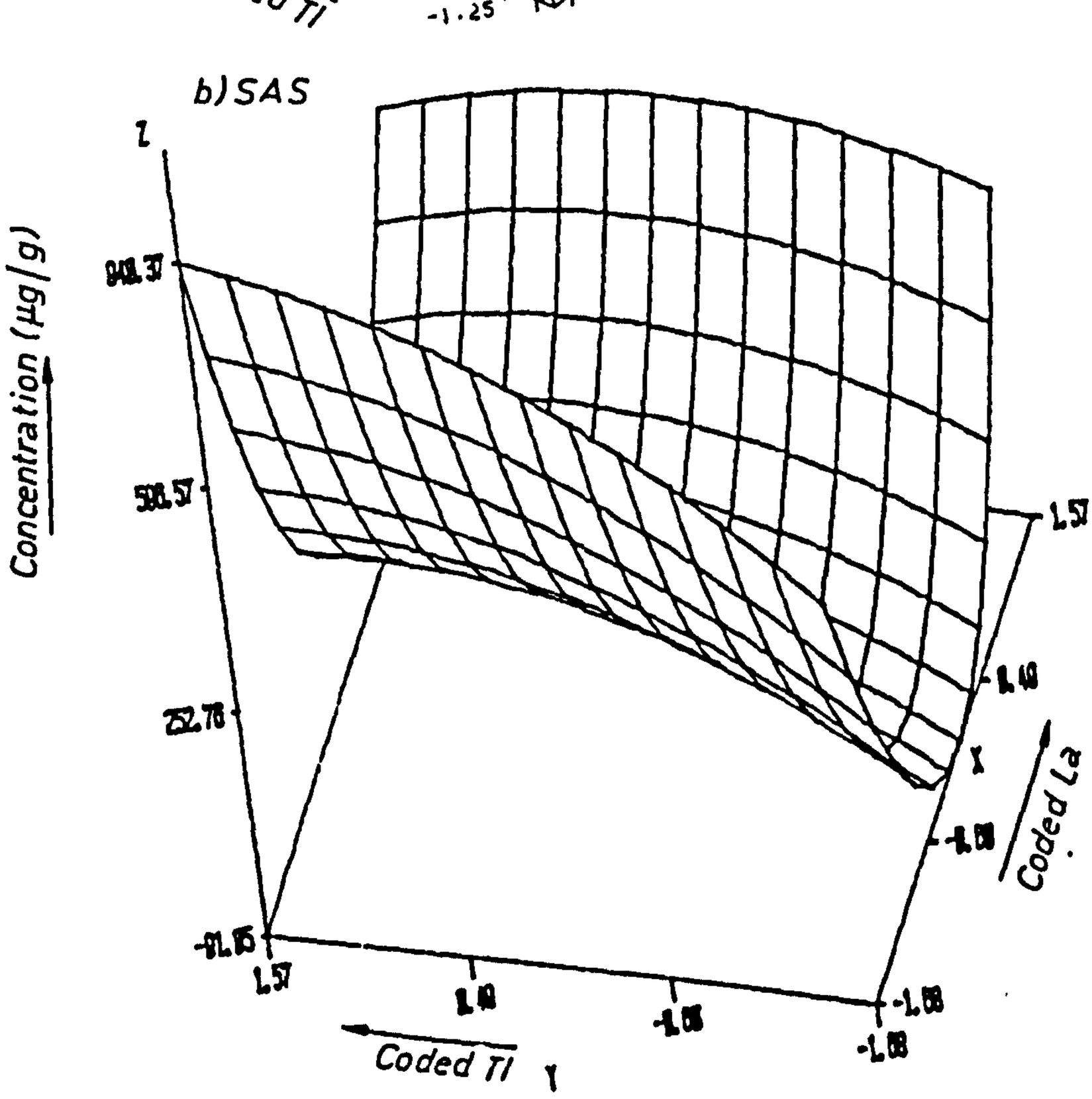

Confirmation of the value being a real effect was given by Figures 6.55 a & b. The former depicts the surface at levels of lead which are low and constant (-1.68, 5 x 10^{-4} $\mu g/cm^3$), thus as the level of La is increased in the solution so the level of La increases in the shoots. However, at high levels of lead (+1.68, 5 $\mu g/cm^3$), the highest levels of La in the tissue are found at low levels of La in the nutrient solution. Presumably lead at these higher levels is an extremely good competitor so preventing uptake of La.

k) Interactive Effect Between La and Pb on Thallium in Plant Tissues

The surfaces (Figure 6.56) for the thallium content in root tissues indicate that both lanthanum and lead decrease the level of thallium in such tissues. Probably these metals detoxify the thallium by competition. This observation shows that heavy metals can play an important role in the uptake of other heavy metals into both the roots and shoots of the plant. Therefore, the plants may grow and exhibit reduced levels of, say, thallium. This interaction effect has not been described previously. Such effects, which reflect the complexity of the natural laws governing metal uptake, would have been difficult to demonstrate if RSM had not been used.

l) Interactive Effects between La and Ag on Lead in Plant Tissues

Figure 6.57 illustrates that the level of lead in the roots is decreased by increasing the concentrations of lanthanum and silver in the nutrient solution. There appears to be little effect on the lead uptake when the Ag or La concentrations are increased. As their concentration increases there is a gradual decrease particularly along the silver axis for the lead taken up. Along the La axis the surface is almost planar signifying little competition between the lead and lanthanum.

FIG. 6.55 RESPONSE SURFACE FOR LANTHANUM TAKEN UP BY SHOOTS OF COCKS FOOT SEEDLING

a) AT CODED Pb = -1.68

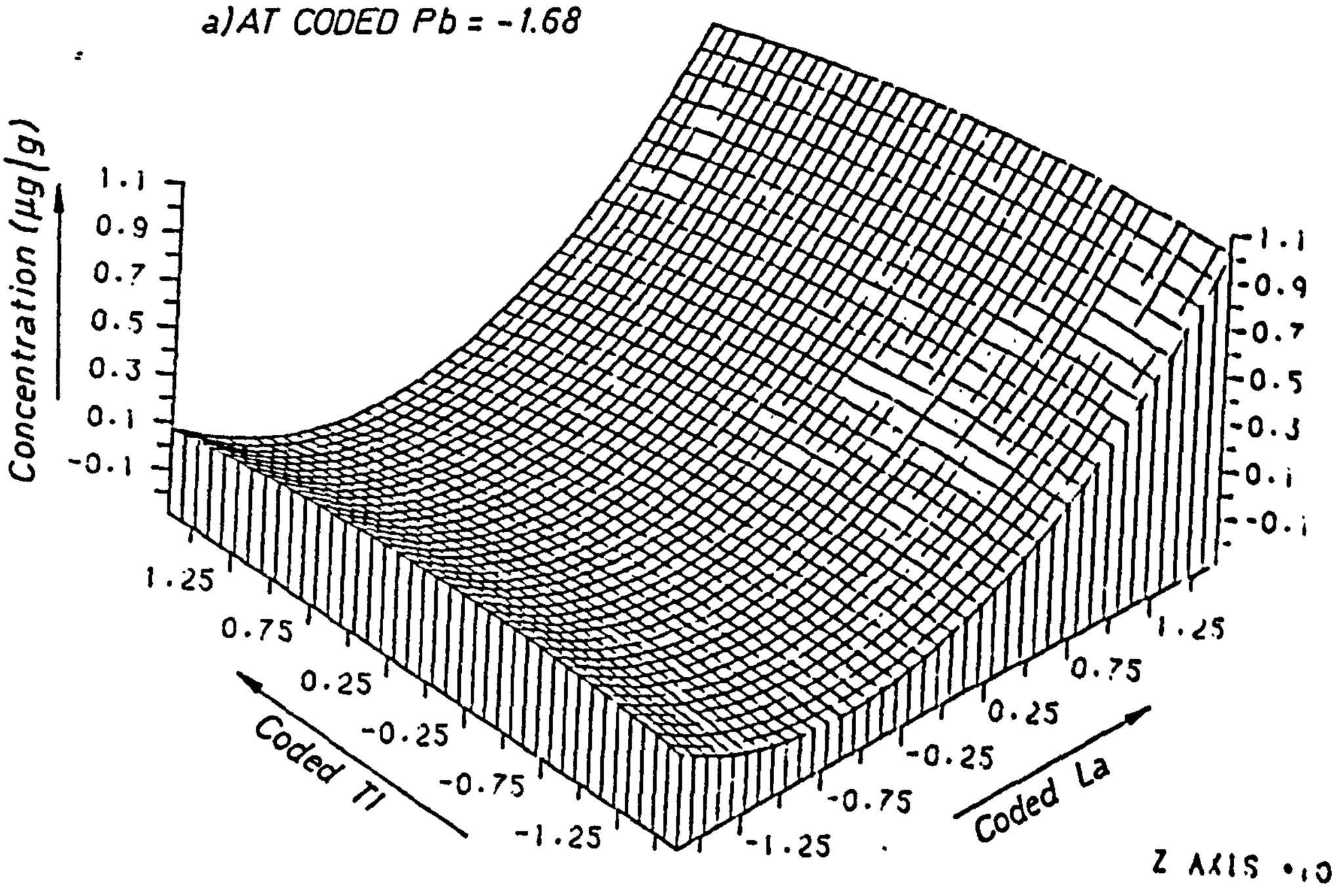

b) AT CODED Pb = +1.68

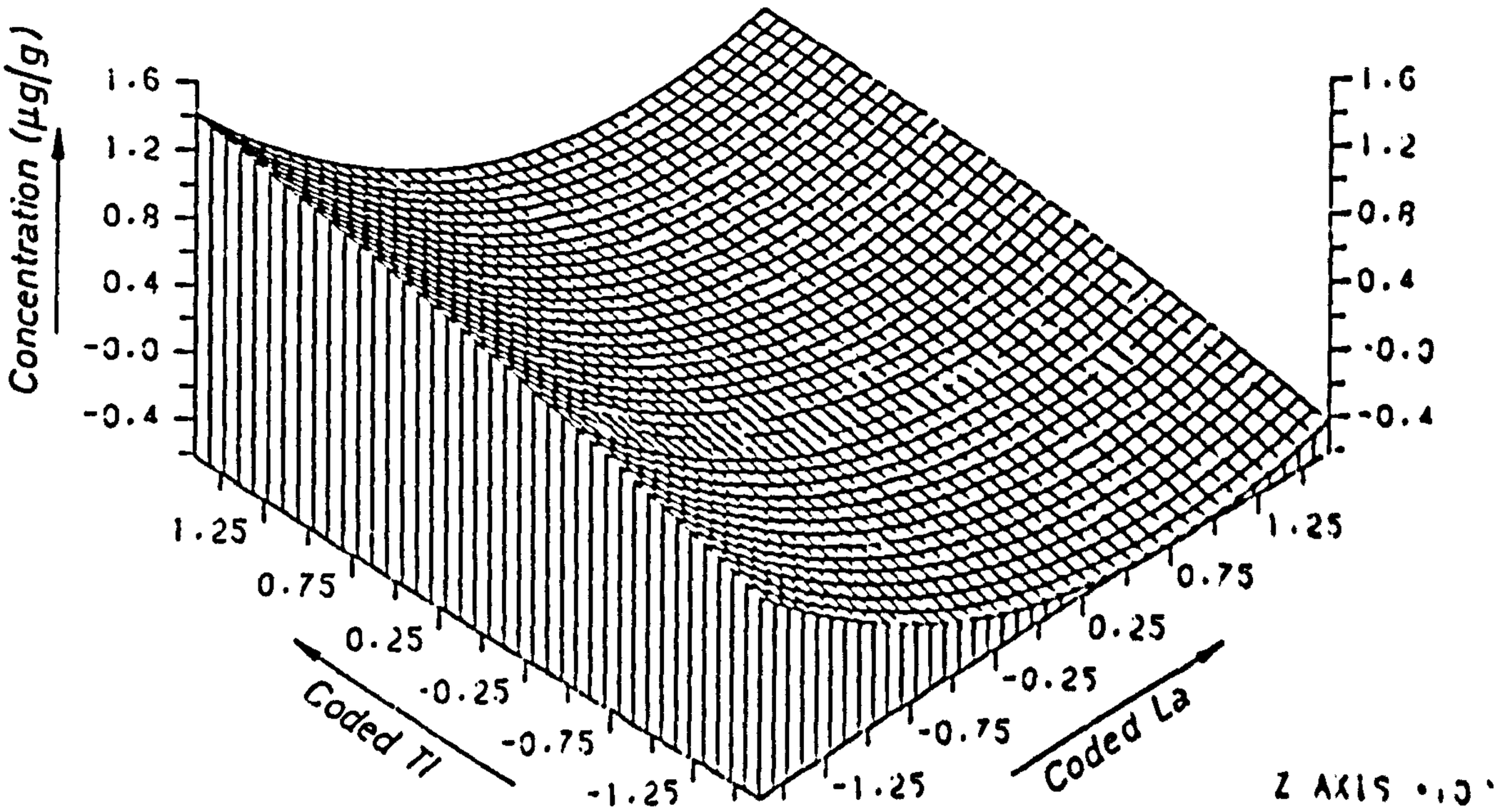

FIG.6.56 RESPONSE SURFACE FOR THALLIUM TAKEN UP BY ROOTS OF COCKS FOOT SEEDLING AT CODED TI = 0

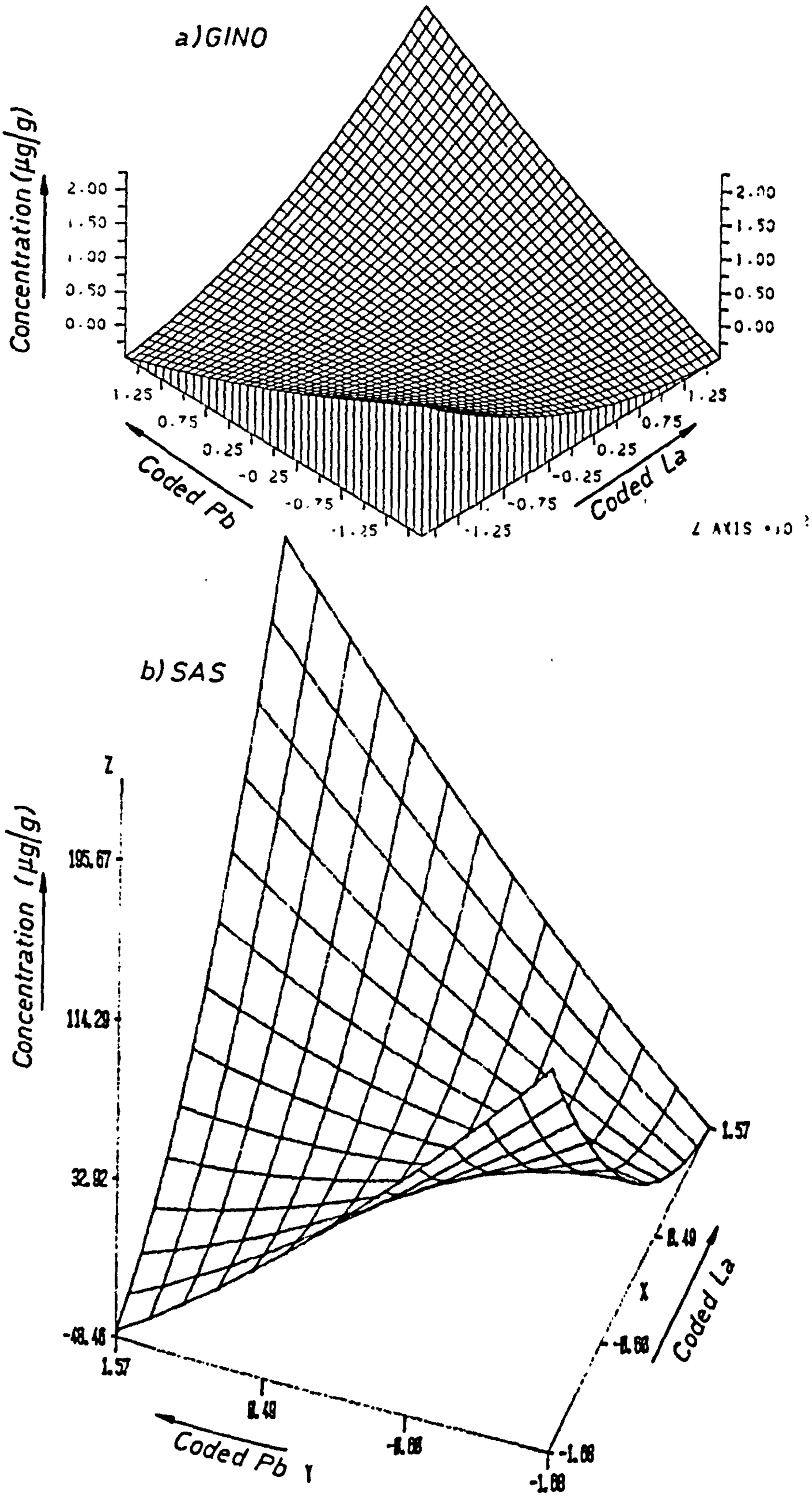

FIG 6.57 RESPONSE SURFACE FOR LEAD TAKEN UP BY ROOTS OF COCKS FOOT SEEDLING AT CODED Pb = 0

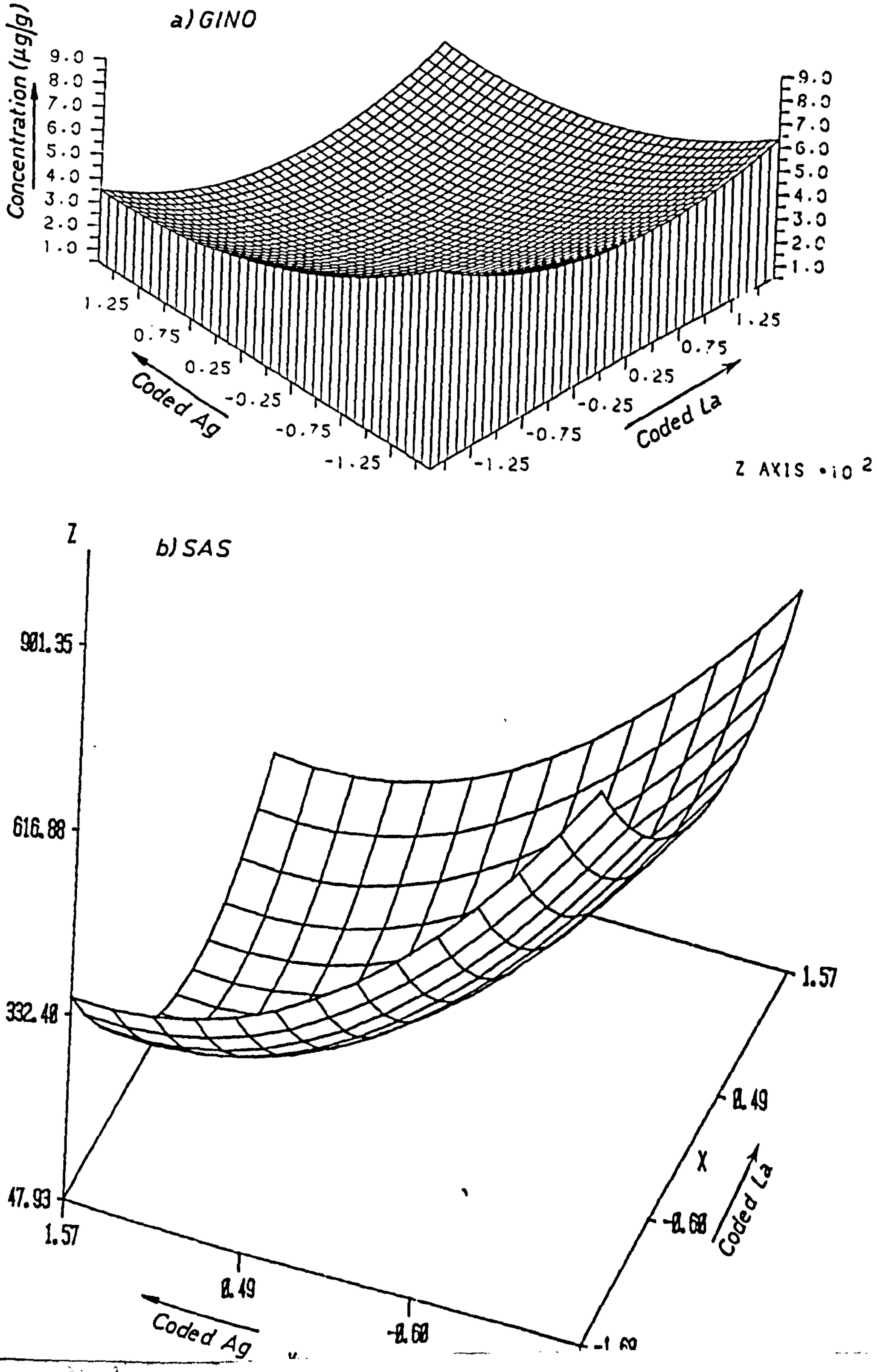

Surfaces of very different shape but similar to each other for roots and shoots were obtained when thallium was added to the nutrient solution instead of Ag (see Figures 6.58 and 6.59). Clearly when the concentration of lead added to the nutrient solution was increased, it was expected that the level of lead in the plant tissues would increase. In fact, however, the lead level does not increase in the manner expected; initially it is quite the reverse, until a coded level of 0 (0.05 $\mu g/cm^3$) when the level of lead found in the shoots decreases quite markedly. Above this coded value the lead content of the shoots begins to increase (see Figure 6.60). The effects appear to hold over all the concentration of the thallium added. There must be some interaction between Pb and Tl. This is expected due to the similarity in the ionic radii for these two elements.

What is remarkable is the change in shape when progressing from coded levels of -1.68 for Tl to 0 (see Figures 6.60 and 6.61a). The surface retains a similar shape but is rotated through 90^{o}. On moving to +1.68 (see Figure 6.61b), the surface returns to that displayed at the -1.68 level but the levels of metals are depressed. Clearly a much more detailed investigation with intermediate values of metal concentration should be undertaken.

m) Interaction Effects between Pb and Ag on the Yield of Plants

Figure 6.62 depicts the effects of the metals on the dry weight of the Cock's Foot species. At low concentrations of lead and silver in the nutrient solution, the plant produced high yields of tissue, both roots and shoots. When the concentration of the metal increased in the nutrient solution, the yield of the plant was reduced. The observation directly indicates the toxicity of these metals to the plant.

FIG. 6.58 RESPONSE SURFACE FOR LEAD TAKEN UP BY ROOTS OF COCKS FOOT SEEDLING AT CODED La = 0

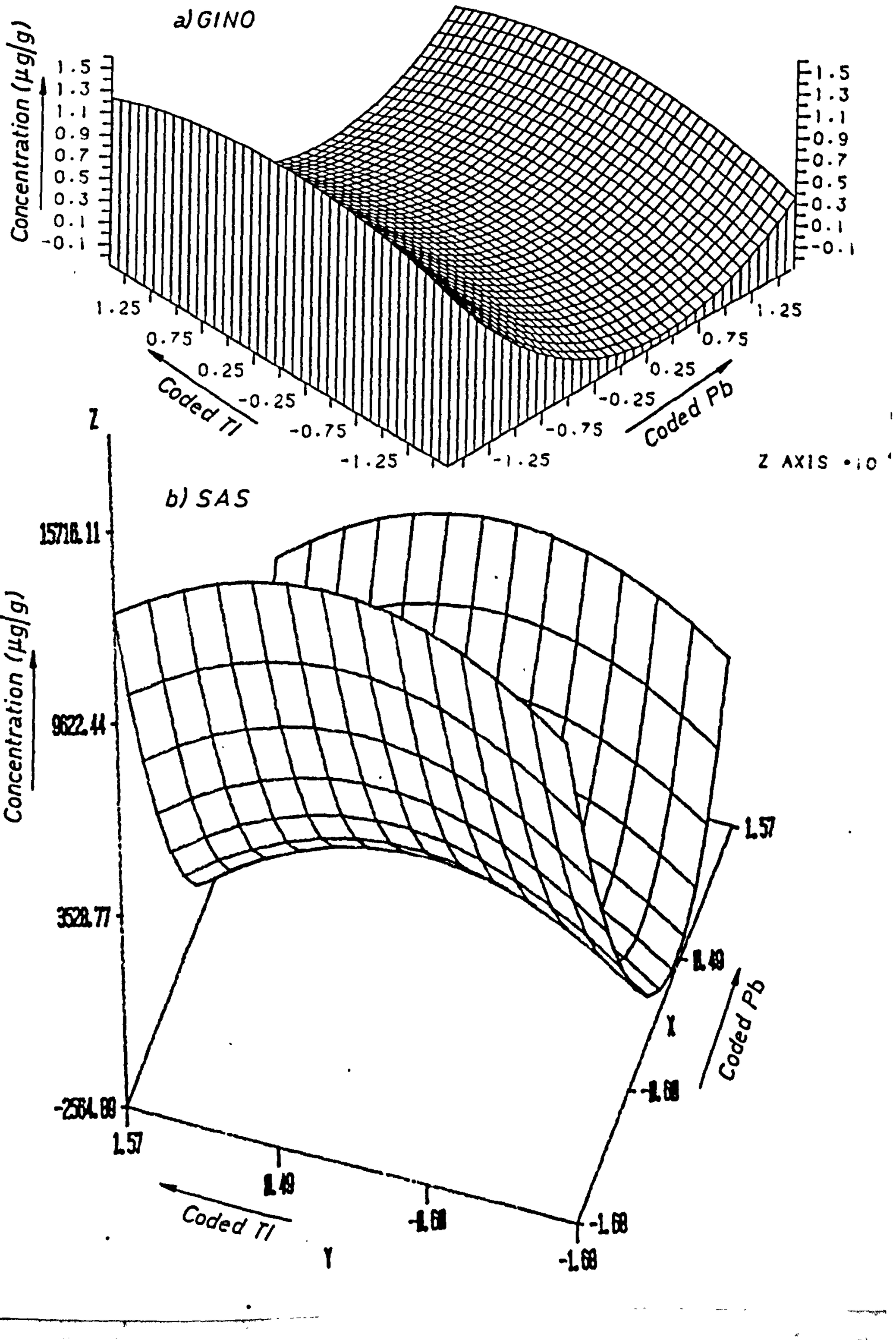

FIG. 6.59 RESPONSE SURFACE FOR LEAD TAKEN UP BY SHOOTS OF COCKS FOOT SEEDLING AT CODED La = 0

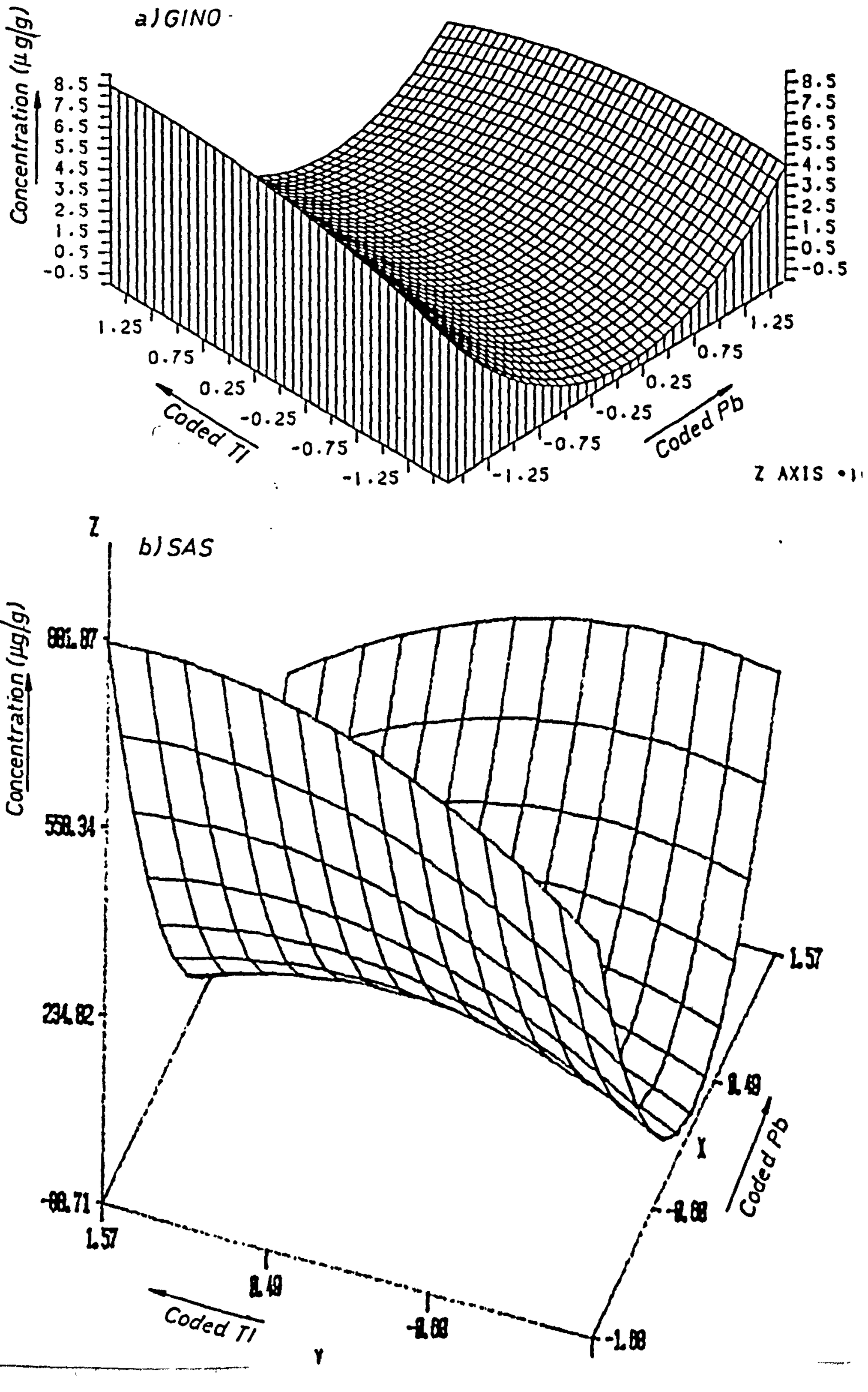

FIG. 6.60 RESPONSE SURFACE FOR LEAD TAKEN UP BY SHOOTS OF COCKS FOOT SEEDLING AT CODED TI = 0

FIG. 6.61 RESPONSE SURFACE FOR LEAD TAKEN UP BY SHOOTS OF COCKS FOOT SEEDLING

a) At coded TI = -1.68

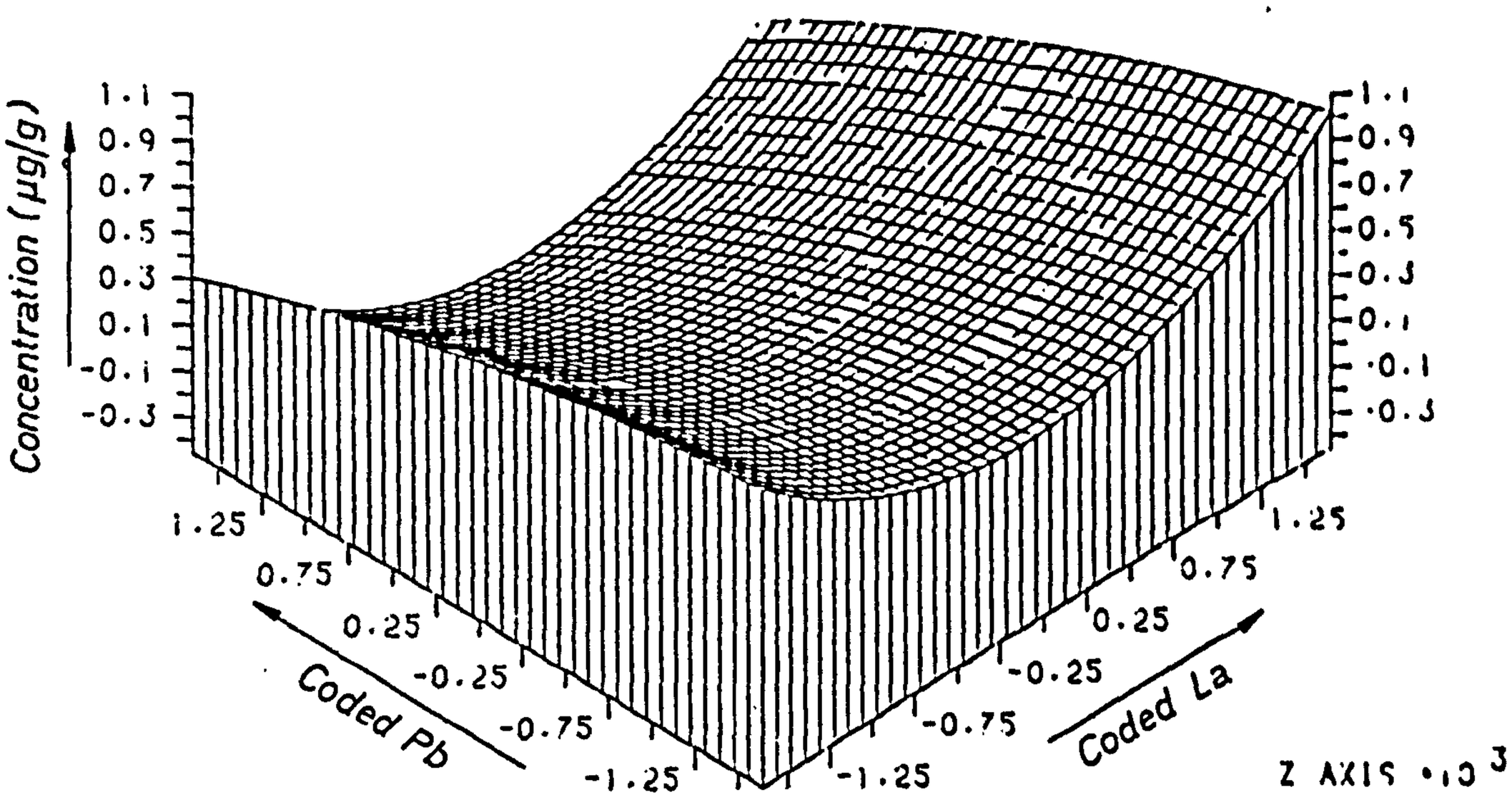

b) At coded TI = +1.68

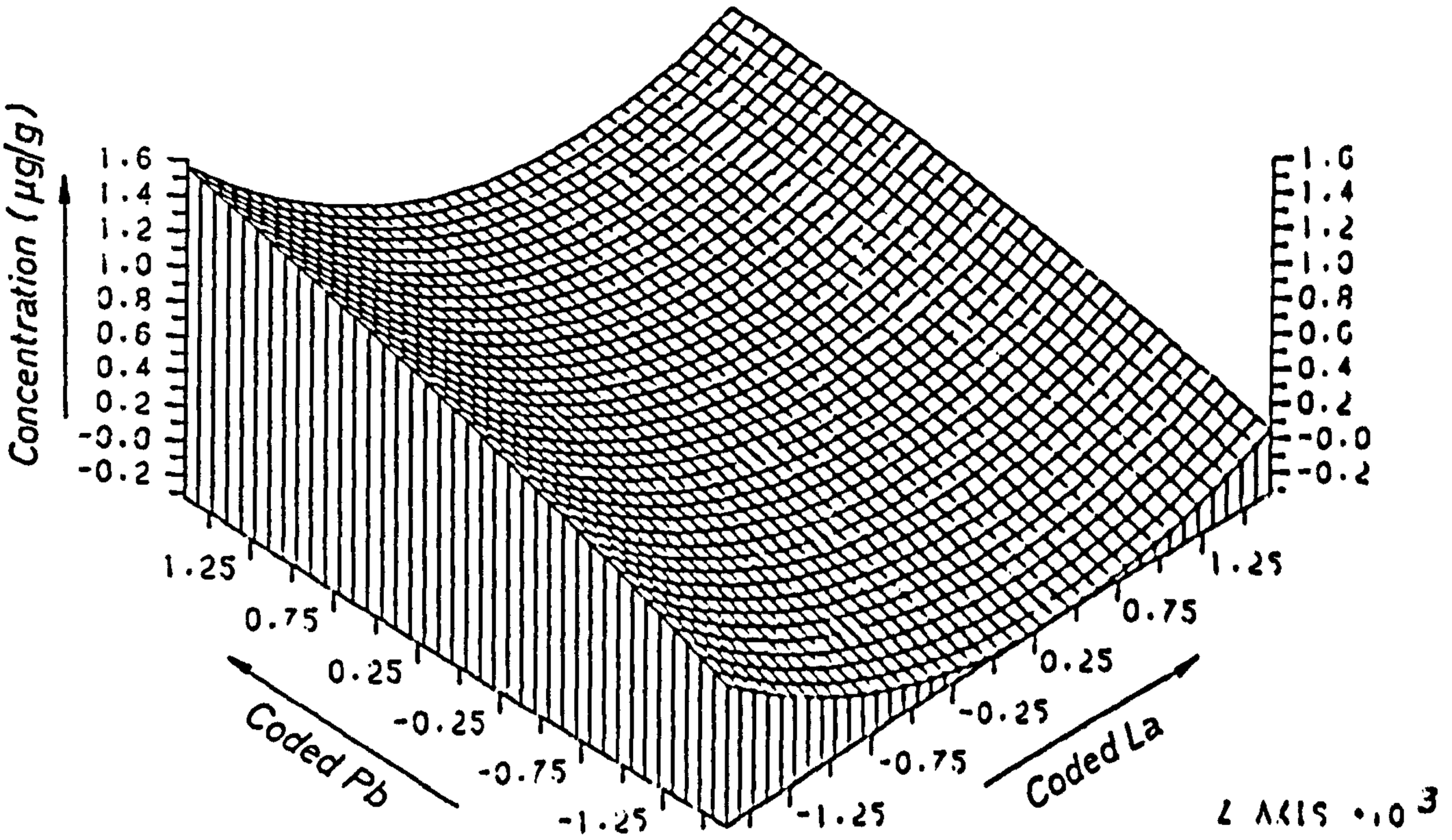

FIG. 6.62 RESPONSE SURFACE FOR DRY WEIGHT OF ROOTS OF COCKS FOOT SEEDLING AT CODED La = 0

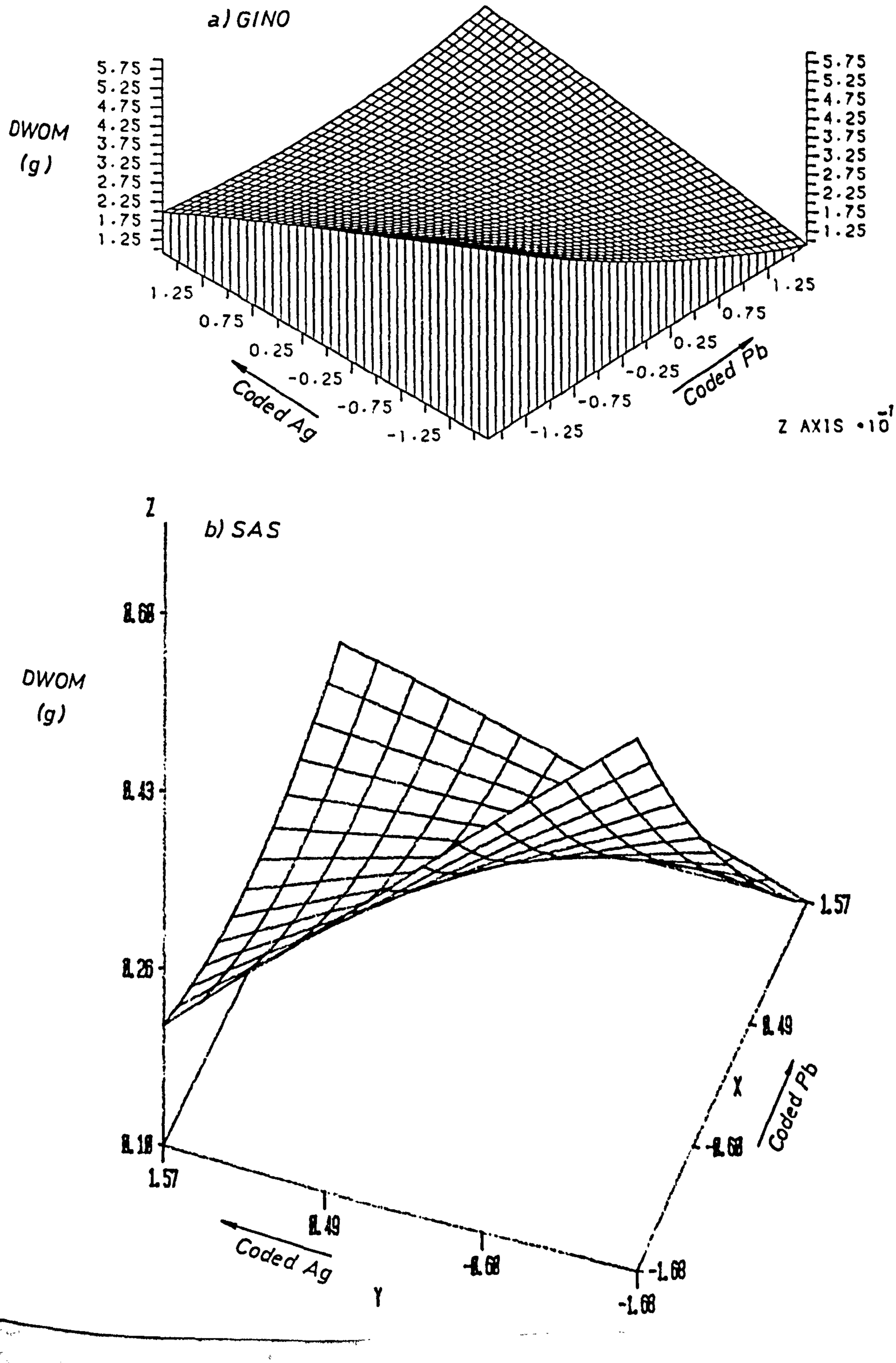

For some responses, particularly the root length parameter; the yield appeared to increase with increase in concentration of toxic metals. Negative numbers were predicted by both statistical packages. Obviously this result is incorrect and presumably there must be a major interference on root growth by trivalent metals. Trivalent metals, in particular Al, are known to inhibit cell division of roots (33,34). Attempts to find a linear regression equation between root length and dry weight to yield of roots failed with a correlation coefficient of less than 0.6. Thus a poor quality relationship exists between root length and dry weight of roots in such circumstances. Therefore it is not a reliable guide to use the root length response as a parameter in such studies when using spiked trivalent metals in the nutrient solution.

A further complicating factor is that these particular plants were initially grown in double strength phosphate solution. However, because of the insolubilities of lead and lanthanum phosphates, phosphate was not present in the nutrient solution during the spiking stages of the experiment. Therefore, the response in root length may be due to a phosphate deficiency since phosphate is essential for root cell elongation and division. During the planning stages of the experiment, it had been hoped that sufficient phosphate would have been taken up by the plant during the initial acclimatisation period to overcome this particular difficulty. From the computer generated surfaces clearly this was not the case and much more detailed planning must be carried out when using trivalent metal ions as additives.

n) Comparison between the Interactive Effects between Metals on the Measured Responses of the Plants

The magnitude of the coefficients B_{12}, B_{13} and B_{23} (see Table 6.19) may be considered as a measure of the intensity of the interaction between the metals added to the nutrient solution and the plant responses. The listing below is the sequence in order of magnitude.

La * Pb (B_{12})

Roots : Fe > Mg > Cu > Zn > Mn > Tl > La > Pb

Shoots : Mn > Cu > DWOM > Tl > Zn > Fe > Mg > Pb > La

La * Tl(B_{13})

Roots : Pb > DWOM > Tl > Zn > Mn > Cu > La > Mg > Fe

Shoots : Pb > Zn > Cu > Tl > DWOM > Mn > Mg > Fe > La

Pb * Tl(B_{23})

Roots : Mg > Cu > La > Zn > DWOM > Tl > Pb > Mn > Fe

Shoots : La > Mg > Fe > DWOM > Tl > Zn > Cu > Mn > Pb

The optimum plant responses in roots and shoots estimated from the coded values of lanthanum, lead and thallium in the nutrient solution are listed in Tables 6.25 and 6.26 respectively.

Table 6.25 : Levels of La, Pb and Tl added to Nutrient Solution Estimated to Produce Optimum Responses by Roots of Cock's Foot Seedlings

*Type of Response		Coded Value of x			Corresponding Actual Concentration Added ($\mu g/cm^3$)			Estimated Response
		La	Pb	Tl				
		x_1	x_2	x_3	La	Pb	Tl	Values in $\mu g/g$ except where stated
(i)	La	0.009	-0.251	0.418	0.257	0.025	0.03	1234
	Pb	-0.382	-0.104	-0.321	0.088	0.037	4.1×10^{-4}	875
	Tl	0.880	0.7960	1.778	2.744	0.400	1.30	65
	Cu	0.187	0.6077	-0.385	0.417	0.261	3.4×10^{-3}	907
	Zn	1.76	-0.3411	-1.355	29.97	0.0198	2.4×10^{-4}	1005
(ii)	Fe	-0.173	-0.336	0.5111	0.156	0.020	0.040	5561
	Mg	0.340	0.337	0.697	0.632	0.1252	0.067	2652
	Mn	0.870	0.445	-0.93	2.670	0.1679	6.8×10^{-4}	980
(iii)	DWOM	-.780	-2.665	2.187	0.030	3.59×10^{-5}	4.000	0.1380
	R.L.	0.391	1.453	0.220	0.726	2.597	0.018	6.20

i) Metals added as spiking elements

ii) Metals already in Hoagland's solution as essential for plant growth

iii) Biological response parameter

DWOM = Dry weight of plants per treatment (g)

R.L. = Root length (cm)

Table 6.26 : Levels of La, Pb and Tl Added to Nutrient Solution Estimated to Produce Optimum Responses by Shoots of Cock's Foot Seedlings

*Type of Response		Coded Value of x			Corresponding Actual Concentration Added ($\mu g/cm^3$)			Estimated Response
		La	Pb	Tl				
		x_1	x_2	x_3	La	Pb	Tl	Values in $\mu g/g$ except where stated
	La	0.2815	0.054	0.899	0.5390	0.059	0.117	307
(i)	Pb	-0.002	0.2661	-0.190	0.2498	0.100	5.9×10^{-3}	270
	Tl	-0.100	0.0063	-0.002	0.1914	0.050	9.9×10^{-3}	779
	Cu	0.1450	0.3140	-0.192	0.3724	0.1176	5.9×10^{-3}	35
	Zn	-0.481	0.1140	0.058	0.0679	0.068	0.0110	29
(ii)	Fe	0.813	0.3960	1.80	2.287	0.1469	1.33	226
	Mg	-0.660	-0.4260	-1.85	0.0418	0.0157	6.5×10^{-5}	125
	Mn	0.650	-0.386	-0.11	1.181	0.0175	7.4×10^{-3}	42
(iii)	DWOM	0.225	-0.350	0.04	0.4629	0.0193	0.0111	0.1580

i) Metals added as spiking elements

ii) Metals already in Hoagland's solution as essential for plant growth

iii) Biological response parameter

DWOM = Dry weight of plants per treatment (g)

R.L. = Root length (cm)

When lanthanum, lead and silver were added to the nutrient solution, the interactive effects between the metals (see Table 6.20) on plant responses were as follows :-

La * Pb (B_{12})

Roots : Fe > Mg > Cu > Zn > La > DWOM > Mn > Ag > Pb

Shoots : Cu > Mn > Mg > DWOM > Ag > Zn > Fe > La > Pb

La * Ag (B_{13})

Roots : La > Pb > DWOM > Mn > Zn > Cu > Ag > Mg > Fe

Shoots : Fe > La > Cu > Ag > DWOM > Mn > Zn > Mg > Pb

Pb * Ag (B_{23})

Roots : La > Cu > Zn > Ag > Mn > DWOM > R.L. > Mg > Fe > Pb

Shoots : Cu > DWOM > Pb > Mg > Mn > Zn > Ag > La > Fe

The optimum plant responses in roots and shoots estimated from the coded values of lanthanum, lead and silver in the nutrient solution are given in Tables 6.27 and 6.28 respectively.

Table 6.27 : Levels of La, Pb and Ag Added to Nutrient Solution Estimated to Produce Optimum Responses by Roots of Cock's Foot Seedlings

*Type of Response		Coded Value of x			Corresponding Actual Concentration Added ($\mu g/cm^3$)			Estimated Response
		La	Pb	Ag	La	Pb	Ag	
		x_1	x_2	x_3				Values in $\mu g/g$ except where stated
	La	1.615	-1.23	-2.13	20.00	1.77×10^{-3}	6.2×10^{-5}	1630
(i)	Pb	0.367	0.005	1.366	0.68	0.05	0.830	488
	Ag	0.942	1.423	-0.41	3.24	2.37	6.70×10^{-3}	115
	Cu	-1.616	1.636	-1.04	311×10^{-3}	4.27	1.21×10^{-3}	490
	Zn	0.026	0.113	-0.23	0.260	0.068	0.010	611
(ii)	Fe	-0.006	0.643	-0.41	0.240	0.287	6.70×10^{-3}	649
	Mg	1.654	-0.889	0.40	22.47	4.47×10^{-3}	0.060	325
	Mn	0.117	-1.063	-0.20	3.98	2.79×10^{-3}	0.0118	35
	DWOM	0.950	1.558	0.640	3.31	3.30	0.142	0.2120
(iii)	R.L.	1.98	1.47	-1.52	54.00	2.72	3.2×10^{-4}	13.37

i) Metals added as spiking elements

ii) Metals already in Hoagland's solution as essential for plant growth

iii) Biological response parameter

DWOM = Dry weight of plants per treatment (g)

R.L. = Root length (cm)

Table 6.28 : Levels of La, Pb and Ag Added to Nutrient Solution Estimated to Produce Optimum Responses by Shoots of Cock's Foot Seedlings

*Type of Response		Coded Value of x			Corresponding Actual Concentration Added ($\mu g/cm^3$)			Estimated Response
		Al x_1	Pb x_2	Ag x_3	Al	Pb	Ag	Values in $\mu g/g$ except where stated
	La	-0.590	0.009	-0.190	0.050	0.051	0.012	490
(i)	Pb	0.072	-0.474	1.253	0.305	0.0138	0.614	150
	Ag	-0.157	1.744	0.3668	0.1639	2.333	0.0553	1.65
	Cu	-0.421	-1.897	0.861	0.0800	1.1×10^{-4}	0.2118	68
	Zn	0.265	-0.1250	0.782	0.5160	0.0356	0.170	63
(ii)	Fe	-0.236	-0.535	0.595	0.1322	0.0117	0.102	97
	Mg	0.0191	0.0112	-0.335	0.2645	0.0516	8×10^{-3}	774
	Mn	-1.929	1.210	1.782	1.32×10^{-3}	1.309	2.586	132
(iii)	DWOM	0.429	1.260	-0.518	0.8057	1.537	4.9×10^{-3}	0.618

i) Metals added as spiking elements

ii) Metals already in Hoagland's solution as essential for plant growth

iii) Biological response parameter

DWOM = Dry weight of plants per treatment (g)

R.L. = Root length (cm)

2) Lolium perenne Seedlings

Figures 6.63 and 6.64 depict the interactive effects between Al and Pb on iron uptake into the shoots on the one hand and Al and Ag on the other. The surfaces indicate that initially Al reduced the level of iron uptake. The effects are due to lead being particularly weak, those due to silver being more pronounced. The observations in these Figures are in agreement with Lee et alia (35). However, when the concentration of the added metals in combination tend towards the maximum experimental levels, then the level of iron taken up increased markedly.

A comparison between the interactive effects (see Table 6.21) between Al, Pb and Tl in the nutrient solution on the Lolium perenne responses can be deduced as follows :-

Al * Pb (B_{12})

Roots : Al > DWOM > Tl > Fe > Pb

Shoots : Fe > DWOM > Tl > Al > Pb

Al * Tl (B_{13})

Roots : Al > DWOM > Tl > Fe > Pb

Shoots : Pb > DWOM > Tl > Al > Fe

Pb * Tl (B_{23})

Roots : Pb > Fe > Al > DWOM > Tl

Shoots : Pb > Al > DWOM > Fe > Tl

The optimum plant responses in roots and shoots estimated from the coded values of Al, Pb and Tl in the nutrient solution are listed in Tables 6.29 and 6.30.

FIG. 6.63 RESPONSE SURFACE FOR IRON TAKEN UP BY SHOOTS OF LOLIUM PERENNE SEEDLING AT CODED TI = 0

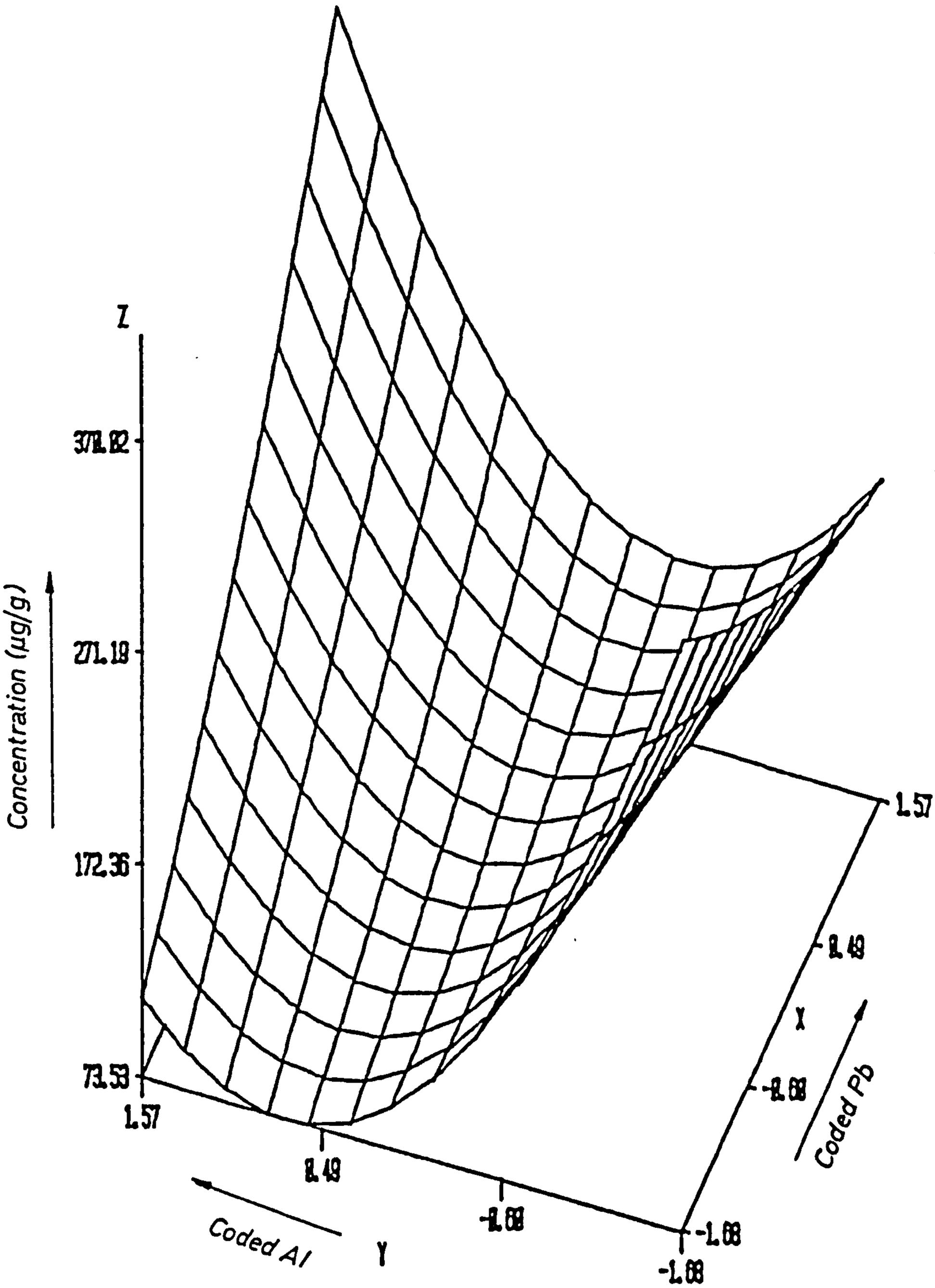

FIG. 6.64 RESPONSE SURFACE FOR IRON TAKEN UP BY SHOOTS OF LOLIUM PERENNE SEEDLING AT CODED Pb = 0

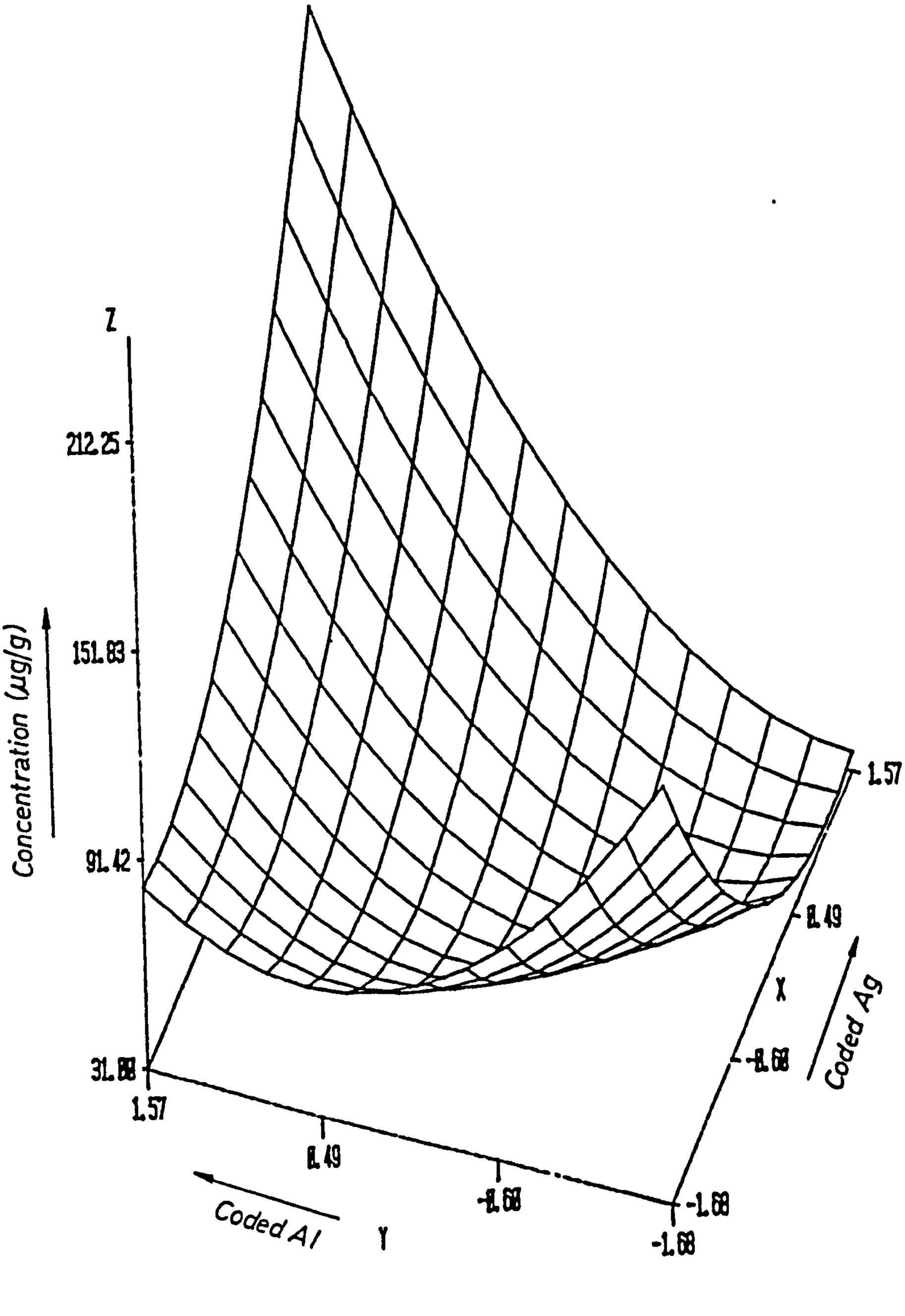

Table 6.29 : Levels of Al, Pb and Tl Added to Nutrient Solution Estimated to Produce Optimum Responses by Roots of Lolium perenne Seedlings

*Type of Response		Coded Value of x			Corresponding Actual Concentration Added ($\mu g/cm^3$)			Estimated Response
		Al	Pb	Tl				
		x_1	x_2	x_3	Al	Pb	Tl	Values in $\mu g/g$ except where stated
	Al	-1.10	0.400	1.981	2.52×10^{-3}	0.148	2.175	263
(i)	Pb	0.795	0.318	-0.440	0.434	0.118	3.0×10^{-3}	189
	Tl	-0.057	0.368	-0.451	0.0429	0.136	2.9×10^{-3}	8.67
(ii)	Fe	0.326	-0.136	-0.360	0.I2I5	0.0346	3.1×10^{-3}	725
(iii)	DWOM	-0.133	-1.340	-0.360	0.0349	1.3×10^{-3}	3.76×10^{-3}	0.477
	R.L.	-0.191	-0.295	-0.620	0.0298	0.0224	4.4×10^{-3}	16.00

i) Metals added as spiking elements

ii) Metals already in Hoagland's solution as essential for plant growth

iii) Biological response parameter

DWOM = Dry weight of plants per treatment (g)

R.L. = Root length (cm)

Table 6.30 : Levels of Al, Pb and Tl Added to Nutrient Solution Estimated to Produce Optimum Responses by Shoots of Lolium perenne Seedlings

*Type of Response		Coded Value of x			Corresponding Actual Concentration Added ($\mu g/cm^3$)			Estimated Response
		Al	Pb	Tl	Al	Pb	Tl	
		x_1	x_2	x_3				Values in $\mu g/g$ except where stated
	Al	0.228	-0.086	0.096	0.093	0.039	0.0130	83.40
(i)	Pb	-0.025	-0.427	0.0208	0.0468	0.0157	0.0105	75
	Tl	-0.796	0.5190	-0.470	5.7×10^{-3}	0.205	2.78×10^{-3}	4
(ii)	Fe	1.436	-1.513	0.75	2.480	8.2×10^{-4}	0.0760	187
(iii)	DWOM	-0.423	-0.809	0.22	0.0158	5.5×10^{-3}	0.0180	0.998

i) Metals added as spiking elements

ii) Metals already in Hoagland's solution as essential for plant growth

iii) Biological response parameter

DWOM = Dry weight of plants per treatment (g)

R.L. = Root length (cm)

When aluminium, lead and silver were added to the nutrient solution, the comparison between the interactive effects between the metals (see Table 6.22) on the plant responses produced the following sequence :-

Al * Pb (B_{12})

Roots : DWOM > Al > Ag > Fe > Pb

Shoots : Al > R.L. > Ag > Pb > Fe

Al * Ag (B_{13})

Roots : Pb > DWOM > Al > Fe > Ag

Shoots : Fe > DWOM > Pb > Ag > Al

Pb * Ag (B_{23})

Roots : Fe > DWOM > Al > Ag > Pb

Shoots : Ag > Pb > DWOM > Al > Fe

The optimum plant responses in roots and shoots were estimated from the coded values of Al, Pb and Ag in the nutrient solution and are listed in Tables 6.31 and 6.32 respectively.

Table 6.31: Levels of Al, Pb and Ag Added to Nutrient Solution Estimated to Produce Optimum Responses by Roots of Lolium perenne Seedlings

*Type of Response		Coded Value of x			Corresponding Actual Concentration Added ($\mu g/cm^3$)			Estimated Response
		Al	Pb	Ag	Al	Pb	Ag	
		x_1	x_2	x_3				Values in $\mu g/g$ except where stated
(i)	Al	-0.172	0.747	0.517	0.0314	0.3814	0.0831	44
	Pb	0.124	0.954	0.777	0.070	0.6694	0.1686	105
	Ag	-0.035	-0.432	0.354	0.0455	0.0154	0.0534	22
(ii)	Fe	0.901	0.819	0.0043	0.579	0.4638	0.0206	951
(iii)	DWOM	-0.058	-0.071	0.0214	0.0428	0.04132	0.0216	0.635
	R.L.	-0.691	-0.490	-0.568	7.66×10^{-3}	0.0132	4.36×10^{-3}	18.00

i) Metals added as spiking elements

ii) Metals already in Hoagland's solution as essential for plant growth

iii) Biological response parameter

DWOM = Dry weight of plants per treatment (g)

R.L. = Root length (cm)

Table 6.32 : Levels of Al, Pb and Ag Added to Nutrient Solution Estimated to Produce Optimum Responses by Shoots of Lolium perenne Seedlings

*Type of Response		Coded Value of x			Corresponding Actual Concentration Added ($\mu g/cm^3$)			Estimated Response
		Al	Pb	Ag	Al	Pb	Ag	
		x_1	x_2	x_3				Values in $\mu g/g$ except where stated
	Al	0.510	-1.120	-1.813	0.200	2.39×10^{-3}	1.48×10^{-4}	21.0
(i)	Pb	-0.227	-0.693	-0.891	0.0270	7.6×10^{-3}	2.20×10^{-3}	19.6
	Ag	0.774	1.367	-0.590	0.410	2.056	4.10×10^{-3}	2.0
(ii)	Fe	0.202	-0.285	-0.979	0.0867	0.0231	1.42×10^{-3}	197
(iii)	DWOM	0.009	-0.167	0.0139	0.0513	0.0318	0.0212	0.935

i) Metals added as spiking elements

ii) Metals already in Hoagland's solution as essential for plant growth

iii) Biological response parameter

DWOM = Dry weight of plants per treatment (g)

R.L. = Root length (cm)

The results in Tables 6.25 to 6.32 indicate the optimum level of metals in these plants, their root length and dry weight. The levels of these parameters probably indicate the maximum or minimum which can be tolerated by the plant with detriment. Above this level of metal burden, the plant suffers and may initiate mechanisms such as increasing the uptake of essential metal, e.g. iron, in order to ameliorate any damage.

The preceding discussion, although lengthy, is necessarily very incomplete but offers an indication of the results to be achieved by using this type of experimental design. In many cases, the effect of addition of two toxic metals is simply additive with the minimum of interaction, as depicted by the number of almost planar type surfaces encountered (see Figure 6.37). However, in certain cases with very curved surfaces (see Figure 6.58) the overall effect is clearly not linearly additive and a high degree of interaction is indicated. The present study has been largely an exploratory one, designed to indicate the possibilities of the system. Clearly such a system is capable of much further development. The original experiment and application to other species both tolerant and non-tolerant must be made. However, better fitment of the data is necessary; it will need to be over a much narrower set of metal levels. Box et alia's (9) approach to experimental design stresses this point but as a very rough working hypothesis it is satisfactory to a first approximation. It should not be expected that a simple quadratic equation could represent (in a quantitative manner) such a response over a wide range of concentrations. Much further experimentation around the regions of optimal response must be made.

6.4 REFERENCES

1. Box, G.E.P., Biometrics, 10, 16 (1954).
2. Box, G.E.P., Hunter, W.G. and Hunter, J.S., "Statistics for Experiments : An Introduction to Design, Data Analysis and Model Building", John Wiley & Sons Inc., Chap. 15, p. 510 (1978).
3. Mead, R. and Pike, D.J., Biometrics, 31, 803 (1975).
4. Davies, O.L. (Ed.), The Design and Analysis of Industrial Experiments, published for Imperial Chemical Industries Ltd. by Oliver and Boyd, Chap. 11, p. 495 (1954).
5. Hill, W.J. and Hunter, W.G., Technometrics, 8, 571 (1966).
6. Draper, N.R. and Stoneman, D.M., Technometrics, 10, 177 (1968).
7. De Baun, R.M., Technometrics, 1, 1 (1959).
8. Deming, S.N., Anal. Chem., 43, 1726 (1971).
9. Box, G.E.P. and Wetz, J., Technical Report No. 9, p. 12 (1973).
10. Minitab Reference Manual, p. 67 (1981).
11. SAS Reference Manual, p. 98G3D (1982).
12. Rose, A. and Smith, H., Ind. & Eng. Chem., 55, 25 (1963).
13. Tidwell, P.W., Ind. & Eng. Chem., 52, 511 (1960).
14. Rubin, T.B., Mitchell, T.J. and Goldstein, G., Anal. Chem., 43, 717 (1971).
15. Hader, R.J., Harward, M.E., Mason, D. and Moore, D.P., Proc. Soil Sci. Soc. Am., 21, 59 (1957).
16. Moore, D.P., Harward, M.E., Mason, D.D., Hader, R.J., Lott, W.L. and Jackson, W.A., Proc. Soil Sci. Soc. Am., 21, 65 (1957).
17. Aia, M.A., Goldsmith, R.L. and Mooney, R.W., Ind. & Eng. Chem., 53, 57 (1961).
18. Morgan, S.L. and Jacques, C.A., J. Chromatogr. Sci., 16, 500 (1978).

19. Britton, H.T.S., Hydrogen Ions : Their Determination and Importance of Pure Industrial Chemistry, Chapman & Hall Ltd., London, p. 358 (1955).

20. Trefry, J.H. and Metz, S., Anal. Chem., 56, 745 (1984).

21. Gambrell, S., Khalid, R.A. and Patrick, W.H., Environ. Sci. Technol., 14, 431 (1980).

22. Rendell, P.S., Batley, G.E. and Cameron, A.J., Environ. Sci. Technol., 14, 315 (1980).

23. Gadde, R.R. and Laitinen, H.A., Anal. Chem., 46, 2022 (1974).

24. Davis, J.A. and Leckie, J.O., Environ. Sci. Technol., 12, 1309 (1978).

25. Murray, D.J., Healy, T.W. and Fuerstenan, D.W., Adv. Chem. Ser., 79, 74 (1968).

26. Green, J.B. and Monahan, S.E., Can. J. Chem., 55, 3248 (1977).

27. Beckett, P.H.T. and Davis, R.D., New Phytol., 81, 155 (1978).

28. Brar, M.S. and Sekhon, G.S., Plant and Soil, 45, 137 (1976).

29. Brar, M.S. and Sekhon, G.S., Plant and Soil, 45, 145 (1976).

30. Wallace, A., Mueller, R.T. and Alexander, G.V., Commun. in Soil Sci. and Plant Analysis, 7, 43 (1976).

31. Martell, A.E. and Smith, R.M., Critical Stability Constants, Volume 1 : Amino Acids, p. 49, Plenum Press, New York (1974).

32. Chaudhry, F.M., Sharif, M., Latif, A. and Qureshi, R.H., Plant and Soil, 38, 573 (1973).

33. Wood, M., Cooper, J.E. and Holding, A.J., Soil Bio. Chem., 15, 123 (1983).

34. Wood, M., Copper, J.E. and Holding, A.J., Plant and Soil, 78, 381 (1984).

35. Lee, J. and Pritchard, M.W., Plant and Soil, 82, 101 (1984).

CHAPTER 7

CONCLUSIONS AND SUGGESTIONS FOR FURTHER WORK

In the initial Experimental chapters samples collected from the Mendip Hills were found to be heavily contaminated with lead, reflecting the mining history of this site. In the water samples, the lead was present as both labile and complexed forms. Unfortunately no information was obtained about the effect of particle size due to contamination effects.

There was little lead contamination in the Iraqi samples. Therefore, it was difficult to find the chemical form of the lead.

Thus high copper levels were found in the samples collected from the Caradon Hill area and were in the following order :-

Drain Luckett > Caradon secondary rock > Caradon Native sediment. Most of the copper in these samples was associated with the Fe-Mn oxide and residual phases, but the bioavailability of copper was also in the above order.

Sediments from the Restronguet Creek and Penhallow Moor areas were found to be highly contaminated with iron and zinc, but also contained Ca, Mn, Cu, Cd and Pb. Different associations and bioavailability of each metal within the sediments were found. For example, in the Adit Bridge No. 8 sediment, the majority of the copper was found within the organic fraction. The association was expected because of the very high affinity copper (II) displays towards organic matter; this sediment had a particularly high organic carbon content (4.93%). However, the organic fraction is the penultimate fraction attacked by the sequential acidic leaching scheme which probably signifies that this copper is in the least available form bar that present in the residual phase. The Restronguet Creek sediment, on the other hand, contained some organic carbon (0.38%) but in this case the Cu(II) was associated with the residual phase. This is probably because the organic content here consists of paraffins

and similar mineral oils due to the commercial merchant traffic in the estuary and Carrick Roads, rather than the fulvic and humic acids of the freshwater sediment which chelate the copper.

Of the purification methods studied, Chelex-100 resin proved to be simple and removed most lead in the background electrolyte. Mercury cathode electrolysis was not suitable for purification of 1 M HAc + 1 M NaAc containing 0.01 M EDTA Na_2. It may be suitable for 1 M HAc + 1 M NaAc without EDTA.

The results for thallium determination indicate that GFAAS and electroanalytical techniques are sensitive for thallium (10 ng/cm^3). With the latter technique, thallium must be separated from any lead and cadmium present to avoid interference effects. The pH of the background electrolyte was found to be very important for the determination of thallium by DPASV. At high pH, thallium becomes a less electroactive species.

Thallium was taken up by Lolium perenne seedlings. The element critical levels were found to be approximately 1.9 and 0.056 mg/kg of Tl for roots and shoots respectively.of Lolium perenne seedlings, expressed on a dry weight basis. Therefore, further work must be carried out to investigate :-

i) how thallium is taken up by plants;

ii) in which part of the plant thallium is associated;

iii) what is the relationship between the uptake of thallium and potassium by plants; and

iv) what is the effect of thallium on enzyme activity.

However, although the determination of Tl in plant tissue was satisfactory, the same cannot be said for the recovery of the element from soil samples. Much further work remains to be carried out before the procedures can be used for soil analyses. The association of thallium,

especially with organic rich soils, is complex and needs clarification.

The use of volatile derivatives for the determination of metals in solutions is a possible but not altogether attractive reality. Although the proposition of the chelation of metals using solution extraction techniques followed by GLC has been proposed for almost three decades now, it has not achieved real status as an analytical procedure and it is not difficult to see why. Using the trifluoroacetylacetonates of Al, Cr, Fe and La as examples, attempts were made to develop suitable determination procedures. The complexes were relatively easily prepared and characterised on a large scale. The relative volatility of metals with TFA follow the order :- Fe > Al > Cr > La.

Thus the aluminium complex was prepared in two ways :-

i) on a large scale, as a solid, and

ii) in dilute solution and solvent extraction.

Comparison of both procedures indicated that the reaction in (ii) did not proceed to completion. Such a conclusion has been reached by other workers and it is unfortunate that these procedures are not satisfactory. It appears that GLC has little to offer the analyst interested in routine metal determinations; perhaps HPLC may fare better. However, much detailed examination of the chelation reactions and separation conditions are required.

The peak height of silver obtained by DC-ASV in 0.1 M KNO_3 + 0.002 M EDTA was higher than in 0.2 M NH_4OH + 0.2 M NH_4NO_3, possibly due to the formation of the electro-inactive species $[Ag(NH_3)_2]^+$ in the latter.

Silver and lead are taken up by the roots of plants and transported to the shoots. From the results obtained by studying the uptake of silver and lead with time, the metal accumulations decrease with increase in time, possibly due to the dilution of metals by plant growth.

Lanthanum in soils and sediments was determined by XRF. The sample

is easy to prepare prior to analysis. However, lanthanum in plant tissues requires a high weight of ashed sample to analyse by XRF. Therefore, Dc-plasma and ICP/MS were used for the lanthanum determination. The results obtained by determination of lanthanum by GFAAS indicated the advantage of statistical design and tantalum foil over the classical pyrolytic graphite tube.

The estimation of the critical levels of aluminium, silver, lanthanum and thallium indicated the toxicity of these metals to Lolium perenne seedlings was as follows :-

Tl > Ag > Al > La.

Further work must be carried out to investigate the mechanism of toxicity of each metal.

Investigation of the distribution of aluminium and lanthanum in Lolium perenne and Holcus lanatus species was carried out. There was a different association for each metal within the plant. In general, lanthaum accumulated in higher levels than aluminium in the same species, possibly indicating an exclusions of aluminium from the plant.

The amount of metal released from two contaminated sediments as a function of pH and time was studied using a 2^5 factorial design. The quantities released did not vary as much as expected indicating a slightly unsuitable choice of experimental conditions. However, pH appeared to be a more significant factor than time, although various other factors such as particle size, etc., were ignored. But the 3D-system of presentation of data especially the SAS package is a highly satisfactory method of presenting data and should be further developed. A major problem appeared to be the readsorption of various elements such as calcium and lead back into the sediments. Presumably the metal is released by one phase e.g. carbonate and readsorbed by the Fe-Mn oxides. It may be that a pH scale of 0.5 to 5 combined with short times

(5 to 60 minutes) would give a larger change in metal released. The shorter time would reduce the readsorption of metals onto the sediments.

Studies of the interactive effect of combinations of metals upon the yield of plants and uptake of metals by plants have shown that the natural laws governing such interactions are complex and may be represented by a second-order polynomial to first approximation. A detailed comparison between tolerant and non-tolerant forms of the same species would be very beneficial, firstly over a series of wide ranges of metal concentration, followed by a more detailed examination of the more interesting regions of the response surface. Already seeds of such species Goginan (Agrostis tenuis), Merlin (Festuca rubra) and Prays (A. tenuis) are available, while the Holcus lanatus species from Hallen may also be very interesting to study. The latter appears to be more difficult to cultivate and may present reproducibility problems. Further research in this area is needed; statistical analysis of different experimental designs may then enable a more complete understanding of the interaction of metals with the measure response to be made. However, the responses so far measured have been very basic ones, macro in nature e.g. dry weight yield, total concentration of metal taken up. What is clearly required is a whole series of well designed experiments involved with the more biochemical responses of a plant to such stresses, e.g. enzyme activity, etc.

APPENDICES

APPENDIX 1 (GINO)

a)Production of Regression Equation

```
Minitab -log ''filename''
---read 'filename' c1 -c8
---let c11 =c1 *c1
---let c22 =c2 *c2
---let c33 =c3 *c3
---let c12 =c1 *c2
---let c13 =c1 *c3
---let c23 =c2 *c3
---regress c4  9 c1.—c3,c11—c13,c22,c23,c33
---end
---stop
```

b) Generation of Surfaces

Three dimensional response surface produced by using Hein Program while contour plot generated by the following program(see next page);

hex2.fortran

```
%global ansi77
real pxl, pxh, pyl, pyh
real w(10000), az(20,20)
real x(1000), y(1000), z(1000)

ndim=1000
nw=10000
open (8, form="formatted", file="datafile")

call readingraphnumbers(x,y,z,npts,ndim,xmin,xmax,ymin,ymax,$9999)
call vterm
call piccle

call rangrd(npts,x,y,z,20,xmin,xmax,20,ymin,ymax,az,nw,w)

iview = 0
call grdcon(20,xmin,xmax,20,ymin,ymax,az,10,0)

call devend

9999 close(8)
end
subroutine readingraphnumbers(x, y, z, npts, ndim, xmin, xmax, ymin,Ymax,
```

```
real x(ndim), y(ndim), z(ndim)
integer npts, ndim
real xmin, xmax, ymin, ymax
xmin=999999
ymin=999999
xmax=-999999
ymax=-999999
npts=0

10 continue
        read(8,*,end=9000,err=9999)x1,y1,z1
npts=npts+1
if (npts.gt.ndim) goto 9998
xmin = min(xmin, x1)
ymin = min(ymin, y1)
xmax = max(xmax, x1)
ymax = max(ymax, y1)
x(npts) = x1
y(npts) = y1
z(npts) = z1
goto 10

9000 return
   1 format(v)

9998 print '(//, "ERROR : too many data points")'
return 1
9999 print '(//, "ERROR : in reading data")'
return 1
end
```

APPENDIX 2 (SAS)

a) Production of Regression Equation

```
data hussian;
infile metal;
input x1 -x3   y1 -y5 ;
proc  print;
run;
proc sort;by x1 -x3 ;
proc rsreg;
  model y1 =x1 -x3 /lackfit;
  run;
```

b) Generation of 3-D plot of Response Surface

```
data hussian;
do x -1.68 to +1.68 by 0.25;
do y -1.68 to +1.68 by 0.25;
z=B0 +B1 x+B2 y+B11  x*x+B22 y*y+B12  x*y;
output;end;end;
proc g3d;
plot y*x=z/caxis=green  ctext=green;
proc g3d;
plot y*x=z/tilt=45 rotate=45;
```

c)Procedure for GLM

```
data homam:
infile abas;
input a $ b $ c $ y @@;
proc GLM;
class a b c;
model y=a b c a*b a*c b*c a*b*c;
```